

GLIOBLASTOMA

Cover image: Primary diagnosis of a right frontal glioblastoma following acquisition of axial slices of T1-weighted gadolinium-enhanced MRI (left) and 18F-FDG PET (right). See page 158, chapter 9 for details.

GLIOBLASTOMA

Edited by

STEVEN DE VLEESCHOUWER

Department of Neurosurgery, University Hospitals Leuven, Leuven, Belgium



Codon Publications
Brisbane, Australia

Glioblastoma

ISBN: 978-0-9944381-2-6

DOI: <http://dx.doi.org/10.15586/codon.glioblastoma.2017>

Edited by

Steven De Vleeschouwer, MD, PhD

Department of Neurosurgery, University Hospitals Leuven, Leuven, Belgium

Published by

Codon Publications

Brisbane, QLD 4122, Australia

Copyright© 2017 Codon Publications

This open access book is published under Creative Commons Attribution 4.0 International (CC BY 4.0). <https://creativecommons.org/licenses/by-nc/4.0/>

Users are allowed to share (copy and redistribute the material in any medium or format) and adapt (remix, transform, and build upon the material for any non-commercial purpose), as long as the authors and the publisher are explicitly identified and properly acknowledged as the original source.

Notice to the user

The views and opinions expressed in this book are believed to be accurate at the time of publication. The publisher, editors or authors cannot be held responsible or liable for any errors, omissions or consequences arising from the use of the information contained in this book. The publisher makes no warranty, implicit or explicit, with respect to the contents of this book, or its use.

First Published in September 2017

Printed in Australia

A free online version is available at <http://codonpublications.com>

CONTENTS

Foreword	ix
Prof. Dr. med. W. Stummer	
Preface	xi
Steven De Vleeschouwer	
Contributors	xiii
Section I Understanding Glioblastoma in the Lab	1
1 Glioblastoma Genomics: A Very Complicated Story	3
Melanie Y. Lombardi, Mahfoud Assem	
2 Molecular Genetics of Secondary Glioblastoma	27
Alireza Mansouri, Jason Karamchandani, Sunit Das	
3 Epigenetic Mechanisms of Glioblastoma	43
Peiyao Li, Minghua Wu	
4 Cancer Stem-Like Cells in Glioblastoma	59
Mathilde Cheray, Gaëlle Bégaud, Elise Deluche, Alexandre Nivet, Serge Battu, Fabrice Lalloué, Mireille Verdier, Barbara Bessette	
5 Molecular Mechanisms of Glioma Cell Motility	73
Angela Armento, Jakob Ehlers, Sonja Schötterl, Ulrike Naumann	
6 Noncoding RNAs in Glioblastoma	95
Ying Zhang, Nichola Cruickshanks, Mary Pahunski, Fang Yuan, Anindya Dutta, David Schiff, Benjamin Purow, Roger Abounader	
7 Mouse Models of Glioblastoma	131
Noriyuki Kijima, Yonehiro Kanemura	

Section II: Managing Glioblastoma in the Clinic	141
8 Epidemiology and Outcome of Glioblastoma	143
Ahmad Faleh Tamimi, Malik Juweid	
9 PET Imaging in Glioblastoma: Use in Clinical Practice	155
Antoine Verger, Karl-Josef Langen	
10 PET for Therapy Response Assessment in Glioblastoma	175
Julie Bolcaen, Marjan Acou, Benedicte Descamps, Ken Kersemans, Karel Deblaere, Christian Vanhove, Ingeborg Goethals	
11 Current Standards of Care in Glioblastoma Therapy	197
Catarina Fernandes, Andreia Costa, Lígia Osório, Rita Costa Lago, Paulo Linhares, Bruno Carvalho, Cláudia Caeiro	
12 Surgical Management of Glioblastoma	243
Salvador Manrique-Guzmán, Tenoch Herrada-Pineda, Francisco Revilla-Pacheco	
13 Cortical Mapping in the Resection of Malignant Cerebral Gliomas	263
Jehad Zakaria, Vikram C. Prabhu	
14 Recurring Glioblastoma: A Case for Reoperation?	281
Joost Dejaegher, Steven De Vleeschouwer	
15 Pediatric Glioblastoma	297
Kuntal Kanti Das, Raj Kumar	
Section III: Upcoming Cutting-Edge Innovations	313
16 Glioblastoma: To Target the Tumor Cell or the Microenvironment?	315
Steven De Vleeschouwer, Gabriele Bergers	

17	Maximizing Local Access to Therapeutic Deliveries in Glioblastoma. Part I: Targeted Cytotoxic Therapy	341
	Waldemar Debinski, Waldemar Priebe, Stephen Tatter	
18	Maximizing Local Access to Therapeutic Deliveries in Glioblastoma. Part II: Arborizing Catheter for Convection-Enhanced Delivery in Tissue Phantoms	359
	Egleide Y. Elenes, Christopher G. Rylander	
19	Maximizing Local Access to Therapeutic Deliveries in Glioblastoma. Part III: Irreversible Electroporation and High-Frequency Irreversible Electroporation for the Eradication of Glioblastoma	373
	Melvin F. Lorenzo, Christopher B. Arena, Rafael V. Davalos	
20	Maximizing Local Access to Therapeutic Deliveries in Glioblastoma. Part IV: Image-Guided, Remote-Controlled Opening of the Blood–Brain Barrier for Systemic Brain Tumor Therapy	395
	Anirudh Sattiraju, Yao Sun, Kiran Kumar Solingapuram Sai, King C.P. Li, Akiva Mintz	
21	Maximizing Local Access to Therapeutic Deliveries in Glioblastoma. Part V: Clinically Relevant Model for Testing New Therapeutic Approaches	405
	John Rossmeisl	
	Index	427

Doi: <http://dx.doi.org/10.15586/codon.glioblastoma.2017>

FOREWORD

Glioblastomas remain a conundrum in neuro-oncology, and the perception of a given generation of physicians and clinician scientists has somehow always been that progress is tedious, if visible at all. Looking beyond generations, however, it is clear that progress in understanding the molecular genesis of these tumors, their genetics and epigenetics, and also their clinical therapy is being made. Over the years, the prognosis of these tumors has been slowly improving as therapies are becoming more complex. Gone are the days in which the basic tenets of therapy were surgery by the youngest and the least experienced neurosurgeons, without early imaging to assess resection rates, followed by simple radiotherapy. Current surgical strategies are complex, encompassing complex intraoperative imaging combined with sophisticated mapping and monitoring, striving for maximal resections while maintaining function and quality of life. These are standard in specialized centers. State-of-the art surgery is followed by molecular classification of tumors and multidisciplinary decisions regarding chemotherapy and radiotherapy. Second and third operations are not uncommon, as are second courses of radiotherapy and varying, individualized chemotherapy regimens. Patients can now participate in a large number of clinical trials. Thus, even though glioblastoma remains a devastating tumor, the knowledge about this disease is rapidly expanding.

This book, edited by Steven De Vleeschouwer, MD, PhD, is a timely, unique, and exhaustive compilation of preclinical and clinical knowledge and concepts regarding glioblastomas. It clearly goes beyond a simple guide for the clinical neuro-oncologist, as it also targets basic and clinician scientists devoted to the expanding field of neuro-oncology. This book covers genetics; epigenetics; stem cells; experimental methods; epidemiology; imaging; clinical surgical, radio-oncological, and oncological management; and provides an exciting outlook at future concepts and treatment approaches.

I strongly recommend this book to anybody active in the field of neuro-oncology, preclinically, clinically, or both.

Prof. Dr. med. W. Stummer
Department of Neurosurgery
University of Münster
September 2017

Doi: <http://dx.doi.org/10.15586/codon.glioblastoma.2017.fr>

PREFACE

Glioblastoma is the most common and the most malignant variant in the wide spectrum of intrinsic glial brain tumors. Although it can affect children, its incidence increases with age. To date, no uniform etiology has been identified. The pathogenesis in genetic and epigenetic terms is gradually being unraveled. Unlike most aggressive malignancies, glioblastoma only seems to thrive in the exclusive microenvironment of the brain and as such, extracranial metastasis is rare. Nevertheless, individual glioblastoma cells display an unmatched capacity to invade surrounding brain areas and thus exert a locally destructive influence on brain tissue and function. This finding, together with the intrinsic and extrinsic heterogeneity of the tumor, and its environment, makes glioblastoma one of the most difficult cancers to treat. In spite of significant improvements in surgical techniques, radiation technology, and systemic therapies, glioblastoma continues to be an incurable disease causing an enormous individual and societal burden. Although a slow, incremental improvement in survival rates has been noticed in those patients who are fit enough to get an intense, multimodal treatment schedule, the medical need still is widely unmet. Therefore, physicians and basic scientists will have to join forces to create some long-awaited breakthroughs for patients with this devastating disease.

This book, aimed at students, basic scientists, and physicians dedicated to neuro-oncological research and care to its full extent, is divided into three sections, focusing on a better understanding of the disease biology, an inclusive diagnostic and therapeutic management of the disease in the clinic, and an outreach to upcoming new insights and technical innovations.

Section I gives a comprehensive overview on the molecular genetics, biological hallmarks, and the current state-of-the-art preclinical animal models in glioblastoma research. Chapter 1 guides us through the complicated story of glioblastoma genomics and discusses validated and upcoming biomarkers with a potential to improve diagnosis and treatment. In Chapter 2, the genetic identity of secondary glioblastomas, an important minority subgroup, is highlighted as an example of how molecular genetics directly impacts clinical decision-making. Chapter 3 introduces the reader to the fascinating world of epigenetics and its role in pathogenesis, therapy response, and prognosis. Glioma cancer stem cell as the niche for glioma initiation and therapy resistance is the central topic of Chapter 4. In Chapter 5, which discusses glioma cell motility, the most important driver of glioblastoma invasiveness in a healthy brain is being thoroughly discussed, and in Chapter 6, the regulatory role of both microRNAs and long non-coding RNA is being explained showing their steadily mounting importance in understanding glioblastoma biology. Finally in Chapter 7, a concise and clear overview is given of the most widely used small animal models for preclinical research in malignant glioma.

Section II deals with the many diagnostic, therapeutic, and prognostic management challenges physicians are facing every day. Chapter 8 nicely rehearses the epidemiological factors involved in disease and outcome. In Chapter 9, an extensive overview is given of PET imaging options that are increasingly being used in

the neuro-oncological field, and Chapter 10 further elaborates on the potential of different PET tracers as promising tools to assess therapy response versus disease progression, as a highly relevant item in the clinical arena since pseudo-progression and pseudo-responses are known to interrupt our classical decision-making based on MRI imaging and clinical performance of the patient. In Chapter 11, in a central position in the book, a bright and critical appraisal is being performed on the current standard-of-care in glioblastoma therapy, including both conventional radiotherapy and chemotherapy but also newer approaches based on medical evidence. After a comprehensive update on the surgical management of glioblastoma in Chapter 12, intraoperative cortical brain mapping is highlighted in Chapter 13. Challenges and considerations in the context of recurrent glioblastoma are described in Chapter 14 from a surgeon's point of view. The peculiar aspects of pediatric glioblastoma, as a separate disease entity, are dealt with in Chapter 15 to conclude this clinical section on glioblastoma.

Section III has six chapters that try to capture innovative approaches and techniques that might have the potential to gain impact in the field in the coming years. Chapter 16 elaborates on a comprehensive overview of the glioblastoma tumor microenvironment as an underexplored gateway to the tumor, lodging quite some new targets for therapy in the near future. In Chapter 17, combined targeting of cytotoxic compounds is described as a promising tool to maximize local access to therapeutic deliveries in glioblastoma. Chapter 18 elaborates on further improvements on the development of arborizing, multi-channel catheters for convection-enhanced delivery, and Chapter 19 introduces irreversible electroporation as a selective and powerful technique to destroy glioblastoma tumor cells. In Chapter 20, the authors discuss how to improve drug delivery by overcoming the blood–brain barrier, and in Chapter 21 the audience will discover how canine models can instruct us on the values of new therapeutic approaches.

We are confident that this book will enable students, scientists, and physicians to widen their understanding of glioblastoma as a complex brain cancer with an ongoing high medical need, and develop potential game-changing innovations in the field of neuro-oncology.

Steven De Vleeschouwer, MD, PhD
Department of Neurosurgery
University Hospitals Leuven, Belgium
Laboratory of Experimental Neurosurgery and Neuroanatomy
KU Leuven, Belgium
September 2017
Doi: <http://dx.doi.org/10.15586/codon.glioblastoma.2017.pr>

CONTRIBUTORS

AHMAD FALEH TAMIMI, MD, PHD

Department of Neurosurgery, Jordan University Hospital and Medical School, University of Jordan, Amman, Jordan

AKIVA MINTZ, MD, PHD

Department of Radiology, Columbia University Medical Center New York, USA

ALEXANDRE NIVET, MD

Radiotherapy Department, University Hospital, Limoges, France

ALIREZA MANSOURI, MD, MSC

Division of Neurosurgery, University of Toronto, Toronto, Ontario, Canada

ANDREIA COSTA, MD

Department of Medical Oncology, Centro Hospitalar de São João, Porto, Portugal

ANGELA ARMENTO, PHD

Hertie Institute for Clinical Brain Research and Center Neurology Department of Vascular Neurology, Molecular Neuro-Oncology University of Tübingen, Tübingen, Germany

ANINDYA DUTTA, MD, PHD

Department of Biochemistry and Molecular Genetics, University of Virginia Charlottesville, Virginia, USA; Cancer Center, University of Virginia, Charlottesville, Virginia, USA

ANIRUDH SATTIRAJU, BS

Department of Radiology, Brain Tumor Center of Excellence, Wake Forest Baptist Medical Center Comprehensive Cancer Center, Winston-Salem, North Carolina, USA

ANTOINE VERGER, MD, PHD

Department of Nuclear Medicine & Nancyclotep Imaging platform CHRU Nancy, Lorraine University, Nancy, France; IADI, INSERM, UMR 947, Lorraine University, Nancy, France

BARBARA BESSETTE, PHD

EA3842 HCP, Faculty of Medicine, Limoges, France

BENEDICTE DESCAMPS, MSC, PHD

IBiTech-MEDISIP, Department of Electronics and Information Systems,
Ghent University, Ghent, Belgium

BENJAMIN PUROW, MD

Department of Neurology, University of Virginia, Charlottesville, Virginia, USA;
Cancer Center, University of Virginia, Charlottesville, Virginia, USA

BRUNO CARVALHO, MD

Department of Neurosurgery, Centro Hospitalar de São João Porto, Portugal;
Faculty of Medicine of the University of Porto, Porto, Portugal

CATARINA FERNANDES, MD

Department of Medical Oncology, Centro Hospitalar de São João Porto, Portugal

CHRISTIAN VANHOVE, PHD

IBiTech-MEDISIP, Department of Electronics and Information Systems, Ghent
University, Ghent, Belgium

CHRISTOPHER B. ARENA, PHD

School of Biomedical Engineering and Sciences Virginia Tech-Wake Forest
University, Blacksburg, Virginia, USA; Laboratory for Therapeutic Directed
Energy Department of Physics, Elon University; Elon, North Carolina, USA

CHRISTOPHER RYLANDER, PHD

Department of Mechanical Engineering, The University of Texas at Austin,
Austin, Texas, USA

CLÁUDIA CAEIRO, MD

Department of Medical Oncology, Centro Hospitalar de São João Porto, Portugal

DAVID SCHIFF, MD

Department of Neurology, University of Virginia Charlottesville, Virginia, USA;
Cancer Center, University of Virginia, Charlottesville, Virginia, USA

EGLIDE Y ELENES, MSBE

Department of Biomedical Engineering, The University of Texas at Austin, Austin, Texas, USA

ELISE DELUCHE, MD

Oncology Department, University Hospital Limoges, France

FABRICE LALLOUÉ, PHD

EA3842 HCP, Faculty of Medicine, Limoges, France

FANG YUAN, BS

Department of Microbiology Immunology and Cancer Biology University of Virginia, Charlottesville, Virginia, USA

FRANCISCO REVILLA-PACHECO, MD, FACS

ABC Neurological Center, Neurosurgery Department Mexico City, Mexico

GABRIELE BERGERS, PHD

VIB-KU Leuven Center for Cancer Biology, Campus Gasthuisberg, Leuven, Belgium

GAËLLE BÉGAUD, PHD

EA3842 HCP, Faculty of Medicine, Limoges, France; Laboratory of Analytical Chemistry, Faculty of Pharmacy Limoges, France

INGEBORG GOETHALS, MD, PHD

Department of Nuclear Medicine, Ghent University Hospital Ghent, Belgium

JAKOB EHLERS (CAND. MED.)

Hertie Institute for Clinical Brain Research and Center Neurology Department of Vascular Neurology, Molecular Neuro-oncology University of Tübingen, Tübingen, Germany

JASON KARAMCHANDANI, MD

Department of Pathology, Montreal Neurological Institute, McGill University, Montreal, Quebec, Canada

JEHAD ZAKARIA, MD

Department of Neurological Surgery, Loyola University Medical Center/Stritch School of Medicine, Maywood, Illinois, USA

**JOHN ROSSMEISL, DVM, MS, DIPLOMATE ACVIM
(SAIM AND NEUROLOGY)**

Neurology and Neurosurgery, Brain Tumor Center of Excellence
Wake Forest Baptist Medical Center Comprehensive Cancer Center
Winston Salem, North Carolina, USA; School of Biomedical Engineering and
Sciences, Virginia Tech-Wake Forest University; Blacksburg, Virginia, USA;
Virginia-Maryland Regional College of Veterinary Medicine; and Blacksburg,
Virginia, USA; Virginia Tech, Blacksburg, Virginia, USA

JOOST DEJAEGER, MD

Department of Neurosurgery, University Hospitals Leuven, Leuven, Belgium

JULIE BOLCAEN, MSC, PHD

Department of Nuclear Medicine, Ghent University Hospital Ghent, Belgium

KAREL DEBLAERE, MD, PHD

Department of Radiology and Medical Imaging, Ghent University Hospital Ghent,
Belgium

KARL-JOSEF LANGEN, MD, PHD

Department of Nuclear Medicine, University of Aachen, Aachen, Germany;
Institute of Neuroscience and Medicine Forschungszentrum Jülich, Jülich,
Germany

KEN KERSEMANS, MSC, PHD

Department of Nuclear Medicine, Ghent University Hospital Ghent, Belgium

KING C.P. LI, MD, MBA

Carle-Illinois College of Medicine, Urbana, Illinois, USA

KIRAN KUMAR SOLINGAPURAM SAI, PHD

Department of Radiology, Brain Tumor Center of Excellence, Wake Forest
Baptist Medical Center Comprehensive Cancer Center, Winston-Salem,
North Carolina, USA

KUNTAL KANTI DAS, MS, MCH

Department of Neurosurgery, Sanjay Gandhi Postgraduate Institute of Medical
Sciences Lucknow, India

LÍGIA OSÓRIO, MD

Department of Radiotherapy, Centro Hospitalar de São João Porto, Portugal

MAHFOUD ASSEM, PHARMD, PHD

Biopharmaceutical Sciences Department, School of Pharmacy, Medical College of Wisconsin, Milwaukee, Wisconsin, USA

MALIK JUWEID, MD

Department of Radiology and Nuclear medicine, Jordan University Hospital and Medical School, University of Jordan Amman, Jordan

MARJAN ACOU, MD

Department of Radiology and Medical Imaging, Ghent University Hospital Ghent, Belgium

MARY PAHUSKI, MS

Department of Microbiology Immunology and Cancer Biology University of Virginia, Charlottesville, Virginia, USA

MATHILDE CHERAY, PHD

Department of Oncology-Pathology, Cancer Centrum Karolinska Stockholm, Sweden

MELANIE Y. LOMBARDI, PHARMD

South University School of Pharmacy, Columbia, South Carolina, USA

MELVIN F. LORENZO, BS

School of Biomedical Engineering and Sciences, Virginia Tech-Wake Forest University, Blacksburg, Virginia, USA

MINGHUA WU, PHD

The Key Laboratory of Carcinogenesis of the Chinese Ministry of Health Cancer Research Institute, Central South University, Changsha, Hunan, China; The Key Laboratory of Carcinogenesis and Cancer Invasion of the Chinese Ministry of Education Cancer Research Institute, Central South University Changsha, Hunan, China

MIREILLE VERDIER, PHD

EA3842 HCP, Faculty of Medicine, Limoges, France

NICHOLA CRUICKSHANKS, PHD

Department of Microbiology Immunology and Cancer Biology
University of Virginia, Charlottesville, Virginia, USA

NORIYUKI KIJIMA, MD, PHD

Department of Neurosurgery, Osaka National Hospital, National Hospital
Organization, Osaka, Japan

PAULO LINHARES, MD

Department of Neurosurgery, Centro Hospitalar de São João Porto, Portugal;
Faculty of Medicine of the University of Porto, Porto, Portugal

PEIYAO LI, PHD

The Key Laboratory of Carcinogenesis of the Chinese Ministry of Health
Cancer Research Institute, Central South University, Changsha, Hunan, China;
The Key Laboratory of Carcinogenesis and Cancer Invasion of the Chinese
Ministry of Education Cancer Research Institute Central South University,
Changsha, Hunan, China

RAFAEL V. DAVALOS, PHD

School of Biomedical Engineering and Sciences, Virginia Tech-Wake Forest
University, Blacksburg, Virginia, USA

RAJ KUMAR, MS, MCH

Department of Neurosurgery, Sanjay Gandhi Postgraduate Institute of Medical
Sciences, Lucknow, India

RITA COSTA LAGO, MD

Department of Radiotherapy, Centro Hospitalar de São João Porto, Portugal

ROGER ABOUNADER, MD, PHD

Department of Microbiology Immunology and Cancer Biology University of
Virginia, Charlottesville, Virginia, USA; Department of Neurology, University of
Virginia; Charlottesville, Virginia, USA; Cancer Center, University of Virginia,
Charlottesville, Virginia, USA

SALVADOR MANRIQUE-GUZMAN, MD, MSC

ABC Neurological Center, Neurosurgery Department, Mexico City, Mexico

SERGE BATTU, PHD

EA3842 HCP, Faculty of Medicine, Limoges, France; Laboratory of Analytical Chemistry, Faculty of Pharmacy Limoges, France

SONJA SCHÖTTERL, MSC

Hertie Institute for Clinical Brain Research and Center Neurology Department of Vascular Neurology, Molecular Neuro-oncology University of Tübingen, Tübingen, Germany

STEPHEN TATTER, MD, PHD

Department of Neurosurgery, Wake Forest Baptist Medical Center, Winston-Salem, North Carolina, USA

STEVEN DE VLEESCHOUWER, MD, PHD

Department of Neurosurgery University Hospitals Leuven, Leuven, Belgium

SUNIT DAS, MD, PHD

Division of Neurosurgery and Li Ka Shing Knowledge Institute, St. Michael's Hospital, Labatt Brain Tumour Research Centre, Hospital for Sick Children, University of Toronto, Toronto, Canada

TENOCH HERRADA-PINEDA, MD

ABC Neurological Center, Neurosurgery Department Mexico City, Mexico

ULRIKE NAUMANN, PHD

Hertie Institute for Clinical Brain Research and Center Neurology Department of Vascular Neurology, Molecular Neuro-oncology University of Tübingen, Tübingen, Germany

VIKRAM C. PRABHU MD, FACS, FAANS

Department of Neurological Surgery, Loyola University Medical Center/ Stritch School of Medicine Maywood, Illinois, USA

WALDEMAR DEBINSKI, MD, PHD

Director, Brain Tumor Center of Excellence, Thomas K. Hearn, Jr. Brain Tumor Research Center; Professor of Cancer Biology, Radiation Oncology Microbiology and Immunology, Translational Science Institute and Neurosurgery, Wake Forest Baptist Medical Center Comprehensive Cancer Center, Winston-Salem, North Carolina, USA

WALDEMAR PRIEBE, PHD

Department of Experimental Therapeutics, Division of Cancer Medicine,
University of Texas MD Anderson Cancer Center, Houston, Texas, USA

YAO SUN, PHD

Department of Radiology, Brain Tumor Center of Excellence, Wake Forest
Baptist Medical Center Comprehensive Cancer Center, Winston-Salem,
North Carolina, USA

YING ZHANG, MD, PHD

Department of Microbiology Immunology and Cancer Biology University of
Virginia, Charlottesville, Virginia, USA

YONEHIRO KANEMURA, MD, PHD

Department of Neurosurgery, Osaka National Hospital, National Hospital
Organization, Osaka, Japan; Division of Regenerative Medicine, Institute for
Clinical Research, Osaka National Hospital, National Hospital Organization,
Osaka, Japan

Doi: <http://dx.doi.org/10.15586/codon.glioblastoma.2017.cont>

Section I

**Understanding
Glioblastoma in the Lab**

1

Glioblastoma Genomics: A Very Complicated Story

MELANIE Y. LOMBARDI¹ • MAHFOUD ASSEM²

¹South University School of Pharmacy, Columbia, SC, USA;

²Biopharmaceutical Sciences Department, School of Pharmacy, Medical College of Wisconsin, Milwaukee, WI, USA

Author for correspondence: Mahfoud Assem, Biopharmaceutical Sciences Department, School of Pharmacy, Medical College of Wisconsin, Milwaukee, WI, USA. E-mail:massem@mcw.edu

Doi: <http://dx.doi.org/10.15586/codon.glioblastoma.2017.ch1>

Abstract: Glioblastoma is a deadly disease that has not shown improvement despite the development of new diagnostic tools and innovative targeted therapies. This grim outcome is mainly related to a complex intra- and inter-individual heterogeneity resulting from severe genetic instability. Understanding glioblastoma biology may establish a foundation to improve prophylaxis, early diagnosis, prognosis, and treatment prediction, thus leading to a better outcome. Recent advances in technologies such as genomics, epigenomics, transcriptomics, and proteomics have led to unprecedented discoveries of potential prognostic and predictive markers. Several of these biomarkers are in deep need of validation to be used in clinical routine. In this chapter, we will discuss the most accomplished recent advances in the genomics of glioblastoma and insight into personalized medicine using validated, and not yet validated, biomarkers that may have great potential to improve patients' outcomes.

Key words: Glioblastoma; Heterogeneity; Prognosis; Subtypes; Targeted therapies

In: *Glioblastoma*. Steven De Vleeschouwer (Editor), Codon Publications, Brisbane, Australia
ISBN: 978-0-9944381-2-6; Doi: <http://dx.doi.org/10.15586/codon.glioblastoma.2017>

Copyright: The Authors.

Licence: This open access article is licenced under Creative Commons Attribution 4.0 International (CC BY 4.0). <https://creativecommons.org/licenses/by-nc/4.0/>

Introduction

Glioblastoma (GBM) is the most frequent type of primary tumors of the central nervous system in adults, and its very poor prognosis has not significantly improved despite the development of innovative diagnostic strategies and new therapies (1, 2). Complex and poorly reproducible diagnoses and the inability to accurately predict sensitivity or resistance to chemotherapy regimens, as well as less than optimal CNS bioavailability, have contributed to the poor prognosis for patients with glioblastoma. Therefore, understanding the molecular mechanisms underlying its aggressive behavior may lead to better management, appropriate therapies, and good outcomes. Cancer progression is promoted by somatic evolution, a process in which an accumulation of mutations causes the genome of a cancer cell to deviate from that of a healthy cell. Some cancers, such as colon cancer, have a very well-defined sequence of events leading to their development. GBM development is however remarkable in that it occurs via a complex network of different genetic and molecular aberrations, leading to significant changes in major signaling pathways. In recent years, substantiated data have emerged and demonstrated that tumors are made of multiple populations of cancerous cells harboring specific genetic alterations in addition to the classical founder genetic abnormalities (3). This heterogeneity in tumors results from the characterized genetic instability and increased mutation rates that accompany all neoplasms and from a Darwinian selection of the fittest clones through genetic and epigenetic modifications (4). GBMs are lethal as they disperse extensively throughout the brain parenchyma, making maximal surgical resection unattainable and also because of a high level of vascularization. Thus, the need for tumor-specific drug targets and pharmacological agents to inhibit cell migration, dispersal, and angiogenesis is indeed immense. There are no inheritable traits that are predisposing to GBM development; therefore, all characterized genetic alterations are somatic and acquired aberrations. This chapter will discuss some of the most commonly affected signaling pathways and their relevance for possible use into a personalized medicine approach.

Pathogenesis of Glioblastoma

ONCOGENIC PATHWAYS

The most frequently altered pathway involves receptor tyrosine kinases (RTKs) (5–7). RTKs are cell-surface receptors that bind growth factors (GFs). GF binding occurs via cross-linking, inducing the dimerization of two adjacent receptors and a conformational shift. This shift activates the kinase function of the RTK allowing cross-phosphorylation of tyrosine residues in preparation for downstream signaling cascades (Figure 1A). Epidermal growth factor receptor (EGFR) signaling functions in the proliferation, migration, differentiation, and survival of all types of central nervous system cells (8). In GBM cells, EGFR signaling can be activated either through overexpression of the receptor or its ligand, amplification of the *EGFR* locus, and/or receptor mutation (9). It is important to note that any combination of these alterations may coexist within the same tumor. The oncogenic

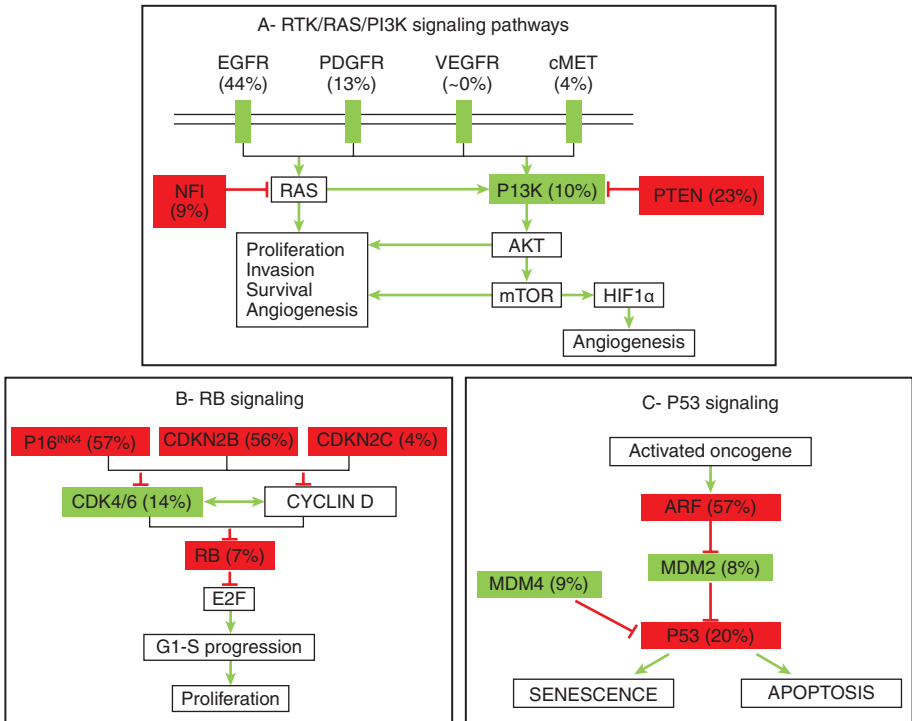


Figure 1 Genetic alterations in major key pathways altered in glioblastoma. Mutations, deletions, and amplifications in (A) RTK/RAS/PI3K, (B) RB, and (C) p53 signaling pathways are shown. Green boxes indicate activating mutation and amplifications. Red boxes indicate inactivating alterations such as mutations and deletions. Frequency of alterations are shown in each box. (Adapted from Ref. (7))

properties of EGFR are associated with constitutive activation and uncontrolled increases in phosphorylation activity. The majority of GBMs that overexpress EGFR also have mutation of the *EGFR* gene. The most common mutation is the EGFRvIII, which corresponds to the loss of exons 2–7, leading to a deletion of 267 amino-acids in the extracellular domain making the receptor ligand independent and constitutively active. This mutation is never observed in healthy tissues and secondary GBM (10).

Another commonly modified pathway in GBM is the Ras pathway. Increases in Ras pathway activity are seen in nearly all GBMs; however, Ras mutations are rare in this population (11). In the absence of mutated Ras, these high levels can be attributed to increased activation of upstream factors, such as the EGFR (Figure 1A). Ras is a guanosine-binding protein (G protein) that cycles between an inactive state when bound to GDP and an active form when bound to GTP. Active Ras (Ras-GTP) promotes progression through the cell cycle, survival, and migration through a cascade of downstream effectors. The Phosphatidylinositol-4,5-Bisphosphate 3-Kinase/Phosphatase and Tensin Homolog/serine threonine kinase Akt (PI3K/PTEN/Akt) pathway is also initiated by growth factor–receptor

interactions (Figure 1A). Upon growth factor receptor activation, PI3K is drawn to the cell membrane, resulting in the generation of the secondary messenger phosphatidylinositol (3,4,5)-trisphosphate (PIP3) (12). Akt is a downstream effector of PIP3 that leads to cell proliferation and inhibition of apoptosis. PTEN normally acts as a negative regulator of PI3K and terminates the PIP3 signal. In GBM, the tumor suppressor function of PTEN is frequently inactivated, either by loss of heterozygosity (LOH) or mutation-induced constitutive activation of PI3K, resulting in increased PI3K availability. Unopposed PI3K-mediated signaling has been implicated in GBM pathogenesis (13).

The retinoblastoma (RB) pathway plays a key role in the cell cycle. In cells that are dormant, or nonproliferating, RB is hypo-phosphorylated and actively binds to the transcription factor E2F. RB binding to E2F prevents the transcription of genes that are necessary for mitosis and the cell cycle is halted at the G1/S check-point. In proliferating cells, GFs induce Cyclin D1 formation and activation of cyclin-dependent kinase-cyclin (CDK/cyclin) complexes. Active CDK/cyclin complexes phosphorylate RB, resulting in the release of E2F. Free E2F induces transcription of genes that promote DNA synthesis and cell proliferation occurs (14). Negative regulation of the RB pathway can be accomplished by cyclin-dependent kinase inhibitor proteins (CDKN) belonging to the INK family. One example is the CDKN2A-p16^{INK4a}, which competes with cyclins for CDK binding to prevent RB phosphorylation (15). Certain GBM cells can override this negative regulation via methylation of the RB promoter and gene silencing. Alteration of the RB pathway leads to substantial cell cycle imbalances (Figure 1B). The TP53 pathway also functions in cell cycle control, DNA damage response, cell death, and differentiation. When DNA damage occurs, the cell becomes stressed and activates the TP53 pathway. To allow time for DNA repair to occur, TP53 increases transcription of p21, a CDKN that binds cyclin proteins and inhibits their functions to halt progression through the G1 phase of the cell cycle (16). If there is more damage than can be repaired quickly, TP53 will induce cell death to prevent division of cells containing mutated or damaged DNA. The TP53 pathway has negative feedback loops. TP53 induces transcription of MDM2, a proto-oncogene, which leads to the degradation of TP53 and prevention of DNA repair. To maintain TP53 activity, the CDKN2A-p14^{ARF} inactivates MDM2 via degradation. MDM4, a regulator of TP53, can inactivate TP53 via binding of the transcriptional activation domain (17). In human gliomas, TP53 mutations are often missense mutations that target exons crucial for DNA binding. Other alterations seen in GBMs are MDM2 amplification, MDM4 amplification, and CDKN2A-p14^{ARF} deletion (7) (Figure 1C). Currently, there are no defined sequence of events that definitively lead to GBM development. Any number or combination of these pathways may contribute to GBM formation. Although these pathways are well defined, the complexity of GBM is enhanced by high levels of variability both between different tumors, as well as within a single tumor.

INTRATUMOR HETEROGENEITY

Intratumor heterogeneity is defined as the presence of multiple different cell sub-populations within a single tumor from one patient (18). Tumor heterogeneity allows a tumor to respond to selective pressures, thus contributing to tumor

aggressiveness, growth, and treatment failure (19). Heterogeneity poses a significant challenge to the design of effective new drug therapies. There are currently two proposed mechanisms for the development of intratumor heterogeneity: cancer stem cells that may possess varying degrees of stemness, the ability to self-renew and differentiate into different tumor cell types, and clonal evolution that may enhance genetic diversity within the affected tissues (20, 21). Intratumor heterogeneity is spatially defined from the core of the tumor to the periphery. The core of a GBM tumor is an area of high proliferation and inflammation. The core is comprised of a zone of necrosis surrounded by the tumor zone. The margin between the tumor tissue and brain parenchyma is called the interface. Tumor cell density decreases throughout the interface as distance from the core increases (Figure 2) (22). The outermost area is known as the peripheral brain zone (PBZ), and it consists of mainly brain parenchymal tissue with isolated infiltrates (23). These isolated infiltrates dispersed throughout normal brain tissues in the PBZ help to explain why total surgical resection is impossible and recurrence is nearly inevitable. Studies have shown that biopsies taken from the core and interface zones had much higher levels of genomic alterations compared to biopsies of tissues from the PBZ, suggesting that changes in gene expression are dependent upon tumor area. These results are clear evidence that tumor fragments from the same patient may be classified into different molecular subtypes (23). Tumor recurrence in the primary site or in surrounding brain parenchyma is all too often a great challenge despite new therapies and interventions. This is related to astrocytic tumor diffusion and invasion properties that are linked to the migrating glioma stem cells (24).

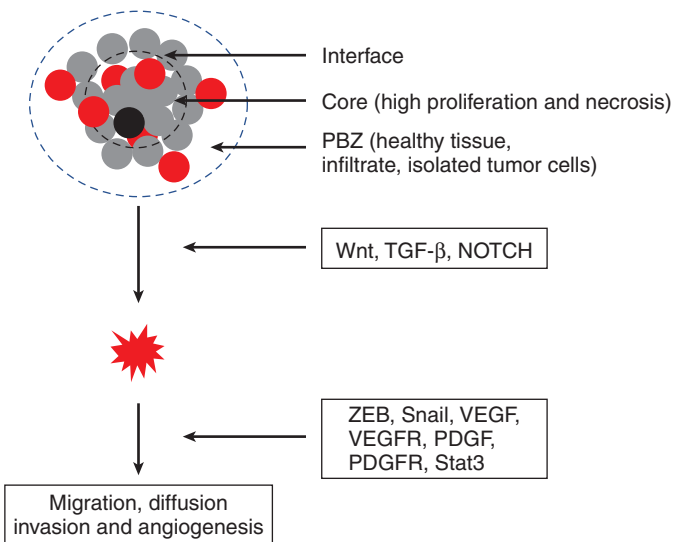


Figure 2 Pathogenesis of epithelial to mesenchymal transition (EMT). EMT is a programmed pathway for clonal outgrowth of localized tumors to colonize surrounding areas and promote angiogenesis. This process is a cross talk between glioblastoma stem cells (red circles), clonal cancer cells (gray and black circles [necrotic]), and epithelial cells via genetic reprogramming, implicating several genes and transcription factors. (Adapted from Ref. (22).)

EPITHELIAL TO MESENCHYMAL TRANSITION

The epithelial to mesenchymal transition (EMT) is a programmed event in which epithelial cells, through a genetic reprogramming or selection, acquire a mesenchymal phenotype. This process results from alterations in cell architecture and behaviors following cell–cell and cell–extracellular matrix interactions (25), leading to clonal outgrowth of localized tumors to promote a mesenchymal phenotype, conferring an unusual property for the cell to colonize surrounding areas and activate angiogenesis (26). It has been demonstrated that tumors with high EMT activation are associated with hyper-vascularization and worse outcomes. Aberrant activation of several signaling pathways and EMT regulators can lead to oncogenic EMT and cancer progression (Figure 2). Wnt, TGF- β , and NOTCH pathways among other signaling pathways have been shown to play major roles in EMT (27). They act via modulating several EMT key transcription factors such as Snai1, Slug, ZEB1, ZEB2, Twist1, and Twist2 (27). Specifically, positive correlation has been found between activation of NOTCH signaling pathway and the expression of EMT markers such as Snail in GBM specimens (28). Further studies have revealed that NOTCH acts upstream of Snai1 to confer invasive ability and mesenchymal phenotype to glioma cells (28). Moreover, recent transcriptomic studies have shown that among many cancer signature genes, mesenchymal genes are overexpressed at the expenditure of proneural genes in several GBM biopsies from patients with poor prognosis (29). Specifically, C/EBP β and STAT3 have been shown to act as mesenchymal driving genes of prognostic value (29). Patients with tumors that are double-positive for C/EBP β and STAT3 have shorter survival when compared to patients with tumors that are single- or double-negative (29). This confirms that these two genes are global regulators of mesenchymal transformation in stem cells and that they are necessary in the maintenance of the aggressive mesenchymal phenotype in glioma cells both *in vitro* and *in vivo* (29), and highlights potential cross talk between glioblastoma stem cell (GSC) theory and the EMT process.

EMT can generate cancer cells with stem-like properties (30). Indeed, upon acquisition of EMT phenotype, GSCs acquire both stemness and mesenchymal properties. Unlike tumors that metastasize, this double property may explain tumor invasion that is one of the hallmarks of recurrent GBM. It has been shown that high expression of Slug (EMT marker) correlates with higher grade glioma and is associated with high levels of the GSC marker, CD44, which also has been reported to promote glioblastoma cells migration, invasion, and angiogenesis (31, 32).

GBM tumors are extensively vascularized resulting from an overactivated angiogenesis, a process of forming new blood vessels which is a critical step for supplying oxygen for tumor growth (33). However, it is often an inefficient process, leading to tumors with areas of hypoxia, necrosis, and edema (34). Mechanisms of new blood vessel formation include differentiation of GSC into vascular endothelium in addition to the generation of new vessels that involves recruitment of endothelial progenitor cells (35). In response to hypoxia, the hypoxia inducible factor-1 (HIF-1 α) is frequently activated in GBM (36) and induces VEGF expression (36) (Figure 1A). There is increasing evidence that

GSCs are maintained with a vascular niche which in turn is maintained with VEGF secreted by GSCs and acting through VEGFR-2/KDR (37). This shows that VEGF pathway might be the rate-limiting step of angiogenesis expansion. VEGFRs and PDGFRs are structurally and functionally related growth factor receptors that function in the promotion of angiogenesis and are well-known targets of cancer cells. The angiogenesis transition is believed to be a balance between pro- and anti-angiogenesis factors (38). Several other mediators have been shown to play roles in GBM angiogenesis. Such factors are represented by NOTCH, angiopoietins, PDGF, FGF, integrins, ephrins, and IL-8 (39–41). Conversely, many endogenous inhibitors such as angiostatin, thrombospondins, endostatin, tumstatin, and interferons oppose the action of these mediators (38). Several angiogenesis inhibitor drugs are used in recent clinical trials, most commonly targeting VEGF, VEGFR, PDGF and PDGFR, the key players in the angiogenesis pathway.

Classification of Glioblastoma Based on Genetic Markers

GENOMIC ABNORMALITIES OF PRIMARY AND SECONDARY GBM

Most GBMs are primary tumors that arise in the absence of prior disease. Primary GBMs are aggressive, highly invasive neoplasms that are more commonly seen in the elderly. Secondary GBMs are much less common and typically affect people below the age of 45. Secondary GBMs develop from low-grade astrocytoma and are associated with better prognosis. Primary and secondary GBMs are histologically indistinguishable, yet they evolve from different genetic precursors and show distinctive genetic alterations that can allow for differentiation (42, 43) (Table 1). The alterations seen most frequently in primary GBM are EGFR amplification or mutation, PTEN deletion or mutation, and CDKN2A-p16^{INK4a} deletion (44). Amplification or mutation of EGFR results in constitutive activity, increased proliferation, and survival of mutated cells. PTEN deletions or mutations are almost exclusively seen in the advanced stages of disease in primary GBM. CDKN2A-p16^{INK4a} deletions can be found in both primary and secondary GBMs, although it is more common in primary GBMs. The clinical relevance of CDKN2A-p16^{INK4a} deletions is yet to be determined. Genetic alterations common to secondary GBM include TP53 mutations and Isocitrate Dehydrogenase 1/2 (IDH1/2) mutations (42, 45). TP53 mutations are detectable in the early stages of disease in secondary GBM. IDH1/2 mutations rarely occur in primary GBMs, and have recently been identified as alterations that frequently occur in low-grade gliomas and in the pathway to secondary GBMs. IDH1 mutations are considered the most reliable indicator to differentiate primary from secondary GBM (45). Platelet-derived growth factor receptor (PDGFR) gene amplification is also known to occur in secondary GBM. Even though much time and effort has gone into developing a standard for the classification of GBM, there are still some alterations that cannot be limited to one subclass over another. A more comprehensive list of commonly seen alterations in primary versus secondary GBMs can be found in Table 1, although the list is not all inclusive.

TABLE 1

Major Genomic, Epigenomic, Transcriptomic, and Proteomic Differences between Primary and Secondary GBM

	Primary	Secondary
Genetic alterations	EGFR Amplification CDKN2A-p16 ^{INK4a} deletion LOH ^a of chromosome 10 PTEN mutation	IDH1/2 mutation LOH of 22q, 13q, 19q TP53 mutation
Gene/protein expression profiles	Centrosome-associated protein 350 Enolase 1 Fas IGFBP2 ^b MMP-9 ^c Survivin Tenascin-X-precursor VEGF ^d VEGF fms-related TK	ADAMTS-19 ^e ASCL1 ^f Cadherin-related tumor suppressor homolog precursor DUOX2 ^g ERCC6 ^h HNRPA3 ⁱ Loss of TIMP-3 ^j PDGFR TP53 WNT-11 ^k protein precursor
Promoter methylation	–	CDKN2A-p14 ^{ARF} CDKN2A-p16 ^{INK4a} MGMT ₁ RB TIMP-3

^aLoss of heterozygosity; ^binsulin-like growth factor binding protein 2; ^cmatrix metalloproteinase 9; ^dvascular endothelial growth factor; ^ea disintegrin and metalloproteinase with thrombospondin motifs 19; ^fAchaete-Scute Family BHLH Transcription Factor 1; ^gdual oxidase 2; ^hexcision repair cross-complementation group 6; ⁱheterogenous nuclear ribonucleoprotein A3; ^jtissue inhibitor of metalloproteinases 3; ^kWnt family member 11; ^lO-6-Methylguanine-DNA Methyltransferase.

GENOME-, EPIGENOME-, AND TRANSCRIPTOME-BASED CLASSIFICATION

Initiation and progression of GBM are linked to genetic and epigenetic aberrations. Genetic subgroups of GBM have unique gene expression profiles. Based on these profiles, GBMs can be stratified into four clusters: mesenchymal, classical (or proliferative), proneural, and neural (Figure 3). These molecular subtypes are also associated with different spatial zones of a GBM tumor. Mesenchymal GBMs have overexpression of mesenchymal and astrocytic markers in addition to neurofibromin 1 (NF1) deletion. NF1 normally functions as a negative regulator of the Ras pathway. The classical subtype displays high-level proliferation and is associated with EGFR amplification, Chr.10 monosomy, and CDKN2A-p16^{INK4a} deletion. Proneural subtype GBMs present with alterations in TP53, PDGFRA, PIK3C, and IDH1. These GBMs are seen most in younger

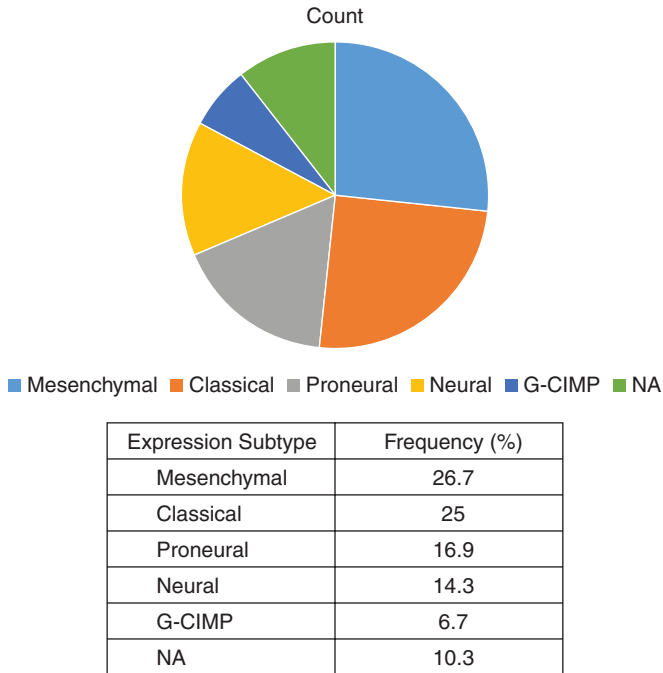


Figure 3 Summary of GBM subtypes based on transcriptomics and methylation status analyses. Unsupervised clustering of GBMs delineates several molecular subtypes. These include proneural, neural, proliferative (or classical), mesenchymal, and G-CIMP. Their frequency is shown. (Adapted from ATLAS-TCGA.) NA: Not analyzed.

patients and are associated with favorable outcomes. Neural subtype GBMs show a strong composition of genes involved in nervous system development and function (46). The mesenchymal and classical subtypes are typically associated with more aggressive high-grade gliomas, while the proneural subtype represents less aggressive high-grade gliomas. Despite this fact, mesenchymal, classical, and proneural subtypes are all associated with tumor tissue. The neural subtype is associated with the interface and PBZ and is classified as a nonenhancing region (23). Another cluster of tumors has been recently identified based on the CpG island methylator phenotype, or G-CIMP tumors (Figure 3). These tumors have distinct copy number alterations, DNA methylation patterns, and transcriptomic profiles compared to the other four subsets of GBMs and are associated with a very favorable outcome (Table 2). The disease process of GBM is characterized by unique sets of molecular changes in cells and their microenvironment. It is increasingly evident that these processes not only differ from patient to patient but also differ between subtypes within the same tumor. These differences shed light on the difficulties seen when trying to develop new targeted drug therapies.

TABLE 2**Summary of Glioblastoma Subtypes Based on Genomics Data (adapted from Refs. (7, 45) and ATLAS-TCGA)**

Gene	Proneural/Neural	Classical	Mesenchymal	G-CIMP
Age	Young	Old	Old	Young
Prognosis	Good	Poor	Poor	Good
Active process	Neurogenesis	Proliferation	Angiogenesis	Neurogenesis
Cell marker	Neuroblast	Stem cell	Stem cell	Neuroblast and nonneuroblast
Chromosomal aberration	Normal Chrs.7 and 10	Gain of Chr.7 Loss of Chr.10	Gain of Chr.7 Loss of Chr.10	Gain of Chrs.8 and 10 IDH1 mutations
EGFR/PTEN loci	Normal EGFR Intact PTEN	EGFR amplified Loss of PTEN	EGFR amplified Loss of PTEN	Normal EGFR Intact PTEN
Altered pathway	NOTCH, TP53, PDGFRA, PIK3C, IDH	AKT, CDKN2A	Met, NF1	MYC

Genomic Landscape of Glioblastoma

COMMON SOMATIC MUTATION ABERRATIONS

Somatic aberrations are nonheritable mutations that can arise spontaneously in somatic cells due to errors that occur in DNA replication or from exposure to environmental mutagens. The resulting changes from these mutations can lead to cellular transformation and cancer progression. Many researchers have focused their efforts on identifying genes relevant to GBM progression by targeting genes with the highest density of missense mutations. A challenge to this method is that higher missense mutations counts may also be associated with higher silent mutation counts and thus be indicative of relaxed purifying selection rather than positive selection (47). One approach to determining which genes are under positive selection in GBM is to identify parallel mutations. Parallel, or recurrent, mutations are identical nucleotide substitutions found at the same site in tumors from different patients. Parallel mutations provide powerful evidence of positive selection on GBM genes because independent random fixation of the same mutation in different patients is highly improbable (47). Genes that are significantly mutated and that display parallelism include EGFR, TP53, PTEN, RB, and IDH1 (Table 3). The advantage of using parallelism is the ability to identify sites under positive selection in GBM when the overall mutation count is not statistically significant. For example, PDGFRA is a known oncogene that shows parallelism, but it is not significantly mutated. Research focusing solely on mutation counts would not classify PDGFRA as a significant mutation in GBM pathogenesis, which could preclude PDGFRA from further investigation (48).

TABLE 3**Most Frequently Mutated Genes Observed in TCGA Glioblastoma Database**

Genes	Number of mutations	Number of patients	Frequency (%)
PTEN	69	131	23.02
EGFR	73	117	20.62
TP53	69	115	20.27
PIK3R1	32	60	10.65
NF1; PIK3CA; SPTA1	28	51	8.93
FLG; PCLO	24	47	8.25
RYR2	21	39	6.87
RB1	20	39	6.87
HMCN1	19	35	6.19
AHNAK2; MUC17	18	33	5.84
IDH1	15	29	5.15
SYNE1; TCHH	14	27	4.81
OBSCN	13	23	4.12
RELN	12	23	4.12
KEL	11	21	3.78
FBN3; GABRA6; MROH2B	10	19	3.44
LZTR1; SEMA3C	9	18	3.09
PDGFRA	10	18	3.09
CNTNAP2; DMD; RBM47	9	18	3.09
BCOR; KMT2C; RPL5; STAG2; TAF1L	8	16	2.75
GRIN2A; HCN1; MYH2	8	14	2.41
ABCB1; ADAMTS16; AFF2; FGD5; GRM3; KIF2B; LRFN5; MYH8; NLRP5; OR8K3; PCDHA1; PCDHA3	7	14	2.41

COMMON COPY NUMBER ABERRATIONS

Copy number aberrations (CNAs) are somatic changes to chromosome structure that result in either a gain or loss of copies in sections of DNA. CNAs are different from copy number variations (CNVs) in that CNAs occur in somatic tissues, whereas CNVs occur in germline tissues and are present in all cells of the organism, not solely in the tumor tissue. The most common CNAs seen in GBM include loss, or partial loss, of chromosomes 9 and 10; polysomy of chromosomes 7, 19, and 20; focal deletion of CDKN2A/B locus (9p21.3); and focal high-level amplifications of EGFR locus (7p11.2) (5, 7) (Figure 4 and Table 4). CNAs targeting chromosomes 7 and 10 are some of the earliest events in GBM tumor evolution.

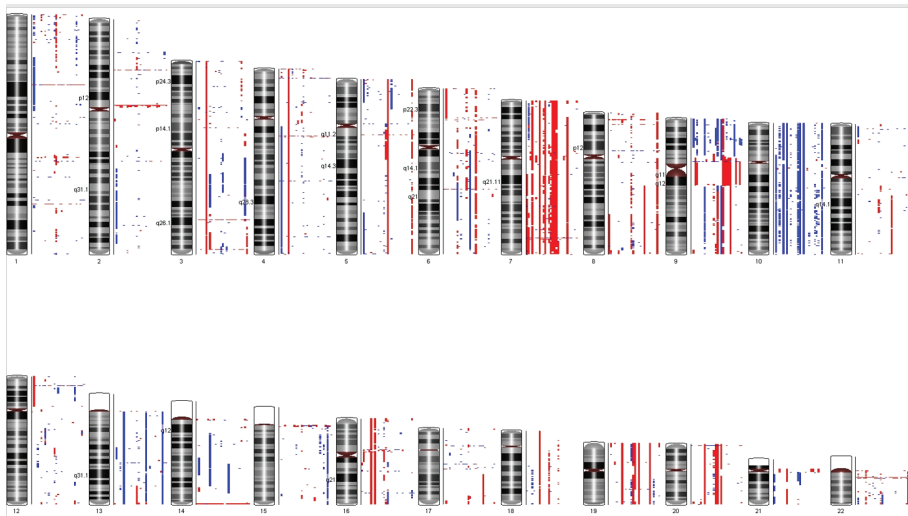


Figure 4 Genomic landscape of glioblastoma. Digital karyotype showing major CNA observed in glioblastoma. Major gain (red) and loss (blue) events are shown. (Adapted from Refs. (5, 7) and ATLAS-TCGA.) Clustering was performed using PartekGS software (Partek, St. Louis, MO).

TABLE 4

Most Frequent Copy Number Alterations (CNAs) and the Corresponding Genes Observed in TCGA Glioblastoma Database

Gene	Cytoband	CNA	Number of patients	Frequency (%)
CDKN2A	9p21	DEL	323	57.37
CDKN2B	9p21	DEL	315	55.95
EGFR	7p12	AMP	246	43.69
MTAP	9p21	DEL	239	42.45
CDK4	12q14	AMP	80	14.21
PDGFRA	4q12	AMP	72	12.79
MLL3	9p22	DEL	67	11.90
CHIC2	4q11	AMP	66	11.72
KIT	4q12	AMP	52	9.24
MDM4	1q32	AMP	48	8.53
FIP1L1	4q12	AMP	48	8.53
MDM2	12q14.3-q15	AMP	47	8.35
DDIT3	12q13.1-q13.2	AMP	46	8.17
PTEN	10q23.3	DEL	41	7.28
GLI1	12q13.2-q13.3	AMP	37	6.57

TABLE 4**Most Frequent Copy Number Alterations (CNAs) and the Corresponding Genes Observed in TCGA Glioblastoma Database (Continued)**

Gene	Cytoband	CNA	Number of patients	Frequency (%)
KDR	4q11-q12	AMP	35	6.22
TEK	9p21	DEL	34	6.04
LRIG3	12q14.1	AMP	22	3.91
SOX2	3q26.3-q27	AMP	21	3.73
CDKN2C	1p32	DEL	20	3.55
MET	7q31	AMP	19	3.37
CDK6	7q21-q22	AMP	19	3.37
IGFBP7	4q12	AMP	18	3.20
DCUN1D1	3q26.3	AMP	18	3.20
KLHL6	3q27.3	AMP	17	3.02
PIK3CA	3q26.3	AMP	16	2.84
AKAP9	7q21-q22	AMP	15	2.66
CCND2	12p13	AMP	15	2.66
FRS2	12q15	AMP	14	2.49
EPHB3	3q27.1	AMP	14	2.49
FGF6	12p13	AMP	14	2.49
FAS	10q24.1	DEL	13	2.31
IKZF1	7p12.2	AMP	13	2.31
MAGI2	7q21	AMP	13	2.31
SMO	7q32.3	AMP	13	2.31
PTPRD	9p23-p24.3	DEL	13	2.31
NFIB	9p24.1	DEL	13	2.31
FGF23	12p13.3	AMP	13	2.31
MYCN	2p24.3	AMP	12	2.13
KMT2C	7q36.1	AMP	12	2.13
XRCC2	7q36.1	AMP	12	2.13
SBDS	7q11.21	AMP	12	2.13
MAP3K13	3q27	AMP	12	2.13
HIP1	7q11.23	AMP	12	2.13
GRM3	7q21.1-q21.2	AMP	12	2.13
ABC1	7q21.12	AMP	12	2.13
RB1	13q14.2	DEL	11	1.95
BTG2	1q32	AMP	11	1.95
JAZF1	7p15.2-p15.1	AMP	11	1.95

Aberrations in other known GBM drivers include focal amplification of PDGFRA, sex determining region Y-box (SOX2, involved in the determination of cell fate), MDM2, and MDM4. These aberrations can occur at different steps in the tumor development process (23).

Potential Biomarkers for Prognosis and New Therapeutic Prediction

Several clinical trials are evaluating efficacy of numerous new targeted therapies with or without a predictive biomarker (Table 5).

TABLE 5

Targeted Therapeutic Agents Currently Used in Several Ongoing Clinical Trials for Patients with Glioblastoma (Obtained from clinicaltrials.gov) and Their Official FDA Approval

Target	Class	Name	FDA approval
EGFR	Tyrosine kinase inhibitors	Panitumumab (Vectibix®)	For metastatic colorectal cancer, KRAS wild type
		Gefitinib (Iressa®)	For advanced nonsmall-cell lung cancer
		Erlotinib (Tarceva®)	For advanced nonsmall-cell lung cancer and pancreatic cancer
		Lapatinib (Tykerb®)	For breast cancer as combination therapy
		AEE788 (also a VEGFR inhibitor)	–
	Vandetanib (Caprelsa®, also a VEGFR and RET inhibitor)	For metastatic medullary thyroid cancer	
	Monoclonal antibodies	Cetuximab (Erbix®)	For KRAS wild-type metastatic colorectal cancer and squamous cell carcinoma of the head and neck
Ras	Farnesyltransferase inhibitors	Tipifarnib (Zarnestra®)	–
		Lonafarnib (Sarasar®)	–
Raf	Tyrosine kinase inhibitors	Sorafenib (Nexavar®, also a VEGFR and PDGFR inhibitor)	For advanced renal cell carcinoma and hepatocellular carcinoma
PDGFR	Tyrosine kinase inhibitors	Imatinib (Gleevec®)	For treatment of multiple cancers, most notably Philadelphia chromosome-positive chronic myelogenous leukemia

TABLE 5**Targeted Therapeutic Agents Currently Used in Several Ongoing Clinical Trials for Patients with Glioblastoma (Obtained from clinicaltrials.gov) and Their Official FDA Approval (Continued)**

Target	Class	Name	FDA approval
		Dasatinib (Sprycel®)	For chronic myelogenous leukemia and Philadelphia chromosome-positive acute lymphoblastic leukemia
		Sunitinib (Sutent®, also a VEGFR inhibitor)	Mainly for treatment of renal cell carcinoma and imatinib-resistant gastrointestinal stromal tumors
	Small molecule	Crenolanib	–
VEGFR	Tyrosine kinase inhibitors	Vatalanib (also a PDGFR inhibitor)	–
		Cediranib (Recentin®)	–
		Axitinib (Inlyta®)	For advanced renal cell carcinoma
VEGFR	Small molecule	Carboxyamidotriazole	–
		Pazopanib (Votrient®)	For advanced renal cell carcinoma and advanced soft tissue sarcoma
		Lenvatinib (Lenvima®)	–
IL-2	Monoclonal antibodies	Basiliximab (Simulect®)	For the prophylaxis of acute rejection for renal transplant
		Daclizumab (Zenapax®)	For relapsing multiple sclerosis
PD-1	Monoclonal antibody	Nivolumab (Opdivo®)	For squamous cell head and neck cancer, Hodgkin lymphoma, metastatic melanoma, nonsmall-cell lung cancer, advanced renal cancer, and urothelial carcinoma
PD-L1	Monoclonal antibody	Durvalumab	–
NF-κB	Proteasome inhibitor	Bortezomib (Velcade®)	For mantle cell lymphoma and multiple myeloma
TGF-β2	Antisense oligodeoxynucleotide	Trabedersen	–
Tenascin	Monoclonal antibody	I ¹³¹ 81C6 (Neuradiab®)	–
PARP	Small molecule	Olaparib (Lynparza®)	For advanced ovarian cancer

Table continued on following page

TABLE 5**Targeted Therapeutic Agents Currently Used in Several Ongoing Clinical Trials for Patients with Glioblastoma (Obtained from clinicaltrials.gov) and Their Official FDA Approval (Continued)**

Target	Class	Name	FDA approval
FLT3	Tyrosine kinase inhibitor	Tandutinib, also inhibits c-KIT and PDGFR	–
Rb	Cyclin-dependent kinase inhibitor	Ribociclib (Kisqali®)	For advanced breast cancer
BRAF	Small molecule	Dabrafenib (Tafinlar®)	For metastatic melanoma in patients with BRAF mutations
mTOR	Small molecule	Sapanisertib	–

CLINICALLY RELEVANT ABERRATIONS (BIOMARKERS)

Although there appears to be a motif of common aberrations, only a select few have been associated with clinical relevance. Specifically, EGFR amplification, IDH1/2 mutations, and MGMT promoter methylation are currently regarded as having clinical significance. EGFR amplifications are associated with high-grade malignancy, poor prognosis, and shorter survival time (49). Currently, EGFR status can be used to predict patient response to EGFR-targeted therapies. Gefitinib and erlotinib are small molecule tyrosine kinase inhibitors that act to prevent phosphorylation of tyrosine residues and block downstream signaling. Both gefitinib and erlotinib have been rigorously tested for use in GBM; however, they have not been proven effective for monotherapy (50). Furthermore, targeting the mutation EGFRvIII using vaccine alone or in combination with tyrosine kinases inhibitors and temozolomide has been shown to improve *in vitro* cytotoxicity, to significantly reduce tumor development in xenograft models and in clinical trial by eliminating EGFRvIII-expressing cells and targeting its downstream target genes (51).

IDH1 mutations have been shown to exhibit characteristics associated with better prognosis. IDH1 mutations are typically found in younger patients that have high frequencies of TP53 mutations, and are currently used as positive predictors of prognosis. Wild-type IDH1 functions to convert α -ketoglutarate to isocitrate; however, a mutated IDH1 results in the formation of 2-hydroxyglutarate (2HG) (52). The consequences associated with the formation of 2HG are yet to be determined and is currently thought to function as an oncogenic metabolite (53). Serum levels of 2HG are being used to identify IDH1 mutations in patients with acute myeloid Leukemia (AML). MGMT promoter methylation is one of the most relevant prognostic markers and can also be used to predict therapeutic response to alkylating agents such as carmustine and temozolomide. The normal function of MGMT is to repair DNA damage, which would counteract the apoptotic effects of temozolomide. Silencing MGMT would lead to enhanced cytotoxic activity of temozolomide. It has been shown that patients that have MGMT

promoter methylation have clinically significant increases in survival time when given temozolomide concurrently with radiation therapy (54). This is related to MGMT methylation that sensitizes tumor cells to alkylating agents, leading thus to increased survival time. One of the many challenges associated with glioblastoma is the lack of standardized testing for these prognostic markers. Per the guidelines published by the National Comprehensive Cancer Network (NCCN) for glioblastoma, patients under the age of 70 years are recommended to receive temozolomide therapy regardless of their methylation status, and there is no mention of IDH1 and/or 2HG testing. Even though this testing is noninvasive, it has not yet been implemented as part of a standardized protocol.

TEMOZOLOMIDE AND GLIADEL WAFER

Temozolomide (Temodar®) and carmustine (BCNU, Gliadel®) are chemotherapeutic alkylating agents that function as prodrugs and are noncell cycle specific. The Gliadel wafer is a polymer that contains 3.85% carmustine and is applied locally immediately following surgical resection of the GBM tumor (55). These agents exploit a weakness in mismatch repair function when given to patients with silenced MGMT. Although they fall under the same broad classification, their mechanisms of action differ. Temozolomide forms the active intermediate MTIC [(methyl-triazene-1-yl)-imidazole-4-carboxamide]. MTIC can methylate the 6-OH on guanine. This methylation causes guanine to mispair with thymine, resulting in DNA double-strand breaks and cellular apoptosis. Carmustine can be more specifically classified as a nitrosourea. Upon activation, it forms active metabolites that are capable of DNA alkylation, DNA and RNA strand cross-linking, and protein carbamylation. The cross-linking effects of carmustine result in inhibition of DNA synthesis, RNA production, and translation. Carbamylation of proteins may inhibit enzyme processes necessary for cell survival. Collectively, these actions contribute to its cytotoxic nature. Recent studies have shown that MGMT promoter methylation (MGMT inactive or silenced) in GBM patients treated with Gliadel, radiotherapy, and TMZ was associated with significantly improved overall survival and progression-free survival (PFS) compared to patients with active MGMT. Therefore, MGMT methylation status can be used as a predictive marker for these therapies.

GROWTH FACTOR RECEPTOR INHIBITORS

There are many growth factor receptor inhibitors currently in use across several cancer types. Growth factor receptor inhibitors can be stratified into two main subclasses, monoclonal antibodies (mAbs) and small molecules. mAbs exert their effects extracellularly and can target either the ligand growth factor or the transmembrane tyrosine kinase receptor. Once bound, mAbs can inhibit signaling pathways and may induce cell death via apoptosis, complement activation, or effector cell activation. Small molecule growth factor receptor inhibitors were developed to penetrate the cell membrane and act on the cytoplasmic tyrosine kinase domain to inhibit its enzyme activity and disrupt signaling.

Recent clinical trials have attempted to translate the predictive qualities of EGFR status to GBM. Cetuximab is a mAb that targets the EGFR to prevent

receptor dimerization. Gefitinib and erlotinib are small molecule EGFR tyrosine kinase inhibitors that act to prevent phosphorylation of tyrosine residues and block downstream signaling. Cetuximab, gefitinib, and erlotinib, although tested for use in GBM, have not been proven effective (50, 56). Aside from EGFR inhibitors, studies have also been done targeting growth factor receptor inhibitors that target angiogenic pathways. Several EGFR mutations have been discovered and some are associated with an oncogenic activity or have a predictive power. Specifically, the point mutations A289V, G598V, R108K, and T263P were shown to predict *in vitro* response to erlotinib (57). Their relevance is much less studied than the T790M mutation that was shown to be oncogenic and to predict response to several TK inhibitors drugs in lung cancers (58). Indeed, patients with this mutation have been shown to not respond to erlotinib, afatinib, and gefitinib (first-generation TK inhibitors) but respond remarkably to second-generation TK inhibitors such as osimertinib (59). However, the therapeutic relevance of these mutations is under investigation in several clinical trials or still needs to be studied in GBM.

ANGIOGENESIS INHIBITORS

Bevacizumab is a mAb that targets VEGF ligand to prevent its binding to VEGFR. It is the only mAb that has been approved for GBM treatment. Bevacizumab studies have shown a significant improvement in PFS over radiotherapy alone (60). Small molecule inhibitors of VEGFR and PDGFR, such as sorafenib and pazopanib, have been studied in GBM and have shown no significant clinical benefit. Apart from bevacizumab, most clinical trials testing targeted therapies for GBM have been unsuccessful. This lack of response may be attributed to the vast number of overlapping pathways, resulting in the development of GBM. Combination therapy design studies are ongoing (Table 5); however, they are not without challenge. A study combining the EGFR inhibitor erlotinib and the mammalian target of rapamycin (mTOR) inhibitor temsirolimus resulted in dose-limiting toxicity without showing any significant benefit (61). Several clinical trials evaluated bevacizumab and irinotecan combination in high-grade gliomas including GBM (62, 63). This combination significantly improved PFS and overall median survival (62, 63) despite development of severe side effects. However, long-term use of bevacizumab is associated with emergence of resistance, high recurrence, rapid disease progression, and failure to respond to other chemotherapy (64, 65). Thus, there is a necessity to combine therapies that target multiple pathways simultaneously.

MISCELLANEOUS AGENTS

All of the previously mentioned agents target well-known pathways in GBM, yet little progress has been made in developing effective treatments. Some researchers have shifted their focus away from these aberrations and have developed alternative approaches to determining potential therapies. One such approach was to determine subtype-specific drugs for each of the four accepted GBM subtypes. Candidate drugs were chosen based on their association to subtype-specific genes and predicted patient phenotypes. The drugs chosen for the classical subtype

included irinotecan, a topoisomerase poison, and paclitaxel, an anti-microtubule agent, to target CDK6. For the mesenchymal subtype, pravastatin, a cholesterol-lowering agent, was chosen to target the gene ITGB2, which encodes for integrin beta chain. Clomipramine, an antidepressant, was selected for the proneural subtype targeting the gene SLC1A1, a solute carrier transporter. Lastly, the GABA antagonist bicuculline was selected for the neural subtype based on its association with the gene CALM2, which encodes calmodulin. These subtype-specific drugs showed significant inhibitory effects on GBM cell clonogenicity and synergistically reversed temozolomide resistance in MGMT methylation negative patients. Further studies must be done to refine this approach, though it does show promise (66).

Conclusion

Omic-based personalized medicine encompasses the utilization of data gathered via genomics, transcriptomics, proteomics, and metabolomics to create patient-specific therapies and/or regimens for successful treatment of disease. There is a common expectation that with an understanding of the changes occurring in gene and protein expression, one would be able to establish the most effective pharmacotherapy for the patient in question. However, intratumor heterogeneity confounds current efforts to solidify molecular biomarkers. Genetic alterations are not common to all tumor tissues within the same patient and between patients, and thus cannot be effectively targeted using the same protocol and therefore need an individualized approach to implement a personalized medicine of this deadly disease. Utilizing Omic-based technologies, it is foreseeable that soon GBM might be treated much in the same way that HIV is currently treated. Upon diagnosis, HIV patients have resistance testing done for their specific strain of the virus. Based on that information, a practitioner has different combination therapies to choose from to suit each patient individually. Ultimately, the goal would be for a patient sample taken during tumor resection, before and after treatments, to be sequenced and analyzed by several omic technologies, and to design a regimen that includes a combination of therapies to target patient-specific aberrations and development of resistance. Combination therapies will require management of toxicities, drug interactions, and therapeutic response monitoring.

Acknowledgments: The results shown here are in whole or part based upon data generated by the TCGA Research Network: <http://cancergenome.nih.gov/>, and data were downloaded/analyzed from the ATLAS-TCGA Data portal: <https://cbiportal.gdc.cancer.gov>.

Conflict of interest: The authors declare no potential conflicts of interest with respect to research, authorship, and/or publication of the manuscript.

Copyright and permission statement: To the best of our knowledge, the materials included in this chapter do not violate copyright laws. All original sources have been appropriately acknowledged and/or referenced. Where relevant, appropriate permissions have been obtained from the original copyright holder(s).

References

1. Deorah S, Lynch CF, Sibenaller ZA, Ryken TC. Trends in brain cancer incidence and survival in the United States: Surveillance, Epidemiology, and End Results Program, 1973 to 2001. *Neurosurg Focus*. 2006;20(4):E1. <http://dx.doi.org/10.3171/foc.2006.20.4.E1>
2. Reardon DA, Herndon JE, 2nd, Peters KB, Desjardins A, Coan A, Lou E, et al. Bevacizumab continuation beyond initial bevacizumab progression among recurrent glioblastoma patients. *Br J Cancer*. 2012;107(9):1481–7. <http://dx.doi.org/10.1038/bjc.2012.415>
3. Loeb LA. Human cancers express mutator phenotypes: Origin, consequences and targeting. *Nat Rev Cancer*. 2011;11:450–7. <http://dx.doi.org/10.1038/nrc3063>
4. Gerlinger M, Swanton C. How Darwinian models inform therapeutic failure initiated by clonal heterogeneity in cancer medicine. *Br J Cancer*. 2010;103:1139–43. <http://dx.doi.org/10.1038/sj.bjc.6605912>
5. Assem M, Sibenaller Z, Agarwal S, Al-Keilani MS, Alqudah MAY, Ryken TC. Enhancing diagnosis, prognosis and therapeutic outcome prediction of gliomas using genomics. *OMICS*. 2012;16(3):113–22. <http://dx.doi.org/10.1089/omi.2011.0031>
6. Agarwal S, Al-Keilani MS, Alqudah MAY, Sibenaller Z, Ryken TC, Assem M. Tumor derived mutations of protein tyrosine phosphatase receptor type K affect its function and alter sensitivity to chemotherapeutics in glioma. *PLoS One*. 2013;8(5):e62852. <http://dx.doi.org/10.1371/journal.pone.0062852>
7. The Cancer Genome Atlas (TCGA) Research Network. Comprehensive genomic characterization defines human glioblastoma genes and core pathways. *Nature*. 2008;455:1061–8. <http://dx.doi.org/10.1038/nature07385>
8. Nicholas MK, Lukas RV, Jafri NF, Faoro L, Salgia R. Epidermal growth factor receptor-mediated signal transduction in the development and therapy of gliomas. *Clin Cancer Res*. 2006;12:7261–70. <http://dx.doi.org/10.1158/1078-0432.CCR-06-0874>
9. Huang PH, Xu AM, White FM. Oncogenic EGFR signaling networks in glioma. *Sci Signal*. 2009;2:re6. <http://dx.doi.org/10.1126/scisignal.287re6>
10. Sugawa N, Exstrand AJ, James CD, Collins VP. Identical splicing of aberrant epidermal growth factor receptor transcripts from amplified rearranged genes in human glioblastoma. *Proc Natl Sci U S A*. 1990; 87:8602–6. <http://dx.doi.org/10.1073/pnas.87.21.8602>
11. Rajasekhar VK, Viale A, Socci ND, Wiedmann M, Hu X, Holland EC. Oncogenic Ras and Akt signaling contribute to glioblastoma formation by differential recruitment of existing mRNAs to polysomes. *Mol Cell*. 2003;12:889–901. [http://dx.doi.org/10.1016/S1097-2765\(03\)00395-2](http://dx.doi.org/10.1016/S1097-2765(03)00395-2)
12. Oh T, Ivan ME, Sun MZ. PI3K pathway inhibitors: Potential prospects as adjuncts to vaccine immunotherapy for glioblastoma. *Immunotherapy*. 2014;6(6):737–53. <http://dx.doi.org/10.2217/imt.14.35>
13. Koul D. PTEN signaling pathways in glioblastoma. *Cancer Biol Ther*. 2008;7:1321–5. <http://dx.doi.org/10.4161/cbt.7.9.6954>
14. Furnari FB, Fenton T, Bachoo RM, Mukasa A, Stommel JM, Stegh A, et al. Malignant astrocytic glioma: Genetics, biology, and paths to treatment. *Genes Dev*. 2007;21:2683–710. <http://dx.doi.org/10.1101/gad.1596707>
15. Knudsen ES, Wang JY. Targeting the RB-pathway in cancer therapy. *Clin Cancer Res*. 2010;16:1094–9. <http://dx.doi.org/10.1158/1078-0432.CCR-09-0787>
16. Van Meir EG, Hadjipanayis CG, Norden AD, Shu HK, Wen PY, Olson JJ. Exciting new advances in neuro-oncology: The avenue to a cure for malignant glioma. *CA Cancer J Clin*. 2010;60:166–193. <http://dx.doi.org/10.3322/caac.20069>
17. Shangary S, Wang S. Small-molecule inhibitors of the MDM2-p53 protein-protein interaction to reactivate p53 function: A novel approach for cancer therapy. *Annu Rev Pharmacol Toxicol*. 2009;49:223–41. <http://dx.doi.org/10.1146/annurev.pharmtox.48.113006.094723>
18. Sturm D, Bender S, Jones DT, Lichter P, Grill J, Becher O, et al. Paediatric and adult glioblastoma: Multiform (epi)genomic culprits emerge. *Nat Rev Cancer*. 2014;14:92–107. <http://dx.doi.org/10.1038/nrc3655>
19. Yap TA, Gerlinger M, Futreal PA, Pusztai L, Swanton C. Intratumor heterogeneity: Seeing the wood for the trees. *Sci Transl Med*. 2012;4:127ps110. <http://dx.doi.org/10.1126/scitranslmed.3003854>

20. Gerlinger M, Rowan AJ, Horswell S, Larkin J, Endesfelder D, Gronroos E, et al. Intratumor heterogeneity and branched evolution revealed by multiregion sequencing. *N Engl J Med*. 2012;366:883–92. <http://dx.doi.org/10.1056/NEJMoa1113205>
21. Stieber D, Golebiewska A, Evers L, Lenkiewicz E, Brons NH, Nicot N, et al. Glioblastomas are composed of genetically divergent clones with distinct tumorigenic potential and variable stem cell-associated phenotypes. *Acta Neuropathol*. 2014;127:203–19. <http://dx.doi.org/10.1007/s00401-013-1196-4>
22. Lombard A, Goffart N, Rogister B. Glioblastoma circulating cells: Reality, trap or illusion? *Stem Cell Int*. 2015;2015:182985. <http://dx.doi.org/10.1155/2015/182985>
23. Aubry M, de Tayrac M, Etcheverry A. “From the core to beyond the margin”: A genomic picture of glioblastoma intratumor heterogeneity. *Oncotarget*. 2015;6(14):12094–109. <http://dx.doi.org/10.18632/oncotarget.3297>
24. Brabletz T, Jung A, Spaderna S, Hlubek F, Kirchner T. Migrating cancer stem cells—An integrated concept of malignant tumour progression. *Nat Rev Cancer*. 2005;5(9):744–9. <http://dx.doi.org/10.1038/nrc1694>
25. Radisky DC. Epithelial-mesenchymal transition. *J Cell Sci*. 2005;118(19):4325–6. <http://dx.doi.org/10.1242/jcs.02552>
26. Kalluri R, Weinberg RA. The basics of epithelial-mesenchymal transition. *J Clin Invest*. 2009;119(6):1420. <http://dx.doi.org/10.1172/JCI39104>
27. Gaoliang Ouyang (2011). Epithelial-Mesenchymal Transition and Cancer Stem Cells, *Cancer Stem Cells - The Cutting Edge*, Prof. Stanley Shostak (Ed.), ISBN: 978-953-307-580-8, InTech, Available from: <http://www.intechopen.com/books/cancer-stem-cells-the-cutting-edge/epithelial-mesenchymal-transition-andcancer-stem-cells>.
28. Zhang X, Chen T, Zhang J, Mao Q, Li S, Xiong W, et al. Notch1 promotes glioma cell migration and invasion by stimulating β -catenin and NF- κ B signaling via AKT activation. *Cancer Sci*. 2012;103(2):181–90. <http://dx.doi.org/10.1111/j.1349-7006.2011.02154.x>
29. Carro MS, Lim WK, Alvarez MJ, Bollo RJ, Zhao X, Snyder EY, et al. The transcriptional network for mesenchymal transformation of brain tumours. *Nature*. 2009;463(7279):318–25. <http://dx.doi.org/10.1038/nature08712>
30. Mani SA, Guo W, Liao M, Eaton EN, Ayyanan A, Zhou AY, et al. The epithelialmesenchymal transition generates cells with properties of stem cells. *Cell*. 2008;133(4):704–15. <http://dx.doi.org/10.1016/j.cell.2008.03.027>
31. Merzak A, Koocheckpour S, Pilkington GJ. CD44 mediates human glioma cell adhesion and invasion in vitro. *Cancer Res*. 1994;54(15):3988–92.
32. Cheng W, Kandel JJ, Yamashiro DJ, Canoll P, Anastassiou D. A multi-cancer mesenchymal transition gene expression signature is associated with prolonged time to recurrence in glioblastoma. *PLoS One*. 2012;7(4):e34705. <http://dx.doi.org/10.1371/journal.pone.0034705>
33. Bouck N. P53 and angiogenesis. *Biochim Biophys Acta*. 1996;1287(1):63–6. [http://dx.doi.org/10.1016/0304-419x\(96\)00005-4](http://dx.doi.org/10.1016/0304-419x(96)00005-4)
34. Long DM. Capillary ultrastructure and the blood-brain barrier in human malignant brain tumors. *J Neurosurg*. 1970;32(2):127. <http://dx.doi.org/10.3171/jns.1970.32.2.0127>
35. Ricci-Vitiani L, Pallini R, Biffoni M, Todaro M, Invernici G, Cenci T, et al. Tumour vascularization via endothelial differentiation of glioblastoma stem-like cells. *Nature*. 2010;468(7325):824–8. <http://dx.doi.org/10.1038/nature09557>
36. Semenza GL. Targeting HIF-1 for cancer therapy. *Nat Rev Cancer*. 2003;3(10):721–32. <http://dx.doi.org/10.1038/nrc1187>
37. Bao S, Wu Q, Sathornsumetee S, Hao Y, Li Z, Hjelmeland AB, et al. Stem cell-like glioma cells promote tumor angiogenesis through vascular endothelial growth factor. *Cancer Res*. 2006;66(16):7843–8. <http://dx.doi.org/10.1158/0008-5472.CAN-06-1010>
38. Bergers G, Benjamin LE. Tumorigenesis and the angiogenic switch. *Nat Rev Cancer*. 2003;3(6):401–10. <http://dx.doi.org/10.1038/nrc1093>
39. Carmeliet P, Jain RK. Molecular mechanisms and clinical applications of angiogenesis. *Nature*. 2011;473(7347):298–307. <http://dx.doi.org/10.1038/nature10144>

40. Weis SM, Cheresh DA. Tumor angiogenesis: Molecular pathways and therapeutic targets. *Nat Med*. 2011;17(11):1359–70. <http://dx.doi.org/10.1038/nm.2537>
41. Norden AD, Drappatz J, Wen PY. Novel anti-angiogenic therapies for malignant gliomas. *Lancet Neurol*. 2008;7(12):1152–60. [http://dx.doi.org/10.1016/S1474-4422\(08\)70260-6](http://dx.doi.org/10.1016/S1474-4422(08)70260-6)
42. Ohgaki H, Dessen P, Jourde B, Horstmann S, Nishikawa T, Di Patre PL, et al. Genetic pathways to glioblastoma: A population-based study. *Cancer Res*. 2004;64:6892–9. <http://dx.doi.org/10.1158/0008-5472.CAN-04-1337>
43. Brennan CW, Verhaak RG, McKenna A, Campos B, Noushmehr H, Salama SR, et al. TCGA Research Network: The somatic genomic landscape of glioblastoma. *Cell*. 2013;155:462–77. <http://dx.doi.org/10.1016/j.cell.2013.09.034>
44. Crespo I, Vital AL, Nieto AB, Rebelo O, Tao H, Lopes MC, et al. Detailed characterization of alterations of chromosomes 7, 9, and 10 in glioblastomas as assessed by single-nucleotide polymorphism arrays. *J Mol Diagn*. 2011;13:634–47. <http://dx.doi.org/10.1016/j.jmoldx.2011.06.003>
45. Jiao Y, Killela PJ, Reitman ZJ, Rasheed AB, Heaphy CM, de Wilde RF, et al. Frequent ATRX, CIC, FUBP1 and IDH1 mutations refine the classification of malignant gliomas. *Oncotarget*. 2012;3:709–22. <http://dx.doi.org/10.18632/oncotarget.588>
46. Phillips HS, Kharbanda S, Chen R, Forrester WF, Soriano RH, Wu TD, et al. Molecular subclasses of high-grade glioma predict prognosis, delineate a pattern of disease progression, and resemble stages in neurogenesis. *Cancer Cell*. 2006;9(3):157–173. <http://dx.doi.org/10.1016/j.ccr.2006.02.019>
47. Shpak M, Goldberg MM, Cowperthwaite MC. Rapid and convergent evolution in the Glioblastoma multiforme genome. *Genomics*. 2015;105(3):159–167. <http://dx.doi.org/10.1016/j.ygeno.2014.12.010>
48. Cheng F, Jia P, Wang Q. Studying tumorigenesis through network evolution and somatic mutational perturbations in the cancer interactome. *Mol Biol Evol*. 2014;31(8): 2156–69. <http://dx.doi.org/10.1093/molbev/msu167>
49. Jeuken J, Sijben A, Alenda C, Rijntjes J, Dekkers M, Boots- Sprenger S, et al. Robust detection of EGFR copy number changes and EGFR variant III: Technical aspects and relevance for glioma diagnostics. *Brain Pathol*. 2009;19:661–671. <http://dx.doi.org/10.1111/j.1750-3639.2009.00320.x>
50. Van den Bent MJ, Brandes AA, Rampling R, Kouwenhoven MC, Kros JM, Carpentier AF, et al. Randomized phase II trial of erlotinib versus temozolomide or carmustine in recurrent glioblastoma: EORTC brain tumor group study 26034. *J Clin Oncol*. 2009;27:1268–74. <http://dx.doi.org/10.1200/JCO.2008.17.5984>
51. Sampson JH, Aldape KD, Archer GE, Coan A, Desjardins A, Friedman AH, et al. Greater chemotherapy-induced lymphopenia enhances tumor-specific immune responses that eliminate EGFRvIII-expressing tumor cells in patients with glioblastoma. *Neuro Oncol*. 2011;13(3):324–33. <http://dx.doi.org/10.1093/neuonc/noq157>
52. Sanson M, Marie Y, Paris S, Idhah A, Laffaire J, Ducray F, et al. Isocitrate dehydrogenase 1 codon 132 mutation is an important prognostic biomarker in gliomas. *J Clin Oncol*. 2009;27:4150–4. <http://dx.doi.org/10.1200/JCO.2009.21.9832>
53. Dang L, White DW, Gross S, Bennett BD, Bittinger MA, Driggers EM, et al. Cancer-associated IDH1 mutations produce 2-hydroxyglutarate. *Nature*. 2009;462(7274):739–44. <http://dx.doi.org/10.1038/nature08617>
54. Zawlik I, Vaccarella S, Kita D, Mittelbronn M, Franceschi S, Ohgaki H. Promoter methylation and polymorphisms of the MGMT gene in glioblastomas: A population-based study. *Neuroepidemiology*. 2009;32:21–29. <http://dx.doi.org/10.1159/000170088>
55. Fleming AB, Saltzman WM. Pharmacokinetics of the carmustine implant. *Clin Pharmacokinet*. 2002;41(6):403–19. <http://dx.doi.org/10.2165/00003088-200241060-00002>
56. Uhm JH, Ballman KV, Wu W, et al. Phase II evaluation of gefitinib in patients with newly diagnosed grade 4 astrocytoma: Mayo/North Central Cancer Treatment Group Study N0074. *Int J Radiat Oncol Biol Phys*. 2011;80:347–53. <http://dx.doi.org/10.1016/j.ijrobp.2010.01.070>
57. Lee JC, Vivanco I, Beroukhi R, Huang JH, Feng WL, DeBiasi RM, et al. Epidermal growth factor receptor activation in glioblastoma through novel missense mutations in the extracellular domain. *Cancer Res*. 2006;66(12):e485.

58. Balias TE, Rizzo RC. Quantitative prediction of fold resistance for inhibitors of EGFR. *Biochemistry*. 2009;48(35):8435–48. <http://dx.doi.org/10.1021/bi900729a>
59. Janne PA, Yang JC, Kim DW, Planchard D, Ohe Y, Ramalingam SS, et al. AZD9291 in EGFR inhibitor-resistant non-small-cell lung cancer. *N Engl J Med*. 2015;372(18):1689–99. <http://dx.doi.org/10.1056/NEJMoa1411817>
60. Chinot OL, Wick W, Mason W, Henriksson R, Saran F, Nishikawa R, et al. Bevacizumab plus radiotherapy-temozolomide for newly diagnosed glioblastoma. *N Engl J Med*. 2014;370:709–22. <http://dx.doi.org/10.1056/NEJMoa1308345>
61. Wen PY, Chang SM, Lamborn KR, Kuhn JG, Norden AD, Cloughesy TF, et al. Phase I/II study of erlotinib and temsirolimus for patients with recurrent malignant gliomas: North American Brain Tumor Consortium trial 04–02. *Neuro Oncol*. 2014;16(4):567–78. <http://dx.doi.org/10.1093/neuonc/not247>
62. Gilbert MR, Pugh SL, Aldape K, Sorensen AG, Mikkelsen T, Penas-Prado M, et al. NRG oncology RTOG 0625: A randomized phase II trial of bevacizumab with either irinotecan or dose-dense temozolomide in recurrent glioblastoma. *J Neurooncol*. 2017;131(1):193–9. <http://dx.doi.org/10.1007/s11060-016-2288-5>
63. Vredenburgh JJ, Desjardins A, Herndon JE, Marcello J, Reardon DA, Quinn JA, et al. Bevacizumab plus irinotecan in recurrent glioblastoma multiforme. *J Clin Oncol*. 2007;25(30):4722–9. <http://dx.doi.org/10.1200/JCO.2007.12.2440>
64. Ellis LM, Hicklin DJ. Pathways mediating resistance to vascular endothelial growth factor–targeted therapy. *Clin Cancer Res*. 2008;14(20):6371–5. <http://dx.doi.org/10.1158/1078-0432.CCR-07-5287>
65. Quant EC, Norden AD, Drappatz J, Muzikansky A, Doherty L, LaFrankie D, et al. Role of a second chemotherapy in recurrent malignant glioma patients who progress on bevacizumab. *Neuro Oncol*. 2009;11(5):550–5. <http://dx.doi.org/10.1215/15228517-2009-006>
66. Oh Y, Cho H, Kim J, Lee J, Rho K, Seo Y, et al. Translational validation of personalized treatment strategy based on genetic characteristics of GBM. *PLOS One*. 2014;9(8):1–11. <http://dx.doi.org/10.1371/journal.pone.0103327>

2

Molecular Genetics of Secondary Glioblastoma

ALIREZA MANSOURI¹ • JASON KARAMCHANDANI² • SUNIT DAS^{1,3,4}

¹Division of Neurosurgery, University of Toronto, Toronto, ON, Canada;

²Department of Pathology, Montreal Neurological Institute, McGill University, Montreal, QC, Canada; ³Li Ka Shing Knowledge, St. Michael's Hospital, University of Toronto, Toronto, Canada; ⁴Labatt Brain Tumour Research Centre, Hospital for Sick Children, University of Toronto, Toronto, Canada

Author for correspondence: Sunit Das, Division of Neurosurgery, University of Toronto, Toronto, Canada. E-mail: sunit.das@utoronto.ca

Doi: <http://dx.doi.org/10.15586/codon.glioblastoma.2017.ch2>

Abstract: Glioblastoma (GBM, WHO grade IV astrocytoma) is among the most common adult brain tumors and one that is invariably fatal. GBM is classified as either primary (de novo) or secondary in origin. Secondary GBMs are derived from previously lower grade (WHO grades II or III) gliomas. While secondary GBMs present with similar clinical characteristics as their primary counterparts, the molecular pathways involved in their pathogenesis distinguish the two and have functional consequences for their behavior. Although a large number of histologic markers are routinely utilized to distinguish primary from secondary GBM, advances in genomic and bioinformatics techniques have drastically improved classification of high-grade gliomas and our understanding of the molecular pathways that influence tumor behavior and response to treatment. The significant influence of molecular identity on tumor behavior has been recognized by the most recent WHO classification of CNS tumors, wherein specific molecular markers have been integrated as part of tumor subtype identification process, as a supplement to traditional histological analysis. Indeed, the change heralds a new era for neuro-oncology, one that is moving toward targeted

In: *Glioblastoma*. Steven De Vleeschouwer (Editor), Codon Publications, Brisbane, Australia
ISBN: 978-0-9944381-2-6; Doi: <http://dx.doi.org/10.15586/codon.glioblastoma.2017>

Copyright: The Authors.

Licence: This open access article is licenced under Creative Commons Attribution 4.0 International (CC BY 4.0). <https://creativecommons.org/licenses/by-nc/4.0/>

therapeutics as part of the standard of care. Thus, a comprehensive grasp of this diverse landscape is necessary. In this chapter, we provide an overview of our latest understanding of the molecular diversity of GBM, specifically as it pertains to primary and secondary GBMs, and how it influences prognostication and therapeutic decision-making.

Key words: Alpha thalassemia/mental retardation syndrome X-linked (ATRX); Isocitrate dehydrogenase (IDH); Low-grade glioma; Secondary glioblastoma

Introduction

Glioblastoma (GBM, WHO grade IV astrocytoma) is the most common malignant primary brain tumor among adults. Despite aggressive therapy, the current median survival is approximately 15 months (1). In addition to the diffusely infiltrative nature of these tumors, which prevents complete surgical resection, tumor recurrence and ultimate patient demise is also largely attributed to the significant molecular and cellular heterogeneity of these lesions, which inevitably results in treatment resistance and tumor recurrence. GBMs are further classified into primary (de novo) and secondary tumors that, while they present with similar clinical characteristics, are derived from previously lower grade (WHO grades II or III) gliomas. While both categories are diffuse in nature, the molecular pathways involved, along with functional tumor behavior, treatment strategy, and clinical outcomes are different (2, 3). Although clinical and imaging biomarkers can be used to distinguish primary from secondary GBM, advances in genomic and bioinformatics techniques have drastically improved classification of high-grade gliomas and our understanding of the molecular pathways that influence tumor behavior and response to treatment. The significant influence of molecular identity on tumor behavior has been recognized by the most recent WHO classification of CNS tumors, wherein specific molecular markers have been integrated as part of tumor subtype identification process, as a supplement to traditional histological analysis (4). Indeed, the change heralds a new era for neuro-oncology, one that is moving toward targeted therapeutics as part of the standard of care. Thus, a comprehensive grasp of this diverse landscape is necessary. In this chapter, we provide an overview of our latest understanding of the molecular diversity of GBM, specifically as it pertains to primary and secondary GBMs, and how it influences prognostication and therapeutic decision-making.

Distinguishing Primary and Secondary GBMs

Primary and secondary GBMs are histologically indistinguishable. Historically, the distinction between the two has been based on clinical history. With a more in-depth understanding of the genetic, epigenetic, and molecular profile of these tumors, however, the distinction has become clearer (Table 1) (5).

TABLE 1

Key Characteristics of *IDH*-Wildtype and *IDH*-Mutant Glioblastomas (adapted from Ref. (5).)

	<i>IDH</i> -WT GBM	<i>IDH</i> -mutant GBM
Synonym	Primary glioblastoma	Secondary glioblastoma
Precursor lesion	Identified de novo	Diffuse astrocytoma Anaplastic astrocytoma
Proportion of glioblastomas	~90%	~10%
Median age at diagnosis	~62 years	~44 years
M:F ratio	1.42:1	1.05:1
Median length of clinical history at diagnosis	4 months	15 months
Median overall survival		
Surgery + radiotherapy	9.9 months	24 months
Surgery + RT + CTX	15 months	31 months
Location	Supratentorial	Preferentially frontal
Necrosis	Extensive	Limited
<i>TERT</i> promoter mutations	72%	26%
<i>TP53</i> mutations	27%	81%
<i>ATRX</i> mutations	Exceptional	71%
<i>EGFR</i> amplification	35%	Exceptional
<i>PTEN</i> mutations	24%	Exceptional

ATRX, adult thalassemia mental retardation x-linked; CTX, chemotherapy; *EGFR*, epidermal growth factor receptor; GBM, Glioblastoma multiforme; *IDH*, Isocitrate dehydrogenase; *PTEN*, phosphatase and tensin homolog; *TERT*, telomerase reverse transcriptase; *TP53*, tumor protein 53; RT, radiotherapy.

EPIDEMIOLOGY OF SECONDARY GBM

The incidence of secondary GBMs based on clinical and imaging criteria is somewhat lower than that estimated by isocitrate dehydrogenase (*IDH*) status (5% vs. 6–13%, respectively) (2, 6, 7). Furthermore, patients with a clinical diagnosis of secondary GBM are on average 17 years younger than those with primary GBM (2, 7); this bias toward a younger patient cohort correlates very closely with *IDH1* status, as patients with *IDH* mutations are substantially younger (8, 9). The clinical course is substantially longer in patients with *IDH*-mutant GBM, indicative of a less aggressive behavior (2, 6, 8).

ANATOMIC PREVALENCE OF SECONDARY GBM

Interestingly, *IDH*-mutant GBM has a predilection for the frontal lobe and typically present with seizure rather than neurological deficit. The same has been demonstrated for *IDH*-mutant Grade II astrocytomas and oligodendrogliomas, including tumor with 1p/19q co-deletion (10). These findings support a hypothesis that the precursor cell of origin among *IDH*-mutant tumor subtypes is shared,

and suggest that these tumors may arise from mutations within a cell population that is independent of the cell populations at risk during development of de novo GBM (11).

MOLECULAR LANDSCAPE OF SECONDARY GBM

Amplification of the *EGFR* gene and activating mutations of its protein product are hallmarks of primary GBM and appear to be exclusive of *TP53* mutations (12). *PTEN* amplification and loss of chromosome 10 are additional features of primary GBMs (3, 13). Both primary and secondary GBMs have in common loss of heterozygosity (LOH) at chromosome 10q (14–16); although *PTEN* is also located on chromosome 10, mutations in this gene are only observed in primary GBM. Therefore, additional genetic events must be responsible for oncogenesis of high-grade gliomas that is shared among both primary and secondary tumors.

One of the earliest events, if not the initial event, in gliomagenesis is mutation of the *IDH1* or *IDH2* gene. Mutations in the promoter of the telomerase reverse transcriptase (*TERT*) gene lead to enhanced telomerase activity, which results in maintenance of telomere length and promotion of cell survival. Interestingly, *TERT* mutation is shared among both primary and secondary GBMs, potentially rendering this mutation as an early event in the process of tumorigenesis (17). In addition to these mutations, secondary GBM originating from a lower grade astrocytoma will frequently display mutations in the *TP53* and *ATRX* (adult thalassemia mental retardation x-linked) genes, while anaplastic tumors arising from a lower grade oligodendroglioma lineage will have co-deletions of 1p and 19q (2, 3, 18). There are several key signaling pathways involved in this transformation as well, and knowledge of mutations in genes involved in these processes and pathways is critical for an in-depth understanding of the biology of secondary GBM and in working toward targeted therapeutics. We will review these pathways in detail below.

Molecular Classification of GBMs Based on Gene Expression

In 2010, Verhaak and colleagues analyzed somatic mutations, DNA copy-number alterations, and gene expression profiling to group GBMs into discrete categories (19). Through this work, they were able to establish four subtypes of GBMs (Classic, Proneural, Neural, and Mesenchymal) based on the specific clustering of molecular and gene expression profiles. The Classic category demonstrated a greater preponderance of *EGFR* amplification, decreased rates of *TP53* mutation, along with *p16INK4A* and *p14ARF* deletion. Histologically, the Classic subtype demonstrated features more consistent with astrocytes. The Proneural category was found to have a greater rate of *PDGFR* amplification, *TP53* mutation, LOH, and *IDH1* mutation. These tumors had histological features most consistent with oligodendrocytes. Moreover, patients harboring the Proneural subtypes were younger and responded better to therapy. The Neural subtype was found to have a greater degree of neuronal marker expression and the histology was consistent with a combination of oligodendroglial, astrocytic, and neuronal features. The Mesenchymal subtype was found to have a greater degree of *NF1* mutations,

along with alterations of *PTEN* and *Akt*. Histologically, these tumors demonstrated a greater degree of necrosis and inflammatory features. Furthermore, astroglial and microglial cell signatures were commonly noted. This landmark study established the concept of differential behavior of GBMs that may be similar histologically but differ substantially from a molecular and gene expression perspective.

Mechanisms of Gliomagenesis

Gliomagenesis is a multicomponent process involving several genetic mutations affecting numerous molecular pathways (Figure 1). When considering tumor phylogeny, *IDH* mutation is critical to deciphering whether the identified tumor is a primary GBM or a GBM arising from secondary progression of a lower grade glioma. It is now established that while *IDH* mutations are early events in the process of gliomagenesis in secondary GBM, additional genes and their end products are altered during this process and these include *ATRX* mutation, loss of tumor suppressor genes such as *TP53* and *RB1*, and mutations in the promoter of *TERT* (5). Alterations of chromosomes 1, 7, 10, and 19, each harboring a distinct subset of tumor suppressor/promoter genes, are pivotal as well. Distinct pathways that have been identified as part of the core drivers of gliomagenesis include the *EGFR/PTEN/Akt/mTOR*, *TP53/MDM2/p14ARF*, and the *p16INK4a/RB1* pathways, which will be elaborated upon in the subsequent sections.

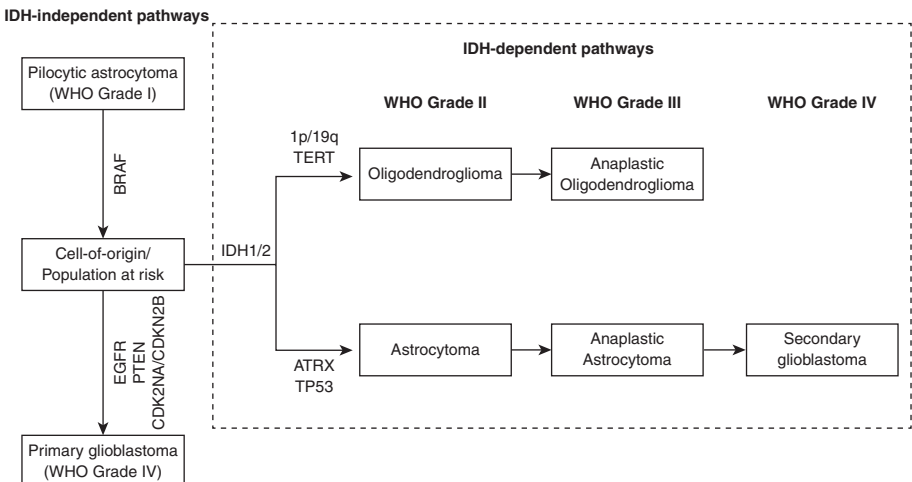


Figure 1 Molecular pathways to gliomagenesis. While the cell of origin in glioma is yet to be identified, large-scale expression and copy-number analyses have determined multiple molecular processes that result in glioma formation. Primary glioblastomas (and most Grade I gliomas) arise via an *IDH*-independent pathway. Conversely, *IDH* mutation is an early if not initiating event in the development of low-grade astrocytomas and oligodendrogliomas. By definition, secondary glioblastomas arise from malignant degeneration of an *IDH*-mutant lower grade tumor.

IDH AND GLIOMA INITIATION

First reported by Parsons and colleagues in 2008, a number of recent studies have since confirmed recurrent somatic mutations in the *IDH1* and *IDH2* genes (R132H and R172K as the canonical mutations in these genes, respectively) in a significant proportion of patients with gliomas. Further, patients who harbored tumors with an *IDH* mutation exhibit distinct disease characteristics relative to patients with a glioma with wild-type (WT) *IDH*. In 615 WHO grade II/III gliomas, *IDH* mutations were identified in 79% of the patient tumors (17). In another series of 457 WHO grade II/III gliomas, 80.7% of the patients were found to harbor an *IDH* mutation (20). The Cancer Genome Atlas Research Network found an *IDH* mutation in 226 (80.1%) of 282 WHO grade II/III gliomas (21). Based on these results, the WHO now recognizes *IDH* mutation as a critical biomarker in the classification of gliomas (4).

The *IDH* enzymes catalyze the oxidative conversion of isocitrate to α -ketoglutarate (α -KG). *IDH* mutations confer a gain-of-function neomorphic activity, converting α -KG to R-2-hydroxyglutarate (R-2-HG), instead of its racemic enantiomer S-2-HG. Although 2-HG is a trace metabolic product in normal cells, it is markedly elevated in *IDH*-mutant gliomas and in other malignancies, such as acute myeloid leukemia (22–24). The oncogenic effect of *IDH* mutation is thought to be twofold. First, 2-HG is considered an oncometabolite that may play a role in the process of glioma development, and progression or resistance to treatment. Although the exact role of *IDH1* mutation in gliomagenesis had initially been hampered by difficulties in establishing *in vitro* cultures with *IDH1* mutations (25), recent reports have demonstrated that increased levels of 2-HG result in increased activity of HIF-1- α and increased levels of its downstream targets such as VEGF. In addition, 2HG also affects collagen maturation, resulting in defective basement membranes that are potentially pivotal to glioma progression (25). Second, *IDH* mutation results in decreased production of α -KG, which impairs the function of many α -KG-dependent dioxygenases, including but not limited to histone demethylases (e.g., collagen prolyl-4-hydroxylase, prolyl hydroxylases, and the ten-eleven translocation (TET) family of DNA hydroxylases) (26). Change in histone methylation is thought to also interfere with the terminal differentiation of cells and may predispose cells harboring mutant *IDH* to malignant transformation (27). Based on the above evidence, *IDH1/2* mutations have been termed as lineage markers by some authors (11), and it is now accepted as a more definitive marker of secondary GBM than any other clinical or pathological criterion (28).

ATRX, TP53, AND 1p/19q

The great majority of low-grade astrocytomas carry a *p53* mutation while most oligodendrogliomas demonstrate loss of chromosomes 1p and 19q (26, 29–33). Biopsy-based studies suggest that the *IDH1* mutation occurs prior to either *p53* mutation or 1p and 19q loss (26, 33). Following *IDH*-mediated oncogenesis, acquisition of *p53* and *ATRX* mutations occurs in the setting of development of an astrocytoma (34, 35), while loss of chromosomes 1p and 19q occurs in the setting of development of an oligodendroglioma. While both subgroups are capable with time of undergoing further malignant degeneration, the current WHO

classification system only considers progression to secondary GBM as an endpoint of astrocytoma progression. It is conceivable that all GBMs that harbor an *IDH* mutation are secondary tumors. In one study, the small subgroup of patients with primary GBM carrying an *IDH* mutation (3.4%) was younger than noncensored primary GBM patients and harbored frequent *p53* mutations and an absence of EGFR amplification, features consistent with secondary GBMs (8). These findings suggest that these tumors could represent cases of a rapidly progressive secondary GBM, rather than a true primary GBM. Conversely, it can be argued that all GBMs harboring a WT *IDH* are biologically primary GBMs: cases of secondary GBM without an *IDH* mutation likely represent a progression from an undergraded, lower grade, or anaplastic glioma (8). These assumptions are borne out by recent data that show that gliomas lacking mutation in *IDH* or having chromosomal loss at 1p and 19q cluster by expression analysis and DNA copy-number profiling (21) and portend a severe prognosis (17). With an increased understanding of molecular markers and their incorporation into clinical trials, the disparity between molecular markers and histopathology-based diagnostics methods becomes more evident. For now, the current WHO classification system posits that, despite histopathological features such as neo-vascularity and necrosis, a high-grade glioma with *IDH1* mutation and 1p/19q co-deletion should be considered an anaplastic oligodendroglioma. Conversely, from a biological perspective, a histological anaplastic astrocytoma with WT *IDH* is now considered a GBM (36). These modifications in the classification system have been corroborated by outcomes data emerging from clinical trials. Together, these findings confirm the integral role of *IDH* and 1p/19q status in determining patient survival.

TERT PROMOTER MUTATION

Mutations in the *TERT* gene are thought to prevent cell senescence through increased telomere length, thus promoting tumorigenesis in several cancers, including GBM (37). The contribution of *TERT* mutation to tumor aggressiveness however is not clear. Focusing on a sample of GBM cases, Mosrati et al. found that *TERT* promoter mutation was associated with a shorter overall survival (37). Interestingly, this mutation was found in both primary and secondary tumors. More recently, Eckel-Passow et al. found that, while GBMs had a higher proportion of *TERT* mutations in isolation (74% of cases) or had neither *TERT* or *IDH* mutations or loss of chromosome 1p and 19q (what they termed “triple negative” tumors, making up 17% of cases), lower grade gliomas were much less likely to be “triple negative” (7% of cases) or harbor a *TERT* mutation in isolation (10% of cases) (16). These findings suggest that while *TERT* promoter mutation is integral to tumorigenesis and may contribute to the overall aggressiveness of the tumor, its role is modified by other key mutations.

THE G-CIMP PHENOTYPE

Methylation of the promoter region of the *MGMT* gene is more frequently found in secondary GBMs compared to primary GBMs (75% vs. 36%) (38), and it is frequently associated with mutations in *IDH1/2* and *TP53* and utilized as a strong predictive marker for response to chemotherapy in GBM patients. In fact,

IDH mutation has been shown to mediate widespread changes in chromosome structure and remodeling of the DNA methylome, resulting in the establishment of the glioma CpG island methylator phenotype (G-CIMP). Introduction of mutant *IDH1* into primary human astrocytes was found to be sufficient to alter specific histone methylation marks and induce extensive DNA hypermethylation in a manner that resembles the changes observed in G-CIMP+ lower grade gliomas. Furthermore, the epigenomic alterations resulting from mutant *IDH1* activate specific gene expression programs that are associated with G-CIMP+ proneural glioblastoma, but not other glioblastoma subtypes, and are associated with longer survival. Based on these data, *IDH* mutation is likely the molecular basis of G-CIMP in gliomas, highlighting the interplay between genomic and epigenomic changes in cancers including GBM.

In GBM, the proneural subtype is predominantly associated with *IDH1/2* mutations and these are further subclassified as either CIMP+ or CIMP- (of which the G-CIMP+ shows better prognosis). The proneural subtype by itself, however, appears to bear little prognostic significance unless considered in association with the *IDH1/2* mutation status (39). In fact, Turcan et al. have demonstrated that the *IDH1* mutation alone is capable of remodeling the genomic methylation profile of the tumor, thus promoting the CIMP+ profile (40). Interestingly, WT *IDH1* status promoted hypomethylation at numerous foci and CIMP- low-grade gliomas lacked *IDH1* mutation. In addition, decreased expression of *ATRX* is associated with downregulation of *MGMT* expression via promoter hypermethylation (41). Therefore, *ATRX* mutation status not only predicts cell of origin but also has a significant prognostic role as well (34, 42, 43).

Genetics of Glioma Progression

EGFR/PTEN/AKT/MTOR PATHWAY

Activation of the *PI3K/Akt* pathway results in increased cell proliferation via downregulation of p27, thereby influencing cell-cycle progression (44), inactivation of pro-apoptotic genes (45), and increased transcription of pro-survival genes under the influence of NFκB (46). PI3K is recruited to the cell surface and activated through EGFR. Once phosphorylated, PI3K activates PIP3 via phosphorylation, which induces activation of downstream molecules such as Akt—a serine/threonine kinase (47)—promoting cell survival and proliferation (48).

EGFR is a tyrosine kinase growth factor receptor situated in the cell membrane. Amplification of the *EGFR* gene and mutation of the protein product are key contributors to the activation of this receptor tyrosine kinase (RTK) pathway in primary GBM. The most common of the *EGFR*-activating mutants is the EGFRvIII variant, in which gene mutation results in a truncated protein product that is constitutively active. Mutations in Akt itself, however, are not common in gliomas (49).

PTEN is the second most commonly mutated tumor suppressor gene in all cancers after *p53* (50), and *PTEN* mutation is found in approximately 40% of GBMs, predominantly in the primary form (51). *PTEN* is a tumor suppressor and one of its functions is dephosphorylation of PIP3, thus preventing activation of Akt and mTOR (47). Through this role, *PTEN* is central in inhibiting cell

proliferation and regulating the ability of cells in migration and invasion (52). Loss of PTEN function, either through genetic or epigenetic modifications, is a common component of the *Akt/PI3K/mTOR* activation pathway in cancer.

TP53/MDM2/P14ARF PATHWAY

Although mutations of the *TP53* gene have been identified in both primary and secondary GBMs, its role appears to be predominantly related to the latter, where the mutation is an early event in gliomagenesis (2). While *p53* mutations in primary GBM appear to involve all exons indiscriminately, they are predominantly focused at codons 248 and 273, particularly involving CpG sites, in secondary GBM (2). This discrepancy suggests that *p53* mutation in secondary GBM is a specific and stereotyped event in secondary GBM ontology, while *p53* mutation in primary GBM is potentially a consequence of widespread genomic instability (3).

MDM2 amplification appears to be specific to primary GBMs that lack the *p53* mutation (53, 54). In normal cells, WT *p53* induces the expression of MDM2, which in turn inhibits the function of WT *p53*. Furthermore, WT *p53* inhibits the function of *p14ARF*, which would normally inhibit the downregulation of *p53* by MDM2. This autoregulatory loop is disrupted when any of the above is dysfunctional, adversely affecting cell-cycle control, DNA damage repair, cell proliferation/differentiation, and neovascularization (55).

P16INK4A/RB1 PATHWAY

Either through homozygous deletion or promoter methylation, the alteration of *p16INK4a* is an important step in both primary and secondary GBMs (56). Conversely, methylation of the *RB1* promoter, correlating with decreased *RB1* expression, is more specific to secondary GBM (57). The *p16INK4a/RB1* pathway is critical to cell-cycle control (58), as *RB1* regulates the progression of the cell cycle from G1 to the S phase by preventing the release of the E2F transcription factor. The latter enables the transcription of genes required for cell-cycle progression, in addition to *p14ARF*. The phosphorylation of *RB1*, via the CDK4/cyclin D complex, inhibits this function enabling the progression of the cell cycle along with increased *p53* expression via the activated *p14ARF*. WT *p16INK4a* serves as an additional checkpoint by binding to CDK4 and inhibiting the function of the CDK4/cyclin D complex. Therefore, altered expression of any of these genes results in an inability to control cell-cycle progression. The central role of cell-cycle regulation in the genesis of secondary GBM has also been confirmed with cDNA expression profile analysis (59).

Effect of Treatment on Glioma Transformation

By virtue of the inherent heterogeneity of these tumors, it is expected that not all of the cells within a glioma will respond to chemotherapy and radiation, inevitably resulting in tumor progression/recurrence. Further, recent evidence suggests

that chemotherapy and radiation may actually result in mutations that promote tumor cell survival. This pro-mutational ability has been most extensively studied in the setting of temozolamide (TMZ) and ionizing radiation.

TEMOZOLAMIDE AND LGG PROGRESSION

An alkylating agent, TMZ is an integral component of the standard treatment regimen for patients with GBM. Accumulating evidence from numerous studies suggests that acquired treatment resistance following TMZ administration is multifactorial and rooted in transcriptional, metabolomic, genomic, and epigenomic changes that lead to this phenotype (60–67).

Costello and colleagues undertook genome sequence analysis of 23 initial and matched recurrent human gliomas to address two questions: (i) What is the extent to which mutations in initial tumors differ from mutations in their subsequent recurrent tumors? (ii) How does chemotherapy with TMZ affect the mutational profile of recurrent tumors? The authors found an average of 33 somatic coding mutations in each initial tumor, of which an average of 54% were also detected at recurrence (shared mutations), including mutations in *IDH1*, *TP53*, and *ATRX*. All other somatic mutations were identified only in the initial tumor or only in the recurrent tumor from a given patient (private mutations), though overall, the initial and recurrent gliomas displayed a broad spectrum of genetic relatedness. Interestingly, in multiple patients, the recurrent tumors shared $\leq 25\%$ of mutations detected in the initial tumors, suggesting that these tumors were seeded by cells derived from the initial tumor at an early stage of its evolution, and that tumor recurrence can occur as the result of either linear or branched evolution.

Their findings regarding the effect of TMZ on tumor evolution and recurrence were as striking. Although the initial tumors and most of the recurrent tumors in their cohort had 0.2 to 4.5 mutations per megabase (Mb), 6 of the 10 patients treated with TMZ had recurrent tumors that were hypermutated; that is, they harbored 31.9 to 90.9 mutations per Mb. Overall, 97% of these were C>T/G>A transitions predominantly occurring at CpC and CpT dinucleotides, which is a signature of TMZ-induced mutagenesis distinct from nonhypermutated tumors. Further, acquisition of DNA mismatch repair (MMR) pathway dysfunction, which results in resistance to TMZ, appeared to exacerbate hypermutation in the face of continued TMZ therapy. The authors postulated that introduction of thousands of de novo mutations could drive the evolution of TMZ-resistant glioma cells to higher states of malignant potential. Indeed, all six recurrent tumors that showed evidence of TMZ-induced hypermutation underwent malignant progression to GBM. Many of these tumors developed mutations in pathways described as critical to gliomagenesis, including Akt-mTOR and the p16/RB. Treatment-induced somatic mutations were recently longitudinally studied in a patient with a 5-year survival period following initial diagnosis (68). Using whole exome sequencing, the investigators demonstrated that each successive therapy selected for resistant clones of tumor cells and that these had arisen via the process of chromothripsis. In addition, this approach enabled the provision of personalized therapy for this patient, based on the identification of target clonal populations sensitive to available treatment, which was critical for this long-term survival. Given the evidence derived from such analyses, it is clear that the genome of GBMs is dynamic and in

order to offer true personalized treatment, the genome of each successive tumor population must be investigated thoroughly.

Stepaneko et al. extended these findings with *in vitro* studies that demonstrated that long-term exposure of glioma cells to TMZ induces chromosomal instability, leading to alteration of cell growth, invasiveness, migration, and response to re-treatment (69). Among the TMZ-resistant cell lines, some responded to temsirolimus, an mTOR inhibitor. Interestingly, although TMZ has been shown to induce the transformation of glioma nonstem-like cells into glioma stem-like cells, the sensitivity of both differentiated and stem-like cells to TMZ was similar (70, 71). These findings further highlight the importance of the evolution of the genetic network that infers TMZ resistance in GBM.

EFFECT OF RADIATION ON GLIOMA BEHAVIOR

The introduction of radiation therapy to the armamentarium of therapy in patients with GBM has been a significant contribution. However, similar to TMZ, radiation is thought to promote malignant progression of gliomas as well. Based on transcription profiling of patient-derived radiation-resistant GBM cells, the mesenchymal subtype was the most commonly identified (72). *In vitro* studies have also demonstrated a proneural to mesenchymal transition among oligodendroglioma cell cultures that were irradiated (73). The authors proposed that the activation of the STAT3 transcription factor following radiation was contributory, given that its inhibition prevented this transition. Furthermore, Jak2 inhibition in mice undergoing radiation prolonged their survival. Alternative mechanisms such as activation of the *TNF- α /NF κ B* pathway may also be involved (72). Other post-translational effects of radiation exposure, such as the stabilization of HIF-1 α , promoting angiogenesis, have been proposed (74). Therefore, a combination of intrinsic cell changes and modifications to the tumor microenvironment may be responsible for the radiation-induced malignant progression noted in gliomas.

Conclusion

The recent publication of the modified WHO classification for CNS tumors, integrating molecular signatures into histological-based classifications, is timely and reflects the field's evolution. Based on our understanding of the vast intratumoral heterogeneity among GBMs, the logical next step is to establish biomarkers that would be predictive of treatment response, identify clonal populations that are potentially resistant to therapy, and develop combination therapies tailored to the specific pathways involved within the entirety of the tumor. Analysis of initial and recurrent tumor samples may be helpful for better clonal evolution analysis.

Acknowledgment: Sunit Das is supported by grants and awards from the American College of Surgeons, Canadian Institutes of Health Research, and Megan's Walk.

Conflict of interest: The authors declare no potential conflicts of interest with respect to research, authorship, or publication of this manuscript.

Copyright and permission statement: To the best of our knowledge, the materials included in this chapter do not violate copyright laws. All original sources have been appropriately acknowledged and/or referenced. Where relevant, appropriate permissions have been obtained from the original copyright holder(s).

References

1. Stupp R, Mason WP, van den Bent MJ, Weller M, Fisher B, Taphoorn MJ, et al. Radiotherapy plus concomitant and adjuvant temozolomide for glioblastoma. *N Engl J Med*. 2005;352(10):987–96. <http://dx.doi.org/10.1056/NEJMoa043330>
2. Ohgaki H, Dessen P, Jourde B, Horstmann S, Nishikawa T, Di Patre PL, et al. Genetic pathways to glioblastoma: A population-based study. *Cancer Res*. 2004;64(19):6892–9. <http://dx.doi.org/10.1158/0008-5472.CAN-04-1337>
3. Ohgaki H, Kleihues P. Genetic pathways to primary and secondary glioblastoma. *Am J Pathol*. 2007;170(5):1445–53. <http://dx.doi.org/10.2353/ajpath.2007.070011>
4. Louis DN, Perry A, Reifenberger G, von Deimling A, Figarella-Branger D, Cavenee WK, et al. The 2016 World Health Organization classification of tumors of the central nervous system: A summary. *Acta Neuropathol*. 2016;131(6):803–20. <http://dx.doi.org/10.1007/s00401-016-1545-1>
5. Costello JF, Plass C, Arap W, Chapman VM, Held WA, Berger MS, et al. Cyclin-dependent kinase 6 (CDK6) amplification in human gliomas identified using two-dimensional separation of genomic DNA. *Cancer Res*. 1997;57(7):1250–4.
6. Ohgaki H, Kleihues P. Population-based studies on incidence, survival rates, and genetic alterations in astrocytic and oligodendroglial gliomas. *J Neuropathol Exp Neurol*. 2005;64(6):479–89. <http://dx.doi.org/10.1093/jnen/64.6.479>
7. Dropcho EJ, Soong SJ. The prognostic impact of prior low grade histology in patients with anaplastic gliomas: A case-control study. *Neurology*. 1996;47(3):684–90. <http://dx.doi.org/10.1212/WNL.47.3.684>
8. Nobusawa S, Watanabe T, Kleihues P, Ohgaki H. IDH1 mutations as molecular signature and predictive factor of secondary glioblastomas. *Clin Cancer Res*. 2009;15(19):6002–7. <http://dx.doi.org/10.1158/1078-0432.CCR-09-0715>
9. Ichimura K, Pearson DM, Kocalkowski S, Backlund LM, Chan R, Jones DT, et al. IDH1 mutations are present in the majority of common adult gliomas but rare in primary glioblastomas. *Neuro Oncol*. 2009;11(4):341–7. <http://dx.doi.org/10.1215/15228517-2009-025>
10. Lai A, Kharbanda S, Pope WB, Tran A, Solis OE, Peale F, et al. Evidence for sequenced molecular evolution of IDH1 mutant glioblastoma from a distinct cell of origin. *J Clin Oncol*. 2011;29(34):4482–90. <http://dx.doi.org/10.1200/JCO.2010.33.8715>
11. Ohgaki H, Kleihues P. The definition of primary and secondary glioblastoma. *Clin Cancer Res*. 2013;19(4):764–72. <http://dx.doi.org/10.1158/1078-0432.CCR-12-3002>
12. Watanabe K, Tachibana O, Sata K, Yonekawa Y, Kleihues P, Ohgaki H. Overexpression of the EGF receptor and p53 mutations are mutually exclusive in the evolution of primary and secondary glioblastomas. *Brain Pathol*. 1996;6(3):217–23; discussion 23–4. <http://dx.doi.org/10.1111/j.1750-3639.1996.tb00848.x>
13. Fujisawa H, Reis RM, Nakamura M, Colella S, Yonekawa Y, Kleihues P, et al. Loss of heterozygosity on chromosome 10 is more extensive in primary (de novo) than in secondary glioblastomas. *Lab Invest*. 2000;80(1):65–72. <http://dx.doi.org/10.1038/labinvest.3780009>
14. Ichimura K, Schmidt EE, Miyakawa A, Goike HM, Collins VP. Distinct patterns of deletion on 10p and 10q suggest involvement of multiple tumor suppressor genes in the development of astrocytic gliomas of different malignancy grades. *Genes Chromosomes Cancer*. 1998;22(1):9–15. [http://dx.doi.org/10.1002/\(SICI\)1098-2264\(199805\)22:1%3C9::AID-GCC2%3E3.0.CO;2-1](http://dx.doi.org/10.1002/(SICI)1098-2264(199805)22:1%3C9::AID-GCC2%3E3.0.CO;2-1)
15. Karlbom AE, James CD, Boethius J, Cavenee WK, Collins VP, Nordenskjold M, et al. Loss of heterozygosity in malignant gliomas involves at least three distinct regions on chromosome 10. *Human Genet*. 1993;92(2):169–74. <http://dx.doi.org/10.1007/BF00219686>

16. Rasheed BK, McLendon RE, Friedman HS, Friedman AH, Fuchs HE, Bigner DD, et al. Chromosome 10 deletion mapping in human gliomas: A common deletion region in 10q25. *Oncogene*. 1995;10(11):2243–6.
17. Eckel-Passow JE, Lachance DH, Molinaro AM, Walsh KM, Decker PA, Sicotte H, et al. Glioma groups based on 1p/19q, IDH, and TERT promoter mutations in tumors. *N Engl J Med*. 2015;372(26):2499–508. <http://dx.doi.org/10.1056/NEJMoa1407279>
18. Nakamura M, Yang F, Fujisawa H, Yonekawa Y, Kleihues P, Ohgaki H. Loss of heterozygosity on chromosome 19 in secondary glioblastomas. *J Neuropathol Exp Neurol*. 2000;59(6):539–43. <http://dx.doi.org/10.1093/jnen/59.6.539>
19. Verhaak RG, Hoadley KA, Purdom E, Wang V, Qi Y, Wilkerson MD, et al. Integrated genomic analysis identifies clinically relevant subtypes of glioblastoma characterized by abnormalities in PDGFRA, IDH1, EGFR, and NF1. *Cancer Cell*. 2010;17(1):98–110. <http://dx.doi.org/10.1016/j.ccr.2009.12.020>
20. Ceccarelli M, Barthel FP, Malta TM, Sabedot TS, Salama SR, Murray BA, et al. Molecular profiling reveals biologically discrete subsets and pathways of progression in diffuse glioma. *Cell*. 2016;164(3):550–63. <http://dx.doi.org/10.1016/j.cell.2015.12.028>
21. Cancer Genome Atlas Research Network, Brat DJ, Verhaak RG, Aldape KD, Yung WK, Salama SR, et al. Comprehensive, integrative genomic analysis of diffuse lower-grade gliomas. *N Engl J Med*. 2015;372(26):2481–98. <http://dx.doi.org/10.1056/NEJMoa1402121>
22. Dang L, White DW, Gross S, Bennett BD, Bittinger MA, Driggers EM, et al. Cancer-associated IDH1 mutations produce 2-hydroxyglutarate. *Nature*. 2009;462(7274):739–44. <http://dx.doi.org/10.1038/nature08617>
23. Fathi AT, Nahed BV, Wander SA, Iafrate AJ, Borger DR, Hu R, et al. Elevation of urinary 2-hydroxyglutarate in IDH-mutant glioma. *Oncologist*. 2016;21(2):214–19. <http://dx.doi.org/10.1634/theoncologist.2015-0342>
24. Fathi AT, Sadrzadeh H, Borger DR, Ballen KK, Amrein PC, Attar EC, et al. Prospective serial evaluation of 2-hydroxyglutarate, during treatment of newly diagnosed acute myeloid leukemia, to assess disease activity and therapeutic response. *Blood*. 2012;120(23):4649–52. <http://dx.doi.org/10.1182/blood-2012-06-438267>
25. Sasaki M, Knobbe CB, Itsumi M, Elia AJ, Harris IS, Chio, II, et al. D-2-hydroxyglutarate produced by mutant IDH1 perturbs collagen maturation and basement membrane function. *Genes Dev*. 2012;26(18):2038–49. <http://dx.doi.org/10.1101/gad.198200.112>
26. Watanabe T, Nobusawa S, Kleihues P, Ohgaki H. IDH1 mutations are early events in the development of astrocytomas and oligodendrogliomas. *Am J Pathol*. 2009;174(4):1149–53. <http://dx.doi.org/10.2353/ajpath.2009.080958>
27. Lu C, Ward PS, Kapoor GS, Rohle D, Turcan S, Abdel-Wahab O, et al. IDH mutation impairs histone demethylation and results in a block to cell differentiation. *Nature*. 2012;483(7390):474–8. <http://dx.doi.org/10.1038/nature10860>
28. Parsons DW, Jones S, Zhang X, Lin JC, Leary RJ, Angenendt P, et al. An integrated genomic analysis of human glioblastoma multiforme. *Science*. 2008;321(5897):1807–12. <http://dx.doi.org/10.1126/science.1164382>
29. Louis DN, Ohgaki H, Wiestler OD, Cavenee WK, Burger PC, Jouvet A, et al. The 2007 WHO classification of tumours of the central nervous system. *Acta Neuropathol*. 2007;114(2):97–109. <http://dx.doi.org/10.1007/s00401-007-0243-4>
30. Okamoto Y, Di Patre PL, Burkhard C, Horstmann S, Jourde B, Fahey M, et al. Population-based study on incidence, survival rates, and genetic alterations of low-grade diffuse astrocytomas and oligodendrogliomas. *Acta Neuropathol*. 2004;108(1):49–56. <http://dx.doi.org/10.1007/s00401-004-0861-z>
31. Watanabe T, Nakamura M, Kros JM, Burkhard C, Yonekawa Y, Kleihues P, et al. Phenotype versus genotype correlation in oligodendrogliomas and low-grade diffuse astrocytomas. *Acta Neuropathol*. 2002;103(3):267–75. <http://dx.doi.org/10.1007/s004010100464>
32. Reifenberger G, Louis DN. Oligodendroglioma: Toward molecular definitions in diagnostic neurooncology. *J Neuropathol Exp Neurol*. 2003;62(2):111–26. <http://dx.doi.org/10.1093/jnen/62.2.111>
33. Kim YH, Nobusawa S, Mittelbronn M, Paulus W, Brokinkel B, Keyvani K, et al. Molecular classification of low-grade diffuse gliomas. *Am J Pathol*. 2010;177(6):2708–14. <http://dx.doi.org/10.2353/ajpath.2010.100680>

34. Jiao Y, Killela PJ, Reitman ZJ, Rasheed AB, Heaphy CM, de Wilde RF, et al. Frequent ATRX, CIC, FUBP1 and IDH1 mutations refine the classification of malignant gliomas. *Oncotarget*. 2012;3(7):709–22. <http://dx.doi.org/10.18632/oncotarget.588>
35. Liu XY, Gerges N, Korshunov A, Sabha N, Khuong-Quang DA, Fontebasso AM, et al. Frequent ATRX mutations and loss of expression in adult diffuse astrocytic tumors carrying IDH1/IDH2 and TP53 mutations. *Acta Neuropathol*. 2012;124(5):615–25. <http://dx.doi.org/10.1007/s00401-012-1031-3>
36. Aldape K, Zadeh G, Mansouri S, Reifenberger G, von Deimling A. Glioblastoma: Pathology, molecular mechanisms and markers. *Acta Neuropathol*. 2015;129(6):829–48. <http://dx.doi.org/10.1007/s00401-015-1432-1>
37. Mosrati MA, Malmstrom A, Lysiak M, Krysztofiak A, Hallbeck M, Milos P, et al. TERT promoter mutations and polymorphisms as prognostic factors in primary glioblastoma. *Oncotarget*. 2015;6(18):16663–73. <http://dx.doi.org/10.18632/oncotarget.4389>
38. Nakamura M, Watanabe T, Yonekawa Y, Kleihues P, Ohgaki H. Promoter methylation of the DNA repair gene MGMT in astrocytomas is frequently associated with G:C → A:T mutations of the TP53 tumor suppressor gene. *Carcinogenesis*. 2001;22(10):1715–19. <http://dx.doi.org/10.1093/carcin/22.10.1715>
39. Brennan CW, Verhaak RG, McKenna A, Campos B, Noushmehr H, Salama SR, et al. The somatic genomic landscape of glioblastoma. *Cell*. 2013;155(2):462–77. <http://dx.doi.org/10.1016/j.cell.2013.09.034>
40. Turcan S, Rohle D, Goenka A, Walsh LA, Fang F, Yilmaz E, et al. IDH1 mutation is sufficient to establish the glioma hypermethylator phenotype. *Nature*. 2012;483(7390):479–83. <http://dx.doi.org/10.1038/nature10866>
41. Cai J, Chen J, Zhang W, Yang P, Zhang C, Li M, et al. Loss of ATRX, associated with DNA methylation pattern of chromosome end, impacted biological behaviors of astrocytic tumors. *Oncotarget*. 2015;6(20):18105–15. <http://dx.doi.org/10.18632/oncotarget.3906>
42. Wiestler B, Capper D, Holland-Letz T, Korshunov A, von Deimling A, Pfister SM, et al. ATRX loss refines the classification of anaplastic gliomas and identifies a subgroup of IDH mutant astrocytic tumors with better prognosis. *Acta Neuropathol*. 2013;126(3):443–51. <http://dx.doi.org/10.1007/s00401-013-1156-z>
43. Cai J, Yang P, Zhang C, Zhang W, Liu Y, Bao Z, et al. ATRX mRNA expression combined with IDH1/2 mutational status and Ki-67 expression refines the molecular classification of astrocytic tumors: Evidence from the whole transcriptome sequencing of 169 samples. *Oncotarget*. 2014;5(9):2551–61. <http://dx.doi.org/10.18632/oncotarget.1838>
44. Narita Y, Nagane M, Mishima K, Huang HJ, Furnari FB, Cavenee WK. Mutant epidermal growth factor receptor signaling down-regulates p27 through activation of the phosphatidylinositol 3-kinase/Akt pathway in glioblastomas. *Cancer Res*. 2002;62(22):6764–9.
45. Datta SR, Dudek H, Tao X, Masters S, Fu H, Gotoh Y, et al. Akt phosphorylation of BAD couples survival signals to the cell-intrinsic death machinery. *Cell*. 1997;91(2):231–41. [http://dx.doi.org/10.1016/S0092-8674\(00\)80405-5](http://dx.doi.org/10.1016/S0092-8674(00)80405-5)
46. Ozes ON, Mayo LD, Gustin JA, Pfeffer SR, Pfeffer LM, Donner DB. NF- κ B activation by tumour necrosis factor requires the Akt serine-threonine kinase. *Nature*. 1999;401(6748):82–5. <http://dx.doi.org/10.1038/43466>
47. LoPiccolo J, Blumenthal GM, Bernstein WB, Dennis PA. Targeting the PI3K/Akt/mTOR pathway: Effective combinations and clinical considerations. *Drug Resist Updat*. 2008;11(1–2):32–50. <http://dx.doi.org/10.1016/j.drug.2007.11.003>
48. Bao ZS, Chen HM, Yang MY, Zhang CB, Yu K, Ye WL, et al. RNA-seq of 272 gliomas revealed a novel, recurrent PTPRZ1-MET fusion transcript in secondary glioblastomas. *Genome Res*. 2014;24(11):1765–73. <http://dx.doi.org/10.1101/gr.165126.113>
49. Carpten JD, Faber AL, Horn C, Donoho GP, Briggs SL, Robbins CM, et al. A transforming mutation in the pleckstrin homology domain of AKT1 in cancer. *Nature*. 2007;448(7152):439–44. <http://dx.doi.org/10.1038/nature05933>
50. Stokoe D. *Pten*. *Curr Biol*. 2001;11(13):R502. [http://dx.doi.org/10.1016/S0960-9822\(01\)00303-7](http://dx.doi.org/10.1016/S0960-9822(01)00303-7)
51. Tohma Y, Gratas C, Biernat W, Peraud A, Fukuda M, Yonekawa Y, et al. PTEN (MMAC1) mutations are frequent in primary glioblastomas (de novo) but not in secondary glioblastomas. *J Neuropathol Exp Neurol*. 1998;57(7):684–9. <http://dx.doi.org/10.1097/00005072-199807000-00005>

52. Tamura M, Gu J, Matsumoto K, Aota S, Parsons R, Yamada KM. Inhibition of cell migration, spreading, and focal adhesions by tumor suppressor PTEN. *Science*. 1998;280(5369):1614–17. <http://dx.doi.org/10.1126/science.280.5369.1614>
53. Reifenberger G, Liu L, Ichimura K, Schmidt EE, Collins VP. Amplification and overexpression of the MDM2 gene in a subset of human malignant gliomas without p53 mutations. *Cancer Res*. 1993;53(12):2736–9.
54. Biernat W, Kleihues P, Yonekawa Y, Ohgaki H. Amplification and overexpression of MDM2 in primary (de novo) glioblastomas. *J Neuropathol Exp Neurol*. 1997;56(2):180–5. <http://dx.doi.org/10.1097/00005072-199702000-00009>
55. Stott FJ, Bates S, James MC, McConnell BB, Starborg M, Brookes S, et al. The alternative product from the human CDKN2A locus, p14(ARF), participates in a regulatory feedback loop with p53 and MDM2. *EMBO J*. 1998;17(17):5001–14. <http://dx.doi.org/10.1093/emboj/17.17.5001>
56. Nakamura M, Watanabe T, Klangby U, Asker C, Wiman K, Yonekawa Y, et al. p14ARF deletion and methylation in genetic pathways to glioblastomas. *Brain Pathol*. 2001;11(2):159–68. <http://dx.doi.org/10.1111/j.1750-3639.2001.tb00388.x>
57. Nakamura M, Yonekawa Y, Kleihues P, Ohgaki H. Promoter hypermethylation of the RB1 gene in glioblastomas. *Lab Invest*. 2001;81(1):77–82. <http://dx.doi.org/10.1038/labinvest.3780213>
58. Sherr CJ, Roberts JM. CDK inhibitors: Positive and negative regulators of G1-phase progression. *Genes Dev*. 1999;13(12):1501–12. <http://dx.doi.org/10.1101/gad.13.12.1501>
59. Tso CL, Freije WA, Day A, Chen Z, Merriman B, Perlina A, et al. Distinct transcription profiles of primary and secondary glioblastoma subgroups. *Cancer Res*. 2006;66(1):159–67. <http://dx.doi.org/10.1158/0008-5472.CAN-05-0077>
60. Lamoral-Theys D, Le Mercier M, Le Calve B, Rynkowski MA, Bruyere C, Decaestecker C, et al. Long-term temozolomide treatment induces marked amino metabolism modifications and an increase in TMZ sensitivity in Hs683 oligodendroglioma cells. *Neoplasia*. 2010;12(1):69–79. <http://dx.doi.org/10.1593/neo.91360>
61. Swilar D, Dyavaiah M, Brown AR, Tang JB, Li J, McDonald PR, et al. Alkylation sensitivity screens reveal a conserved cross-species functionome. *Mol Cancer Res*. 2012;10(12):1580–96. <http://dx.doi.org/10.1158/1541-7786.MCR-12-0168>
62. Ye F, Zhang Y, Liu Y, Yamada K, Tso JL, Menjivar JC, et al. Protective properties of radiochemoresistant glioblastoma stem cell clones are associated with metabolic adaptation to reduced glucose dependence. *PLoS One*. 2013;8(11):e80397. <http://dx.doi.org/10.1371/journal.pone.0080397>
63. Auger N, Thillet J, Wanherdrick K, Idbaih A, Legrier ME, Dutrillaux B, et al. Genetic alterations associated with acquired temozolomide resistance in SNB-19, a human glioma cell line. *Mol Cancer Ther*. 2006;5(9):2182–92. <http://dx.doi.org/10.1158/1535-7163.MCT-05-0428>
64. Hiddingh L, Raktoc RS, Jeuken J, Hulleman E, Noske DP, Kaspers GJ, et al. Identification of temozolomide resistance factors in glioblastoma via integrative miRNA/mRNA regulatory network analysis. *Sci Rep*. 2014;4:5260. <http://dx.doi.org/10.1038/srep05260>
65. Kumar DM, Patil V, Ramachandran B, Nila MV, Dharmalingam K, Somasundaram K. Temozolomide-modulated glioma proteome: Role of interleukin-1 receptor-associated kinase-4 (IRAK4) in chemosensitivity. *Proteomics*. 2013;13(14):2113–24. <http://dx.doi.org/10.1002/pmic.201200261>
66. Sun S, Wong TS, Zhang XQ, Pu JK, Lee NP, Day PJ, et al. Protein alterations associated with temozolomide resistance in subclones of human glioblastoma cell lines. *J Neuro Oncol*. 2012;107(1):89–100. <http://dx.doi.org/10.1007/s11060-011-0729-8>
67. Anderson JC, Duarte CW, Welaya K, Rohrbach TD, Bredel M, Yang ES, et al. Kinomic exploration of temozolomide and radiation resistance in Glioblastoma multiforme xenografts. *Radiother Oncol*. 2014;111(3):468–74. <http://dx.doi.org/10.1016/j.radonc.2014.04.010>
68. Erson-Omay EZ, Henegariu O, Omay SB, Harmanci AS, Youngblood MW, Mishra-Gorur K, et al. Longitudinal analysis of treatment-induced genomic alterations in gliomas. *Genome Med*. 2017;9(1):12. <http://dx.doi.org/10.1186/s13073-017-0401-9>
69. Stepanenko AA, Andreieva SV, Korets KV, Mykytenko DO, Baklaushev VP, Huleyuk NL, et al. Temozolomide promotes genomic and phenotypic changes in glioblastoma cells. *Cancer Cell Int*. 2016;16:36. <http://dx.doi.org/10.1186/s12935-016-0311-8>

70. Auffinger B, Tobias AL, Han Y, Lee G, Guo D, Dey M, et al. Conversion of differentiated cancer cells into cancer stem-like cells in a glioblastoma model after primary chemotherapy. *Cell Death Differ.* 2014;21(7):1119–31. <http://dx.doi.org/10.1038/cdd.2014.31>
71. Fouse SD, Nakamura JL, James CD, Chang S, Costello JF. Response of primary glioblastoma cells to therapy is patient specific and independent of cancer stem cell phenotype. *Neuro Oncol.* 2014;16(3):361–71. <http://dx.doi.org/10.1093/neuonc/not223>
72. Bhat KP, Balasubramanian V, Vaillant B, Ezhilarasan R, Hummelink K, Hollingsworth F, et al. Mesenchymal differentiation mediated by NF-kappaB promotes radiation resistance in glioblastoma. *Cancer Cell.* 2013;24(3):331–46. <http://dx.doi.org/10.1016/j.ccr.2013.08.001>
73. Lau J, Ilkhanizadeh S, Wang S, Miroshnikova YA, Salvatierra NA, Wong RA, et al. STAT3 blockade inhibits radiation-induced malignant progression in glioma. *Cancer Res.* 2015;75(20):4302–11. <http://dx.doi.org/10.1158/0008-5472.CAN-14-3331>
74. Kim YH, Yoo KC, Cui YH, Uddin N, Lim EJ, Kim MJ, et al. Radiation promotes malignant progression of glioma cells through HIF-1alpha stabilization. *Cancer Lett.* 2014;354(1):132–41. <http://dx.doi.org/10.1016/j.canlet.2014.07.048>

3

Epigenetic Mechanisms of Glioblastoma

PEIYAO LI^{1,2} • MINGHUA WU^{1,2}

¹The Key Laboratory of Carcinogenesis of the Chinese Ministry of Health, Cancer Research Institute, Central South University, Changsha, Hunan, China; ²The Key Laboratory of Carcinogenesis and Cancer Invasion of the Chinese Ministry of Education, Cancer Research Institute, Central South University, Changsha, Hunan, China

Author for correspondence: Minghua Wu, The Key Laboratory of Carcinogenesis of the Chinese Ministry of Health, Cancer Research Institute, Central South University, Changsha, Hunan 410008, China.
E-mail: wuminghua554@aliyun.com

Doi: <http://dx.doi.org/10.15586/codon.glioblastoma.2017.ch3>

Abstract: Aberrant DNA methylation is a common event in the genesis and progression of tumors. The application of next-generation sequencing enables the identification and mapping of DNA methylation and its derivatives, 5fC and 5hmC, to base-pair resolution. This chapter describes nine novel hypermethylation genes and six hypomethylation genes, identified by constructing a DNA methylation profile, in glioblastoma. Abnormal promoter methylation and histone modifications were associated with differential expression of miRNAs in glioblastoma: miR-185 reversed global DNA methylation and the methylation level of the hypermethylation genes by targeting DNMT; and miR-101 regulated histone methylation of hypomethylation genes by targeting EED, EZH2, and DNMT3A. The long noncoding RNA CASC2c directly bound to miR-101 via microRNA response elements, and there was a reciprocal repression between CASC2c and miR-101. Despite being competitors they both led to the overexpression of their target hypomethylation genes CPEB1, PRDM16, and LMO3.

In: *Glioblastoma*. Steven De Vleeschouwer (Editor), Codon Publications, Brisbane, Australia
ISBN: 978-0-9944381-2-6; Doi: <http://dx.doi.org/10.15586/codon.glioblastoma.2017>

Copyright: The Authors.

Licence: This open access article is licenced under Creative Commons Attribution 4.0 International (CC BY 4.0). <https://creativecommons.org/licenses/by-nc/4.0/>

Taken together, glioblastoma is a complicated pathological process with deregulated methylation and histone modifications. Focal differentially methylated region and differentially methylated site studies will be helpful for the identification of regulatory elements of transcription. Studies of intragenic and distant intergenic alterations in DNA methylation will help elucidate the nature of epigenetic deregulation in glioblastoma.

Key words: Glioblastoma; Histone modification; lncRNA; Methylation; miRNA

Introduction

Aberrant DNA methylation patterns have been shown to be common events in the genesis and progression of tumors (1). In cancer cells, a general decline in the level of methylated cytosine (genomic hypomethylation) is accompanied by local locus-specific hypermethylation (2, 3). Genomic hypomethylation contributes to genetic instability and proto-oncogene hypomethylation, which is responsible for their stronger expression (4). In addition, functional silencing of tumor-associated genes is usually associated with local promoter hypermethylation (5). Thus, alterations in tumor cell DNA methylation patterns contribute to abnormal gene expression and malignant phenotypes. Glioblastoma multiforme is the most common and aggressive primary central nervous system tumor in adults. Abnormal DNA methylation is responsible for glioblastoma genesis, development, and malignancy progression (6). Promoter hypermethylation and epigenetic silencing of the MGMT gene have been widely described in glioma (7–9). Several genes that are involved in key cellular functions such as the cell cycle (10), tumor suppression (11–15), DNA repair (16, 17), tumor invasion (18), and apoptosis (19) have been shown to be silenced in association with promoter hypermethylation in malignant glioblastoma. Despite these important findings, aberrant DNA methylation on genome-wide scale is still not fully understood in glioblastoma. This chapter describes nine novel hypermethylation genes and six hypomethylation genes, identified by constructing a genome-wide DNA methylation profile, in glioblastoma.

Methylomes of Glioblastoma

DNA METHYLATION PROFILE IN GLIOBLASTOMA

MeDIP-chip was used to investigate the whole-genome differential methylation patterns between glioblastoma and nontumor brain samples (20). A total of 104 hypomethylated and 524 hypermethylated regions were identified in glioblastoma. Of these, 70 hypomethylated and 361 hypermethylated regions were CpG islands (Figure 1A). Thirty hypomethylated and 199 hypermethylated regions were mapped to the unannotated gene regions (Figure 1B). Meanwhile, 74 hypomethylation and 325 hypermethylation regions were mapped to

annotated gene regions comprising the promoter region, intragenic region, and the regions downstream. Furthermore, 81.1% (60 of 74) of hypomethylated and 66.5% (216 of 325) of hypermethylated regions mapped to the promoter regions of annotated genes (Figure 1C). Twenty-seven hypomethylated and 53 hypermethylated regions mapped to CpG islands as well as the promoters of known genes (Figure 1D). Thus, a number of new differential methylation regions (DMRs) were shown to exist in unannotated genomic regions as well as the promoter regions, intragenic regions, and regions downstream of known genes in glioblastoma. The promoter hypermethylated genes exist predominately on chromosomes 1, 2, 3, 17, and x, while the promoter hypomethylated genes were mainly distributed on chromosomes 1, 11, 16, 19, 20, and 22 (Figure 1D). The functional and pathway analyses of these differential promoter methylated genes were performed by the DAVID bioinformatics tools. Most of the differential promoter methylated genes belonged to signaling networks that played critical roles in regulation of transcription, neurological process, ion transport, cell adhesion, apoptosis, and regulation of tumor development (Tables 1 and 2). Promoter hypermethylated genes that were correlated to

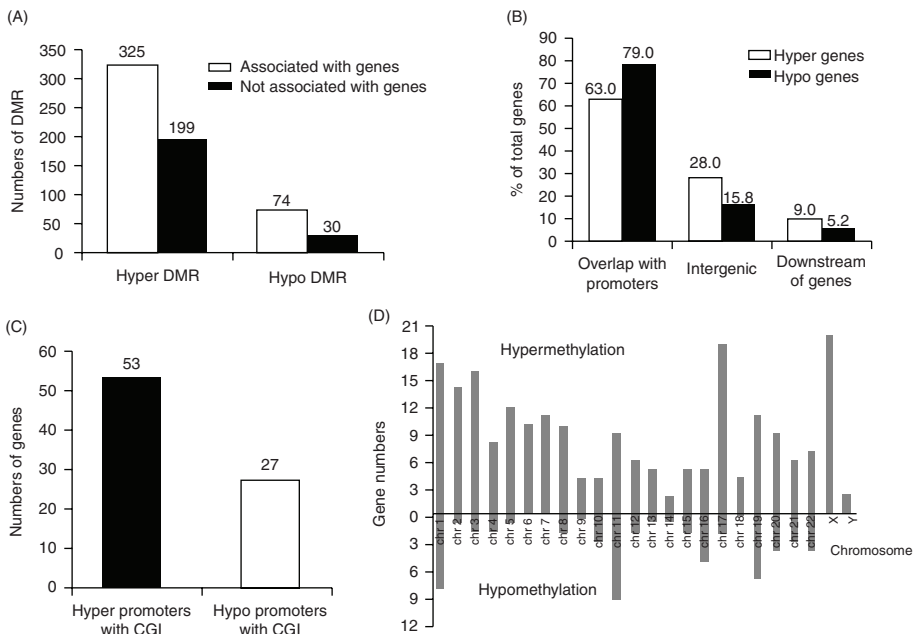


Figure 1 Genome-wide analysis of DMRs in primary glioblastoma. (A) DMRs (differentially methylated regions) are correlated with or without genes. (B) Distribution of DMRs is correlated with genes. Most identified DMRs are mapped to gene promoters. (C) Numbers of DMRs are mapped to both gene promoters and CpG islands. (D) Chromosomal distribution of 60 promoter hypomethylated genes and 216 promoter hypermethylated genes (Zuping Zhang, Guiyuan Li. Study on epigenetic mechanisms of glioma. Doctoral thesis, Central South University, 2009; 12).

TABLE 1

Gene Ontology and KEGG Pathway Enrichment Analysis of Promoter Hypermethylated Genes Identified by MeDIP-Chip (Zuping Zhang. Doctoral thesis. Central South University, 2009)

Gene Ontology Analysis	Promoter Hypermethylation Genes
Cell communication and intracellular signal transduction	22 Genes: ANKDD1A, OPN1MW, PKP1, PCDHB13, PI4KA, HSH2D, KNDC1, KCNMB3SST, DIRAS3, PTAFR, KCNN3, OR10Q1, CD81, ABRA, CASP9, FYN, MBP, OR10H5, RCVRN, GPR31, KCNMB2, TDGF1,
Neurological system process, and synaptic and nerve impulse transmission	20 Genes: SIX3, PI4KA, RCVRN, PCDHB13, OR10H5, MBP, KCNMB2, KCNMB3, CLN3, MPZ, S100P, TRPV1, DLGAP2, PROM1, FYN, SYPL1, SST, GAD1KCNN3, OR10Q1, HTR1D
Negative regulation of biological process, metabolic process, cellular process, and transcription activity	16 Genes: PAIP2, TDGF1, RASSF1, DEDD2, GRLF1, SALL4, RASSF2, TMSB4Y, CFTR, CLN3, GDNF, SIX3, DKK4, SST, ST18, B4GALNT2
Chemical homeostasis, homeostatic process, ion homeostasis, regulation of pH, and biological quality	13 Genes: KCNMB3, CCKAR, CLN3, MPZ, TRPV1, CYP11B2, RPH3AL, DNAJC16, DEDD2, MB, KCNMB2, MBP, EDNRB
Brain development, neurons generation, and migration	9 Genes: FYN, SIX3, CFTR, NNAT, CCKAR, ROBO2, GRLF1, GDNF, LRRC4
Cell and biological adhesion, homophilic cell adhesion, and Cadherin	13 Genes: SDK1, FBLN7, PCDHB13, CLDN18, PKP1, CD300A, ROBO2, PCDHA12, PARVB, FGF6, FLRT1FERMT3, PCDHA8, PCDHA13
Ion transport, calcium channel, cation channel activity, gated channel activity, and ion transmembrane transporter activity	10 Genes: KCNMB3, TRPV1, FYN, CACNG7, KCNN3, TRPV3, CACNG1, SLC5A11, KCNK10, KCNMB2
Migration and motility of cell, localization of cell, cellular morphogenesis during differentiation, and cellular structure morphogenesis	9 Genes: S100P, TDGF1, EDNRB, SST, FYN, CCKAR, GDNF, ROBO2, CFTR
Actin binding and cytoskeletal protein binding	8 Genes: TMSB4Y, PDE4DIP, FYN, PARVB, ABRA, C14 or f49, RPH3AL, PHACTR3
Apoptosis induction by extracellular signals	2 Genes: SST, DEDD2
Neuroactive ligand–receptor interaction	6 Genes: EDNRB, PTAFR, HTR1D, GH2, SST, CCKAR, TRPV1
KEGG Pathway Analysis	Promoter Hypermethylation Genes
MAPK signaling pathway	4 Genes: MAP2K3, CACNG7, FGF6, CACNG1
WNT signaling pathway	1 Gene: DKK4
JAK-STAT signaling pathway	1 Gene: GH2

TABLE 2

Gene Ontology and KEGG Pathway Enrichment Analysis of Promoter Hypomethylation Genes Identified by MeDIP-Chip (Zuping Zhang, Doctoral thesis, Central South University, 2009)

Gene Ontology Analysis	Promoter Hypomethylation genes
Cell communication and intracellular signal transduction	14 Genes: ABR, OR1L6, FKBP8, DRD4, SORBS1, GPIBB, OR10G4, BAD, C9, OR51S1, CCRL2, OR8A1, SFN, MLNR
Protein metabolic, cellular metabolic, and biopolymer metabolic process	11 Genes: CPEB1, C9, FKBP8, TUBB4Q, PRSS33, FUT5, NRBP2, PSMF1, OR51S1, KLHL21, TUBB8
Transport including metal ion transport and cation transport, ion channel activity	10 Genes: ACCN1, ABCC12, SLC5A9, SLC2A9, KCNK4, TUBB4Q, TUBB8, MFSD3, SLC28A1, SORBS1
Hydrolase activity and serine hydrolase activity	5 Genes: ABCC12, OR51S1, TUBB4Q, TUBB8, PRSS33
Regulation of gene expression, transcription, DNA binding, and transcription factor activity	5 Genes: CPEB1, LMO3, PHF13, TOX2, NAT14
Nervous system and organ development, and system development	3 Genes: ACCN1, ABR, IGSF8
Cell death, apoptotic program, and induction of apoptosis	3 Genes: BAD, C9, SFN
KEGG Pathway Analysis	Promoter Hypomethylation Genes
Neuroactive ligand–receptor interaction	3 Genes: SCT, DRD4, MLNR
Insulin signaling pathway	2 Genes: BAD, SORBS1

human tumor development included EDNRB, ARHI, FYN, GIPC2, GDNF, RASSF1, RASSF2, and ARHI (21–25).

NINE NOVEL HYPERMETHYLATION GENES IN GLIOBLASTOMA

Sequenom MassARRAY platform quantitative analysis confirmed that LRRC4, ANKDD1A, GAD1, SIX3, SST, PHOX2B, PCDHA8, HIST1H3E, and PCDHA13 were the nine novel promoter hypermethylation genes in glioblastoma (Figure 2B). LRRC4 (GeneBank: AF196976) is not only a brain-specific gene but also a novel candidate for tumor suppression. Methylation-mediated inactivation of LRRC4, SIX3, and ANKDD1A has been verified as a frequent and glioblastoma-specific

event (15). SIX3 is a novel negative transcriptional regulator and acts as a tumor suppressor that directly represses the transcription of AURKA and AURKB in glioblastoma (26). ANKDD1A inhibits the transcriptional activity of HIF1 α to alter hypoxia microenvironment by directly interacting with FIH1. The tumor-specific methylation of ANKDD1A indicates that it could be used as a potential epigenetic biomarker and also as a possible therapeutic target for glioblastoma.

SIX NEW HYPOMETHYLATION GENES IN GLIOBLASTOMA

Signalmap software was used to select the following 12 genes from the 74 hypomethylated regions screened with the methylation chip: F10, POTEH, CPEB1, LMO3, ELFN2, PRDM16, CD207, BAD, NRBP2, SLITRK5, SLC44A2, and PGP. These genes were tested in a large scale of samples by BSP, which revealed that there is no difference between the methylation levels of CD207, BAD, NRBP2, SLITRK5, SLC44A2, and PGP in glioblastoma tissues and in normal brain tissues. F10 (27), POTEH (28), CPEB1 (29), LMO3 (30), ELFN2, and PRDM16 (31) were hypomethylated in glioblastoma tissues. They were confirmed to be novel hypomethylated genes in glioblastoma. Because of their higher expression, and poor outcomes in patients harboring these genes, these hypomethylated genes could be

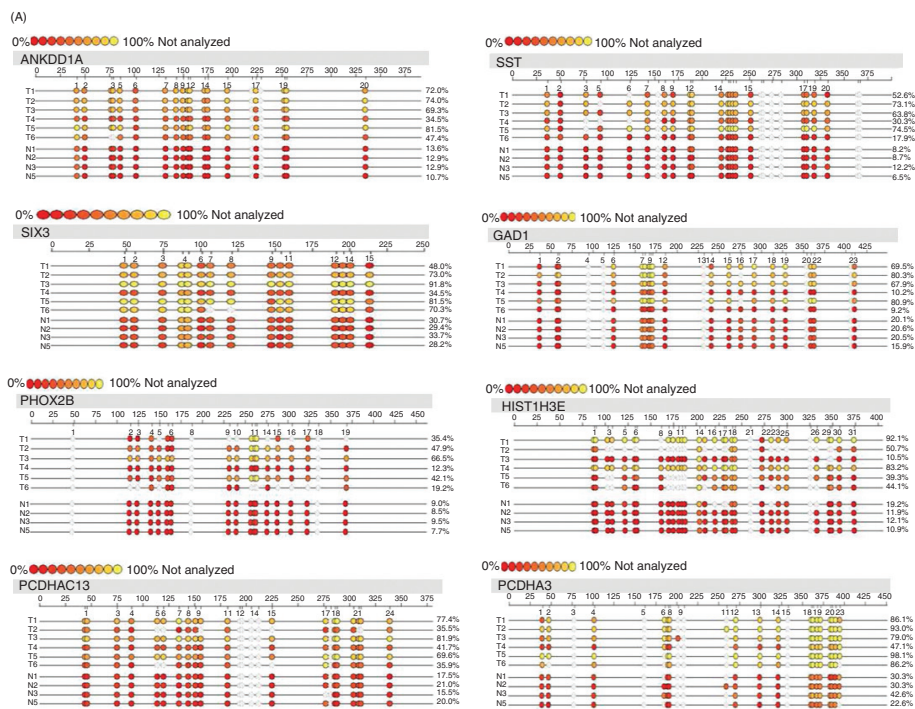


Figure continued on following page

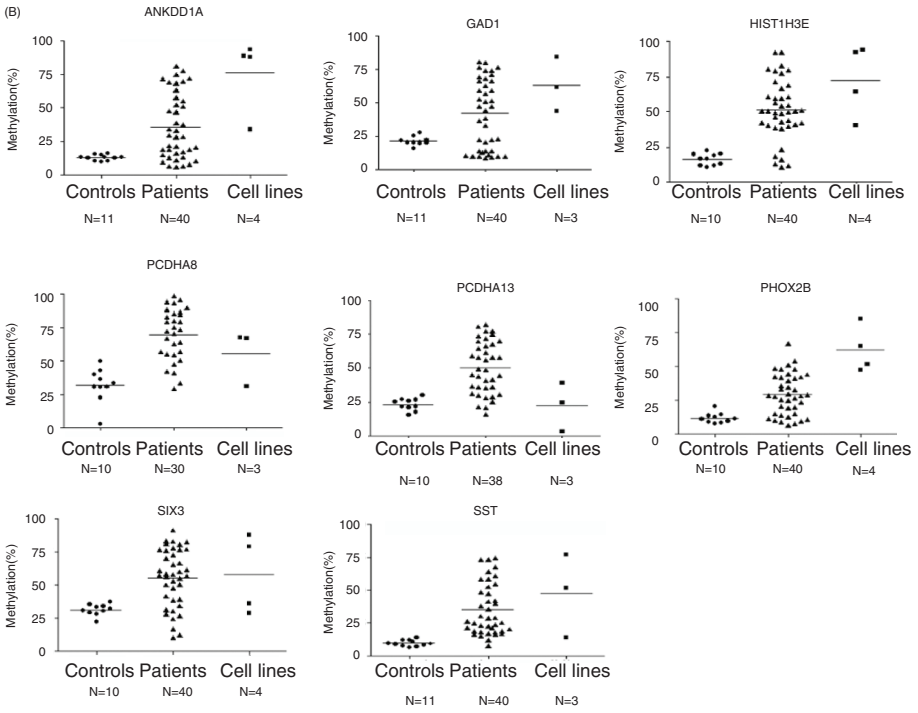


Figure 2 MassARRAY methylation analysis for glioblastoma. (A) MeDIP-chip assay detected hypermethylation genes' promoter methylation levels. Mass ARRAY assay were carried out using patients' samples gDNA screened by microarray. The position of CpG dinucleotides were marked by circles within the sequence (straight line), and the methylation levels were marked by different circle colors. Gray circles represent CpG sites that could not be analyzed. The base-pair position in the gene sequence used the ruler on top and CpG sites number at the bottom. In all tested genes, glioma samples have significant hypermethylation in promoter regions compared with normal controls. N1, N2, N3, and N5 represent normal brain, while T1, T2, T3, T4, T5, and T6 represent glioma samples. Glioma samples and normal samples were matched for age and sex. (B) Methylation levels of eight selected genes were identified by MeDIP-chip in glioma patients, normal controls, and glioma cell lines. DNA methylation was analyzed using MassARRAY assay. The gene names were marked in the top of each graph. N represents the number of cases for this research. In the top of each graph, the results of an individual gene are represented (20).

regarded as important prognostic markers of glioblastoma. While hypomethylation of F10 was correlated to patients' age, high expression of POTEH and hypomethylation of PRDM16 were related to astrocytoma pathology grade (Table 3). Thus, high expression of POTEH and hypomethylation of PRDM16 could be considered as important markers in the progression of glioblastoma. The glioblastoma tissues with a high POTEH expression level or PRDM16 hypomethylation would be more malignant than those with a low POTEH expression level or PRDM16 hypermethylation.

TABLE 3

Correlation between Methylation Status and Protein Expression of Hypomethylation Genes and Clinical Parameters of Astrocytoma Patients

Variables	hypomethylation		Sex		Age(years) ^a		Grade	
	+	-	Male	Female	<median	≥median	Low grade (I+II)	High grade (III+IV)
FX(score)								
<8	12	9	9	12	12	9	10	11
≥8	67	8	45	30	32	43	46	29
P		0.001		0.162		0.239		0.126
POTEH(score)								
<8	27	12	23	16	15	24	29	10
≥8	51	6	31	26	29	28	27	30
P		0.006		0.656		0.230		0.008
CPEB1(score)								
<8	18	7	17	8	14	11	14	11
≥8	25	0	17	8	9	16	12	13
P		0.010		1.000		0.781		0.571
LMO3(score)								
<8	9	4	10	3	8	5	8	5
≥8	34	3	24	13	19	18	18	19
P		0.043		0.508		0.526		0.424
ELFN2(score)								
<8	12	6	11	7	9	9	10	8
≥8	29	3	23	9	18	14	16	16
P		0.034		0.434		0.670		0.706
PRDM16(score)								
<8	7	4	8	3	7	4	7	4
≥8	36	3	26	13	20	19	19	20
P		0.016		0.704		0.468		0.382

Note: Immunohistochemistry score ≥8 represents the high expression; <8 represents the low expression. The high expression of FX, POTEH, CPEB1, ELFN2, LMO3, and PRDM16 were accompanied by their hypomethylation in glioblastoma. And the hypomethylation of POTEH, CPEB1, LMO3, and ELFN2 did not have statistically significant correlation with sex, age, or histological grades. The hypomethylation of F10 was correlated to patients' ages, and high expression of POTEH and hypomethylation of PRDM16 were related to the pathology grade of astrocytoma.

miRNA and Methylation Genes in Glioblastoma

Epigenetic modifications encompass DNA methylation, chromatin remodeling, noncoding RNA expression, and histone tail modifications. Methylation modification is important for a proper genome function by maintaining chromatin structure, chromosome stability, and transcription. Histones are the protein moiety around chromatin, which is packaged by DNA, and their N-terminal tails can suffer a variety of post-translational modifications, such as methylation, acetylation, sumoylation, ubiquitination, phosphorylation, and ADP ribosylation (32, 33). MicroRNAs (miRNAs) are 20–22 nucleotide (nt) noncoding RNAs that bind to the 3' untranslated region of the target mRNA to form RNA-induced silencing complexes, which lead to the down regulation of genes by causing mRNA destabilization and/or translational inhibition (34, 35). miRNAs, as both targets and effectors, play a critical role in regulation of DNA methylation (36–39). Moreover, miRNAs can regulate DNA methylation by targeting the DNA methylation machinery.

THE LRRC4-AP-2-miR-182 LOOP

As miR-381 and miR-182 could facilitate glioblastoma cell growth *in vitro* and *in vivo*, they are regarded as potential therapeutic biomarkers in glioblastoma (40). The downregulation of miR-381 or miR-182 arrested cell cycle of glioblastoma cells in the G₀/G₁ phase and inhibited their proliferation by suppressing E2F3 and upregulating phosphorylated Rb. LRRC4 was the co-target gene of miR-381 and miR-182, and its expression was inversely correlated with miR-381, miR-182, and BRD7 in glioblastoma. Knockdown of miR-182 and miR-381 inhibited LRRC4-mediated binding of AP-2/SP1/E2F6/c-Myc to BRD7 by ERK/MAPK and PI-3K/AKT (40). Transcription of miR-182 was induced by the transcription factor AP-2, as predicted by online software and confirmed by ChIP. miR-182 inhibited the expression of LRRC4, and LRRC4 inhibited the expression and transcription of AP-2 by negatively regulating the ERK/MAPK and PI-3K/AKT signaling pathways. This indicated that the LRRC4-AP-2-miR-182-LRRC4 loop is involved in glioblastoma development (40).

THE LRRC4-miR-185/SP1-DNMT1 LOOP

LRRC4 upregulation induced the expression of miR-185, and the LRRC4-miR-185/SP1-DNMT1-LRRC4 loop played a key role in glioblastoma: miR-185 inhibited cell motility, invasion, and proliferation; and DNMT1, one of the most important DNA methyltransferases, maintained methylation. miR-185 upregulation inhibited DNMT1 and decreased global methylation through HPLC-DAD; it also downregulated the expression of nine novel hypermethylated genes (SIX3, SST, LRRC4, GAD1, PCDHA8, PHOX2B, PCDHA13, ANKDD1A, and HIST1H3E) (20). Thus, miR-185 acts as a tumor suppressor by targeting DNMT1 to decrease global methylation and recover hypermethylation of these genes. The GO methodology is a success-oriented probabilistic system performance analysis technique. Based on GO methodology, miR-185 was also considered to be involved in Rho GTPase activity. RhoA and CDC42 were the direct targets of miR-185, and

the expression of these two molecules was negatively correlated with miR-185 in glioblastoma. Overexpression of miR-185 reduced the growth and migration of glioblastoma cells by inhibiting RhoA, CDC42 directly, and VEGFA indirectly (20). In summary, LRRC4 could regulate miRNAs as a tumor suppressor gene. These processes constitute multiple circuits, including LRRC4-miR-185-DNMT1-LRRC4, LRRC4-SP1-DNMT1-LRRC4, and LRRC4-AP-2-miR-182-LRRC4. These circuits take part in the development of glioblastoma with multiple feedback mechanisms (Figure 3).

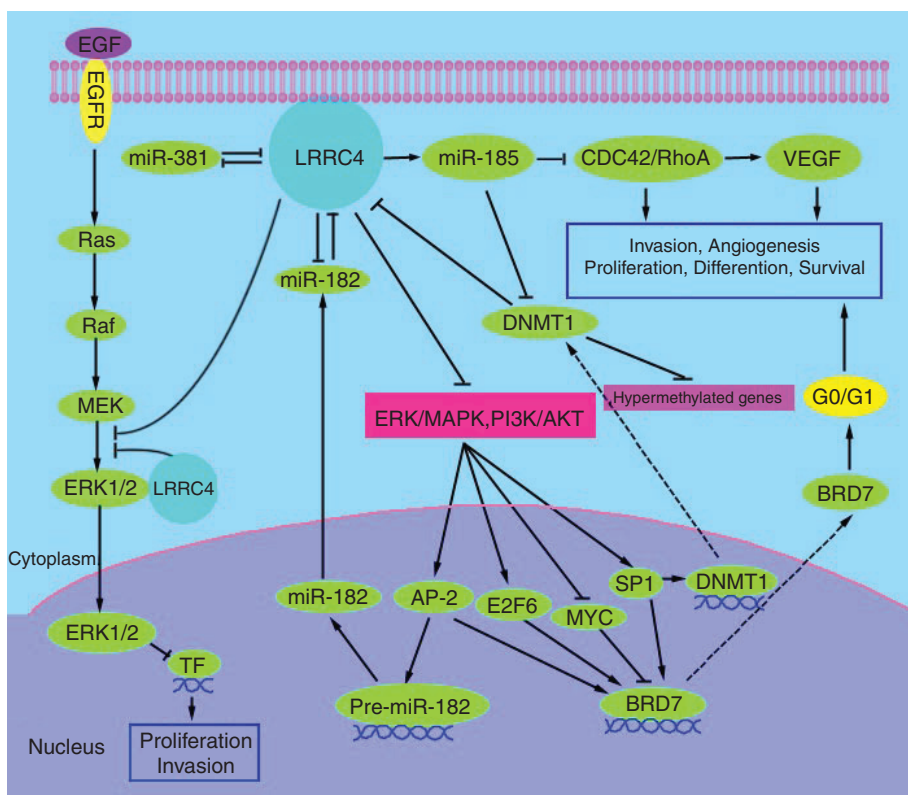


Figure 3 The regulation networks of hypermethylated genes, miRNA, DNMT, transcript factors, and target genes in glioblastoma. LRRC4-AP-2-miR-182-LRRC4loop: LRRC4 is a common target of miR-182 and miR-381, and miR-182 and miR-381 inhibit LRRC4 expression; meanwhile, the re-expression of LRRC4 also decreases miR-182 and miR-381 expression. The transcription of miR-182 is induced by AP-2; however, LRRC4 also inhibits the expression of AP-2 through negatively regulating the ERK/MAPK and PI-3K/AKT signaling pathways. The LRRC4-AP-2-miR-182-LRRC4 loop was formed among LRRC4, miR-182, and AP-2. LRRC4-miR-185-DNMT1-LRRC4 loop: The re-expression of LRRC4 increases miR-185 expression, while miR-185 decreases global methylation by targeting DNMT1 and increases the expression of LRRC4. LRRC4-SP1-DNMT1-LRRC4loop: DNMT1 is positively regulated by SP1, and it increases the expression of LRRC4, while LRRC4 also inhibits SP1 by negatively regulating the ERK/MAPK and PI-3K/AKT signal pathway (Adapted from Mol Cancer 2011;10:124.)

miR-101 AND HYPOMETHYLATION GENES

It has been shown that miR-101 is downregulated in multiple tumors, including glioblastoma, and acts as a tumor suppressor. Interestingly, the novel hypomethylation genes CPEB1, PRDM16, ELFN2, and LMO3 were predicted to be targeted by miR-101. CPEB1, PRDM16, and ELFN2 were verified to be the direct target genes of miR-101; however, LMO3 was not the direct target (Figure 4). miR-101 suppressed CPEB1 expression by reversing the CPEB1 promoter methylation status. Furthermore, miR-101 reversed CPEB1 promoter methylation status by regulating the methylation-related histones H3K27me₃, H3K4me₂, H4K20me₃, and H3K9me₃. In addition, the decreased expression of CPEB1 triggered senescence in a p53-dependent manner (Figure 4). miR-101 downregulated LMO3 expression by reversing the LMO3 promoter methylation status, inhibiting the presence of the methylation-related histones H3K27me₃ and H3K4me₂, and increasing the presence of H4K20me₃ and H3K9me₃ on the promoter. miR-101 reduced the occupancy of H3K27me₃ through suppressing EED, DNMT3A, and EZH2, and reduced the H3K9me₃ occupancy on the LMO3 promoter by PHF8, G9a, SUV39H1, and SUV39H2. Moreover, miR-101 inhibited LMO3 expression by reducing MZF1 and USF (Figure 4). miR-101 also reduced PRDM16 expression by affecting the PRDM16 promoter methylation status. miR-101 was related to an increase in H4K20me₃ and H3K9me₃ and a decrease in the methylation-related histones H3K27me₃ and H3K4me₂ on the PRDM16 promoter. In addition, miR-101 suppressed PRDM16 expression by targeting DNMT3A, which decreased histones H3K27me₃ and H3K4me₂ at the PRDM16 core promoter (Figure 4). In addition, miR-101 also reduced H3K27me₃ occupancy at the core promoter of the hypermethylation gene LRRC4 and reversed the LRRC4 methylation level through targeting EED, EZH2, and DNMT3A (Figure 4).

LncRNA, miRNA, and Methylation in Glioblastoma

INTERACTION OF LNCRNA AND miRNA

lncRNAs regulate gene transcription (41), chromatin remodeling (42), post-transcriptional processing of mRNA (43), and competing endogenous RNA (ceRNA) (44, 45). Emerging evidence suggests that lncRNAs communicate with ncRNAs, mRNAs, proteins, and genomic DNA, and act as tethers, guides, decoys, and scaffolds (46, 47). lncRNAs can participate in the ceRNA regulatory network and act as endogenous miRNA sponges to compete for binding of miRNA through MRE, which is “the letters” of the RNAcode (48). ceRNAs and miRNAs repress reciprocally and form a double-negative feedback loop (49, 50). Online promoterInspector and promoterScan softwares predicted that the CpG island status on the promoter of pre-miR-101-1 and pre-miR-101-2 is not the reason for the lower expression of miR-101. Furthermore, the LOH in chromosomes 1p31(pre-miR-101-1) and 9p24 (pre-miR-101-2) was insufficient to lower the expression of miR-101 in glioblastoma. The software programs DIANA LAB and miRanda were used to search for lncRNAs and there were 18 lncRNAs predicted to form putative binding sites with miR-101. However, only six lncRNAs have been confirmed to

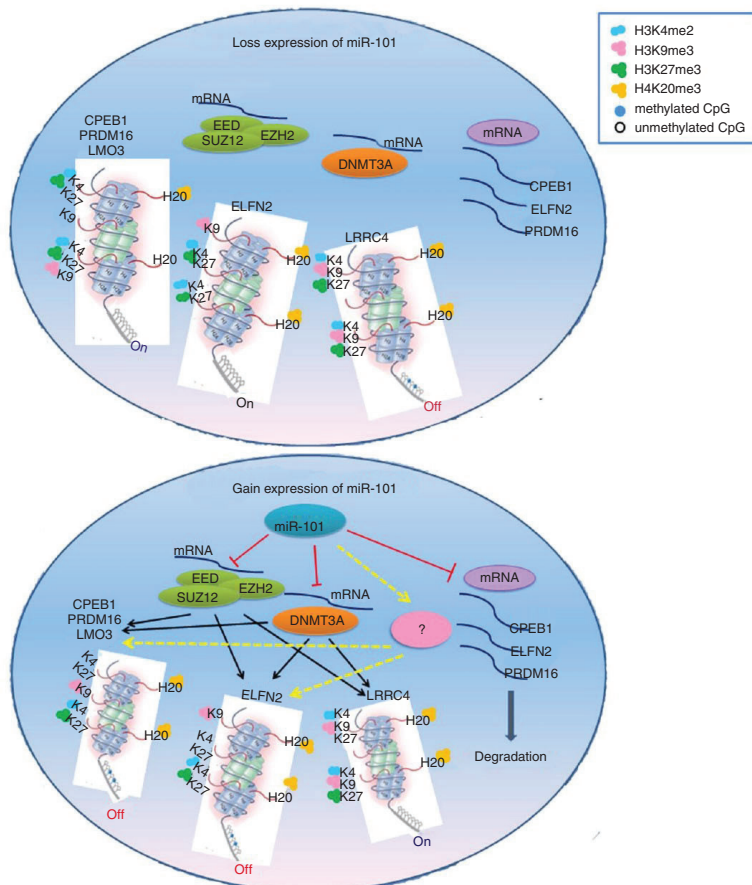


Figure 4 The networks of miRNA, gene methylation, and histone modification in glioblastoma.

The hypomethylated genes CPEB1, PRDM16, and ELFN2 are target genes of miR-101, but LMO3 is not, and the expression of CPEB1, PRDM16, and ELFN2 are inhibited directly by miR-101. Moreover, miR-101 also indirectly suppresses the expression of CPEB1, ELFN2, PRDM16, and LMO3 and affects their methylation levels by targeting EZH2, EED, and DNMT3A and regulating histone methylation; miR-101 decreases the occupancy of H3K4me2 and H3K27me3 at CPEB1, ELFN2, PRDM16, and LMO3 core promoter and increases the H3K9me3 and H4K20me3 occupancy at CPEB1, PRDM16, and LMO3 core promoter by targeting EZH2, EED, and DNMT3A; then, it recovers the methylation levels of CPEB1, ELFN2, PRDM16, and LMO3 gene promoter, and indirectly downregulates the expression of these hypomethylation genes. miR-101 does not bind to 3'UTR of hypermethylated gene LRRC4, but it remains to upregulate the expression of LRRC4. miR-101 decreases the occupancy of H3K27me3 at LRRC4 core promoter and induces hypomethylation of LRRC4 by targeting EZH2, EED, and DNMT3A. In short, miRNAs can not only directly regulate expression of hyper-/hypo- methylation genes by binding to 3'-UTR of genes but also regulate the methylation level and gene expression through histone and DNA methylation modification by targeting histone and DNA methyltransferases (Xiaoping Liu. Doctor's thesis. Central South University, 2012).

show significantly different expression between glioblastoma and normal brain tissues. CASC2c was bound to miR-101 directly by MRE of miR-101, and there was a reciprocal repression between CASC2c and miR-101. The higher expression of CASC2c is one of the reasons for the low expression of miR-101. CASC2c is also the target of miR-101 and commonly exists in the RISC complex with miR-101. A high level of CASC2c positively regulated the expression of pre-miR-101; however, in the processing from pre-miR-101 to mature miR-101, CASC2c negatively regulated the expression of Dicer and inhibited the expression of mature miR-101 in glioblastoma (51). CASC2c is a long noncoding RNA and provided evidence that high expression of CASC2c occurred in glioblastoma. Knockdown CASC2c suppressed the proliferation, migration, and invasion *in vitro* and glioblastoma tumorigenesis *in vivo*.

EFFECT OF LNCRNA ON METHYLATION GENES IN GLIOBLASTOMA

CASC2c functions as a suppressor of miR-101 or as a competitor of its target genes such as CPEB1, PRDM16, and LMO3. The expression of hypomethylation genes CPEB1, PRDM16, and LMO3 was increased in glioblastoma, and the depletion of CASC2c led to their repression. Thus, in normal tissue, CASC2c, miR-101, and target genes keep a balance by competitive restriction. In glioblastoma, because of the high expression of CASC2c; low expression of miR-101; or the overexpression of CPEB1, PRDM16, and LMO3 as a result of hypomethylation status of its promoter, the balance of this regulatory feedback is lost. In terms of complexity of molecular mechanisms in tumors, a cause-and-effect relationship among CASC2c, miR-101, CPEB1, PRDM16, and LMO3 could not be established. Despite this, miR-101 might be a core unit, and MRE of miR-101 is important for the crosstalk among CASC2c, miR-101, and their target genes in glioblastoma.

Conclusion

The application of next-generation sequencing enabled DNA methylation and its derivatives, 5fC and 5hmC, to be mapped at base-pair resolution. These studies have offered novel viewpoints into the distribution, dynamics, and function of DNA methylation in vertebrate genomes. Focal DMRs and DM site studies will be helpful for the discovery of regulatory elements of transcription factors, which may participate in specific gene regulation *in vivo*. Model systems should be used to test the functionality of individual DM sites or DMRs identified in epigenomic profiles. In the near future, studies of intragenic and distant intergenic alterations in DNA methylation will help elucidate the nature of epigenetic deregulation in diseases, especially for glioblastoma.

Acknowledgment: This study was supported by grants from the National Science Foundation of China (81272297), National Key Technology Research and Development program of the Ministry of Science and Technology of China (2014BAI04B02), and Hunan Province Natural Sciences Foundations (2015JJ2167).

Conflict of interest: The authors declare no potential conflicts of interest with respect to research, authorship, and/or publication of this manuscript.

Copyright and permission statement: To the best of our knowledge, the materials included in this chapter do not violate copyright laws. All original sources have been appropriately acknowledged and/or referenced. Where relevant, appropriate permissions have been obtained from the original copyright holders.

References

1. Jones PA, Baylin SB. The epigenomics of cancer. *Cell*. 2007 Feb 23;128(4):683–92. <http://dx.doi.org/10.1016/j.cell.2007.01.029>
2. Baylin SB, Esteller M, Rountree MR, Bachman KE, Schuebel K, Herman JG, et al. Aberrant patterns of DNA methylation, chromatin formation and gene expression in cancer. *Hum Mol Genet*. 2001 Apr;10(7):687–92. <http://dx.doi.org/10.1093/hmg/10.7.687>
3. Laird PW. Cancer epigenetics. *Hum Mol Genet*. 2005 Apr 15;14 Spec No 1:R65–76. <http://dx.doi.org/10.1093/hmg/ddi113>
4. Ehrlich M. DNA methylation in cancer: Too much, but also too little. *Oncogene*. 2002 Aug 12;21(35):5400–13. <http://dx.doi.org/10.1038/sj.onc.1205651>
5. Herman JG, Baylin SB. Gene silencing in cancer in association with promoter hypermethylation. *N Engl J Med*. 2003 Nov 20;349(21):2042–54. <http://dx.doi.org/10.1056/NEJMra023075>
6. Kim TY, Zhong S, Fields CR, Kim JH, Robertson KD. Epigenomic profiling reveals novel and frequent targets of aberrant DNA methylation-mediated silencing in malignant glioma. *Cancer Res*. 2006 Aug 1;66(15):7490–501. <http://dx.doi.org/10.1158/0008-5472.CAN-05-4552>
7. Komine C, Watanabe T, Katayama Y, Yoshino A, Yokoyama T, Fukushima T. Promoter hypermethylation of the DNA repair gene O6-methylguanine-DNA methyltransferase is an independent predictor of shortened progression free survival in patients with low-grade diffuse astrocytomas. *Brain Pathol*. 2003 Apr;13(2):176–84. <http://dx.doi.org/10.1111/j.1750-3639.2003.tb00017.x>
8. Yin D, Xie D, Hofmann WK, Zhang W, Asotra K, Wong R, et al. DNA repair gene O6-methylguanine-DNA methyltransferase: Promoter hypermethylation associated with decreased expression and G:C to A:T mutations of p53 in brain tumors. *Mol Carcinog*. 2003 Jan;36(1):23–31. <http://dx.doi.org/10.1002/mc.10094>
9. Hegi ME, Diserens AC, Godard S, Dietrich PY, Regli L, Ostermann S, et al. Clinical trial substantiates the predictive value of O-6-methylguanine-DNA methyltransferase promoter methylation in glioblastoma patients treated with temozolomide. *Clin Cancer Res*. 2004 Mar 15;10(6):1871–4. <http://dx.doi.org/10.1158/1078-0432.CCR-03-0384>
10. Ohta T, Watanabe T, Katayama Y, Yoshino A, Yachi K, Ogino A, et al. Aberrant promoter hypermethylation profile of cell cycle regulatory genes in malignant astrocytomas. *Oncol Rep*. 2006 Nov;16(5):957–63. <http://dx.doi.org/10.3892/or.16.5.957>
11. Amatyra VJ, Naumann U, Weller M, Ohgaki H. TP53 promoter methylation in human gliomas. *Acta Neuropathol*. 2005 Aug;110(2):178–84. <http://dx.doi.org/10.1007/s00401-005-1041-5>
12. Hesson L, Bieche I, Krex D, Criniere E, Hoang-Xuan K, Maher ER, et al. Frequent epigenetic inactivation of RASSF1A and BLU genes located within the critical 3p21.3 region in gliomas. *Oncogene*. 2004 Mar 25;23(13):2408–19. <http://dx.doi.org/10.1038/sj.onc.1207407>
13. Horiguchi K, Tomizawa Y, Tosaka M, Ishiuchi S, Kurihara H, Mori M, et al. Epigenetic inactivation of RASSF1A candidate tumor suppressor gene at 3p21.3 in brain tumors. *Oncogene*. 2003 Oct 30;22(49):7862–5. <http://dx.doi.org/10.1038/sj.onc.1207082>
14. Wiencke JK, Zheng S, Jelluma N, Tihan T, Vandenberg S, Tamgüney T, et al. Methylation of the PTEN promoter defines low-grade gliomas and secondary glioblastoma. *Neuro Oncol*. 2007 Jul;9(3):271–9. <http://dx.doi.org/10.1215/15228517-2007-003>

15. Zhang Z, Li D, Wu M, Xiang B, Wang L, Zhou M, et al. Promoter hypermethylation-mediated inactivation of *LRRC4* in gliomas. *BMC Mol Biol.* 2008 Nov 3;9:99. <http://dx.doi.org/10.1186/1471-2199-9-99>
16. Fukushima T, Katayama Y, Watanabe T, Yoshino A, Ogino A, Ohta T, et al. Promoter hypermethylation of mismatch repair gene *hMLH1* predicts the clinical response of malignant astrocytomas to nitrosourea. *Clin Cancer Res.* 2005 Feb 15;11(4):1539–44. <http://dx.doi.org/10.1158/1078-0432.CCR-04-1625>
17. Nakamura M, Watanabe T, Yonekawa Y, Kleihues P, Ohgaki H. Promoter methylation of the DNA repair gene *MGMT* in astrocytomas is frequently associated with G:C → A:T mutations of the TP53 tumor suppressor gene. *Carcinogenesis.* 2001 Oct;22(10):1715–19. <http://dx.doi.org/10.1093/carcin/22.10.1715>
18. Waha A, Guntner S, Huang TH, Yan PS, Arslan B, Pietsch T, et al. Epigenetic silencing of the protocadherin family member *PCDH-gamma-A11* in astrocytomas. *Neoplasia.* 2005 Mar;7(3):193–9. <http://dx.doi.org/10.1593/neo.04490>
19. Stone AR, Bobo W, Brat DJ, Devi NS, Van Meir EG, Vertino PM. Aberrant methylation and down-regulation of *TMS1/ASC* in human glioblastoma. *Am J Pathol.* 2004 Oct;165(4):1151–61. [http://dx.doi.org/10.1016/S0002-9440\(10\)63376-7](http://dx.doi.org/10.1016/S0002-9440(10)63376-7)
20. Zhang Z, Tang H, Wang Z, Zhang B, Liu W, Lu H, et al. *Mir-185* targets the DNA methyltransferases 1 and regulates global DNA methylation in human glioma. *Mol Cancer.* 2011 Sep 30;10:124. <http://dx.doi.org/10.1186/1476-4598-10-124>
21. Riemenschneider MJ, Reifenberger J, Reifenberger G. Frequent biallelic inactivation and transcriptional silencing of the *DIRAS3* gene at 1p31 in oligodendroglial tumors with 1p loss. *Int J Cancer.* 2008 Jun 1;122(11):2503–10. <http://dx.doi.org/10.1002/ijc.23409>
22. Yates DR, Rehman I, Abbod MF, Meuth M, Cross SS, Linkens DA, et al. Promoter hypermethylation identifies progression risk in bladder cancer. *Clin Cancer Res.* 2007 Apr 1;13(7):2046–53. <http://dx.doi.org/10.1158/1078-0432.CCR-06-2476>
23. Wu X, Rauch TA, Zhong X, Bennett WP, Latif F, Krex D, et al. CpG island hypermethylation in human astrocytomas. *Cancer Res.* 2010 Apr 1;70(7):2718–27. <http://dx.doi.org/10.1158/0008-5472.CAN-09-3631>
24. Huang KH, Huang SF, Chen IH, Liao CT, Wang HM, Hsieh LL. Methylation of *RASSF1A*, *RASSF2A*, and *HIN-1* is associated with poor outcome after radiotherapy, but not surgery, in oral squamous cell carcinoma. *Clin Cancer Res.* 2009 Jun 15;15(12):4174–80. <http://dx.doi.org/10.1158/1078-0432.CCR-08-2929>
25. Huang J, Lin Y, Li LH, Qing D, Teng XM, Zhang YL, et al. *ARHI*, As a novel suppressor of cell growth and downregulated in human hepatocellular carcinoma, could contribute to hepatocarcinogenesis. *Mol Carcinog.* 2009 Feb;48(2):130–40. <http://dx.doi.org/10.1002/mc.20461>
26. Yu Z, Sun Y, She X, Wang Z, Chen S, Deng Z, et al. *SIX3*, a tumor suppressor, inhibits astrocytoma tumorigenesis by transcriptional repression of *AURKA/B*. *J Hematol Oncol.* 2017 Jun 8;10(1):115. <http://dx.doi.org/10.1186/s13045-017-0483-2>
27. Liu X, Tang H, Wang Z, Huang C, Zhang Z, She X, et al. *F10* gene hypomethylation, a putative biomarker for glioma prognosis. *J Neurooncol.* 2012 May;107(3):479–85. <http://dx.doi.org/10.1007/s11060-011-0775-2>
28. Liu X, Tang H, Zhang Z, Li W, Wang Z, Zheng Y, et al. *POTEH* hypomethylation, a new epigenetic biomarker for glioma prognosis. *Brain Res.* 2011 May 19;1391:125–31. <http://dx.doi.org/10.1016/j.brainres.2011.03.042>
29. Liu X, Yu Z, Li W, Wang Z, Xu G, Li ZH, et al. *CPEB1*, a histone-modified hypomethylated gene, is regulated by miR-101 and involved in cell senescence in glioma. *Cell Death Dis.* 2013 Jun 20;4:e675. <http://dx.doi.org/10.1038/cddis.2013.197>
30. Liu X, Lei Q, Yu Z, Xu G, Tang H, Wang W, et al. *LMO3* MiR-101 reverses the hypomethylation of the *LMO3* promoter in glioma cells. *Oncotarget.* 2015 Apr 10;6(10):7930–43. <http://dx.doi.org/10.18632/oncotarget.3181>
31. Lei Q, Liu X, Fu H, Sun Y, Wang L, Xu G, et al. miR-101 reverses hypomethylation of the *PRDM16* promoter to disrupt mitochondrial function in astrocytoma cells. *Oncotarget.* 2016 Jan 26;7(4):5007–22.

32. Bhaumik SR, Smith E, Shilatifard A. Covalent modifications of histones during development and disease pathogenesis. *Nat Struct Mol Biol.* 2007 Nov;14(11):1008–16. <http://dx.doi.org/10.1038/nsmb1337>
33. Kouzarides T. Chromatin modifications and their function. *Cell.* 2007 Feb 23;128(4):693–705. <http://dx.doi.org/10.1016/j.cell.2007.02.005>
34. Bartel DP. MicroRNAs: Genomics, biogenesis, mechanism, and function. *Cell.* 2004 Jan 23;116(2):281–97. [http://dx.doi.org/10.1016/S0092-8674\(04\)00045-5](http://dx.doi.org/10.1016/S0092-8674(04)00045-5)
35. He L, Hannon GJ. MicroRNAs: Small RNAs with a big role in gene regulation. *Nat Rev Genet.* 2004 Jul;5(7):522–31. <http://dx.doi.org/10.1038/nrg1379>
36. Saito Y, Liang G, Egger G, Friedman JM, Chuang JC, Coetzee GA, et al. Specific activation of microRNA-127 with downregulation of the proto-oncogene bcl6 by chromatin-modifying drugs in human cancer cells. *Cancer Cell.* 2006 Jun;9(6):435–43. <http://dx.doi.org/10.1016/j.ccr.2006.04.020>
37. Fabbri M, Garzon R, Cimmino A, Liu Z, Zanesi N, Callegari E, et al. MicroRNA-29 family reverts aberrant methylation in lung cancer by targeting DNA methyltransferases 3a and 3b. *Proc Natl Acad Sci U S A.* 2007 Oct 2;104(40):15805–10. <http://dx.doi.org/10.1073/pnas.0707628104>
38. Benetti R, Gonzalo S, Jaco I, Muñoz P, Gonzalez S, Schoeftner S, et al. A mammalian microRNA cluster controls DNA methylation and telomere recombination via rbl2-dependent regulation of DNA methyltransferases. *Nat Struct Mol Biol.* 2008 Sep;15(9):998. <http://dx.doi.org/10.1038/nsmb0908-998b>
39. Wu L, Zhou H, Zhang Q, Zhang J, Ni F, Liu C, et al. DNA methylation mediated by a microRNA pathway. *Mol Cell.* 2010 May 14;38(3):465–75. <http://dx.doi.org/10.1016/j.molcel.2010.03.008>
40. Tang H, Liu X, Wang Z, She X, Zeng X, Deng M, et al. Interaction of hsa-miR-381 and glioma suppressor LRRC4 is involved in glioma growth. *Brain Res.* 2011 May 16;1390:21–32. <http://dx.doi.org/10.1016/j.brainres.2011.03.034>
41. Goodrich JA, Kugel JF. Non-coding-RNA regulators of RNA polymerase II transcription. *Nat Rev Mol Cell Biol.* 2006 Aug;7(8):612–16. <http://dx.doi.org/10.1038/nrm1946>
42. Kanduri C. Kcnq1ot1: A chromatin regulatory RNA. *Semin Cell Dev Biol.* 2011 Jun;22(4):343–50. <http://dx.doi.org/10.1016/j.semcdb.2011.02.020>
43. Wang K, Sun T, Li N, Wang Y, Wang JX, Zhou LY, et al. MDRL lncRNA regulates the processing of miR-484 primary transcript by targeting miR-361. *PLoS Genet.* 2014 Jul 24;10(7):e1004467. <http://dx.doi.org/10.1371/journal.pgen.1004467>
44. Cesana M, Cacchiarelli D, Legnini I, Santini T, Sthandier O, Chinappi M, et al. A long noncoding RNA controls muscle differentiation by functioning as a competing endogenous RNA. *Cell.* 2011 Oct 14;147(2):358–69. <http://dx.doi.org/10.1016/j.cell.2011.09.028>
45. Fan M, Li X, Jiang W, Huang Y, Li J, Wang Z. A long non-coding RNA, PTCSC3, as a tumor suppressor and a target of miRNAs in thyroid cancer cells. *Exp Ther Med.* 2013 Apr;5(4):1143–6.
46. Yan B, Yao J, Liu JY, Li XM, Wang XQ, Li YJ, et al. LncRNA-MIAT regulates microvascular dysfunction by functioning as a competing endogenous RNA. *Circ Res.* 2015 Mar 27;116(7):1143–56. <http://dx.doi.org/10.1161/CIRCRESAHA.116.305510>
47. Ebert MS, Sharp PA. Emerging roles for natural microRNA sponges. *Curr Biol.* 2010 Oct 12;20(19):R858–61. <http://dx.doi.org/10.1016/j.cub.2010.08.052>
48. Sumazin P, Yang X, Chiu HS, Chung WJ, Iyer A, Llobet-Navas D, et al. An extensive microRNA-mediated network of RNA-RNA interactions regulates established oncogenic pathways in glioblastoma. *Cell.* 2011 Oct 14;147(2):370–81. <http://dx.doi.org/10.1016/j.cell.2011.09.041>
49. Salmena L, Poliseno L, Tay Y, Kats L, Pandolfi PP. A ceRNA hypothesis: The Rosetta Stone of a hidden RNA language? *Cell.* 2011 Aug 5;146(3):353–8. <http://dx.doi.org/10.1016/j.cell.2011.07.014>
50. Yan L, Zhou J, Gao Y, Ghazal S, Lu L, Bellone S, et al. Regulation of tumor cell migration and invasion by the H19/let-7 axis is antagonized by metformin-induced DNA methylation. *Oncogene.* 2015 Jun 4;34(23):3076–84. <http://dx.doi.org/10.1038/onc.2014.236>
51. Liu C, Sun Y, She X, Tu C, Cheng X, Wang L, et al. CASC2c as an unfavorable prognosis factor interacts with miR-101 to mediate astrocytoma tumorigenesis. *Cell Death Dis.* 2017 Mar 2;8(3):e2639. <http://dx.doi.org/10.1038/cddis.2017.11>

4

Cancer Stem-Like Cells in Glioblastoma

MATHILDE CHERAY¹ • GAËLLE BÉGAUD^{2,3} • ELISE DELUCHE⁴ •
ALEXANDRE NIVET⁵ • SERGE BATTU^{2,3} • FABRICE LALLOUÉ² •
MIREILLE VERDIER*² • BARBARA BESSETTE*²

¹Department of Oncology-Pathology, Cancer Centrum Karolinska, Stockholm, Sweden; ²EA3842 HCP, Faculty of Medicine, Limoges, France; ³Laboratory of Analytical Chemistry, Faculty of Pharmacy, Limoges, France; ⁴Oncology Department, University Hospital, Limoges, France; ⁵Radiotherapy Department, University Hospital, Limoges, France

Author for correspondence: Barbara Bessette, EA3842 HCP, Faculty of Medicine, Limoges, France. E-mail: barbara.bessette@unilim.fr

Doi: <http://dx.doi.org/10.15586/codon.glioblastoma.2017.ch4>

Abstract: Glioblastoma is currently described as the worst brain tumor because of its aggressiveness and poor prognosis. Chemotherapy and irradiation are not curative, and the average survival for patients with glioblastoma is around 15 months. The cellular heterogeneity and infiltrative capability of glioblastoma make complete surgical resection almost impossible. Moreover, the presence of cancer stem-like cells in this tumor leads to therapeutic resistance and tumor recurrence after surgery. Numerous studies have explored the physiology of these cancer stem cells, and attempts have been made to develop devices aimed at isolating this rare population of cells. This chapter describes the complexity of cancer stem cells in glioblastoma. Their role in autophagy, gene regulation by epigenetic modifications, and the challenges in isolating these cells are addressed. This knowledge may pave the way for a better understanding of cancer stem cells in glioblastoma, and the potential development of new therapeutic strategies for this deadly disease.

Key words: Autophagy; Cancer stem cells; Epigenetic; Glioblastoma; SdFFF

* These authors contributed equally to the writing of this chapter.

In: *Glioblastoma*. Steven De Vleeschouwer (Editor), Codon Publications, Brisbane, Australia
ISBN: 978-0-9944381-2-6; Doi: <http://dx.doi.org/10.15586/codon.glioblastoma.2017>

Copyright: The Authors.

Licence: This open access article is licenced under Creative Commons Attribution 4.0 International (CC BY 4.0). <https://creativecommons.org/licenses/by-nc/4.0/>

Introduction

Glioblastoma (GBM) is the most frequent and the most aggressive glial tumor of the central nervous system. Each year, about 240,000 cases of brain tumor are diagnosed worldwide, of which the majority are GBMs. Conventional therapeutic strategy is mainly surgery, in combination with temozolomide chemotherapy and radiation (corresponding to the Stupp protocol) (1). Novel drugs that are being developed include monoclonal antibodies against vascular endothelial growth factor (VEGF), inhibitors of tyrosine kinase receptors (2, 3), and Programmed death-ligand 1 (PD-L1) (4, 5). Despite recent advances, only a few patients with GBM are still alive 5 years after the initial diagnosis (3–10%, depending on the applied protocol). The estimated survival time without progression of the disease hardly exceeds 18 months. Various reasons could explain such a poor outcome: late diagnosis, difficulty to clearly identify the tumor due to its histopathological heterogeneity, relapse of the tumor due to GBM cancer stem-like cells (CSCs), difficulties in identification and isolation of these cells, and paucity of knowledge about the physiology of CSCs. This chapter gives an overview of the complexity of GBM and the ongoing cell sorting methods.

Evolution of Classifications and Diagnosis

Reliable identification of tumors is a prerequisite for the development of efficient therapies. Because of the heterogeneity of the cells found in GBM, interobserver variability is not infrequent (6, 7), and this makes proper identification a difficult task. A tumor that has been initially identified as a GBM could turn out to be of a different type on subsequent analysis (7). These discrepancies justify the need for tools that will allow the unambiguous identification of GBM. GBM is the only solid tumor defined as higher grade tumor (grade IV) in the absence of any metastatic component. All other solid tumors can be classified (e.g., tumor-nodes-metastasis [TNM] classification of colon tumor), depending on their tissue infiltration, degree of cell differentiation, mitotic index, and metastatic invasion (8). Because of the complexity and the heterogeneity of GBM, the 2007 World Health Organization (WHO) classification of brain tumors was based only on the histological profile of the cells, combined with their mitotic index and molecular criteria (9). Different kinds of GBM were listed in this classification: pure astrocytoma, oligoastrocytoma, and neuro-astrocytoma. The 2016 WHO classification developed a new approach (10) that primarily relies on the genetic profile of the tumor. The most notable changes are in the isocitrate dehydrogenase (IDH) status (mutated vs. wild type) and the detection of 1p19q co-deletion. Importantly, if the histological phenotype and the genotype are nonconcordant, then the genotype will take over and will be used to determine the diagnosis and subsequent therapeutic decision-making. This guideline, associated with the mitotic index and the histological nature of the cells, helps to orientate the therapeutic scheme. In this way, the current WHO classification not only allows to determine the nature of the tumor but also enables to make a choice for therapeutic management.

Cancer Stem Cells in Glioblastoma

CANCER STEM CELL IDENTIFICATION

CSCs were initially reported by Singh et al., who described a subpopulation of cells positive for CD133 that were able to initiate tumors *in vivo* (11). Hence, they were termed “tumor initiating cells” (11). Solid tumors such as GBMs are characterized by a high degree of heterogeneity, which has been explained by two different theories. According to the first theory, the stochastic model, tumor cells share the same genetic mutations (homogeneous), and heterogeneity is the result of intrinsic as well as extrinsic factors. According to the second theory, the hierarchy model, cells are intrinsically different in terms of differentiation stage and only a small subset, the CSCs, can initiate tumor growth and progression (12). This subpopulation is increasingly referred to as the cause of tumor onset and recurrence as well as therapeutic resistance. The difficulty encountered in studying CSCs is largely the result of challenges in precisely identifying them (13). Although CD133 is classically associated with this cell subset, it is also expressed in normal neural stem cells; thus, the relevance of this biomarker is still a matter of debate when it comes to GBM stem cells. Indeed, it has been shown that CD133^{neg} cells are also capable of inducing tumors when implanted in rat brains (14). Consequently, it is now recognized that additional markers are needed to identify this subpopulation. Among these markers, CD44 and ABC transporters are probably the most reliable. Recently, our team contributed to identify a new GBM stem-like cell marker, the *KLRC3* gene coding for NKG2E, a protein expressed in natural killer cells (15). We showed that the silencing of *KLRC3* decreased self-renewal, invasion, and proliferation capacities, along with radioresistance and tumorigenicity of the U87-MG GBM cell line. Transcription factors such as sox2, oct4, Bmi1, and nanog are also known to contribute to the stemness properties of CSCs (16). Researchers currently working on this peculiar cell subpopulation consider that seeking more than a single marker is mandatory to identify and/or enrich this population. These potential molecular markers, combined with functional properties, such as self-renewal and cancer-initiation capacities, will enable the identification and enrichment of this subpopulation of cells.

AUTOPHAGY

Similar to many solid tumors, GBM development leads to the formation of hypoxic areas. Uncontrolled proliferation of tumors, especially in the high cellular density pseudo-palisading region, leads to a decrease in O₂ tension. In response to this stress, cancer cells stabilize the hypoxia-inducible factor 1 (HIF-1), which in turn induces overexpression of VEGF (17). The binding of this growth factor to its receptor on endothelial cells promotes neoangiogenesis. This vascularization is characterized by abnormal, dysfunctional, and/or occluded vessels, which are unable to sustain normoxia, hence the formation of hypoxic regions. Although a hypoxic microenvironment could induce cell death in normal conditions, it is also well known to maintain CSCs, especially in GBM (18). While actively proliferating cells are more likely to be found close to the vessels, stem-like cells lie in the central parts of the tumor, the core region, which

contributes to a CSC niche. The core region is more likely to be radioresistant and chemoresistant, and usually necrotic. These different distributions of cells illustrate the GBM heterogeneity. CSC population density and aggressiveness are inversely related to oxygen tension (19).

In the context of vasculature and oxygen supply deficiency, several studies, including ours, demonstrated that autophagy is induced as a cytoprotective mechanism (20, 21). This catabolic process, which is complementary to the ubiquitin–proteasome system, leads altered organelles and proteins to lysosomes where they are degraded. Besides basal physiological level, autophagy is upregulated when cells are subjected to various stresses such as nutrient starvation, oxygen deprivation, or therapy (22). In GBM, hypoxia-induced autophagy promotes cell survival and aggressiveness. This could be explained in part by the pro-survival effects of autophagy in response to antiangiogenic therapy, leading to hypoxia (23). Furthermore, it has been shown that antiangiogenic agents targeting VEGF or its receptor induce expansion of CSCs in tumors implanted in animals, supporting the link between hypoxia-induced autophagy and stemness (24). Another major function of autophagy is to supply metabolic precursors, such as amino acids and/or fatty acids, via the catabolic process, which contributes to energy supply and cellular homeostasis. When microenvironment is unfriendly, autophagy is likely to be enhanced in CSCs to allow cell viability and quiescence (25). Such a response has also been demonstrated during temozolomide chemotherapy or radiotherapy (26, 27). Both treatments are known to favor conservation of the CSC subset, which is responsible for therapy escape and tumor recurrence. Consequently, the use of autophagy inhibitors, such as chloroquine or its analog hydroxychloroquine, combined with classical therapy (i.e., temozolomide), appears to enhance the cytotoxicity against CSCs (28). Prospective studies are needed to better delineate the exact application and efficiency of this combination treatment, where autophagy inhibition could represent an adjuvant cancer therapy.

EPIGENETIC REGULATION

Cells constantly change their state of equilibrium in response to internal and external stimuli. These changes in cell identity are driven by highly coordinated modulation of gene expression, which is achieved largely by changes in the structure and composition of the chromatin, driven by epigenetic modulators. Epigenetic modifications such as histone modification and DNA methylation are crucial for normal development but can also be involved in cancer initiation and progression. Recent discoveries in cellular and genomic reprogramming have highlighted the importance of chromatin modifications in the regulation of CSC in GBM.

HISTONE MODIFICATIONS

Histones can be subjected to posttranslational modifications which alter their interaction with DNA and nuclear proteins. Modifications of the histone tails include methylation, acetylation, and phosphorylation, among others. Chromatin opening through the methylation of H3K4 (Lysine 4 of Histone 3) allows transcription to be performed, whereas chromatin closing through H3K9 and

H3K27 methylations (Lysine 9 and Lysine 27 of Histone 3) constitutes the two main repressive mechanisms in mammalian cells. In a study of 230 gliomas, the global expression of several histone modification markers was assessed using immunocytochemistry. Based on WHO grade, histology, and histone modifications, H3K9ac (acetylation of Lysine 9 of Histone 3), H3K4me2 (dimethylation of Lysine 4 of Histone 3), H3K18ac (acetylation of Lysine 18 of Histone 3), and H4K20me3 (trimethylation of Lysine 20 of Histone 4), 10 distinct prognostic groups were generated, suggesting that aberrant histone modifications can have a role in GBM (29).

In the case of CSCs, it has been demonstrated that CD133 expression is regulated by H3K9me2. CD133-positive cells, which are usually considered as CSCs, were found to be H3K9me2 negative, whereas most cancer cells were found to be H3K9me2 positive. In their study, Tao et al. demonstrated that the G9a-dependent H3K9me2 repression of CD133 was one of the crucial switches for the self-renewal of CSCs, similar to the embryonic stem cells (30). Transcriptional repression by histone methylation is facilitated by polycomb genes like EZH2 and Bmi1 and had been linked to differentiation and self-renewal abilities of CSCs. EZH2 silencing of the BMP pathway in CSCs inhibits their ability to differentiate. Moreover, inhibition of EZH2 or forced expression of methylated-promoter-repressed BMP pathway restores normal differentiation capacity of CSCs. This reduces proliferation and induces terminal differentiation of CSCs, causing loss of self-renewal and a decrease in tumorigenicity of CSCs (31, 32). Bmi1, a key component of the polycomb repressive complex 1 (PRC1), is upregulated in GBM and significantly enriched in the CSC population, but it is not expressed in normal astrocytes. Moreover, its suppression in human CSCs inhibits their growth *in vitro* and *in vivo* (33). Finally, the expression inhibition of Bmi1 by knockdown in a glioma mouse model suppresses the formation of malignant tumors (34).

DNA METHYLATION

DNA methylation, catalyzed by DNA methyltransferases (DNMTs), is a major epigenetic modification that modulates gene expression. DNA methylation patterns are heritable and reversible, conserved during cell division, and involved in cell reprogramming processes. DNA methylation directly represses gene expression via the inhibition of transcription factor recruitment (35). Transcription inhibition could also be indirect through the recruitment of methyl-CpG-binding proteins and their associated repressive chromatin remodeling activities (36). DNA methylation deregulation is found in cancer where hypermethylation of specific tumor suppressor genes (TSGs) leads to the inhibition of their expression. It is known that aberrant DNA methylation is linked to the initiation and the progression of cancer. Global DNA hypomethylation promotes chromosomal instability, reactivation of transposable elements, and loss of imprinting. Local hypomethylation induces oncogene activation, while hypermethylation induces the silencing of TSGs (37). Aberrant DNA methylation patterns have been detected in GBM. A well-studied example is the silencing of the DNA repair enzyme MGMT (O⁶-methylguanine-DNA methyltransferase) following hypermethylation of the MGMT CpG island. Methylation of the MGMT promoter results in defects in DNA repair and is associated with a better response to

treatment with alkylating agents (38). MGMT methylation status is now used in the clinical management of GBM patients as a biomarker for predicting drug responsiveness.

Epigenetic changes like DNA methylation can be involved in the adaptation of CSCs to the environment in such a way that they reinforce the malignant state of the tumor. For example, it has been shown that the resetting of DNA methylation by induction of pluripotent stem cell reprogramming, followed by lineage differentiation, suppresses the malignant properties of GBM (39). Moreover, in CSCs, the cell-surface marker CD133, defined as a CSC-specific marker, is found methylated. In their study, Gopisetty et al. showed that Sp1 and Myc regulate CD133 transcription in CSCs and that promoter methylation and methyl-DNA-binding proteins cause repression of CD133 by excluding transcription-factor binding (40). Expression of the transcriptional coactivator with PDZ-binding motif (TAZ) has been linked to GBM subtype. It has been shown that its silencing in mesenchymal CSCs suppresses the mesenchymal gene expression signature, while expressing TAZ in proneural CSCs, leading to increased expression of mesenchymal signature genes (41).

More recently, taking advantage of the genome-wide analysis technology, it has been shown that specific DNA methylation patterns were associated with CSCs. Concurrent promoter hypermethylation and gene body hypomethylation were observed in a subset of genes, including MGMT, AJAP1, and PTPRN2. These unique DNA methylation signatures were also found in primary GBM-derived xenograft tumors, indicating that they are not tissue culture–related epigenetic changes. Integration of GSC-specific epigenetic signatures with gene expression analysis further identified candidate TSGs that are frequently downregulated in GBMs, such as SPINT2, NEFM, and PENK (42).

Isolation of Cancer Stem Cells in Glioblastoma

Because of their key roles in tumorigenesis, metastasis, and therapeutic relapses, CSCs appear as major biological and therapeutic targets, in particular for GBM (43–46). This cellular status fully justifies the discovery, development, and validation of methods allowing purification and characterization of CSCs (43–46). However, the heterogeneity of the tumor cell population, the rarity of CSCs within the tumor mass (1–5%, depending on the type of cancer (43)), the difficulty in accurately defining their properties, and the criteria on which the sorting and characterization methods are based (44, 45, 47, 48) continue to pose major challenges.

FUNCTIONAL TESTS

CSCs are known to display different properties which give them the ability to relapse, and be more resistant to chemotherapy (49, 50) or radiation therapy (51). These properties are currently being investigated in order to better characterize CSCs. The self-renewal of CSCs (which is one of the properties defining CSCs) can be determined with two different tests: the colony forming

unit approach and the limiting dilution assay. Both tests are based on the ability of a single CSC to proliferate and create a new neurosphere *in vitro* (49). CSCs share common properties with normal stem cells such as their ability to differentiate into specific cell lineage. For GBM, the CSCs should be able to differentiate into neurons, astrocytes, and oligodendrocytes. Moreover, the most important feature of CSCs is their ability to resist treatment (50, 51). In GBM, this property leads to tumor relapse and unfortunately to patient death. The most conventional approach includes the evaluation of the apoptotic impact of temozolomide and/or radiation on CSCs. A strong resistance to these treatments is a characteristic of CSC (52). Finally, the capability of CSC to form a tumor has to be addressed by xenograft or orthotopic cell engraftment (51).

CLASSICAL CELL SORTING METHODS

The classical cell sorting methods are based on the recognition of specific extracellular or intracellular antigens using fluorescent (FACS) or magnetic (MACS) probes. Other methods such as affinity chromatography, panning, and aptamers also use the immunological recognition principle (44, 47, 48). In GBM, some of the most useful markers are SOX2, OCT4, NANOG, CD133, and ABCG2 (44, 45, 53). However, no single marker can be considered a gold standard, and, therefore, a series of markers is mandatory to validate the stemness status. Aldehyde dehydrogenase (ALDH) activity can be used in addition to the above staining. High ALDH expression has been reported in precursor cells of GBM. Another way to separate CSCs from GBM is the detection of the side population using Hoechst staining. However, this labeling could lead to functional modifications of the cell such as induction of cell differentiation and therefore difficulties for *in vitro* studies (culture, graft, etc.) (44, 47).

SEDIMENTATION FIELD-FLOW FRACTIONATION CELL SORTING

Field-flow fractionation (FFF) techniques were developed by J.C. Giddings in the late 1960s (54). FFF methods are considered as gentle methods as cells are sorted by applying low-intensity forces: (i) one corresponding to an external multigravitational field due to the channel rotation and (ii) the other corresponding to hydrodynamic lift-forces due to the flowing of the cells in the mobile phase (Figure 1). The balance of these two forces leads to the focusing of identical subpopulations (with respect to size, density, shape, and rigidity) into thin layers, which are eluted from the flow stream passing through their gravitational center (hyperlayer elution mode) (55). Sedimentation field-flow fractionation (SdFFF) is a gentle (low flow rate and low external field to limit shear forces exerted on cells) and noninvasive method, which takes into account, without any labeling, a complex matrix of cell properties such as the size, the cell-cycle position (related to the density), or the rigidity of the cytoskeleton, which are the major properties of stem cells. Usually, the largest and less dense cells (the most differentiated) are eluted first, while the smallest and the most dense cells (low nucleo-cytoplasmic ratio corresponding to stem cells) are eluted last. This elution order also depends on the ploidy or the

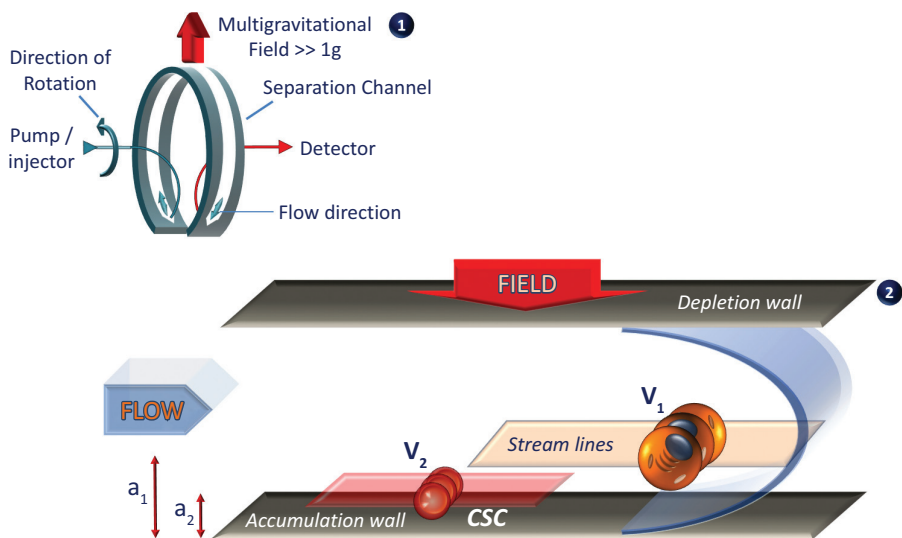


Figure 1 (1) Schematic representation of an SdFFF separation channel and its implementation in the chromatographic chain. (2) Schematic representation of hyperlayer elution mode and cell elution order depending on the size. a : distance from the center of gravity of the cell to the accumulation wall. V : velocity of cells.

position in the cell cycle; the cells eluted in the last fraction are usually in the G0/G1 phase (56, 57).

Our first work on CSC isolation began with human neuroblastoma cell lines (SKNSH-SY5Y, IMR-32) and was then followed by the U87-MG human GBM cell line analysis (58–60). We demonstrated that cells eluted in the ultimate part of the fractogram (Figure 2) overexpressed vimentin and CD133, presented the ability to form neurospheres in defined culture medium, and were resistant to Fas-induced apoptosis. To increase the purity and the diversity of subpopulations with different degrees of differentiation, we developed an analytical SdFFF protocol using different external fields. The following four cell culture conditions were tested: normal (+ FBS), defined (– FBS), normoxia, and hypoxia ($O_2 < 0.1\%$). Defined culture medium and hypoxia mimicked the conditions found in the tumor niche and yielded an enriched CSC population. The use of two different fields in SdFFF allowed the separation of differentiated cells at 25 g, while a lower field of 15 g favored the isolation of CSCs. Eight different subpopulations were identified based on the expression of CD133, NCAM, nestin, Oct4, A2B5, cell-cycle position, ALDH activity, and clonogenicity (Figure 2). As described in Figure 2, differentiated cells are eluted in the fraction F1 of cells cultured in normal culture medium under normoxia, at 25 g. The most undifferentiated cells were obtained by collecting fraction F3 at 15 g from cells cultured in defined medium under hypoxic conditions. These populations should be further used to identify CSC properties or to test their sensitivity to therapy.

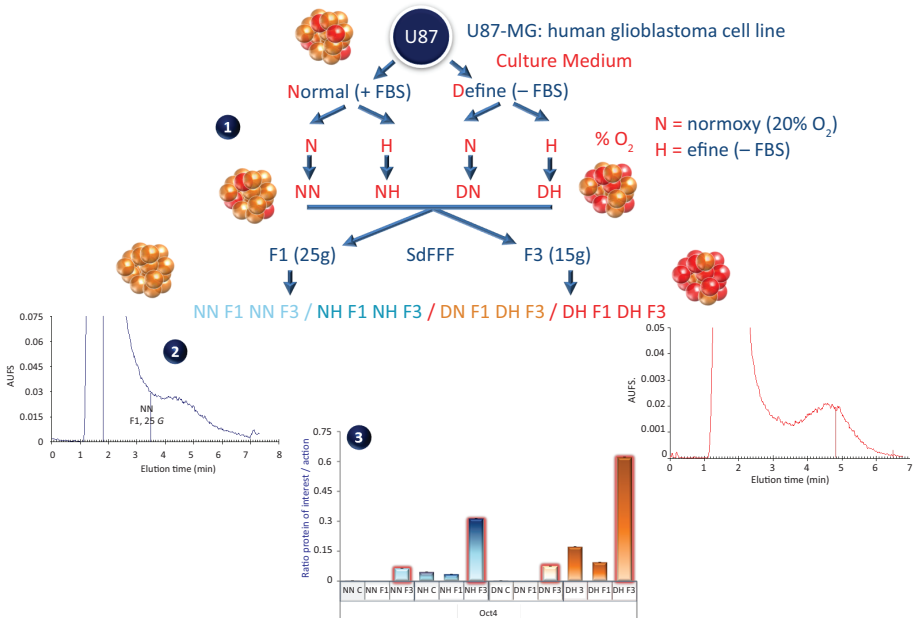


Figure 2 Representation of the global method used to enrich CSCs from human glioblastoma cell line. Four conditions are established with different media and oxygen tensions, namely, NN, NH, DN, and DH, in order to obtain a matrix of CSCs enrichment (1). CSC level is increased by the use of SdFFF cell sorting method (2: representative fractograms). Oct4 stem cell marker expression (3) in subpopulations obtained after SdFFF sorting (F1/F3), compared to crude (C) populations. Concerning fractograms (2), the optimal elution conditions were: injection of 2×10^5 U87-MG cells; flow rate: 0.80 mL/min; mobile phase: sterile PBS, pH = 7.4; and external multi-gravitational field strength: 15 or 25.00 ± 0.02 g (312 or 412 ± 0.2 rpm). These optimal elution conditions allowed cell separation under the biocompatible hyperlayer elution mode. Time-dependent fractions F1 and F3 corresponded to differentiated and cancer stem cells, respectively.

Conclusion

Despite current advances in the study of GBM and the physiology of GBM CSCs, it remains impossible to cure GBM. To develop a better therapy, one of the steps would be the development of new methods such as SdFFF that allow the isolation of CSCs without causing any cellular modification. The ability of tumor cells to adapt to their environment is of great interest and mechanisms by which tumor cells communicate with their microenvironment are increasingly being investigated. Studies concerning exosomes (vesicles excreted from cells) and their role in cancer progression underline new point of views on tumors including GBM (61, 62). Numerous studies are also being performed on the epigenetic profile of tumor cells, which could be involved in cell reprogramming and adaptation to their environment. Together, these approaches could enable a better understanding of the role of CSCs in GBM initiation and progression, and help develop novel therapeutics in the days to come.

Acknowledgment: This work was supported by grants from Conseil Régional du Limousin, Ligue Nationale Contre le Cancer (comités de la Creuse, Corrèze et de la Haute Vienne), and CORC (Comité d'Organisation de la Recherche sur le Cancer du Limousin). The authors thank Dr. Michel Guilloton for his help in editing the manuscript.

Conflict of interest: The authors declare no potential conflicts of interest with respect to research, authorship, and/or publication of this manuscript.

Copyright and permission statement: To the best of our knowledge, the materials included in this chapter do not violate copyright laws. All original sources have been appropriately acknowledged and/or referenced. Where relevant, appropriate permissions have been obtained from the original copyright holder(s).

References

1. Stupp R, Mason WP, van den Bent MJ, Weller M, Fisher B, Taphoorn MJ, et al. Radiotherapy plus concomitant and adjuvant temozolomide for glioblastoma. *N Engl J Med.* 2005 Mar 10;352(10):987–96. <http://dx.doi.org/10.1056/NEJMoa043330>
2. Erdem-Eraslan L, van den Bent MJ, Hoogstrate Y, Naz-Khan H, Stubbs A, van der Spek P, et al. Identification of patients with recurrent glioblastoma who may benefit from combined bevacizumab and CCNU therapy: A report from the BELOB trial. *Cancer Res.* 2016 Feb 01;76(3):525–34. <http://dx.doi.org/10.1158/0008-5472.CAN-15-0776>
3. Schafer N, Gielen GH, Kebir S, Wieland A, Till A, Mack F, et al. Phase I trial of dovitinib (TKI258) in recurrent glioblastoma. *J Cancer Res Clin Oncol.* 2016;142(7):1581–9. <http://dx.doi.org/10.1007/s00432-016-2161-0>
4. Tang X, Li Q, Zhu Y, Zheng D, Dai J, Ni W, et al. The advantages of PD1 activating chimeric receptor (PD1-ACR) engineered lymphocytes for PDL1(+) cancer therapy. *Am J Transl Res.* 2015;7(3):460–73.
5. Heiland DH, Haaker G, Delev D, Mercas B, Masalha W, Heynckes S, et al. Comprehensive analysis of PD-L1 expression in glioblastoma multiforme. *Oncotarget.* 2017 Jun 27;8(26):42214–25. <http://dx.doi.org/10.18632/oncotarget.15031>
6. Scott CB, Nelson JS, Farnan NC, Curran WJ, Jr., Murray KJ, Fischbach AJ, et al. Central pathology review in clinical trials for patients with malignant glioma. A report of Radiation Therapy Oncology Group 83-02. *Cancer.* 1995 Jul 15;76(2):307–13. [http://dx.doi.org/10.1002/1097-0142\(19950715\)76:2%3C307::AID-CNCR2820760222%3E3.0.CO;2-L](http://dx.doi.org/10.1002/1097-0142(19950715)76:2%3C307::AID-CNCR2820760222%3E3.0.CO;2-L)
7. Kim BY, Jiang W, Beiko J, Prabhu SS, DeMonte F, Gilbert MR, et al. Diagnostic discrepancies in malignant astrocytoma due to limited small pathological tumor sample can be overcome by IDH1 testing. *J Neuro Oncol.* 2014 Jun;118(2):405–12. <http://dx.doi.org/10.1007/s11060-014-1451-0>
8. Lo DS, Pollett A, Siu LL, Gallinger S, Burkes RL. Prognostic significance of mesenteric tumor nodules in patients with stage III colorectal cancer. *Cancer.* 2008 Jan 01;112(1):50–4. <http://dx.doi.org/10.1002/cncr.23136>
9. Louis DN, Ohgaki H, Wiestler OD, Cavenee WK, Burger PC, Jouvet A, et al. The 2007 WHO classification of tumours of the central nervous system. *Acta Neuropathol.* 2007 Aug;114(2):97–109. <http://dx.doi.org/10.1007/s00401-007-0243-4>
10. Louis DN, Perry A, Reifenberger G, von Deimling A, Figarella-Branger D, Cavenee WK, et al. The 2016 World Health Organization classification of tumors of the central nervous system: A summary. *Acta Neuropathol.* 2016 Jun;131(6):803–20. <http://dx.doi.org/10.1007/s00401-016-1545-1>
11. Singh SK, Hawkins C, Clarke ID, Squire JA, Bayani J, Hide T, et al. Identification of human brain tumour initiating cells. *Nature.* 2004 Nov 18;432(7015):396–401. <http://dx.doi.org/10.1038/nature03128>

12. Catalano V, Gaggianesi M, Spina V, Iovino F, Dieli F, Stassi G, et al. Colorectal cancer stem cells and cell death. *Cancers*. 2011 Apr 11;3(2):1929–46. <http://dx.doi.org/10.3390/cancers3021929>
13. Abbaszadegan MR, Bagheri V, Razavi MS, Momtazi AA, Sahebkar A, Gholamin M. Isolation, identification, and characterization of cancer stem cells: A review. *J Cell Physiol*. 2017 Aug;232(8):2008–18.
14. Wang J, Sakariassen PO, Tsinkalovsky O, Immervoll H, Boe SO, Svendsen A, et al. CD133 negative glioma cells form tumors in nude rats and give rise to CD133 positive cells. *Int J Cancer*. 2008 Feb 15;122(4):761–8. <http://dx.doi.org/10.1002/ijc.23130>
15. Cheray M, Bessette B, Lacroix A, Melin C, Jawhari S, Pinet S, et al. KLRC3, a Natural Killer receptor gene, is a key factor involved in glioblastoma tumourigenesis and aggressiveness. *J Cell Mol Med*. 2017 Feb;21(2):244–53. <http://dx.doi.org/10.1111/jcmm.12960>
16. Yi Y, Hsieh IY, Huang X, Li J, Zhao W. Glioblastoma stem-like cells: Characteristics, microenvironment, and therapy. *Front Pharmacol*. 2016;7:477. <http://dx.doi.org/10.3389/fphar.2016.00477>
17. Kaur B, Khwaja FW, Severson EA, Matheny SL, Brat DJ, Van Meir EG. Hypoxia and the hypoxia-inducible-factor pathway in glioma growth and angiogenesis. *Neuro Oncol*. 2005 Apr;7(2):134–53. <http://dx.doi.org/10.1215/S1152851704001115>
18. Heddleston JM, Li Z, McLendon RE, Hjelmeland AB, Rich JN. The hypoxic microenvironment maintains glioblastoma stem cells and promotes reprogramming towards a cancer stem cell phenotype. *Cell Cycle*. 2009 Oct 15;8(20):3274–84. <http://dx.doi.org/10.4161/cc.8.20.9701>
19. Persano L, Rampazzo E, Basso G, Viola G. Glioblastoma cancer stem cells: Role of the microenvironment and therapeutic targeting. *Biochem Pharmacol*. 2013 Mar 01;85(5):612–22. <http://dx.doi.org/10.1016/j.bcp.2012.10.001>
20. Hu YL, DeLay M, Jahangiri A, Molinaro AM, Rose SD, Carbonell WS, et al. Hypoxia-induced autophagy promotes tumor cell survival and adaptation to antiangiogenic treatment in glioblastoma. *Cancer Res*. 2012 Apr 01;72(7):1773–83. <http://dx.doi.org/10.1158/0008-5472.CAN-11-3831>
21. Jawhari S, Bessette B, Hombourger S, Durand K, Lacroix A, Labrousse F, et al. Autophagy and TrkC/NT-3 signaling joined forces boost the hypoxic glioblastoma cell survival. *Carcinogenesis*. 2017;38(6):592–603. <http://dx.doi.org/10.1093/carcin/bgx029>
22. Feng Y, Yao Z, Klionsky DJ. How to control self-digestion: Transcriptional, post-transcriptional, and post-translational regulation of autophagy. *Trends Cell Biol*. 2015 Jun;25(6):354–63. <http://dx.doi.org/10.1016/j.tcb.2015.02.002>
23. Jawhari S, Ratinaud MH, Verdier M. Glioblastoma, hypoxia and autophagy: A survival-prone “menage-a-trois.” *Cell Death Dis*. 2016 Oct 27;7(10):e2434. <http://dx.doi.org/10.1038/cddis.2016.318>
24. Piao Y, Liang J, Holmes L, Zurita AJ, Henry V, Heymach JV, et al. Glioblastoma resistance to anti-VEGF therapy is associated with myeloid cell infiltration, stem cell accumulation, and a mesenchymal phenotype. *Neuro Oncol*. 2012 Nov;14(11):1379–92. <http://dx.doi.org/10.1093/neuonc/nos158>
25. Guan JL, Simon AK, Prescott M, Menendez JA, Liu F, Wang F, et al. Autophagy in stem cells. *Autophagy*. 2013 Jun 01;9(6):830–49. <http://dx.doi.org/10.4161/auto.24132>
26. Ojha R, Bhattacharyya S, Singh SK. Autophagy in cancer stem cells: A potential link between chemoresistance, recurrence, and metastasis. *BioRes Open Access*. 2015;4(1):97–108. <http://dx.doi.org/10.1089/biores.2014.0035>
27. Koukourakis MI, Mitrakas AG, Giatromanolaki A. Therapeutic interactions of autophagy with radiation and temozolomide in glioblastoma: Evidence and issues to resolve. *Br J Cancer*. 2016 Mar 01;114(5):485–96. <http://dx.doi.org/10.1038/bjc.2016.19>
28. Rangwala R, Leone R, Chang YC, Fecher LA, Schuchter LM, Kramer A, et al. Phase I trial of hydroxychloroquine with dose-intense temozolomide in patients with advanced solid tumors and melanoma. *Autophagy*. 2014 Aug;10(8):1369–79. <http://dx.doi.org/10.4161/auto.29118>
29. Liu BL, Cheng JX, Zhang X, Wang R, Zhang W, Lin H, et al. Global histone modification patterns as prognostic markers to classify glioma patients. *Cancer Epidemiol Biomarkers Prev*. 2010 Nov;19(11):2888–96. <http://dx.doi.org/10.1158/1055-9965.EPI-10-0454>
30. Tao H, Li H, Su Y, Feng D, Wang X, Zhang C, et al. Histone methyltransferase G9a and H3K9 dimethylation inhibit the self-renewal of glioma cancer stem cells. *Mol Cell Biochem*. 2014 Sep;394(1–2):23–30. <http://dx.doi.org/10.1007/s11010-014-2077-4>

31. Lee J, Son MJ, Woolard K, Donin NM, Li A, Cheng CH, et al. Epigenetic-mediated dysfunction of the bone morphogenetic protein pathway inhibits differentiation of glioblastoma-initiating cells. *Cancer Cell*. 2008 Jan;13(1):69–80. <http://dx.doi.org/10.1016/j.ccr.2007.12.005>
32. Suva ML, Riggi N, Janiszewska M, Radovanovic I, Provero P, Stehle JC, et al. EZH2 is essential for glioblastoma cancer stem cell maintenance. *Cancer Res*. 2009 Dec 15;69(24):9211–18. <http://dx.doi.org/10.1158/0008-5472.CAN-09-1622>
33. Abdouh M, Facchino S, Chatoov W, Balasingam V, Ferreira J, Bernier G. BMI1 sustains human glioblastoma multiforme stem cell renewal. *J Neurosci*. 2009 Jul 15;29(28):8884–96. <http://dx.doi.org/10.1523/JNEUROSCI.0968-09.2009>
34. Bruggeman SW, Hulsman D, Tanger E, Buckle T, Blom M, Zevenhoven J, et al. Bmi1 controls tumor development in an Ink4a/Arf-independent manner in a mouse model for glioma. *Cancer Cell*. 2007 Oct;12(4):328–41. <http://dx.doi.org/10.1016/j.ccr.2007.08.032>
35. Prendergast GC, Ziff EB. Methylation-sensitive sequence-specific DNA binding by the c-Myc basic region. *Science*. 1991 Jan 11;251(4990):186–9. <http://dx.doi.org/10.1126/science.1987636>
36. Robertson KD. DNA methylation and chromatin—Unraveling the tangled web. *Oncogene*. 2002 Aug 12;21(35):5361–79. <http://dx.doi.org/10.1038/sj.onc.1205609>
37. Esteller M. Epigenetics in cancer. *N Engl J Med*. 2008 Mar 13;358(11):1148–59. <http://dx.doi.org/10.1056/NEJMra072067>
38. Paz MF, Yaya-Tur R, Rojas-Marcos I, Reynes G, Pollan M, Aguirre-Cruz L, et al. CpG island hypermethylation of the DNA repair enzyme methyltransferase predicts response to temozolomide in primary gliomas. *Clin Cancer Res*. 2004 Aug 01;10(15):4933–8.
39. Stricker SH, Feber A, Engstrom PG, Caren H, Kurian KM, Takashima Y, et al. Widespread resetting of DNA methylation in glioblastoma-initiating cells suppresses malignant cellular behavior in a lineage-dependent manner. *Genes Dev*. 2013 Mar 15;27(6):654–69. <http://dx.doi.org/10.1101/gad.212662.112>
40. Gopisetty G, Xu J, Sampath D, Colman H, Puduvali VK. Epigenetic regulation of CD133/PROM1 expression in glioma stem cells by Sp1/myc and promoter methylation. *Oncogene*. 2013 Jun 27;32(26):3119–29. <http://dx.doi.org/10.1038/onc.2012.331>
41. Bhat KP, Salazar KL, Balasubramanian V, Wani K, Heathcock L, Hollingsworth F, et al. The transcriptional coactivator TAZ regulates mesenchymal differentiation in malignant glioma. *Genes Dev*. 2011 Dec 15;25(24):2594–609. <http://dx.doi.org/10.1101/gad.176800.111>
42. Lee EJ, Rath P, Liu J, Ryu D, Pei L, Noonpalle SK, et al. Identification of Global DNA Methylation signatures in glioblastoma-derived cancer stem cells. *J Genet Genomics*. 2015 Jul 20;42(7):355–71.
43. Boman BM, Wicha MS. Cancer stem cells: A step toward the cure. *J Clin Oncol*. 2008 Jun 10;26(17):2795–9. <http://dx.doi.org/10.1200/JCO.2008.17.7436>
44. Islam F, Gopalan V, Smith RA, Lam AKY. Translational potential of cancer stem cells: A review of the detection of cancer stem cells and their roles in cancer recurrence and cancer treatment. *Exp Cell Res*. 2015 Jul 1;335(1):135–47. <http://dx.doi.org/10.1016/j.yexcr.2015.04.018>
45. Lathia JD, Mack SC, Mulkearns-Hubert EE, Valentim CLL, Rich JN. Cancer stem cells in glioblastoma. *Genes Dev*. 2015 Jun;29(12):1203–17. <http://dx.doi.org/10.1101/gad.261982.115>
46. Gilbert CA, Ross AH. Cancer stem cells: Cell culture, markers, and targets for new therapies. *J Cell Biochem*. 2009 Dec 1;108(5):1031–8. <http://dx.doi.org/10.1002/jcb.22350>
47. Diogo MM, da Silva CL, Cabral JMS. Separation technologies for stem cell bioprocessing. *Biotechnol Bioeng*. 2012 Nov;109(11):2699–709. <http://dx.doi.org/10.1002/bit.24706>
48. Tirino V, Desiderio V, Paino F, De Rosa A, Papaccio F, La Noce M, et al. Cancer stem cells in solid tumors: An overview and new approaches for their isolation and characterization. *Faseb J*. 2013 Jan;27(1):13–24. <http://dx.doi.org/10.1096/fj.12-218222>
49. Salmaggi A, Boiardi A, Gelati M, Russo A, Calatuzzolo C, Ciusani E, et al. Glioblastoma-derived tumorspheres identify a population of tumor stem-like cells with angiogenic potential and enhanced multidrug resistance phenotype. *Glia*. 2006 Dec;54(8):850–60. <http://dx.doi.org/10.1002/glia.20414>
50. Lu C, Shervington A. Chemoresistance in gliomas. *Mol Cell Biochem*. 2008 May;312(1–2):71–80. <http://dx.doi.org/10.1007/s11010-008-9722-8>

51. Bao S, Wu Q, McLendon RE, Hao Y, Shi Q, Hjelmeland AB, et al. Glioma stem cells promote radio-resistance by preferential activation of the DNA damage response. *Nature*. 2006 Dec 07;444(7120):756–60. <http://dx.doi.org/10.1038/nature05236>
52. Ishiguro T, Ohata H, Sato A, Yamawaki K, Enomoto T, Okamoto K. Tumor-derived spheroids: Relevance to cancer stem cells and clinical applications. *Cancer Sci*. 2017 Mar;108(3):283–9. <http://dx.doi.org/10.1111/cas.13155>
53. Podberezin M, Wen J, Chang C-C. Cancer stem cells A review of potential clinical applications. *Arch Pathol Lab Med*. 2013 Aug;137(8):1111–16. <http://dx.doi.org/10.5858/arpa.2012-0494-RA>
54. Giddings JC. Field-flow fractionation: Analysis of macromolecular, colloidal, and particulate materials. *Science*. 1993;260(5113):1456–65. <http://dx.doi.org/10.1126/science.8502990>
55. Bégaud-Grimaud G, Battu S, Leger DY, Cardot PJP. Mammalian cell sorting with sedimentation field flow fractionation. In: Williams SKR, Caldwell KD, editors. *Field-flow fractionation in biopolymer analysis*. Wien: Springer-Verlag; 2012; 223–253.
56. Guglielmi L, Battu S, Le Bert M, Faucher JL, Cardot PJP, Denizot Y. Mouse embryonic stem cell sorting for the generation of transgenic mice by sedimentation field-flow fractionation. *Anal Chem*. 2004;76:1580–5. <http://dx.doi.org/10.1021/ac030218e>
57. Mélin C, Perraud A, Akil H, Jauberteau MO, Cardot P, Mathonnet M, et al. Cancer stem cell sorting from colorectal cancer cell lines by sedimentation field flow fractionation. *Anal Chem*. 2012;84(3):1549–56. <http://dx.doi.org/10.1021/ac202797z>
58. Bégaud-Grimaud G, Battu S, Lazcoz P, Castresana JS, Jauberteau MO, Cardot PJP. Study of the phenotypic relationship in the IMR-32 human neuroblastoma cell line by sedimentation field flow fractionation. *Int J Oncol*. 2007;31:883–92. <http://dx.doi.org/10.3892/ijo.31.4.883>
59. Bertrand J, Bégaud-Grimaud G, Bessette B, Verdier M, Battu S, Jauberteau MO. Cancer stem cells from human glioma cell line are resistant to fas-induced apoptosis. *Int J Oncol*. 2009;34:717–27.
60. Lautrette C, Cardot PJP, Vermot-Desroche C, Wijdenes J, Jauberteau MO, Battu S. SdFFF purification of immature neural cells from a human tumor neuroblastoma cell line. *J Chromatogr B*. 2003;791:149–60. [http://dx.doi.org/10.1016/S1570-0232\(03\)00229-0](http://dx.doi.org/10.1016/S1570-0232(03)00229-0)
61. Pinet S, Bessette B, Vedrenne N, Lacroix A, Richard L, Jauberteau MO, et al. TrkB-containing exosomes promote the transfer of glioblastoma aggressiveness to YKL-40-inactivated glioblastoma cells. *Oncotarget*. 2016 Aug 02;7(31):50349–64.
62. Gourlay J, Morokoff AP, Luwor RB, Zhu HJ, Kaye AH, Styli SS. The emergent role of exosomes in glioma. *J Clin Neurosci*. 2017 Jan;35:13–23.

5

Molecular Mechanisms of Glioma Cell Motility

ANGELA ARMENTO* • JAKOB EHLERS* • SONJA SCHÖTTERL* •
ULRIKE NAUMANN

Department of Vascular Neurology, Hertie Institute for Clinical Brain Research and Center Neurology, University of Tübingen, Tübingen, Germany

Author for correspondence: Ulrike Naumann, Department of Vascular Neurology, Hertie Institute for Clinical Brain Research and Center Neurology, University of Tübingen, Otfried-Müller-Str. 27, DE-72076 Tübingen, Germany.
E-mail: ulrike.naumann@uni-tuebingen.de

Doi: <http://dx.doi.org/10.15586/codon.glioblastoma.2017.ch5>

Abstract: Gliomas are the most common intracranial tumors in humans. The most malignant among these tumors is glioblastoma (GBM), with an incidence of 3–5 out of 100,000 persons in Western countries. GBM arises either *de novo* (primary GBM) or develops from a lower grade glioma (secondary GBM). The prognosis is poor. GBMs are lethal tumors and even optimal surgical resection, followed by chemotherapy and irradiation, results in a median survival of about 12–15 months. One characteristic that is responsible for GBM malignancy, and its worse prognosis, is the highly infiltrative growth of GBM cells into the healthy brain. GBM cell migration and invasion is a very complex process that is regulated by several factors, which include changes in the migrating cell itself as well as the tumor microenvironment. This chapter provides an overview of routes of invasion of glioma cells, the signaling pathways that drive glioma cell motility, and the processes through which glioma cells modulate their surrounding environment.

Key words: Glioma migration; Invasion; Molecular mechanisms

* These authors contributed equally for authorship.

In: *Glioblastoma*. Steven De Vleeschouwer (Editor), Codon Publications, Brisbane, Australia
ISBN: 978-0-9944381-2-6; Doi: <http://dx.doi.org/10.15586/codon.glioblastoma.2017>

Copyright: The Authors.

Licence: This open access article is licenced under Creative Commons Attribution 4.0 International (CC BY 4.0). <https://creativecommons.org/licenses/by-nc/4.0/>

Introduction

Glioblastoma (GBM), the most malignant brain tumor, has a complex biology, and despite decades of research, much is still unknown. GBM separates itself from lower grade gliomas by exhibiting central necrosis and microvascular proliferation. It is characterized by a rapid and highly infiltrative growth. In GBM, extracranial metastases are extremely rare; tumor cell invasion and migration are the main features of GBM spreading (1). The invasive nature of GBM leads to local destruction of healthy tissues, and is the main source of recurrence (2). Even with the best imaging methods available, it is difficult to detect cells that had migrated away from the primary tumor. Glioma cells are able to migrate far away from the original tumor and can even cross into the contralateral hemisphere making complete surgical resection of GBM impossible (3). Invasion of glioma cells into the healthy brain also leads to the escape of these cells from irradiation and chemotherapy. Therefore, understanding the biology of glioma cell motility is of great importance for developing novel therapeutic approaches to treat GBM patients.

Glioma cells mainly use two routes to invade the healthy brain: the perivascular space around blood vessels and axons (4). Whether glioma cells exclusively use one route over the other, or whether other roads are also utilized, is not fully understood. In addition, it is not known how glioma cells decide to choose one pathway over the other for invasion. There are several cellular and environmental requirements that set the stage for a glioma cell to move. For example, migrating cells show changes in energy metabolism that are often induced by hypoxic conditions (5, 6). Cytokines, chemokines, nutrition deprivation, and hypoxia lead to changes in the expression of transcription factors (TFs), and subsequently to altered protein expression (7). In this regard, differential expression of ion channels, neurotransmitters, proteases, chemokines, and cytokines has been described in moving versus resting glioma cells (2). Besides transcriptional changes, the cytoskeleton of the glioma cell has to be rearranged to allow cell movement, cell adhesion has to be reduced, and the tumor cell has to be shrunk to fit into the small perivascular space. Furthermore, the extracellular matrix (ECM) has to be remodeled or destroyed to allow glioma cell invasion (8). Even the interaction of glioma cells with adjacent nonneoplastic cells like astrocytes or endothelial cells is important for glioma cell migration (9, 10). This chapter gives an overview of different processes and mechanisms glioma cells use to migrate and invade, and the signaling cascades that regulate the motility of glioma cells.

Infiltration of Diffuse Glioma

PATTERNS OF GLIOMA CELL INFILTRATION

Glioma cells infiltrate into the healthy brain parenchyma using preexisting structures like blood vessels or myelinated nerve fibers of white matter tracts, both of which present high mechanical rigidity (11, 12). ECM stiffness is a major regulator of cell motility. The movement of cells toward a more rigid ECM area is called

mechanotaxis (13). A more rigid ECM, as in the perivascular space, promotes glioma cell migration (14). Stiffness varies with the grade of glioma. It is known that invasive GBM produces stiffness-promoting factors like collagen, fibronectin (FN), and laminin. Furthermore, glioma cells overexpress components of the basal membrane of the cerebral vasculature, for example, tenascin (TN)-C, which is associated with glioma progression (15). Glioma cells are recruited to the perivascular space around blood vessels by chemoattractants like bradykinin, which is produced by endothelial cells (16). Also, overexpression of chemokine receptors on glioma cells has been associated with perivascular invasion (17). Cell movement along white matter tracts, a second known route of glioma cell invasion, is mediated by a variety of proteins called axonal guidance molecules (see the section “Axonal Guidance Molecules”), which act as attracting or repelling factors.

HYPOXIA

The center of GBM is characterized by necrosis, surrounded by an area where tumor cells deal with hypoxia and nutrient starvation. Around the necrotic region, the population of “pseudopalisading” cells become prominent. These glioma cells activate migratory processes in an attempt to escape hypoxia and to reach oxygen-rich areas adjacent to blood vessels (18). Some of the pro-migratory and pro-invasive factors produced or activated in response to hypoxic conditions include: metalloproteases like MMP-9, A Disintegrin, and Metalloproteinase (ADAM)-17 (19, 20); galectins (21); epithelial to mesenchymal transition (EMT) transcriptional regulators like SLUG and SNAIL and the zinc-finger E-Box-binding homeobox proteins ZEB-1 and ZEB-2 (22, 23); and CXCR4 and CXCR7, the latter mediating glioma cell migration toward stromal-derived factor (SDF)-1 α /CXCL12 (24, 25).

THE “GO OR GROW” OF TUMOR CELLS

Migration and proliferation of glioma cells are mutually exclusive. This phenomenon, called “Go or Grow,” was first discovered in astrocytoma cells, where proliferation and migration are timely separated (26). The “Go or Grow” is modulated by changes in the microenvironment like hypoxia or nutrient depletion, which prompts a tumor cell to “Go” in order to reach a more favorable environment and re-settle there, or to “Grow” if the environment provides enough oxygen and nutrients. The pentose phosphate pathway (PPP) is mainly used during proliferation, and glycolysis is used as the energy source during migration (5). Other parameters that influence the “Go or Grow” of glioma cells are the cell volume, cytoskeleton dynamics, and the ECM composition (27). Differential activation of TFs has been reported: increased NF- κ B activity in migrating cells, and c-myc in proliferating cells (28). Also, changes in miRNAs expression modulate the “Go or Grow”: elevated miR-451 expression is associated with a shorter GBM patient survival and higher proliferation (29), whereas mir-9, being highly expressed in glioma cells, inhibits proliferation but promotes migration (30). Understanding the process of “Go or Grow” in glioma is of central importance since it is known that ionizing irradiation used for the treatment of GBM promotes the “Go” and thereby the invasive phenotype of glioma cells (31, 32).

Extracellular Matrix

ECM constitutes 10–20% of brain volume. It is produced by the surrounding cells. ECM not only has a structural function but also a major role in brain development, cell survival, migration, maturation, differentiation, and tissue homeostasis (33, 34). The main components of the brain ECM are proteoglycans, hyaluronan, link-proteins like TN-C, and others (Figure 1) (35). Another ECM type in the brain is the basement membrane that covers blood vessels and is part of the perivascular space. Deregulated ECM dynamics is a hallmark of cancer. The ECM of glioma differs from that of the healthy brain. Whereas universal ECM components are expressed uniformly in healthy brains (36), in high-grade glioma fibrous proteins and laminin are upregulated (15, 37). Besides, the interaction of the ECM component hyaluronan with its receptor CD44, both being overexpressed in glioma cells, is a major requirement for glioma invasion (38–40). For glioma cells to invade the healthy brain tissue, the intact ECM has to be destroyed and remodeled. ECM degrading and remodeling enzymes include several MMPs, A Disintegrin and Metalloproteinase with Thrombospondin Motifs (ADAMTS), the serine protease plasmin, 6-O-sulfatases, heparanases, cathepsins, and urokinase (uPa). These enzymes are not only regulated at the transcriptional and translational levels but also post-translationally by their functionally inhibitory pro-domains or by selective natural proteinase inhibitors (41).

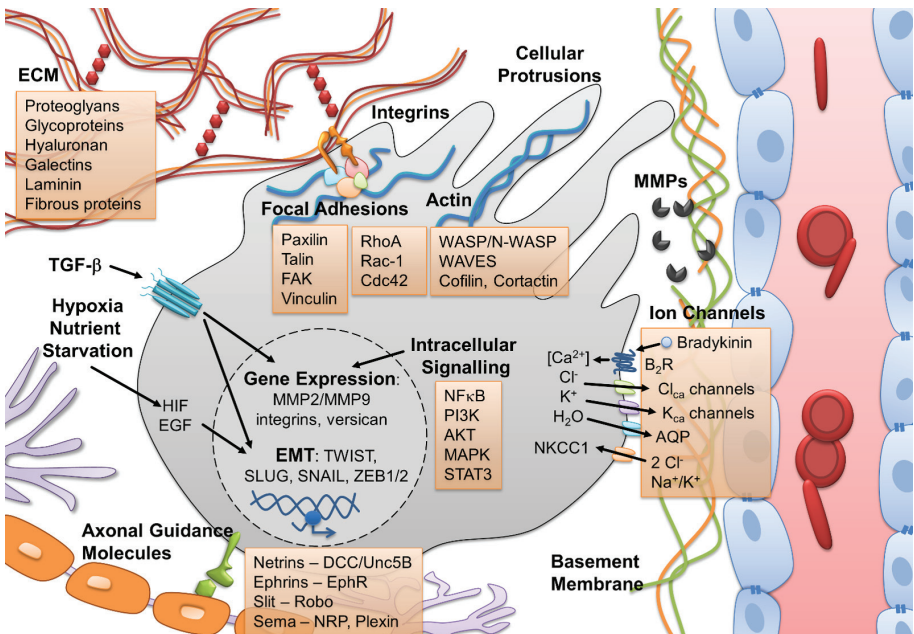


Figure 1 Mechanisms involved in the migration and invasion of glioblastoma (GBM). The migrational phenotype of GBM cells is regulated by a complex interplay of different factors, signaling cascades, as well as cellular and environmental features.

MATRIX-METALLOPROTEINASES

MMPs are a family of secreted or membrane-anchored endoproteinases (42). Their main function is the degradation and remodeling of the ECM. MMP expression in the normal brain is low. In glioma, MMPs are overexpressed or activated. MMP-2 and MMP-9 are of interest for invasive processes in gliomas as their expression correlates with tumor grade and progression (43, 44). MMP-2 and MMP-9 convert latent pro-migratory transforming growth factor (TGF)- β into its active form, which in turn induces MMP-2 in a feedback loop (see the section “The Role of TGF- β in Glioma Cell Motility” (45–47)). MMP-9 expression or activity can be regulated by: activation of signal transducer and activator of transcription (STAT)3; epidermal growth factor (EGF); FN; vitronectin (VN); interleukin (IL)-1 β ; tumor necrosis factor (TNF)- α ; and TGF- β (47–52). Furthermore, glioma cells exploit MMP-14 that is expressed by surrounding microglia cells (53). MMP-14 activates MMP-2 by cleaving its pro-peptide (54, 55). Furthermore, MMP-3, -7, -12, -13, -16, -19, and -26 are also highly expressed and mostly associated with enhanced glioma invasion (56–63). MMPs are inhibited by the four tissue inhibitors of metalloproteinases (TIMP), TIMP-1–4. They inhibit all MMPs but also have other functions including MMP activation. TIMP-2 can form a ternary complex with pro-MMP-2 and MMP-14 that is necessary for efficient MMP-2 activation (55, 64). High TIMP-1 levels and TIMP-3 silencing are associated with a poor prognosis for glioma patients (65–68). Due to these paradoxical effects, the important role of TIMPs in glioma invasion remains elusive.

INTEGRINS—THE LINK BETWEEN THE ECM AND CELLS

Integrins are catalytic inactive heterodimeric transmembrane glycoproteins responsible for cell–ECM interactions. They are the link between the ECM and the cytoskeleton and important for signal transduction. To date, 24 integrins composed of different combinations of 18 α - and 8 β -subunits have been identified (69). The $\alpha\beta$ combination determines ligand specificity. Typical ECM ligands for integrins are laminin, collagen, and FN, which are part of the basement membrane in the brain and are expressed by high-grade gliomas (70). Other integrin ligands are thrombospondin (TSP), osteopontin (OPN), VN, and TN-C, all being overexpressed in gliomas. Upon ligand binding, integrins form clusters, leading to activation of the focal adhesion kinase (FAK) and finally to enhanced migration (71). FAK is active and overexpressed in gliomas, and its expression correlates with the tumor grade (72–74). Upon integrin clustering, the cytoplasmic domain attaches to cytoskeletal components to form focal adhesion points at the leading edge of migrating cells (75). This adhesion points give cells a polarity which enable them to move forward. In GBM, integrin β 1 is overexpressed and is associated with migration (76, 77). Integrin α 9 β 1 expression correlates with glioma grade and influences MMP-9 expression (78, 79). Furthermore, integrin α 5 β 1 can stimulate MMP-2 expression upon interaction with angiopoietin (80). In addition, integrin α v β 3 and α v β 5 expression is associated with disease progression. Both can bind to the latency-associated peptide (LAP) of the LAP-TGF- β complex and thereby release active TGF- β (81, 82). In summary, integrins are substantial for glioma cell migration, establishing the link between the brain ECM and the tumor cells (Figure 1).

CHONDROITIN SULFATE PROTEOGLYCANs, GLYCOPROTEINS, AND GALECTINS

One important class of proteoglycans are chondroitin sulfate proteoglycans (CSPG), which are overexpressed in glioma and associated with increased glioma invasion (83). A subgroup of CSPG, the lecticans, forms tertiary complexes with hyaluronan and TN-R. Three of them, versican, BEHAB/brevican, and neurocan, are overexpressed in glioma and enhance glioma motility (84–86).

Invasion-promoting ECM glycoproteins secreted in glioma are: Secreted Protein Acidic and Rich in Cysteine (SPARC); TN-C supporting cell adhesion through integrin binding; OPN and VN (87–90). In addition, TSP-1, a multifunctional matrix glycoprotein, is implicated in cell adhesion, migration, invasion, and activation of TGF- β (91; see the section “The Role of TGF- β in Glioma Cell Motility”). Galectins are soluble lectins with specificity for β -galactoside which allow them to bind to proteoglycans and glycoproteins in the brain ECM (92). In malignant gliomas, galectin-1, -3, and -8 are overexpressed and promote glioma cell migration and invasion by modulating the actin cytoskeleton (93–96).

Migration-Associated Changes of the Cytoskeleton

Cell migration is a multistep process initiated by binding of chemoattractants or pro-migratory factors to cell surface receptors, followed by the activation or inactivation of diverse small GTPases and cytoskeleton reorganization (97). The resulting structures are called filopodia, lamellipodia, and podosomes. Turnover of adhesion site formation at the cell front and disruption at the rear is essential for cell movement (98).

SMALL GTPASES

The most important and well-characterized small GTPases associated with cytoskeletal remodeling are: RhoA, which is responsible for coordination of contractility at the cell body and cell rear; RAC-1 that regulates protrusion formation at the leading edge; and CDC42 that modulates cell polarity (99). RAC-1 protein levels correlate with tumor grade in astrocytomas. In addition, RAC-1 is hyperactivated in GBM (100). Enhanced activity of CDC42 and RAC-1 has been reported in infiltrating glioma cells (101). Migration-associated small GTPase activity is regulated by a variety of factors and signals. Rho GTPase activity is mediated by several receptors and effectors. In GBM, two members of the TNF receptor superfamily act through RAC-1: TNF-like weak inducer of apoptosis (TWAK) and TNF receptor superfamily member 19 (TROY) (99, 102). EGFRvIII, a truncated and constitutively active EGF receptor, and Platelet Growth Factor Receptor alpha (PDGFR α) activate RAC-1-mediated migration through tyrosine protein kinase SRC-dependent DOCK180 phosphorylation (103, 104). RAC-1 is also activated by the IQ-domain GTPase-Activating Protein (IQGAP)-1/ADP-Ribosylation Factor 6 (ARF6), neurotensin, and ephrinB3 signaling (105–107). RAC-1 activity is further modulated by CDC42 (104, 108) as well as by axonal guidance molecules (see the section “Axonal Guidance Molecules”). RhoA activity correlates with

increased glioma cell migration. Functional evidence for the role of RhoA has been demonstrated via inhibition of the RhoA effector ROCK, which leads to enhanced invasion due to the fact that ROCK, together with mDia, coordinates stress fiber formation and focal adhesion, thereby exacerbating migration. The activity of Rho and RAC GTPases is tightly regulated by three main proteins: guanine nucleotide exchange factors (GEFs), GTPase-activating proteins (GAPs), and guanine nucleotide dissociation inhibitors. Many GEFs (e.g., Ect2, ARHGEF7 [βPIX], SWAP, SGEF, Vav3, Trio, Dock180, and Dock9) have been correlated with glioma pathology, higher tumor grade, and glioma invasion, in particular when co-localized with small GTPases (99).

ACTIN REARRANGEMENT, ADHESION COMPLEXES, AND CELLULAR PROTRUSIONS

Nonmotile cells show nonpolarized cell morphology. In these cells, the machinery for actin filament and protrusions formation is inactive. Protrusion formation and actin polymerization requires, besides actin, at least six other proteins: the Arp2/3 complex; an Arp2/3 complex-activating nucleation promoting factor (NPF); a barbed-end capping protein; cofilin and profilin, the latter binding both ADP-bound and ATP-bound actin monomers (109). Lamellipodia are flat, branched, sheet-like actin membrane protrusions that drive cell migration by attaching to the substrate and generating force at the leading edge. Filopodia are thin, finger-like projections beyond the lamellipodial edge, composed of long, bundled, and unbranched actin filaments. No Arp2/3 complex or cofilin are present in filopodia. Invadopodia/podosomes are ventral membrane protrusions responsible for ECM degradation with a not yet well-characterized actin organization (98).

The Wiskott–Aldrich Syndrome (WASP) family consists of two principal classes of proteins: WASPs and SCAR/WAVEs. WASP/N-WASP induces invadopodia and podosome formation, while WAVEs are key regulators of lamellipodia. Cofilin, involved in de-polymerization and polymerization of actin filaments, is highly expressed in migrating GBM cells. It is phosphorylated and inactivated by LIM1/2 kinase. For proper migration and protrusion formation, cofilin and LIM kinase activity must be perfectly balanced. Invadopodia formation is dependent on the activity of cortactin, an actin-binding protein (98).

During cell movement, focal adhesion complexes (FACs) are formed to connect the rearranged actin cytoskeleton to the ECM. While integrin clustering is the first step for FAC formation, microtubule extension promotes FAC disruption. Several studies reported a transport of integrins from the rear to the front of the cell during migration, maintaining the focal adhesion turnover. The presence of large focal adhesions creates more links to actin stress fibers and makes cell movement more difficult (110). The molecular structure of FAC includes integrins, intracellularly bound to paxillin and talin, which subsequently recruit FAK and vinculin. FAK then phosphorylates alpha-actinin, leading to cross-links with actin filaments. The resulting structures lead to alterations of the cell morphology and the generation of traction force necessary to move the cell body. Recent reports indicate that focal adhesion protein expression, like talin and alpha-actinin, is related to the invasiveness of glioma cells (111).

Ion Channels and Their Contribution to Glioma Cell Migration

AUTOCRINE GLUTAMATE SIGNALING

Gliomas express glutamate receptors (GluRs) like α -amino-3-hydroxy-5-methylisoxazole-4-propionic acid receptors (AMPA), N-methyl-D-aspartate (NMDA) receptors, and metabotropic mGluRs. AMPARs are composed of four types of subunits: GluR1–4. Through autocrine glutamate signaling, they contribute to enhanced glioma cell invasion (112, 113). The subunits, especially GluR2, influence the cation permeability of AMPAR. In the presence of GluR2, the channel is Ca^{2+} impermeable, the situation in the mature and healthy brain (114, 115). In glioma, GluR2 is not expressed, leading to high Ca^{2+} permeability (116, 117). Artificial GluR2 overexpression in glioma cells inhibits migration (117, 118). Overexpression of GluR1 positively correlates with glioma cell adhesion to collagen, whereas stimulation of AMPAR leads to detachment from the ECM. In a mouse glioma model, overexpression of GluR1 results in enhanced invasion of glioma cells into the perivascular space similar to patterns described in human GBM.

HYDRODYNAMIC MODEL OF GLIOMA CELL MIGRATION

Glioma cells migrate through the extracellular space in the brain. To aid such migration, they reduce their volume by more than 30% by releasing cytoplasmic water (119). For this purpose, glioma cells exploit ion channels which normally function as membrane potential regulators (Figure 1). Unlike adult neurons, glioma cells have high intracellular Cl^- levels (120). This is due to the constitutive expression and prolonged activity of the $\text{Na}^+/\text{K}^+/\text{Cl}^-$ cotransporter 1 (NKCC1) that correlates with glioma grade and invasiveness (121). Upon opening of Cl^- channels, the outflow of Cl^- is accompanied by the efflux of water through aquaporins due to osmotic forces, leading to volume shrinkage. In glioma, the chloride channels ClC-2 and ClC-3 are functionally expressed, and blocking them reduces glioma migration (122–124).

The K^+ gradient, regulated by Na^+/K^+ -ATPase, is essential for invasion (125). The KCa family of Ca^{2+} -activated K^+ channels, especially KCa3.1 , is overexpressed in 32% of the glioma patients, and its expression correlates with patient survival (126). KCa3.1 is localized at the leading edge of migrating cells, and its inhibition results in reduced migration (127, 128). The bradykinin receptor B_2 (B_2R) is also expressed at the leading edge of migrating glioma cells. It is a critical attractor of glioma cells toward the vasculature, and an activator of ion channels (127, 129). Binding of bradykinin to B_2R leads to increases in intracellular Ca^{2+} which induces the opening of the KCa3.1 and ClC-3 channels, resulting in the efflux of Cl^- , K^+ , and water (16, 127, 130). As a result, the glioma cells shrink which enable them to migrate through the narrow space of the brain.

Axonal Guidance Molecules

Glioma cell movement can also occur along myelinated neuronal axons of white matter tracts. A multitude of proteins act as axonal guidance molecules by either attracting or repelling axonal growth cones and modulating neural cell motility

during development (Figure 1). The most prominent axonal guidance molecules are: ephrins (Eph); netrins; Slits and their roundabout (Robo) receptors; semaphorins (Sema) and their receptors plexin and neuropilin (NRP) (131).

EPHRINS

Ephrins serve as ligands of ephrin receptors (EphRs), a family of proteins containing nine EphR class A and five EphR class B members. Interaction of Eph and EphR regulates cell–cell interaction by forward (Eph to EphR) or reverse (EphR to Eph) signaling. Eph regulates cell migration, adhesion, morphology, differentiation, proliferation, and survival through Jun-N-terminal kinase (JNK), STAT3, PKB/AKT, Rho GTPase, and paxillin pathways. Recent studies have detected an abnormal expression of EphB1 receptors in brain tumors (132). Eph proteins have a dual role in glioma cell migration: negative regulation that inhibits migration and positive regulation that promotes migration (133, 134). Therefore, it could be postulated that these proteins might serve as regulators of the “Go or Grow” behavior of GBM.

NETRINS AND SLIT/ROBO

Netrins are a family of laminin-related proteins. Netrin-1, the most prominent representative of the netrin family, is widely expressed in fetal and adult brain tissues. Its expression is associated with progression of various types of human cancers. Netrin-1 binds to UNC5-family dependence receptor (DR) deleted in colorectal cancer (DCC), or other UNC5 molecules. While the absence of netrin-1, DCC/UNC induces apoptosis, the absence of the DRs or enhanced netrin-1 expression is tumorigenic. Netrin expression is associated with poor patient prognosis in lower grade gliomas. In GBM cells, elevated netrin expression activates notch signaling, finally resulting in the gain of stemness and enhancement of invasiveness of these cells (135).

Slit (Slit 1–3) and the Robo receptor family proteins are evolutionarily conserved molecules. During normal development, secreted Slit proteins regulate axon guidance and neuronal precursor cell migration by mediating chemo-repulsive signals on cells expressing Robo. In glioma, Slit2 and Robo1 provide different patterns. By hypermethylation of its promoter, the expression of Slit is low in most gliomas (136), whereas the expression of Robo1 is high. Slit2/Robo1 signaling inhibits glioma cell migration and invasion by inactivation of CDC42 signaling. *In vivo*, Slit-2 mitigates infiltration of glioma cells into the healthy brain (137), indicating that a chemo-repulsive signal transmitted by the interaction of Slit2/Robo1 participates in glioma cell migration or guidance (138).

SEMAPHORINS AND THEIR RECEPTORS

Semaphorins (Sema), originally identified as guidance molecules that navigate axon growth in the brain, fall into eight subclasses of secreted, membrane-anchored, and transmembrane proteins (139). Class 3 semaphorins (Sema3) transfer their function through a receptor complex consisting of plexins and neuropilin (NRP)-1 and -2 (140, 141). Downstream signaling of Sema involves RhoA,

RAC-1, and cofilin, leading to the reorganization of the cytoskeleton (142). In GBM cells, inactivation of RhoA by Sema3F leads to the collapse of the cytoskeleton, whereas inhibition of Sema3F promotes cell motility (143, 144). Similar effects have been observed for Sema3G (145), and higher expression of Sema3G in GBM patients has been associated with a better prognosis (146). While Sema3A, 3B, and 3F show antitumorigenic properties in many cancers, other Sema3 family members are associated with tumor progression. Overexpression of Sema3C promotes cell invasion of prostate cancer cell lines, whereas enhanced expression of Sema3E induces metastasis in lung cancer (147, 148). Regarding this dual function of semaphorins, it should be kept in mind that the signaling complexes of Semas and their Robo receptors as well as the downstream signaling cascades that are modulated by Semas are complex and interconnected, which then might finally determine whether they work in a pro- or anti-migratory fashion.

The Role of TGF- β in Glioma Cell Motility

The TGF- β superfamily of cytokines consists of TGF- β 1–3 which are master regulators of inflammation and cell differentiation. They play a key role in tumor progression and metastasis (149). After binding to the TGF- β receptor (TGF β -R)-I, TGF β -RII is phosphorylated. This in turn phosphorylates SMAD2/3, which then combines with SMAD4. This complex translocates to the nucleus and regulates gene expression (150). TGF- β is heavily secreted by glioma cells *in vitro* and *in vivo*. TGF- β promotes a mesenchymal phenotype in GBM cells, enhancing invasion and migration *in vitro*, and in an orthotopic mouse model (151). TGF- β also stimulates the production of reactive oxygen species (ROS), and activates ERK1/2, JNK, and NF κ B. NF κ B finally upregulates the expression of MMP-9 (152). Other mechanisms of TGF- β influencing the ECM and promoting migration include the upregulation of integrin α v β 3 and the versican isoforms V0/V1 (84, 153). Furthermore, TGF- β suppresses phosphatase and tensin homolog (PTEN) in glioma cells through enhanced miR10a/b expression (154). In patient samples, TGFBI1 (TGF- β 1-induced transcript 1) expression was found to be correlated with tumor grade, and activation of EMT pathways (152). In reaction to radiation treatment, the invasion capability of glioma cells is enhanced and TGF- β is upregulated. This suggests a role for TGF- β in treatment resistance (155).

EMT-Like Processes

EMT is a process by which epithelial cells lose their polarity and cell–cell adhesion, resulting in a mesenchymal phenotype characterized by enhanced motility, chemoresistance, and stem-like properties. EMT is involved in various biological functions such as wound healing, embryonic development, and fibrosis (156). In epithelial carcinoma, EMT is a well-established driver of invasion and metastasis (157), and even though gliomas are nonepithelial tumors, EMT-like processes have been described (158). Among the signals that have been shown to induce EMT in glioma are TGF- β , EGF, and Hypoxia-Inducible Factor (HIF; Figure 1) (159).

TWIST, SNAIL, SLUG, AND ZEB

TWIST1 and TWIST2 are helix-loop-helix TFs involved in EMT during development and cancer progression (160). In glioma, TWIST was found to be a possible prognostic marker, and its expression correlates with tumor grade (161, 162). TWIST overexpression promotes invasion of glioma cells *in vitro* and in orthotopic glioma xenotransplants *in vivo* by inducing the expression of EMT-associated genes like MMP-2 and FN-1. The SNAIL family of transcriptional repressors consisting of SNAIL/SNAI1 and SLUG/SNAI2 is known to drive invasion and metastasis in various carcinomas (163). SNAIL binds to E-box DNA sequences of genes related to an epithelial phenotype through carboxy-terminal zinc-finger domains, thereby suppressing their expression. Knockdown of SNAIL in glioma cells by siRNA diminished glioma migration and invasion (164, 165). In GBM, the Rho family GTPase (RND)-3 has been shown to promote the degradation of SNAIL *in vitro* and *in vivo*, while downregulation of RND3 strongly induces SNAIL expression and migration (166). SLUG expression was found to correlate with histologic grade and invasive phenotype in glioma, whereas knockdown of SLUG attenuated invasion and prolonged survival in an intracranial mouse model (167).

The TFs Zinc-finger E-box Binding homeobox proteins (ZEB)-1 and -2 also bind to E-boxes of DNA sequences, thereby repressing cell polarity-associated genes such as E-cadherin/CDH1, cell-adhesion molecules, and stemness-inhibiting miR-200 (168, 169). In GBM patients, ZEB-1 overexpression correlated with poor overall survival. Glioma cells implanted in mice brain were less invasive after knockdown of ZEB-1. ZEB-1 and PDGFR α were found to be co-expressed in tissue samples from GBM patients, while high expression of both ZEB-1 and activated PDGFR α was identified to significantly coincide with poor survival. The same study further established Protein Tyrosine Phosphatase/Nonreceptor type (PTPN)-1 as a regulator of ZEB-1-induced and PDGFR-induced EMT in glioma (170). EMT may also be directly promoted by the microenvironment of GBM. Both the hypoxic marker HIF1 α and ZEB-1 were shown to colocalize in hypoxic areas of human GBM. In glioma cells, the suppression of HIF1 α negatively affected the level of ZEB-1 (22). ZEB-2 was overexpressed in glioma tissue samples compared to healthy brain tissue, and higher expression of ZEB-2 correlated with glioma pathology grading. Knockdown of ZEB-2 showed an upregulation of E-cadherin, whereas N-cadherin and SNAIL were repressed (171).

CADHERINS

Cadherins are Ca²⁺-dependent transmembrane molecules with an important role in cell to cell adhesion, recognition, and signaling (172). In epithelial cancers, the loss of E-cadherin and an increased expression of N-cadherin, the so-called “cadherin switch,” is considered to be a hallmark of EMT (173). In tissues of GBM and healthy brain, the expression of E-cadherin is generally only marginal (174, 175). However, in a minor subset of GBM showing epithelial differentiation, high expression of E-cadherin is observed, correlating with poorer clinical outcome compared to GBM with low or no E-cadherin expression. Glioma cells with high E-cadherin expression show greater invasion when orthotopically implanted in mice (176). In contrast to its role in carcinoma, N-cadherin is frequently

downregulated in GBM compared to the healthy brain (177, 178). N-cadherin overexpression has been shown to decrease glioma invasion *in vitro* and *in vivo* (179). Interestingly, the role of N-cadherin in glioma is postulated not only to be determined by its expression level but also by its distribution in the cell membrane (180). ZEB-1 knockdown in GBM cells showed a loss of invasiveness and concentration of N-cadherin to the juxtaposed membranes between adjacent cells; the axon-guidance molecule Robo-1 mediated by ZEB-1 can reverse this process by severing the anchorage of N-cadherin to the cytoskeleton (181).

Conclusion

Migration and invasion of glioma cells in the brain follow different migratory routes. It is a complex process regulated by the surrounding environmental conditions, and interconnected by diverse signaling cascades. Understanding the process of migration and invasion of glioma cells is of central importance since these characteristics make GBM aggressive and complete resection impossible. Identifying the molecular mechanisms that govern the motility of GBM cells will help develop new therapeutic strategies to treat this deadly tumor.

Conflict of interest: The authors declare no potential conflicts of interest with respect to research, authorship, and/or publication of this manuscript.

Copyright and permission statement: To the best of our knowledge, the materials included in this chapter do not violate copyright laws. All original sources have been appropriately acknowledged and/or referenced. Where relevant, appropriate permissions have been obtained from the original copyright holder(s).

References

1. Johansen MD, Rochat P, Law I, Scheie D, Poulsen HS, Muhic A. Presentation of two cases with early extracranial metastases from glioblastoma and review of the literature. *Case Rep Oncol Med.* 2016;2016:8190950. <http://dx.doi.org/10.1155/2016/8190950>
2. Demuth T, Berens ME. Molecular mechanisms of glioma cell migration and invasion. *J Neuro-Oncol.* 2004;70(2):217–28. <http://dx.doi.org/10.1007/s11060-004-2751-6>
3. Altieri R, Zenga F, Fontanella MM, Cofano F, Agnoletti A, Spena G, et al. Glioma surgery: Technological advances to achieve a maximal safe resection. *Surg Technol Int.* 2015;27:297–302.
4. Cuddapah VA, Robel S, Watkins S, Sontheimer H. A neurocentric perspective on glioma invasion. *Nat Rev Neurosci.* 2014;15(7):455–65. <http://dx.doi.org/10.1038/nrn3765>
5. Kathagen-Buhmann A, Schulte A, Weller J, Holz M, Herold-Mende C, Glass R, et al. Glycolysis and the pentose phosphate pathway are differentially associated with the dichotomous regulation of glioblastoma cell migration versus proliferation. *Neuro Oncol.* 2016;18(9):1219–29. <http://dx.doi.org/10.1093/neuonc/now024>
6. Höring E, Harter PN, Seznec J, Schittenhelm J, Bühring HJ, Bhattacharyya S, et al. The “go or grow” potential of gliomas is linked to the neuropeptide processing enzyme carboxypeptidase E and mediated by metabolic stress. *Acta Neuropathol.* 2012;124(1):83–97. <http://dx.doi.org/10.1007/s00401-011-0940-x>
7. Lu DY, Leung YM, Cheung CW, Chen YR, Wong KL. Glial cell line-derived neurotrophic factor induces cell migration and matrix metalloproteinase-13 expression in glioma cells. *Biochem Pharmacol.* 2010;80(8):1201–9. <http://dx.doi.org/10.1016/j.bcp.2010.06.046>

8. Gladson CL. The extracellular matrix of gliomas: Modulation of cell function. *J Neuropathol Exp Neurol.* 1999;58(10):1029–40. <http://dx.doi.org/10.1097/00005072-199910000-00001>
9. Bougnaud S, Golebiewska A, Oudin A, Keunen O, Harter PN, Mader L, et al. Molecular cross-talk between tumour and brain parenchyma instructs histopathological features in glioblastoma. *Oncotarget.* 2016;7(22):31955–71. <http://dx.doi.org/10.18632/oncotarget.7454>
10. da Fonseca AC, Badie B. Microglia and macrophages in malignant gliomas: Recent discoveries and implications for promising therapies. *Clin Dev Immunol.* 2013;2013:264124.
11. Rao JS. Molecular mechanisms of glioma invasiveness: The role of proteases. *Nat Rev Cancer.* 2003;3(7):489–501. <http://dx.doi.org/10.1038/nrc1121>
12. Lefranc F, Brotchi J, Kiss R. Possible future issues in the treatment of glioblastomas: Special emphasis on cell migration and the resistance of migrating glioblastoma cells to apoptosis. *J Clin Oncol.* 2005;23(10):2411–22. <http://dx.doi.org/10.1200/JCO.2005.03.089>
13. Lo CM, Wang HB, Dembo M, Wang YL. Cell movement is guided by the rigidity of the substrate. *Biophys J.* 2000;79(1):144–52. [http://dx.doi.org/10.1016/S0006-3495\(00\)76279-5](http://dx.doi.org/10.1016/S0006-3495(00)76279-5)
14. Ulrich TA, de Juan Pardo EM, Kumar S. The mechanical rigidity of the extracellular matrix regulates the structure, motility, and proliferation of glioma cells. *Cancer Res.* 2009;69(10):4167–74. <http://dx.doi.org/10.1158/0008-5472.CAN-08-4859>
15. Mahesparan R, Read TA, Lund-Johansen M, Skaftnesmo KO, Bjerkvig R, Engebraaten O. Expression of extracellular matrix components in a highly infiltrative in vivo glioma model. *Acta Neuropathol.* 2003;105(1):49–57.
16. Montana V, Sontheimer H. Bradykinin promotes the chemotactic invasion of primary brain tumors. *J Neurosci.* 2011;31(13):4858–67. <http://dx.doi.org/10.1523/JNEUROSCI.3825-10.2011>
17. Yadav VN, Zamler D, Baker GJ, Kadiyala P, Erdreich-Epstein A, DeCarvalho AC, et al. CXCR4 increases in-vivo glioma perivascular invasion, and reduces radiation induced apoptosis: A genetic knockdown study. *Oncotarget.* 2016;7(50):83701–19.
18. Brat DJ, Van Meir EG. Vaso-occlusive and prothrombotic mechanisms associated with tumor hypoxia, necrosis, and accelerated growth in glioblastoma. *Lab Invest.* 2004;84(4):397–405. <http://dx.doi.org/10.1038/labinvest.3700070>
19. Szalad A, Katakowski M, Zheng X, Jiang F, Chopp M. Transcription factor Sp1 induces ADAM17 and contributes to tumor cell invasiveness under hypoxia. *J Exp Clin Cancer Res.* 2009;28:129. <http://dx.doi.org/10.1186/1756-9966-28-129>
20. Wang Y, Liu T, Yang N, Xu S, Li X, Wang D. Hypoxia and macrophages promote glioblastoma invasion by the CCL4-CCR5 axis. *Oncol Rep.* 2016;36(6):3522–8. <http://dx.doi.org/10.3892/or.2016.5171>
21. Le Mercier M, Fortin S, Mathieu V, Kiss R, Lefranc F. Galectins and gliomas. *Brain Pathol.* 2010;20(1):17–27. <http://dx.doi.org/10.1111/j.1750-3639.2009.00270.x>
22. Joseph JV, Conroy S, Pavlov K, Sontakke P, Tomar T, Eggens-Meijer E, et al. Hypoxia enhances migration and invasion in glioblastoma by promoting a mesenchymal shift mediated by the HIF1alpha-ZEB1 axis. *Cancer Lett.* 2015;359(1):107–16. <http://dx.doi.org/10.1016/j.canlet.2015.01.010>
23. Kahlert UD, Suwala AK, Raabe EH, Siebzehnrubl FA, Suarez MJ, Orr BA, et al. ZEB1 promotes invasion in human fetal neural stem cells and hypoxic glioma neurospheres. *Brain Pathol.* 2015;25(6):724–32. <http://dx.doi.org/10.1111/bpa.12240>
24. Esencay M, Sarfraz Y, Zagzag D. CXCR7 is induced by hypoxia and mediates glioma cell migration towards SDF-1alpha. *BMC Cancer.* 2013;13:347. <http://dx.doi.org/10.1186/1471-2407-13-347>
25. Zagzag D, Lukyanov Y, Lan L, Ali MA, Esencay M, Mendez O, et al. Hypoxia-inducible factor 1 and VEGF upregulate CXCR4 in glioblastoma: Implications for angiogenesis and glioma cell invasion. *Lab Invest.* 2006;86(12):1221–32. <http://dx.doi.org/10.1038/labinvest.3700482>
26. Giese A, Loo MA, Tran N, Haskett D, Coons SW, Berens ME. Dichotomy of astrocytoma migration and proliferation. *Int J Cancer.* 1996;67(2):275–82. [http://dx.doi.org/10.1002/\(SICI\)1097-0215\(19960717\)67:2%3C275::AID-IJC20%3E3.0.CO;2-9](http://dx.doi.org/10.1002/(SICI)1097-0215(19960717)67:2%3C275::AID-IJC20%3E3.0.CO;2-9)
27. Hatzikirou H, Basanta D, Simon M, Schaller K, Deutsch A. “Go or grow”: The key to the emergence of invasion in tumour progression? *Math Med Biol.* 2012;29(1):49–65. <http://dx.doi.org/10.1093/imammb/dqq011>

28. Dhruv HD, McDonough Winslow WS, Armstrong B, Tuncali S, Eschbacher J, et al. Reciprocal activation of transcription factors underlies the dichotomy between proliferation and invasion of glioma cells. *PLoS One*. 2013;8(8):e72134. <http://dx.doi.org/10.1371/journal.pone.0072134>
29. Godlewski J, Nowicki MO, Bronisz A, Nuovo G, Palatini J, De Lay M, et al. MicroRNA-451 regulates LKB1/AMPK signaling and allows adaptation to metabolic stress in glioma cells. *Mol Cell*. 2010;37(5):620–32. <http://dx.doi.org/10.1016/j.molcel.2010.02.018>
30. Tan X, Wang S, Yang B, Zhu L, Yin B, Chao T, et al. The CREB-miR-9 negative feedback minicircuitry coordinates the migration and proliferation of glioma cells. *PLoS One*. 2012;7(11):e49570. <http://dx.doi.org/10.1371/journal.pone.0049570>
31. Wild-Bode C, Weller M, Rimmer A, Dichgans J, Wick W. Sublethal irradiation promotes migration and invasiveness of glioma cells: Implications for radiotherapy of human glioblastoma. *Cancer Res*. 2001;61(6):2744–50.
32. Huber SM, Butz L, Stegen B, Klumpp D, Braun N, Ruth P, et al. Ionizing radiation, ion transports, and radioresistance of cancer cells. *Front Physiol*. 2013;4:212. <http://dx.doi.org/10.3389/fphys.2013.00212>
33. Novak U, Kaye AH. Extracellular matrix and the brain: Components and function. *J Clin Neurosci*. 2000;7(4):280–90. <http://dx.doi.org/10.1054/jocn.1999.0212>
34. Cragg B. Brain extracellular space fixed for electron microscopy. *Neurosci Lett*. 1979;15(2–3):301–6. [http://dx.doi.org/10.1016/0304-3940\(79\)96130-5](http://dx.doi.org/10.1016/0304-3940(79)96130-5)
35. Dityatev A, Seidenbecher CI, Schachner M. Compartmentalization from the outside: The extracellular matrix and functional microdomains in the brain. *Trends Neurosci*. 2010;33(11):503–12. <http://dx.doi.org/10.1016/j.tins.2010.08.003>
36. Lau LW, Cua R, Keough MB, Haylock-Jacobs S, Yong VW. Pathophysiology of the brain extracellular matrix: A new target for remyelination. *Nat Rev Neurosci*. 2013;14(10):722–9. <http://dx.doi.org/10.1038/nrn3550>
37. Serres E, Debarbieux F, Stanchi F, Maggiorola L, Grall D, Turchi L, et al. Fibronectin expression in glioblastomas promotes cell cohesion, collective invasion of basement membrane in vitro and orthotopic tumor growth in mice. *Oncogene*. 2014;33(26):3451–62. <http://dx.doi.org/10.1038/onc.2013.305>
38. Wiranowska M, Ladd S, Moscinski LC, Hill B, Haller E, Mikecz K, et al. Modulation of hyaluronan production by CD44 positive glioma cells. *Int J Cancer*. 2010;127(3):532–42. <http://dx.doi.org/10.1002/ijc.25085>
39. Park JB, Kwak HJ, Lee SH. Role of hyaluronan in glioma invasion. *Cell Adh Migr*. 2008;2(3):202–7. <http://dx.doi.org/10.4161/cam.2.3.6320>
40. Bouterfa H, Janka M, Meese E, Kerkau S, Roosen K, Tonn JC. Effect of changes in the CD44 gene on tumour cell invasion in gliomas. *Neuropathol Appl Neurobiol*. 1997;23(5):373–9. <http://dx.doi.org/10.1111/j.1365-2990.1997.tb01311.x>
41. Lu P, Weaver VM, Werb Z. The extracellular matrix: A dynamic niche in cancer progression. *J Cell Biol*. 2012;196(4):395–406. <http://dx.doi.org/10.1083/jcb.201102147>
42. Konnecke H, Bechmann I. The role of microglia and matrix metalloproteinases involvement in neuroinflammation and gliomas. *Clin Dev Immunol*. 2013;2013:914104. <http://dx.doi.org/10.1155/2013/914104>
43. Forsyth PA, Wong H, Laing TD, Rewcastle NB, Morris DG, Muzik H, et al. Gelatinase-A (MMP-2), gelatinase-B (MMP-9) and membrane type matrix metalloproteinase-1 (MT1-MMP) are involved in different aspects of the pathophysiology of malignant gliomas. *Br J Cancer*. 1999;79(11–12):1828–35. <http://dx.doi.org/10.1038/sj.bjc.6990291>
44. Wang M, Wang T, Liu S, Yoshida D, Teramoto A. The expression of matrix metalloproteinase-2 and -9 in human gliomas of different pathological grades. *Brain Tumor Pathol*. 2003;20(2):65–72. <http://dx.doi.org/10.1007/BF02483449>
45. Wick W, Platten M, Weller M. Glioma cell invasion: Regulation of metalloproteinase activity by TGF-beta. *J Neurooncol*. 2001;53(2):177–85.
46. Imai K, Hiramatsu A, Fukushima D, Pierschbacher MD, Okada Y. Degradation of decorin by matrix metalloproteinases: Identification of the cleavage sites, kinetic analyses and transforming growth factor-beta1 release. *Biochem J*. 1997;322(Pt 3):809–14. <http://dx.doi.org/10.1042/bj3220809>

47. Yu Q, Stamenkovic I. Cell surface-localized matrix metalloproteinase-9 proteolytically activates TGF-beta and promotes tumor invasion and angiogenesis. *Genes Dev.* 2000;14(2):163–76.
48. Natesh K, Bhosale D, Desai A, Chandrika G, Pujari R, Jagtap J, et al. Oncostatin-M differentially regulates mesenchymal and proneural signature genes in gliomas via STAT3 signaling. *Neoplasia.* 2015;17(2):225–37. <http://dx.doi.org/10.1016/j.neo.2015.01.001>
49. Beliveau A, Mott JD, Lo A, Chen EI, Koller AA, Yaswen P, et al. Raf-induced MMP9 disrupts tissue architecture of human breast cells in three-dimensional culture and is necessary for tumor growth in vivo. *Genes Dev.* 2010;24(24):2800–11. <http://dx.doi.org/10.1101/gad.1990410>
50. Milner R, Crocker SJ, Hung S, Wang X, Frausto RF, del Zoppo GJ. Fibronectin- and vitronectin-induced microglial activation and matrix metalloproteinase-9 expression is mediated by integrins alpha5beta1 and alphavbeta5. *J Immunol.* 2007;178(12):8158–67. <http://dx.doi.org/10.4049/jimmunol.178.12.8158>
51. Lin CC, Kuo CT, Cheng CY, Wu CY, Lee CW, Hsieh HL, et al. IL-1 beta promotes A549 cell migration via MAPKs/AP-1- and NF-kappaB-dependent matrix metalloproteinase-9 expression. *Cell Signal.* 2009;21(11):1652–62. <http://dx.doi.org/10.1016/j.cellsig.2009.07.002>
52. Esteve PO, Chicoine E, Robledo O, Aoudjit F, Descoteaux A, Potworowski EF, et al. Protein kinase C-zeta regulates transcription of the matrix metalloproteinase-9 gene induced by IL-1 and TNF-alpha in glioma cells via NF-kappa B. *J Biol Chem.* 2002;277(38):35150–5. <http://dx.doi.org/10.1074/jbc.M108600200>
53. Markovic DS, Vinnakota K, Chirasani S, Synowitz M, Raguet H, Stock K, et al. Gliomas induce and exploit microglial MT1-MMP expression for tumor expansion. *Proc Natl Acad Sci USA.* 2009;106(30):12530–5. <http://dx.doi.org/10.1073/pnas.0804273106>
54. Sato H, Takino T, Okada Y, Cao J, Shinagawa A, Yamamoto E, et al. A matrix metalloproteinase expressed on the surface of invasive tumour cells. *Nature.* 199;370(6484):61–5.
55. Murphy G, Stanton H, Cowell S, Butler G, Knauper V, Atkinson S, et al. Mechanisms for pro matrix metalloproteinase activation. *APMIS.* 1999;107(1):38–44. <http://dx.doi.org/10.1111/j.1699-0463.1999.tb01524.x>
56. Sarkar S, Nuttall RK, Liu S, Edwards DR, Yong VW. Tenascin-C stimulates glioma cell invasion through matrix metalloproteinase-12. *Cancer Res.* 2006;66(24):11771–80. <http://dx.doi.org/10.1158/0008-5472.CAN-05-0470>
57. Wang J, Li Y, Wang J, Li C, Yu K, Wang Q. Increased expression of matrix metalloproteinase-13 in glioma is associated with poor overall survival of patients. *Med Oncol.* 2012;29(4):2432–7. <http://dx.doi.org/10.1007/s12032-012-0181-4>
58. Yeh WL, Lu DY, Lee MJ, Fu WM. Leptin induces migration and invasion of glioma cells through MMP-13 production. *Glia.* 2009;57(4):454–64. <http://dx.doi.org/10.1002/glia.20773>
59. Wang H, Li XT, Wu C, Wu ZW, Li YY, Yang TQ, et al. miR-132 can inhibit glioma cells invasion and migration by target MMP16 in vitro. *Onco Targets Ther.* 2015;8:3211–18.
60. Laurent M, Martinerie C, Thibout H, Hoffman MP, Verrecchia F, Le Bouc Y, et al. NOVH increases MMP3 expression and cell migration in glioblastoma cells via a PDGFR-alpha-dependent mechanism. *FASEB J.* 2003;17(13):1919–21.
61. Deng Y, Li W, Li Y, Yang H, Xu H, Liang S, et al. Expression of Matrix Metalloproteinase-26 promotes human glioma U251 cell invasion in vitro and in vivo. *Oncol Rep.* 2010;23(1):69–78.
62. Rome C, Arsaut J, Taris C, Couillaud F, Loiseau H. MMP-7 (matrilysin) expression in human brain tumors. *Mol Carcinog.* 2007;46(6):446–52. <http://dx.doi.org/10.1002/mc.20293>
63. Lettau I, Hattermann K, Held-Feindt J, Brauer R, Sedlacek R, Mentlein R. Matrix metalloproteinase-19 is highly expressed in astroglial tumors and promotes invasion of glioma cells. *J Neuropathol Exp Neurol.* 2010;69(3):215–23. <http://dx.doi.org/10.1097/NEN.0b013e3181ce9f67>
64. Jackson HW, Defamie V, Waterhouse P, Khokha R. TIMPs: Versatile extracellular regulators in cancer. *Nat Rev Cancer.* 2017;17(1):38–53. <http://dx.doi.org/10.1038/nrc.2016.115>
65. Crocker M, Ashley S, Giddings I, Petrik V, Hardcastle A, Aherne W, et al. Serum angiogenic profile of patients with glioblastoma identifies distinct tumor subtypes and shows that TIMP-1 is a prognostic factor. *Neuro Oncol.* 2011;13(1):99–108. <http://dx.doi.org/10.1093/neuonc/noq170>
66. Aaberg-Jessen C, Christensen K, Offenberg H, Bartels A, Dreehsen T, Hansen S, et al. Low expression of tissue inhibitor of metalloproteinases-1 (TIMP-1) in glioblastoma predicts longer patient survival. *J Neurooncol.* 2009;95(1):117–28. <http://dx.doi.org/10.1007/s11060-009-9910-8>

67. Nakamura M, Ishida E, Shimada K, Kishi M, Nakase H, Sakaki T, et al. Frequent LOH on 22q12.3 and TIMP-3 inactivation occur in the progression to secondary glioblastomas. *Lab Invest.* 2005;85(2):165–75. <http://dx.doi.org/10.1038/labinvest.3700223>
68. Zhang L, Wang M, Wang W, Mo J. Incidence and prognostic value of multiple gene promoter methylations in gliomas. *J Neurooncol.* 2014;116(2):349–56. <http://dx.doi.org/10.1007/s11060-013-1301-5>
69. Desgrosellier JS, Cheresh DA. Integrins in cancer: Biological implications and therapeutic opportunities. *Nat Rev Cancer.* 2010;10(1):9–22. <http://dx.doi.org/10.1038/nrc2748>
70. D'Abaco GM, Kaye AH. Integrins: Molecular determinants of glioma invasion. *J Clin Neurosci.* 2007;14(11):1041–8. <http://dx.doi.org/10.1016/j.jocn.2007.06.019>
71. Mitra SK, Schlaepfer DD. Integrin-regulated FAK-Src signaling in normal and cancer cells. *Curr Opin Cell Biol.* 2006;18(5):516–23. <http://dx.doi.org/10.1016/j.ceb.2006.08.011>
72. Wang D, Grammer JR, Cobbs CS, Stewart JE, Jr., Liu Z, Rhoden R, et al. p125 focal adhesion kinase promotes malignant astrocytoma cell proliferation in vivo. *J Cell Sci.* 2000;113(Pt 23):4221–30.
73. Hecker TP, Grammer JR, Gillespie GY, Stewart J, Jr., Gladson CL. Focal adhesion kinase enhances signaling through the Shc/extracellular signal-regulated kinase pathway in anaplastic astrocytoma tumor biopsy samples. *Cancer Res.* 2002;62(9):2699–707.
74. Gutenberg A, Bruck W, Buchfelder M, Ludwig HC. Expression of tyrosine kinases FAK and Pyk2 in 331 human astrocytomas. *Acta Neuropathol.* 2004;108(3):224–30. <http://dx.doi.org/10.1007/s00401-004-0886-3>
75. Ridley AJ, Schwartz MA, Burridge K, Firtel RA, Ginsberg MH, Borisy G, et al. Cell migration: Integrating signals from front to back. *Science.* 2003;302(5651):1704–9. <http://dx.doi.org/10.1126/science.1092053>
76. Gingras MC, Roussel E, Bruner JM, Branch CD, Moser RP. Comparison of cell adhesion molecule expression between glioblastoma multiforme and autologous normal brain tissue. *J Neuroimmunol.* 1995;57(1–2):143–53. [http://dx.doi.org/10.1016/0165-5728\(94\)00178-Q](http://dx.doi.org/10.1016/0165-5728(94)00178-Q)
77. Tynes BB, Larsen LF, Ness GO, Mahesparan R, Edvardsen K, Garcia-Cabrera I, et al. Stimulation of glioma-cell migration by laminin and inhibition by anti-alpha3 and anti-beta1 integrin antibodies. *Int J Cancer.* 1996;67(6):777–84. [http://dx.doi.org/10.1002/\(SICI\)1097-0215\(19960917\)67:6%3C777::AID-IJC5%3E3.0.CO;2-O](http://dx.doi.org/10.1002/(SICI)1097-0215(19960917)67:6%3C777::AID-IJC5%3E3.0.CO;2-O)
78. Brown MC, Staniszewska I, Lazarovici P, Tuszynski GP, Del Valle L, Marcinkiewicz C. Regulatory effect of nerve growth factor in alpha9beta1 integrin-dependent progression of glioblastoma. *Neuro Oncol.* 2008;10(6):968–80. <http://dx.doi.org/10.1215/15228517-2008-0047>
79. Veeravalli KK, Ponnala S, Chetty C, Tsung AJ, Gujrati M, Rao JS. Integrin alpha9beta1-mediated cell migration in glioblastoma via SSAT and Kir4.2 potassium channel pathway. *Cell Signal.* 2012;24(1):272–81. <http://dx.doi.org/10.1016/j.cellsig.2011.09.011>
80. Hu B, Jarzynka MJ, Guo P, Imanishi Y, Schlaepfer DD, Cheng SY. Angiopoietin 2 induces glioma cell invasion by stimulating matrix metalloprotease 2 expression through the alphavbeta1 integrin and focal adhesion kinase signaling pathway. *Cancer Res.* 2006;66(2):775–83. <http://dx.doi.org/10.1158/0008-5472.CAN-05-1149>
81. Ludbrook SB, Barry ST, Delves CJ, Horgan CM. The integrin alphavbeta3 is a receptor for the latency-associated peptides of transforming growth factors beta1 and beta3. *Biochem J.* 2003;369(Pt 2):311–18. <http://dx.doi.org/10.1042/bj20020809>
82. Bello L, Francolini M, Marthyn P, Zhang J, Carroll RS, Nikas DC, et al. Alpha(v)beta3 and alpha(v)beta5 integrin expression in glioma periphery. *Neurosurgery.* 2001;49(2):380–9; discussion 90.
83. Sim H, Hu B, Viapiano MS. Reduced expression of the hyaluronan and proteoglycan link proteins in malignant gliomas. *J Biol Chem.* 2009;284(39):26547–56. <http://dx.doi.org/10.1074/jbc.M109.013185>
84. Onken J, Moeckel S, Leukel P, Leidgens V, Baumann F, Bogdahn U, et al. Versican isoform V1 regulates proliferation and migration in high-grade gliomas. *J Neurooncol.* 2014;120(1):73–83. <http://dx.doi.org/10.1007/s11060-014-1545-8>
85. Viapiano MS, Hockfield S, Matthews RT. BEHAB/brevican requires ADAMTS-mediated proteolytic cleavage to promote glioma invasion. *J Neurooncol.* 2008;88(3):261–72. <http://dx.doi.org/10.1007/s11060-008-9575-8>

86. Varga I, Hutoczi G, Szemcsak CD, Zahuczky G, Toth J, Adamecz Z, et al. Brevican, neurocan, tenascin-C and versican are mainly responsible for the invasiveness of low-grade astrocytoma. *Pathol Oncol Res*. 2012;18(2):413–20. <http://dx.doi.org/10.1007/s12253-011-9461-0>
87. Rempel SA, Golembieski WA, Fisher JL, Maile M, Nakeff A. SPARC modulates cell growth, attachment and migration of U87 glioma cells on brain extracellular matrix proteins. *J Neurooncol*. 2001;53(2):149–60. <http://dx.doi.org/10.1023/A:1012201300188>
88. Brosicke N, Faissner A. Role of tenascins in the ECM of gliomas. *Cell Adh Migr*. 2015;9(1–2):131–40. <http://dx.doi.org/10.1080/19336918.2014.1000071>
89. Jan HJ, Lee CC, Shih YL, Hueng DY, Ma HI, Lai JH, et al. Osteopontin regulates human glioma cell invasiveness and tumor growth in mice. *Neuro Oncol*. 2010;12(1):58–70. <http://dx.doi.org/10.1093/neuonc/nop013>
90. Fukushima Y, Tamura M, Nakagawa H, Itoh K. Induction of glioma cell migration by vitronectin in human serum and cerebrospinal fluid. *J Neurosurg*. 2007;107(3):578–85. <http://dx.doi.org/10.3171/JNS-07/09/0578>
91. Amagasaki K, Sasaki A, Kato G, Maeda S, Nukui H, Naganuma H. Antisense-mediated reduction in thrombospondin-1 expression reduces cell motility in malignant glioma cells. *Int J Cancer*. 2001;94(4):508–12. <http://dx.doi.org/10.1002/ijc.1497>
92. Strik HM, Kolodziej M, Oertel W, Basecke J. Glycobiology in malignant gliomas: Expression and functions of galectins and possible therapeutic options. *Curr Pharm Biotechnol*. 2012;13(11):2299–307. <http://dx.doi.org/10.2174/138920112802502051>
93. Metz C, Doger R, Riquelme E, Cortes P, Holmes C, Shaughnessy R, et al. Galectin-8 promotes migration and proliferation and prevents apoptosis in U87 glioblastoma cells. *Biol Res*. 2016;49(1):33. <http://dx.doi.org/10.1186/s40659-016-0091-6>
94. Toussaint LG, 3rd, Nilson AE, Goble JM, Ballman KV, James CD, Lefranc F, et al. Galectin-1, a gene preferentially expressed at the tumor margin, promotes glioblastoma cell invasion. *Mol Cancer*. 2012;11:32. <http://dx.doi.org/10.1186/1476-4598-11-32>
95. Camby I, Belot N, Lefranc F, Sadeghi N, de Launoit Y, Kaltner H, et al. Galectin-1 modulates human glioblastoma cell migration into the brain through modifications to the actin cytoskeleton and levels of expression of small GTPases. *J Neuropathol Exp Neurol*. 2002;61(7):585–96. <http://dx.doi.org/10.1093/jnen/61.7.585>
96. Debray C, Vereecken P, Belot N, Teillard P, Brion JP, Pandolfo M, et al. Multifaceted role of galectin-3 on human glioblastoma cell motility. *Biochem Biophys Res Commun*. 2004;325(4):1393–8. <http://dx.doi.org/10.1016/j.bbrc.2004.10.181>
97. Mitra SK, Hanson DA, Schlaepfer DD. Focal adhesion kinase: In command and control of cell motility. *Nat Rev Mol Cell Biol*. 2005;6(1):56–68. <http://dx.doi.org/10.1038/nrm1549>
98. Yamaguchi H, Condeelis J. Regulation of the actin cytoskeleton in cancer cell migration and invasion. *Biochim Biophys Acta*. 2007;1773(5):642–52. <http://dx.doi.org/10.1016/j.bbamcr.2006.07.001>
99. Fortin Ensign SP, Mathews IT, Symons MH, Berens ME, Tran NL. Implications of Rho GTPase signaling in glioma cell invasion and tumor progression. *Front Oncol*. 2013;3:241. <http://dx.doi.org/10.3389/fonc.2013.00241>
100. Salhia B, Tran NL, Chan A, Wolf A, Nakada M, Rutka F, et al. The guanine nucleotide exchange factors trio, Ect2, and Vav3 mediate the invasive behavior of glioblastoma. *Am J Pathol*. 2008;173(6):1828–38. <http://dx.doi.org/10.2353/ajpath.2008.080043>
101. Hirata E, Yukinaga H, Kamioka Y, Arakawa Y, Miyamoto S, Okada T, et al. In vivo fluorescence resonance energy transfer imaging reveals differential activation of Rho-family GTPases in glioblastoma cell invasion. *J Cell Sci*. 2012;125(Pt 4):858–68. <http://dx.doi.org/10.1242/jcs.089995>
102. Paulino VM, Yang Z, Kloss J, Ennis MJ, Armstrong BA, Loftus JC, et al. TROY (TNFRSF19) is overexpressed in advanced glial tumors and promotes glioblastoma cell invasion via Pyk2-Rac1 signaling. *Mol Cancer Res*. 2010;8(11):1558–67. <http://dx.doi.org/10.1158/1541-7786.MCR-10-0334>
103. Feng H, Hu B, Jarzynka MJ, Li Y, Keezer S, Johns TG, et al. Phosphorylation of dedicator of cytokinesis 1 (Dock180) at tyrosine residue Y722 by Src family kinases mediates EGFRvIII-driven glioblastoma tumorigenesis. *Proc Natl Acad Sci U S A*. 2012;109(8):3018–23. <http://dx.doi.org/10.1073/pnas.1121457109>

104. Feng H, Hu B, Liu KW, Li Y, Lu X, Cheng T, et al. Activation of Rac1 by Src-dependent phosphorylation of Dock180(Y1811) mediates PDGFR α -stimulated glioma tumorigenesis in mice and humans. *J Clin Invest.* 2011;121(12):4670–84. <http://dx.doi.org/10.1172/JCI58559>
105. Hu B, Shi B, Jarzynka MJ, Yiin JJ, D'Souza-Schorey C, Cheng SY. ADP-ribosylation factor 6 regulates glioma cell invasion through the IQ-domain GTPase-activating protein 1-Rac1-mediated pathway. *Cancer Res.* 2009;69(3):794–801. <http://dx.doi.org/10.1158/0008-5472.CAN-08-2110>
106. Servotte S, Camby I, Debeir O, Deroanne C, Lambert CA, Lapiere CM, et al. The in vitro influences of neurotensin on the motility characteristics of human U373 glioblastoma cells. *Neuropathol Appl Neurobiol.* 2006;32(6):575–84. <http://dx.doi.org/10.1111/j.1365-2990.2006.00760.x>
107. Nakada M, Drake KL, Nakada S, Niska JA, Berens ME. Ephrin-B3 ligand promotes glioma invasion through activation of Rac1. *Cancer Res.* 2006;66(17):8492–500. <http://dx.doi.org/10.1158/0008-5472.can-05-4211>
108. Fortin SP, Ennis MJ, Schumacher CA, Zylstra-Diegel CR, Williams BO, Ross JT, et al. Cdc42 and the guanine nucleotide exchange factors Ect2 and trio mediate Fn14-induced migration and invasion of glioblastoma cells. *Mol Cancer Res.* 2012;10(7):958–68. <http://dx.doi.org/10.1158/1541-7786.MCR-11-0616>
109. Nicholson-Dykstra S, Higgs HN, Harris ES. Actin dynamics: Growth from dendritic branches. *Curr Biol.* 2005;15(9):R346–57. <http://dx.doi.org/10.1016/j.cub.2005.04.029>
110. Nagano M, Hoshino D, Koshikawa N, Akizawa T, Seiki M. Turnover of focal adhesions and cancer cell migration. *Int J Cell Biol.* 2012;2012:310616. <http://dx.doi.org/10.1155/2012/310616>
111. Sen S, Ng WP, Kumar S. Contributions of talin-1 to glioma cell–matrix tensional homeostasis. *J R Soc Interface.* 2012;9(71):1311–17. <http://dx.doi.org/10.1098/rsif.2011.0567>
112. Lyons SA, Chung WJ, Weaver AK, Ogunrinu T, Sontheimer H. Autocrine glutamate signaling promotes glioma cell invasion. *Cancer Res.* 2007;67(19):9463–71. <http://dx.doi.org/10.1158/0008-5472.CAN-07-2034>
113. Rojas A, Dingledine R. Ionotropic glutamate receptors: Regulation by G-protein-coupled receptors. *Mol Pharmacol.* 2013;83(4):746–52. <http://dx.doi.org/10.1124/mol.112.083352>
114. Kim DY, Kim SH, Choi HB, Min C, Gwag BJ. High abundance of GluR1 mRNA and reduced Q/R editing of GluR2 mRNA in individual NADPH-diaphorase neurons. *Mol Cell Neurosci.* 2001;17(6):1025–33. <http://dx.doi.org/10.1006/mcne.2001.0988>
115. Isaac JT, Ashby MC, McBain CJ. The role of the GluR2 subunit in AMPA receptor function and synaptic plasticity. *Neuron.* 2007;54(6):859–71. <http://dx.doi.org/10.1016/j.neuron.2007.06.001>
116. Maas S, Patt S, Schrey M, Rich A. Underediting of glutamate receptor GluR-B mRNA in malignant gliomas. *Proc Natl Acad Sci U S A.* 2001;98(25):14687–92. <http://dx.doi.org/10.1073/pnas.251531398>
117. Ishiuchi S, Tsuzuki K, Yoshida Y, Yamada N, Hagimura N, Okado H, et al. Blockage of Ca(2+)-permeable AMPA receptors suppresses migration and induces apoptosis in human glioblastoma cells. *Nat Med.* 2002;8(9):971–8. <http://dx.doi.org/10.1038/nm746>
118. Beretta F, Bassani S, Binda E, VerPELLI C, Bello L, Galli R, et al. The GluR2 subunit inhibits proliferation by inactivating Src-MAPK signalling and induces apoptosis by means of caspase 3/6-dependent activation in glioma cells. *Eur J Neurosci.* 2009;30(1):25–34. <http://dx.doi.org/10.1111/j.1460-9568.2009.06804.x>
119. Watkins S, Sontheimer H. Hydrodynamic cellular volume changes enable glioma cell invasion. *J Neurosci.* 2011;31(47):17250–9. <http://dx.doi.org/10.1523/JNEUROSCI.3938-11.2011>
120. Habela CW, Ernest NJ, Swindall AF, Sontheimer H. Chloride accumulation drives volume dynamics underlying cell proliferation and migration. *J Neurophysiol.* 2009;101(2):750–7. <http://dx.doi.org/10.1152/jn.90840.2008>
121. Garzon-Muvdi T, Schiapparelli P, ap Rhys C, Guerrero-Cazares H, Smith C, Kim DH, et al. Regulation of brain tumor dispersal by NKCC1 through a novel role in focal adhesion regulation. *PLoS Biol.* 2012;10(5):e1001320. <http://dx.doi.org/10.1371/journal.pbio.1001320>
122. Olsen ML, Schade S, Lyons SA, Amaral MD, Sontheimer H. Expression of voltage-gated chloride channels in human glioma cells. *J Neurosci.* 2003;23(13):5572–82.
123. Soroceanu L, Manning TJ, Jr., Sontheimer H. Modulation of glioma cell migration and invasion using Cl(-) and K(+) ion channel blockers. *J Neurosci.* 1999;19(14):5942–54.

124. Lui VC, Lung SS, Pu JK, Hung KN, Leung GK. Invasion of human glioma cells is regulated by multiple chloride channels including CLC-3. *Anticancer Res.* 2010;30(11):4515–24.
125. Chen D, Song M, Mohamad O, Yu SP. Inhibition of Na⁺/K⁺-ATPase induces hybrid cell death and enhanced sensitivity to chemotherapy in human glioblastoma cells. *BMC Cancer.* 2014;14:716. <http://dx.doi.org/10.1186/1471-2407-14-716>
126. Turner KL, Honasoge A, Robert SM, McFerrin MM, Sontheimer H. A proinvasive role for the Ca(2+)-activated K(+) channel KCa3.1 in malignant glioma. *Glia.* 2014;62(6):971–81. <http://dx.doi.org/10.1002/glia.22655>
127. Cuddapah VA, Turner KL, Seifert S, Sontheimer H. Bradykinin-induced chemotaxis of human gliomas requires the activation of KCa3.1 and CLC-3. *J Neurosci.* 2013;33(4):1427–40. <http://dx.doi.org/10.1523/JNEUROSCI.3980-12.2013>
128. D'Alessandro G, Catalano M, Sciacaluga M, Chece G, Cipriani R, Rosito M, et al. KCa3.1 channels are involved in the infiltrative behavior of glioblastoma in vivo. *Cell Death Dis.* 2013;4:e773.
129. Thompson EG, Sontheimer H. A role for ion channels in perivascular glioma invasion. *Eur Biophys J.* 2016;45(7):635–48. <http://dx.doi.org/10.1007/s00249-016-1154-x>
130. Seifert S, Sontheimer H. Bradykinin enhances invasion of malignant glioma into the brain parenchyma by inducing cells to undergo amoeboid migration. *J Physiol.* 2014;592(22):5109–27. <http://dx.doi.org/10.1113/jphysiol.2014.274498>
131. Chedotal A, Kerjan G, Moreau-Fauvarque C. The brain within the tumor: New roles for axon guidance molecules in cancers. *Cell Death Differ.* 2005;12(8):1044–56. <http://dx.doi.org/10.1038/sj.cdd.4401707>
132. Wei W, Wang H, Ji S. Paradoxes of the EphB1 receptor in malignant brain tumors. *Cancer Cell Intl.* 2017;17:21. <http://dx.doi.org/10.1186/s12935-017-0384-z>
133. Holmberg J, Armulik A, Senti KA, Edoff K, Spalding K, Momma S, et al. Ephrin-A2 reverse signaling negatively regulates neural progenitor proliferation and neurogenesis. *Genes Dev.* 2005;19(4):462–71. <http://dx.doi.org/10.1101/gad.326905>
134. Nakada M, Niska JA, Miyamori H, McDonough WS, Wu J, Sato H, et al. The phosphorylation of EphB2 receptor regulates migration and invasion of human glioma cells. *Cancer Res.* 2004;64(9):3179–85. <http://dx.doi.org/10.1158/0008-5472.can-03-3667>
135. Ylivinkka I, Sihto H, Tynninen O, Hu Y, Laakso A, Kivisaari R, et al. Motility of glioblastoma cells is driven by netrin-1 induced gain of stemness. *J Exp Clin Cancer Res.* 2017;36(1):9. <http://dx.doi.org/10.1186/s13046-016-0482-0>
136. Dickinson RE, Dallol A, Bieche I, Krex D, Morton D, Maher ER, et al. Epigenetic inactivation of SLIT3 and SLIT1 genes in human cancers. *Br J Cancer.* 2004;91(12):2071–8. <http://dx.doi.org/10.1038/sj.bjc.6602222>
137. Yiin JJ, Hu B, Jarzynka MJ, Feng H, Liu KW, Wu JY, et al. Slit2 inhibits glioma cell invasion in the brain by suppression of Cdc42 activity. *Neuro Oncol.* 2009;11(6):779–89. <http://dx.doi.org/10.1215/15228517-2009-017>
138. Mertsch S, Schmitz N, Jeibmann A, Geng JG, Paulus W, Senner V. Slit2 involvement in glioma cell migration is mediated by Robo1 receptor. *J Neurooncol.* 2008;87(1):1–7. <http://dx.doi.org/10.1007/s11060-007-9484-2>
139. Tessier-Lavigne M, Goodman CS. The molecular biology of axon guidance. *Science.* 1996;274(5290):1123–33. <http://dx.doi.org/10.1126/science.274.5290.1123>
140. Kong Y, Janssen BJ, Malinauskas T, Vangoor VR, Coles CH, Kaufmann R, et al. Structural basis for plexin activation and regulation. *Neuron.* 2016;91(3):548–60. <http://dx.doi.org/10.1016/j.neuron.2016.06.018>
141. Janssen BJ, Malinauskas T, Weir GA, Cader ME, Siebold C, Jones EY. Neuropilins lock secreted semaphorins onto plexins in a ternary signaling complex. *Nat Struct Mol Biol.* 2012;19(12):1293–9. <http://dx.doi.org/10.1038/nsmb.2416>
142. Derijck AA, Van Erp S, Pasterkamp RJ. Semaphorin signaling: Molecular switches at the midline. *Trends Cell Biol.* 2010;20(9):568–76. <http://dx.doi.org/10.1016/j.tcb.2010.06.007>
143. Li X, Law JW, Lee AY. Semaphorin 5A and plexin-B3 regulate human glioma cell motility and morphology through Rac1 and the actin cytoskeleton. *Oncogene.* 2012;31(5):595–610.
144. Li X, Lee AY. Semaphorin 5A and plexin-B3 inhibit human glioma cell motility through RhoGDIalpha-mediated inactivation of Rac1 GTPase. *J Biol Chem.* 2010;285(42):32436–45. <http://dx.doi.org/10.1074/jbc.M110.120451>

145. Zhou X, Ma L, Li J, Gu J, Shi Q, Yu R. Effects of SEMA3G on migration and invasion of glioma cells. *Oncology Rep.* 2012;28(1):269–75.
146. Karayan-Tapon L, Wager M, Guilhot J, Levillain P, Marquant C, Clarhaut J, et al. Semaphorin, neuropilin and VEGF expression in glial tumours: SEMA3G, a prognostic marker? *Br J Cancer.* 2008;99(7):1153–60. <http://dx.doi.org/10.1038/sj.bjc.6604641>
147. Herman JG, Meadows GG. Increased class 3 semaphorin expression modulates the invasive and adhesive properties of prostate cancer cells. *Int J Oncol.* 2007;30(5):1231–8. <http://dx.doi.org/10.3892/ijo.30.5.1231>
148. Christensen C, Ambartsumian N, Gilestro G, Thomsen B, Comoglio P, Tamagnone L, et al. Proteolytic processing converts the repelling signal Sema3E into an inducer of invasive growth and lung metastasis. *Cancer Res.* 2005;65(14):6167–77. <http://dx.doi.org/10.1158/0008-5472.CAN-04-4309>
149. Massague J. TGF-beta signaling in development and disease. *FEBS Lett.* 2012;586(14):1833. <http://dx.doi.org/10.1016/j.febslet.2012.05.030>
150. Massaouf J, Hata A. TGF-beta signalling through the Smad pathway. *Trends Cell Biol.* 1997;7(5):187–92. [http://dx.doi.org/10.1016/S0962-8924\(97\)01036-2](http://dx.doi.org/10.1016/S0962-8924(97)01036-2)
151. Joseph JV, Conroy S, Tomar T, Eggens-Meijer E, Bhat K, Copray S, et al. TGF-beta is an inducer of ZEB1-dependent mesenchymal transdifferentiation in glioblastoma that is associated with tumor invasion. *Cell Death Dis.* 2014;5:e1443. <http://dx.doi.org/10.1038/cddis.2014.395>
152. Hsieh HL, Wang HH, Wu WB, Chu PJ, Yang CM. Transforming growth factor-beta1 induces matrix metalloproteinase-9 and cell migration in astrocytes: Roles of ROS-dependent ERK- and JNK-NF-kappaB pathways. *J Neuroinflammation.* 2010;7:88. <http://dx.doi.org/10.1186/1742-2094-7-88>
153. Platten M, Wick W, Wild-Bode C, Aulwurm S, Dichgans J, Weller M. Transforming growth factors beta(1) (TGF-beta(1)) and TGF-beta(2) promote glioma cell migration via up-regulation of alpha(V) beta(3) integrin expression. *Biochem Biophys Res Commun.* 2000;268(2):607–11. <http://dx.doi.org/10.1006/bbrc.2000.2176>
154. Liu S, Sun J, Lan Q. TGF-beta-induced miR10a/b expression promotes human glioma cell migration by targeting PTEN. *Mol Med Rep.* 2013;8(6):1741–6.
155. Canazza A, Calatozzolo C, Fumagalli L, Bergantin A, Ghielmetti F, Fariselli L, et al. Increased migration of a human glioma cell line after in vitro CyberKnife irradiation. *Cancer Biol Ther.* 2011;12(7):629–33. <http://dx.doi.org/10.4161/cbt.12.7.16862>
156. Thiery JP, Acloque H, Huang RY, Nieto MA. Epithelial-mesenchymal transitions in development and disease. *Cell.* 2009;139(5):871–90. <http://dx.doi.org/10.1016/j.cell.2009.11.007>
157. Chaffer CL, Weinberg RA. A perspective on cancer cell metastasis. *Science.* 2011;331(6024):1559–64. <http://dx.doi.org/10.1126/science.1203543>
158. Iwadata Y. Epithelial-mesenchymal transition in glioblastoma progression. *Oncol Lett.* 2016;11(3):1615–20. <http://dx.doi.org/10.3892/ol.2016.4113>
159. Moustakas A, Heldin CH. Signaling networks guiding epithelial-mesenchymal transitions during embryogenesis and cancer progression. *Cancer Sci.* 2007;98(10):1512–20. <http://dx.doi.org/10.1111/j.1349-7006.2007.00550.x>
160. Khan MA, Chen HC, Zhang D, Fu J. Twist: A molecular target in cancer therapeutics. *Tumour Biol.* 2013;34(5):2497–506. <http://dx.doi.org/10.1007/s13277-013-1002-x>
161. Elias MC, Tozer KR, Silber JR, Mikheeva S, Deng M, Morrison RS, et al. TWIST is expressed in human gliomas and promotes invasion. *Neoplasia.* 2005;7(9):824–37. <http://dx.doi.org/10.1593/neo.04352>
162. Nordfors K, Haapasalo J, Makela K, Granberg KJ, Nykter M, Korja M, et al. Twist predicts poor outcome of patients with astrocytic glioma. *J Clin Pathol.* 2015;68(11):905–12. <http://dx.doi.org/10.1136/jclinpath-2015-202868>
163. Wang Y, Shi J, Chai K, Ying X, Zhou BP. The role of snail in EMT and tumorigenesis. *Curr Cancer Drug Targets.* 2013;13(9):963–72. <http://dx.doi.org/10.2174/15680096113136660102>
164. Han SP, Kim JH, Han ME, Sim HE, Kim KS, Yoon S, et al. SNAIL1 is involved in the proliferation and migration of glioblastoma cells. *Cell Mol Neurobiol.* 2011;31(3):489–96. <http://dx.doi.org/10.1007/s10571-010-9643-4>
165. Myung JK, Choi SA, Kim SK, Wang KC, Park SH. Snail plays an oncogenic role in glioblastoma by promoting epithelial mesenchymal transition. *Int J Clin Exp Pathol.* 2014;7(5):1977–87.

166. Liu B, Dong H, Lin X, Yang X, Yue X, Yang J, et al. RND3 promotes Snail 1 protein degradation and inhibits glioblastoma cell migration and invasion. *Oncotarget*. 2016;7(50):82411–23. <http://dx.doi.org/10.18632/oncotarget.12396>
167. Yang HW, Menon LG, Black PM, Carroll RS, Johnson MD. SNAI2/Slug promotes growth and invasion in human gliomas. *BMC Cancer*. 2010;10:301. <http://dx.doi.org/10.1186/1471-2407-10-301>
168. Hill L, Browne G, Tulchinsky E. ZEB/miR-200 feedback loop: At the crossroads of signal transduction in cancer. *Int J Cancer*. 2013;132(4):745–54. <http://dx.doi.org/10.1002/ijc.27708>
169. Wellner U, Schubert J, Burk UC, Schmalhofer O, Zhu F, Sonntag A, et al. The EMT-activator ZEB1 promotes tumorigenicity by repressing stemness-inhibiting microRNAs. *Nat Cell Biol*. 2009;11(12):1487–95. <http://dx.doi.org/10.1038/ncb1998>
170. Zhang L, Zhang W, Li Y, Alvarez A, Li Z, Wang Y, et al. SHP-2-upregulated ZEB1 is important for PDGFRalpha-driven glioma epithelial-mesenchymal transition and invasion in mice and humans. *Oncogene*. 2016;35(43):5641–52. <http://dx.doi.org/10.1038/onc.2016.100>
171. Qi S, Song Y, Peng Y, Wang H, Long H, Yu X, et al. ZEB2 mediates multiple pathways regulating cell proliferation, migration, invasion, and apoptosis in glioma. *PLoS One*. 2012;7(6):e38842. <http://dx.doi.org/10.1371/journal.pone.0038842>
172. Maitre JL, Heisenberg CP. Three functions of cadherins in cell adhesion. *Curr Biol*. 2013;23(14):R626–33. <http://dx.doi.org/10.1016/j.cub.2013.06.019>
173. Thiery JP. Epithelial-mesenchymal transitions in tumour progression. *Nat Rev Cancer*. 2002;2(6):442–54. <http://dx.doi.org/10.1038/nrc822>
174. Asano K, Kubo O, Tajika Y, Takakura K, Suzuki S. Expression of cadherin and CSF dissemination in malignant astrocytic tumors. *Neurosurg Rev*. 2000;23(1):39–44.
175. Redies C. Cadherins in the central nervous system. *Prog Neurobiol*. 2000;61(6):611–48. [http://dx.doi.org/10.1016/S0301-0082\(99\)00070-2](http://dx.doi.org/10.1016/S0301-0082(99)00070-2)
176. Lewis-Tuffin LJ, Rodriguez F, Giannini C, Scheithauer B, Necela BM, Sarkaria JN, et al. Misregulated E-cadherin expression associated with an aggressive brain tumor phenotype. *PLoS One*. 2010;5(10):e13665. <http://dx.doi.org/10.1371/journal.pone.0013665>
177. Camand E, Peglion F, Osmani N, Sanson M, Etienne-Manneville S. N-cadherin expression level modulates integrin-mediated polarity and strongly impacts on the speed and directionality of glial cell migration. *J Cell Sci*. 2012;125(Pt 4):844–57. <http://dx.doi.org/10.1242/jcs.087668>
178. Musumeci G, Magro G, Cardile V, Coco M, Marzagalli R, Castrogiovanni P, et al. Characterization of matrix metalloproteinase-2 and -9, ADAM-10 and N-cadherin expression in human glioblastoma multiforme. *Cell Tissue Res*. 2015;362(1):45–60. <http://dx.doi.org/10.1007/s00441-015-2197-5>
179. Asano K, Duntsch CD, Zhou Q, Weimar JD, Bordelon D, Robertson JH, et al. Correlation of N-cadherin expression in high grade gliomas with tissue invasion. *J Neurooncol*. 2004;70(1):3–15. <http://dx.doi.org/10.1023/B:NEON.0000040811.14908.f2>
180. Perego C, Vanoni C, Massari S, Raimondi A, Pola S, Cattaneo MG, et al. Invasive behaviour of glioblastoma cell lines is associated with altered organisation of the cadherin-catenin adhesion system. *J Cell Sci*. 2002;115(Pt 16):3331–40.
181. Siebzehnrubl FA, Silver DJ, Tugertimur B, Deleyrolle LP, Siebzehnrubl D, Sarkisian MR, et al. The ZEB1 pathway links glioblastoma initiation, invasion and chemoresistance. *EMBO Mol Med*. 2013;5(8):1196–212. <http://dx.doi.org/10.1002/emmm.201302827>

6

Noncoding RNAs in Glioblastoma

YING ZHANG¹ • NICHOLA CRUICKSHANKS¹ • MARY PAHUSKI¹ •
FANG YUAN¹ • ANINDYA DUTTA² • DAVID SCHIFF^{3,4} •
BENJAMIN PUROW^{3,4} • ROGER ABOUNADER^{1,3,4}

¹Department of Microbiology, Immunology, and Cancer Biology, University of Virginia, Charlottesville, VA, USA; ²Department of Biochemistry and Molecular Genetics, University of Virginia, Charlottesville, VA, USA; ³Department of Neurology, University of Virginia, Charlottesville, VA, USA; ⁴Cancer Center, University of Virginia, Charlottesville, VA, USA

Author for correspondence: Roger Abounader, Department of Microbiology, Immunology, and Cancer Biology, University of Virginia, Old Medical School, Room 4819, PO Box 800168, Charlottesville, VA 22908, USA. E-mail: ra6u@virginia.edu

Doi: <http://dx.doi.org/10.15586/codon.glioblastoma.2017.ch6>

Abstract: The vast majority of the human genome is transcribed into noncoding RNAs. Among these, microRNAs (miRNA) and long noncoding RNAs (lncRNA) are frequently deregulated in cancer, where they regulate a wide variety of functions. Glioblastoma (GBM) is the most common and the most deadly primary human brain tumor. This chapter reviews the deregulation, functions, mechanisms of action, and clinical applications of miRNAs and lncRNAs in GBM. miRNAs are short noncoding RNAs that broadly and profoundly regulate gene expression. Numerous miRNAs are deregulated in GBM, where their expression levels can serve as diagnostic and prognostic biomarkers. miRNAs can act as oncogenes or tumor suppressors in GBM by regulating the expression of numerous tumor-suppressive or oncogenic proteins. miRNAs regulate all GBM malignancy parameters including tumor cell proliferation, cell survival, invasion, angiogenesis, cancer stem cells, immune escape, and therapy resistance. miRNAs are also secreted in body fluids, where they can be used as biomarkers. Because of

In: *Glioblastoma*. Steven De Vleeschouwer (Editor), Codon Publications, Brisbane, Australia
ISBN: 978-0-9944381-2-6; Doi: <http://dx.doi.org/10.15586/codon.glioblastoma.2017>

Copyright: The Authors.

Licence: This open access article is licenced under Creative Commons Attribution 4.0 International (CC BY 4.0). <https://creativecommons.org/licenses/by-nc/4.0/>

their deep involvement in GBM malignancy, efforts are under way to also exploit miRNAs as therapeutic agents or targets. lncRNAs are a diverse group of noncoding RNAs that are >200 nucleotides long. Several lncRNAs are deregulated in GBM, where their expressions can associate with clinical parameters. lncRNAs regulate GBM functions including tumor cell proliferation, survival, invasion, cancer stem cell differentiation, and therapy resistance. lncRNAs exert their actions via transcriptional, post-transcriptional, and epigenetic mechanisms that are only partly understood. Studying noncoding RNAs is important for the understanding, management, and development of future therapies for GBM.

Key words: Cancer stem cells; Glioblastoma; Glioma; Long noncoding RNA; microRNA

Introduction

The vast majority (>80%) of the human genome is transcribed into RNA. However, only ~2% of RNA is translated into proteins. Consequently, the vast majority of cellular RNAs are noncoding RNAs (ncRNAs). ncRNAs function as crucial regulators of biological, physiological, and pathological processes and are not evolutionary junk as previously thought. In the last decade, the small ncRNAs (microRNAs; 17–22 nucleotides) and long ncRNAs (lncRNAs; >200 nucleotides) have been extensively studied in cancer and have furthered our understanding and knowledge of cancer initiation and progression, and offered new therapeutic avenues. A large number of studies have shown that microRNAs and lncRNAs play important roles in almost every aspect of cancer, including tumor initiation, progression, and resistance to therapy, as well as providing biomarkers for diagnosis and prognosis and serving as therapeutic agents or targets. This chapter reviews the roles of microRNAs and lncRNAs in glioblastoma (GBM).

Glioblastoma

Gliomas are the most common and most malignant primary human brain tumors. They are extremely aggressive tumors that account for the majority of deaths due to primary brain neoplasms (1). Despite the most advanced treatment with combinations of surgery, radiotherapy, and chemotherapy, the most commonly diagnosed grade IV GBM is associated with an average life expectancy of only 14 months. The origin of gliomas is largely unknown, but there is increasing speculation that they might arise from glioma stem cells (GSCs), which might consist of transformed normal neural stem cells (NSCs). GBM malignancy is driven by the deregulation of molecules and pathways that control tumor cell proliferation, survival, invasion, and stem cell differentiation (2). The Cancer Genome Atlas (TCGA) classified these molecular deregulations as belonging to three major pathways: Receptor tyrosine kinase (RTK), p53, and Rb pathways (3). Factors responsible for GBM malignancy and poor prognosis include rapid cell proliferation, resistance to apoptosis, invasion of the surrounding brain, high levels of angiogenesis, immune evasion, and the existence of therapy-resistant GSCs.

MicroRNAs

MicroRNAs (miRNAs) are short, noncoding, endogenous RNAs (17–22 nucleotides) that post-transcriptionally regulate gene expression. More than 3,000 human miRNAs have been identified to date (4, 5). Around two-thirds of miRNA coding genes are located in introns (6, 7). One-third of miRNAs are transcribed as independent single transcriptional units or in clusters (6–8). MiRNA genes are transcribed by RNA polymerase II as pri-miRNA and then processed into pre-miRNA by the RNase III enzyme Drosha and its interacting partner DGCR8 or Pasha. The pre-miRNA is exported to the cytoplasm by exportin-5 and converted into a mature duplex by the Dicer complex (9–11). Mature miRNAs regulate their targets by incorporating into the RNA-induced silencing complex (RISC) and directing it to the targeted mRNA 3' untranslated region (3'UTR) (12). MiRNAs directly cleave the mRNA or inhibit protein synthesis, according to the degree of complementarities with their targets' 3' untranslated regions (3'UTR) (Figure 1). Notably, single miRNAs can regulate the expressions of numerous genes and most genes are regulated by multiple miRNAs. Computational predictions of miRNA targets suggest that more than 60% of human protein expressions are regulated by miRNAs (13). miRNAs are frequently deregulated in human cancers via genetic, epigenetic, transcriptional, and processing mechanisms (14–19). Deregulation of miRNA expression has been associated with cancer initiation, progression, and metastasis (20, 21). By targeting the mRNAs of oncogenes or tumor suppressors, miRNAs can act as tumor suppressors or oncogenes, respectively. miRNAs regulate all aspects of cancer biology including cell cycle, proliferation, death, apoptosis, migration, invasion, metastasis, angiogenesis, tumor microenvironment, tumor immunology, and cancer stem cell biology (5) (Figure 2). Thus, correcting miRNA deficiencies by either antagonizing or restoring miRNA function may provide a therapeutic benefit.

miRNA DEREGULATION AND ASSOCIATION WITH CLINICAL PARAMETERS IN GBM

Several studies have shown that miRNA expression is deregulated in GBM. Recent reviews (22, 23) summarized the differentially expressed miRNAs in GBM and showed that 256 miRNAs were significantly overexpressed and 95 miRNAs were significantly downregulated in GBM as compared to the normal brain tissue. There follows a brief survey of select deregulated miRNAs in GBM.

MiR-21 was the first miRNA to be linked with glioma malignancy. Most reports describe miR-21 as an oncogenic miRNA. MiR-21 levels are elevated in human glioma cells and tissues as compared to normal glial cells and/or brain (24–26). In addition, miR-21 levels in gliomas correlate with tumor grade, and low miR-21 levels in human tumors are associated with slightly better survival according to the TCGA database (27, 28).

Several reports have implicated miR-221/222 in glioma malignancy. A screening study identified miR-221 as one of the most frequently upregulated miRNAs in human glioma tumors and cell lines (29). MiR-221 upregulation was confirmed in a subsequent study which also found that miR-221 levels are further increased

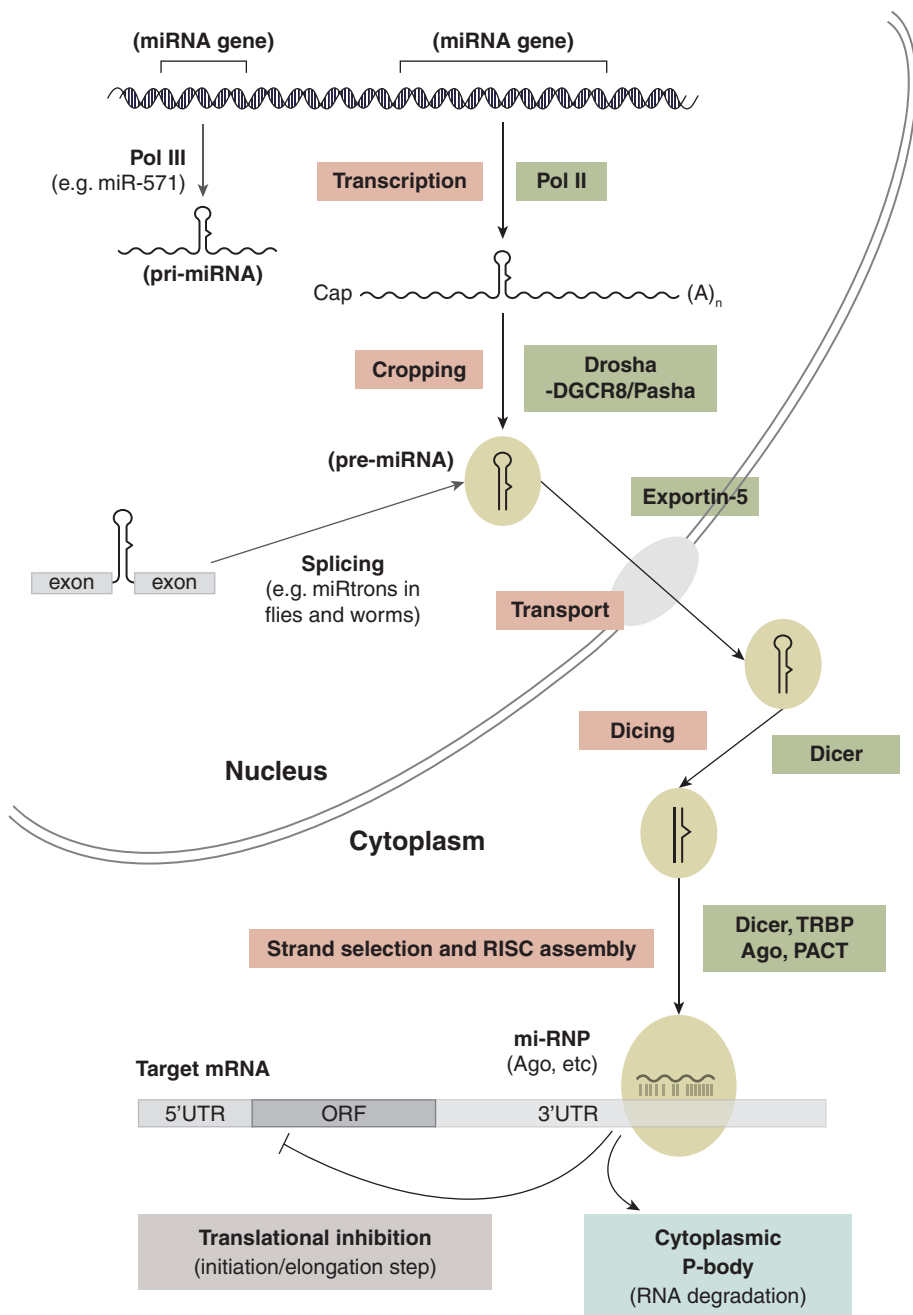


Figure 1 miRNA biogenesis and functions. Black lines indicate the canonical pathway, with minor pathways depicted in gray lines. Modified with permission from Lee and Dutta (5).

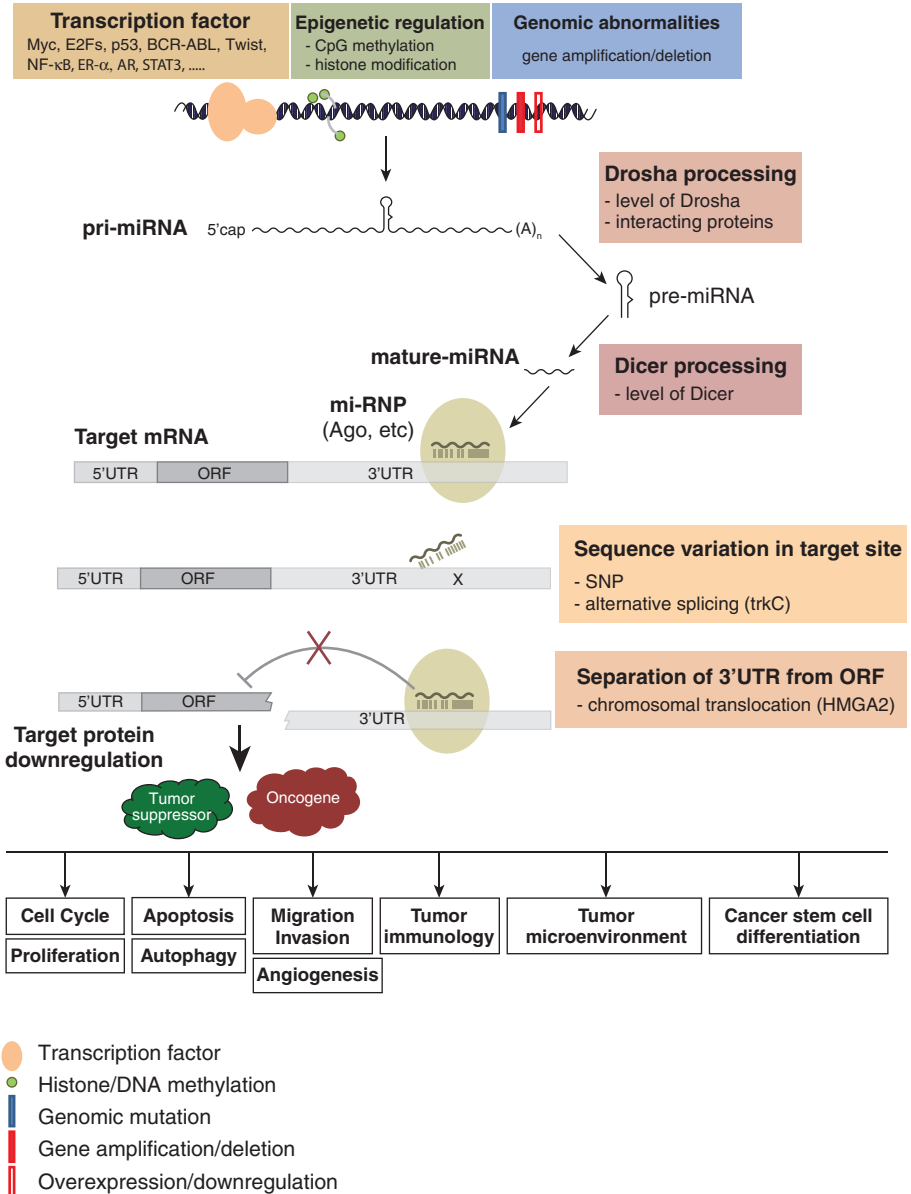


Figure 2 Mechanisms of miRNA deregulation in cancer. Modified with permission from Lee and Dutta (5).

in higher grade tumors (30). TCGA data show that miR-221/222 downregulation in human tumors is associated with a better patient prognosis.

MiR-181a, miR-181b, and miR-181c were reported to be downregulated in GBM cells and tumors (29). miR-181a and, to a greater extent, miR-181b were subsequently described as tumor suppressors (31). Moreover, miR-181b and miR-181c were significantly downregulated in patients who responded to radiation therapy and temozolomide (TMZ) in comparison to patients with progressive disease. It was therefore proposed that expression levels of miR-181b and miR-181c could serve as a predictive marker of response to therapy in GBM patients (32).

Two high-profile publications identified miR-26a as a regulator of the tumor suppressor PTEN in gliomas (33, 34). The first publication showed that miR-26a gene is frequently amplified in human gliomas and that this is associated with monoallelic PTEN loss. The second publication used a multidimensional genomic data set of GBM from TCGA to identify miR-26a as a cooperating component of a frequently occurring amplicon that also contains CDK4 and CENTG1, two oncogenes that regulate the RB1 and PI3K/AKT pathways, respectively.

Analysis of human specimens showed that miR-34a expression is downregulated in GBM tissues compared to normal brain and in mutant p53 gliomas as compared with wild-type p53 gliomas. MiR-34a was also downregulated in GBM cell lines compared to astrocytes. MiR-34a levels in human gliomas were inversely correlated to RTK MET, measured in the same tumors (35).

MiR-148a expression was elevated in human GBM specimens, cell lines, and GSC compared with normal human brain and astrocytes. High expression of miR-148a significantly correlated with survival in TCGA samples. Therefore, miR-148a can serve as a prognostic oncogenic miRNA in GBM (36).

MiR-10b expression was upregulated in glioma samples as compared to non-neoplastic brain tissues, and expression levels were associated with higher grade tumors. Several lines of evidence suggest that miR-10b plays a role in glioma invasion (37, 38).

A recent study identified miR-182 as a prognostic marker for glioma progression and patient survival (39). miR-182 was upregulated in glioma cell lines and primary glioma specimens as compared to normal brain. miR-182 expression levels in the tumors significantly correlated with tumor grade and clinical features. The 5-year survival rates of patients with low miR-182 levels were significantly better than the survival rates of patients with high miR-182 levels. Additional miRNAs that are differentially expressed in GBM are listed in Table 1.

SECRETED miRNAs AS GBM BIOMARKERS

GBM cells shed microvesicles with cytoplasmic contents including substantial quantities of miRNAs that are stably preserved to allow quantitation in patient serum and cerebrospinal fluid. The quantification of miRNAs in fluid samples would permit noninvasive determination of GBM features based on miRNA signatures (40, 41). Interestingly, microvesicle shedding by GBM cells enables them to “share” miRNAs with surrounding cells, modifying nearby stromal cells, and essentially terraforming their environment (42). There are many examples of miRNAs released from tumor cells that indicate the importance

TABLE 1 Deregulated miRNAs with Their Correlations with Survival, Targets, and Functions in Glioblastoma

miRNA	Survival correlation			Function	
	Expression in GBM (glioma)	Survival correlation	Targets	Overexpression	Anti-miR
Let-7	Down		KRAS	Migration↓, Proliferation↓, <i>In vivo</i> tumor growth↓	
Hsa-miR-7	Down		FAK, EGFR, AKT <i>PI3K</i> , <i>RAF1</i>	Viability↓, Migration↓, Invasiveness↓, Proliferation↓, <i>In vivo</i> tumor growth↓, Radiosensitivity↓, GSC proliferation and invasion↓	
Hsa-miR-9	Up (Up in high-grade tumor)		CAMTA1		
Hsa-miR-10ab	Up (Up in TMZ-resistant tumor)	Y	HOXD10		
Hsa-miR-15a	Up (Up in high-grade tumor)				
Hsa-miR-15b	(Down in high-grade tumor)		CCNE1	Proliferation↑	Proliferation↓
Hsa-miR-16	Up (Up in high-grade tumor)				
Hsa-miR-17-92 cluster	Up (Disputed in high-grade tumor, CD133+ cells)		POLD2, TGFβ-RII, CTGF, CAMTA1, ATG7	Angiogenesis↑, Growth↑, GSC apoptosis↑, proliferation↓	Viability↓, Apoptosis↑, Proliferation↓
Hsa-miR-18a	Up (Up in low-grade tumor)		Smad4, CTGF	Angiogenesis↑, Growth↑	Viability↓, Apoptosis↑, Proliferation↓

Table continued on following page

TABLE 1 Deregulated miRNAs with Their Correlations with Survival, Targets, and Functions in Glioblastoma (Continued)

miRNA	Expression in GBM (glioma)	Survival correlation	Targets	Function	
				Overexpression	Anti-miR
Hsa-miR-19a	Disputed (Up in high-grade tumor)		CTGF		Viability↓, Apoptosis↑, Proliferation↓
Hsa-miR-20a	Up (Up in high-grade tumor)		TGFβ-RII, CTGF	Angiogenesis↑, Growth↑	Viability↓, Proliferation↓
Hsa-miR-21	Up (Up in high-grade tumor)	Y	RECK, TIMP3, APAF1, NP32A, SMARCA4, Sptyl2, Caspases, PTEN, Cdc25A, HNRPK, TAp63, RRF1P1, PDCCD4, p53	Invasiveness↑	Invasiveness↓, Apoptosis↑, Viability↓, Proliferation↓, In vivo tumor volume↓, Chemosensitivity↑, Radiosensitizes↑
Hsa-miR-23a	(Down in high-grade tumor)				
Hsa-miR-25	Up (Up in high-grade tumor)		Mdm2, TSC1	In vivo tumor growth ↓	
Hsa-miR-26a	Up	Y	PTEN, Rb1 and MAP3K2/ MEKK2	In vivo tumor growth ↑	
Hsa-miR-28	Up (Up in high-grade tumor)		KRAS		
Hsa-miR-30bc	Disputed		SIRT1, MET, NOTCH1/2, MsiI, PDGFRA,	Viability↓, Proliferation↓, Apoptosis↑, Invasiveness↓, In vivo tumor growth ↓, Differentiation↑, GSC stemness↓	
Hsa-miR-34a	Down (Down in GSCs, Down in proneural subtype)				

TABLE 1 Deregulated miRNAs with Their Correlations with Survival, Targets, and Functions in Glioblastoma (Continued)

miRNA	Expression in GBM (glioma)	Survival correlation	Targets	Function	
				Overexpression	Anti-miR
Hsa-miR-93	Up		Integrin- β 8	Angiogenesis \uparrow , Proliferation \uparrow , <i>In vivo</i> tumor growth \uparrow	
Hsa-miR-96	Up		KRAS		
Hsa-miR-100	Down		ATM	Radiosensitivity \uparrow	
Hsa-miR-124/137	Down	Y	PTBP1, STAT3	Proliferation \downarrow , Migration \downarrow , Invasiveness \downarrow , Stemness \downarrow , GSC differentiation \uparrow	
Hsa-miR-125b	Down		Bmf, MAZ	Invasiveness \uparrow , Apoptosis \downarrow , Proliferation \uparrow	
Hsa-miR-128	Down		WEE1, p70S6K1, Msi1, E2F3a, Bmi-1, EGFR, PDGFR α	Angiogenesis \downarrow , Proliferation \downarrow , <i>In vivo</i> tumor growth \downarrow , inhibition of GSC stemness and self-renewal \downarrow	
Hsa-miR-130b	Up (Up in high-grade tumor)				
Hsa-miR-133a	(Down in high-grade tumor)				
Hsa-miR-134	Up		KRAS and STAT5B		

Table continued on following page

TABLE 1 Deregulated miRNAs with Their Correlations with Survival, Targets, and Functions in Glioblastoma (Continued)

miRNA	Expression in GBM (glioma)	Survival correlation	Targets	Function	
				Overexpression	Anti-miR
Hsa-miR-135b	Up (Up in GSCs)				
Hsa-miR-137	Down (Down in late-stage tumor)		CDK6, Msi1, Cox-2	Proliferation↓, Invasiveness↓, Migration↓, <i>In vivo</i> tumor growth↓	
Hsa-miR-140	Up (Up in high-grade tumor)				
Hsa-miR-141	Disputed (UP in GSCs)				
Hsa-miR-146b-5p	Down		EGFR, MMP16	Invasiveness↓, Migration↓, Proliferation↓, <i>In vivo</i> tumor growth ↓	
Hsa-miR-148a	Up	Y		Proliferation↑, Apoptosis↓, Angiogenesis↑, <i>In vivo</i> tumor growth ↑	Proliferation↓, Apoptosis↑
Hsa-miR-150	Down in high-grade tumor				
Hsa-miR-153	Down		Bcl-2, Mcl-1, Irs-2	Proliferation↓, Viability↓, Apoptosis↑	
Hsa-miR-181abc	Down		Bcl-2	Proliferation↓, Apoptosis↑, Invasiveness↓, Chemosensitivity and Radiosensitivity↑	

TABLE 1
Deregulated miRNAs with Their Correlations with Survival, Targets, and Functions in Glioblastoma (Continued)

miRNA	Expression in GBM (glioma)	Survival correlation	Targets	Function	
				Overexpression	Anti-miR
Hsa-miR-182/183	Up (Up at late-stage tumor)	Y			
Hsa-miR-184	Down (Down in high-grade tumor)		Akt2	Apoptosis ↑, Invasiveness ↓	
Hsa-miR-193	Up		KRAS		
Hsa-miR-195	Up in TMZ resistant)		CCND3, E2F3, CCND1	Proliferation ↓, Invasiveness ↓	Chemoresensitivity, Viability ↓
Hsa-miR-196ab	Up	Y			
Hsa-miR-197	(Down in high-grade tumor)				
Hsa-miR-200c	Up (High in GSCs)				
Hsa-miR-205	Disputed (High in GSCs)		VEGF-A	Proliferation ↓, Apoptosis ↑, Invasiveness ↓	
Hsa-miR-210	Up (Up in high-grade tumor)	Y	HIF3α	Enhanced vasculogenesis	Reduced vascular density and tumor growth <i>in vivo</i>
Hsa-miR-218	Down (Down in mesenchymal subtype)		IKK-β, HIF2α	Invasiveness ↓	
Hsa-miR-221/222	Up (Up in high-grade tumor, CD133+ cells)	Y	P27, Akt, PUMA, P57, PTPμ, BIRC1, NIAF, ICAM-1	Proliferation ↑, Invasiveness ↑, <i>In vivo</i> tumor growth ↑, Apoptosis ↓, Migration ↑	Proliferation ↓, Apoptosis ↑, <i>In vivo</i> tumor volume ↓, STAT1/2 upregulation

Table continued on following page

TABLE 1 Deregulated miRNAs with Their Correlations with Survival, Targets, and Functions in Glioblastoma (Continued)

miRNA	Expression in GBM (glioma)	Survival correlation	Targets	Function	
				Overexpression	Anti-miR
Hsa-miR-296	Up				Reduced angiogenesis
Hsa-miR-297	Down				
Hsa-miR-301a	Up (Up in GSCs)				
Hsa-miR-326	Down		NOTCH 1/2, PKM2	Proliferation↓, Apoptosis↑, Viability↓, Invasiveness↓, <i>In vivo</i> tumor growth↓, GSC stemness↓	
Hsa-miR-328	(Up in invading cells)	Y	SFRP1, ABCG2	Invasiveness↑	Invasiveness↓
Hsa-miR-335	Up		Daam1	Viability↑, Invasiveness↑	Apoptosis↑, Invasiveness↓, <i>In vivo</i> tumor growth↓
Hsa-miR-339-5p	Down (Down in GSCs)		ICAM-1		
Hsa-miR-363	Up (Up in GSCs)		Bim, Caspase3	Proliferation↑, Apoptosis↓	Proliferation↓, Apoptosis↑
Hsa-miR-365a	(Down in GSCs)		KRAS, MAX	Proliferation↓, Invasiveness↓, Cell cycle↓	Proliferation↑, Migration↑
Hsa-miR-367-302	Up, (Up in GSCs)				
Hsa-miR-371-373	Up, (Up in GSCs)				

TABLE 1 Deregulated miRNAs with Their Correlations with Survival, Targets, and Functions in Glioblastoma (Continued)

miRNA	Expression in GBM (glioma)	Survival correlation	Targets	Function	
				Overexpression	Anti-miR
Hsa-miR-451	Disputed, (Up in GSCs)	High with poor survival Y	CAB39	Proliferation↓, Invasion↓, Stemness↓, Neurosphere formation↓, Sensitized cells to glucose deprivation	Migration↑
Hsa-miR-455	(Up in TMZ resistant)				
Hsa-miR-497	(Down in high-grade tumor)				
Hsa-miR-548b	(Down in high-grade tumor)				
Hsa-miR-582-5p	Up (Up in GSCs)		Caspase 3/9	Proliferation↑, Apoptosis↓	Proliferation↓, Apoptosis↑

of their roles in the modulation of the microenvironment in GBM (Table 2). MiR-21 is upregulated (43), while miR-205 is downregulated in patient plasma (44, 45). Many more miRNAs have been described as highly expressed in peripheral blood as compared to normal samples (46). MiR-454-3p was highly expressed in the plasma of GBM patients as compared to healthy controls and was lower in low-grade glioma. Furthermore, miR-454-3p expression in the postoperative plasma is markedly downregulated in comparison to preoperative plasma, and a correlation of worsening prognosis of glioma was observed with increasing miR-454-3p expression (47). MiR-29 levels in serum can serve to distinguish the progression of malignancy from stage I–II to stage III–IV (48). In addition, a huge increase in miR-210 expression was found in serum samples of GBM patients compared to controls and this was associated with tumor grade and poor outcome (48). A study of serum miRNA profiles found a significant difference of miRNA levels between untreated high-grade astrocytomas (grade III–IV) and controls in a genome-wide miRNA analysis. Seven miRNAs (miR-15b*, miR-23a, miR-133a, miR-150*, miR-197, miR-497, and miR-548b-5p) were markedly decreased in grade II–IV patients and showed high specificity (97.87%) and sensitivity (88.00%) for the prediction of malignant astrocytomas (48, 49).

MiRNAs in GSCs

GSCs are major contributors to therapy resistance in gliomas. It was shown that CD133+ tumor cells, presumably GSCs, represent the cellular population that confers glioma radioresistance and could be the source of tumor recurrence after radiation (50). It was hypothesized that GSCs originate from transformed NSCs. This hypothesis was recently supported by a study that found that gliomas display a miRNA expression profile reminiscent of neural precursor cells (51). Discussed below are select critical miRNAs that have been implicated in the regulation of GSCs (summarized in Figure 3 and Table 1). A study assessed the effects of miR-124 and miR-137 on the differentiation of mouse NSCs, mouse oligodendrogloma-derived stem cells, and human GSCs (26). Transfection of miR-124 or miR-137 induced morphological changes and marker expressions consistent with neuronal differentiation in mouse NSCs, mouse oligodendrogloma-derived stem cells derived from S100 β -v-erbB tumors, and CD133+ human GBM-derived stem cells. This study therefore implicated miR-124 and miR-137 in the differentiation of NSCs and GSCs. A subsequent report examined the miRNA profiles of GSC and nonstem cell populations and found that several miRNAs including miR-451, miR-486, and miR-425 were upregulated in the GSCs (53). The expression of miR-451 is regulated by SMADs, which have been previously associated with GSC regulation, through binding to promoter region of miR-451 gene (54). Two studies uncovered critical roles of miRNA-34a in GSCs (35, 55). It was first shown that miR-34a is downregulated in human GBM and exerts potent tumor-suppressive effects in glioma cells and stem cells via direct inhibition of MET, NOTCH1, and NOTCH2 expressions. NOTCH is a critical regulator of normal and cancer stem cell maintenance (56–58). NOTCH pathway activation enhances the stemness, proliferation, and radioresistance of GSCs (57–60). These studies therefore implicated miR-34a in the regulation of GSCs partly via regulation of

TABLE 2
Deregulated lncRNAs with Their Correlations with Survival, Targets/Mechanisms of Action and Functions in Glioblastoma

lncRNA	Expression in GBM (glioma)	Survival correlation	Targets/Mechanisms of action	Function	
				Overexpression	Under-expression
<i>linc-RoR</i>	Down		KLF4	Proliferation↓, Sphere formation↓	Proliferation↑, Sphere formation↑,
<i>ADAMTS9-AS2</i>	Down	Y		Migration↓	Migration↑
<i>CRNDE</i>	Up	Y	polycomb repressive complex 2 and CoREST complexes, MiR-384, miR-186	Cell growth↑, Invasion↑, Apoptosis↓	
<i>H19</i>	(Up in high grade)			Invasion↑	
<i>HOTAIR</i>	Up	Y	EZH2, miR-148b-3p		Cell cycle↓, <i>in vivo</i> tumor growth↓
<i>Xist</i>				X-chromosome inactivation↓	
<i>HOTAIRM1</i>	Up				
<i>MEG3</i>	Down		p53	Proliferation↓, Apoptosis↑	
<i>MALAT1</i>	(Up at hypoxic conditions)		AIM1, LAYN, HMMR, SLC26A2, CCT4, ROD1, CTHRC1, and FHL1	Migration↓	
<i>MIR210HG</i>	(Up at hypoxic conditions)			Invasion at hypoxia↑	Angiogenesis↓
<i>GAS5</i>			GR, GREs		Sensitivity GBM cells to erlotinib treatment↑
<i>PNKY</i>			PTBP1	Normal neuronal differentiation	

Table continued on following page

TABLE 2
Deregulated lncRNAs with Their Correlations with Survival, Targets/Mechanisms of Action and Functions in Glioblastoma (Continued)

lncRNA	Expression in GBM (glioma)	Survival correlation	Targets/Mechanisms of action	Function	
				Overexpression	Under-expression
NEAT1	Up		miR-449b-5p		Proliferation↓, Invasion↓, Migration↓
ASLNC22381	Up				GBM recurrence↑
ASLNC2081	Up				GBM recurrence↑
LOC000937	Up				
LINC00152	Up				
LOC04745	Up				
TUNAR	Down			Normal neuronal differentiation	
RP11-713C5.1	Down				
RP11-123M6.2	Down				
LINC00599	Down				
LOC27853	(Up in low grade tumor)				
RP-32L13.3	(Up in low grade tumor)				

TABLE 2 Deregulated lncRNAs with Their Correlations with Survival, Targets/Mechanisms of Action and Functions in Glioblastoma (Continued)

lncRNA	Expression in GBM (glioma)	Survival correlation	Targets/Mechanisms of action	Function	
				Overexpression	Under-expression
MIAT	(Down in low grade tumor)				
RP11-67704.6	(Down in low grade tumor)				
TMEM191A	(Down in low grade tumor)				
LINC01476	Down				
RP11-334C17		Y			
BTAT10		Y			
SOX2OT	(Down in migratory GBM cells)	Y			
LOC100192378	Up				
RP11-112J3.16	Up				
LOC100127888	Up				
HCG4	Down				
FLJ39609	Down				

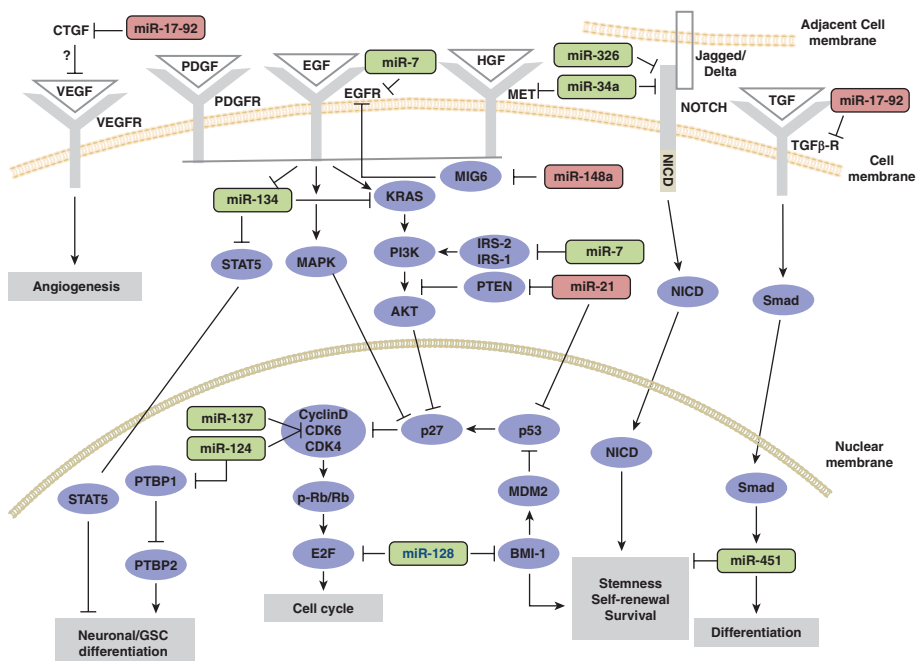


Figure 3 Regulation of glioblastoma stem cell targets and functions by miRNAs. Modified with permission from Zhang et al. (52).

NOTCH expression. The miR-17-92 cluster has been implicated in the regulation of GSC differentiation, apoptosis, and proliferation (61). It was first shown that expression of several members of miR-17-92 was significantly higher in primary astrocytic tumors than in the normal brain and significantly increased with tumor grade. A high-level amplification of the miR-17-92 locus was also detected in one GBM specimen, while inhibition of miR-17-92 induced apoptosis and decreased cell proliferation of GSCs.

Functions and Targets of miRNAs in GBM

CELL PROLIFERATION, VIABILITY, AND STEMNESS

One distinctive characteristic of GBM is uncontrolled proliferation and evasion of programmed cell death. miRNA deregulation is one mechanism for sustained proliferation and evasion of apoptosis through regulation of the cell cycle, apoptosis, and growth signaling pathways.

AP-1-induced miR-21 downregulates tumor suppressors PDCD4 and PTEN. Inhibition of PDCD4 contributes to an increase in AP-1 activity, revealing an AP-1 autoregulatory mechanism in RAS transformation (62). MiR-21 exerts antiapoptotic effects and enhances tumor formation through targeting of p53 and TGF- β signaling

and the mitochondrial apoptotic pathway (63). MiR-21 affects apoptosis and the cell cycle by inhibiting heterogeneous nuclear ribonucleoprotein K (HNPRK); the tumor suppressor homologue of p53 (Tap63); programmed cell death 4 (PDCD4); and possibly also EGFR, cyclin D, and Bcl2 (63–65), as well as ANP32A, SMARCA4, SPRY2, IGFBP3, and LRRFIP1 (4, 66–68). MiR-21 is therefore an important miRNA in gliomas that exerts oncogenic effects by regulating cell proliferation and survival.

MiR-221/222 directly targets the tumor suppressor and negative regulator of the cell cycle, p27 (69, 70). miR-221/222 can inhibit apoptosis by targeting p53-upregulated modulator of apoptosis (PUMA), which acts to induce rapid cell death via binding to Bcl-2 and Bcl-xL. Therefore, overexpression of miR-221/222 and subsequent downregulation of PUMA enhance cell survival while knockdown of miR-221/222 induces apoptosis, thereby reducing tumor growth (71, 72).

MiR-26a regulates the major tumor suppressor PTEN in glioma (33, 34). It was shown that miR-26a can transform cells and promote GBM cell growth by decreasing PTEN, RB1, and MAP3K2/MEKK2 protein expression, thereby increasing AKT activation, promoting proliferation, and decreasing c-JUN N-terminal kinase-dependent apoptosis. Overexpression of miR-26a in PTEN-competent and PTEN-deficient GBM cells promoted tumor growth *in vivo* and increased growth in cells overexpressing CDK4 or CENTG1. MiR-335 is upregulated in GBM and acts to prevent apoptosis and promote cell growth and invasion of astrocytoma cells by targeting the potential tumor suppressor disheveled-associated activator of morphogenesis 1 (DAAM1), as well as regulating RB1 in a p53-dependent manner (73). Inhibition of miR-335 leads to effective suppression of growth and increased apoptosis of astrocytoma cells. Importantly, delivery of a miR-335 antagonist to rat glioma C6 cells prevented tumor growth, resulted in activation of apoptosis, and repressed invasion of astrocytoma xenografts (74).

MiR-34a is a downregulated miRNA in GBM that directly inhibits the expression of MET, NOTCH1, NOTCH2, CDK6, CCND1, and SIRT1 (35, 75–77). MET is a commonly overexpressed and activated RTK in GBM and is responsible for mediating multiple growth-signaling pathways. NOTCH is a critical regulator of cell fate and cancer stem cell maintenance (56–58). CDK6 and CCND1 are well-known cell-cycle regulators. By targeting these important molecules involved in cell proliferation, miR-34a inhibits cell survival, proliferation, and invasion, as well as GSCs self-renewal (35, 55). RTKs are co-deregulated in the majority of GBM. MiR-134 is upregulated in human tumors and GSCs and is regulated by the RTKs, MET, EGFR, and PDGFR (19). MiR-134 inhibits GSCs self-renewal, survival, and xenograft growth and induces GSC differentiation by directly binding to KRAS and STAT5B 3' UTRs. MiR-134 therefore represents an RTK-regulated tumor-suppressive hub that mediates RTK effects on GBM malignancy.

Many more miRNAs, including the tumor-suppressive miR-181, miR-15b, miR-153, miR-184, miR-326, miR-218, and miR-451 (23, 78–80), inhibit proliferation and/or induce apoptosis in GBM. Additional upregulated oncogenic miRNAs that promote glioma cell viability and proliferation include miR-296 (81), miR-125b (82), miR-196a (83), miR-148a (36), miR-363, and miR-582-5p (84, 52).

MIGRATION AND INVASION

The lethality of GBM is partly attributed to extensive and diffuse tumor cell infiltration throughout the brain. The invasive growth of GBM is driven by the modulation of cell-to-cell and cell-to-matrix interactions, degradation, and remodeling of the extracellular matrix, cytoskeletal reorganization, and gain of migratory behavior (85). These processes are regulated by miRNAs. The oncogenic miR-21 promotes GBM invasiveness through suppression of the expression of matrix metalloprotease (MMP) inhibitors. MMPs are a family of enzymes that function in proteolysis of extracellular matrix components and are critical for the migration and invasion properties of tumor cells. By targeting multiple molecules, such as RECK, TIMP3, ANP32A, and SPRY2, miR-21 can induce the expression and activity of various MMPs, increase Ras/Raf binding, and activate ERK phosphorylation, thereby enhancing the invasive potential of GBM cells (27, 68, 86). Several studies reported that miR-146b and miR-10b can also promote GBM invasion (37, 87–89). MiR-146b inhibits MMP16 and leads the increased invasion in GBM, whereas MiR-10b can enhance GBM invasive growth by indirectly modulating MMP14 as well as uPAR and RhoC through direct binding and inhibits upstream target, HOXD10 (37, 88). When treated with antisense miR-10b, GBM cells display reduced growth, invasion, and angiogenesis, as well as enhanced cell death (38, 88, 89). The let-7 family of tumor-suppressive miRNAs is inhibited by Lin28A, which is normally expressed in development but is also found overexpressed in GBM by TCGA data analysis. There is a strong correlation in GBM between Lin28A expression and expression of the pro-invasive HMGA2 gene targeted by let-7 miRNAs, and an inverse correlation with let-7 family members. Overexpression of let-7g can reverse the invasive phenotype of Lin28A-expressing GSCs (90).

ANGIOGENESIS

One of the primary characteristics of GBM is its ability to create extensive microvasculature networks. New blood vessel growth orchestrates the growth of aggressive GBM by supplying a greater quantity of energy and nutrients, in addition to providing infrastructure for invasion. A number of miRNAs have been identified as important regulators of neovascularization in GBM (91). MiR-218 was shown to prevent GBM tumor angiogenesis and cell survival by targeting multiple components of RTK signaling pathways and the hypoxia-inducible factor, HIF2 α (92). MiR-125b is downregulated in both human GBM-associated endothelium and in endothelial cells cultured with conditioned medium from GBM cells (82). Myc-associated zinc finger protein (MAZ), a transcription factor that regulates vascular endothelial growth factor (VEGF), is a target of miR-125b that is overexpressed in GBM-associated endothelium and is driven by VEGF. It was reported that miR-296 is a GBM angiogenic miRNA that is upregulated in tumor-associated endothelial cells. Augmented expression of miR-296 is associated with increased endothelial cell tube formation and enhanced vascularization of tumors, while knockdown of miR-296 results in reduced tumor angiogenesis (81). miR-210-3p is induced under hypoxic growth conditions and directly targets HIF3 α , a negative regulator of hypoxic response that acts through downregulation of VEGF.

Therefore, miR-210-3p overexpression induces HIF, VEGF, and CA9 transcriptional activity, enhancing vasculogenesis, while inhibition of miR-210-3p under hypoxia inhibits HIF-mediated induction of VEGF and CA9, reducing vascular density and tumor growth *in vivo* (93). A member of the miR-17 family, miR-93, plays a role in GBM-associated angiogenesis by targeting integrin B8, a tumor suppressor and inhibitor of angiogenesis (94). MiR-93 was sufficient to enhance angiogenesis and tumor growth and drastically reduce survival in a xenograft model of GBM.

IMMUNE EVASION AND DRUG RESISTANCE

Increased antitumor immune responses have been linked to enhanced survival in many cancers, including GBM (95–101). MiRNAs regulate immune evasion. MiR-124 inhibits STAT3 to enhance T-cell-mediated immune clearance of glioma (102). Treatment of T cells isolated from GBM with miR-124 reversed a block in T-cell proliferation and also reduced expression of signal transducer and activator of transcription 3 and forkhead box P3—ultimately inhibiting the development of immune-suppressive regulatory T cells (102). MiR-124 delivery in mouse GBM xenograft models prolonged survival but only in immunocompetent mice. Dicer, miR-222, and miR-339 expressions were inversely associated with the expression of intercellular cell adhesion molecule (ICAM-1) and they enhanced the susceptibility of tumor cells to antigen-specific lysis by cytotoxic T-lymphocytes. MiR-222 and miR-339 contribute to GBM evasion of the immune system by targeting ICAM-1, which modulates T-cell responses (103). A major challenge of GBM therapy is the resistance to chemotherapy and/or radiotherapy. A number of miRNAs can influence therapeutic sensitivity by targeting multidrug resistance proteins (104). MiR-21 strongly reduces the effect of TMZ on apoptosis, which is mediated through inhibition of proapoptotic proteins Bax and caspase-3 as well as upregulation of antiapoptotic protein Bcl-2 (105). Inhibition of miR-21 can enhance the chemosensitivity of human GBM cells to TMZ and other drugs including paclitaxel, sunitinib, doxorubicin, and VM-26 (106–110). MiR-195, miR-455-3p, and miR-10a* were also implicated in TMZ resistance as they were upregulated in a TMZ resistant variant of the U251 GBM cell line (111). Knockdown of miR-195 was shown to significantly enhance the effectiveness of TMZ. Two studies examined the link between the miRNA levels (32) and TMZ resistance (112) in GBM. They found that miR-221, miR-222, miR-181b, miR-181c, and miR-128 were significantly downregulated in GBM, while miR-21 was overexpressed. MiR-181b and miR-181c had the strongest correlation with responsiveness to TMZ treatment, indicating their potential as predictive markers for response to TMZ therapy. MiR-125b-2 has also been shown to increase resistance of GSCs to TMZ, whereas peptide nucleic acid (PNA) miR-125b inhibitors increase TMZ-induced GSCs apoptosis via mediation of cytochrome c release from the mitochondria, caspase-3, and PARP activation (113). MiR-328 has been found to sensitize GSCs to chemotherapy through downregulating the expression of ATP-binding cassette subfamily G member 2 (ABCG2), a transporter that regulates shuttling of substrates across the cellular membrane (114). MiR-100 has been reported to increase the sensitivity of glioma cells to ionizing radiation through the downregulation of ataxia telangiectasia mutated (ATM) (115).

miRNA Therapeutics

Because miRNAs regulate all aspects of cancer, they represent promising therapeutic agents or targets. The goal of miRNA therapeutics is to replace tumor suppressor miRNAs or inhibit oncogenic miRNAs. There are a host of possible choices for both the therapeutic payload and the delivery vector. A number of reports in GBM describe preclinical efforts to characterize individual oncogenic and tumor-suppressive miRNA that can be targeted *in vitro*, with some evidence of efficacy in mouse models; however, none of them has moved on to clinical trials in GBM patients to date.

As described earlier in this chapter, numerous groups have reported oncogenic and tumor-suppressive miRNAs, affecting cell viability in GBM. Therapeutic efforts targeting oncogenic miRNAs have largely focused on delivering stabilized antisense oligonucleotides complementary to the miRNAs sequence. Preclinical studies with GBM tumor-suppressive miRNAs have consisted of forced overexpression of miRNA mimics. Among the GBM oncogenic miRNAs described in multiple studies, miR-21 and miR-10b figure prominently (38, 116–118). Several of these GBM miR-21 and miR-10b studies have demonstrated preclinical efficacy with delivery of miRNA antisense, some of which are dubbed “antagomiRs” (anti-miR); miR-10b may be an especially powerful oncogenic miRNA in GBM. One group has now shown preclinical efficacy in GBM models with a radically different approach to targeting miR-10b; viral delivery of CRISPR/Cas9 elements was used to eliminate miR-10b expression in GBM (119). Even more studies have identified tumor-suppressive microRNAs in GBM and shown their potential for therapeutic delivery. Among these translational studies of tumor-suppressive miRNAs and their therapeutic potential in GBM, miR-34a has received the most attention (35, 55). Others include miR-326, miR-297, miR-128, and miR-182 (120–124). Most of the published work with tumor-suppressive miRNAs in GBM has involved *ex vivo* transfection prior to GBM cell implantation in the mouse brain, but some studies have reached the higher bar of demonstrating *in vivo* efficacy with tumor-suppressive miRNA delivery to previously established orthotopic GBM in mice. A number of studies have also shown the potential of miRNA-based therapies to indirectly attack GBM, through its vasculature or through immunotherapeutic effects (82, 92, 94, 102, 103).

The problem of efficient delivery of miRNA-based therapies to GBM remains perhaps the biggest challenge. Numerous approaches tested preclinically have involved local delivery, sometimes with the addition of convection-enhanced delivery (CED) to drive better penetration of the agent into the tumor and the nearby brain. These local delivery approaches have typically used lentivirus, adenovirus, or one of a large variety of nanoparticles as vectors to transfect the GBM cells. While in the occasional report naked miRNA or anti-miRNA has been infused, it is typically more efficient to use a viral or nanoparticle vector to get substantial quantities of the payload into GBM cells. It should also be noted that intravenous delivery of miRNA-based therapeutic vectors might be a possibility for GBM; some reports describe approaches targeted to the brain vasculature or designed to pass through the blood–brain barrier or locally disrupt it (124, 125).

One key question for miRNA-based therapies directly targeting GBM cells is whether it is necessary for the therapeutic vector to reach all or nearly all of the

malignant cells to be highly effective. Some therapies might yield a bystander effect allowing for less-than-perfect delivery, but in general, it is likely that delivery will have to be highly efficient. However, this requirement might well be eased substantially by a biologic phenomenon found to be prominent in GBM cells—intercellular sharing of cytoplasmic contents through exosome shedding and uptake (126). This has been found in GBM cells to allow transduced cells to share cytoplasmic contents such as overexpressed miRNAs with adjacent GBM cells (42), which could dramatically reduce the need to reach the overwhelming majority of the GBM cells with any miRNA-based therapy.

Although there are numerous preclinical studies on miRNA-based therapeutic strategies for GBM, none has yet advanced to clinical trials in patients. However, miRNA-based therapeutics have entered clinical trial testing for other cancers, and GBM might not be far behind. A miRNA-34a therapeutic entered a Phase I trial for certain cancers (NCT01829971), enrolling 47 patients, yielding a partial response and four cases of stable disease, but it was marked by significant inflammatory side effects requiring immunosuppressive steroid premedication (127). This immune reaction may represent yet another challenge with miRNA therapeutics in the clinic, and it is hoped that valuable information will be gleaned from the analysis of this trial.

Long Noncoding RNAs

lncRNAs are nonprotein coding transcripts that are longer than 200 nucleotides (nt). lncRNAs are emerging as significant regulators of critical biological functions in human disease, including cancer and GBM (128–132). Over 50,000 human lncRNAs have been identified (133–135) and similar catalogs have been generated from various mouse tissues and model organisms (136–140). lncRNAs can regulate gene expression at the transcriptional, post-transcriptional, and epigenetic levels (141). Recent studies indicate that lncRNAs play important roles in glioma development (142, 143) by regulating several tumorigenic processes such as cellular proliferation and apoptosis (144). Differential expression of specific lncRNAs might correlate with disease progression and cancer malignancy and thus could potentially be used as therapeutic targets and biomarkers for prognosis (145–149).

lncRNA EXPRESSION AND CORRELATION WITH CLINICAL PARAMETERS IN GLIOMAS

One high throughput screening study of 1308 lncRNAs discovered 654 highly upregulated lncRNA in GBM compared to normal brain tissue (150), among which ASLNC22381 and ASLNC2081 were further investigated and found to be involved in GBM recurrence and malignant progression. Another study (145), using a microarray-mining approach, demonstrated aberrant lncRNA expression patterns in two large public cohorts (151, 152). They identified 127 lncRNAs that were differentially expressed between glioma and nontumoral brain tissues. Their analysis found that lncRNAs, CRNDE and HOTAIRM1, were significantly

upregulated in GBM while MEG3 was downregulated. In a clinical trial-based study, 80 GBM specimens were analyzed and 81 sets of lncRNAs were found to be deregulated (153). Another study found 37 lncRNAs that were upregulated and 44 lncRNAs that were downregulated in GBM specimens compared to nontumoral brain tissues based on the profiling analysis of 30 GBM patient samples and 5 GBM cell lines. They found that 147 out of 2448 lncRNAs were differentially expressed in tumor tissues compared to normal brain, and 213 lncRNAs were differentially expressed in tumor cell lines compared to normal astrocytes. Importantly, certain lncRNAs, including CRNDE, HOTAIRM1, and MEG3, were consistently differentially expressed, indicating that they may play a role early in GBM initiation and tumorigenesis (153, 154) (Table 2).

A recent comprehensive study of global lncRNA expression analyzed over 650 brain tumor and 70 normal brain tissues from TCGA and other public databases (155). A total of 611 induced and 677 repressed lncRNAs were identified in glial tumors relative to normal brains. One frequently reported oncogenic lncRNA, CRNDE, was confirmed to be upregulated over 40-fold in GBM. The lncRNA, TUNAR, was also identified as significantly downregulated (14-fold) in both GBM and LGG. Interestingly, TUNAR was found to act as a crucial positive regulator of neuronal development and differentiation in zebrafish, mice, and humans, suggesting that its downregulation is required for increased oncogenic potential and uncontrolled neuronal cell growth (138, 156).

Specific lncRNAs correlate with patient survival. From TCGA data analysis, approximately 500 lncRNAs were associated with poor prognosis, while 200 lncRNAs correlated with better survival outcomes (155). For example, patients displaying high expression of RP11-334C17.6 had a median survival time of 485 days, while patients with lower expression had a median survival time of 380 days (HR = 0.728, 95% CI = 0.6011–0.883, $p = 0.00122$). Patients with high versus low expression of BTAT10 had median survival time of 335 and 485 days, respectively (HR = 1.298, 95% CI = 1.0881–1.548, $p = 0.00374$).

Functions of lncRNAs in GBM

lncRNAs have been implicated in GBM development and malignancy by regulating cell proliferation, apoptosis, GSC self-renewal, differentiation, and response to hypoxic stress (see Table 2).

CELL PROLIFERATION AND APOPTOSIS

MEG3, a lncRNA that is significantly downregulated in GBM (144), acts as a tumor suppressor in GBM cells. Ectopic expression of MEG3 inhibits cell proliferation and via p53 activation. CRNDE, an oncogenic lncRNA in GBM (157) and other cancer types (158), promotes cell proliferation, migration, and invasion while inhibiting apoptosis in GBM cells and GSCs (157, 159, 160). HOTAIR has been shown to regulate cell cycle progression in glioma via interaction with EZH2 (161). Knockdown of HOTAIR or EZH2 leads to cell cycle arrest in GBM cells (161) and inhibition of HOTAIR represses orthotopic GBM tumor growth *in vivo* (162).

MIGRATION AND INVASION

MALAT1 is one lncRNA that was found to regulate cell migration in GBM and lung cancer (163). Although its mechanism in glioma is unclear, initial evidence suggests that MALAT1 regulates cell migration in lung cancer cells through the mediation of several motility-associated molecules, including AIM1, LAYN, HMMR, SLC26A2, CCT4, ROD1, CTHRC1, and FHL1 (164). LncRNA SOX2OT is also downregulated in migratory GBM cells, although its exact mechanism of action is unknown. Increased expression of SOX2OT in GBM correlates with better prognosis (165).

GSC DIFFERENTIATION

A study discovered 39 lncRNAs that were differentially expressed between GSCs and differentiated GBM cells (166), while another lncRNA screening study identified 33 lncRNAs that were expressed in a unique pattern between glioma cells and GSCs (167). Between these independent studies, six lncRNAs were consistently altered in a similar pattern, with LOC100192378, H19, RP11-112J3.16, and LOC100127888 being upregulated, and HCG4 and FLJ39609 being downregulated in GSCs (167). The effects and mechanism of action of these lncRNAs on the biological properties of GSC remains unknown, although H19 has been reported to play an important role in the maintenance of adult hematopoietic stem cells (168).

THERAPEUTIC RESPONSE AND RESISTANCE

Differential expression of lncRNAs has been associated with therapeutic response in GBM patients. Through gene expression profiling of GBM cell lines treated with the EGFR inhibitor erlotinib (ERL), the lncRNA GAS5 was significantly increased after treatment in both ERL-resistant and ERL-sensitive glioma cell lines. Moreover, knockdown of GAS5 sensitized GBM cells to ERL treatment (169). GAS5 is reportedly upregulated in growth-arrested cells and sensitizes mammalian cells to apoptosis, by suppressing genes responsive to glucocorticoid (170). GAS5 may also sensitize mammalian cells to apoptosis through binding to the DNA-binding domain of the glucocorticoid receptor (GR) and competing with target genes of glucocorticoid response elements (GREs).

MECHANISMS OF ACTION OF LNCRNA IN GBM

Little is known about the regulation of lncRNA expression in GBM. c-Myc, a transcription factor, has been found to induce the expression of the lncRNA H19 in GBM cells (171). Additional transcription factors, c-Myc, NFKB, E2F6, TAF1, and SMAD, which are well-known regulators in GBM (172–175), have been found to possess several binding sites in the promoter region of the lncRNA, CRNDE, which may mediate these important signaling pathways. Similarly, the lncRNA, HOTAIRM1, is highly overexpressed in GBM, and its gene promoter sequence has been bound by NFKB, PU.1, and USF-1 (176). The lncRNA, GASS, functions as a decoy GRE by binding to the DNA-binding domain of the GR and competing with target genes of GREs. Thus, GASS acts to suppress GR-induced transcriptional activity and may

enhance ERL effects in GBM (132, 170). Through interaction with EZH2, lncRNA HOTAIR regulates cell cycle progression in glioma. Proteins with bromodomain and extraterminal (BET) domain are potential therapeutic targets in cancer and GBM, as treatment of GBM samples with a BET inhibitor decreases GBM growth and causes reduced HOTAIR expression. Interestingly, a protein with a BET domain has been found to directly bind the HOTAIR promoter (177). PNKY plays an important role in neuronal differentiation and chromatin-state maps of the PNKY/BRN2 locus in GSCs and shows widespread active chromatin marks at their promoters (178). PNKY can bind to PTBP1, which is upregulated in GBM, and plays a role as a driver gene in GBM tumor growth as well as in the V-SVZ neurogenic lineage (179). CRNDE, an oncogenic lncRNA, induces cell proliferation, migration, and invasion, and inhibits apoptosis in GBM cells and GSCs via the activation of multiple signaling pathways. It functions as a sponge by binding miRNAs, such as miR-384, resulting in the downregulation of piwi-like RNA-mediated gene silencing 4 (PIWIL4) and STAT3 protein in GBM cells (160). CRNDE also upregulates X-linked inhibitor of apoptosis (XIAP) and the evolutionarily conserved serine/threonine protein kinase, PAK7, by binding and inhibiting miR-186, which targets XIAP and PAK7 in GBM cells (159). The lncRNA, nuclear-enriched abundant transcript 1 (NEAT1), is essential for the formation of nuclear body paraspeckles (180) and is upregulated in GBM tissues. Inhibition of NEAT1 reduces cell proliferation, invasion, and migration. NEAT1 exerts its oncogenic effects through the direct binding of miR-449b-5p, leading to upregulation of the RTK MET (180).

Conclusion

MicroRNAs and long noncoding RNAs are frequently deregulated in cancer and GBM, where they regulate all aspects of malignancy, including tumor cell proliferation, survival, migration, and invasion, as well as cancer stem cells, angiogenesis, tumor immune responses, therapy resistance, and the microenvironment. Studying these noncoding RNAs could lead to a better understanding of GBM initiation and progression. MiRNAs and lncRNAs could also be clinically exploited for diagnostic, prognostic, and therapeutic purposes. However, more research is required, especially in the case of lncRNAs, for a better understanding and efficient clinical exploitation of this large and important class of regulatory molecules in cancer and GBM.

Acknowledgment: This article was supported by NIH R01 NS045209 (Roger Abounader).

Conflict of interest: The authors declare no potential conflicts of interest with respect to research, authorship, and/or publication of this manuscript.

Copyright and permission statement: To the best of our knowledge, the materials included in this chapter do not violate copyright laws. All original sources have been appropriately acknowledged and/or referenced. Where relevant, appropriate permissions have been obtained from the original copyright holder(s).

References

1. Wen PY, Kesari S. Malignant gliomas in adults. *N Engl J Med*. 2008;359(5):492–507. <http://dx.doi.org/10.1056/NEJMra0708126>
2. Abounader R, Laterra J. Scatter factor/hepatocyte growth factor in brain tumor growth and angiogenesis. *Neuro Oncol*. 2005;7(4):436–51. <http://dx.doi.org/10.1215/S1152851705000050>
3. Cancer Genome Atlas Research Network. Comprehensive genomic characterization defines human glioblastoma genes and core pathways. *Nature*. 2008;455(7216):1061–8. <http://dx.doi.org/10.1038/nature07385>
4. Londin E, Loher P, Telonis AG, Quann K, Clark P, Jing Y, et al. Analysis of 13 cell types reveals evidence for the expression of numerous novel primate- and tissue-specific microRNAs. *Proc Natl Acad Sci U S A*. 2015;112(10):E1106–15. <http://dx.doi.org/10.1073/pnas.1420955112>
5. Lee YS, Dutta A. MicroRNAs in cancer. *Annu Rev Pathol*. 2009;4:199–227. <http://dx.doi.org/10.1146/annurev.pathol.4.110807.092222>
6. Fire A, Xu S, Montgomery MK, Kostas SA, Driver SE, Mello CC. Potent and specific genetic interference by double-stranded RNA in *Caenorhabditis elegans*. *Nature*. 1998;391(6669):806–11. <http://dx.doi.org/10.1038/35888>
7. Lagos-Quintana M, Rauhut R, Lendeckel W, Tuschl T. Identification of novel genes coding for small expressed RNAs. *Science*. 2001;294(5543):853–8. <http://dx.doi.org/10.1126/science.1064921>
8. Lee RC, Ambros V. An extensive class of small RNAs in *Caenorhabditis elegans*. *Science*. 2001;294(5543):862–4. <http://dx.doi.org/10.1126/science.1065329>
9. Lau NC, Lim LP, Weinstein EG, Bartel DP. An abundant class of tiny RNAs with probable regulatory roles in *Caenorhabditis elegans*. *Science*. 2001;294(5543):858–62. <http://dx.doi.org/10.1126/science.1065062>
10. Bentwich I, Avniel A, Karov Y, Aharonov R, Gilad S, Barad O, et al. Identification of hundreds of conserved and nonconserved human microRNAs. *Nat Genet*. 2005;37(7):766–70. <http://dx.doi.org/10.1038/ng1590>
11. Berezikov E, Guryev V, van de Belt J, Wienholds E, Plasterk RH, Cuppen E. Phylogenetic shadowing and computational identification of human microRNA genes. *Cell*. 2005;120(1):21–4. <http://dx.doi.org/10.1016/j.cell.2004.12.031>
12. Yu J, Wang F, Yang GH, Wang FL, Ma YN, Du ZW, et al. Human microRNA clusters: Genomic organization and expression profile in leukemia cell lines. *Biochem Biophys Res Commun*. 2006;349(1):59–68. <http://dx.doi.org/10.1016/j.bbrc.2006.07.207>
13. Lewis BP, Burge CB, Bartel DP. Conserved seed pairing, often flanked by adenosines, indicates that thousands of human genes are microRNA targets. *Cell*. 2005;120(1):15–20. <http://dx.doi.org/10.1016/j.cell.2004.12.035>
14. Dews M, Homayouni A, Yu D, Murphy D, Sevignani C, Wentzel E, et al. Augmentation of tumor angiogenesis by a Myc-activated microRNA cluster. *Nat Genet*. 2006;38(9):1060–5. <http://dx.doi.org/10.1038/ng1855>
15. Sylvestre Y, De Guire V, Querido E, Mukhopadhyay UK, Bourdeau V, Major F, et al. An E2F/miR-20a autoregulatory feedback loop. *J Biol Chem*. 2007;282(4):2135–43. <http://dx.doi.org/10.1074/jbc.M608939200>
16. Hafner M, Renwick N, Brown M, Mihailovic A, Holoch D, Lin C, et al. RNA-ligase-dependent biases in miRNA representation in deep-sequenced small RNA cDNA libraries. *RNA*. 2011;17(9):1697–712. <http://dx.doi.org/10.1261/rna.2799511>
17. Hermeking H. p53 enters the microRNA world. *Cancer Cell*. 2007;12(5):414–8. <http://dx.doi.org/10.1016/j.ccr.2007.10.028>
18. He L, He X, Lim LP, de Stanchina E, Xuan Z, Liang Y, et al. A microRNA component of the p53 tumour suppressor network. *Nature*. 2007;447(7148):1130–4. <http://dx.doi.org/10.1038/nature05939>
19. Zhang Y, Kim J, Mueller AC, Dey B, Yang Y, Lee DH, et al. Multiple receptor tyrosine kinases converge on microRNA-134 to control KRAS, STAT5B, and glioblastoma. *Cell Death Differ*. 2014;21(5):720–34. <http://dx.doi.org/10.1038/cdd.2013.196>

20. Melo SA, Esteller M. Dysregulation of microRNAs in cancer: Playing with fire. *FEBS Lett.* 2011;585(13):2087–99. <http://dx.doi.org/10.1016/j.febslet.2010.08.009>
21. Calin GA, Sevignani C, Dumitru CD, Hyslop T, Noch E, Yendamuri S, et al. Human microRNA genes are frequently located at fragile sites and genomic regions involved in cancers. *Proc Natl Acad Sci U S A.* 2004;101(9):2999–3004. <http://dx.doi.org/10.1073/pnas.0307323101>
22. Moller HG, Rasmussen AP, Andersen HH, Johnsen KB, Henriksen M, Duroux M. A systematic review of microRNA in glioblastoma multiforme: Micro-modulators in the mesenchymal mode of migration and invasion. *Mol Neurobiol.* 2013;47(1):131–44. <http://dx.doi.org/10.1007/s12035-012-8349-7>
23. Shea A, Harish V, Afzal Z, Chijioko J, Kedir H, Dusmatova S, et al. MicroRNAs in glioblastoma multiforme pathogenesis and therapeutics. *Cancer Med.* 2016;5(8):1917–46. <http://dx.doi.org/10.1002/cam4.775>
24. Conti A, Aguenouz M, La Torre D, Tomasello C, Cardali S, Angileri FF, et al. miR-21 and 221 upregulation and miR-181b downregulation in human grade II-IV astrocytic tumors. *J Neurooncol.* 2009;93(3):325–32. <http://dx.doi.org/10.1007/s11060-009-9797-4>
25. Chan JA, Krichevsky AM, Kosik KS. MicroRNA-21 is an antiapoptotic factor in human glioblastoma cells. *Cancer Res.* 2005;65(14):6029–33. <http://dx.doi.org/10.1158/0008-5472.CAN-05-0137>
26. Silber J, Lim DA, Petritsch C, Persson AI, Maunakea AK, Yu M, et al. miR-124 and miR-137 inhibit proliferation of glioblastoma multiforme cells and induce differentiation of brain tumor stem cells. *BMC Med.* 2008;6:14. <http://dx.doi.org/10.1186/1741-7015-6-14>
27. Gabriely G, Wurdinger T, Kesari S, Esau CC, Burchard J, Linsley PS, et al. MicroRNA 21 promotes glioma invasion by targeting matrix metalloproteinase regulators. *Mol Cell Biol.* 2008;28(17):5369–80. <http://dx.doi.org/10.1128/MCB.00479-08>
28. Malzkorn B, Wolter M, Liesenberg F, Grzendowski M, Stuhler K, Meyer HE, et al. Identification and functional characterization of microRNAs involved in the malignant progression of gliomas. *Brain Pathol.* 2010;20(3):539–50. <http://dx.doi.org/10.1111/j.1750-3639.2009.00328.x>
29. Ciafre SA, Galardi S, Mangiola A, Ferracin M, Liu CG, Sabatino G, et al. Extensive modulation of a set of microRNAs in primary glioblastoma. *Biochem Biophys Res Commun.* 2005;334(4):1351–8. <http://dx.doi.org/10.1016/j.bbrc.2005.07.030>
30. Conrad ME, Barton JC. Factors affecting the absorption and excretion of lead in the rat. *Gastroenterology.* 1978;74(4):731–40.
31. Shi L, Cheng Z, Zhang J, Li R, Zhao P, Fu Z, et al. hsa-mir-181a and hsa-mir-181b function as tumor suppressors in human glioma cells. *Brain Res.* 2008;1236:185–93. <http://dx.doi.org/10.1016/j.brainres.2008.07.085>
32. Slaby O, Lakomy R, Fadrus P, Hrstka R, Kren L, Lzicarova E, et al. MicroRNA-181 family predicts response to concomitant chemoradiotherapy with temozolomide in glioblastoma patients. *Neoplasma.* 2010;57(3):264–9. http://dx.doi.org/10.4149/neo_2010_03_264
33. Huse JT, Brennan C, Hambardzumyan D, Wee B, Pena J, Rouhanifard SH, et al. The PTEN-regulating microRNA miR-26a is amplified in high-grade glioma and facilitates gliomagenesis in vivo. *Genes Dev.* 2009;23(11):1327–37. <http://dx.doi.org/10.1101/gad.1777409>
34. Kim H, Huang W, Jiang X, Pennicooke B, Park PJ, Johnson MD. Integrative genome analysis reveals an oncomir/oncogene cluster regulating glioblastoma survivorship. *Proc Natl Acad Sci U S A.* 2010;107(5):2183–8. <http://dx.doi.org/10.1073/pnas.0909896107>
35. Li Y, Guessous F, Zhang Y, Dipierro C, Kefas B, Johnson E, et al. MicroRNA-34a inhibits glioblastoma growth by targeting multiple oncogenes. *Cancer Res.* 2009;69(19):7569–76. <http://dx.doi.org/10.1158/0008-5472.CAN-09-0529>
36. Kim J, Zhang Y, Skalski M, Hayes J, Kefas B, Schiff D, et al. microRNA-148a is a prognostic oncomiR that targets MIG6 and BIM to regulate EGFR and apoptosis in glioblastomas. *Cancer Res.* 2014;74(5):1541–53. <http://dx.doi.org/10.1158/0008-5472.CAN-13-1449>
37. Sasayama T, Nishihara M, Kondoh T, Hosoda K, Kohmura E. MicroRNA-10b is overexpressed in malignant glioma and associated with tumor invasive factors, uPAR and RhoC. *Int J Cancer.* 2009;125(6):1407–13. <http://dx.doi.org/10.1002/ijc.24522>
38. Guessous F, Alvarado-Velez M, Marcinkiewicz L, Zhang Y, Kim J, Heister S, et al. Oncogenic effects of miR-10b in glioblastoma stem cells. *J Neurooncol.* 2013;112(2):153–63. <http://dx.doi.org/10.1007/s11060-013-1047-0>

39. Jiang L, Mao P, Song L, Wu J, Huang J, Lin C, et al. miR-182 as a prognostic marker for glioma progression and patient survival. *Am J Pathol.* 2010;177(1):29–38. <http://dx.doi.org/10.2353/ajpath.2010.090812>
40. Akers JC, Ramakrishnan V, Kim R, Skog J, Nakano I, Pingle S, et al. MiR-21 in the extracellular vesicles (EVs) of cerebrospinal fluid (CSF): A platform for glioblastoma biomarker development. *PLoS One.* 2013;8(10):e78115. <http://dx.doi.org/10.1371/journal.pone.0078115>
41. Tepluyk NM, Mollenhauer B, Gabriely G, Giese A, Kim E, Smolsky M, et al. MicroRNAs in cerebrospinal fluid identify glioblastoma and metastatic brain cancers and reflect disease activity. *Neuro Oncol.* 2012;14(6):689–700. <http://dx.doi.org/10.1093/neuonc/nos074>
42. Li CC, Eaton SA, Young PE, Lee M, Shuttleworth R, Humphreys DT, et al. Glioma microvesicles carry selectively packaged coding and non-coding RNAs which alter gene expression in recipient cells. *RNA Biol.* 2013;10(8):1333–44. <http://dx.doi.org/10.4161/rna.25281>
43. Wang Q, Li P, Li A, Jiang W, Wang H, Wang J, et al. Plasma specific miRNAs as predictive biomarkers for diagnosis and prognosis of glioma. *J Exp Clin Cancer Res.* 2012;31:97. <http://dx.doi.org/10.1186/1756-9966-31-97>
44. Sun J, Liao K, Wu X, Huang J, Zhang S, Lu X. Serum microRNA-128 as a biomarker for diagnosis of glioma. *Int J Clin Exp Med.* 2015;8(1):456–63.
45. Yue X, Lan F, Hu M, Pan Q, Wang Q, Wang J. Downregulation of serum microRNA-205 as a potential diagnostic and prognostic biomarker for human glioma. *J Neurosurg.* 2016;124(1):122–8. <http://dx.doi.org/10.3171/2015.1.JNS141577>
46. Barciszewska AM. MicroRNAs as efficient biomarkers in high-grade gliomas. *Folia Neuropathol.* 2016;54(4):369–74. <http://dx.doi.org/10.5114/fn.2016.64812>
47. Shao N, Wang L, Xue L, Wang R, Lan Q. Plasma miR-454-3p as a potential prognostic indicator in human glioma. *Neurol Sci.* 2015;36(2):309–13. <http://dx.doi.org/10.1007/s10072-014-1938-7>
48. Yu X, Li Z. Serum microRNAs as potential noninvasive biomarkers for glioma. *Tumour Biol.* 2016;37(2):1407–10. <http://dx.doi.org/10.1007/s13277-015-4515-7>
49. Yang C, Wang C, Chen X, Chen S, Zhang Y, Zhi F, et al. Identification of seven serum microRNAs from a genome-wide serum microRNA expression profile as potential noninvasive biomarkers for malignant astrocytomas. *Int J Cancer.* 2013;132(1):116–27. <http://dx.doi.org/10.1002/ijc.27657>
50. Bao S, Wu Q, McLendon RE, Hao Y, Shi Q, Hjelmeland AB, et al. Glioma stem cells promote radioresistance by preferential activation of the DNA damage response. *Nature.* 2006;444(7120):756–60. <http://dx.doi.org/10.1038/nature05236>
51. Lavon I, Zrihan D, Granit A, Einstein O, Fainstein N, Cohen MA, et al. Gliomas display a microRNA expression profile reminiscent of neural precursor cells. *Neuro Oncol.* 2010;12(5):422–33. <http://dx.doi.org/10.1093/neuonc/nop061>
52. Zhang Y, Dutta A, Abounader R. The role of microRNAs in glioma initiation and progression. *Fron Biosci.* 2012;17:700–12. <http://dx.doi.org/10.2741/3952>
53. Gal H, Pandi G, Kanner AA, Ram Z, Lithwick-Yanai G, Amariglio N, et al. MIR-451 and Imatinib mesylate inhibit tumor growth of glioblastoma stem cells. *Biochem Biophys Res Commun.* 2008;376(1):86–90. <http://dx.doi.org/10.1016/j.bbrc.2008.08.107>
54. Piccirillo SG, Reynolds BA, Zanetti N, Lamorte G, Binda E, Broggi G, et al. Bone morphogenetic proteins inhibit the tumorigenic potential of human brain tumour-initiating cells. *Nature.* 2006;444(7120):761–5. <http://dx.doi.org/10.1038/nature05349>
55. Guessous F, Zhang Y, Kofman A, Catania A, Li Y, Schiff D, et al. microRNA-34a is tumor suppressive in brain tumors and glioma stem cells. *Cell Cycle.* 2010;9(6):1031–6. <http://dx.doi.org/10.4161/cc.9.6.10987>
56. Fan X, Matsui W, Khaki L, Stearns D, Chun J, Li YM, et al. Notch pathway inhibition depletes stem-like cells and blocks engraftment in embryonal brain tumors. *Cancer Res.* 2006;66(15):7445–52. <http://dx.doi.org/10.1158/0008-5472.CAN-06-0858>
57. Shih AH, Holland EC. Notch signaling enhances nestin expression in gliomas. *Neoplasia.* 2006;8(12):1072–82. <http://dx.doi.org/10.1593/neo.06526>
58. Fan X, Khaki L, Zhu TS, Soules ME, Talsma CE, Gul N, et al. NOTCH pathway blockade depletes CD133-positive glioblastoma cells and inhibits growth of tumor neurospheres and xenografts. *Stem Cells.* 2010;28(1):5–16.

59. Wang J, Wakeman TP, Lathia JD, Hjelmeland AB, Wang XF, White RR, et al. Notch promotes radioreistance of glioma stem cells. *Stem Cells*. 2010;28(1):17–28.
60. Zhang XP, Zheng G, Zou L, Liu HL, Hou LH, Zhou P, et al. Notch activation promotes cell proliferation and the formation of neural stem cell-like colonies in human glioma cells. *Mol Cell Biochem*. 2008;307(1–2):101–8.
61. Ernst A, Campos B, Meier J, Devens F, Liesenberg F, Wolter M, et al. De-repression of CTGF via the miR-17-92 cluster upon differentiation of human glioblastoma spheroid cultures. *Oncogene*. 2010;29(23):3411–22. <http://dx.doi.org/10.1038/onc.2010.83>
62. Talotta F, Cimmino A, Matarazzo MR, Casalino L, De Vita G, D'Esposito M, et al. An autoregulatory loop mediated by miR-21 and PDCD4 controls the AP-1 activity in RAS transformation. *Oncogene*. 2009;28(1):73–84. <http://dx.doi.org/10.1038/onc.2008.370>
63. Papagiannakopoulos T, Shapiro A, Kosik KS. MicroRNA-21 targets a network of key tumor-suppressive pathways in glioblastoma cells. *Cancer Res*. 2008;68(19):8164–72. <http://dx.doi.org/10.1158/0008-5472.CAN-08-1305>
64. Chen Y, Liu W, Chao T, Zhang Y, Yan X, Gong Y, et al. MicroRNA-21 down-regulates the expression of tumor suppressor PDCD4 in human glioblastoma cell T98G. *Cancer Lett*. 2008;272(2):197–205. <http://dx.doi.org/10.1016/j.canlet.2008.06.034>
65. Zhou X, Ren Y, Moore L, Mei M, You Y, Xu P, et al. Downregulation of miR-21 inhibits EGFR pathway and suppresses the growth of human glioblastoma cells independent of PTEN status. *Lab Invest*. 2010;90(2):144–55. <http://dx.doi.org/10.1038/labinvest.2009.126>
66. Gaur AB, Holbeck SL, Colburn NH, Israel MA. Downregulation of Pdc4 by mir-21 facilitates glioblastoma proliferation in vivo. *Neuro Oncol*. 2011;13(6):580–90. <http://dx.doi.org/10.1093/neuonc/nor033>
67. Yang CH, Yue J, Pfeffer SR, Fan M, Paulus E, Hosni-Ahmed A, et al. MicroRNA-21 promotes glioblastoma tumorigenesis by down-regulating insulin-like growth factor-binding protein-3 (IGFBP3). *J Biol Chem*. 2014;289(36):25079–87. <http://dx.doi.org/10.1074/jbc.M114.593863>
68. Kwak HJ, Kim YJ, Chun KR, Woo YM, Park SJ, Jeong JA, et al. Downregulation of Spry2 by miR-21 triggers malignancy in human gliomas. *Oncogene*. 2011;30(21):2433–42. <http://dx.doi.org/10.1038/onc.2010.620>
69. Gillies JK, Lorimer IA. Regulation of p27Kip1 by miRNA 221/222 in glioblastoma. *Cell Cycle*. 2007;6(16):2005–9. <http://dx.doi.org/10.4161/cc.6.16.4526>
70. Zhang C, Kang C, You Y, Pu P, Yang W, Zhao P, et al. Co-suppression of miR-221/222 cluster suppresses human glioma cell growth by targeting p27kip1 in vitro and in vivo. *Int J Oncol*. 2009;34(6):1653–60.
71. Zhang CZ, Zhang JX, Zhang AL, Shi ZD, Han L, Jia ZF, et al. MiR-221 and miR-222 target PUMA to induce cell survival in glioblastoma. *Mol Cancer*. 2010;9:229. <http://dx.doi.org/10.1186/1476-4598-9-229>
72. Chen L, Zhang J, Han L, Zhang A, Zhang C, Zheng Y, et al. Downregulation of miR-221/222 sensitizes glioma cells to temozolomide by regulating apoptosis independently of p53 status. *Oncol Rep*. 2012;27(3):854–60.
73. Shu M, Zheng X, Wu S, Lu H, Leng T, Zhu W, et al. Targeting oncogenic miR-335 inhibits growth and invasion of malignant astrocytoma cells. *Mol Cancer*. 2011;10:59. <http://dx.doi.org/10.1186/1476-4598-10-59>
74. Shu M, Zhou Y, Zhu W, Wu S, Zheng X, Yan G. Activation of a pro-survival pathway IL-6/JAK2/STAT3 contributes to glial fibrillary acidic protein induction during the cholera toxin-induced differentiation of C6 malignant glioma cells. *Mol Oncol*. 2011;5(3):265–72. <http://dx.doi.org/10.1016/j.molonc.2011.03.003>
75. Sun F, Fu H, Liu Q, Tie Y, Zhu J, Xing R, et al. Downregulation of CCND1 and CDK6 by miR-34a induces cell cycle arrest. *FEBS Lett*. 2008;582(10):1564–8. <http://dx.doi.org/10.1016/j.febslet.2008.03.057>
76. Bueno MJ, Malumbres M. MicroRNAs and the cell cycle. *Biochim Biophys Acta*. 2011;1812(5):592–601. <http://dx.doi.org/10.1016/j.bbadis.2011.02.002>
77. Luan S, Sun L, Huang F. MicroRNA-34a: A novel tumor suppressor in p53-mutant glioma cell line U251. *Arch Med Res*. 2010;41(2):67–74. <http://dx.doi.org/10.1016/j.arcmred.2010.02.007>

78. Zhang JM, Sun CY, Yu SZ, Wang Q, An TL, Li YY, et al. [Relationship between miR-218 and CDK6 expression and their biological impact on glioma cell proliferation and apoptosis]. *Zhonghua bing li xue za zhi Chin J Pathol.* 2011;40(7):454–9.
79. Xia H, Yan Y, Hu M, Wang Y, Wang Y, Dai Y, et al. MiR-218 sensitizes glioma cells to apoptosis and inhibits tumorigenicity by regulating ECOP-mediated suppression of NF-kappaB activity. *Neuro Oncol.* 2013;15(4):413–22. <http://dx.doi.org/10.1093/neuonc/nos296>
80. Nan Y, Han L, Zhang A, Wang G, Jia Z, Yang Y, et al. MiRNA-451 plays a role as tumor suppressor in human glioma cells. *Brain Res.* 2010;1359:14–21. <http://dx.doi.org/10.1016/j.brainres.2010.08.074>
81. Wurdinger T, Tannous BA, Saydam O, Skog J, Grau S, Soutschek J, et al. miR-296 regulates growth factor receptor overexpression in angiogenic endothelial cells. *Cancer Cell.* 2008;14(5):382–93. <http://dx.doi.org/10.1016/j.ccr.2008.10.005>
82. Smits M, Wurdinger T, van het Hof B, Drexhage JA, Geerts D, Wesseling P, et al. Myc-associated zinc finger protein (MAZ) is regulated by miR-125b and mediates VEGF-induced angiogenesis in glioblastoma. *FASEB J.* 2012;26(6):2639–47. <http://dx.doi.org/10.1096/fj.11-202820>
83. Yang G, Han D, Chen X, Zhang D, Wang L, Shi C, et al. MiR-196a exerts its oncogenic effect in glioblastoma multiforme by inhibition of IkappaBalpha both in vitro and in vivo. *Neuro Oncol.* 2014;16(5):652–61. <http://dx.doi.org/10.1093/neuonc/not307>
84. Floyd DH, Zhang Y, Dey BK, Kefas B, Breit H, Marks K, et al. Novel anti-apoptotic microRNAs 582-5p and 363 promote human glioblastoma stem cell survival via direct inhibition of caspase 3, caspase 9, and Bim. *PLoS One.* 2014;9(5):e96239. <http://dx.doi.org/10.1371/journal.pone.0096239>
85. Kalluri R, Weinberg RA. The basics of epithelial-mesenchymal transition. *J Clin Invest.* 2009;119(6):1420–8. <http://dx.doi.org/10.1172/JCI39104>
86. Schramedei K, Morbt N, Pfeifer G, Lauter J, Rosolowski M, Tomm JM, et al. MicroRNA-21 targets tumor suppressor genes ANP32A and SMARCA4. *Oncogene.* 2011;30(26):2975–85. <http://dx.doi.org/10.1038/onc.2011.15>
87. Li Y, Wang Y, Yu L, Sun C, Cheng D, Yu S, et al. miR-146b-5p inhibits glioma migration and invasion by targeting MMP16. *Cancer Lett.* 2013;339(2):260–9. <http://dx.doi.org/10.1016/j.canlet.2013.06.018>
88. Sun L, Yan W, Wang Y, Sun G, Luo H, Zhang J, et al. MicroRNA-10b induces glioma cell invasion by modulating MMP-14 and uPAR expression via HOXD10. *Brain Res.* 2011;1389:9–18. <http://dx.doi.org/10.1016/j.brainres.2011.03.013>
89. Lin J, Teo S, Lam DH, Jayaseelan K, Wang S. MicroRNA-10b pleiotropically regulates invasion, angiogenicity and apoptosis of tumor cells resembling mesenchymal subtype of glioblastoma multiforme. *Cell Death Dis.* 2012;3:e398. <http://dx.doi.org/10.1038/cddis.2012.134>
90. Mao XG, Hutt-Cabezas M, Orr BA, Weingart M, Taylor I, Rajan AK, et al. LIN28A facilitates the transformation of human neural stem cells and promotes glioblastoma tumorigenesis through a pro-invasive genetic program. *Oncotarget.* 2013;4(7):1050–64. <http://dx.doi.org/10.18632/oncotarget.1131>
91. Wang S, Olson EN. AngiomiRs—key regulators of angiogenesis. *Curr Opin Genet Dev.* 2009;19(3):205–11. <http://dx.doi.org/10.1016/j.gde.2009.04.002>
92. Mathew LK, Skuli N, Mucaj V, Lee SS, Zinn PO, Sathyan P, et al. miR-218 opposes a critical RTK-HIF pathway in mesenchymal glioblastoma. *Proc Natl Acad Sci U S A.* 2014;111(1):291–6. <http://dx.doi.org/10.1073/pnas.1314341111>
93. Agrawal R, Pandey P, Jha P, Dwivedi V, Sarkar C, Kulshreshtha R. Hypoxic signature of microRNAs in glioblastoma: Insights from small RNA deep sequencing. *BMC Genomics.* 2014;15:686. <http://dx.doi.org/10.1186/1471-2164-15-686>
94. Fang L, Deng Z, Shatseva T, Yang J, Peng C, Du WW, et al. MicroRNA miR-93 promotes tumor growth and angiogenesis by targeting integrin-beta8. *Oncogene.* 2011;30(7):806–21. <http://dx.doi.org/10.1038/onc.2010.465>
95. Brooks WH, Markesbery WR, Gupta GD, Roszman TL. Relationship of lymphocyte invasion and survival of brain tumor patients. *Ann Neurol.* 1978;4(3):219–24. <http://dx.doi.org/10.1002/ana.410040305>
96. Jacobs JF, Idema AJ, Bol KF, Grotenhuis JA, de Vries IJ, Wesseling P, et al. Prognostic significance and mechanism of Treg infiltration in human brain tumors. *J Neuroimmunol.* 2010;225(1–2):195–9. <http://dx.doi.org/10.1016/j.jneuroim.2010.05.020>

97. Kong LY, Wu AS, Doucette T, Wei J, Priebe W, Fuller GN, et al. Intratumoral mediated immunosuppression is prognostic in genetically engineered murine models of glioma and correlates to immunotherapeutic responses. *Clin Cancer Res.* 2010;16(23):5722–33. <http://dx.doi.org/10.1158/1078-0432.CCR-10-1693>
98. Palma L, Di Lorenzo N, Guidetti B. Lymphocytic infiltrates in primary glioblastomas and recidivous gliomas. Incidence, fate, and relevance to prognosis in 228 operated cases. *J Neurosurg.* 1978;49(6):854–61. <http://dx.doi.org/10.3171/jns.1978.49.6.0854>
99. Safdari H, Hochberg FH, Richardson EP, Jr. Prognostic value of round cell (lymphocyte) infiltration in malignant gliomas. *Surg Neurol.* 1985;23(3):221–6. [http://dx.doi.org/10.1016/0090-3019\(85\)90086-2](http://dx.doi.org/10.1016/0090-3019(85)90086-2)
100. von Hanwehr RI, Hofman FM, Taylor CR, Apuzzo ML. Mononuclear lymphoid populations infiltrating the microenvironment of primary CNS tumors. Characterization of cell subsets with monoclonal antibodies. *J Neurosurg.* 1984;60(6):1138–47. <http://dx.doi.org/10.3171/jns.1984.60.6.1138>
101. Yang I, Tihan T, Han SJ, Wrench MR, Wiencke J, Sughrue ME, et al. CD8+ T-cell infiltrate in newly diagnosed glioblastoma is associated with long-term survival. *J Clin Neurosci.* 2010;17(11):1381–5. <http://dx.doi.org/10.1016/j.jocn.2010.03.031>
102. Wei J, Wang F, Kong LY, Xu S, Doucette T, Ferguson SD, et al. miR-124 inhibits STAT3 signaling to enhance T cell-mediated immune clearance of glioma. *Cancer Res.* 2013;73(13):3913–26. <http://dx.doi.org/10.1158/0008-5472.CAN-12-4318>
103. Ueda R, Kohanbash G, Sasaki K, Fujita M, Zhu X, Kastenhuber ER, et al. Dicer-regulated microRNAs 222 and 339 promote resistance of cancer cells to cytotoxic T-lymphocytes by down-regulation of ICAM-1. *Proc Natl Acad Sci U S A.* 2009;106(26):10746–51. <http://dx.doi.org/10.1073/pnas.0811817106>
104. Hassan A, Mosley J, Singh S, Zinn PO. A comprehensive review of genomics and noncoding RNA in gliomas. *Top Magn Reson Imaging.* 2017;26(1):3–14. <http://dx.doi.org/10.1097/rmr.0000000000000111>
105. Shi L, Chen J, Yang J, Pan T, Zhang S, Wang Z. MiR-21 protected human glioblastoma U87MG cells from chemotherapeutic drug temozolomide induced apoptosis by decreasing Bax/Bcl-2 ratio and caspase-3 activity. *Brain Res.* 2010;1352:255–64. <http://dx.doi.org/10.1016/j.brainres.2010.07.009>
106. Li Y, Li W, Yang Y, Lu Y, He C, Hu G, et al. MicroRNA-21 targets LRRFIP1 and contributes to VM-26 resistance in glioblastoma multiforme. *Brain Res.* 2009;1286:13–8. <http://dx.doi.org/10.1016/j.brainres.2009.06.053>
107. Costa PM, Cardoso AL, Nobrega C, Pereira de Almeida LF, Bruce JN, Canoll P, et al. MicroRNA-21 silencing enhances the cytotoxic effect of the antiangiogenic drug sunitinib in glioblastoma. *Hum Mol Genet.* 2013;22(5):904–18. <http://dx.doi.org/10.1093/hmg/dds496>
108. Wong ST, Zhang XQ, Zhuang JT, Chan HL, Li CH, Leung GK. MicroRNA-21 inhibition enhances in vitro chemosensitivity of temozolomide-resistant glioblastoma cells. *Anticancer Res.* 2012;32(7):2835–41.
109. Barker CA, Chang M, Chou JF, Zhang Z, Beal K, Gutin PH, et al. Radiotherapy and concomitant temozolomide may improve survival of elderly patients with glioblastoma. *J Neurooncol.* 2012;109(2):391–7. <http://dx.doi.org/10.1007/s11060-012-0906-4>
110. Ren Y, Zhou X, Mei M, Yuan XB, Han L, Wang GX, et al. MicroRNA-21 inhibitor sensitizes human glioblastoma cells U251 (PTEN-mutant) and LN229 (PTEN-wild type) to taxol. *BMC Cancer.* 2010;10:27. <http://dx.doi.org/10.1186/1471-2407-10-27>
111. Ujifuku K, Mitsutake N, Takakura S, Matsuse M, Saenko V, Suzuki K, et al. miR-195, miR-455-3p and miR-10a(*) are implicated in acquired temozolomide resistance in glioblastoma multiforme cells. *Cancer Lett.* 2010;296(2):241–8. <http://dx.doi.org/10.1016/j.canlet.2010.04.013>
112. Zhang S, Han L, Wei J, Shi Z, Pu P, Zhang J, et al. Combination treatment with doxorubicin and microRNA-21 inhibitor synergistically augments anticancer activity through upregulation of tumor suppressing genes. *Int J Oncol.* 2015;46(4):1589–600. <http://dx.doi.org/10.3892/ijo.2015.2841>
113. Shi L, Zhang S, Feng K, Wu F, Wan Y, Wang Z, et al. MicroRNA-125b-2 confers human glioblastoma stem cells resistance to temozolomide through the mitochondrial pathway of apoptosis. *Int J Oncol.* 2012;40(1):119–29.
114. Turrini E, Haenisch S, Laechelt S, Diewock T, Bruhn O, Cascorbi I. MicroRNA profiling in K-562 cells under imatinib treatment: Influence of miR-212 and miR-328 on ABCG2 expression. *Pharmacogenet Genomics.* 2012;22(3):198–205. <http://dx.doi.org/10.1097/FPC.0b013e328350012b>

115. Ng WL, Yan D, Zhang X, Mo YY, Wang Y. Over-expression of miR-100 is responsible for the low-expression of ATM in the human glioma cell line: M059J. *DNA repair*. 2010;9(11):1170–5. <http://dx.doi.org/10.1016/j.dnarep.2010.08.007>
116. Krichevsky AM, King KS, Donahue CP, Khrapko K, Kosik KS. A microRNA array reveals extensive regulation of microRNAs during brain development. *RNA*. 2003;9(10):1274–81. <http://dx.doi.org/10.1261/rna.5980303>
117. Lee TJ, Yoo JY, Shu D, Li H, Zhang J, Yu JG, et al. RNA nanoparticle-based targeted therapy for glioblastoma through inhibition of oncogenic miR-21. *Mol Ther*. 2017;25(7):1544–55. <http://dx.doi.org/10.1016/j.ymthe.2016.11.016>
118. Gabriely G, Yi M, Narayan RS, Niers JM, Wurdinger T, Imitola J, et al. Human glioma growth is controlled by microRNA-10b. *Cancer Res*. 2011;71(10):3563–72. <http://dx.doi.org/10.1158/0008-5472.CAN-10-3568>
119. El Fatimy R, Subramanian S, Uhlmann EJ, Krichevsky AM. Genome editing reveals glioblastoma addiction to microRNA-10b. *Mol Ther*. 2017;25(2):368–78. <http://dx.doi.org/10.1016/j.ymthe.2016.11.004>
120. Kefas B, Comeau L, Erdle N, Montgomery E, Amos S, Purov B. Pyruvate kinase M2 is a target of the tumor-suppressive microRNA-326 and regulates the survival of glioma cells. *Neuro Oncol*. 2010;12(11):1102–12. <http://dx.doi.org/10.1093/neuonc/neoq080>
121. Kefas B, Comeau L, Floyd DH, Seleverstov O, Godlewski J, Schmittgen T, et al. The neuronal microRNA miR-326 acts in a feedback loop with notch and has therapeutic potential against brain tumors. *J Neurosci*. 2009;29(48):15161–8. <http://dx.doi.org/10.1523/JNEUROSCI.4966-09.2009>
122. Kefas B, Floyd DH, Comeau L, Frisbee A, Dominguez C, Dipierro CG, et al. A miR-297/hypoxia/DGK-alpha axis regulating glioblastoma survival. *Neuro Oncol*. 2013;15(12):1652–63. <http://dx.doi.org/10.1093/neuonc/not118>
123. Godlewski J, Nowicki MO, Bronisz A, Williams S, Otsuki A, Nuovo G, et al. Targeting of the Bmi-1 oncogene/stem cell renewal factor by microRNA-128 inhibits glioma proliferation and self-renewal. *Cancer Res*. 2008;68(22):9125–30. <http://dx.doi.org/10.1158/0008-5472.CAN-08-2629>
124. Kouri FM, Hurley LA, Daniel WL, Day ES, Hua Y, Hao L, et al. miR-182 integrates apoptosis, growth, and differentiation programs in glioblastoma. *Genes Dev*. 2015;29(7):732–45. <http://dx.doi.org/10.1101/gad.257394.114>
125. Teplyuk NM, Uhlmann EJ, Gabriely G, Volfovsky N, Wang Y, Teng J, et al. Therapeutic potential of targeting microRNA-10b in established intracranial glioblastoma: First steps toward the clinic. *EMBO Mol Med*. 2016;8(3):268–87. <http://dx.doi.org/10.15252/emmm.201505495>
126. Skog J, Wurdinger T, van Rijn S, Meijer DH, Gainche L, Sena-Estevés M, et al. Glioblastoma microvesicles transport RNA and proteins that promote tumour growth and provide diagnostic biomarkers. *Nat Cell Biol*. 2008;10(12):1470–6. <http://dx.doi.org/10.1038/ncb1800>
127. Beg MS, Brenner AJ, Sachdev J, Borad M, Kang YK, Stoudemire J, et al. Phase I study of MRX34, a liposomal miR-34a mimic, administered twice weekly in patients with advanced solid tumors. *Invest New Drugs*. 2017;35(2):180–8. <http://dx.doi.org/10.1007/s10637-016-0407-y>
128. Rinn JL, Chang HY. Genome regulation by long noncoding RNAs. *Annu Rev Biochem*. 2012;81:145–66. <http://dx.doi.org/10.1146/annurev-biochem-051410-092902>
129. Batista PJ, Chang HY. Long noncoding RNAs: Cellular address codes in development and disease. *Cell*. 2013;152(6):1298–307. <http://dx.doi.org/10.1016/j.cell.2013.02.012>
130. Mercer TR, Mattick JS. Structure and function of long noncoding RNAs in epigenetic regulation. *Nat Struct Mol Biol*. 2013;20(3):300–7. <http://dx.doi.org/10.1038/nsmb.2480>
131. Heo JB, Lee YS, Sung S. Epigenetic regulation by long noncoding RNAs in plants. *Chromosome Res*. 2013;21(6–7):685–93. <http://dx.doi.org/10.1007/s10577-013-9392-6>
132. Ramos AD, Attenello FJ, Lim DA. Uncovering the roles of long noncoding RNAs in neural development and glioma progression. *Neurosci Lett*. 2016;625:70–9. <http://dx.doi.org/10.1016/j.neulet.2015.12.025>
133. Iyer MK, Niknafs YS, Malik R, Singhal U, Sahu A, Hosono Y, et al. The landscape of long noncoding RNAs in the human transcriptome. *Nat Genet*. 2015;47(3):199–208SS.
134. Cabili MN, Trapnell C, Goff L, Koziol M, Tazon-Vega B, Regev A, et al. Integrative annotation of human large intergenic noncoding RNAs reveals global properties and specific subclasses. *Gene Dev*. 2011;25(18):1915–27. <http://dx.doi.org/10.1101/gad.17446611>

135. Derrien T, Johnson R, Bussotti G, Tanzer A, Djebali S, Tilgner H, et al. The GENCODE v7 catalog of human long noncoding RNAs: Analysis of their gene structure, evolution, and expression. *Genome Res.* 2012;22(9):1775–89. <http://dx.doi.org/10.1101/gr.132159.111>
136. Mercer TR, Qureshi IA, Gokhan S, Dinger ME, Li GY, Mattick JS, et al. Long noncoding RNAs in neuronal-glia fate specification and oligodendrocyte lineage maturation. *BMC Neurosci.* 2010;11:14. <http://dx.doi.org/10.1186/1471-2202-11-14>
137. Belgard TG, Marques AC, Oliver PL, Abaan HO, Sirey TM, Hoerder-Suabedissen A, et al. A transcriptomic atlas of mouse neocortical layers. *Neuron.* 2011;71(4):605–16. <http://dx.doi.org/10.1016/j.neuron.2011.06.039>
138. Ulitsky I, Shkumatava A, Jan CH, Sive H, Bartel DP. Conserved function of lincRNAs in vertebrate embryonic development despite rapid sequence evolution. *Cell.* 2011;147(7):1537–50. <http://dx.doi.org/10.1016/j.cell.2011.11.055>
139. Guttman M, Amit I, Garber M, French C, Lin MF, Feldser D, et al. Chromatin signature reveals over a thousand highly conserved large non-coding RNAs in mammals. *Nature.* 2009;458(7235):223–7. <http://dx.doi.org/10.1038/nature07672>
140. Ramos AD, Diaz A, Nellore A, Delgado RN, Park KY, Gonzales-Roybal G, et al. Integration of genome-wide approaches identifies lincRNAs of adult neural stem cells and their progeny in vivo. *Cell Stem Cell.* 2013;12(5):616–28. <http://dx.doi.org/10.1016/j.stem.2013.03.003>
141. Mercer TR, Dinger ME, Mattick JS. Long non-coding RNAs: Insights into functions. *Nat Rev Genet.* 2009;10(3):155–9. <http://dx.doi.org/10.1038/nrg2521>
142. Bian EB, Li J, Xie YS, Zong G, Li J, Zhao B. LncRNAs: New players in gliomas, with special emphasis on the interaction of lncRNAs with EZH2. *J Cell Physiol.* 2015;230(3):496–503. <http://dx.doi.org/10.1002/jcp.24549>
143. Sun YZ, Wang Z, Zhou D. Long non-coding RNAs as potential biomarkers and therapeutic targets for gliomas. *Med Hypotheses.* 2013;81(2):319–21. <http://dx.doi.org/10.1016/j.mehy.2013.04.010>
144. Wang PJ, Ren ZQ, Sun PY. Overexpression of the long non-coding RNA MEG3 impairs in vitro glioma cell proliferation. *J Cell Biochem.* 2012;113(6):1868–74. <http://dx.doi.org/10.1002/jcb.24055>
145. Zhang XQ, Sun S, Pu JKS, Tsang ACO, Lee D, Man VOY, et al. Long non-coding RNA expression profiles predict clinical phenotypes in glioma. *Neurobiol Dis.* 2012;48(1):1–8. <http://dx.doi.org/10.1016/j.nbd.2012.06.004>
146. Amit D, Matouk IJ, Lavon I, Birman T, Galula J, Abu-Lail R, et al. Transcriptional targeting of glioblastoma by diphtheria toxin-A driven by both H19 and IGF2-P4 promoters. *Int J Clin Exp Med.* 2012;5(2):124–35.
147. Qi P, Du X. The long non-coding RNAs, a new cancer diagnostic and therapeutic gold mine. *Modern Pathol.* 2013;26(2):155–65. <http://dx.doi.org/10.1038/modpathol.2012.160>
148. Spizzo R, Almeida MI, Colombatti A, Calin GA. Long non-coding RNAs and cancer: A new frontier of translational research? *Oncogene.* 2012;31(43):4577–87. <http://dx.doi.org/10.1038/onc.2011.621>
149. Wahlestedt C. Targeting long non-coding RNA to therapeutically upregulate gene expression. *Nat Rev Drug Discov.* 2013;12(6):433–46. <http://dx.doi.org/10.1038/nrd4018>
150. Han L, Zhang KL, Shi ZD, Zhang JX, Zhu JL, Zhu SJ, et al. LncRNA profile of glioblastoma reveals the potential role of lncRNAs in contributing to glioblastoma pathogenesis. *Int J Oncol.* 2012;40(6):2004–12.
151. Gravendeel L, Kouwenhoven M, Gevaert O, de Rooij J, Stubbs A, Duijnm J, et al. Intrinsic gene expression profiles of gliomas are a better predictor of survival than histology. *Neuro Oncol.* 2009;11(5):602. <http://dx.doi.org/10.1158/0008-5472.can-09-2307>
152. Sun LX, Hui AM, Su Q, Vortmeyer A, Kotliarov Y, Pastorino S, et al. Neuronal and glioma-derived stem cell factor induces angiogenesis within the brain. *Cancer Cell.* 2006;9(4):287–300. <http://dx.doi.org/10.1016/j.ccr.2006.03.003>
153. Murat A, Migliavacca E, Gorlia T, Lambiv WL, Shay T, Hamou MF, et al. Stem cell-related “Self-Renewal” signature and high epidermal growth factor receptor expression associated with resistance to concomitant chemoradiotherapy in glioblastoma. *J Clin Oncol.* 2008;26(18):3015–24. <http://dx.doi.org/10.1200/JCO.2007.15.7164>

154. Grzmil M, Morin PJ, Lino MM, Merlo A, Frank S, Wang YH, et al. MAP kinase-interacting kinase 1 regulates SMAD2-dependent TGF-beta signaling pathway in human glioblastoma. *Cancer Res.* 2011;71(6):2392–402. <http://dx.doi.org/10.1158/0008-5472.CAN-10-3112>
155. Reon BJ, Anaya J, Zhang Y, Mandell J, Purow B, Abounader R, et al. Expression of lncRNAs in low-grade gliomas and glioblastoma multiforme: An in silico analysis. *PLoS Med.* 2016;13(12):e1002192. <http://dx.doi.org/10.1371/journal.pmed.1002192>
156. Lin NW, Chang KY, Li ZH, Gates K, Rana ZA, Dang JS, et al. An evolutionarily conserved long noncoding RNA TUNA controls pluripotency and neural lineage commitment. *Mol Cell.* 2014;53(6):1005–19. <http://dx.doi.org/10.1016/j.molcel.2014.01.021>
157. Zheng J, Liu XB, Wang P, Xue YX, Ma J, Qu CB, et al. CRNDE promotes malignant progression of glioma by attenuating miR-384/PIWIL4/STAT3 axis. *Mol Ther.* 2016;24(7):1199–215. <http://dx.doi.org/10.1038/mt.2016.71>
158. Graham LD, Pedersen SK, Brown GS, Ho T, Kassir Z, Moynihan AT, et al. Colorectal neoplasia differentially expressed (CRNDE), a novel gene with elevated expression in colorectal adenomas and adenocarcinomas. *Genes Cancer.* 2011;2(8):829–40. <http://dx.doi.org/10.1177/1947601911431081>
159. Zheng J, Li XD, Wang P, Liu XB, Xue YX, Hu Y, et al. CRNDE affects the malignant biological characteristics of human glioma stem cells by negatively regulating miR-186. *Oncotarget.* 2015;6(28):25339–55. <http://dx.doi.org/10.18632/oncotarget.4509>
160. Wang Y, Wang Y, Li J, Zhang Y, Yin H, Han B. CRNDE, a long-noncoding RNA, promotes glioma cell growth and invasion through mTOR signaling. *Cancer Lett.* 2015;367(2):122–8. <http://dx.doi.org/10.1016/j.canlet.2015.03.027>
161. Zhang K, Sun X, Zhou X, Han L, Chen L, Shi Z, et al. Long non-coding RNA HOTAIR promotes glioblastoma cell cycle progression in an EZH2 dependent manner. *Oncotarget.* 2015;6(1):537–46.
162. Zhou X, Ren Y, Zhang J, Zhang C, Zhang K, Han L, et al. HOTAIR is a therapeutic target in glioblastoma. *Oncotarget.* 2015;6(10):8353–65. <http://dx.doi.org/10.18632/oncotarget.3229>
163. Gutschner T, Hammerle M, Eissmann M, Hsu J, Kim Y, Hung G, et al. The noncoding RNA MALAT1 is a critical regulator of the metastasis phenotype of lung cancer cells. *Cancer Res.* 2013;73(3):1180–9. <http://dx.doi.org/10.1158/0008-5472.CAN-12-2850>
164. Tano K, Mizuno R, Okada T, Rakwal R, Shibato J, Masuo Y, et al. MALAT-1 enhances cell motility of lung adenocarcinoma cells by influencing the expression of motility-related genes. *FEBS Lett.* 2010;584(22):4575–80. <http://dx.doi.org/10.1016/j.febslet.2010.10.008>
165. Zhang XQ, Sun S, Lam KF, Kiang KM, Pu JK, Ho AS, et al. A long non-coding RNA signature in glioblastoma multiforme predicts survival. *Neurobiol Dis.* 2013;58:123–31. <http://dx.doi.org/10.1016/j.nbd.2013.05.011>
166. Aldaz B, Sagardoy A, Nogueira L, Guruceaga E, Grande L, Huse JT, et al. Involvement of miRNAs in the differentiation of human glioblastoma multiforme stem-like cells. *PLoS One.* 2013;8(10):e77098. <http://dx.doi.org/10.1371/journal.pone.0077098>
167. Zarkoob H, Taube JH, Singh SK, Mani SA, Kohandel M. Investigating the link between molecular subtypes of glioblastoma, epithelial-mesenchymal transition, and CD133 cell surface protein. *PLoS One.* 2013;8(5):e64169. <http://dx.doi.org/10.1371/journal.pone.0064169>
168. Venkatraman A, He XC, Thorvaldsen JL, Sugimura R, Perry JM, Tao F, et al. Maternal imprinting at the H19-Igf2 locus maintains adult haematopoietic stem cell quiescence. *Nature.* 2013;500(7462):345–9. <http://dx.doi.org/10.1038/nature12303>
169. Garcia-Claver A, Lorente M, Mur P, Campos-Martin Y, Mollejo M, Velasco G, et al. Gene expression changes associated with erlotinib response in glioma cell lines. *Eur J Cancer.* 2013;49(7):1641–53. <http://dx.doi.org/10.1016/j.ejca.2013.01.002>
170. Kino T, Hurt DE, Ichijo T, Nader N, Chrousos GP. Noncoding RNA gas5 is a growth arrest- and starvation-associated repressor of the glucocorticoid receptor. *Sci Signal.* 2010;3(107):ra8. <http://dx.doi.org/10.1126/scisignal.2000568>
171. Barsyte-Lovejoy D, Lau SK, Boutros PC, Khosravi F, Jurisica I, Andrulis IL, et al. The c-Myc oncogene directly induces the H19 noncoding RNA by allele-specific binding to potentiate tumorigenesis. *Cancer Res.* 2006;66(10):5330–7. <http://dx.doi.org/10.1158/0008-5472.CAN-06-0037>

172. Atkinson GP, Nozell SE, Benveniste ET. NF-kappaB and STAT3 signaling in glioma: Targets for future therapies. *Expert Rev Neurother.* 2010;10(4):575–86. <http://dx.doi.org/10.1586/ern.10.21>
173. Herms JW, von Loewenich FD, Behnke J, Markakis E, Kretzschmar HA. c-myc oncogene family expression in glioblastoma and survival. *Surg Neurol.* 1999;51(5):536–42. [http://dx.doi.org/10.1016/S0090-3019\(98\)00028-7](http://dx.doi.org/10.1016/S0090-3019(98)00028-7)
174. Moustakas A, Souchelnytskyi S, Heldin CH. Smad regulation in TGF-beta signal transduction. *J Cell Sci.* 2001;114(Pt 24):4359–69.
175. ten Dijke P, Hill CS. New insights into TGF-beta-Smad signalling. *Trends Biochem Sci.* 2004;29(5):265–73. <http://dx.doi.org/10.1016/j.tibs.2004.03.008>
176. Yang JH, Li JH, Jiang S, Zhou H, Qu LH. ChIPBase: A database for decoding the transcriptional regulation of long non-coding RNA and microRNA genes from ChIP-Seq data. *Nucleic Acids Res.* 2013;41(Database issue):D177–87. <http://dx.doi.org/10.1093/nar/gks1060>
177. Pastori C, Kapranov P, Penas C, Peschansky V, Volmar CH, Sarkaria JN, et al. The Bromodomain protein BRD4 controls HOTAIR, a long noncoding RNA essential for glioblastoma proliferation. *Proc Natl Acad Sci U S A.* 2015;112(27):8326–31. <http://dx.doi.org/10.1073/pnas.1424220112>
178. Suva ML, Rheinbay E, Gillespie SM, Patel AP, Wakimoto H, Rabkin SD, et al. Reconstructing and reprogramming the tumor-propagating potential of glioblastoma stem-like cells. *Cell.* 2014;157(3):580–94. <http://dx.doi.org/10.1016/j.cell.2014.02.030>
179. Ferrarese R, Harsh GR, Yadav AK, Bug E, Maticzka D, Reichardt W, et al. Lineage-specific splicing of a brain-enriched alternative exon promotes glioblastoma progression. *J Clin Invest.* 2014;124(7):2861–76. <http://dx.doi.org/10.1172/JCI68836>
180. Zhen L, Yun-Hui L, Hong-Yu D, Jun M, Yi-Long Y. Long noncoding RNA NEAT1 promotes glioma pathogenesis by regulating miR-449b-5p/c-Met axis. *Tumour Biol.* 2016;37(1):673–83. <http://dx.doi.org/10.1007/s13277-015-3843-y>

7

Mouse Models of Glioblastoma

NORIYUKI KIJIMA¹ • YONEHIRO KANEMURA^{1,2}

¹Department of Neurosurgery, Osaka National Hospital, National Hospital Organization, Osaka, Japan; ²Division of Regenerative Medicine, Institute for Clinical Research, Osaka National Hospital, National Hospital Organization, Osaka, Japan

Author for correspondence: Noriyuki Kijima, Department of Neurosurgery, Osaka National Hospital, National Hospital Organization, Osaka, Japan.
E-mail: norikiji@onh.go.jp

Doi: <http://dx.doi.org/10.15586/codon.glioblastoma.2017.ch7>

Abstract: Glioblastoma is one of the most common malignant brain tumors. The prognosis for glioblastoma is still very poor despite intensive treatment by surgery, radiation, and chemotherapy. To develop new therapies for glioblastoma, preclinical mouse models are essential for analyzing the biology of glioblastoma, identifying new therapeutic targets, and evaluating the potential of new therapeutic strategies. Current preclinical glioblastoma models are classified into two categories: xenografts and genetically engineered mouse models. Xenografts are classified into two categories: glioblastoma cell-line xenografts and patient-derived xenografts. Glioblastoma cell-line xenografts generally have the advantages of high engraftment and growth rates, but it is doubtful whether glioblastoma cell-line xenografts reflect the true biological nature of glioblastoma. Patient-derived xenografts retain both the genetic and histological features of the primary tumor, and thus are expected to be good preclinical models in translational glioblastoma research. However, they cannot fully reflect the host's antitumor immunity in human glioblastoma. Glioblastoma genetically engineered mouse models make it possible to pinpoint genetic alterations involved in tumor initiation and progression, but tumors are usually composed of cells with specific, homogeneous genetic changes, and thus cannot completely reflect the intratumoral genomic and phenotypic heterogeneity of glioblastoma. Presently, patient-derived xenografts and glioblastoma

In: *Glioblastoma*. Steven De Vleeschouwer (Editor), Codon Publications, Brisbane, Australia
ISBN: 978-0-9944381-2-6; Doi: <http://dx.doi.org/10.15586/codon.glioblastoma.2017>

Copyright: The Authors.

Licence: This open access article is licenced under Creative Commons Attribution 4.0 International (CC BY 4.0). <https://creativecommons.org/licenses/by-nc/4.0/>

genetically engineered mouse models are excellent glioblastoma mouse models for current use, but more work is needed to establish mouse models that fully recapitulate human glioblastoma.

Key words: Chemically induced mouse model; Genetically engineered mouse model; Glioblastoma; Preclinical model; Xenograft

Introduction

Glioblastoma is one of the most common malignant brain tumors. The prognosis for glioblastoma is still very poor; despite intensive treatment by surgery, radiation, and chemotherapy, the median survival is only about 15 months (1). Thus, there is an urgent need for more effective treatments, and various therapies for glioblastoma have been tested or are in development. To develop new therapies, preclinical mouse models are essential for analyzing the biology of glioblastoma, identifying new therapeutic targets, and evaluating the potential of new therapeutic strategies. Current preclinical glioblastoma models are classified into three categories: xenografts, genetically engineered mouse (GEM) models, and syngenic murine models (2, 3). In this chapter, we summarize the currently available mouse models of glioblastoma, the advantages and disadvantages of each model, and the prospects for developing better mouse models.

Xenografts

Glioblastoma xenografts are classified into two categories: glioblastoma cell-line xenografts and patient-derived xenografts.

GLIOBLASTOMA CELL-LINE XENOGRAPTS

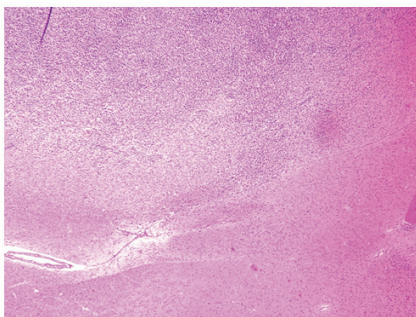
Commercially available glioblastoma cell lines include U87, U251, T98G, and A172, among others. These traditional glioblastoma cell lines are the most common models used in both *in vitro* and *in vivo* glioblastoma research. These glioblastoma cell lines, which were originally derived from glioblastoma patients, are usually cultured in serum-containing medium and xenografted into immunodeficient mice such as nude mice, NOD/SCID mice, and NOD/SCID gamma mice.

Glioblastoma cell-line xenografts generally have the advantages of high engraftment and growth rates, good reproducibility, and reliable disease growth and progression. Moreover, immortalized cell lines can be readily expanded for an unlimited number of passages *in vitro*, yielding a large number of tumor cells for experimental use (3). However, studies have reported that glioblastoma cell-line xenografts do not reflect the clinical characteristics of the original patient tumors (4); that is, the xenografted tumors are usually circumscribed and do not show single-cell invasion, tumor necrosis, or microvascular proliferation (5, 6). They also show differences in MHC (7) and integrin expression (3), suggesting that the xenografted tumors differ phenotypically from the original patient tumors. Genotypes of glioblastoma cell-line xenograft models also differ from the original

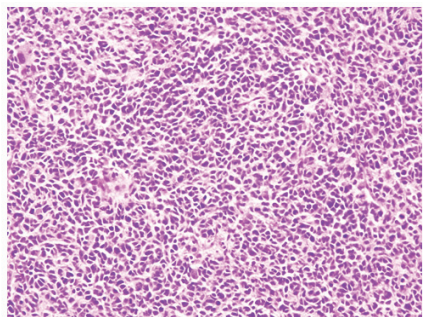
patient tumors (3); profiles from array-comparative genomic hybridization (aCGH) and whole-genome sequencing of glioblastoma cell lines are quite different from those typically found in primary glioblastoma (8, 9). Thus, it is doubtful whether glioblastoma cell-line xenografts reflect the true biological nature of glioblastoma, and this is a disadvantage in preclinical trials. Due to their genomic and transcriptomic deviations from glioblastoma *in situ*, glioblastoma cell lines are poor models for glioblastoma (3, 10).

PATIENT-DERIVED XENOGRAFTS

Patient-derived xenografts (PDX) (11, 12), a recent focus of glioblastoma research, are used extensively in translational research. The PDX model has the advantage of retaining both the genetic and histological features of the primary tumor from which it was derived (Figure 1). Because the tumors are propagated in successive generations of mice, PDX cells are not subjected to stresses that can arise in cell cultures (13, 14). There is some controversy as to whether PDX models are best established by injecting freshly biopsied tumor tissue (15, 16) or cultured tumor spheres into mice (17), and whether orthotopic or subcutaneous xenograft is preferable. PDX models are generally established by injecting glioblastoma tumor spheres produced under serum-free neurosphere-culture conditions, into immunodeficient mice. Tumor spheres have several advantages over serum-cultured glioblastoma cell lines: the tumor spheres retain a molecular profile similar to that of the patient's original tumor, thus maintaining tumor heterogeneity (18, 19); their molecular profile is stable over time, and they are both tumorigenic and phenotypically similar to the patient's original tumor, even in aspects such as single-cell invasion and tumor angiogenesis (20, 21). However, not all human gliomas are successfully cultured as tumor spheres; reported success rates vary from 10 to 20% (3, 22). Thus, one group took an alternative approach of using a serum-free cell-culture system to generate monolayer cultures on laminin-coated plates (23). At present, however, there is little molecular evidence for preferring adherent culture over sphere culture. The generation of tumorigenic cell populations



Representative picture of a H&E image from patient-derived orthotopic glioblastoma xenograft.($\times 40$) day 70



Representative picture of a H&E image from patient-derived orthotopic glioblastoma xenograft.($\times 200$) day 70

Figure 1 Representative picture of a H&E image from patient-derived orthotopic glioblastoma xenograft.

from human glioblastomas using neurosphere culture has significantly advanced our knowledge of specific subpopulations within human primary tumors. Even though their phenotypes *in vivo* are not necessarily predictable, these cell populations are an important tool for studying the tumorigenicity and progression of glioblastoma *in vivo*.

Another method for establishing PDX models is to inject tissues from fresh brain-tumor biopsies into immunodeficient mice. The biopsy tissue is generally minced with surgical blades and placed in flasks containing standard serum-supplemented tissue-culture medium (24). Under these conditions, tumor spheroids form quickly, and the spheroids maintain the architecture of the original tissue, including the endothelium, extracellular matrix components, and resident macrophages (24). PDX models from fresh brain-tumor biopsies display diffuse single-cell infiltration when implanted into the brain of immunodeficient rats or mice (15, 25, 26), and these biopsy xenograft models preserve other histological features of human glioblastoma. In one study, however, spheroids derived from a fresh brain-tumor biopsy failed to form tumors in the mouse brain (16). Thus, technological standardization is needed to establish highly reproducible PDX models from tumor spheroids.

Both cultured tumor spheres and tumor biopsy tissues maintain the genetic and phenotypical features of the original patient tumors when injected into immunodeficient mice. However, in theory, tumor biopsy tissues may have advantages over tumor spheres in that they maintain the original tissue architecture, complete with endothelium, extracellular matrix components, and resident macrophages. Thus, the injected biopsy tissue has a greater potential for reflecting the biological features of the original human glioblastoma. However, more studies are necessary to confirm the superiority of one method over the other.

Another controversy related to PDX models is whether orthotopic or subcutaneous xenografts are better. While orthotopic xenografts more closely mimic the clinical situation, subcutaneous xenografts, usually accomplished by transplanting the patient-derived tumor spheres or freshly biopsied tissue directly into the flanks of immunodeficient mice (27), are less technically challenging than orthotopic xenografts and are easily passaged *in vivo*. PDX is very useful not only in preclinical models of glioblastoma but also for verifying molecular changes and signaling pathways in various types of cancer. Thus, PDX models are expected to remain a mainstay in translational glioblastoma research.

Genetically Engineered Mouse Models

GEM preclinical models of glioblastoma have been reported to reflect the histology and biology of human glioblastoma. In many GEM glioblastoma models (3), gene expression is manipulated using Tet-regulation or Cre-inducible gene alleles to express or inactivate genes at a specific time or duration or in specific cells. GEM glioblastoma models can also be established by somatic-cell gene transfers using retroviral or adenoviral vectors to deliver Cre recombinase, such as in the RCAS/Tva system (28). Glioblastoma GEM models make it possible to pinpoint genetic alterations involved in tumor initiation and progression. These models are also useful for testing therapeutic strategies.

Syngenic Mouse Models

Syngenic mouse models of glioblastoma have long been used as indispensable tools for glioblastoma research. These models (GL261, GL26, CT-2A, and P560) (29) are established from spontaneous or chemically induced murine glioma. GL261, GL26, and CT-2A are from chemically induced mouse models of glioblastoma while P560 is from spontaneous mouse models of glioblastoma. GL261 models are perhaps the most extensively used syngenic mouse models of glioblastoma. These models are reported to recapitulate histologic and biological characteristics of glioblastoma. Furthermore, these models use immunocompetent mice, and thus are suitable for analyzing glioblastoma tumor immunology and immunotherapeutic research.

Advantages and Disadvantages of Each Type of Glioblastoma Mouse Model

GLIOBLASTOMA CELL-LINE XENOGRAPTS

Although cell lines in serum-containing media are readily established from human glioblastoma, it is difficult to establish cell lines from low-grade gliomas such as oligodendrogliomas (30, 31). More importantly, extensive clonal selection occurs after glioma cells are suspended in serum-containing medium, and further selection occurs during cell passaging. It is therefore highly doubtful that biological information obtained from glioblastoma cell-line xenografts can contribute to an accurate understanding of the biology of human glioblastoma. The glioblastoma cell lines are so different from the original patient tumors that it might be impossible to recapitulate the complex genetic and phenotypic traits of human gliomas with these cell lines.

PATIENT-DERIVED XENOGRAPTS

Unlike xenografts from glioblastoma cell lines, PDXs have the advantage of maintaining the histological and genetic features of the original tumor when engrafted into immunodeficient mice. It should also be emphasized that PDX models are highly variable, reflecting the inter-patient heterogeneity of glioblastoma, but are advantageous because of their clinical relevancy. However, PDX models also have shortcomings. They cannot be established from all patient tumors, especially from low-grade gliomas. Even if engraftment is successful, it usually takes between 2 and 11 months to obtain tumors (25). Furthermore, standardization and experimental planning may be difficult because PDX models are as variable as the glioblastomas they are derived from (3). However, once established, PDX models can contribute to the development of personalized treatment for individual patients. Another disadvantage of the PDX model is that it can only be established in immunodeficient mice such as nude, NOD-SCID, or NOD-SCID-gamma mice. The immune system in these mice differs innately from that of the host; thus, current PDX models do not represent the host immune system.

GENETICALLY ENGINEERED MOUSE MODELS

GEM models are particularly useful for identifying the molecular events responsible for tumor initiation and progression, and can also offer insight into the sequence of events underlying the genetic alterations occurring in response to specific mutations. GEM models are also useful for analyzing the role of the microenvironment in tumor biology (32).

However, it is not certain whether the gene changes involved in these models truly mirror the tumor-associated events in human glioblastomas. GEM tumors are usually composed of cells with specific, homogeneous genetic changes, and thus cannot completely reflect the intratumoral genomic and phenotypic heterogeneity of glioblastoma. In addition, GEM models are sometimes at a disadvantage in therapeutic studies because tumor initiation cannot be controlled, and thus the time of tumor formation is not highly reproducible.

SYNGENIC MOUSE MODEL

Syngenic mouse models use immunocompetent mice; thus, the greatest advantage of these models is that they recapitulate host immunity and are considered to be suitable for analyzing glioblastoma tumor immunology and immunotherapeutic research.

Preclinical findings from these mouse models have already been tested as clinical trials in human glioblastoma patients such as dendritic cell vaccines pulsed with whole tumor homogenate (33). These findings came from studies using GL261 models.

However, it remains to be seen whether murine glioma models faithfully reflect human glioblastoma; thus, further studies are needed to conclude on this.

Future Prospects for Mouse Models of Glioblastoma

Table 1 summarizes the characteristics of currently available mouse models of glioblastoma. At present, none of the animal models mentioned fully recapitulate human glioblastoma development and progression. Glioblastoma cell-line xenografts do not reflect the genetic background of human glioblastoma. PDX, GEM, and syngenic models better reflect phenotypic features of glioblastoma, and are thus the best of the currently available models for analyzing glioblastoma development and therapeutic strategies.

The value of PDX models in predicting human clinical-trial drug responses was recently highlighted by a study of 1000 PDX cancer models from various primary sites (34), and by the establishment of a large-scale breast-cancer PDX biobank (35). This type of large-scale PDX bank is likely to prove valuable for predicting human responses to clinical trials of new glioblastoma drugs, and should help make it possible to tailor therapy to the individual patient. However, since PDX models do not reflect the tumor microenvironment of the glioblastoma and are established in immunodeficient mice, they cannot fully reflect the host's antitumor immunity in human glioblastoma. Thus, PDX models can be improved by developing models that recapitulate human immunity and the human glioblastoma

TABLE 1

Characteristics of Each Glioblastoma Mouse Model

Model	Advantage	Disadvantage
Cell-line xenograft	High engraftment and growth rates Good reproducibility Reliable disease growth and progression	Does not recapitulate genetic and phenotypical feature of original tumor Need to use immunodeficient mice
Patient-derived xenograft	Recapitulate genetic and phenotypical feature of original tumor	Relatively low engraftment and growth rates Need to use immunodeficient mice
Genetically engineered mouse model	Identify the molecular events responsible for tumor initiation and progression Analyze the role of the microenvironment	Does not completely reflect the intratumoral genomic and phenotypic heterogeneity Tumor initiation cannot be controlled
Syngenic mouse model	Suitable for tumor immunity and immunotherapeutic research	Might be different from human glioblastoma

microenvironment. In the continued search for models that more fully reflect human glioblastoma, it will be particularly useful to compare the phenotypes developed in xenograft models with those obtained in various GEM models (3).

Conclusion

In this chapter, we summarized the currently available mouse models of glioblastoma. Each mouse model has its own advantages and disadvantages; thus, it is important to choose appropriate models depending on the purpose of the research. PDX, GEM, and syngenic models are excellent glioblastoma mouse models for current use and preclinical translational research for glioblastoma. However, further work is needed to establish mouse models that fully recapitulate human glioblastoma.

Conflict of interest: The authors declare no potential conflicts of interest with respect to research, authorship, and/or publication of the article.

Copyright and permission statement: To the best of our knowledge, the materials included in this chapter do not violate copyright laws. All original sources have been appropriately acknowledged and/or referenced. Where relevant, appropriate permissions have been obtained from the original copyright holder(s).

References

1. Stupp R, Mason WP, van den Bent MJ, Weller M, Fisher B, Taphoorn MJ, et al. Radiotherapy plus concomitant and adjuvant temozolomide for glioblastoma. *N Engl J Med*. 2005;352(10):987–96. <http://dx.doi.org/10.1056/NEJMoa043330>

2. Qazi M, Mann A, van Ommeren R, Venugopal C, McFarlane N, Vora P, et al. Generation of murine xenograft models of brain tumors from primary human tissue for in vivo analysis of the brain tumor-initiating cell. *Methods Mol Biol.* 2014;1210:37–49. http://dx.doi.org/10.1007/978-1-4939-1435-7_4
3. Huszthy PC, Daphu I, Niclou SP, Stieber D, Nigro JM, Sakariassen PØ, et al. In vivo models of primary brain tumors: Pitfalls and perspectives. *Neuro Oncol.* 2012;14(8):979–93. <http://dx.doi.org/10.1093/neuonc/nos135>
4. Martens T, Laabs Y, Günther HS, Kemming D, Zhu Z, Witte L, et al. Inhibition of glioblastoma growth in a highly invasive nude mouse model can be achieved by targeting epidermal growth factor receptor but not vascular endothelial growth factor receptor-2. *Clin Cancer Res.* 2008;14(17):5447–58. <http://dx.doi.org/10.1158/1078-0432.CCR-08-0147>
5. Mahesparan R, Read TA, Lund-Johansen M, Skafnesmo KO, Bjerkvig R, Engebraaten O. Expression of extracellular matrix components in a highly infiltrative in vivo glioma model. *Acta Neuropathol.* 2003;105(1):49–57.
6. Kijima N, Hosen N, Kagawa N, Hashimoto N, Kinoshita M, Oji Y, et al. Wilms' tumor 1 is involved in tumorigenicity of glioblastoma by regulating cell proliferation and apoptosis. *Anticancer Res.* 2014;34(1):61–7.
7. Anderson RC, Elder JB, Brown MD, Mandigo CE, Parsa AT, Kim PD, et al. Changes in the immunologic phenotype of human malignant glioma cells after passaging in vitro. *Clin Immunol.* 2002;102(1):84–95. <http://dx.doi.org/10.1006/clim.2001.5152>
8. Ernst A, Hofmann S, Ahmadi R, Becker N, Korshunov A, Engel F, et al. Genomic and expression profiling of glioblastoma stem cell-like spheroid cultures identifies novel tumor-relevant genes associated with survival. *Clin Cancer Res.* 2009;15(21):6541–50. <http://dx.doi.org/10.1158/1078-0432.CCR-09-0695>
9. Clark MJ, Homer N, O'Connor BD, Chen Z, Eskin A, Lee H, et al. U87MG decoded: The genomic sequence of a cytogenetically aberrant human cancer cell line. *PLoS Genet.* 2010;6(1):e1000832. <http://dx.doi.org/10.1371/journal.pgen.1000832>
10. Li A, Walling J, Kotliarov Y, Center A, Steed ME, Ahn SJ, et al. Genomic changes and gene expression profiles reveal that established glioma cell lines are poorly representative of primary human gliomas. *Mol Cancer Res.* 2008;6(1):21–30. <http://dx.doi.org/10.1158/1541-7786.MCR-07-0280>
11. Jin K, Teng L, Shen Y, He K, Xu Z, Li G. Patient-derived human tumour tissue xenografts in immunodeficient mice: A systematic review. *Clin Transl Oncol.* 2010;12(7):473–80. <http://dx.doi.org/10.1007/s12094-010-0540-6>
12. Hidalgo M, Amant F, Biankin AV, Budinská E, Byrne AT, Caldas C, et al. Patient-derived xenograft models: An emerging platform for translational cancer research. *Cancer Discov.* 2014;4(9):998–1013. <http://dx.doi.org/10.1158/2159-8290.CD-14-0001>
13. Daniel VC, Marchionni L, Hierman JS, Rhodes JT, Devereux WL, Rudin CM, et al. A primary xenograft model of small-cell lung cancer reveals irreversible changes in gene expression imposed by culture in vitro. *Cancer Res.* 2009;69(8):3364–73. <http://dx.doi.org/10.1158/0008-5472.CAN-08-4210>
14. Fichtner I, Rolff J, Soong R, Hoffmann J, Hammer S, Sommer A, et al. Establishment of patient-derived non-small cell lung cancer xenografts as models for the identification of predictive biomarkers. *Clin Cancer Res.* 2008;14(20):6456–68. <http://dx.doi.org/10.1158/1078-0432.CCR-08-0138>
15. Fei XF, Zhang QB, Dong J, Diao Y, Wang ZM, Li RJ, et al. Development of clinically relevant orthotopic xenograft mouse model of metastatic lung cancer and glioblastoma through surgical tumor tissues injection with trocar. *J Exp Clin Cancer Res.* 2010;29(1):84. <http://dx.doi.org/10.1186/1756-9966-29-84>
16. Kim KM, Shim JK, Chang JH, Lee JH, Kim SH, Choi J, et al. Failure of a patient-derived xenograft for brain tumor model prepared by implantation of tissue fragments. *Cancer Cell Int.* 2016;16:43. <http://dx.doi.org/10.1186/s12935-016-0319-0>
17. Kang SG, Cheong JH, Huh YM, Kim EH, Kim SH, Chang JH. Potential use of glioblastoma tumor-sphere: Clinical credentialing. *Arch Pharm Res.* 2015;38(3):402–7. <http://dx.doi.org/10.1007/s12272-015-0564-0>
18. Lee J, Kotliarova S, Kotliarov Y, Li A, Su Q, Donin NM, et al. Tumor stem cells derived from glioblastomas cultured in bFGF and EGF more closely mirror the phenotype and genotype of primary tumors

- than do serum-cultured cell lines. *Cancer Cell*. 2006;9(5):391–403. <http://dx.doi.org/10.1016/j.ccr.2006.03.030>
19. Chen R, Nishimura MC, Bumbaca SM, Kharbanda S, Forrest WF, Kasman IM, et al. A hierarchy of self-renewing tumor-initiating cell types in glioblastoma. *Cancer Cell*. 2010;17(4):362–75. <http://dx.doi.org/10.1016/j.ccr.2009.12.049>
 20. Günther HS, Schmidt NO, Phillips HS, Kemming D, Kharbanda S, Soriano R, et al. Glioblastoma-derived stem cell-enriched cultures form distinct subgroups according to molecular and phenotypic criteria. *Oncogene*. 2008;27(20):2897–909. <http://dx.doi.org/10.1038/sj.onc.1210949>
 21. Wakimoto H, Mohapatra G, Kanai R, Curry WT Jr, Yip S, Nitta M, et al. Maintenance of primary tumor phenotype and genotype in glioblastoma stem cells. *Neuro Oncol*. 2012;14(2):132–44. <http://dx.doi.org/10.1093/neuonc/nor195>
 22. Wan F, Zhang S, Xie R, Gao B, Campos B, Herold-Mende C, et al. The utility and limitations of neurosphere assay, CD133 immunophenotyping and side population assay in glioma stem cell research. *Brain Pathol*. 2010;20(5):877–89. <http://dx.doi.org/10.1111/j.1750-3639.2010.00379.x>
 23. Pollard SM, Yoshikawa K, Clarke ID, Danovi D, Stricker S, Russell R, et al. Glioma stem cell lines expanded in adherent culture have tumor-specific phenotypes and are suitable for chemical and genetic screens. *Cell Stem Cell*. 2009;4(6):568–80. <http://dx.doi.org/10.1016/j.stem.2009.03.014>
 24. Bjerkvig R, Tønnesen A, Laerum OD, Backlund EO. Multicellular tumor spheroids from human gliomas maintained in organ culture. *J Neurosurg*. 1990;72(3):463–75. <http://dx.doi.org/10.3171/jns.1990.72.3.0463>
 25. Wang J, Miletic H, Sakariassen PØ, Huszthy PC, Jacobsen H, Brekkå N, et al. A reproducible brain tumour model established from human glioblastoma biopsies. *BMC Cancer*. 2009;9:465. <http://dx.doi.org/10.1186/1471-2407-9-465>
 26. Sakariassen PØ, Prestegarden L, Wang J, Skafnesmo KO, Mahesparan R, Molthoff C, et al. Angiogenesis-independent tumor growth mediated by stem-like cancer cells. *Proc Natl Acad Sci U S A*. 2006;103(44):16466–71. <http://dx.doi.org/10.1073/pnas.0607668103>
 27. Taillandier L, Antunes L, Angioi-Duprez KS. Models for neuro-oncological preclinical studies: Solid orthotopic and heterotopic grafts of human gliomas into nude mice. *J Neurosci Methods*. 2003;125(1–2):147–57. [http://dx.doi.org/10.1016/S0165-0270\(03\)00043-8](http://dx.doi.org/10.1016/S0165-0270(03)00043-8)
 28. Federspiel MJ, Bates P, Young JA, Varmus HE, Hughes SH. A system for tissue-specific gene targeting: Transgenic mice susceptible to subgroup A avian leukemia virus-based retroviral vectors. *Proc Natl Acad Sci U S A*. 1994;91(23):11241–5. <http://dx.doi.org/10.1073/pnas.91.23.11241>
 29. Oh T, Fakurnejad S, Sayegh ET, Clark AJ, Ivan ME, Sun MZ, et al. Immunocompetent murine models for the study of glioblastoma immunotherapy. *J Transl Med*. 2014;29(12):107. <http://dx.doi.org/10.1186/1479-5876-12-107>
 30. Kelly JJ, Blough MD, Stechishin OD, Chan JA, Beauchamp D, Perizzolo M, et al. Oligodendroglioma cell lines containing t(1;19)(q10;p10). *Neuro Oncol*. 2010;12(7):745–55. <http://dx.doi.org/10.1093/neuonc/noq031>
 31. Grippo MC, Penteado PF, Carelli EF, Cruz-Höfling MA, Verinaud L. Establishment and partial characterization of a continuous human malignant glioma cell line: NG97. *Cell Mol Neurobiol*. 2001;21(4):421–8. <http://dx.doi.org/10.1023/A:1012662423863>
 32. Charles N, Holland EC. The perivascular niche microenvironment in brain tumor progression. *Cell Cycle*. 2010;9(15):3012–3021. <http://dx.doi.org/10.4161/cc.9.15.12710>
 33. Ni HT, Spellman SR, Jean WC, Hall WA, Low WC. Immunization with dendritic cells pulsed with tumor extract increases survival of mice bearing intracranial gliomas. *J Neurooncol*. 2001;51(1):1–9. <http://dx.doi.org/10.1023/A:1006452726391>
 34. Gao H, Korn JM, Ferretti S, Monahan JE, Wang Y, Singh M, et al. High-throughput screening using patient-derived tumor xenografts to predict clinical trial drug response. *Nat Med*. 2015;21(11):1318–25. <http://dx.doi.org/10.1038/nm.3954>
 35. Bruna A, Rueda OM, Greenwood W, Batra AS, Callari M, Batra RN, et al. A Biobank of breast cancer explants with preserved intra-tumor heterogeneity to screen anticancer compounds. *Cell*. 2016;167(1):260–74. <http://dx.doi.org/10.1016/j.cell.2016.08.041>

Section II

Managing Glioblastoma in the Clinic

8

Epidemiology and Outcome of Glioblastoma

AHMAD FALEH TAMIMI¹ • MALIK JUWEID²

¹Department of Neurosurgery, Jordan University Hospital and Medical School, University of Jordan, Amman, Jordan; ²Department of Radiology and Nuclear Medicine, Jordan University Hospital and Medical School, University of Jordan, Amman, Jordan

Author for correspondence: Ahmad Faleh Tamimi, Department of Neurosurgery, Jordan University Hospital and Medical School, University of Jordan, Amman, Jordan. E-mail: aftamimi@hotmail.com

Doi: <http://dx.doi.org/10.15586/codon.glioblastoma.2017.ch8>

Abstract: Glioblastoma (GBM) is the most aggressive malignant primary brain tumor. With an incidence rate of 3.19 per 100,000 persons in the United States and a median age of 64 years, it is uncommon in children. The incidence is 1.6 times higher in males compared to females and 2.0 times higher in Caucasians compared to Africans and Afro-Americans, with lower incidence in Asians and American Indians. GBM is commonly located in the supratentorial region (frontal, temporal, parietal, and occipital lobes) and is rarely located in cerebellum. Genetic and environmental factors have been investigated in GBM. Risk factors include prior radiotherapy, decreased susceptibility to allergy, immune factors and immune genes, as well as some single nucleotide polymorphisms detected by genomic analysis. Use of anti-inflammatory medication has been found to be protective against GBM. Survival from GBM is poor; only few patients survive 2.5 years and less than 5% of patients survive 5 years following diagnosis. Survival rates for patients with GBM have shown no notable improvement in population statistics in the last three decades. Molecular epidemiology integrates molecular technology into epidemiological studies and outcomes. The future of the epidemiology of

In: *Glioblastoma*. Steven De Vleeschouwer (Editor), Codon Publications, Brisbane, Australia ISBN: 978-0-9944381-2-6; Doi: <http://dx.doi.org/10.15586/codon.glioblastoma.2017>

Copyright: The Authors.

Licence: This open access article is licenced under Creative Commons Attribution 4.0 International (CC BY 4.0). <https://creativecommons.org/licenses/by-nc/4.0/>

GBM will depend on multicenter studies generating large clinical data sets of genomic data potentially leading to further understanding of the roles of genes and environment in the development of this devastating disease.

Key words: Brain tumors; Epidemiology; Glioblastoma; Outcome.

Introduction

Glioblastoma (GBM) is the most aggressive diffuse glioma of astrocytic lineage and is considered a grade IV glioma based on the WHO classification (1). GBM is the most common malignant primary brain tumor making up 54% of all gliomas and 16% of all primary brain tumors (2). GBM remains an incurable tumor with a median survival of only 15 months (3). Treatment is complex, initially consisting of maximally safe surgical resection followed by radiation therapy (RT) and concurrent Temozolomide (TMZ) chemotherapy (4). The terms “primary GBM” and “secondary GBM” were first used by the German neuropathologist Hans Joachim Sherer in Antwerp in 1940 (5). Nowadays, GBM comprised of primary and secondary types, constituting distinct disease entities which evolve through different genetic pathways, affect patients at different ages, and likely differ in prognosis and response to therapy (5). Primary *de novo* GBM accounts for more than 80% of GBM (6), occurs in older patients (mean age = 64 years), and typically shows epidermal growth factor receptor (EGFR) over expression, PTN (MMC 1) mutation, CDKN2A (p16) deletion, and less frequently MDM2 amplification. Secondary GBM develops from lower grade astrocytoma or oligodendrogliomas, occurs in younger patients (mean age = 45 years), and often contains TP53 mutations as the earliest detectable alteration (5). Mutations in isocitrate dehydrogenase-1 (IDH1) and IDH2 are present in 70–80% of low-grade glioma and secondary GBM, and in only 5–10% of primary GBM (7–9). Strong link has been found between IDH mutations and genome-wide glioma cytosine–phosphate–guanine I and methylator phenotype (G-CIMP) across all subtypes of glioma (10). The WHO recently added a rare subtype of GBM termed “GBM-0,” with oligodendroglioma component, defined as GBM having areas resembling anaplastic oligodendroglioma, with features of GBM and necrosis without microvascular proliferation (7). According to the 2016 WHO classification of GBM multiforme, this tumor has been separated from the classical identity and is currently classified into three groups: GBM IDH-wild type (including giant cell GBM, gliosarcoma, and epithelioid GBM), GBM IDH-mutant, and GBM NOS (1). The average annual age-adjusted incidence rate (IR) of GBM is 3.19 per 100,000 persons in the United States (11), with the age-adjusted GBM rates being 2.5 times higher in European Americans than in African Americans (12).

Incidence of Glioblastoma

The average annual age-adjusted IR of GBM is variable, ranging from 0.59 per 100,000 persons to 3.69 per 100,000 persons (11, 13–17), and is the highest among malignant primary brain tumors (Table 1).

TABLE 1**Age-adjusted Incidence per 100,000 Persons (ICD-O Morphology Code 9450) in Different Countries**

Region	Years	Overall	Ref
United States	2006–2010	3.19	2
Australia	2000–2008	3.40	13
England	1999–2003	2.05	14
Korea	2005	0.59	15
Greece	2005–2007	3.69	17
Jordan	2012–2013	0.89	16

AGE

GBM is primarily diagnosed at older age with a median age of 64 at diagnosis (2, 18). The incidence increases with age peaking at 75–84 years and drops after 85 years (2). The age at diagnosis tends to be higher for primary GBM (mean age of 55 and median age of 64) (2, 18) than for secondary GBM (mean age of 40 years) (19). GBM is uncommon in children (2). DNA methylation patterns for pediatric and adult groups are similar, but there are distinct clusters that are predominantly found in children and adolescents. Two of these correspond strictly to recurrent age-specific mutations in H3F3A. Another type was enriched for DPGFRA alterations and consists of patients from a more widespread age range (20). Age-adjusted and age-specific IRs for GBM according to age at diagnosis and gender are shown in Figure 1 (11).

GENDER AND SITE

Overall, the incidence of GBM is higher in males than in females (3.97 vs. 2.53 in the United States) (2). The male-to-female ratio is increased for each brain subsite except for the posterior fossa (18). The IR of primary GBMs is higher in men with reported male-to-female ratio of 1:0.33, while the IR of secondary GBMs is higher in women with reported male-to-female ratio of (0.65:1) (20).

GBM is most commonly located in the supratentorial region (frontal, temporal parietal, and occipital lobes), with the highest incidence in the frontal lobe, multiple lobes (overlapping tumors), followed by the temporal and parietal lobes (18). GBM is rarely located in the cerebellum and is very rare in the spinal cord (21, 22), with different tumor behavior found at these locations (21). Cerebellar location of GBM is more common in younger patients (50–56 years of age); supratentorial location is prevalent in older patients (62–64 years of age) and cerebellar location is rare (0.4–3.4%) in this age bracket (23). Cerebellar GBM is less common in Whites and is smaller in size (22–24). For spinal cord GBMs, the mean age is 27 years, with a male predominance; 53% of these tumors are seen in those aged less than 18 years (25).

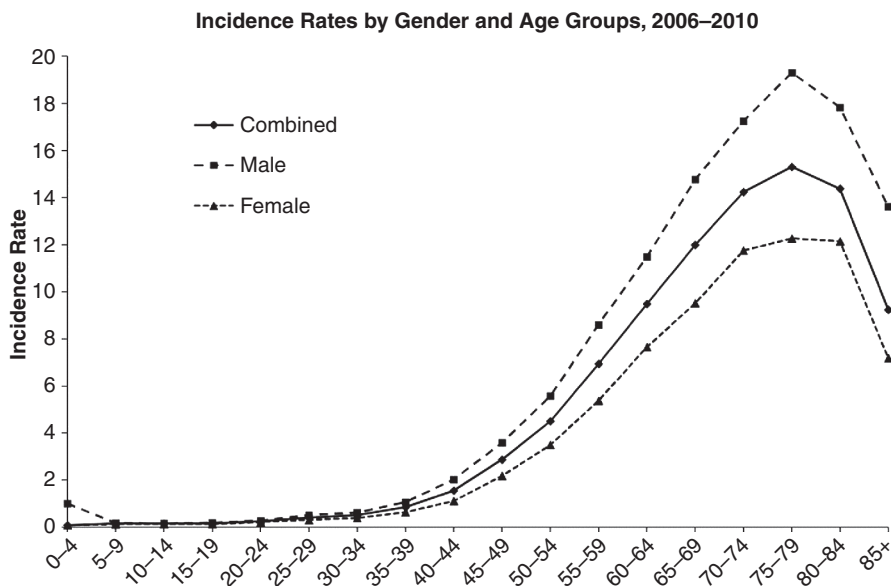


Figure 1 Age-adjusted and age-specific incidence rates for glioblastoma at diagnosis and gender, CBTRUS statistical report: NPCR and SEER, 2006–2010. X-axis, age groups; Y-axis, incidence rates. Rates are per 100,000 and age-adjusted to the 2000 US standard population. NPCR, CDC's National Program of Cancer Registries; SEER, NCI's Surveillance, Epidemiology, and End Results program. (Adapted from Ref. (11).)

ETHNICITY AND GENETICS

Whites have the highest IR of GBM followed by Blacks; age-adjusted GBM rate is 2.5 times higher in European Americans than in African Americans and more common in non-Hispanics than in Hispanics (12) (Figure 2) (11). Associations between XRCC1 polymorphisms and glioma are still controversial. However, a recent meta-analysis showed that the Arg399Gln polymorphism was associated with an increased risk of glioma in Asians and of GBM in Caucasians. However, Arg194Trp/Arg280His polymorphisms probably have no influence on glioma in different ethnicities (26).

There is increased incidence of GBM in patients with hereditary tumor syndromes, for example, Turcot syndrome (27) and Li-Fraumeni syndrome (5). Otherwise, GBM occurs sporadically without known genetic predisposition (28).

Classification of GBM

GBM is a grade IV glioma according to the WHO 2007 classification and is the most common and lethal primary malignancy of the central nervous system. Despite multidisciplinary treatments such as surgery, chemotherapy, and radiotherapy, the median survival time for patients with GBM is only 14.6 months (4). Due to its high degree of invasiveness, radical tumor resection is not curative.

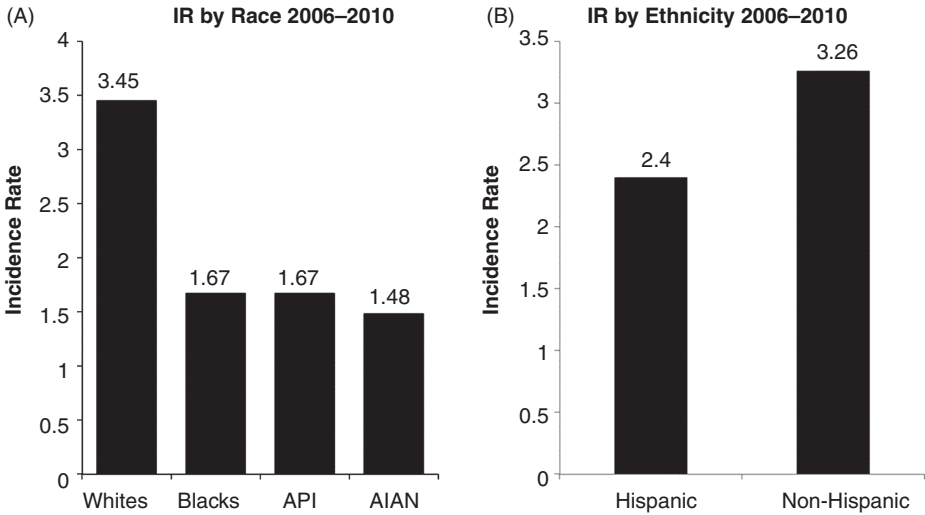


Figure 2 (A) Average annual age-adjusted incidence rates of glioblastoma by race, CBTRUS statistical report: NPCR and SEER, 2006 to 2010. X-axis, race; Y-axis, incidence rates. (B) Average annual age-adjusted incidence rates of glioblastoma by ethnicity, CBTRUS statistical report: NPCR and SEER, 2006 to 2010. X-axis, ethnicity; Y-axis, incidence rates. Rates are per 100,000. AIAN, Asian Indian Alaskan Native. (Adapted from Ref. (11).)

There is experimental evidence that GBM contains a subpopulation of highly tumorigenic cells (GBM stem cells) from which recurrent GBM is thought to derive (29–31), and that GBM has the capacity to differentiate into multiple lineages of tumor genesis (29, 31, 32).

As stated above, GBMs can be classified into primary and secondary GBMs. Primary GBM occurs *de novo* without evidence of a less malignant precursor, whereas secondary GBM develops from initially low-grade diffuse astrocytoma (WHO grade II diffuse astrocytoma) or anaplastic astrocytoma (Grade III). The majority of GBMs (90%) are primary (33), and patients with primary GBM tend to be older (mean age = 55 years) than those with secondary GBM (mean age = 40 years). Genetic alterations more typical for primary GBM are EGFR overexpression, PTN mutation, and loss of chromosome 10 (5, 6, 34, 35), whereas genetic alterations more commonly seen in secondary GBM include IDH1 mutations, TP53 mutations, and 19q loss (5, 6, 20, 36–39). IDH1 mutation is associated with better outcome and increased overall survival (33). Interestingly, IDH1 mutations are also found in 80% of diffuse astrocytoma and anaplastic astrocytoma, the precursors of secondary GBM, and in less than 5% of primary GBM (8, 40–42). Thus, the IDH1 mutation is a reliable objective molecular marker for secondary GBM over clinical and pathological criteria (33).

Molecular diagnosis will contribute to a better understanding and classification of brain tumors (42). The classification of GBM based on gene expression distinguishes between four subtypes: proneural, neural, classical, and mesenchymal. Aberrations and gene expression of EGFR, NF1, and PDGFRA/IDH1 define classical, mesenchymal, and proneural GBMs, respectively. Genes of normal brain cell types show a strong relationship between subtypes and different neural lineages

and the response to aggressive treatment differs by subtype, with prominent benefits in the classical and little or no benefit in the proneural subtype (35). GBMs have significant genetic heterogeneity and tumor subtypes with genetic alterations, which carry prognostic significance (5). In 2010, GBM was classified into four different molecular subtypes (35): classical, mesenchymal, proneural, and neural subtypes based on characteristic genetic alterations and distinct molecular profiles (33, 42–44). Each subtype harbors distinct genetic alterations and expression profiles (42, 44). Loss of chromosomal 10 is frequently observed in classical subtype as well as mutations in TP53 and IHD1. The mesenchymal subtype is enriched in the gene expression pattern of astrocytes as well as microglial markers. Proneural subtype is enriched in proneural genes expressed in oligodendrocytes and characterized by alterations in TP53, platelet-derived growth receptor (PDGFR), and ILDH1 (5, 8, 35–37). The proneural subtype is also associated with younger age at diagnosis (31). Neural subtype is the most similar to the astrocytic and oligodendrocytic markers. Finally, a group with only telomerase reverse transcripts (TERT) mutation is found in primarily grade IV gliomas (45). According to the 2016 WHO classification of CNS tumors, GBM is divided into the following groups:

- (i) GBM, IDH-wild type (about 90% of cases) corresponding most frequently to the clinically defined primary or *de novo* GBM and predominant in patients aged over 55 years (5, 33).
- (ii) GBM, IDH-mutant (about 10% of cases) corresponding closely to the so-called secondary GBM, with a history of prior lower grade diffuse glioma, and preferentially occurring in younger patients (5, 33).
- (iii) GBM, NOS, a diagnosis that is reserved for those tumors for which full IDH evaluation cannot be performed.

One provisional new variant of GBM has been added to the classification: epithelioid GBM. It joins giant cell GBM and gliosarcoma under the umbrella of IDH-wild type GBM. Epithelioid GBM features large epithelioid cells, with abundant eosinophilic cytoplasm, vesicular chromatin, and prominent nucleoli (often resembling melanoma cells), and variably present rhabdoid cells. GBM with primitive neuronal component was added as a pattern in GBM. This pattern, previously referred to in the literature as GBM with PNET-like component, usually comprised of a diffuse astrocytoma of any grade (or oligodendroglioma in rare cases) that has well-demarcated nodules containing primitive cells that display neuronal differentiation, and sometimes has MYC or MYCN amplification. These tumors also have a tendency for craniospinal fluid dissemination (46). About a quarter of them develop in patients with a previously known lower grade glioma precursor, a subset of which shows R132H IDH1 immunoreactivity in both the glial and primitive neuronal components (47).

Survival and Prognostic Factors

RISK FACTORS

Factors associated with GBM risk are prior radiation, decreased susceptibility to allergy, immune factors and immune genes, and some nucleotide polymorphisms, detected by genome-wide association (48, 49). The lower risk of GBM in people with

asthma and other allergic conditions is consistent with findings that have been confirmed by objective evidence from asthma and other allergies-related germline polymorphism in patients with GBM and in controls. Genotypes that increase asthma risk are associated with decreased GBM risk (49). Nevertheless, both familiar aggregation of glioma and the inverse association of allergies and immune-related conditions with glioma have been shown consistently (48). A lower risk of gliomas has been associated with allergy or atopic disease (e.g., asthma, eczema, psoriasis) (50–52). A short-term (less than 10 years) use of anti-inflammatory medication is also associated with a protective effect against GBM (52). The use of cyclooxygenase-2 (COX-2) inhibitors is still controversial where a positive effect in laboratory investigation in reducing the gliomagenesis was achieved *in vivo* and *in vitro* (53). However, in clinical setting, the use of COX-2 inhibitor was unrelated to glioma risk (54).

Other factors associated with GBM risk are high socioeconomic status and a person's height (18, 55). There is no substantial evidence of GBM association with lifestyle characteristics, such as cigarette smoking, alcohol consumption, drug use, or dietary exposure to nitrous compounds (56). Inconsistent and indefinite reports have been published regarding the association of GBM with the use of mobile phones (57, 58). Prognostic factors that affect the survival of GBM patients include the resectability of the tumor, its location, size, multifocality, as well as advanced age, comorbidities, and the patient's general condition (59).

Outcome and Prognostic Factors

GBM is an aggressive neoplasm with a median survival of only 3 months in untreated patients (60). Surgery remains an important component in the management of GBM. Surgery enables a histological confirmation of the clinical diagnosis and also has decompressive and cytoreductive effects, with an advantage of increased survival with complete resection (61). Tumor fluorescence derived from 5 aminolevulinic acid enabled a more complete resection of contrast-enhancing tumor, leading to improved progression-free-survival in patients with GBM (61). The main contraindications to resective surgery are poor performance status (Karnofsky of less than 70), advanced age, and eloquent location (19). The combination of radiotherapy and TMZ chemotherapy is the most effective adjuvant therapy shown to prolong survival following primary resection. Radiotherapy followed by TMZ results in significantly prolonged survival compared with radiotherapy alone (4). Treatment of GBM remains challenging. The current experience in GBM treatment shows that several targets should be approached. Therefore, rational combinations between established treatments and new approaches aiming, for example, at inhibition of angiogenesis, induction of apoptosis, or inhibition of several signal transduction pathways might offer the best opportunity to improve prognosis.

Conclusion

GBM is still the most malignant primary brain tumor with clear predominance in males. The management and outcome of GBM have remained stable for almost the last four decades. However, recent advances in genetic and molecular research

will open a new horizon in the future of management and outcome of this devastating tumor.

Conflict of interest: The authors declare no potential conflicts of interest with respect to research, authorship, and/or publication of this manuscript.

Copyright and permission statement: To the best of our knowledge, the materials included in this chapter do not violate copyright laws. All original sources have been appropriately acknowledged and/or referenced. Where relevant, appropriate permissions have been obtained from the original copyright holder(s).

References

1. Louis N, Perry A, Reifenberge RG, von Deimling A, Figarella-Branger D, Cavenee WK, et al. The 2016 World Health Organization classification of tumors of the central nervous system: A summary. *Acta Neuropathol.* 2016;131:803–20. <http://dx.doi.org/10.1007/s00401-016-1545-1>
2. Ostrom QT, Gittleman H, Farah P, Ondracek A, Chen Y, Wolinsky Y, et al. CBTRUS statistical report: Primary brain and central nervous system tumors diagnosed in the United States in 2006–2010. *Neuro Oncol.* 2013;15(Suppl):2ii–56.
3. Koshy M, Villano JL, Dolecek TA, Howard A, Mahmood U, Chmura SJ, et al. Improved survival time trends of glioblastoma using the SEER 17 population-based registries. *J Neuro Oncol.* 2012;107(1):207–12. <http://dx.doi.org/10.1007/s11060-011-0738-7>
4. Stupp R, Mason WP, van den Bent MJ, Weller M, Fisher B, Taphoorn MJ, et al. Radiotherapy plus concomitant and adjuvant Temozolomide for glioblastoma. *N Engl J Med.* 2005;352:987–96. <http://dx.doi.org/10.1056/NEJMoa043330>
5. Kleihues P, Ohgaki H. Primary and secondary glioblastomas: From concept to clinical diagnosis. *Neuro Oncol.* 1999;1:44–51. <http://dx.doi.org/10.1215/15228517-1-1-44>
6. Ohgaki H, Dessen P, Jourde B, Horstmann S, Nishikawa T, Di Patre PL, et al. Genetic pathways to glioblastoma: A population-based study. *Cancer Res.* 2004;64:6892–9. <http://dx.doi.org/10.1158/0008-5472.CAN-04-1337>
7. Appin CL, Gao J, Chisolm C, Torian M, Alexis D, Vincentelli C, et al. Glioblastoma with oligodendroglioma component(GMB-O) molecular genetic and clinical characteristics. *Brain Pathol.* 2013;23(4):454–61. <http://dx.doi.org/10.1111/bpa.12018>
8. Yan H, Parsons DW, Jin G, McLendon R, Rasheed BA, Yuan W. IDH1 and IDH2 mutations in gliomas. *N Engl J Med.* 2009;360:765–73. <http://dx.doi.org/10.1056/NEJMoa0808710>
9. Hartmann C, Hentschel B, Wick W, Capper D, Felsberg J, Simon M, et al. Patients with IDH1 wild type anaplastic astrocytomas exhibit worse prognosis than IDH1-mutated glioblastomas, and IDH1 mutation status accounts for the unfavorable prognostic effect of higher age: Implications for classification of gliomas. *Acta Neuropathol.* 2010;120:707–18. <http://dx.doi.org/10.1007/s00401-010-0781-z>
10. Nushmehr H, Weisenberger DJ, Diefes K, Phillips HS, Pujara K, Berman BP, et al. Identification of a CpG island methylator phenotype that defines a distinct subgroup of glioma. *Cancer Cell.* 2010;17(5):510–22. <http://dx.doi.org/10.1016/j.ccr.2010.03.017>
11. Thakkar J, Dolecek TA, Horbinski C, Ostrom QT, Lightner DD, Barnholtz-Sloan JS, et al. Epidemiologic and molecular prognostic review of glioblastoma. *Cancer Epidemiol. Biomarkers Rev.* 2014;23(10):1985–96. <http://dx.doi.org/10.1158/1055-9965.EPI-14-0275>
12. Song W, Ruder AM, Hu L, Li Y, Ni R, Shao W, et al. Genetic epidemiology of glioblastoma multiforme: Confirmatory and new findings from analyses of human leukocyte antigen alleles and motifs. *PLoS One.* 2009 Sept 23;4(9):e7157.
13. Dobes M, Khurana VG, Shadbol TB, Smith SF, Sme R, Dexter M, et al. Increasing incidence of glioblastoma and meningioma, and decreasing incidence of Schwannoma (2000–2008); Findings of a multi-centric Australian study. *Surg Neurol Int.* 2011;2:176. <http://dx.doi.org/10.4103/2152-7806.90696>

14. Arora RS, Altson RD, Eden TO, Estlin EJ, Moran A, Birch JM. Age-incidence patterns of primary CNS tumors in children, adolescents and adults in England. *Neuro Oncol.* 2009;11(4):403–13. <http://dx.doi.org/10.1215/15228517-2008-097>
15. Lee CH, Jung KW, Yoo H, Park S, Lee SH. Epidemiology of primary brain and central nervous system tumors in Korea. *J Korean Neurosurg Soc.* 2010;48(2):145–52. <http://dx.doi.org/10.3340/jkns.2010.48.2.145>
16. Tamimi AF, Tamimi I, Abdelaziz M, Saleh Q, Obeidat F, Al-Husseini M, et al. Epidemiology of malignant and non-malignant primary brain tumors in Jordan. *Neuroepidemiology.* 2015;45:100–8. <http://dx.doi.org/10.1159/000438926>
17. Gausia SK, Markou M, Voulgaris S, Bai M, Polyzoidis K, Kyritsis A, et al. Descriptive epidemiology of cerebral gliomas in northwest Greece and study of potential predisposing factors, 2005–2007. *Neuroepidemiology.* 2009;33(2):89–95. <http://dx.doi.org/10.1159/000222090>
18. Chakrabarti I, Cockburn M, Cozen W, Wang YP, Preston-Martin S. A population-based description of glioblastoma multiforme in Los Angeles County, 1974–1999. *Cancer.* 2005;104:2798–06. <http://dx.doi.org/10.1002/cncr.21539>
19. Taylor A, Karajannis MA, Harter DH. Glioblastoma multiforme: State of art and future therapeutics. *Surg Neurol Int.* 2014;5:64. <http://dx.doi.org/10.4103/2152-7806.132138>
20. Sturm D, Bender S, Jones DT, Lichter P, Grill J, Becher O, et al. Pediatric and adult glioblastoma: Multiform (epi) genomic culprits emerge. *Nat Rev Cancer.* 2014;14(2):92–107. <http://dx.doi.org/10.1038/nrc3655>
21. Engelhard HH, Villano JL, Porter KR, Stewart AK, Barua M, Barker FG, et al. Clinical presentation, histology, and treatment in 430 patients with primary tumors of the spinal cord, spinal meninges, or cauda equine. *J Neurosurg Spine.* 2010;13:67–77. <http://dx.doi.org/10.3171/2010.3.SPINE09430>
22. Adams H, Chaichana KL, Avendano J, Liu B, Raza SM, Quinones-Hinojosa A. Adult cerebellar glioblastoma: Understanding survival and prognostic factors using a population-based database from 1973–2009. *World Neurosurg.* 2013;80(6):e181–3. <http://dx.doi.org/10.1016/j.wneu.2013.02.010>
23. Babu R, Sharma R, Karikari IO, Owens TR, Friedman AH, Adamson C. Outcome and prognostic factors in adult cerebellar glioblastoma. *J Clin Neurosci.* 2013;20:1117–21. <http://dx.doi.org/10.1016/j.jocn.2012.12.006>
24. Jeswani S, Nuno M, Folkerts V, Mukherjee D, Black KL, Patil CG. Comparison of survival between cerebellar and supratentorial glioblastoma patients: Surveillance, epidemiology, and end results (SEER) analysis. *Neurosurgery.* 2013;73:240–6. <http://dx.doi.org/10.1227/01.neu.0000430288.85680.37>
25. Konar SK, Maiti TK, Bir SC, Kalakoti P, Bollam P, Nanda A. Predictive factors determining the overall outcome of primary spinal glioblastoma multiforme: An integrative survival analysis. *World Neurosurg.* 2016;86:341–8. <http://dx.doi.org/10.1016/j.wneu.2015.08.078>
26. Jiang L, Fang X, Bao Y, Zhou JY, Shen XY, Ding MH, et al. Association between the XRCC1 polymorphisms and glioma risk: A meta-analysis of case-control studies. *PLoS One.* 2013;8(1):e55597. <http://dx.doi.org/10.1371/journal.pone.0055597>
27. Hamilton SR, Liu B, Parsons RE, Papadopoulos N, Jen J, Powell SM, et al. The molecular basis of Turcot's syndrome. *N Engl J Med.* 1995 Mar 30;332(13):839–47. <http://dx.doi.org/10.1056/NEJM199503303321302>
28. Krex D, Klink B, Hartmann C, von Deimling A, Pietsch T, Simon M, et al. German glioma network long-term survival with glioblastoma multiforme. *Brain.* 2007;130(10):596–606. <http://dx.doi.org/10.1093/brain/awm204>
29. Wang R, Chadalavada K, Wilshire J, Kowalik U, Hovinga KE, Fligelman B, et al. Glioblastoma stem-like cells give rise to tumor endothelium. *Nature.* 2010;468:829–3. <http://dx.doi.org/10.1038/nature09624>
30. Dirks PB. Brain tumor stem cells: Bringing order to the chaos of brain cancer. *J Clin Oncol.* 2008;26:2916–24. <http://dx.doi.org/10.1200/JCO.2008.17.6792>
31. Chen J, McKay RM, Parada LF. Malignant glioma: Lessons from genomics, mouse models, and stem cells. *Cell.* 2012;149:36–47. <http://dx.doi.org/10.1016/j.cell.2012.03.009>
32. Pollard SM, Yoshikawa K, Clarke ID, Danovi D, Stricker S, Russell R, et al. Glioma stem cell lines expanded in adherent culture have tumor-specific phenotypes and are suitable for chemical and genetic screens. *Cell Stem Cell.* 2009;4:568–80. <http://dx.doi.org/10.1016/j.stem.2009.03.014>

33. Ohgaki H, Kleihues P. The definition of primary and secondary glioblastoma. *Clin Cancer Res.* 2013;19:764–72. <http://dx.doi.org/10.1158/1078-0432.CCR-12-3002>
34. Fueyo J, Alemany R, Gomez-Manzano C, Fuller GN, Khan A, Conrad CA, et al. Preclinical characterization of the antiangioma activity of a tropism-enhanced adenovirus targeted to the retinoblastoma pathway. *J Natl Cancer Inst.* 2003;95:652–60. <http://dx.doi.org/10.1093/jnci/95.9.652>
35. Verhaak RG, Hoadley KA, Purdom E, Wang V, Qi Y, Wilkerson MD, et al. Integrated genomic analysis identifies clinically relevant subtypes of glioblastoma characterized by abnormalities in PDGFRA, IDH1, EGFR, and NF1. *Cancer Cell.* 2010;17:98–10. <http://dx.doi.org/10.1016/j.ccr.2009.12.020>
36. Arjona D, Rey JA, Taylor SM. Early genetic changes involved in low-grade astrocytic tumor development. *Curr Mol Med.* 2006;6:645–50. <http://dx.doi.org/10.2174/156652406778195017>
37. Furnari FB, Fenton T, Bachoo RM, Mukasa A, Stommel JM, Stegh A, et al. Malignant astrocytic glioma: Genetics, biology, and paths to treatment. *Genes Dev.* 2007;21:683–710. <http://dx.doi.org/10.1101/gad.1596707>
38. Nakamura M, Yang F, Fujisawa H, Yonekawa Y, Kleihues P, Ohgaki H. Loss of heterozygosity on chromosome 19 in secondary glioblastomas. *J Neuropathol Exp Neurol.* 2000;59:539–43. <http://dx.doi.org/10.1093/jnen/59.6.539>
39. Watanabe K, Tachibana O, Sata K, Yonekawa Y, Kleihues P, Ohgaki H. Overexpression of the EGF receptor and p53 mutations are mutually exclusive in the evolution of primary and secondary glioblastomas. *Brain Pathol.* 1996;6:217–23. <http://dx.doi.org/10.1111/j.1750-3639.1996.tb00848.x>
40. Dillman RO, Duma CM, Schiltz PM, DePriest C, Ellis RA, Okamoto K, et al. Intracavitary placement of autologous lymphokine-activated killer (LAK) cells after resection of recurrent glioblastoma. *J Immunother.* 2004;27:398–404. <http://dx.doi.org/10.1097/00002371-200409000-00009>
41. Watanabe T, Nobusawa S, Kleihues P, Ohgaki H. IDH1 mutations are early events in the development of astrocytomas and oligodendrogliomas. *Am J Pathol.* 2009;174:1149–53. <http://dx.doi.org/10.2353/ajpath.2009.080958>
42. Phillips HS, Kharbanda S, Chen R, Forrest WF, Soriano RH, Wu TD, et al. Molecular subclasses of high grade glioma predict prognosis, delineate a patterns of disease progression and resemble stages in neurogenesis. *Cancer Cell.* 2006;9:157–73. <http://dx.doi.org/10.1016/j.ccr.2006.02.019>
43. Murat A, Migliavacca E, Gorlia T, Lambiv WL, Shay T, Hamou MF, et al. Stem cell-related “self-renewal” signature and high epidermal growth factor receptor expression associated with resistance to concomitant chemo radiotherapy in glioblastoma. *J Clin Oncol.* 2008;26:3015–24. <http://dx.doi.org/10.1200/JCO.2007.15.7164>
44. Brennan C, Momota H, Hambardzumyan D, Ozawa T, Tandon A, Pedraza A, et al. Glioblastoma subclasses can be defined by activity among signal transduction pathways and associated genomic alterations. *PLoS One.* 2009;4:e7752. <http://dx.doi.org/10.1371/journal.pone.0007752>
45. Reuss DE, Kratz A, Sahn F, Capper D, Schrimpf D, Koelsche C, et al. Adult IDH wild type astrocytomas biologically and clinically resolve into other tumor entities. *Acta Neuropathol.* 2015;130(3):407–17. <http://dx.doi.org/10.1007/s00401-015-1454-8>
46. Perry A, Miller CR, Gujrati M, Scheithauer BW, Zambrano SC, Jos SC, et al. Malignant gliomas with primitive neuroectodermal tumor-like components: A clinicopathologic and genetic study of 53 cases. *Brain Pathol.* 2009;19:81–90. <http://dx.doi.org/10.1111/j.1750-3639.2008.00167.x>
47. Joseph NM, Phillips J, Dahiya S, Felicella M, Tihan T, Bra DJ, et al. Diagnostic implications of IDH1-R132H and OLIG2 expression patterns in rare and challenging glioblastoma variants. *Mod Pathol.* 2013;26:315–26. <http://dx.doi.org/10.1038/modpathol.2012.173>
48. Wrensch W, Fisher JL, Schwartzbaum A, Bondy M, Berger M, Aldape KD. Molecular epidemiology of gliomas in adults. *Neurosurgical Focus.* 2005;19(5):1–11. <http://dx.doi.org/10.3171/foc.2005.19.5.6>
49. Schwartzbaum JA, Fisher JL, Aldape KD, Wrensch M. Epidemiology and molecular pathology of Glioblastoma multiforme. *Nat Clin Pract Neurol.* 2006;2:494–503. <http://dx.doi.org/10.1038/ncpneuro0289>
50. Brenner AV, Butler MA, Wang SS, Ruder AM, Rothman N, Schulte PA, et al. Single-nucleotide polymorphisms in selected cytokine genes and risk of adult glioma Carcinogenesis. 2007;28(12):2543–47. <http://dx.doi.org/10.1093/carcin/bgm210>

51. Lachance DH, Yang P, Johnson DR, Decker PA, Kollmeyer TM, McCoy LS, et al. Associations of high-grade glioma with glioma risk alleles and histories of allergy and smoking. *Am J Epidemiol.* 2011;174(5):574–81. <http://dx.doi.org/10.1093/aje/kwr124>
52. Scheurer ME, Amirian S, Davlin TL, Rice T, Wrensch M, Bondy ML. Effects of antihistamine and anti-inflammatory medication use on risk of specific glioma histologies. *Int J Cancer.* 2011;129(9):2290–6. <http://dx.doi.org/10.1002/ijc.25883>
53. Fujita M, Kohanbash G, Fellows-Mayle W, Hamilton RL, Komohara Y, Decker SA, et al. COX-2 blockade suppresses gliomagenesis by inhibiting myeloid-derived suppressor cells. *Cancer Res.* 2011;71(7):2664–74. <http://dx.doi.org/10.1158/0008-5472.CAN-10-3055>
54. Seliger C, Meier CR, Becker C, Jick SS, Bogdahn U, Hau P, et al. Use of selective cyclooxygenase-2 inhibitors, other analgesics, and risk of glioma. *PLoS One.* 2016;11(2):1–12. <http://dx.doi.org/10.1371/journal.pone.0149293>
55. Kitahara CM, Wang SS, Melin BS, Wang Z, Braganza M, Albanes D, et al. Association between adult height, genetic susceptibility and risk of glioma. *Int J Epidemiol.* 2012 Aug;41(4):1075–85. <http://dx.doi.org/10.1093/ije/dys114>
56. Hoschberg F, Toniolo P, Cole P, Scalcman M. Nonoccupational risk indicators of glioblastoma in adults. *J Neuroincol.* 1999;8:55–60.
57. Deltour I, Auvinen A, Feychting M, Johansen C, Klæboe L, Sankila R, et al. Mobile phone use and incidence of glioma in the Nordic countries 1979–2008: Consistency check. *Epidemiology.* 2012;23(2):301–7. <http://dx.doi.org/10.1097/EDE.0b013e3182448295>
58. Benson VS, Pirie K, Schuz J, Reeves GK, Beral V, Green J. Mobil phone use and risk of brain neoplasms and other cancers: Prospective study. *Int J Epidemiol.* 2013;43(3):792–802. <http://dx.doi.org/10.1093/ije/dyt072>
59. Nieder C, Grosu A, Astner S, Molls M. Treatment of unresectable glioblastoma multiforme. *Anticancer Res.* 2005;1(25):4605–10.
60. Malmstrom A, Gronberg BH, Marosi C, Stupp R, Frappaz D, Schultz H, et al. Temozolamide versus standard 6-week radiotherapy versus hypo fractionates radiotherapy in patients older than 60 years with glioblastoma. The Nordic randomized phase 3 trial. *Lancet Oncol.* 2012;13:916–26. [http://dx.doi.org/10.1016/S1470-2045\(12\)70265-6](http://dx.doi.org/10.1016/S1470-2045(12)70265-6)
61. Stummer W, Reulen H-J, Meinert T, Pichlmeier U, Schumacher W, Tonn JC, et al. Extent of resection and survival in glioblastoma multiforme: Identification of and adjustment for bias. *Neurosurgery.* 2008;62(3):564–76. <http://dx.doi.org/10.1227/01.neu.0000317304.31579.17>

9

PET Imaging in Glioblastoma: Use in Clinical Practice

ANTOINE VERGER^{1,2} • KARL-JOSEF LANGEN^{3,4}

¹Department of Nuclear Medicine & Nancyclotep Imaging Platform, CHRU Nancy, Lorraine University, France; ²IADI, INSERM, UMR 947, Lorraine University, Nancy, France; ³Department of Nuclear Medicine, University of Aachen, Aachen, Germany; ⁴Institute of Neuroscience and Medicine, Forschungszentrum Jülich, Jülich, Germany

Author for correspondence: Antoine Verger, Service de Médecine Nucléaire, Hôpital de Brabois, 54500 Vandoeuvre les Nancy, France.
Email: a.verger@chru-nancy.fr

Doi: <http://dx.doi.org/10.15586/codon.glioblastoma.2017.ch9>

Abstract: Positron emission tomography (PET) is a nuclear medicine imaging method with increasing relevance for the diagnosis, prognostication, and monitoring of glioblastomas. PET provides additional insight beyond magnetic resonance imaging (MRI) into the biology of gliomas, which can be used for noninvasive grading, differential diagnosis, delineation of tumor extent, planning of surgery, and radiotherapy and post-treatment monitoring. In clinical practice, two classes of radiotracers have been used predominantly for imaging purposes, namely glucose metabolism tracers and amino acid transport tracers. Both classes of tracers can provide information on grading and prognosis of gliomas, but amino acid tracers, which exhibit lower uptake in normal brain tissue, are better suited for delineation of tumor extent, treatment planning, or follow-up than ¹⁸F-2-fluoro-2-deoxy-D-glucose (¹⁸F-FDG). Owing to the progress in PET imaging using radio-labeled amino acids in recent years, the Response Assessment in Neuro-Oncology (RANO) working group, an international effort to develop new standardized response criteria for clinical trials in brain tumors, has recently recommended amino acid PET as an additional tool in the diagnostic assessment of brain tumors.

In: *Glioblastoma*. Steven De Vleeschouwer (Editor), Codon Publications, Brisbane, Australia
ISBN: 978-0-9944381-2-6; Doi: <http://dx.doi.org/10.15586/codon.glioblastoma.2017>

Copyright: The Authors.

Licence: This open access article is licenced under Creative Commons Attribution 4.0 International (CC BY 4.0). <https://creativecommons.org/licenses/by-nc/4.0/>

These developments as well as multimodality imaging should improve the diagnostic assessment of these tumors.

Keywords: ^{11}C -MET PET; ^{18}F -FDG PET; ^{18}F -FDopa PET; ^{18}F -FET PET; Glioblastoma

Introduction

The incidence of primary malignant brain and central nervous system tumors in the general population was estimated at 3 per 100,000 in 2008, with a higher incidence rate in developed countries than in developing countries (1). Among these tumors, glioblastomas account for approximately 60–70% of malignant gliomas (2, 3). With maximum safe resection, radiotherapy, and concurrent and adjuvant temozolomide, in clinical trial populations, the median survival is 12–15 months (4–7). Unfortunately, after initial treatment, these tumors invariably recur. Initial diagnosis, prognosis, and targeted treatment of these tumors thus represent very active areas of investigation.

In this setting, neuroimaging plays a key role in the assessment of these tumors (8). Magnetic resonance imaging (MRI), the current imaging gold standard, has offered limited insight to date with regard to grade of malignancy, tumor delineation, differentiation between necrotic tissues and recurrent tumor, as well as the management of therapeutic interventions such as surgery or radiotherapy (9, 10). In fact, although a rapidly enlarging or enhancing lesion on MRI with or without clinical symptoms is usually considered a progressing tumor, imaging the extent of contrast enhancement in malignant gliomas has limited accuracy due to the difficulty in distinguishing between progressive tumor and treatment-induced changes such as radiation necrosis (11).

Positron emission tomography (PET) is a nuclear medicine method with an increasing relevance especially due to the improved availability of radioactively labeled amino acids, allowing widespread applications in diagnosis, therapy planning, and therapy monitoring of glioblastomas (9, 10). PET provides additional insight beyond MRI into the biology of gliomas which can be used for noninvasive grading, differential diagnosis, delineation of tumor extent, planning of surgery and radiotherapy, post-treatment monitoring, and prognostication. Among PET radiotracers, ^{18}F -2-fluoro-2-deoxy-D-glucose (^{18}F -FDG) is the most widely studied and validated tracer to date. In addition, ^{18}F -FDG is widespread in clinical nuclear medicine and is of low cost (8). In instances of suspicious low-grade glioma, it is able to identify anaplastic transformation and displays good prognostic value. Indeed, tumor cells are characterized by increased glycolytic metabolism, in parallel with cell proliferation and loss of differentiation. ^{18}F -FDG is an appropriate, albeit nonspecific radiotracer for noninvasively assessing the biological aggressiveness of tumors *in vivo*, as previously suggested in many cancer types (12). However, a high ^{18}F -FDG uptake in surrounding normal brain tissue limits its use for the imaging of cerebral gliomas which may not be visualized in a large fraction of primary and recurrent tumors (13).

Due to the relatively low tracer uptake in normal gray matter, amino acid PET tracers can detect gliomas with greater sensitivity than ^{18}F -FDG in primary

and recurrent tumors and are helpful in differentiating recurrent tumors from treatment-induced changes (14). ^{11}C -methyl-methionine (^{11}C -MET) is the most studied and validated amino acid tracer. It is a natural amino acid avidly taken up by glioma cells, with only a low uptake in normal cerebral tissue. A smaller portion of ^{11}C -MET is metabolized by decarboxylation. However, several experiments have suggested that during PET studies, tumor uptake of ^{11}C -MET mainly reflects increased amino acid transport (15). Its major drawback lies in the short half-life of the ^{11}C -carbon, only 20 min, and thus requires close proximity to a cyclotron, thereby limiting its use in routine nuclear medicine centers. To overcome the drawbacks of the short-lived MET, ^{18}F -labeled amino acids have been developed in order to expand amino acid tracer utilization, namely O-(2-[^{18}F]-fluoroethyl)-L-tyrosine (^{18}F -FET) and 3,4-dihydroxy-6-[^{18}F]-fluoro-L-phenylalanine (^{18}F -FDOPA). ^{18}F -FET is increasingly used in Europe as a tracer for both high-grade gliomas as well as low-grade gliomas, owing to its several advantages including synthesis by an efficient nucleophilic reaction, elevated uptake by tumor tissues, low uptake by inflammatory tissues, and high stability (16). Similar to ^{11}C -MET and ^{18}F -FET, ^{18}F -FDOPA is incorporated into cells through amino acid transporters that are overexpressed in gliomas, and its transport and uptake are independent of the blood-brain barrier (17). Of note, a striatal uptake has nonetheless been reported in the case of ^{18}F -FDOPA, which may lead to difficulties in delineating gliomas in these areas (17).

The aim of this chapter is to define clinical practice PET indications in glioblastomas for the purposes of diagnosis, delineation of glioma extent, as well as its value in treatment planning, follow-up, and prognostication. The following mainly focuses on imaging tracers of glucose metabolism (^{18}F -FDG) and amino acid transport (^{11}C -MET, ^{18}F -FET, and ^{18}F -FDOPA), since these compounds are already part of current clinical practice. Future perspectives in novel radiotracers and technical improvements are also outlined.

Primary Diagnosis/Differential Diagnosis

^{18}F -FDG is useful for differentiating high-grade gliomas from other types of brain tumors (18). In the specific setting of glioblastomas, ^{18}F -FDG is particularly sensitive at the initial stage of the diagnosis (19, 20), an example of which is given in Figure 1. In a study involving 31 newly diagnosed glioblastomas, Colavolpe et al. found an uptake of ^{18}F -FDG in these tumors with a tumor-to-background ratio max (TBRmax) of 1.4 ± 0.8 (12). However, differential diagnosis at the initial stage with ^{18}F -FDG may be difficult to achieve due to the low specificity of this radiotracer. Indeed, brain lymphomas can display a higher glucose metabolism uptake than high-grade gliomas (21). Moreover, nonneoplastic neurological diseases can mimic brain neoplasms on ^{18}F -FDG, including pyogenic abscesses, tuberculosis, fungal infections, or sarcoidosis (22). Studies comparing the ^{18}F -FDG and amino acid tracer uptake in the assessment of brain tumors demonstrated significantly higher tumor to brain contrast with amino acid PET than with ^{18}F -FDG (23–25), demonstrating a higher sensitivity of amino acid tracers for glioblastoma detection.

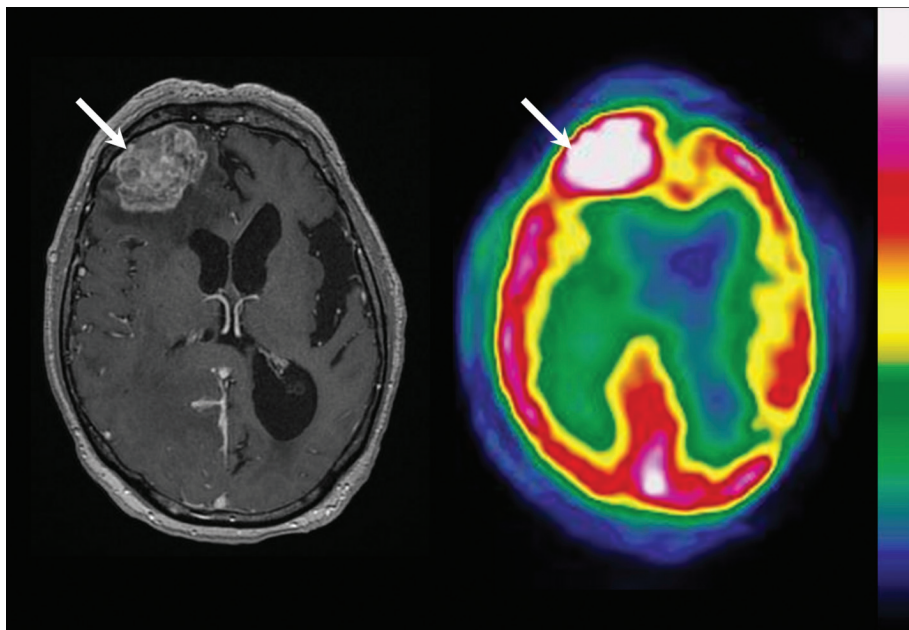


Figure 1 Primary diagnosis of a right frontal glioblastoma in a 79-year-old man following acquisition of axial slices of T1-weighted gadolinium-enhanced MRI (left side) and ^{18}F -FDG PET (right side). The right frontal glioblastoma is contrast-enhanced on MRI (white arrow) and shows an extensive uptake of ^{18}F -FDG PET (white arrow), despite the high uptake in surrounding normal brain tissue.

^{18}F -FET has shown comparable results to ^{11}C -MET in the detection of brain gliomas (26). Approximately 95% of high-grade gliomas, including glioblastomas, display a significant uptake of ^{18}F -FET (27–29), leading to a high sensitivity of ^{18}F -FET for tumor detection. A study conducted in rats demonstrated that ^{18}F -FET uptake was absent in macrophages, a common inflammatory mediator, in contrast to accumulation of ^{18}F -FDG in these cells (30). Nevertheless, in patient studies, unspecific FET uptake has been observed in nonneoplastic brain lesions (28, 31). Despite its limited specificity (32), ^{18}F -FDOPA is also a sensitive tool for diagnosing glioblastomas with similar results to ^{11}C -MET (33). For instance, in a study of 23 histologically confirmed tumors, ^{18}F -FDOPA had a TBRmax of 2.50 ± 0.73 for 18 high-grade tumors, 3 of which were glioblastomas (24).

In the diagnosis of gliomas, noninvasive tumor grading may be helpful in order to define aggressive forms at initial stages with poor prognosis. In this instance, ^{18}F -FDG is helpful to detect glioblastomas, since low-grade gliomas often appear as hypometabolic lesions, particularly when compared with cortical uptake (34). However, due to its high uptake in gray matter, tumor to brain ratios of ^{18}F -FDG uptake are low (1.23 ± 0.69) for high-grade tumors, leading to a poorer tumor imaging contrast in comparison to amino acid tracers (24). ^{18}F -FDOPA uptake was found to be significantly higher in high-grade tumors compared to low-grade tumors in newly diagnosed but nonrecurrent tumors that

had been previously treated in a series of 59 gliomas of which 25 were glioblastomas (35). In another study, ^{18}F -FDOPA uptake was significantly different in high-grade and low-grade gliomas or for both newly diagnosed and recurrent gliomas in a series of 31 gliomas of which 5 were glioblastomas (17). Similarly, several studies, including those on glioblastomas, have shown significantly different TBRmax between high-grade and low-grade gliomas with ^{11}C -MET (36–38), although other study results are more controversial (39, 40).

For ^{18}F -FET, it has been shown that a TBRmax < 2.5 excludes a high-grade tumor with high probability (27). Furthermore, ^{18}F -FET accuracy for tumor grading can be markedly improved by assessing dynamic PET data, which typically show steadily increasing time–activity curves in low-grade gliomas, as opposed to an early activity peak around 10–20 min after injection, followed by decreased uptake in high-grade gliomas (41, 42). Accordingly, in a study combining MRI and dynamic ^{18}F -FET data for initial glioma grading (43), the authors concluded that on multivariate logistic regression analysis, a negative slope of the tumor FET time–activity curve remains the best predictor of high-grade glioma. Analysis of dynamic data was not helpful for tumor grading neither with ^{11}C -MET (44) nor with ^{18}F -FDOPA (45, 46). Altogether, PET is helpful in the diagnostic evaluation of glioblastomas at the initial stage by means of glycolytic or amino acid metabolism-based tracers. Differential diagnosis with nonneoplastic lesions, however, is poorer with ^{18}F -FDG due to its low specificity. On the contrary, all commonly used PET tracers can contribute to the differentiation of glioblastomas from low-grade gliomas, especially ^{18}F -FET, when using dynamic data.

Delineation of Glioma Extent

The accurate definition of initial tumor volume as well as extent of recurrence is essential in treatment planning. Accordingly, PET data provide valuable additional information compared with MRI, which suffers from high interindividual variability in delineation of glioblastoma target volumes (47). Furthermore, multiple histopathological and postmortem series have demonstrated the limitations of conventional MRI in defining the extent of gliomas (48, 49). Amino acid PET tracers are the better candidates for this indication compared with ^{18}F -FDG, which exhibits high uptake in normal brain tissue (13). In a study involving 12 patients with recurrent glioblastoma, the metabolically active tumor volume as defined by ^{11}C -MET PET was substantially underestimated by contrast enhancement in MRI. These findings support the notion that information derived from ^{11}C -MET uptake in addition to contrast-enhanced MRI may be helpful in optimized targeting of the tumor mass by surgery and radiotherapy (50).

Similarly, some studies in which the radiological findings were compared with the histological findings in tissue samples obtained by biopsy or open surgery have provided evidence that FET PET detects the solid mass of gliomas and metabolically active tumor areas more reliably than MRI (51, 52). Furthermore, in a study of initial diagnosis of 56 gliomas, 24 of which were glioblastomas, ^{18}F -FET showed considerably higher TBRmax and larger tumor volumes when compared to regional cerebral blood volume maps derived from perfusion-weighted

MR imaging (53). In addition, postoperative ^{18}F -FET PET has been shown to reveal residual tumor with higher sensitivity than MRI as well as show larger tumor volumes (54). In this latter series of 62 patients with recurrent glioblastoma, ^{18}F -FET was thus recommended as a helpful adjunct in addition to MRI for postoperative assessment of residual tumor (54). Similar results have been obtained with ^{18}F -FDOPA PET in progressive or recurrent glioblastomas where a larger tumor extent was identified when compared with MRI-derived regional cerebral blood volume maps (55). Accordingly, ^{18}F -FDOPA PET-based tumor volumes have been shown to extend beyond the contrast-enhancing volume on conventional MRI (56). In addition, initial nonenhancing glioblastoma areas were also identified with this radiotracer since they were subsequently followed by abnormal MRI contrast enhancement (57).

Value in Treatment Planning

BIOPSY AND RESECTION

PET enables better identification of intra-tumor heterogeneity compared with standard MRI in addition to delineating tumor extent with much greater accuracy. The identification of malignant foci, commonly defined as “hot spots” in heterogeneous gliomas and a specific characteristic of glioblastomas (58), is essential for biopsy planning. The objective is to ensure that the most biologically aggressive portion of the tumor, which ultimately determines the patient’s prognosis as well as treatment, is not under-sampled (56, 59). Similar to the delineation of tumor extent, amino acid tracers are more suitable than ^{18}F -FDG in identifying malignant foci in gliomas. In a study aimed at guiding stereotactic brain biopsy of gliomas by using ^{18}F -FDG and ^{11}C -MET, the authors showed that all 32 gliomas, 10 of which were glioblastomas, exhibited an area of abnormal ^{11}C -MET uptake, whereas only 7 glioblastomas showed abnormal ^{18}F -FDG uptake (60). An example of superiority of ^{11}C -MET in comparison to ^{18}F -FDG is given in Figure 2. In another study aimed at comparing performances with MRI, stereotactic PET-guided biopsies were also performed with ^{18}F -FDOPA PET. Thirteen of the 16 high-grade biopsy specimens were obtained from regions of elevated ^{18}F -FDOPA uptake, while MRI contrast enhancement was present in only 6 of the aforementioned 16 samples (56). These observations, in accordance with previous results, thus underscore the potential benefit of using PET amino acid tracers in determining the most aggressive portion of the tumor.

Of particular interest, in a study using a combination of ^{18}F -FDG and ^{11}C -MET, surgical tumor resection based on PET tracer uptake was found to be significantly associated with longer survival in glioblastoma patients when compared with surgical resection based on MRI contrast enhancement (61). Thus, in addition to its value in biopsy planning, PET data provide added prognostic value with regard to surgical resection outcome (61). It has moreover been suggested that patients with glioblastomas may potentially benefit from maximal PET-guided tumor resection since lower biological tumor volume (BTV) before treatment with ^{18}F -FET was independent of clinical prognostic factors: patients with smaller tumor volumes had significantly longer progression-free and overall survival (62).

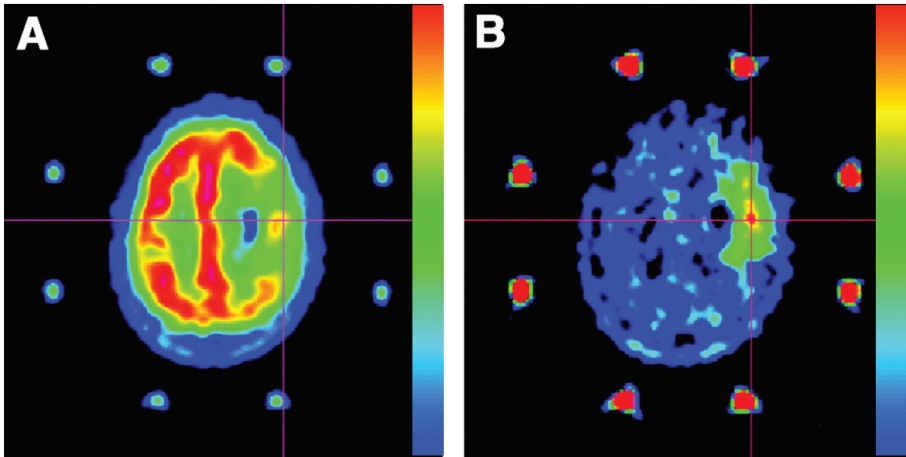


Figure 2 PET performed with ^{18}F -FDG (A) and ^{11}C -MET (B) in a 62-year-old woman with a glioblastoma in the left prerolandic cortical area. Uptake of ^{18}F -FDG was reduced in the tumor area except for one area of uptake equivalent to that in the surrounding gray matter. Uptake of ^{11}C -MET was higher in the tumor than in the surrounding cortex, allowing the definition of a target for biopsy. When PET images obtained with the two tracers were co-recorded, the highest focus of ^{11}C -MET uptake corresponded to the hot spot of ^{18}F -FDG uptake (intersecting lines). (Adapted from *J Nucl Med* 2004;45:1293–1298. Copyright: The Society of Nuclear Medicine and Molecular Imaging, Inc. Reproduced with Permission.)

RADIATION

In radiotherapy treatment planning, ^{18}F -FDG PET can provide prognostic information. Indeed, ^{18}F -FDG PET volumes are predictive of survival and time to tumor progression in the treatment of patients with glioblastomas (63). However, ^{18}F -FDG uptake abnormalities generally demonstrate a smaller region of uptake contained within the MRI abnormality, with only an occasional extension outside of the MRI target (63). ^{18}F -FDG PET is therefore of limited value for radiation treatment planning except for the definition of target volumes in radiation dose escalation. PET amino acid tracers are thus better suited to delineate tumor volume prior to radiotherapy. Accordingly, in a study of 39 patients with high-grade gliomas before radiotherapy, the region of ^{11}C -MET uptake was larger and detected up to 45 mm beyond MRI contrast enhancement in 29 patients (15). Similarly, high-grade glioma contours obtained with ^{18}F -FDOPA PET-based consensus target volumes were larger than MRI-based volumes (64). ^{11}C -MET PET was also found to provide supplementary information to MRI data, whereby BTV defined with ^{11}C -MET PET included all localizations of recurrences in a series of 52 glioblastomas (65). Thus, these pretreatment ^{11}C -MET PET volumes appear to identify areas at highest risk of recurrence for patients with glioblastomas since inadequate PET-gross-tumor-volume coverage was associated with increased risk of noncentral failures (66).

Of note, in re-irradiated patients, significant longer survival times have been reported using image fusion in treatment planning when compared with treated patients based on MRI/CT alone (67). Large BTC on ^{18}F -FET PET is accordingly

an independent prognostic factor of poor overall survival and of progression-free survival in newly diagnosed glioblastoma patients, to the detriment of other prognosis factors such as clinical factors or MRI-based tumor volume (62, 68). A number of centers have accordingly begun to integrate amino acid imaging into CT-based and MRI-based radiotherapy planning (69), particularly in high-grade gliomas and in instances when high-precision radiotherapy is to be given, or in the setting of dose escalation studies, or for re-irradiation of recurrent tumors (70, 71). In this context, ^{11}C -MET /CT/MRI fusion has also been proposed to optimize hypofractionated stereotactic radiotherapy by intensity-modulated radiation therapy (HS-IMRT) in recurrent glioblastomas, with good treatment tolerance and a median survival time of 11 months (72).

Follow-up: Treatment Response, Progression, Pseudoprogression, and Radionecrosis

The extent of MRI contrast enhancement is usually considered an indicator of treatment response or progression (73). However, contrast enhancement after radiotherapy with or without concomitant temozolomide can mimic tumor progression and is termed “pseudoprogression.” This phenomenon typically occurs within the first 12 weeks after chemoradiation with concurrent temozolomide or radiotherapy alone (74, 75). Moreover, contrast enhancement is linked to nonspecific post-therapeutic effects, in the specific setting of post-radiation effects, occurring several months later than pseudoprogression (76). It is relatively similar to that observed in tumor recurrence thus impeding the differential diagnosis between radionecrosis and recurrence. Finally, since the introduction of antiangiogenic agents such as bevacizumab, the phenomenon of pseudoresponse further complicates the assessment of treatment response using standard MRI alone (74, 77).

^{18}F -FDG PET shows a decreased metabolic rate of cerebral glucose after radiotherapy or chemotherapy even if hypermetabolism is observed in the early phase after radiotherapy mostly due to the inflammatory process (20, 78, 79). ^{18}F -FDG nevertheless displays low specificity between radionecrosis and tumor recurrence (80) as well as a weak added value to MRI (81). In contrast, amino acid tracers appear to be better tools to provide sensitive monitoring of the response to various treatment options as well as the early detection of tumor recurrence, including an improved differentiation of tumor recurrence from post-therapeutic effects (82).

^{11}C -MET is considered as very helpful in the assessment of these patients because the decrease in amino acid in the metabolically active tumor volume is a sign of treatment response associated with long-term outcome (83, 84). Accordingly, combined assessment with MRI and ^{11}C -MET at 8 weeks can differentiate true responders, that is, those predicted to show a more favorable prognosis, from pseudoresponders (85). ^{18}F labeled amino acid tracers can also determine treatment response after chemotherapy with a higher accuracy than MRI alone. A comparative illustration between ^{18}F -FET PET and contrast-enhanced MRI is shown in Figure 3. For example, in a study involving 25 patients with glioblastoma after early completion of radiochemotherapy, a decrease in both ^{18}F -FET

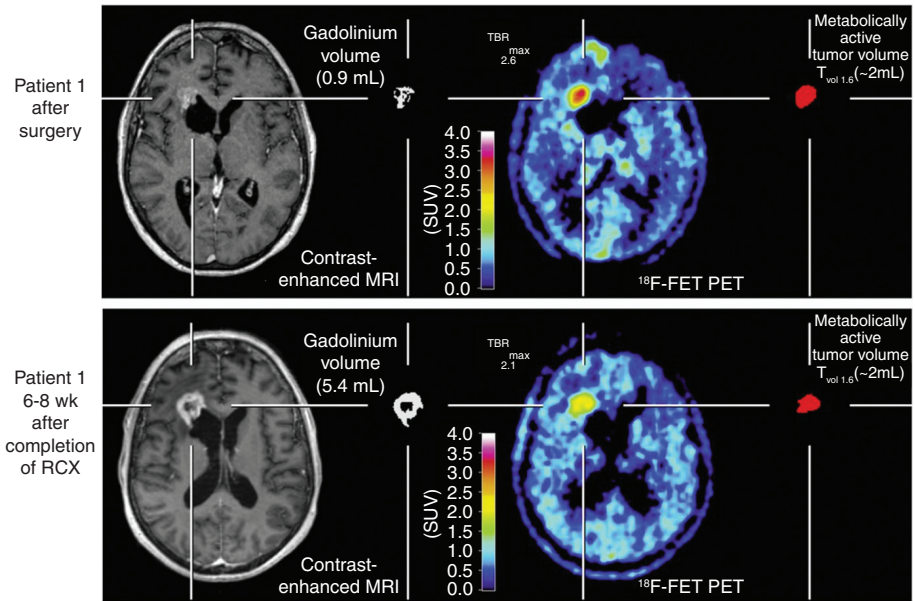


Figure 3 ^{18}F -FET-PET in a 59-year-old woman with glioblastoma. Brain imaging was performed after surgery (upper panel; MRI-/FET-1) and 6–8 weeks after completion of radiochemotherapy (lower panel; MRI-/FET-3). Contrast-enhanced MRI with corresponding contrast-enhanced volume is shown on the left and ^{18}F -FET PET with corresponding metabolic volume on the right. Enlargement of contrast-enhanced volume on MRI 6–8 weeks after completion of radiochemotherapy (lower panel) is suggestive of tumor progression, whereas ^{18}F -FET PET conversely indicates responsiveness with decreasing amino acid uptake (reduction of TBRmax) and unchanged metabolic volume. (Adapted from *J Nucl Med* 2012;53:1048–1057. Copyright: Society of Nuclear Medicine and Molecular Imaging, Inc. Reproduced with Permission.)

TBR(max) and TBR(mean) was found to be a highly significant and independent statistical predictor of progression-free survival and overall survival. On the contrary, contrast enhancement volume changes had no significant predictive value for survival (86).

Otherwise, it has been shown that ^{18}F -FET PET is able to differentiate pseudoprogression from early tumor progression within the first 12 weeks after completion of radiochemotherapy with concomitant temozolomide. In patients with pseudoprogression, ^{18}F -FET uptake was found to be significantly lower than in patients with early progression (TBRmax 1.9 ± 0.4 vs. 2.8 ± 0.5 , TBRmean 1.8 ± 0.2 vs. 2.3 ± 0.3). Performances for diagnosis of pseudoprogression with ^{18}F -FET PET were high in sensitivity, specificity, and accuracy by using TBRmax reaching up to respectively, 100, 91, and 96% (87). Moreover, a rapid increase in radiotracer uptake in time activity curves (shorter time to peak) was more frequently present in patients with tumor progression (87). Furthermore, a recent study has even proposed an original method of clustering based on textural ^{18}F -FET PET features that could distinguish pseudoprogression from true tumor progression (88). In addition, ^{18}F -FET PET has also been found to provide valuable information in assessing the elusive phenomenon of late pseudoprogression (89).

^{18}F -FDOPA can identify treatment responders to antiangiogenic therapy as early as 2 weeks after treatment initiation and thus could be an efficient tool in case of suspicion of pseudoresponse (90). In a study involving antiangiogenic therapy, a decrease in ^{18}F -FDOPA PET tracer uptake was associated with longer progression-free survival and overall survival (91). Furthermore, in this latter study, the volume fraction of increased ^{18}F -FDOPA PET uptake measured at two time points after bevacizumab treatment also enabled to stratify long-term and short-term progression-free survival as well as overall survival (91). Responders based on ^{18}F -FDOPA PET data survived 3.5 times longer (12.1 months vs. 3.5 months of median overall survival) than nonresponders, which was much higher than responders based solely on MRI (90). Similar results have been reported for ^{18}F -FET (92–94).

With regard to the differential diagnosis between tumor recurrence and radionecrosis, ^{11}C -MET provides a better sensitivity and clearer delineation of the suspected recurrence (83). In a comparative study, ^{11}C -MET was found to be superior to ^{18}F -FDG for diagnostic accuracy in distinguishing glioma recurrence from radiation necrosis (95). Similarly, in a prospective comparison with ^{18}F -FDG PET, ^{18}F -FDOPA PET had a diagnostic accuracy of 100% for the diagnosis of glioblastoma recurrence versus 92.8% with ^{18}F -FDG PET (96). In addition, in a study of 110 glioblastoma patients, ^{18}F -FDOPA PET detected recurrence with high accuracy while lesion-to-normal-tissue ratios were predictive of progression-free survival (97). Finally, ^{18}F -FDOPA PET is also able to distinguish tumor recurrence from treatment-related changes (24), an example of which is depicted in Figure 4.

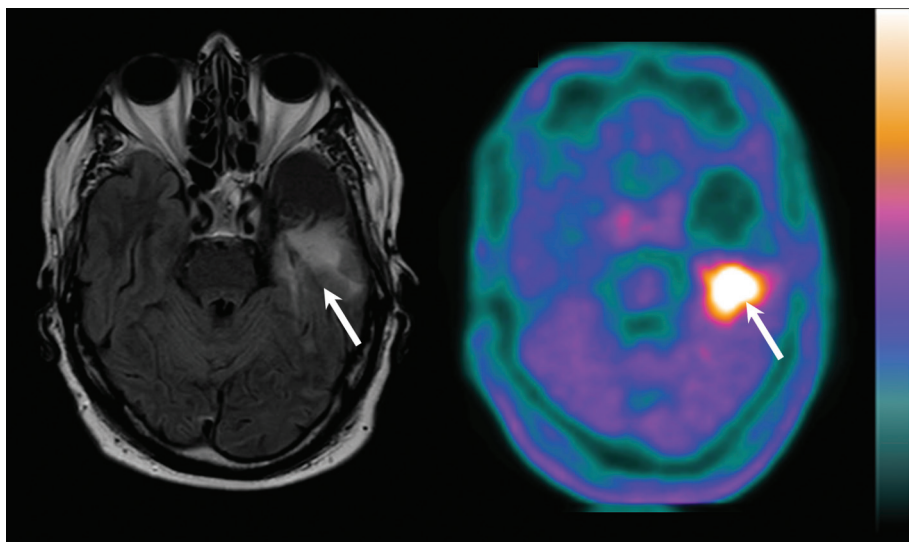


Figure 4 Left temporal glioblastoma recurrence in a 66-year-old man after surgery and adjuvant radiochemotherapy. The axial slice of Fluid-Attenuated Inversion Recovery (FLAIR)-weighted MRI (left side) shows a hypersignal at the posterior area of the exeresis cavity (white arrow), making the distinction between tumor recurrence and post-therapeutic effects somewhat challenging. The axial slice of ^{18}F -FDOPA PET shows an intense uptake in the same area (white arrow), which is strongly in favor of tumor recurrence.

In a similar manner, static and dynamic ^{18}F -FET PET parameters can differentiate progressive or recurrent glioma from treatment-related nonneoplastic changes with a higher accuracy than conventional MRI, especially with regard to glioblastoma recurrence (98, 99).

Prognostication

^{18}F -FDG provides an additional prognostic value to MRI (100) in newly diagnosed (12) or recurrent glioblastomas (101). Indeed, the tumor-to-normal brain tissue ratio has been reported to predict overall survival in a newly diagnosed glioblastoma subgroup, independently of age, Karnofsky performance status, histological grade, and surgery (12). In addition, in a series of 20 recurrent glioblastomas, ^{18}F -FDG uptake was found to be the most powerful predictor of both progression-free survival and overall survival, using either univariate or multivariate analysis, among all variables tested, including histological grade, Karnofsky performance status, steroid intake, and number of previous treatments (101).

Prognostic value is also a feature of amino acid tracers. Indeed, ^{11}C -MET uptake is correlated to prognostic, histological, and molecular parameters in gliomas at initial stage (102). Moreover, a prospective multicenter trial investigating the role of pretreatment ^{18}F -FET PET in newly diagnosed glioblastoma found BTV prior to radiochemotherapy to be highly prognostic of outcome (62). Furthermore, ^{18}F -FET PET time-activity curves before treatment and their changes after radiochemotherapy were also related to outcome, whereby patients with increasing time-activity curves experienced longer overall survival (62). This latter observation is in accordance with results of previous studies investigating amino acid PET in malignant glioma prior to therapy in which volumetry of ^{11}C -MET uptake was a pretreatment prognostic marker in patients with malignant glioma (103). Interestingly, tumor-to-normal brain tissue ratio using ^{18}F -FDOPA PET was also reported as an independent predictor of survival, along with the size of recurrent tumor on MRI in patients with suspected recurrent glioblastomas (104). More recently, a combination of two radiotracers was used to define a metabolic tumor volume in hypoxia, with the latter expressed as the volume of ^{18}F -FDG / ^{18}F -fluoromisonidazole (^{18}F -FMISO) double-positive, and ^{18}F -FMISO used as a radiotracer of hypoxia. This metabolic tumor volume in hypoxia was a significant predictor of progression-free survival and overall survival in glioblastoma patients (105).

Future Perspectives: Novel Radiotracers and Multimodality

Several other radiotracers have been developed for diagnosis, prognosis, or follow-up of glioblastomas (106). Among the better-known compounds, the aforementioned ^{18}F -FMISO, a nitroimidazole derivative, was developed as a PET imaging agent of hypoxia (107), through the trapping of its metabolites into hypoxic cells (108). Hypoxia in tumors is a pathophysiological consequence of

structurally and functionally disturbed angiogenesis along with a deterioration in the ability of oxygen to diffuse through the tissues and is associated with progression and resistance to radiotherapy (109). ^{18}F -FMISO uptake has been found in high-grade gliomas, but not in low-grade gliomas, along with a significant relationship between its uptake and expression of the angiogenesis marker VEGF-R1. Thus, ^{18}F -FMISO may have a role in directing and monitoring targeted hypoxic therapy (110).

Another radiotracer, ^{18}F -fluorothymidine (^{18}F -FLT), is a thymidine analog developed for the purpose of imaging tumor cell proliferation (111). ^{18}F -FLT has been used in diagnosis and assessment of glioma grading, in differentiating tumor recurrence from radionecrosis, in assessing response to treatment, and in predicting overall survival (112). In an image-guided biopsy study, results demonstrated that ^{18}F -FLT, while a useful marker of cell proliferation, and although correlated with regional variations in cell proliferation, was unable to identify the margin of gliomas (113). This is due to the fact that ^{18}F -FLT is not able to penetrate the intact blood–brain barrier and normally accumulates only in areas with contrast enhancement on MRI (114, 115).

^{11}C -Choline has been used as a marker of cell membrane phospholipids in brain tumors, exhibiting a significant correlation of uptake with the degree of glioma malignancy (116). However, as is the case with ^{18}F -FLT, tracer uptake is limited to areas with blood–brain barrier disruption and therefore this tracer offers limited additional information compared to a contrast-enhanced MRI. It should nevertheless be emphasized that, despite their many advantages, the majority of these radiotracers as well as multiple others are not widely available and are only used in a limited number of centers since they require well-experienced staff with on-site radiochemistry equipment and cyclotron. These radiotracers are currently available only in research centers. Furthermore, future perspectives also include multimodality imaging. Accordingly, technological innovations in glioma imaging assessment such as simultaneous acquisition of anatomic and functional images with the integration of PET–MRI data appear to be of particular promise for research, diagnosis, and treatment of glioblastomas. Fully integrated PET/MRI scanners are now available and the number of scanner installations and published studies is steadily on the rise (117–119). Furthermore, hybrid PET–MRI systems offer improved patient comfort due to a significant reduction in measurement time and improved spatial and temporal co-recording of PET and MRI data. Hybrid PET–MR allows comparing amino acid PET data with advanced MR parameters including perfusion-weighted imaging, magnetic resonance spectroscopy, and diffusion-weighted imaging (118).

In addition to this technical multimodality and the concomitant efforts of using various radiopharmaceuticals to characterize multiple biological targets (61, 105), currently used multiparametric imaging also integrates the development and applications of innovative methods of image processing and analysis (120). While common metrics such as standard uptake value (SUV) or BTM or TBR only partially describes the properties of pathological lesions, novel parameters such as shape and uptake heterogeneity may provide additional information on the biological profile associated with tumor aggressiveness or degree of response to specific treatment and, consequently, with prognosis (121).

Conclusion

In summary, PET is a nuclear medicine imaging method with increasing relevance in diagnosis, therapy monitoring, and prognostication of glioblastomas. In clinical practice, currently used radiotracers are focused on imaging of glucose metabolism and amino acid transport. Both classes of tracers can provide information on grading and prognosis of gliomas, but amino acid tracers, which exhibit lower uptake in normal brain tissue, are better suited for delineation of tumor extent, treatment planning, and follow-up than ^{18}F -FDG. Although the use of PET in the diagnosis of glioblastomas is still at an early stage of development in clinical practice, development of novel radiotracers and recent innovations in multimodality imaging are expected to enhance its use in the assessment of these tumors in the near future.

Acknowledgment: The authors thank Pierre Pothier for the editing this article.

Conflict of interest: The authors declare no potential conflicts of interest with respect to research, authorship, and/or publication of this article.

Copyright and permission statement: To the best of our knowledge, the materials included in this chapter do not violate copyright laws. All original sources have been appropriately acknowledged and/or referenced. Where relevant, appropriate permissions have been obtained from the original copyright holder(s).

References

1. Ferlay J, Shin H-R, Bray F, Forman D, Mathers C, Parkin DM. Estimates of worldwide burden of cancer in 2008: GLOBOCAN 2008. *Int J Cancer*. 2010 Dec;127(12):2893–917. <http://dx.doi.org/10.1002/ijc.25516>
2. Ostrom QT, Gittleman H, Farah P, Ondracek A, Chen Y, Wolinsky Y, et al. CBTRUS statistical report: Primary brain and central nervous system tumors diagnosed in the United States in 2006–2010. *Neuro-Oncology*. 2013 Nov;15(Suppl 2):ii1–56. <http://dx.doi.org/10.1093/neuonc/not151>
3. Louis DN, Ohgaki H, Wiestler OD, Cavenee WK, Burger PC, Jouvet A, et al. The 2007 WHO classification of tumours of the central nervous system. *Acta Neuropathol (Berl)*. 2007 Aug;114(2):97–109. <http://dx.doi.org/10.1007/s00401-007-0243-4>
4. Ahmed R, Oborski MJ, Hwang M, Lieberman FS, Mountz JM. Malignant gliomas: Current perspectives in diagnosis, treatment, and early response assessment using advanced quantitative imaging methods. *Cancer Manage Res*. 2014;6:149–70.
5. Stupp R, Mason WP, van den Bent MJ, Weller M, Fisher B, Taphoorn MJB, et al. Radiotherapy plus concomitant and adjuvant temozolomide for glioblastoma. *N Engl J Med*. 2005 Mar;352(10):987–96. <http://dx.doi.org/10.1056/NEJMoa043330>
6. Chinot OL, Wick W, Mason W, Henriksson R, Saran F, Nishikawa R, et al. Bevacizumab plus radiotherapy-temozolomide for newly diagnosed glioblastoma. *N Engl J Med*. 2014 Feb;370(8):709–22. <http://dx.doi.org/10.1056/NEJMoa1308345>
7. Weller M, van den Bent M, Hopkins K, Tonn JC, Stupp R, Falini A, et al. EANO guideline for the diagnosis and treatment of anaplastic gliomas and glioblastoma. *Lancet Oncol*. 2014 Aug;15(9):e395–403. [http://dx.doi.org/10.1016/S1470-2045\(14\)70011-7](http://dx.doi.org/10.1016/S1470-2045(14)70011-7)

8. Chen W, Silverman DHS. Advances in evaluation of primary brain tumors. *Semin Nucl Med.* 2008 Jul;38(4):240–50. <http://dx.doi.org/10.1053/j.semnuclmed.2008.02.005>
9. Heiss W-D. [PET in gliomas. Overview of current studies]. *Nukl Nucl Med.* 2014 Aug;53(4):163–171. <http://dx.doi.org/10.3413/Nukmed-0662-14-04>
10. Dhermain F. Radiotherapy of high-grade gliomas: Current standards and new concepts, innovations in imaging and radiotherapy, and new therapeutic approaches. *Chin J Cancer.* 2014 Jan;33(1):16–24. <http://dx.doi.org/10.5732/cjc.013.10217>
11. Levivier M, Becerra A, De Witte O, Brotschi J, Goldman S. Radiation necrosis or recurrence. *J Neurosurg.* 1996 Jan;84(1):148–9.
12. Colavolpe C, Metellus P, Mancini J, Barrie M, Béquet-Boucard C, Figarella-Branger D, et al. Independent prognostic value of pre-treatment 18-FDG-PET in high-grade gliomas. *J Neurooncol.* 2012 May;107(3):527–35. <http://dx.doi.org/10.1007/s11060-011-0771-6>
13. Demetriades AK, Almeida AC, Bhargoo RS, Barrington SF. Applications of positron emission tomography in neuro-oncology: A clinical approach. *Surg J R Coll Surg Edinb Irel.* 2014 Jun;12(3):148–57. <http://dx.doi.org/10.1016/j.surge.2013.12.001>
14. von Neubeck C, Seidlitz A, Kitzler HH, Beuthien-Baumann B, Krause M. Glioblastoma multiforme: Emerging treatments and stratification markers beyond new drugs. *Br J Radiol.* 2015 Sep;88(1053):20150354. <http://dx.doi.org/10.1259/bjr.20150354>
15. Grosu A-L, Weber WA, Riedel E, Jeremic B, Nieder C, Franz M, et al. L-(methyl-11C) methionine positron emission tomography for target delineation in resected high-grade gliomas before radiotherapy. *Int J Radiat Oncol Biol Phys.* 2005 Sep;63(1):64–74. <http://dx.doi.org/10.1016/j.ijrobp.2005.01.045>
16. Wang L, Lieberman BP, Ploessl K, Kung HF. Synthesis and evaluation of ¹⁸F labeled FET prodrugs for tumor imaging. *Nucl Med Biol.* 2014 Jan;41(1):58–67. <http://dx.doi.org/10.1016/j.nucmedbio.2013.09.011>
17. Janvier L, Olivier P, Blonski M, Morel O, Vignaud J-M, Karcher G, et al. Correlation of SUV-derived indices with tumoral aggressiveness of gliomas in static 18F-FDOPA PET: Use in clinical practice. *Clin Nucl Med.* 2015 Sep;40(9):e429–35. <http://dx.doi.org/10.1097/RLU.0000000000000897>
18. Kosaka N, Tsuchida T, Uematsu H, Kimura H, Okazawa H, Itoh H. 18F-FDG PET of common enhancing malignant brain tumors. *AJR Am J Roentgenol.* 2008 Jun;190(6):W365–9. <http://dx.doi.org/10.2214/AJR.07.2660>
19. De Witte O, Lefranc F, Levivier M, Salmon I, Brotschi J, Goldman S. FDG-PET as a prognostic factor in high-grade astrocytoma. *J Neurooncol.* 2000 Sep;49(2):157–63. <http://dx.doi.org/10.1023/A:1026518002800>
20. Spence AM, Muzi M, Graham MM, O'Sullivan F, Link JM, Lewellen TK, et al. 2-[(18F)]Fluoro-2-deoxyglucose and glucose uptake in malignant gliomas before and after radiotherapy: Correlation with outcome. *Clin Cancer Res Off J Am Assoc Cancer Res.* 2002 Apr;8(4):971–9.
21. Yamashita K, Yoshiura T, Hiwatashi A, Togao O, Yoshimoto K, Suzuki SO, et al. Differentiating primary CNS lymphoma from glioblastoma multiforme: Assessment using arterial spin labeling, diffusion-weighted imaging, and ¹⁸F-fluorodeoxyglucose positron emission tomography. *Neuroradiology.* 2013 Feb;55(2):135–43. <http://dx.doi.org/10.1007/s00234-012-1089-6>
22. Omuro AM, Leite CC, Mokhtari K, Delattre J-Y. Pitfalls in the diagnosis of brain tumours. *Lancet Neurol.* 2006 Nov;5(11):937–48. [http://dx.doi.org/10.1016/S1474-4422\(06\)70597-X](http://dx.doi.org/10.1016/S1474-4422(06)70597-X)
23. Chung J-K, Kim YK, Kim S, Lee YJ, Paek S, Yeo JS, et al. Usefulness of 11C-methionine PET in the evaluation of brain lesions that are hypo- or isometabolic on 18F-FDG PET. *Eur J Nucl Med Mol Imaging.* 2002 Feb;29(2):176–82. <http://dx.doi.org/10.1007/s00259-001-0690-4>
24. Chen W, Silverman DHS, Delaloye S, Czernin J, Kamdar N, Pope W, et al. 18F-FDOPA PET imaging of brain tumors: Comparison study with 18F-FDG PET and evaluation of diagnostic accuracy. *J Nucl Med Off Publ Soc Nucl Med.* 2006 Jun;47(6):904–11.
25. Plotkin M, Blechschmidt C, Auf G, Nyuyki F, Geworski L, Denecke T, et al. Comparison of F-18 FET-PET with F-18 FDG-PET for biopsy planning of non-contrast-enhancing gliomas. *Eur Radiol.* 2010 Oct;20(10):2496–502. <http://dx.doi.org/10.1007/s00330-010-1819-2>
26. Grosu A-L, Astner ST, Riedel E, Nieder C, Wiedenmann N, Heinemann F, et al. An interindividual comparison of O-(2-[18F]fluoroethyl)-L-tyrosine (FET)- and L-[methyl-11C]methionine (MET)-PET

- in patients with brain gliomas and metastases. *Int J Radiat Oncol Biol Phys*. 2011 Nov;81(4):1049–58. <http://dx.doi.org/10.1016/j.ijrobp.2010.07.002>
27. Rapp M, Heinzl A, Galldiks N, Stoffels G, Felsberg J, Ewelt C, et al. Diagnostic performance of 18F-FET PET in newly diagnosed cerebral lesions suggestive of glioma. *J Nucl Med*. 2013 Feb;54(2):229–35
 28. Hutterer M, Nowosielski M, Putzer D, Jansen NL, Seiz M, Schocke M, et al. [18F]-fluoro-ethyl-L-tyrosine PET: A valuable diagnostic tool in neuro-oncology, but not all that glitters is glioma. *Neuro Oncol*. 2013 Mar;15(3):341–51 <http://dx.doi.org/10.1093/neuonc/nos300>
 29. Jansen NL, Suchorska B, Wenter V, Schmid-Tannwald C, Todica A, Eigenbrod S, et al. Prognostic significance of dynamic 18F-FET PET in newly diagnosed astrocytic high-grade glioma. *J Nucl Med Off Publ Soc Nucl Med*. 2015 Jan;56(1):9–15. <http://dx.doi.org/10.2967/jnumed.114.144675>
 30. Spaeth N, Wyss MT, Weber B, Scheidegger S, Lutz A, Verwey J, et al. Uptake of 18F-fluorocholine, 18F-fluoroethyl-L-tyrosine, and 18F-FDG in acute cerebral radiation injury in the rat: Implications for separation of radiation necrosis from tumor recurrence. *J Nucl Med Off Publ Soc Nucl Med*. 2004 Nov;45(11):1931–8.
 31. Floeth FW, Pauleit D, Sabel M, Reifenberger G, Stoffels G, Stummer W, et al. 18F-FET PET differentiation of ring-enhancing brain lesions. *J Nucl Med Off Publ Soc Nucl Med*. 2006 May;47(5):776–82.
 32. Sala Q, Metellus P, Taieb D, Kaphan E, Figarella-Branger D, Guedj E. 18F-DOPA, a clinically available PET tracer to study brain inflammation? *Clin Nucl Med*. 2014 Apr;39(4):e283–5. <http://dx.doi.org/10.1097/RLU.0000000000000383>
 33. Becherer A, Karanikas G, Szabó M, Zetting G, Asenbaum S, Marosi C, et al. Brain tumour imaging with PET: A comparison between [18F]fluorodopa and [11C]methionine. *Eur J Nucl Med Mol Imaging*. 2003 Nov;30(11):1561–7. <http://dx.doi.org/10.1007/s00259-003-1259-1>
 34. Dunet V, Pomoni A, Hottinger A, Nicod-Lalonde M, Prior JO. Performance of 18F-FET versus 18F-FDG-PET for the diagnosis and grading of brain tumors: Systematic review and meta-analysis. *Neuro-Oncology*. 2016 Mar;18(3):426–34. <http://dx.doi.org/10.1093/neuonc/nov148>
 35. Fueger BJ, Czernin J, Cloughesy T, Silverman DH, Geist CL, Walter MA, et al. Correlation of 6-18F-fluoro-L-dopa PET uptake with proliferation and tumor grade in newly diagnosed and recurrent gliomas. *J Nucl Med Off Publ Soc Nucl Med*. 2010 Oct;51(10):1532–8. <http://dx.doi.org/10.2967/jnumed.110.078592>
 36. Sato N, Suzuki M, Kuwata N, Kuroda K, Wada T, Beppu T, et al. Evaluation of the malignancy of glioma using 11C-methionine positron emission tomography and proliferating cell nuclear antigen staining. *Neurosurg Rev*. 1999 Dec;22(4):210–14. <http://dx.doi.org/10.1007/s101430050018>
 37. Sadeghi N, Salmon I, Decaestecker C, Levivier M, Metens T, Wikler D, et al. Stereotactic comparison among cerebral blood volume, methionine uptake, and histopathology in brain glioma. *AJNR Am J Neuroradiol*. 2007 Mar;28(3):455–61.
 38. Shinozaki N, Uchino Y, Yoshikawa K, Matsutani T, Hasegawa A, Saeki N, et al. Discrimination between low-grade oligodendrogliomas and diffuse astrocytoma with the aid of 11C-methionine positron emission tomography. *J Neurosurg*. 2011 Jun;114(6):1640–7. <http://dx.doi.org/10.3171/2010.11.JNS10553>
 39. Ceysens S, Van Laere K, de Groot T, Goffin J, Bormans G, Mortelmans L. [11C]methionine PET, histopathology, and survival in primary brain tumors and recurrence. *AJNR Am J Neuroradiol*. 2006 Aug;27(7):1432–7.
 40. Yamamoto A, Hosoya T, Takahashi N, Iwahara S, Munakata K. Quantification of left ventricular regional functions using ECG-gated myocardial perfusion SPECT—Validation of left ventricular systolic functions—. *Ann Nucl Med*. 2006 Aug;20(7):449–56. <http://dx.doi.org/10.1007/BF02987253>
 41. Pöppel G, Kreth FW, Mehrkens JH, Herms J, Seelos K, Koch W, et al. FET PET for the evaluation of untreated gliomas: Correlation of FET uptake and uptake kinetics with tumour grading. *Eur J Nucl Med Mol Imaging*. 2007 Dec;34(12):1933–42. <http://dx.doi.org/10.1007/s00259-007-0534-y>
 42. Lohmann P, Herzog H, Rota Kops E, Stoffels G, Judov N, Filss C, et al. Dual-time-point O-(2-[(18F]fluoroethyl)-L-tyrosine PET for grading of cerebral gliomas. *Eur Radiol*. 2015 Oct;25(10):3017–24. <http://dx.doi.org/10.1007/s00330-015-3691-6>

43. Dunet V, Maeder P, Nicod-Lalonde M, Lhermitte B, Pollo C, Bloch J, et al. Combination of MRI and dynamic FET PET for initial glioma grading. *Nucl Nucl Med.* 2014 Aug;53(4):155–61. <http://dx.doi.org/10.3413/Nukmed-0650-14-03>
44. Moulin-Romsée G, D'Hondt E, de Groot T, Goffin J, Sciort R, Mortelmans L, et al. Non-invasive grading of brain tumours using dynamic amino acid PET imaging: Does it work for 11C-methionine? *Eur J Nucl Med Mol Imaging.* 2007 Dec;34(12):2082–7. <http://dx.doi.org/10.1007/s00259-007-0557-4>
45. Kratochwil C, Combs SE, Leotta K, Afshar-Oromieh A, Rieken S, Debus J, et al. Intra-individual comparison of ¹⁸F-FET and ¹⁸F-DOPA in PET imaging of recurrent brain tumors. *Neuro-Oncology.* 2014 Mar;16(3):434–40. <http://dx.doi.org/10.1093/neuonc/not199>
46. Schiepers C, Chen W, Cloughesy T, Dahlbom M, Huang S-C. 18F-FDOPA kinetics in brain tumors. *J Nucl Med Off Publ Soc Nucl Med.* 2007 Oct;48(10):1651–61. <http://dx.doi.org/10.2967/jnumed.106.039321>
47. Wee CW, Sung W, Kang H-C, Cho KH, Han TJ, Jeong B-K, et al. Evaluation of variability in target volume delineation for newly diagnosed glioblastoma: A multi-institutional study from the Korean Radiation Oncology Group. *Radiat Oncol Lond Engl.* 2015 Jul;10:137. <http://dx.doi.org/10.1186/s13014-015-0439-z>
48. Johnson PC, Hunt SJ, Drayer BP. Human cerebral gliomas: Correlation of postmortem MR imaging and neuropathologic findings. *Radiology.* 1989 Jan;170(1 Pt 1):211–17. <http://dx.doi.org/10.1148/radiology.170.1.2535765>
49. Watanabe M, Tanaka R, Takeda N. Magnetic resonance imaging and histopathology of cerebral gliomas. *Neuroradiology.* 1992;34(6):463–9. <http://dx.doi.org/10.1007/BF00598951>
50. Galldiks N, Ullrich R, Schroeter M, Fink GR, Jacobs AH, Kracht LW. Volumetry of [(11)C]-methionine PET uptake and MRI contrast enhancement in patients with recurrent glioblastoma multiforme. *Eur J Nucl Med Mol Imaging.* 2010 Jan;37(1):84–92. <http://dx.doi.org/10.1007/s00259-009-1219-5>
51. Pauleit D, Floeth F, Hamacher K, Riemenschneider MJ, Reifenberger G, Müller H-W, et al. O-(2-[¹⁸F]fluoroethyl)-L-tyrosine PET combined with MRI improves the diagnostic assessment of cerebral gliomas. *Brain J Neurol.* 2005 Mar;128(Pt 3):678–87. <http://dx.doi.org/10.1093/brain/awh399>
52. Lopez WOC, Cordeiro JG, Albicker U, Doostkam S, Nikkha G, Kirch RD, et al. Correlation of (18) F-fluoroethyl tyrosine positron-emission tomography uptake values and histomorphological findings by stereotactic serial biopsy in newly diagnosed brain tumors using a refined software tool. *OncoTargets Ther.* 2015;8:3803–15. <http://dx.doi.org/10.2147/OTT.S87126>
53. Filss CP, Galldiks N, Stoffels G, Sabel M, Wittsack HJ, Turowski B, et al. Comparison of 18F-FET PET and perfusion-weighted MR imaging: A PET/MR imaging hybrid study in patients with brain tumors. *J Nucl Med Off Publ Soc Nucl Med.* 2014 Apr;55(4):540–5. <http://dx.doi.org/10.2967/jnumed.113.129007>
54. Buchmann N, Kläsner B, Gempt J, Bauer JS, Pyka T, Delbridge C, et al. (18)F-Fluoroethyl-L-tyrosine positron emission tomography to delineate tumor residuals after glioblastoma resection: A comparison with standard postoperative magnetic resonance imaging. *World Neurosurg.* 2016 May;89:420–6. <http://dx.doi.org/10.1016/j.wneu.2016.02.032>
55. Cicone F, Filss CP, Minniti G, Rossi-Espagnet C, Papa A, Scaringi C, et al. Volumetric assessment of recurrent or progressive gliomas: Comparison between F-DOPA PET and perfusion-weighted MRI. *Eur J Nucl Med Mol Imaging.* 2015 May;42(6):905–15. <http://dx.doi.org/10.1007/s00259-015-3018-5>
56. Pafundi DH, Laack NN, Youland RS, Parney IF, Lowe VJ, Giannini C, et al. Biopsy validation of 18F-DOPA PET and biodistribution in gliomas for neurosurgical planning and radiotherapy target delineation: Results of a prospective pilot study. *Neuro-Oncology.* 2013 Aug;15(8):1058–67. <http://dx.doi.org/10.1093/neuonc/not002>
57. Ledezma CJ, Chen W, Sai V, Freitas B, Cloughesy T, Czernin J, et al. 18F-FDOPA PET/MRI fusion in patients with primary/recurrent gliomas: Initial experience. *Eur J Radiol.* 2009 Aug;71(2):242–8. <http://dx.doi.org/10.1016/j.ejrad.2008.04.018>
58. Lindberg OR, McKinney A, Engler JR, Koshkakarayan G, Gong H, Robinson AE, et al. GBM heterogeneity as a function of variable epidermal growth factor receptor variant III activity. *Oncotarget.* 2016 Nov 29;7(48):79101–79116. <http://dx.doi.org/10.18632/oncotarget.12600>

59. Pirotte B, Goldman S, Brucher JM, Zomosa G, Baleriaux D, Brotchi J, et al. PET in stereotactic conditions increases the diagnostic yield of brain biopsy. *Stereotact Funct Neurosurg.* 1994;63(1-4):144-9.
60. Pirotte B, Goldman S, Massager N, David P, Wikler D, Vandesteene A, et al. Comparison of 18F-FDG and 11C-methionine for PET-guided stereotactic brain biopsy of gliomas. *J Nucl Med Off Publ Soc Nucl Med.* 2004 Aug;45(8):1293-8.
61. Pirotte BJM, Levivier M, Goldman S, Massager N, Wikler D, Dewitte O, et al. Positron emission tomography-guided volumetric resection of supratentorial high-grade gliomas: A survival analysis in 66 consecutive patients. *Neurosurgery.* 2009 Mar;64(3):471-481. <http://dx.doi.org/10.1227/01.NEU.0000338949.94496.85>
62. Suchorska B, Jansen NL, Linn J, Kretschmar H, Janssen H, Eigenbrod S, et al. Biological tumor volume in 18FET-PET before radiochemotherapy correlates with survival in GBM. *Neurology.* 2015 Feb;84(7):710-19. <http://dx.doi.org/10.1212/WNL.0000000000001262>
63. Tralins KS, Douglas JG, Stelzer KJ, Mankoff DA, Silbergeld DL, Rostomily RC, et al. Volumetric analysis of 18F-FDG PET in glioblastoma multiforme: Prognostic information and possible role in definition of target volumes in radiation dose escalation. *J Nucl Med Off Publ Soc Nucl Med.* 2002 Dec;43(12):1667-73.
64. Kosztyla R, Chan EK, Hsu F, Wilson D, Ma R, Cheung A, et al. High-grade glioma radiation therapy target volumes and patterns of failure obtained from magnetic resonance imaging and 18F-FDOPA positron emission tomography delineations from multiple observers. *Int J Radiat Oncol Biol Phys.* 2013 Dec;87(5):1100-6. <http://dx.doi.org/10.1016/j.ijrobp.2013.09.008>
65. Navarria P, Reggiori G, Pessina F, Ascolese AM, Tomatis S, Mancosu P, et al. Investigation on the role of integrated PET/MRI for target volume definition and radiotherapy planning in patients with high grade glioma. *Radiother Oncol J Eur Soc Ther Radiol Oncol.* 2014 Sep;112(3):425-9. <http://dx.doi.org/10.1016/j.radonc.2014.09.004>
66. Lee IH, Piert M, Gomez-Hassan D, Junck L, Rogers L, Hayman J, et al. Association of 11C-methionine PET uptake with site of failure after concurrent temozolomide and radiation for primary glioblastoma multiforme. *Int J Radiat Oncol Biol Phys.* 2009 Feb;73(2):479-85. <http://dx.doi.org/10.1016/j.ijrobp.2008.04.050>
67. Grosu AL, Weber WA, Franz M, Stärk S, Piert M, Thamm R, et al. Reirradiation of recurrent high-grade gliomas using amino acid PET (SPECT)/CT/MRI image fusion to determine gross tumor volume for stereotactic fractionated radiotherapy. *Int J Radiat Oncol Biol Phys.* 2005 Oct;63(2):511-19. <http://dx.doi.org/10.1016/j.ijrobp.2005.01.056>
68. Poulsen SH, Urup T, Grunnet K, Christensen IJ, Larsen VA, Jensen ML, et al. The prognostic value of FET PET at radiotherapy planning in newly diagnosed glioblastoma. *Eur J Nucl Med Mol Imaging.* 2017 Mar;44(3):373-381.
69. Lundemann M, Costa JC, Law I, Engelholm SA, Muhic A, Poulsen HS, et al. Patterns of failure for patients with glioblastoma following O-(2-[(18)F]fluoroethyl)-L-tyrosine PET- and MRI-guided radiotherapy. *Radiother Oncol.* 2017 Mar;122(3):380-386.
70. Rickhey M, Koelbl O, Eilles C, Bogner L. A biologically adapted dose-escalation approach, demonstrated for 18F-FET-PET in brain tumors. *Strahlenther Onkol Organ Dtsch Rontgengesellschaft Al.* 2008 Oct;184(10):536-42. <http://dx.doi.org/10.1007/s00066-008-1883-6>
71. Weber DC, Zilli T, Buchegger F, Casanova N, Haller G, Rouzaud M, et al. [(18)F]Fluoroethyltyrosine-positron emission tomography-guided radiotherapy for high-grade glioma. *Radiat Oncol Lond Engl.* 2008 Dec ;3:44. <http://dx.doi.org/10.1186/1748-717X-3-44>
72. Miwa K, Matsuo M, Ogawa S, Shinoda J, Yokoyama K, Yamada J, et al. Re-irradiation of recurrent glioblastoma multiforme using 11C-methionine PET/CT/MRI image fusion for hypofractionated stereotactic radiotherapy by intensity modulated radiation therapy. *Radiat Oncol Lond Engl.* 2014;9:181. <http://dx.doi.org/10.1186/1748-717X-9-181>
73. Macdonald DR, Cascino TL, Schold SC, Cairncross JG. Response criteria for phase II studies of supratentorial malignant glioma. *J Clin Oncol Off J Am Soc Clin Oncol.* 1990 Jul;8(7):1277-80. <http://dx.doi.org/10.1200/JCO.1990.8.7.1277>
74. Brandsma D, Stalpers L, Taal W, Sminia P, van den Bent MJ. Clinical features, mechanisms, and management of pseudoprogression in malignant gliomas. *Lancet Oncol.* 2008 May;9(5):453-61. [http://dx.doi.org/10.1016/S1470-2045\(08\)70125-6](http://dx.doi.org/10.1016/S1470-2045(08)70125-6)

75. Wen PY, Macdonald DR, Reardon DA, Cloughesy TF, Sorensen AG, Galanis E, et al. Updated response assessment criteria for high-grade gliomas: Response assessment in Neuro-Oncology Working Group. *J Clin Oncol*. 2010 Apr;28(11):1963–72. <http://dx.doi.org/10.1200/JCO.2009.26.3541>
76. Shah AH, Snelling B, Bregy A, Patel PR, Tememe D, Bhatia R, et al. Discriminating radiation necrosis from tumor progression in gliomas: A systematic review what is the best imaging modality? *J Neurooncol*. 2013 Apr;112(2):141–52. <http://dx.doi.org/10.1007/s11060-013-1059-9>
77. Brandsma D, van den Bent MJ. Pseudoprogression and pseudoresponse in the treatment of gliomas. *Curr Opin Neurol*. 2009 Dec;22(6):633–8. <http://dx.doi.org/10.1097/WCO.0b013e328332363e>
78. Rozental JM, Levine RL, Mehta MP, Kinsella TJ, Levin AB, Algan O, et al. Early changes in tumor metabolism after treatment: The effects of stereotactic radiotherapy. *Int J Radiat Oncol Biol Phys*. 1991 May;20(5):1053–60. [http://dx.doi.org/10.1016/0360-3016\(91\)90204-H](http://dx.doi.org/10.1016/0360-3016(91)90204-H)
79. Charnley N, West CM, Barnett CM, Brock C, Bydder GM, Glaser M, et al. Early change in glucose metabolic rate measured using FDG-PET in patients with high-grade glioma predicts response to temozolomide but not temozolomide plus radiotherapy. *Int J Radiat Oncol Biol Phys*. 2006 Oct;66(2):331–8. <http://dx.doi.org/10.1016/j.ijrobp.2006.04.043>
80. Nihashi T, Dahabreh IJ, Terasawa T. Diagnostic accuracy of PET for recurrent glioma diagnosis: A meta-analysis. *AJNR Am J Neuroradiol*. 2013 May;34(5):944–50, S1–11.
81. Chao ST, Suh JH, Raja S, Lee SY, Barnett G. The sensitivity and specificity of FDG PET in distinguishing recurrent brain tumor from radionecrosis in patients treated with stereotactic radiosurgery. *Int J Cancer*. 2001 Jun 20;96(3):191–7. <http://dx.doi.org/10.1002/ijc.1016>
82. Galldiks N, Langen K-J. Amino acid PET—An imaging option to identify treatment response, post-therapeutic effects, and tumor recurrence? *Front Neurol*. 2016;7:120. <http://dx.doi.org/10.3389/fneur.2016.00120>
83. Van Laere K, Ceyssens S, Van Calenbergh F, de Groot T, Menten J, Flamen P, et al. Direct comparison of 18F-FDG and 11C-methionine PET in suspected recurrence of glioma: Sensitivity, inter-observer variability and prognostic value. *Eur J Nucl Med Mol Imaging*. 2005 Jan;32(1):39–51. <http://dx.doi.org/10.1007/s00259-004-1564-3>
84. Galldiks N, Kracht LW, Burghaus L, Thomas A, Jacobs AH, Heiss W-D, et al. Use of 11C-methionine PET to monitor the effects of temozolomide chemotherapy in malignant gliomas. *Eur J Nucl Med Mol Imaging*. 2006 May;33(5):516–24. <http://dx.doi.org/10.1007/s00259-005-0002-5>
85. Beppu T, Terasaki K, Sasaki T, Sato Y, Tomabechi M, Kato K, et al. MRI and 11C-methyl-L-methionine PET Differentiate Bevacizumab True Responders After Initiating Therapy for Recurrent Glioblastoma. *Clin Nucl Med*. 2016 Nov;41(11):852–7. <http://dx.doi.org/10.1097/RLU.0000000000001377>
86. Galldiks N, Langen K-J, Holy R, Pinkawa M, Stoffels G, Nolte KW, et al. Assessment of treatment response in patients with glioblastoma using O-(2-18F-fluoroethyl)-L-tyrosine PET in comparison to MRI. *J Nucl Med*. 2012 Jul;53(7):1048–57. <http://dx.doi.org/10.2967/jnumed.111.098590>
87. Galldiks N, Dunkl V, Stoffels G, Hutterer M, Rapp M, Sabel M, et al. Diagnosis of pseudoprogression in patients with glioblastoma using O-(2-[18F]fluoroethyl)-L-tyrosine PET. *Eur J Nucl Med Mol Imaging*. 2015 Apr;42(5):685–95. <http://dx.doi.org/10.1007/s00259-014-2959-4>
88. Kebir S, Khurshid Z, Gaertner FC, Essler M, Hattingen E, Fimmers R, et al. Unsupervised consensus cluster analysis of [18F]-fluoroethyl-L-tyrosine positron emission tomography identified textural features for the diagnosis of pseudoprogression in high-grade glioma. *Oncotarget*. 2017 Jan 31;8(5):8294–8304.
89. Kebir S, Fimmers R, Galldiks N, Schäfer N, Mack F, Schaub C, et al. Late pseudoprogression in glioblastoma: Diagnostic value of dynamic O-(2-[18F]fluoroethyl)-L-tyrosine PET. *Clin Cancer Res Off J Am Assoc Cancer Res*. 2016 May;22(9):2190–6. <http://dx.doi.org/10.1158/1078-0432.CCR-15-1334>
90. Schwarzenberg J, Czernin J, Cloughesy TF, Ellingson BM, Pope WB, Grogan T, et al. Treatment response evaluation using 18F-FDOPA PET in patients with recurrent malignant glioma on bevacizumab therapy. *Clin Cancer Res Off J Am Assoc Cancer Res*. 2014 Jul;20(13):3550–9. <http://dx.doi.org/10.1158/1078-0432.CCR-13-1440>
91. Harris RJ, Cloughesy TF, Pope WB, Nghiemphu PL, Lai A, Zaw T, et al. 18F-FDOPA and 18F-FLT positron emission tomography parametric response maps predict response in recurrent malignant

- gliomas treated with bevacizumab. *Neuro-Oncology*. 2012 Aug;14(8):1079–89. <http://dx.doi.org/10.1093/neuonc/nos141>
92. Hutterer M, Nowosielski M, Putzer D, Waitz D, Tinkhauser G, Kostron H, et al. O-(2-18F-fluoroethyl)-L-tyrosine PET predicts failure of antiangiogenic treatment in patients with recurrent high-grade glioma. *J Nucl Med Off Publ Soc Nucl Med*. 2011 Jun;52(6):856–64. <http://dx.doi.org/10.2967/jnumed.110.086645>
 93. Galldiks N, Rapp M, Stoffels G, Dunkl V, Sabel M, Langen K-J. Earlier diagnosis of progressive disease during bevacizumab treatment using O-(2-18F-fluoroethyl)-L-tyrosine positron emission tomography in comparison with magnetic resonance imaging. *Mol Imaging*. 2013 Aug;12(5):273–6.
 94. Galldiks N, Rapp M, Stoffels G, Fink GR, Shah NJ, Coenen HH, et al. Response assessment of bevacizumab in patients with recurrent malignant glioma using [18F]Fluoroethyl-L-tyrosine PET in comparison to MRI. *Eur J Nucl Med Mol Imaging*. 2013 Jan;40(1):22–33. <http://dx.doi.org/10.1007/s00259-012-2251-4>
 95. Takenaka S, Asano Y, Shinoda J, Nomura Y, Yonezawa S, Miwa K, et al. Comparison of (11)C-methionine, (11)C-choline, and (18)F-fluorodeoxyglucose-PET for distinguishing glioma recurrence from radiation necrosis. *Neurol Med Chir (Tokyo)*. 2014;54(4):280–9. <http://dx.doi.org/10.2176/nmc.0a2013-0117>
 96. Karunanithi S, Sharma P, Kumar A, Khangembam BC, Bandopadhyaya GP, Kumar R, et al. 18F-FDOPA PET/CT for detection of recurrence in patients with glioma: Prospective comparison with 18F-FDG PET/CT. *Eur J Nucl Med Mol Imaging*. 2013 Jul;40(7):1025–35. <http://dx.doi.org/10.1007/s00259-013-2384-0>
 97. Herrmann K, Czernin J, Cloughesy T, Lai A, Pomykala KL, Benz MR, et al. Comparison of visual and semiquantitative analysis of 18F-FDOPA-PET/CT for recurrence detection in glioblastoma patients. *Neuro-Oncology*. 2014 Apr;16(4):603–9. <http://dx.doi.org/10.1093/neuonc/not166>
 98. Galldiks N, Stoffels G, Filss C, Rapp M, Blau T, Tscherpel C, et al. The use of dynamic O-(2-18F-fluoroethyl)-L-tyrosine PET in the diagnosis of patients with progressive and recurrent glioma. *Neuro-Oncology*. 2015 Sep;17(9):1293–300. <http://dx.doi.org/10.1093/neuonc/nov088>
 99. Pöppel G, Götz C, Rächinger W, Gildehaus F-J, Tonn J-C, Tatsch K. Value of O-(2-[18F]fluoroethyl)-L-tyrosine PET for the diagnosis of recurrent glioma. *Eur J Nucl Med Mol Imaging*. 2004 Nov;31(11):1464–70. <http://dx.doi.org/10.1007/s00259-004-1590-1>
 100. Chiang GC, Galla N, Ferraro R, Kovanlikaya I. The added prognostic value of metabolic tumor size on FDG-PET at first suspected recurrence of glioblastoma multiforme: FDG-PET for prognosis of recurrent glioblastoma. *J Neuroimaging*. 2017 Mar;27(2):243–247. <http://dx.doi.org/10.1111/jon.12386>
 101. Colavolpe C, Chinot O, Metellus P, Mancini J, Barrie M, Bequet-Boucard C, et al. FDG-PET predicts survival in recurrent high-grade gliomas treated with bevacizumab and irinotecan. *Neuro-Oncology*. 2012 May;14(5):649–57. <http://dx.doi.org/10.1093/neuonc/nos012>
 102. Lopci E, Riva M, Olivari L, Raneri F, Soffietti R, Piccardo A, et al. Prognostic value of molecular and imaging biomarkers in patients with supratentorial glioma. *Eur J Nucl Med Mol Imaging*. 2017 Jul;44(7):1155–1164. <http://dx.doi.org/10.1007/s00259-017-3618-3>
 103. Galldiks N, Dunkl V, Kracht LW, Vollmar S, Jacobs AH, Fink GR, et al. Volumetry of [11C]-methionine positron emission tomographic uptake as a prognostic marker before treatment of patients with malignant glioma. *Mol Imaging*. 2012 Dec;11(6):516–27.
 104. Karunanithi S, Sharma P, Kumar A, Gupta DK, Khangembam BC, Ballal S, et al. Can (18)F-FDOPA PET/CT predict survival in patients with suspected recurrent glioma? A prospective study. *Eur J Radiol*. 2014 Jan;83(1):219–25. <http://dx.doi.org/10.1016/j.ejrad.2013.09.004>
 105. Toyonaga T, Yamaguchi S, Hirata K, Kobayashi K, Manabe O, Watanabe S, et al. Hypoxic glucose metabolism in glioblastoma as a potential prognostic factor. *Eur J Nucl Med Mol Imaging*. 2016 Oct 18; <http://dx.doi.org/10.1007/s11060-016-2077-1>
 106. Frosina G. Positron emission tomography of high-grade gliomas. *J Neurooncol*. 2016 May;127(3):415–25.
 107. Rasey JS, Koh W, Evans ML, Peterson LM, Lewellen TK, Graham MM, et al. Quantifying regional hypoxia in human tumors with positron emission tomography of [18F]fluoromisonidazole: A pretherapy study of 37 patients. *Int J Radiat Oncol*. 1996 Sep;36(2):417–28. [http://dx.doi.org/10.1016/S0360-3016\(96\)00325-2](http://dx.doi.org/10.1016/S0360-3016(96)00325-2)

108. Whitmore GF, Varghese AJ. The biological properties of reduced nitroheterocyclics and possible underlying biochemical mechanisms. *Biochem Pharmacol.* 1986 Jan;35(1):97–103. [http://dx.doi.org/10.1016/0006-2952\(86\)90565-4](http://dx.doi.org/10.1016/0006-2952(86)90565-4)
109. Brown JM. Therapeutic targets in radiotherapy. *Int J Radiat Oncol.* 2001 Feb;49(2):319–26. [http://dx.doi.org/10.1016/S0360-3016\(00\)01482-6](http://dx.doi.org/10.1016/S0360-3016(00)01482-6)
110. Cher LM, Murone C, Lawrentschuk N, Ramdave S, Papenfuss A, Hannah A, et al. Correlation of hypoxic cell fraction and angiogenesis with glucose metabolic rate in gliomas using 18F-fluoromisonidazole, 18F-FDG PET, and immunohistochemical studies. *J Nucl Med Off Publ Soc Nucl Med.* 2006 Mar;47(3):410–18.
111. Shields AF, Grierson JR, Dohmen BM, Machulla H-J, Stayanoff JC, Lawhorn-Crews JM, et al. Imaging proliferation in vivo with [F-18]FLT and positron emission tomography. *Nat Med.* 1998 Nov;4(11):1334–6. <http://dx.doi.org/10.1038/3337>
112. Zhao F, Cui Y, Li M, Fu Z, Chen Z, Kong L, et al. Prognostic value of 3'-deoxy-3'-18F-fluorothymidine ([18F] FLT PET) in patients with recurrent malignant gliomas. *Nucl Med Biol.* 2014 Sep;41(8):710–15. <http://dx.doi.org/10.1016/j.nucmedbio.2014.04.134>
113. Hart MG, Ypma RJF, Romero-Garcia R, Price SJ, Suckling J. Graph theory analysis of complex brain networks: New concepts in brain mapping applied to neurosurgery. *J Neurosurg.* 2016 Jun;124(6):1665–78. <http://dx.doi.org/10.3171/2015.4.JNS142683>
114. Chen W, Cloughesy T, Kamdar N, Satyamurthy N, Bergsneider M, Liao L, et al. Imaging proliferation in brain tumors with 18F-FLT PET: Comparison with 18F-FDG. *J Nucl Med Off Publ Soc Nucl Med.* 2005 Jun;46(6):945–52.
115. Jacobs AH, Thomas A, Kracht LW, Li H, Dittmar C, Garlip G, et al. 18F-fluoro-L-thymidine and 11C-methylmethionine as markers of increased transport and proliferation in brain tumors. *J Nucl Med Off Publ Soc Nucl Med.* 2005 Dec;46(12):1948–58.
116. Ohtani T, Kurihara H, Ishiuchi S, Saito N, Oriuchi N, Inoue T, et al. Brain tumour imaging with carbon-11 choline: Comparison with FDG PET and gadolinium-enhanced MR imaging. *Eur J Nucl Med.* 2001 Nov;28(11):1664–70. <http://dx.doi.org/10.1007/s002590100620>
117. Shah NJ, Oros-Peusquens A-M, Arrubla J, Zhang K, Warbrick T, Mauler J, et al. Advances in multimodal neuroimaging: Hybrid MR-PET and MR-PET-EEG at 3 T and 9.4 T. *J Magn Reson San Diego Calif.* 1997. 2013 Apr;229:101–15.
118. Neuner I, Kaffanke JB, Langen K-J, Kops ER, Tellmann L, Stoffels G, et al. Multimodal imaging utilising integrated MR-PET for human brain tumour assessment. *Eur Radiol.* 2012 Dec;22(12):2568–80. <http://dx.doi.org/10.1007/s00330-012-2543-x>
119. Deuschl C, Moenninghoff C, Goericke S, Kirchner J, Köppen S, Binse I, et al. Response assessment of bevacizumab therapy in GBM with integrated 11C-MET-PET/MRI: A feasibility study. *Eur J Nucl Med Mol Imaging.* 2017 Mar 3; <http://dx.doi.org/10.1007/s00259-017-3661-0>
120. Guedj E, Cammilleri S, Verger A. Predictive medicine: towards a multi-parametric imaging for a personal risk stratification. *Eur J Nucl Med Mol Imaging.* 2016 Sep 27;44(2):196–198.
121. Visvikis D, Hatt M, Tixier F, Cheze Le Rest C. The age of reason for FDG PET image-derived indices. *Eur J Nucl Med Mol Imaging.* 2012 Nov;39(11):1670–2. <http://dx.doi.org/10.1007/s00259-012-2239-0>

10

PET for Therapy Response Assessment in Glioblastoma

JULIE BOLCAEN¹ • MARJAN ACOU² • BENEDICTE DESCAMPS³ •
KEN KERSEMANS¹ • KAREL DEBLAERE² • CHRISTIAN VANHOVE³ •
INGEBORG GOETHALS¹

¹Department of Nuclear Medicine, Ghent University Hospital, Ghent, Belgium; ²Department of Radiology and Medical Imaging, Ghent University Hospital, Ghent, Belgium; ³IBiTech-MEDISIP, Department of Electronics and Information Systems, Ghent University, Ghent, Belgium

Author of correspondence: Julie Bolcaen, Department of Nuclear Medicine, Ghent University Hospital, Ghent, Belgium. E-mail: Julie.Bolcaen@ugent.be

Doi: <http://dx.doi.org/10.15586/codon.glioblastoma.2017.ch10>

Abstract: Glioblastoma (GB) is the most malignant and the most common type of glioma in adults, accounting for 60–70% of all malignant gliomas. Despite the current therapy, the clinical course of GB is usually rapid, with a mean survival time of approximately 1 year. For therapy response assessment in GB, magnetic resonance imaging (MRI) is the method of choice. In 2010, the Response Assessment in Neuro-Oncology (RANO) was introduced, including the tumor size (in 2D) as measured on T2-weighted and Fluid Attenuated Inversion Recovery (FLAIR)-weighted images, in addition to the contrast-enhancing tumor part. Although the RANO criteria addressed some of the limitations of the previous MacDonald criteria for therapy evaluation in high-grade glioma, treatment-related side effects hamper correct response assessment. To address the above-mentioned drawbacks in the follow-up of GB, incorporating changes in tumor biology measured by advanced MRI and positron emission tomography (PET) imaging, which may precede anatomical changes of the tumor volume, is promising. Imaging biomarkers capable of predicting response at an early time point after treatment initiation are the premise of personalized treatment enabling change or

In: *Glioblastoma*. Steven De Vleeschouwer (Editor), Codon Publications, Brisbane, Australia
ISBN: 978-0-9944381-2-6; Doi: <http://dx.doi.org/10.15586/codon.glioblastoma.2017>

Copyright: The Authors.

Licence: This open access article is licenced under Creative Commons Attribution 4.0 International (CC BY 4.0). <https://creativecommons.org/licenses/by-nc/4.0/>

discontinuation of therapy to prevent ineffective treatment or adverse events of treatment. In this chapter, an overview of applicable PET tracers for the therapy response assessment in GB and the determination of tumor recurrence versus treatment-related effects is given.

Key words: Glioblastoma; MRI; PET; Radiation necrosis; Therapy response

Introduction

Gliomas are the most common primary brain tumors with a peak incidence in the fifth and sixth decade of life (1, 2). The highest grade of gliomas (WHO grade IV) are called glioblastoma (GB). GBs account for more than half of all glial tumors, are a highly invasive solid tumor type, and are most often found in cerebral hemispheres, particularly in frontal, parietal, and temporal lobes, although they can be situated in any lobe. They can arise *de novo* (primary GB) or after progression of a low-grade glioma (secondary GB) (2–4). Usually, GBs are poorly delineated, heterogeneous tumors with necrosis, hemorrhage, and increased vascularity. Central necrosis is the hallmark of GBs and may occupy as much as 80% of total tumor mass (2). GB cell infiltration into the surrounding brain parenchyma renders a complete surgical resection mostly impossible without producing significant neurological injury. Residual glioma cells at the tumor margins frequently lead to tumor recurrence (3). In patients with suspected brain tumor, after medical history taking and clinical examination, the most important diagnostic procedure is magnetic resonance imaging (MRI) of the brain with a contrast-enhancing agent. However, the diagnosis should be confirmed via a stereotactic biopsy or, when appropriate, via resection. Functional and molecular imaging has gained a lot of attention in the last decade. Before confirmation of the diagnosis via tissue analysis, MR spectroscopy (MRS), perfusion weighted MRI (PWI), and positron emission tomography (PET) imaging can be helpful. After the diagnosis has been confirmed pathologically, these imaging modalities can be even more valuable. In particular, they may be useful for planning of radiation therapy (RT) and even more established in clinical practice for the monitoring during therapy, post-treatment surveillance, and prognostication (5, 6).

Treatment of Glioblastoma

Surgical resection remains one of the most effective treatments for cerebral gliomas (7, 8). It has been shown that patients who had a gross total resection also have a better response to subsequent adjuvant treatments than those who had only a partial resection or biopsy (7). However, in about half of the patients, (total) resection is not possible (9). The current standard of care for patients with GB has slowly evolved over the course of several decades. In the early 1960s, systemic corticosteroids were shown to have a beneficial impact on patients' quality of life by reducing peritumoral edema. Shortly thereafter, whole brain radiation therapy (WBRT) became recognized as an effective adjuvant therapy.

However, the dose was limited by potential toxicity to the surrounding normal brain (3). New developments in RT enabled to shape the radiation dose conform to the tumor target, limiting the dose to normal tissues, resulting in so-called conformal RT. Intensity-modulated radiation therapy (IMRT) allows even greater control over the shape of the dose distribution using variable intensities of the radiation beam (10, 11). In an effort to complement the beneficial effects of corticosteroids and RT, systemic chemotherapeutic agents were also studied (3). In 2005, Stupp et al. established the superiority of surgery and combined chemoradiation therapy with temozolomide (TMZ) over surgery and RT alone. As a result, for newly diagnosed GB patients with a good performance status, the standard of care now includes maximal surgical resection followed by combined external beam RT (60 Gy in 30 fractions) and TMZ, followed by maintenance TMZ (12–14). TMZ is an oral deoxyribonucleic acid (DNA) alkylating agent with good blood brain barrier (BBB) penetration. It is usually well tolerated with thrombocytopenia as its main and dose-limiting toxicity. In contrast to TMZ, nitrosoureas such as lomustine (CCNU), carmustine (BCNU), nimustine (ACNU), or fotemustine can induce prolonged leukopenia and thrombocytopenia, requiring dose reductions for the subsequent cycles, or a change of regimen. Nitrosoureas are now second-choice agents relative to TMZ for glioma treatment. In high-risk, low-grade gliomas, RT followed by procarbazine, CCNU, and vincristine (PCV) constitutes a new standard of care due to prolonged survival reported in the RTOG 9802 trial (15). The most recent development with respect to novel therapies for GB involves the use of angiogenesis inhibitors, such as bevacizumab, which improve the quality of life of patients due to their capacity to reduce vessel leakiness, resulting in diminished intracranial edema (16). Despite the current therapy for GB, the clinical course of GB tumors is usually rapid, with a mean survival time between 6 and 12 months (2).

THErapy RESPONSE ASSESSMENT OF GLIOBLASTOMA

Several prognostic factors have been identified in patients with GB, such as age, Karnofsky performance status, neurological status, WHO tumor grade, tumor location, extent of surgery, genetic and molecular biomarker status, and concomitant TMZ (17, 18). For therapy response assessment in GB, MRI is the method of choice. Until 2010, mainly MacDonald criteria were used for assessing response to therapy in high-grade glioma (HGG). Although the MacDonald criteria were developed primarily for computed tomography (CT) scans, they have been extrapolated to MRI. The criteria are based on two-dimensional (2D) tumor measurements on CT or MRI, in addition to a clinical assessment and corticosteroid use and dose (19). In the MacDonald criteria, a significant increase ($\geq 25\%$) in the contrast-enhancing lesion is used as a reliable marker for tumor progression. However, contrast enhancement after the administration of gadolinium is nonspecific and primarily reflects the passage of contrast material across a disrupted BBB. Furthermore, in 20–30% of patients, pathological contrast enhancement on MRI subsiding without any change in therapy is shown on the first post-irradiation MRI. This phenomenon, known as *pseudoprogression*, likely results from a combination of transiently increased permeability of the tumor vasculature from irradiation, treatment-induced necrosis, and post-operative infarcts, and should always

be considered in the first 3 months after concurrent chemoradiation for gliomas (19–21). In addition, it is worth mentioning that pseudoprogression may be reinforced by chemotherapy with TMZ (9, 19, 22). This treatment-related effect complicates the determination of tumor progression immediately after the completion of RT and may result in premature discontinuation of effective adjuvant therapy (19, 22). Furthermore, since the introduction of antiangiogenic agents, another phenomenon known as “*pseudoresponse*” occurred. These agents can produce a marked decrease in contrast enhancement as early as 1–2 days after initiation of therapy, which may be partly a result of normalization of abnormally permeable tumor vessels and not a true anti-glioma effect as a nonenhancing tumor may continue to grow (19, 20). This normalization of BBB disruption is often combined with a regression of perifocal edema followed by an improvement of neurological symptoms and consequently a reduction of corticosteroid use (22). In an attempt to more accurately assess treatment response, new criteria for Response Assessment in Neuro-Oncology (RANO) were introduced in 2010, including the tumor size (in 2D) as measured on T2-weighted and Fluid Attenuated Inversion Recovery (FLAIR)-weighted images, in addition to the contrast-enhancing tumor part. Although the RANO criteria addressed some of the limitations of the MacDonald criteria for evaluation of therapy in HGG, the abovementioned treatment-related side effects hamper correct response assessment. The proposed new response criteria suggest that within the first 3 months after completion of RT, progression can only be determined if the majority of the new enhancement is outside of the radiation field or if there is pathologic confirmation of progressive disease. This means that response assessment shortly after the end of RT is not accepted (22). Furthermore, increased enhancement and FLAIR/T2 hyperintense signal abnormalities can also occur due to treatment-related inflammation, post-surgical changes, subacute irradiation effects, and radiation necrosis (RN) (19). As such, tumor recurrence cannot be accurately distinguished from treatment effects on CT or conventional MRI (9).

DIFFERENTIATION BETWEEN TREATMENT-RELATED EFFECTS AND GLIOBLASTOMA RECURRENCE

Early and late therapy-related effects on brain tissues are an unwanted but unavoidable consequences of RT (7). The incidence is increasing with more frequent use of stereotactic radiosurgery and combined modality therapy for brain tumors. These therapy-related effects on the brain, such as radiation injury, also add to the complexity of imaging response and recurrence patterns, which is particularly important in patients with HGG in whom recurrence is commonly seen (20, 21). Radiation injury is known to potentially target glial cells and vascular endothelial cells and has been divided into acute, early-delayed, and late-delayed reactions (20, 23). Acute RN (during RT to 3 months after completion of RT) is a consequence of injury to the vasculature, more specifically radiation-induced endothelial cell apoptosis, leading to capillary leakiness and edema. Up to 12 weeks following RT, early-delayed injury can occur due to a delay in myelin synthesis (injury to oligodendrocytes). However, pseudoprogression must be considered. Late vascular changes include vessel wall thickening, with resulting occlusive vasculopathy, perivascular parenchymal coagulative necrosis,

and inflammation. Late delayed reactions are reported to occur in 3–24% of patients from 3 months to 13 years after the completion of RT (23–26). The risk increases with increasing radiation dose, fraction size, irradiated volume, and the (concomitant) administration of chemotherapy (24). The pattern of radiation injury may vary from diffuse periventricular white matter lesions to focal or multifocal lesions and may occur even distant from the original site of treatment (27). Differentiation between RN and recurrent brain tumor presents a diagnostic dilemma as both entities frequently develop at the resection site and often have a similar appearance on conventional MRI (20, 21). Both types of lesions can have similar clinical presentations, such as seizures, focal neurologic deficits, and increased intracranial pressure (25). Obviously, a correct diagnosis is important for further patient management. RN may require the administration of steroids, whereas tumor recurrence necessitates second-line treatment (20, 28). A definite diagnosis requires a biopsy. Unfortunately, a biopsy is subject to sampling error, is invasive, and can lead to potential complications such as brain hemorrhage (21).

To address the abovementioned drawbacks in the follow-up of GB, incorporating changes in tumor biology measured by advanced MRI and PET imaging, which may precede anatomical changes of the tumor volume, is promising (9, 29, 30). Imaging biomarkers able to predict response at an early time point after treatment initiation are the premise of personalized treatment enabling change or discontinuation of therapy to prevent ineffective treatment or adverse events of treatment. Moreover, identification of treatment failure may help reduce costs. This is highly relevant because the expense of newer systemic treatment options (e.g., bevacizumab) is considerably higher than conventional alkylating chemotherapy (e.g., lomustine) (31). Currently, MRI techniques that interrogate the vascular density and permeability of tumor vasculature, such as dynamic contrast-enhanced MRI (DCE-MRI), diffusion-weighted MRI (DWI), perfusion-weighted MRI (PWI), and metabolite concentrations using MRS, are being evaluated as imaging biomarkers of tumor response in treatment trials (9). Using DWI, higher apparent diffusion coefficients (ADCs) were found in RN compared to tumor recurrence due to an increase in water in the interstitial spaces resulting from cell necrosis (32). Choline/creatine and choline/*N*-acetylaspartate ratios as measured by MRS may also add valuable information in differentiating recurrent tumor from RN, and even a higher diagnostic accuracy was achieved when combining DWI with MRS (32, 33). PWI, such as dynamic susceptibility contrast-enhanced MRI (DSC-MRI), was found to distinguish tumor recurrence from RN by using cerebral blood volume (CBV) maps (9, 34–36). Furthermore, the use of the amide proton transfer MRI signal of endogenous cellular proteins and peptides as an imaging biomarker has been shown to be able to differentiate viable glioma from RN in rats (37). Although advanced MRI techniques may yield promising results, a major disadvantage is the current lack of standardization and validation, which hampers the translation into the clinic. In the remainder of this chapter, the focus is on the use of PET for therapy response assessment in GB. In the future, incorporation of these advanced imaging techniques into the RANO criteria is necessary, but it needs standardization and requires rigorous clinical validation before they can be recommended and incorporated into response criteria (19). Currently, the decision tree given in Figure 1 can be proposed for the follow-up of HGG (38).

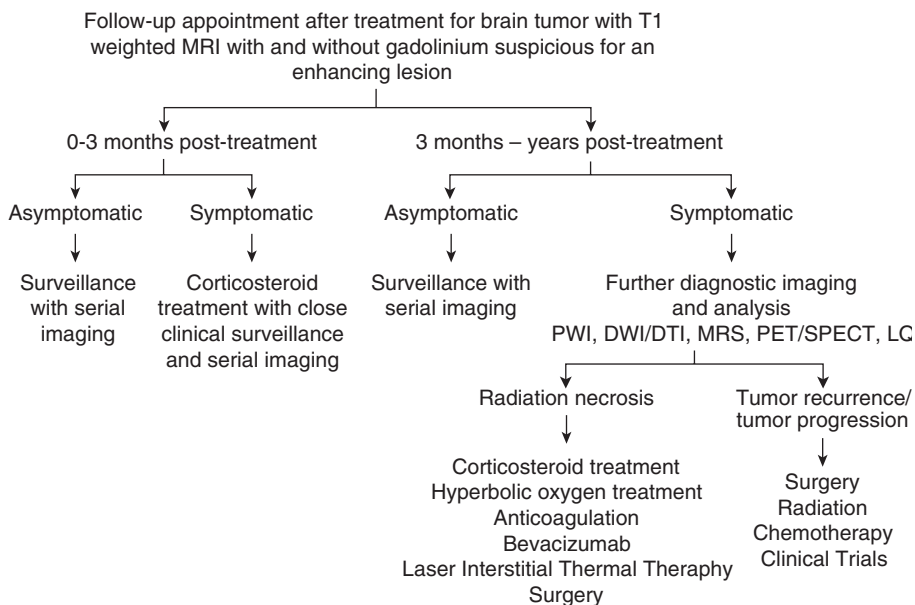


Figure 1 Decision tree for post-treatment follow-up in high-grade gliomas. (Adapted from Ref. (38).)

PET for Therapy Response Assessment in GB

In the past decades, a variety of molecular targets have been addressed by specific PET tracers in neuro-oncology and could be used for therapy response evaluation in HGG, see Figure 2 (39–44).

^{18}F -FLUORODEOXYGLUCOSE (^{18}F -FDG) PET

^{18}F -Fluorodeoxyglucose (^{18}F -FDG) is the most common clinically utilized PET tracer due to its high potential to detect tumors in the body based on increased energy demand of malignant tumors. ^{18}F -FDG PET measures cellular glucose metabolism as a function of the enzyme hexokinase (40, 41, 45). ^{18}F -FDG-6- PO_4 accumulates in cells over time, leading to signal amplification and making this imaging agent a suitable indicator of hexokinase-II activity as well as a cell's need for glucose (45). In the brain, ^{18}F -FDG exhibits high uptake in normal gray matter, reflecting the metabolic demands of neurons and glia. This high uptake in normal brain parenchyma often makes the localization and the delineation of brain tumors difficult and only co-registration of ^{18}F -FDG PET with MRI allows the rating of glucose metabolism in specific areas of a tumor, see Figure 2A (40, 41). Several studies investigating the potential of ^{18}F -FDG in discriminating tumor recurrence and RN have been performed. However, equivocal results with sensitivities and specificities ranging from 40 to 100% were published (21, 28, 34, 46–48). Besides the high and variable uptake by the normal cortex, radiation

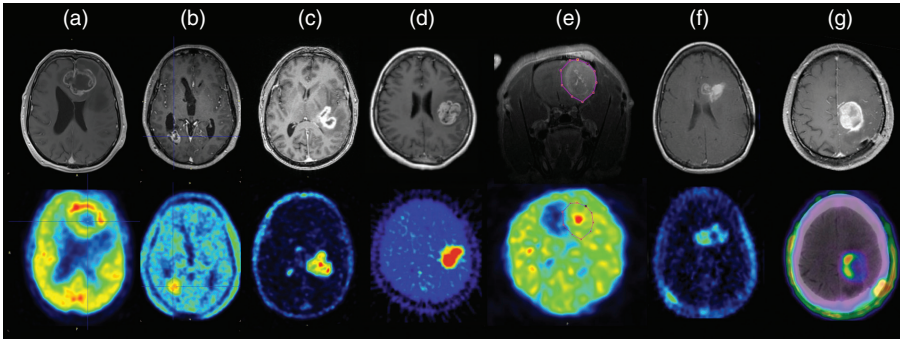


Figure 2 Contrast-enhanced MRI (top row) and multiple PET tracers (bottom row) in glioblastoma. (a) ^{18}F -Fluorodeoxyglucose (^{18}F -FDG), (b) ^{18}F -fluoroethyltyrosine (^{18}F -FET), (c) ^{18}F -Fluoromethylcholine (^{18}F -FCho), (d) ^{18}F -fluoromisonidazole (^{18}F -FMISO) (43) PET in human GB, (e) ^{18}F -fluoroazomycin arabinoside (^{18}F -FAZA) PET of the rat F98 model, (f) ^{18}F -fluorothymidine (^{18}F -FLT) (9) PET, and (g) ^{18}F -AIF-NOTA-PRGD2 (^{18}F -RGD) PET/CT in human GB. (Adapted from Ref. (44).)

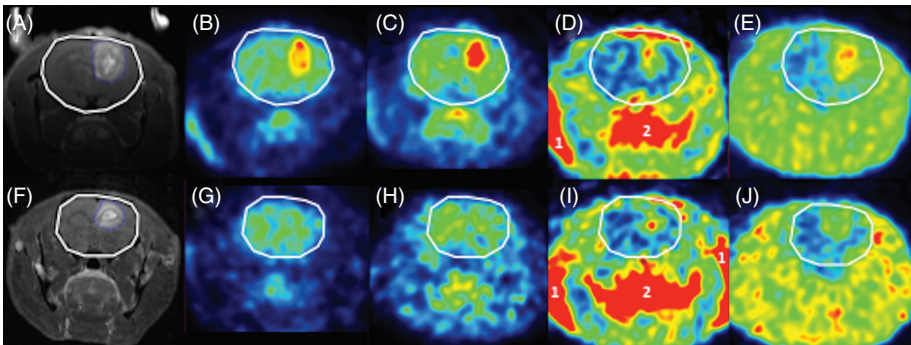


Figure 3 Contrast-enhanced MRI (A and F) and PET of glioblastoma (top row) and radiation necrosis (bottom row). For clarity, the rat brain is contoured in white. ^{18}F -FDG PET 40-60 min post-injection (B,G) and 240 min post-injection (C,H), ^{18}F -FCho PET 10-20 min post-injection (D,I), ^{18}F -FET PET 35-55 min post-injection (E,J) (49).

injury can activate repair mechanisms or lead to inflammation, which can lead to false-positive results (20).

Our research group compared the uptake of ^{18}F -FDG, ^{18}F -fluoromethylcholine (^{18}F -FCho), and ^{18}F -fluoroethyltyrosine (^{18}F -FET) in GB and RN in rats, see Figure 3 (49, 50). We found significantly higher values for the maximum and mean standard uptake value (SUV_{max} and SUV_{mean}) and the maximum and mean lesion to normal tissue ratio (LNR_{max} and LNR_{mean}) on ^{18}F -FDG PET in GB compared to RN. Uptake of ^{18}F -FDG in GB was high, which means that the uptake was higher than that in the cortex. The latter was not shown in RN (51, 52). In the literature, ^{18}F -FDG PET has been found to be of only moderate additional value to MRI for differentiation between glioma recurrence and RN, especially due to low specificity (6, 21, 28, 30, 48, 53, 54). A potentially useful approach for

^{18}F -FDG PET is dual-phase imaging. It was shown previously that delayed ^{18}F -FDG imaging 3–8 h after injection improves the distinction between tumor and normal gray matter because the outflow of glucose was hypothesized to be higher from normal brain tissue than from the tumor. This was confirmed using kinetic modeling (KM) showing that the dephosphorylation rate of FDG-6 phosphate values were not significantly different between tumor and normal brain tissue at early imaging times but was lower in tumor than in normal brain tissue at delayed imaging times (55–58). Applying conventional and delayed ^{18}F -FDG PET, Horkey et al. found that early and late SUVs of the lesion alone did not differentiate between tumor and necrosis. However, the change of LNR_{max} between early and late ^{18}F -FDG images was 95% sensitive, 100% specific, and 96% accurate (58). In our study, we found that differences in LNR_{mean} and LNR_{max} between GB and RN were higher on the delayed PET images compared to the conventional ^{18}F -FDG PET. A plausible explanation is that, like normal brain tissue, necrotic tissue shows increased ^{18}F -FDG excretion at delayed times when compared with tumor (56). Consequently, the LNR increases over time for tumor but remained stable or even decreased for RN (58).

AMINO-ACID PET

Radiolabeled amino acids are the most commonly used PET tracers for imaging brain tumors. An advantage over ^{18}F -FDG is the relatively low uptake of amino acids by normal brain tissue. Therefore, cerebral gliomas can be distinguished from the surrounding normal tissue with higher contrast, see Figure 2B (40, 41). Labeled amino acid tracers developed so far for PET imaging are divided into two categories: tracers actively incorporated into the proteins, such as ^{11}C -Methionine (^{11}C -MET), potentially allowing investigating protein synthesis, and tracers not integrated into proteins, such as ^{18}F -fluoroethyltyrosine (^{18}F -FET) and 3,4-dihydroxy-6- ^{18}F -fluoro-l-phenylalanine (^{18}F -FDOPA), which are valuable tools to evaluate amino acid transport (59). The increased uptake of ^{18}F -FET and ^{18}F -FDOPA by cerebral glioma tissue appears to be caused mainly by increased transport via sodium-independent amino acid transport system L for large neutral amino acids (LATs) and Na^+ -dependent general amino acid transporters $\text{B}^{0,+}$ and B^0 , with a disruption of the BBB not being a prerequisite for intratumoral accumulation (20, 60–62). Most PET studies of cerebral gliomas have been performed with ^{11}C -MET, although the short half-life of ^{11}C (20 min) limits the use of this tracer to the few centers that are equipped with an on-site cyclotron facility. Results with ^{18}F -FET PET are similar to those with ^{11}C -MET (63), and due to its longer half-life (109 min) and lack of (or minimal) uptake in macrophages and inflammatory cells, ^{18}F -FET PET is preferred for clinical use (56, 59, 61, 64–67). The diagnostic potential of ^{18}F -FET PET in brain tumors is well documented, for example, a superior delineation of human gliomas by ^{18}F -FET PET compared with MRI and a high specificity for the detection of gliomas and biopsy site planning (31, 64, 68). Among WHO grades III and IV gliomas, the vast majority (>95%) shows increased ^{18}F -FET uptake. However, a lack of ^{18}F -FET uptake does not exclude a glioma, as approximately one-third of WHO grade II gliomas and most dysembryoplastic neuroepithelial tumors (WHO grade I) are ^{18}F -FET negative (6). Several studies have also indicated that

time–activity curves of ^{18}F -FET uptake contain biological information beyond that of static images, and these data may be helpful for glioma grading (31). In HGGs, uptake patterns of ^{18}F -FDOPA are not significantly different from ^{18}F -FET, but both SUV_{mean} and LNRs were 10–15% higher for ^{18}F -FET than ^{18}F -FDOPA (69).

Current amino acid PET data suggest that deactivation of amino acid transport and/or decrease of the metabolically active tumor volume is a sign of treatment response associated with long-term outcome (6, 70–73). Treatment response and outcome in bevacizumab therapy has been suggested to be better assessed by ^{18}F -FET and ^{18}F -FDOPA, compared to MRI (6, 74–77). Also, reliable monitoring of TMZ and nitrosourea-based chemotherapy effects has been demonstrated in patients with recurrent HGG (9, 31, 64, 66, 70, 71). In a study by Rachinger et al., ^{18}F -FET PET was able to distinguish tumor progression from stable disease with 93% specificity and 100% sensitivity, while the specificity of conventional MRI alone was 50% (78). ^{18}F -FET PET responders, based on a decrease of more than 10% of LNR after completion of therapy, also showed a significant longer overall survival than nonresponders (60). The biological tumor volume on ^{18}F -FET PET prior to chemoradiotherapy and as early as 7–10 days after the completion of treatment in GB was also found to be highly prognostic. Remarkably, the time-to-peak and the shape of the ^{18}F -FET time–activity curve, derived from dynamic PET acquisitions, were shown to have value in therapy response assessment (6, 60, 70, 79, 80).

A promising role of amino acid PET for the distinction between tumor recurrence and benign post-therapeutic changes has also been suggested. The LNR of ^{11}C -MET PET revealed a sensitivity and specificity of 70–80% for the differentiation of brain metastasis recurrence from radiation-related effects (31). A higher diagnostic accuracy was shown by Grosu et al., with ^{11}C -MET able to differentiate tumor tissue from treatment-related changes with a sensitivity of 91% and a specificity of 100% (63). Using ^{18}F -FET PET, the detection of tumor recurrence/progression was even more accurate, with a sensitivity and specificity of 100% and 93%, respectively, compared with 93- and 50% for MRI alone (73, 78). Pöpperl et al. were able to distinguish recurrent tumor and RN with 100% accuracy, applying a threshold of 2.0 for LNR_{max} , and Galldiks et al. suggested that the combined evaluation of the LNR_{mean} of ^{18}F -FET uptake and the pattern of the time–activity curve can differentiate brain metastasis recurrence from RN with high accuracy (70, 73). The lower specificity of ^{11}C -MET may be explained by its higher affinity for macrophages compared with ^{18}F -FET as demonstrated in animal experiments (81, 82). In our study, ^{18}F -FET uptake in GB was more intense and more heterogeneous compared to RN, see Figure 3E. It was already mentioned that focal and high ^{18}F -FET uptake was suspicious for tumor recurrence, whereas low and homogeneous uptake around the resection cavity was considered benign due to post-treatment alterations of the BBB (73). Furthermore, amino acid PET was assumed to be superior to both ^{18}F -FCho PET and ^{18}F -FDG PET for diagnostic accuracy in distinguishing glioma recurrence from RN (6, 49, 50, 83). Using ^{18}F -FDOPA PET, a sensitivity and specificity of more than 80% to distinguish recurrent GB or recurrent brain metastasis and radiation-related effects was shown (25, 84). However, the lack of physiological ^{18}F -FET uptake in the basal ganglia when compared with ^{18}F -FDOPA PET makes ^{18}F -FET the most promising amino acid tracer for PET imaging in brain tumor patients (31).

However, it should be kept in mind that (moderately) increased ^{18}F -FET uptake can also be seen in acute inflammatory lesions such as active multiple sclerosis and brain abscesses (6).

^{18}F -FLUOROMETHYLCHOLINE (^{18}F -FCHO)

Positron-labeled choline analogues appear to be successful as oncological PET probes because a major hallmark of cancer cells is increased lipogenesis (85, 86). Phosphorylation by choline kinase (CK) constitutes an important step in the incorporation of choline into phospholipids, which is an essential component of all cell membranes. In cancer, there is often an increase in the cellular transport and phosphorylation of choline, as well as an increase in the expression of CK, increasing the uptake of radiolabeled choline (87–89). Choline can be labeled with either ^{11}C or ^{18}F . As a tracer, ^{11}C -Cho is biochemically indistinguishable from natural choline; however, the short half-life of ^{11}C has led to the development of ^{18}F -labeled derivatives, such as ^{18}F -Fluoromethylcholine (^{18}F -FCho) (90, 91). Previous *in vitro* studies have clearly documented that these fluorinated choline analogues are suitable substrates for the enzyme CK (90, 92), although the rate of their incorporation in phospholipids may be slower than that of endogenous choline (93). ^{18}F -labeled choline analogues have been investigated as oncological PET probes for the detection of (recurrent) local prostate cancer, but seem to have limited value for tumor and nodal staging. Rapidly proliferating GB cells have increased membrane/fatty acid requirements, which result in a higher ^{18}F -FCho uptake than in healthy brain tissue (86). Kwee et al. showed promising results for ^{18}F -FCho in brain tumor PET imaging with a differential uptake in HGG, brain metastases, and benign lesions (87). One of the assets of this tracer is the very low uptake in normal brain, increasing distinctively the contrast between GB and healthy brain, see Figure 2C. Changes in ^{18}F -FCho uptake may also precede post-treatment anatomical changes on conventional MRI (86). However, only a few studies investigated the potential of ^{18}F -FCho for therapy response assessment in gliomas. Li et al. reported that, for ^{11}C -Choline PET, an $\text{LNR} \leq 1.4$ might predict a longer overall survival in patients with suspected recurrent glioma after treatment (94). Parashar et al. suggested that there was a good correlation between a change in SUV_{max} of the tumor during RT and response (95). However, in the latter study, only one patient with a malignant glioma was included. Our research group recently investigated the potential of ^{18}F -FCho PET for early therapy response assessment in GB patients; see Figure 4 (96). Based on our results, ^{18}F -FCho SUV values pre-RT, during RT, and 1 month post-RT did not predict response. Physiological phenomena, such as therapy-induced perfusion changes due to alteration of BBB, cell repair mechanisms obscuring assessment of true cell death, and aspecific uptake of PET tracers due to infiltrating macrophages, may complicate response assessment. It should also be kept in mind that GBs are very heterogeneous tumors, containing clusters of tumor and normal cells, vascular structures, and necrotic tissues (29), which are not fully captured when using SUV_{max} or SUV_{mean} values. Based on our results, we also noted that in some nonresponders, absolute SUV values decreased during the course of the treatment while the metabolic tumor volume (MTV) increased, indicating that MTV is an important parameter. As such, we found that the ^{18}F -FCho PET-derived parameter, $\text{MTV} \times \text{SUV}_{\text{mean}}$, allowed prediction of therapy

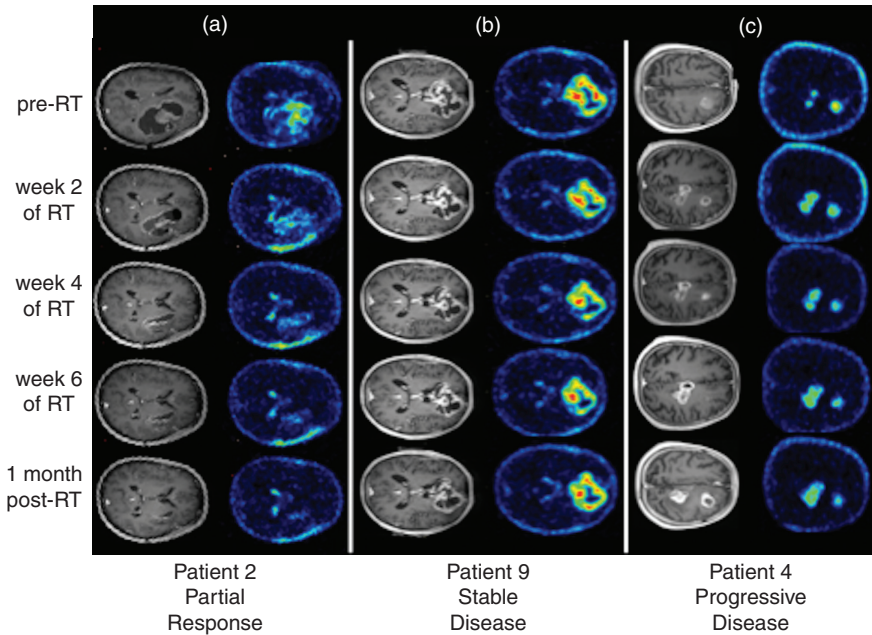


Figure 4 ^{18}F -Fluoromethylcholine (^{18}F -FCho) PET and contrast-enhanced T1-weighted MR images in 3 GB patients (a,b,c). (a) A 47-year old female patient diagnosed with GB in the right frontal and temporal lobe. According to the RANO criteria the patient is categorized as a partial responder. A 60 % decrease in SUV_{max} and SUV_{mean} is observed from pre-RT to 1 month post-RT. (b) A 71-year old male patient diagnosed with a bifrontal GB. According to the RANO criteria, the patient was categorized as stable disease. From pre-RT to 1 month post-RT, SUV_{max} decreased 17 % while SUV_{mean} remained more or less stable. (c) A 66-year old male patient diagnosed with multifocal GB. A new lesion was visible on follow-up MRI, categorizing the patient as progressive disease. From pre-RT to 1 month post-RT SUV_{max} and SUV_{mean} decreased 52 % and 59 % respectively, while MTV increased with > 300 % (96).

response as early as 1 month after the completion of RT. Interestingly, the tumor volume derived from contrast-enhanced MRI was able to predict response earlier, that is, at week 6 during RT. However, due to the possibility of pseudoprogression, inclusion of PET in the RANO criteria might be helpful for early therapy response prediction in HGG.

Finally, ^{18}F -FCho PET was assumed to be promising in differentiating GB from RN (47, 52, 97). ^{18}F -FCho PET was studied in patients with solitary brain lesions and correctly identified patients with RN based on LNR (87). Tan et al. showed higher sensitivity and specificity for ^{11}C -Cho PET compared to MRI and ^{18}F -FDG, and Spaeth et al. noted a higher ^{18}F -FCho uptake in HGG compared to acute radiation injury (52, 97). Although promising results for the differentiation of RN and tumor recurrence in gliomas were reported, in our *in vivo* animal experiment, ^{18}F -FCho was not able to differentiate “pure” GB from “pure” RN; see Figure 3D (87, 97). Using KM and graphical analysis, we tried to interpret these results. However, we could not confirm an increased choline transporter-like protein-mediated transport, nor a higher expression of CK in GBs compared to RN.

The immediate metabolization of choline raises the question if ^{18}F -Fluorobetaine attributes to the detected choline signal, and the uptake in RN is influenced by leakage through the damaged BBB and inflammation (93, 98–101). As such, correlative imaging with MRI is of utmost importance (85). Also, it should be kept in mind that the metabolism of choline tracers in humans is slower than in rodents.

HYPOXIA-PET

Hypoxia is a pathological condition arising in living tissues when oxygen supply does not adequately cover the cellular metabolic demand. Detection of this phenomenon in tumors is of utmost clinical relevance because tumor aggressiveness, metastatic spread, failure to achieve local tumor control, increased rate of recurrence, and ultimate poor outcome are all associated with hypoxia (39, 102, 103). A number of hypoxia tracers are available for PET. The first introduced hypoxia tracer is called ^{18}F -fluoromisonidazole (^{18}F -FMISO). After passive diffusion through the membrane and in the presence of reduced pO_2 , ^{18}F -FMISO undergoes progressive reduction by the nitroreductase enzyme (NTR). This process is reversible in the presence of sufficient O_2 . Conversely, in hypoxic conditions, the reduced ^{18}F -FMISO is covalently bound to the intracellular proteins, resulting in tracer accumulation within the hypoxic cell (39, 40, 45, 88). To date, ^{18}F -FMISO has predominantly been used in a preclinical setting (79, 104). Concerning its use in therapy response assessment, the volume and intensity of hypoxia on ^{18}F -FMISO PET in GB before radiotherapy was strongly associated with poorer time to progression and survival (57). However, the slow uptake of ^{18}F -FMISO in target tissue and slow clearance of unbound ^{18}F -FMISO from nonhypoxic areas stimulated the development of ^{18}F -fluoroazomycin arabinoside (^{18}F -FAZA) with improved pharmacokinetics (39). A highly increased uptake of ^{18}F -FAZA was observed in all glioma types, with a LNR ranging between 2 and 16 due to low uptake in normal brain tissue (105). Also, in the F98 GB rat model, we observed a high LNR on ^{18}F -FAZA PET; see Figure 2D. Further prospective studies are however needed before incorporating hypoxia PET in glioma in the clinic. Another promising role for hypoxia PET lies in the era of PET-guided RT in GB.

^{18}F -FLUOROTHYMININE

DNA synthesis is required for cell growth and proliferation. Nucleotides of the four bases (cytosine, guanine, adenine, and thymidine) are required for DNA synthesis. Of these four nucleosides, thymidine is the only one incorporated exclusively into DNA, and not ribonucleic acid (RNA), providing a measure of DNA synthesis (106). ^{18}F -fluorothymidine (^{18}F -FLT) has been proposed to directly assess DNA synthesis to estimate tumor cell proliferation and has been proposed for therapy monitoring, based on the concept that change in DNA synthesis should be the most direct index of therapeutic effects on tumor proliferation (59). A direct correlation between ^{18}F -FLT uptake and Ki67 expression in tumor cells has been documented (56), leading to the use of this tracer in many tumor types as a surrogate for aggressiveness and an early marker of response (39, 56, 107–111). Obviously, tumor size is an important prognostic indicator, and tumor volume determined by ^{18}F -FLT was assumed to be a better predictor of overall survival than the intensity of uptake (112).

In preclinical GB models, early therapy response to chemotherapeutic and/or anti-angiogenic therapy could be predicted via ^{18}F -FLT PET (113–115). This was confirmed in recurrent glioma patients treated with bevacizumab and irinotecan showing that ^{18}F -FLT is able to predict overall survival and would allow differentiation between recurrent glioma and RN (56, 116, 117). A high LNR of a GB tumor on ^{18}F -FLT PET is visible in Figure 2F (9). However, the sensitivity for the detection of HGG might be lower than required for clinical application, and dependence of ^{18}F -FLT uptake on BBB disruption raises the question of its specificity (59).

NOVEL PET TRACERS

Currently, novel promising glioma PET tracers are under investigation. The value of new amino acid PET tracers, such as α - ^{11}C -methyl-tryptophan and ^{18}F -Fluciclovine as well as glutamine-based amino acid PET tracers has been evaluated with promising results in glioma patients in terms of tumor delineation, prognostication, and the differentiation of tumor recurrence from radiation injury (31, 118–122). Another interesting new PET target is the translocator protein (TSPO), a mitochondrial membrane protein highly expressed in activated microglia, macrophages, and neoplastic cells. Imaging with the TSPO ligand ^{11}C -(R)PK11195 demonstrates increased binding in HGG compared to low-grade gliomas and normal brain parenchyma (123, 124). More recently, the TSPO ligand ^{18}F -DPA-714 has been evaluated in glioma animal models, but results in human glioma patients are pending (31, 125, 126). A novel labeled integrin $\alpha_v\beta_3$ -targeting ^{18}F -AIF-NOTA-PRGD2 (^{18}F -RGD) tracer showed positive results in assessing sensitivity to concurrent chemoradiotherapy in GB. An example is given in Figure 2G (44, 26). Another approach was published by Oborski et al., suggesting the ability to image therapy-induced tumor cellular apoptosis using ^{18}F -2-(5-fluoro-pentyl)-2-methyl-malonic acid (^{18}F -ML-10) for early therapy response assessment of a newly diagnosed GB patient (127).

Conclusion

The identification of new MRI and PET biomarkers and their inclusion in the RANO criteria may be helpful for early therapy response prediction in HGG. However, it is difficult to compare results of individual studies because of methodological differences and varying clinical endpoints (128). As such, standardization and validation are needed first.

Acknowledgment: The authors would like to thank Stichting Luka Hemelaere and Soroptimist International for supporting this work.

Conflict of interest: The authors declare no potential conflicts of interest with respect to research, authorship, and/or publication of this manuscript.

Copyright and permission statement: To the best of our knowledge, the materials included in this chapter do not violate copyright laws. All original sources have been appropriately acknowledged and/or referenced. Where relevant, appropriate permissions have been obtained from the original copyright holder(s).

References

1. Omuro A, DeAngelis LM. Glioblastoma and other malignant gliomas. A clinical review. *JAMA*. 2013;310(17):1842–50. <http://dx.doi.org/10.1001/jama.2013.280319>
2. Drevelegas A, Karkavelas G. Imaging of brain tumors with histological correlations. Berlin: Springer; 2011. Chapter 6, High-grade gliomas; p. 157. <http://dx.doi.org/10.1007/978-3-540-87650-2>
3. Wadajkar AS, Dancy JG, Hersh DS, Anastasiadis P, Tran NL, Woodworth GF, et al. Tumor-targeted nanotherapeutics: Overcoming treatment barriers for glioblastoma. *Wiley Interdiscip Rev Nanomed Nanobiotechnol*. 2017;9(4):1–17. <http://dx.doi.org/10.1002/wnan.1439>
4. Huse JT, Holland EC. Targeting brain cancer: Advances in the molecular pathology of malignant glioma and medulloblastoma. *Nat Rev Cancer*. 2010;10(5):319–31. <http://dx.doi.org/10.1038/nrc2818>
5. Hattingen E, Pilatus U. Brain tumor Imaging. Berlin: Springer; 2016. Chapter, Brain tumor imaging; p. 1–11. <http://dx.doi.org/10.1007/978-3-642-45040-2>
6. Albert NL, Weller M, Suchorska B, Galldiks N, Soffietti R, Kim MM, et al. Response Assessment in Neuro-Oncology working group and European Association for Neuro-Oncology recommendations for the clinical use of PET imaging in gliomas. *Neuro Oncol*. 2016;18(9):1199–208. <http://dx.doi.org/10.1093/neuonc/nov058>
7. Rees JH. Diagnosis and treatment in neuro-oncology: An oncological perspective. *Br J Radiol*. 2011;84:S82–9. <http://dx.doi.org/10.1259/bjr/18061999>
8. Watts C, Sanai N. Surgical approaches for the gliomas. *Handbook Clin Neurol*. 2016;134:51–69. <http://dx.doi.org/10.1016/B978-0-12-802997-8.00004-9>
9. Ahmed R, Oborski MJ, Hwang M, Lieberman FS, Mountz JM. Malignant gliomas: Current perspectives in diagnosis, treatment, and early response assessment using advanced quantitative imaging methods. *Cancer Manag Res*. 2014;6:149–70.
10. Khan FM. The physics of radiation therapy. 5th ed. Baltimore, MD: Wolters Kluwer Health—Lippincott Williams & Wilkins; 2010. Chapter 20, Intensity-modulated radiation therapy; p. 430.
11. Kirsch DG, Tarbell NJ. Conformal radiation therapy for childhood CNS tumors. *Oncologist*. 2004;9(4):442–50. <http://dx.doi.org/10.1634/theoncologist.9-4-442>
12. Stupp R, Dietrich PY, Ostermann Kraljevic S, Pica A, Maillard I, Maeder P, et al. Promising survival for patients with newly diagnosed glioblastoma multiforme treated with concomitant radiation plus temozolomide followed by adjuvant temozolomide. *J Clin Oncol*. 2002;20:1375–82. <http://dx.doi.org/10.1200/JCO.2002.20.5.1375>
13. Anton K, Baehring JM, Mayer T. Glioblastoma multiforme: Overview of current treatment and future perspectives. *Hematol Oncol Clin North Am*. 2012;26(4):825–53. <http://dx.doi.org/10.1016/j.hoc.2012.04.006>
14. Siu A, Wind JJ, Iorgulescu JB, Chan TA, Yamada Y, Sherman JH. Radiation necrosis following treatment of high grade glioma—a review of the literature and current understanding. *Acta Neurochir*. 2012;154(2):191–201. <http://dx.doi.org/10.1007/s00701-011-1228-6>
15. van den Bent MJ. Practice changing mature results of RTOG study 9802: Another positive PCV trial makes adjuvant chemotherapy part of standard of care in low-grade glioma. *Neuro Oncol*. 2014;16(12):1570–4. <http://dx.doi.org/10.1093/neuonc/nou297>
16. de Vries NA, Beijnen JH, van Tellingen O. High-grade glioma mouse models and their applicability for preclinical testing. *Cancer Treat Rev*. 2009;35:714–23. <http://dx.doi.org/10.1016/j.ctrv.2009.08.011>
17. Gorlia T, van den Bent MJ, Hegi ME, Mirimanoff RO, Weller M, Cairncross JG, et al. Nomograms for predicting survival of patients with newly diagnosed glioblastoma: Prognostic factor analysis of EORTC and NCIC trial 26981-22981/CE.3. *Lancet Oncol*. 2008;9:29–38. [http://dx.doi.org/10.1016/S1470-2045\(07\)70384-4](http://dx.doi.org/10.1016/S1470-2045(07)70384-4)
18. Ducray F, Idbaih A, Wang XW, Cheneau C, Labussiere M, Sanson M. Predictive and prognostic factors for gliomas. *Expert Rev Anticancer Ther*. 2011;11:781–9. <http://dx.doi.org/10.1586/era.10.202>
19. Wen PY, Macdonald DR, Reardon DA, Cloughesy TF, Sorensen AG, Galanis E, et al. Updated response assessment criteria for high-grade gliomas: Response assessment in neuro-oncology working group. *J Clin Oncol*. 2010;28:1963–72. <http://dx.doi.org/10.1200/JCO.2009.26.3541>

20. Jain R, Narang J, Sundgren PM, Harschen D, Saksena S, Rock JP, et al. Treatment induced necrosis versus recurrent/progressing brain tumor: Going beyond the boundaries of conventional morphologic imaging. *J Neurooncol.* 2010;100(1):17–29. <http://dx.doi.org/10.1007/s11060-010-0139-3>
21. Chao ST, Suh JH, Raja S, Lee SY, Barnett G. The sensitivity and specificity of FDG PET in distinguishing recurrent brain tumor from radionecrosis in patients treated with stereotactic radiosurgery. *Int J Cancer.* 2001;96:191–7. <http://dx.doi.org/10.1002/ijc.1016>
22. Lutz K, Radbruch A, Wiestler B, Bäumer P, Wick W, Bendszus M. Neuroradiological response criteria for high-grade gliomas. *Clin Neuroradiol.* 2011;21:199–205. <http://dx.doi.org/10.1007/s00062-011-0080-7>
23. Langleben DD, Segall GM. PET in differentiation of recurrent brain tumor from radiation injury. *J Nucl Med.* 2000;41:1861–7.
24. Ruben JD, Dally M, Bailey M, Smith R, McLean CA, Fedele P. Cerebral radiation necrosis: Incidence, outcomes, and risk factors with emphasis on radiation parameters and chemotherapy. *Int J Radiat Oncol Biol Phys.* 2006;65(2):499–508. <http://dx.doi.org/10.1016/j.ijrobp.2005.12.002>
25. Lizarraga KJ, Allen-Auerbach M, Czernin J, DeSalles AA, Yong WH, Phelps ME, et al. 18F-FDOPA PET for differentiating recurrent or progressive brain metastatic tumors from late or delayed radiation injury after radiation treatment. *J Nucl Med.* 2014;55(1):30–6. <http://dx.doi.org/10.2967/jnumed.113.121418>
26. Rahmthulla G, Marko NF, Weil RJ. Cerebral radiation necrosis: A review of the pathobiology, diagnosis and management considerations. *J Clin Neurosci.* 2013;20(4):485–502. <http://dx.doi.org/10.1016/j.jocn.2012.09.011>
27. Giglio P, Gilbert HR. Cerebral radiation necrosis. *Neurologist.* 2003;9:180–8. <http://dx.doi.org/10.1097/01.nrl.0000080951.78533.c4>
28. Van Laere K, Ceyssens S, Van Calenbergh F, de Groot T, Menten J, Flamen P, et al. Direct comparison of 18F-FDG and 11C-methionine PET in suspected recurrence of glioma: Sensitivity, inter-observer variability and prognostic value. *Eur J Nucl Med Mol Imaging.* 2005;32:39–51. <http://dx.doi.org/10.1007/s00259-004-1564-3>
29. Hoekstra CJ, Paglianiti I, Hoekstra OS, Smit EF, Postmus PE, Teule GJ, et al. Monitoring response to therapy in cancer using (18F)-2-fluoro-2-deoxy-D-glucose and positron emission tomography—An overview of different analytical methods. *Eur J Nucl Med.* 2000;27:731–43. <http://dx.doi.org/10.1007/s002590050570>
30. Dhermain FG, Hau P, Lanfermann H, Jacobs AH, van den Bent MJ. Advanced MRI and PET imaging for assessment of treatment response in patients with gliomas. *Lancet Neurol.* 2010;9:906–20. [http://dx.doi.org/10.1016/S1474-4422\(10\)70181-2](http://dx.doi.org/10.1016/S1474-4422(10)70181-2)
31. Galldiks N, Langen KJ. Amino acid PET—An imaging option to identify treatment response, post-therapeutic effects, and tumor recurrence? *Front Neurol.* 2016;28(7):120. <http://dx.doi.org/10.3389/fneur.2016.00120>
32. Shah A, Snelling B, Bregy A, Patel PR, Tememe D, Bhatia R, et al. Discriminating radiation necrosis from tumor progression in gliomas: A systematic review what is the best imaging modality? *J Neurooncol.* 2013;112:141–52. <http://dx.doi.org/10.1007/s11060-013-1059-9>
33. Zeng QS, Li CF, Liu H, Zhen JH, Feng DC. Distinction between recurrent glioma and radiation injury using magnetic resonance spectroscopy in combination with diffusion-weighted imaging. *Int J Radiat Oncol Biol Phys.* 2007;68:151–8. <http://dx.doi.org/10.1016/j.ijrobp.2006.12.001>
34. Kim HS, Goh MJ, Kim N, Chol CG, Kim SJ, Kim JH. Which combination of MR imaging modalities is best for predicting recurrent glioblastoma? Study of diagnostic accuracy and reproducibility. *Radiology.* 2014;273:831–43. <http://dx.doi.org/10.1148/radiol.14132868>
35. Hu LS, Baxter LC, Smith KA, Feuerstein BG, Karis JP, Eschbacher JM, et al. Relative cerebral blood volume values to differentiate high-grade glioma recurrence from posttreatment radiation effect: Direct correlation between image-guided tissue histopathology and localized dynamic susceptibility-weighted contrast-enhanced perfusion MR imaging measurements. *Am J Neuroradiol.* 2009;30:552–8. <http://dx.doi.org/10.3174/ajnr.A1377>
36. Barajas RF Jr, Chang JS, Segal MR, Parsa AT, McDermott MW, Berger MS, et al. Differentiation of recurrent glioblastoma multiforme from radiation necrosis after external beam radiation therapy with

- dynamic susceptibility-weighted contrast-enhanced perfusion MR imaging. *Radiology*. 2009;253:486–96. <http://dx.doi.org/10.1148/radiol.2532090007>
37. Zhou J, Tryggestad E, Wen Z, Lal B, Zhou T, Grossman R, et al. Differentiation between glioma and radiation necrosis using molecular resonance imaging of endogenous proteins and peptides. *Nat Med*. 2011;17:130–4. <http://dx.doi.org/10.1038/nm.2268>
 38. Parvez K, Parvez A, Zadeh G. The diagnosis and treatment of pseudoprogression, radiation necrosis and brain tumor recurrence. *Int J Mol Sci*. 2014;15(7):11832–46. <http://dx.doi.org/10.3390/ijms150711832>
 39. Lopci E, Franzese C, Grimaldi M, Zucali PA, Navarra P, Simonelli M, et al. Imaging biomarkers in primary brain tumours. *Eur J Nucl Med Mol Imaging*. 2015;42(4):597–612. <http://dx.doi.org/10.1007/s00259-014-2971-8>
 40. Demetriades AK1, Almeida AC, Bhangoo RS, Barrington SF. Applications of positron emission tomography in neuro-oncology: A clinical approach. *Surgeon*. 2014;12(3):148–57. <http://dx.doi.org/10.1016/j.surge.2013.12.001>
 41. Hattingen E, Pilatus U. *Brain tumor imaging*. Berlin: Springer; 2016. Chapter, PET imaging of brain tumors; p. 121–35. <http://dx.doi.org/10.1007/978-3-642-45040-2>
 42. Frosina G. Positron emission tomography of high-grade gliomas. *J Neurooncol*. 2016;127:415–25. <http://dx.doi.org/10.1007/s11060-016-2077-1>
 43. Kuge Y, Shiga T, Tamaki N. *Perspectives on nuclear medicine for molecular diagnosis and integrated therapy*. Japan: Springer; 2016. Chapter 18, Hypoxia imaging with 18F-FMISO PET for brain tumors; p. 236. <http://dx.doi.org/10.1007/978-4-431-55894-1>
 44. Zhang H, Liu N, Gao S, Hu X, Zhao W, Tao R, et al. Can an 18F-ALF-NOTA-PRGD2 PET/CT scan predict treatment sensitivity to concurrent chemoradiotherapy in patients with newly diagnosed glioblastoma? *J Nucl Med*. 2016; 57:524–9. <http://dx.doi.org/10.2967/jnumed.115.165514>
 45. James ML, Gambhir SS. A molecular imaging primer: Modalities, imaging agents, and applications. *Physiol Rev*. 2012;92(2):897–965. <http://dx.doi.org/10.1152/physrev.00049.2010>
 46. Doyle WK, Budingger TF, Valk PE, Levin VA, Gutin PH. Differentiation of cerebral radiation necrosis from tumor recurrence by (18F)FDG and 82Rb positron emission tomography. *J Comput Assist Tomogr*. 1987;11(4):563–70. <http://dx.doi.org/10.1097/00004728-198707000-00001>
 47. Kahn D, Follett KA, Bushnell DL, Nathan MA, Piper JG, Madsen M, et al. Diagnosis of recurrent brain tumor: Value of 201Tl SPECT vs 18F-fluorodeoxyglucose PET. *Am J Roentgenol*. 1994;163:1459–65. <http://dx.doi.org/10.2214/ajr.163.6.7992747>
 48. Ricci PE, Karis JP, Heiserman JE, Fram EK, Bice AN, Drayer BP. Differentiating recurrent tumor from radiation necrosis: Time for re-evaluation of positron emission tomography? *Am J Neuroradiol*. 1998;19:407–13.
 49. Bolcaen J, Descamps B, Deblaere K, Boterberg T, De Vos F, Kalala JP, et al. 18F-fluoromethylcholine (FCho), 18F-fluoroethyltyrosine (FET), and 18F-fluorodeoxyglucose (FDG) for the discrimination between high-grade glioma and radiation necrosis in rats: A PET study. *Nucl Med Biol*. 2014;42(1):38–45. <http://dx.doi.org/10.1016/j.nucmedbio.2014.07.006>
 50. Bolcaen J, Lybaert K, Moerman L, Descamps B, Deblaere K, Boterberg T, et al. Kinetic modeling and graphical analysis of 18F-fluoromethylcholine (FCho), 18F-fluoroethyltyrosine (FET) and 18F-fluorodeoxyglucose (FDG) PET for the discrimination between high-grade glioma and radiation necrosis in rats. *PLoS One*. 2016;11(10):e0164208. <http://dx.doi.org/10.1371/journal.pone.0164208>
 51. Spaeth N, Wyss MT, Weber B, Scheidegger S, Lutz A, Verwey J, et al. Uptake of 18F-fluorocholine, 18F-fluoroethyl-L-tyrosine, and 18F-FDG in acute cerebral radiation injury in the rat: Implications for separation of radiation necrosis from tumor recurrence. *J Nucl Med*. 2004;45:1931–8.
 52. Spaeth N, Wyss MT, Pahnke J, Biollaz G, Lutz A, Goepfert K, et al. Uptake of 18F-fluorocholine, 18F-fluoro-ethyl-L-tyrosine and 18F-fluoro-2-deoxyglucose in F98 gliomas in the rat. *Eur J Nucl Med Mol Imaging*. 2006;33:673–82. <http://dx.doi.org/10.1007/s00259-005-0045-7>
 53. Caroline I, Rosenthal MA. Imaging modalities in high-grade gliomas: Pseudoprogression, recurrence, or necrosis? *J Clin Neurosci*. 2012;19(5):633–7. <http://dx.doi.org/10.1016/j.jocn.2011.10.003>
 54. Nihashi T, Dahabreh JJ, Terasawa T. Diagnostic accuracy of PET for recurrent glioma diagnosis: A meta-analysis. *Am J Neuroradiol*. 2013;34(5):944–50. <http://dx.doi.org/10.3174/ajnr.A3324>

55. Mertens K, Acou M, Van Hauwe J, De Ruyck I, Van den Broecke C, Kalala JP, et al. Validation of 18F-FDG PET at conventional and delayed intervals for the discrimination of high-grade from low-grade gliomas: A stereotactic PET and MRI study. *Clin Nucl Med.* 2013;38(7):495–500. <http://dx.doi.org/10.1097/RLU.0b013e318292a753>
56. Chen W. Clinical applications of PET in brain tumors. *J Nucl Med.* 2007;48(9):1468–81. <http://dx.doi.org/10.2967/jnumed.106.037689>
57. Spence AM, Muzi M, Mankoff DA, O'Sullivan SF, Link JM, Lewellen TK, et al. 18F-FDG PET of gliomas at delayed intervals: Improved distinction between tumor and normal gray matter. *J Nucl Med.* 2004;45(10):1653–9.
58. Horky LL1, Hsiao EM, Weiss SE, Drappatz J, Gerbaudo VH. Dual phase FDG-PET imaging of brain metastases provides superior assessment of recurrence versus post-treatment necrosis. *J Neurooncol.* 2011;103(1):137–46. <http://dx.doi.org/10.1007/s11060-010-0365-8>
59. Juweid ME, Hoekstra OS. Positron emission tomography. New York: Springer-Humana press; 2011. Chapter 16, Brain tumors. *Methods Mol Biol.* 2011;727:291–315. <http://dx.doi.org/10.1007/978-1-61779-062-1>
60. Piroth MD, Pinkawa M, Holy R, Nussen S, Stoffels G, Coenen HH, et al. Prognostic value of early (18F)fluoroethyltyrosine positron emission tomography after radiochemotherapy in glioblastoma multiforme. *Int J Radiat Oncol Biol Phys.* 2011;80:176–84. <http://dx.doi.org/10.1016/j.ijrobp.2010.01.055>
61. Becherer A, Karanikas G, Szabó M, Zetting G, Asenbaum S, Marosi C, et al. Brain tumour imaging with PET: A comparison between (18F)fluorodopa and (11C)methionine. *Eur J Nucl Med Mol Imaging.* 2003;30(11):1561–7. <http://dx.doi.org/10.1007/s00259-003-1259-1>
62. Ikotun OF, Marquez BV, Huang C, Masuko K, Daiji M, Masuko T, et al. Imaging the L-type amino acid transporter-1 (LAT1) with Zr-89 immunoPET. *PLoS One.* 2013;15;8(10):e77476.
63. Grosu AL, Astner ST, Riedel E, Nieder C, Wiedenmann N, Heinemann F, et al. An interindividual comparison of O-(2-[18F]fluoroethyl)-L-tyrosine (FET)- and L-[methyl-11C]methionine (MET)-PET in patients with brain gliomas and metastases. *Int J Radiat Oncol Biol Phys.* 2011;81(4):1049–58. <http://dx.doi.org/10.1016/j.ijrobp.2010.07.002>
64. Langen KJ, Hamacher K, Weckesser M, Floeth F, Stoffels G, Bauer D, et al. O-(2-(18F)fluoroethyl)-L-tyrosine: Uptake mechanisms and clinical applications. *Nucl Med Biol.* 2006;33(3):287–94. <http://dx.doi.org/10.1016/j.nucmedbio.2006.01.002>
65. Langen KJ, Tatsch K, Grosu AL, Jacobs AH, Wackesser M, Sabri O. Diagnostics of cerebral gliomas with radiolabeled amino acids. *Dtsch Arztebl Int.* 2008;105(4):55–61.
66. Herholz K, Langen KJ, Schiepers C, Mountz JM. Brain tumors. *Semin Nucl Med.* 2012;42:356–70. <http://dx.doi.org/10.1053/j.semnuclmed.2012.06.001>
67. Walter F, Cloughesy T, Walter MA, Lai A, Nghiemphu P, Wagle N, et al. Impact of 3,4-dihydroxy-6-18F-fluoro-L-phenylalanine PET/CT on managing patients with brain tumors: The referring physician's perspective. *J Nucl Med.* 2012;53(3):393–8. <http://dx.doi.org/10.2967/jnumed.111.095711>
68. Floeth FW, Sabel M, Stoffels G, Pauleit D, Hamacher K, Steiger HJ, et al. Prognostic value of 18F-fluoroethyl-L-tyrosine PET and MRI in small nonspecific incidental brain lesions. *J Nucl Med.* 2008;49:730–7. <http://dx.doi.org/10.2967/jnumed.107.050005>
69. Lapa C, Linsenmann T, Monoranu CM, Samnick S, Buck AK, Bluemel C, et al. Comparison of the amino acid tracers 18F-FET and 18F-DOPA in high-grade glioma patients. *J Nucl Med.* 2014;55:1611–6. <http://dx.doi.org/10.2967/jnumed.114.140608>
70. Galldiks N, Langen KJ, Holy R, Pinkawa M, Stoffels G, Nolte KW, et al. Assessment of treatment response in patients with glioblastoma using O-(2-18F-fluoroethyl)-L-tyrosine PET in comparison to MRI. *J Nucl Med.* 2012;53:1048–57. <http://dx.doi.org/10.2967/jnumed.111.098590>
71. Galldiks N, Kracht LW, Burghaus L, Thomas A, Jacobs AH, Heiss WD, et al. Use of 11C-methionine PET to monitor the effects of temozolomide chemotherapy in malignant gliomas. *Eur J Nucl Med Mol Imaging.* 2006;33(5):516–24. <http://dx.doi.org/10.1007/s00259-005-0002-5>
72. Popperl G, Goldbrunner R, Gildehaus FJ, Kreth FW, Tanner P, Holtmannspötter M, et al. O-(2-[18F]fluoroethyl)-L-tyrosine PET for monitoring the effects of convection-enhanced delivery of paclitaxel in patients with recurrent glioblastoma. *Eur J Nucl Med Mol Imaging.* 2005;32(9):1018–25. <http://dx.doi.org/10.1007/s00259-005-1819-7>

73. Pöpperl G, Götz C, Rachinger W, Schnell O, Gildehaus FJ, Tonn KC, et al. Serial O-(2-(18F)fluoroethyl)-L-tyrosine PET for monitoring the effects of intracavitary radioimmunotherapy in patients with malignant glioma. *Eur J Nucl Med Mol Imaging*. 2006;33:792–800. <http://dx.doi.org/10.1007/s00259-005-0053-7>
74. Galldiks N, Rapp M, Stoffels G, Fink GR, Shah NJ, Coenen HH, et al. Response assessment of bevacizumab in patients with recurrent malignant glioma using [18F]Fluoroethyl-L-tyrosine PET in comparison to MRI. *Eur J Nucl Med Mol Imaging*. 2013;40:22–33. <http://dx.doi.org/10.1007/s00259-012-2251-4>
75. Harris RJ, Cloughesy TF, Pope WB, Nghiemphu PL, Lai A, Zaw T, et al. 18F-FDOPA and 18F-FLT positron emission tomography parametric response maps predict response in recurrent malignant gliomas treated with bevacizumab. *Neuro Oncol*. 2012;14(8):1079–89. <http://dx.doi.org/10.1093/neuonc/nos141>
76. Schwarzenberg J, Czernin J, Cloughesy TF, Ellingson BM, Pope WB, Grogan T, et al. Treatment response evaluation using 18F-FDOPA PET in patients with recurrent malignant glioma on bevacizumab therapy. *Clin Cancer Res*. 2014;20(13):3550–9. <http://dx.doi.org/10.1158/1078-0432.CCR-13-1440>
77. Hutterer M, Nowosielski M, Putzer D, Waitz D, Tinkhauser G, Kostron H, et al. O-(2-(18F-fluoroethyl)-L-tyrosine PET predicts failure of antiangiogenic treatment in patients with recurrent high-grade glioma. *J Nucl Med*. 2011;52:856–64. <http://dx.doi.org/10.2967/jnumed.110.086645>
78. Rachinger W, Goetz C, Pöpperl G, Gildehaus FJ, Kreth FW, Holtmannspötter M, et al. Positron emission tomography with O-(2-(18F) fluoroethyl)-l-tyrosine versus magnetic resonance imaging in the diagnosis of recurrent gliomas. *Neurosurgery*. 2005;57(3):505–11. <http://dx.doi.org/10.1227/01.NEU.0000171642.49553.B0>
79. Suchorska B, Jansen NL, Linn J, Kretzschmar H, Janssen H, Eigenbrod S, et al. Biological tumor volume in 18FET-PET before radiochemotherapy correlates with survival in GBM. *Neurology*. 2015;84(7):710–9. <http://dx.doi.org/10.1212/WNL.0000000000001262>
80. Roelcke U, Bruehlmeier M, Hefti M, Hundsberger T, Nitzsche EU. F-18 choline PET does not detect increased metabolism in F-18 fluoroethyltyrosine-negative low-grade gliomas. *Clin Nucl Med*. 2012;37:e1–3. <http://dx.doi.org/10.1097/RLU.0b013e3182336100>
81. Salber D, Stoffels G, Pauleit D, Reifenberger G, Sabel M, Shah NJ, et al. Differential uptake of (18F) FET and (3H)l-methionine in focal cortical ischemia. *Nucl Med Biol*. 2006;33(8):1029–35. <http://dx.doi.org/10.1016/j.nucmedbio.2006.09.004>
82. Salber D, Stoffels G, Pauleit D, Oros-Peusquens AM, Shah NJ, Klauth P, et al. Differential uptake of O-(2-(18F-fluoroethyl)-L-tyrosine, L-3H-methionine, and 3H-deoxyglucose in brain abscesses. *J Nucl Med*. 2007;48(12):2056–62. <http://dx.doi.org/10.2967/jnumed.107.046615>
83. Takenaka SI, Asano Y, Shinoda J, Nomura Y, Yonezawa S, Miwa K, et al. Comparison of (11)C-methionine, (11)C-choline, and (18)F-fluorodeoxyglucose-PET for distinguishing glioma recurrence from radiation necrosis. *Neurol Med Chir*. 2014;54(4):280–9. <http://dx.doi.org/10.2176/nmc.0a2013-0117>
84. Herrmann K, Czernin J, Cloughesy T, Lai A, Pomykala KL, Benz MR, et al. Comparison of visual and semiquantitative analysis of 18F-FDOPA-PET/CT for recurrence detection in glioblastoma patients. *Neuro Oncol*. 2014;16(4):603–9. <http://dx.doi.org/10.1093/neuonc/not166>
85. Calabria FF, Barbarisi M, Gangemi V, Grillea G, Cascini GL. Molecular imaging of brain tumors with radiolabeled choline PET. *Neurosurg Rev*. 2016;1–10. <http://dx.doi.org/10.1007/s10143-016-0756-1>
86. Mertens K, Slaets D, Lambert B, Acou M, De Vos F, Goethals I. PET with (18)F-labelled choline-based tracers for tumour imaging: A review of the literature. *Eur J Nucl Med Mol Imaging*. 2010;37(11):2188–93. <http://dx.doi.org/10.1007/s00259-010-1496-z>
87. Kwee SA, Ko JP, Jiang CS, Watters MR, Coel MN. Solitary brain lesions enhancing at MR imaging: Evaluation with fluorine 18-fluorocholine PET. *Radiology*. 2007;244:557–65. <http://dx.doi.org/10.1148/radiol.2442060898>
88. Vallabhajosula S. ¹⁸F-labelled positron emission tomographic radiopharmaceuticals in oncology: An overview of radiochemistry and mechanisms of tumor localization. *Sem Nucl Med*. 2007;37:400–19. <http://dx.doi.org/10.1053/j.semnuclmed.2007.08.004>

89. Nakagami K, Uchida T, Ohwada S, Koibuchi Y, Suda Y, Sekine T, et al. Increased choline kinase activity and elevated phosphocholine levels in human colon cancer. *Jpn J Cancer Res.* 1999;90(4):419–24. <http://dx.doi.org/10.1111/j.1349-7006.1999.tb00764.x>
90. DeGrado TR, Coleman RE, Wang S, Baldwin SW, Orr MD, Robertson CN, et al. Synthesis and evaluation of 18F-labeled choline as an oncologic tracer for positron emission tomography: Initial findings in prostate cancer. *Cancer Res.* 2001;61:110–17.
91. Treglia G1, Giovannini E, Di Franco D, Calcagni ML, Rufini V, Picchio M, et al. The role of positron emission tomography using carbon-11 and fluorine-18 choline in tumors other than prostate cancer: A systematic review. *Ann Nucl Med.* 2012;26(6):451–61. <http://dx.doi.org/10.1007/s12149-012-0602-7>
92. Hara T, Kosaka N, Kishi H. Development of (18)F-fluoroethylcholine for cancer imaging with PET: Synthesis, biochemistry, and prostate cancer imaging. *J Nucl Med.* 2002;43:187–99.
93. Bansal A, Shuyan W, Hara T, Harris RA, Degrado TR. Biodisposition and metabolism of (18F)fluorocholine in 9L glioma cells and 9L glioma-bearing fisher rats. *Eur J Nucl Med Mol Imaging.* 2008;35:1192–203. <http://dx.doi.org/10.1007/s00259-008-0736-y>
94. Li W, Ma L, Wang X, Sun J, Wang S, Hu X. 11C-choline PET/CT tumor recurrence detection and survival prediction in post-treatment patients with high-grade gliomas. *Tumor Biol.* 2014;35:12353–60.
95. Parashar B, Wernicke AG, Rice S, Osborne J, Singh P. Early assessment of radiation response using a novel functional imaging modality-[18F] Fluorocholine PET (FCH-PET): A pilot study. *Discov Med.* 2012;14:13–20. <http://dx.doi.org/10.1007/s13277-014-2549-x>
96. Bolcaen J, Acou M, Boterberg T, Vanhove C, De Vos F, Van den Broecke C, et al. ¹⁸F-fluoromethylcholine (¹⁸F-FCho) PET and MRI for the prediction of response in glioblastoma patients according to the RANO criteria. *Nucl Med Commun.* 2017;38(3):242–9.
97. Tan H, Chen L, Guan Y, Lin X. Comparison of MRI, F-18 FDG, and 11C-choline PET/CT for their potentials in differentiating brain tumor recurrence from brain tumor necrosis following radiotherapy. *Clin Nucl Med.* 2011;36:978–81. <http://dx.doi.org/10.1097/RLU.0b013e31822f68a6>
98. Takesh M. Kinetic modeling application to 18F-fluoroethylcholine positron emission tomography in patients with primary and recurrent prostate cancer using two-tissue compartmental model. *World J Nucl Med.* 2013;12(3):101–10. <http://dx.doi.org/10.4103/1450-1147.136734>
99. Challapali A, Sharma R, Hallett WA, Koziowski K, Carroll L, Brickute D, et al. Biodistribution and radiation dosimetry of deuterium-substituted 18F-fluoromethyl-(1,2-²H₄)choline in healthy volunteers. *J Nucl Med.* 2014;55(2):256–63. <http://dx.doi.org/10.2967/jnumed.113.129577>
100. Roivainen A, Forsback S, Grönroos T, Lehikoinen P, Kähkönen M, Sutinen E, et al. Blood metabolism of (methyl-11C)choline; implications for in vivo imaging with positron emission tomography. *Eur J Nucl Med.* 2000;27(1):25–32. <http://dx.doi.org/10.1007/PL00006658>
101. Verwer EE, Oprea-Lager DE, van den Eertwegh AJM, van Moorselaar RJ, Windhorst AD, Schwarte LA, et al. Quantification of 18F-fluorocholine kinetics in patients with prostate cancer. *J Nucl Med.* 2015;56:365–71. <http://dx.doi.org/10.2967/jnumed.114.148007>
102. Nordsmark M, Overgaard J. Tumor hypoxia is independent of hemoglobin and prognostic for locoregional tumor control after primary radiotherapy in advanced head and neck cancer. *Acta Oncol.* 2004;43(4):396–403. <http://dx.doi.org/10.1080/02841860410026189>
103. Rajendran JG, Krohn KA. F-18 fluoromisonidazole for imaging tumor hypoxia: Imaging the microenvironment for personalized cancer therapy. *Sem Nucl Med.* 2015;45(2):151–62. <http://dx.doi.org/10.1053/j.semnucmed.2014.10.006>
104. Galldiks N, Langen KJ. Amino acid PET in neuro-oncology: Applications in the clinic. *Expert Rev Anticancer Ther.* 2017;11:1–3. <http://dx.doi.org/10.1080/14737140.2017.1302799>
105. Postema EJ, McEwan AJ, Riauka TA, Kumar P, Richmond DA, Abrams DN, et al. Initial results of hypoxia imaging using 1-alpha-D-(5-deoxy-5-(18F)-fluoroarabinofuranosyl)-2-nitroimidazole (18F-FAZA). *Eur J Nucl Med Mol Imaging.* 2009;36(10):1565–73. <http://dx.doi.org/10.1007/s00259-009-1154-5>
106. Mankoff DA, Shields AF, Krohn KA. PET imaging of cellular proliferation. *Radiol Clin North Am.* 2005;43(1):153–67. <http://dx.doi.org/10.1016/j.rcl.2004.09.005>

107. Buck AK, Herrmann K, Shen C, Dechow T, Schwaiger M, Wester HJ. Molecular imaging of proliferation in vivo: Positron emission tomography with (18F)fluorothymidine. *Methods*. 2009;48:205–15. <http://dx.doi.org/10.1016/j.ymeth.2009.03.009>
108. Barwick T, Bencherif B, Mountz JM, Avril N. Molecular PET and PET/CT imaging of tumour cell proliferation using F-18 fluoro-L-thymidine: A comprehensive evaluation. *Nucl Med Commun*. 2009;30:908–17. <http://dx.doi.org/10.1097/MNM.0b013e32832ee93b>
109. Bradbury MS, Hambardzumyan D, Zanzonico PB, Schwartz J, Cai S, Burnazi EM, et al. Dynamic small-animal PET imaging of tumor proliferation with 3'-deoxy-3'-18F-fluorothymidine in a genetically engineered mouse model of high-grade gliomas. *J Nucl Med*. 2008;49(3):422–9. <http://dx.doi.org/10.2967/jnumed.107.047092>
110. Jacobs AH, Thomas A, Kracht LW, Li H, Dittmar C, Garlip G, et al. 18F-fluoro-L-thymidine and 11C-methylmethionine as markers of increased transport and proliferation in brain tumors. *J Nucl Med*. 2005;46(12):1948–58.
111. Price SJ, Fryer TD, Cleij MC, Dean AF, Joseph J, Salvador R, et al. Imaging regional variation of cellular proliferation in gliomas using 3'-deoxy-3'-(18F)fluorothymidine positron-emission tomography: An image-guided biopsy study. *Clin Radiol*. 2009;64(1):52–63. <http://dx.doi.org/10.1016/j.crad.2008.01.016>
112. Idema AJ, Hoffmann AL, Boogaarts HD, Troost EG, Wesseling P, Heerschap A, et al. 3'-Deoxy-3'-18F-fluorothymidine PET-derived proliferative volume predicts overall survival in high-grade glioma patients. *J Nucl Med*. 2012;53:1904–10. <http://dx.doi.org/10.2967/jnumed.112.105544>
113. Bao X, Wang MW, Zhang YP, Zhang YJ. Early monitoring antiangiogenesis treatment response of Sunitinib in U87MG Tumor Xenograft by (18)F-FLT MicroPET/CT imaging. *Biomed Res Int*. 2014;2014:218578. <http://dx.doi.org/10.1155/2014/218578>
114. Corroyer-Dulmont A, Pères EA, Gérault AN, Savina A, Bouquet F, Divoux D. Multimodal imaging based on MRI and PET reveals ((18)F)FLT PET as a specific and early indicator of treatment efficacy in a preclinical model of recurrent glioblastoma. *Eur J Nucl Med Mol Imaging*. 2016;43(4):682–94. <http://dx.doi.org/10.1007/s00259-015-3225-0>
115. Viel T, Schelhaas S, Wagner S, Wachsmuth L, Schwegmann K, Kuhlmann M, et al. Early assessment of the efficacy of temozolomide chemotherapy in experimental glioblastoma using (18F)FLT-PET imaging. *PLoS One*. 2013;8(7):e67911. <http://dx.doi.org/10.1371/journal.pone.0067911>
116. Enslow MS, Zollinger LV, Morton KA, Butterfield RI, Kadrmas DJ, Christian PE, et al. Comparison of 18F-fluorodeoxyglucose and 18F-fluorothymidine PET in differentiating radiation necrosis from recurrent glioma. *Clin Nucl Med*. 2012;37(9):854–61. <http://dx.doi.org/10.1097/RLU.0b013e318262c76a>
117. Wardak M, Schiepers C, Cloughesy TF, Dahlbom M, Phelps ME, Huang SC. 18F-FLT and 18F-FDOPA PET kinetics in recurrent brain tumors. *Eur J Nucl Med Mol Imaging*. 2014;41(6):1199–209. <http://dx.doi.org/10.1007/s00259-013-2678-2>
118. Kamson DO, Juhasz C, Buth A, Kupsky WJ, Barger GR, Chakraborty PK, et al. Tryptophan PET in pretreatment delineation of newly-diagnosed gliomas: MRI and histopathologic correlates. *J NeuroOncol*. 2013;112:121–32. <http://dx.doi.org/10.1007/s11060-013-1043-4>
119. Kondo A, Ishii H, Aoki S, Suzuki M, Nagasawa H, Kubota K, et al. Phase IIa clinical study of (18F) fluciclovine: Efficacy and safety of a new PET tracer for brain tumors. *Ann Nucl Med*. 2016;30:608–18. <http://dx.doi.org/10.1007/s12149-016-1102-y>
120. Venneti S, Dunphy MP, Zhang H, Pitter KL, Zanzonico P, Campos C, et al. Glutamine-based PET imaging facilitates enhanced metabolic evaluation of gliomas in vivo. *Sci Transl Med*. 2015;7(274):274ra17. <http://dx.doi.org/10.1126/scitranslmed.aaa1009>
121. Alkonyi B, Barger GR, Mittal S, Muzik O, Chugani DC, Bahl G, et al. Accurate differentiation of recurrent gliomas from radiation injury by kinetic analysis of alpha-11C-methyl-L-tryptophan PET. *J Nucl Med*. 2012;53:1058–64. <http://dx.doi.org/10.2967/jnumed.111.097881>
122. Kamson DO, Mittal S, Robinette NL, Muzik O, Kupsky WJ, Barger GR, et al. Increased tryptophan uptake on PET has strong independent prognostic value in patients with a previously treated high-grade glioma. *Neuro Oncol*. 2014;16:1373–83. <http://dx.doi.org/10.1093/neuonc/nou042>

123. Su Z, Herholz K, Gerhard A, Roncaroli F, Du Plessis D, Jackson A, et al. ((11)C)-(R)PK11195 tracer kinetics in the brain of glioma patients and a comparison of two referencing approaches. *Eur J Nucl Med Mol Imaging*. 2013;40:1406–19. <http://dx.doi.org/10.1007/s00259-013-2447-2>
124. Su Z, Roncaroli F, Durrenberger PF, Coope DJ, Karabatsou K, Hinz R, et al. The 18-kDa mitochondrial translocator protein in human gliomas: A 11C-(R)PK11195 PET imaging and neuropathology study. *J Nucl Med*. 2015;56:512–17. <http://dx.doi.org/10.2967/jnumed.114.151621>
125. Winkeler A, Boisgard R, Awde A, Dubois A, Thézé B, Zheng J, et al. The translocator protein ligand (18F)DPA-714 images glioma and activated microglia in vivo. *Eur J Nucl Med Mol Imaging*. 2012;39:811–23. <http://dx.doi.org/10.1007/s00259-011-2041-4>
126. Awde AR, Boisgard R, Theze B, Dubois A, Zheng J, Dollé F, et al. The translocator protein radioligand 18F-DPA-714 monitors antitumor effect of erufosine in a rat 9L intracranial glioma model. *J Nucl Med*. 2013;54:2125–31. <http://dx.doi.org/10.2967/jnumed.112.118794>
127. Oborski MJ, Laymon CM, Qian Y, Liebermann FS, Nelson AD, Mountz JM. Challenges and approaches to quantitative therapy response assessment in glioblastoma multiforme using the novel apoptosis positron emission tomography tracer F-18 ML-10. *Transl Oncol*. 2014;7(1):111–9. <http://dx.doi.org/10.1593/tlo.13868>
128. Allen-Auerbach M, Weber WA. Measuring response with FDG-PET: Methodological aspects. *The Oncologist*. 2009;14:369–77. <http://dx.doi.org/10.1634/theoncologist.2008-01195>

11

Current Standards of Care in Glioblastoma Therapy

CATARINA FERNANDES¹ • ANDREIA COSTA¹ • LÍGIA OSÓRIO² • RITA COSTA LAGO² • PAULO LINHARES^{3,4} • BRUNO CARVALHO^{3,4} • CLÁUDIA CAEIRO¹

¹Department of Medical Oncology, Centro Hospitalar de São João, Porto, Portugal; ²Department of Radiotherapy, Centro Hospitalar de São João, Porto, Portugal; ³Department of Neurosurgery, Centro Hospitalar de São João, Porto, Portugal; ⁴Faculty of Medicine of the University of Porto, Portugal;

Author for correspondence: Catarina Fernandes, Department of Medical Oncology, Centro Hospitalar de São João, Porto, Portugal. E-mail: ana.catarinaf@gmail.com

Doi: <http://dx.doi.org/10.15586/codon.glioblastoma.2017.ch11>

Abstract: Glioblastoma (GBM) is the most common primary malignant brain tumor in adults. Regardless of ideal multidisciplinary treatment, including maximal surgical resection, followed by radiotherapy plus concomitant and maintenance temozolomide (TMZ), almost all patients experience tumor progression with nearly universal mortality and a median survival of less than 15 months. The addition of bevacizumab to standard treatment with TMZ revealed no increase in overall survival (OS) but improved progression-free survival (PFS). In newly diagnosed GBM, methylation of the O6-methylguanine-DNA methyltransferase (MGMT) promoter has been shown to predict response to alkylating agents, as well as prognosis. Therefore, MGMT promoter status may have a crucial role in the choice of single modality treatment in fragile elderly population. No standard of care is established in recurrent or progressive GBM. Treatment alternatives may include supportive care, surgery, re-irradiation, systemic therapies, and combined modality therapy. Despite numerous clinical trials, the identification of effective therapies is complex because of the lack of appropriate control arms, selection bias, small sample sizes, and disease heterogeneity. Tumor-treating fields plus TMZ represent a major advance in the field of GBM therapy, and should be

In: *Glioblastoma*. Steven De Vleeschouwer (Editor), Codon Publications, Brisbane, Australia ISBN: 978-0-9944381-2-6; Doi: <http://dx.doi.org/10.15586/codon.glioblastoma.2017>

Copyright: The Authors.

Licence: This open access article is licenced under Creative Commons Attribution 4.0 International (CC BY 4.0). <https://creativecommons.org/licenses/by-nc/4.0/>

considered for patients with newly diagnosed GBM with no contraindications. As a disease with such a poor prognosis, treatment of GBM should go beyond improving survival and aim at preserving and even improving the quality of life of both the patient and the caregiver.

Key words: Bevacizumab; Glioblastoma; MGMT; Radiotherapy; Temozolomide

Introduction

Glioblastoma (GBM) is the most common and devastating primary malignant brain tumor in adults, encompassing 16% of all primary brain and central nervous system neoplasms (1). Regardless of advanced diagnostic modalities and ideal multidisciplinary treatment that includes maximal surgical resection, followed by radiotherapy (RT) plus concomitant and maintenance temozolomide (TMZ) chemotherapy, almost all patients experience tumor progression with nearly universal mortality. The median survival from initial diagnosis is less than 15 months, with a 2-year survival rate of 26–33% (2, 3). The addition of bevacizumab to standard treatment revealed no increase in overall survival (OS), but improved progression-free survival (PFS). That finding caused considerable debate regarding whether the combination is cost-effective in first-line treatment (4, 5). In newly diagnosed GBM (nGBM), methylation of O6-methylguanine-DNA methyltransferase (MGMT) promoter has been shown to predict response to alkylating agents; its status may play a crucial role in the choice of single modality treatment in fragile elderly population (6–8).

Currently, no standard of care is established for recurrent or progressive GBM (rGBM) (9). Despite numerous clinical trials, the identification of effective therapies is complex due to the lack of appropriate control arms, selection bias, small sample size, and disease heterogeneity (10). Treatment alternatives may include supportive care, reoperation, re-irradiation, systemic therapies, and combined modality therapy. Therapeutic options need to be carefully weighted, taking into account tumor size and location, previous treatments, age, Karnofsky performance score (KPS), patterns of relapse, and prognostic factors. The association of tumor-treating fields (TTFields) with TMZ represents the first major advance in the field of GBM therapy in approximately a decade and should be considered for newly diagnosed patients with no contraindications (11). As a disease with such a poor prognosis, treatment of GBM should go beyond improving survival and aim at preserving and even improving the quality of life (QoL) of both the patient and the caregiver.

Newly Diagnosed Glioblastoma

SURGERY

Surgery is the initial therapeutic approach for GBM and remains a hallmark in the treatment of malignant brain tumors. Some preoperative issues such as medical conditions of the patient, appropriate imaging and functional studies,

neuropsychological evaluation, and the use of corticosteroid and antiepileptic drugs should be taken into account. While steroids can control cerebral edema and symptoms/signs of intracranial hypertension, thus improving brain conditions for surgical resection, antiepileptic drugs should not be used prophylactically (12). In patients with brain tumors who have not had a seizure, tapering and discontinuing anticonvulsants after the first postoperative week is appropriate (12). Attention should be paid to patients who are going to be operated with cortical stimulation, in an asleep–awake–asleep manner, due to the potential development of stimulation-induced seizures. The goals of surgical treatment are: maximal safe resection; tissue specimen for pathological diagnosis; improving conditions for complementary treatments; delaying clinical worsening; and improving QoL.

While strong predictors of good outcome are essentially patient related, the most important treatment-related predictor is extent of resection (EOR) (13). A more extensive surgical resection is associated with longer life expectancy, achieving the longest survival in those patients who undergo gross total resection followed by RT and TMZ (13–15). An important issue is the fine balance between the aggressive removal and the preservation of function; so the goal is to achieve maximal safe surgical resection. A postoperative magnetic resonance imaging (MRI) should assess the EOR within 72 h of surgery. MRI after 72 h of surgery cannot be relied upon because of inflammatory postoperative changes. It has been postulated that $\geq 98\%$ EOR is necessary to improve survival significantly (16). However, Sanai and colleagues showed that, for oncological purposes, resections of 78% of the tumor volume, associated with chemoradiotherapy, already have prognostic advantages (17). More recently, some authors revealed that more important than the EOR is the amount of the residual volume (18, 19).

Tumors located within eloquent cortex pose a particular surgical challenge due to the high risk of postoperative neurological deficits (20). Muller and colleagues, using functional MRI to map the functional cortex, showed that postoperative neurological deficits occurred in 0% of cases in which the resection margins were beyond 2 cm of the eloquent cortex, in 33% of cases when resection margins were within 1 to 2 cm, and in 50% of cases when resection margins were less than 1 cm (21). Intraoperative electrical stimulation mapping with awake craniotomy decreases the risk of novel neurological deficits, while maximizing the EOR (17, 22). A large meta-analysis demonstrated that resections with the use of intraoperative functional mapping were associated with fewer late severe neurological deficits (3.4% vs. 8.2%) and more extensive resection (75% vs. 58%), although the tumors were more frequently in eloquent locations (100% vs. 96%) (23). Motor evoked potentials and somatosensory evoked potentials can also be recorded during surgery to continuously monitor the integrity of motor and somatosensory pathways.

To increase the EOR, enhancing the visualization of the tumor margins, some fluorescent agents have been used, namely the most widely employed 5-aminolevulinic acid (5-ALA). Panciani and colleagues showed that fluorescence-guided resection revealed a sensitivity of 91.4% and a specificity of 89.2% (24). The use of 5-ALA increases the rate of gross total resection, in randomized controlled trials (65% vs. 35%) and in observational studies (from 25 to 94.3%) (25, 26), and also increases PFS (8.6 vs. 4.8 months) and the 6-month PFS (PFS6)

(46% vs. 28%) (27, 28). The increase in gross total resection rate and PFS was confirmed by three meta-analyses performed to evaluate the literature on 5-ALA. Fluorescein is another option but was not tested in randomized controlled trials (25). Fluorescence near eloquent areas should be managed carefully. A biopsy should be reserved for patients with multiple comorbidities, who would not be able to tolerate a large cranial surgery, or for those with unresectable tumors, and the only benefit is provision of tissue specimen for pathological diagnosis (29). The surgery also allows relieving of the mass effect with concurrent amelioration of symptoms, in patients with increased intracranial hypertension and brain edema, leading to an improvement in the QoL.

COMPLEMENTARY TREATMENT

The current standard of care for patients with nGBM is maximum safe surgical resection followed by concurrent TMZ (75 mg/m²/day for 6 weeks) and RT (60 Gy in 30 fractions) and then six maintenance cycles of TMZ (150–200 mg/m²/day for the first 5 days of a 28-day cycle—sdTMZ), according to the results of the phase III EORTC 26981 (2). Stupp et al. showed an OS and PFS improvement with the combination therapy relative to RT alone (median OS 14.6 vs. 12.1 months; $P < 0.001$) (3). These results were supported by other trials (30–33). A recently published meta-analysis by Feng et al. revealed a median OS of 13.4–19.0 months in the combination treatment group, as opposed to 7.7–17.1 months in the RT-alone group (34).

Age, neurological status (assessed by KPS and Mini Mental State Examination), EOR, IDH (isocitrate dehydrogenase) mutations, and methylation of the MGMT promoter region are established prognostic factors in GBM patients (35, 36). The predictive role of MGMT promoter methylation in response to TMZ has also been established in several studies (3, 37). Nevertheless, the clinical utility of MGMT remains poor, primarily because of a lack of therapeutic options for patients with unmethylated MGMT promoter GBM. The only exception is in the management of elderly patients with GBM. TMZ is an oral chemotherapeutic drug that induces DNA methylation and tumor cytotoxicity through cell cycle arrest. The cytotoxic activity of TMZ and other alkylating agents is apparent by the formation of O6-methylguanine DNA adducts, which are repaired by the enzyme MGMT. Consequently, the primary mechanism of resistance to TMZ is dependent on the MGMT activity (38). It exhibits a linear pharmacokinetics with excellent bioavailability, readily enters the cerebrospinal fluid, and it does not require hepatic metabolism for activation (39). Although evidence suggests that TMZ chemotherapy is associated with few adverse events, risk of hematological complications, fatigue, and infections were increased with its use (40).

DOSE-DENSE TEMOZOLOMIDE

Dose-dense schedules of TMZ (ddTMZ) have been designed to deplete tumor MGMT levels and thereby improve activity of TMZ, particularly in the MGMT unmethylated GBM cohort (41). In the RTOG 0525 phase III trial, 833 patients were randomized to receive sdTMZ or ddTMZ (75–100 mg/m² days 1 through

21 of a 28-day cycle), for 6–12 cycles, after completion of concomitant RT-TMZ. The median OS (16.6 vs. 14.9 months; $P = 0.63$) and the median PFS (5.5 vs. 6.7 months; $P = 0.06$) were not significantly different between the two treatment arms. There was increased grade ≥ 3 toxicity in ddTMZ arm (34% vs. 53%; $P < 0.001$), as well as a greater deterioration on function subscales and QoL (2).

DURATION OF TEMOZOLOMIDE MAINTENANCE THERAPY

RT with concomitant and adjuvant TMZ was initially introduced with six TMZ maintenance cycles (3). In clinical practice, however, many centers continue TMZ therapy beyond six cycles. The impact of this strategy is controversial and has not yet been confirmed in prospective randomized clinical trials. A phase II comparison of 6 versus 12 cycles of TMZ (NCT02209948) is currently underway. Some retrospective studies suggested a benefit in OS with extension of maintenance TMZ (42–45). The major limitation of all these studies, beyond the retrospective nature, is the comparison of patients who were treated with at least seven cycles of TMZ to patients receiving ≤ 6 cycles, who, in most cases, stopped TMZ because of tumor progression. Other limitations are missing information on MGMT methylation and univariate Kaplan–Meier description of OS, but no investigation of significance by multivariate Cox regression (42–45). Data from a large pooled analysis of four clinical trials for nGBM indicates that extended treatment with TMZ beyond six cycles is not associated with improved OS, but prolongs PFS (2, 3, 46–48). A similar analysis was performed in patients enrolled in the German Glioma Network. A total of 61 of the 142 identified patients received at least seven maintenance TMZ cycles (median 11, range 7–20). Patients with extended maintenance TMZ treatment had better PFS (20.5 months vs. 17.2 months; $P = 0.035$) but not OS (32.6 months vs. 33.2 months; $P = 0.126$). However, there was no significant association of prolonged TMZ chemotherapy with PFS or OS adjusted for age, EOR, KPS, presence of residual tumor, MGMT promoter methylation status, or IDH mutation status (49). This study provides Class III evidence that in patients with nGBM, prolonged TMZ chemotherapy does not significantly increase PFS or OS.

GLIADEL (CARMUSTINE) IMPLANTABLE WAFERS

Biodegradable carmustine wafers, implanted into the tumor bed, after near or complete tumor resection, has been approved by the FDA for first-line treatment of GBM and anaplastic glioma. Nevertheless, the use of carmustine wafers remains controversial due to the questionable survival benefit and potential adverse events (50).

OPTIMAL DOSE-FRACTIONATION SCHEDULE FOR EXTERNAL BEAM RADIATION THERAPY

For patients aged under 70 years with good PS ($KPS \geq 60$), the optimal dose-fractionation schedule for external beam RT, following resection or biopsy, is 60 Gy in 2 Gy fractions delivered over 6 weeks. Numerous other dose schedules have been explored without clear benefits. Attention must be paid to ensure that

dose to critical structures (such as brainstem, optic chiasm, optic nerves) is kept within acceptable limits. Risk of radiation necrosis increases with concurrent chemotherapy and larger volume of irradiated brain. The QUANTEC authors emphasize that for most brain tumors, there is no clinical indication to give fractionated RT > 60 Gy (51).

TARGETED THERAPY—IS THERE A PLACE IN NEWLY DIAGNOSED GLIOBLASTOMA?

Since GBM is one of the most vascularized tumors, antiangiogenic therapeutic strategies are very attractive. Bevacizumab is a monoclonal antibody that binds to circulating VEGF-A and inhibits its biological activity by preventing the interaction with the VEGF receptor. This leads to a reduction in endothelial proliferation and vascular growth within the tumor (52). Bevacizumab was approved by the FDA, based on unprecedented response rates (RRs) in rGBM, which led to its evaluation in the postoperative setting of nGBM (Table 1) (64, 65). Two large phase III, randomized, placebo-controlled trials, adding bevacizumab to standard treatment were conducted (4, 5). In the RTOG 0825 trial, median PFS was increased (10.7 vs. 7.3 months), although it did not reach the predefined significance level, and there was no difference in OS between the two treatment groups. The MGMT methylation status and recursive partitioning analysis (RPA) class were prognostic regardless of the study treatment. A decline in QoL and neurocognitive function (NCF) was more frequently observed with bevacizumab (5). In the AVAglio trial, there was a significant increase in PFS (10.6 vs. 6.2 months; $P < 0.001$), but not in OS. Baseline health-related QoL and PS were maintained longer in the bevacizumab group (4). Grade 3 or 4 toxicities occurred more often in the bevacizumab arms of both studies. In RTOG 0825, the crossover from placebo to bevacizumab, at disease progression, was planned and occurred in 48.3% of patients, and in AVAglio, the crossover was about 30%. This may have eliminated a potential survival benefit (4, 5). In both RTOG 0825 and AVAglio, efforts have been made to identify a subset of patients who could benefit from upfront treatment with bevacizumab, but no marker proved consistently effective in predicting either response or resistance to bevacizumab (4, 5).

In summary, these trials have shown that the combination of bevacizumab with standard RT–TMZ for the treatment of nGBM resulted in improved median PFS, without gain in OS. Data regarding QoL and functional status are contradictory. Not surprisingly, there was an increase in adverse events associated with bevacizumab therapy. Cilengitide, a selective $\alpha v\beta 3$ - $\alpha v\beta 5$ -integrin inhibitor, had shown promising results in phase II trials, with more pronounced benefits in GBM with methylated MGMT promoter (66–68). Two prospective randomized trials evaluated the role of cilengitide in combination with standard treatment, in patients with a methylated MGMT gene promoter (CENTRIC) and in those with an unmethylated MGMT status (CORE). They both failed in demonstrating an OS gain (47, 48). Other agents, namely enzastaurin and temsirolimus, have been studied in phase II trials, without any improvement in OS or PFS (41).

TABLE 1 Clinical trials with bevacizumab in the newly diagnosed glioblastoma

Reference	Arm 1	Arm 2	Phase	n	RR (%)		PFS6 (%)		OS (months)	
					Arm 1 versus Arm 2	Arm 1 versus Arm 2	Arm 1 versus Arm 2	Arm 1 versus Arm 2		
RTOG 0825 trial (5)	BVZ/TMZ + RT → TMZ/BVZ	Placebo/TMZ + RT → TMZ/placebo	III	637	-	10.7 vs. 7.3 (<i>P</i> < 0.0007)	-	15.7 vs. 16.1 (<i>P</i> = 0.21)		
AVAglio trial (4)	BVZ/TMZ + RT → TMZ/BVZ	Placebo/TMZ + RT → TMZ/placebo	III	921	-	10.6 vs. 6.2 (<i>P</i> < 0.0001)	-	16.8 vs. 16.7 (<i>P</i> = 0.10)		
(53, 54)	BVZ + RT → BVZ/IRI	TMZ + RT ⊕ TMZ	III (MGMT-nonmethylated)	171	-	9.7 vs. 5.9 (<i>P</i> = 0.0004)	80 vs. 41 (<i>P</i> < 0.0001)	16.6 vs. 17.3 (<i>P</i> = 0.9)		
(55)	BVZ/TMZ + hypo-IMRT → TMZ/BVZ	TMZ + hypo-IMRT → TMZ	II	56	-	12.8 vs. 9.4 (<i>P</i> = 0.58)	84 vs. 83 (<i>P</i> = 0.702)	16.3 in both		
(56)	BVZ/TMZ + hypo-RT → TMZ/BVZ	-	II	40	57	10	93 (1 year)	19		
(57)	TMZ + RT → TMZ/BVZ	-	II	62	-	8.8	-	16.5		
(58)	TMZ + RT → BVZ/EVE	-	II (MGMT-nonmethylated)	48	-	7.3	-	14.2		
(59)	BVZ/TMZ + RT → TMZ/BVZ	-	II	51	-	13.0	85.1	23.0		
(60)	BVZ/TMZ + RT → BVZ/EVE	-	II	68	61	11.3	-	13.9		
(61)	BVZ/TMZ + RT → TMZ/BVZ/TOP	-	II	80	-	11.1	-	17.2		
(62)	BVZ/TMZ + RT → TMZ/BVZ/IRI	-	II	75	-	14.2	-	21.2		
(63)	BVZ/TMZ + RT → TMZ/BVZ	-	II	70	-	13.6	88	19.6		

BVZ, bevacizumab; EVE, everolimus; hypo-IMRT, hypofractionated-intensity-modulated RT; IRI, irinotecan; OS, overall survival; PFS, progression-free survival; PFS6, 6-month PFS; RR, Response Rate; RT, radiotherapy; TMZ, temozolomide; TOP, topotecan.

Recurrent Glioblastoma

SURGERY AT RECURRENCE

When tumor recurs, treatment options include supportive care, reoperation, re-irradiation, systemic therapies, and combined modality therapy. In this setting, the role of reoperation remains unclear. A recent review of the literature, including 28 studies and 2279 patients, who underwent second surgery, showed a median survival from reoperation of 9.7 months and concluded that EOR at reoperation improves OS, even in patients with subtotal resection at initial surgery (69). Nonetheless, clinical and survival benefit is dependent on patient and tumor characteristics, which need to be considered before pursuing a second surgery. The most consistently demonstrated prognostic factor is favorable PS (KPS ≥ 70), which associates with significantly improved PFS and OS, following salvage therapy (70–76). Younger age is the second most frequently reported prognostic factor associated with improved survival (70, 72, 77, 78). Park et al. have devised a scale to predict survival after reoperation based on tumor involvement of pre-specified eloquent/critical brain regions (MSM, motor–speech–middle cerebral artery score), KPS score of 80, and tumor volume (50 cm^3). The scale identified three statistically distinct groups within the validation cohort as well (median survival of 9.2, 6.3, and 1.9 months, respectively) (76). Recently, a new 3-tier scale was developed, including KPS score of 70 and ependymal involvement, allowing identification of groups of patients with significant differences in median OS after reoperation (79). Maximal tumor volume resection should be the surgical goal even in candidates for a second surgery. In this perspective, involvement of eloquent brain usually precludes this objective and is associated with shorter OS (15, 80). Molecular markers' impact in rGBM is still a matter of debate. Brandes et al. reported that MGMT methylation status determined at first surgery seems to be of prognostic value, although it is not predictive of outcome after the second surgery (81).

The DIRECTOR trial, although not aimed at addressing the reoperation issue, allowed the retrospective analysis of EOR and residual tumor volume in approximately two-thirds of the patients, who underwent surgery prior to study entry. Complete resection of enhancing tumor was achieved in 68% of the patients, and in multivariate analysis it was found to be an independent predictor for post-resection survival (82). A multicenter retrospective study, including 503 patients with rGBM submitted to reoperation, concluded that preoperative and postoperative KPS, EOR of first re-resection, and chemotherapy after first re-resection significantly influenced survival after reoperation. Importantly, this study reported a rate of permanent new deficits after first re-resection of 8% (83). In conclusion, evidence suggests higher OS in selected patients who undergo reoperation at the time of GBM recurrence. It should be considered in patients with a good KPS and a favorable preoperative clinical and radiological characteristics. Age <60 years and KPS ≥ 70 are particularly associated with better outcome. Of paramount importance are the preservation of eloquent brain areas and the avoidance of neurological deterioration after second surgery, since that might mitigate the expected survival benefit.

RE-IRRADIATION AND SPECIAL TECHNIQUES

The majority of studies on re-irradiation of gliomas are retrospective and they use a variety of techniques, including brachytherapy, fractionated stereotactic RT (FSRT), radiosurgery, and conformal or intensity-modulated RT, with or without new systemic agents. Furthermore, the published data include a wide range of doses, emphasizing the fact that no standard approach exists (84). Inter-study comparison is difficult because studies have heterogeneous samples, different endpoints, and some patients were treated at first and others at second or third progression. Although the biology of re-irradiation remains to be fully understood, there is now a large body of clinical and animal data that can guide recommendations. Mayer and Sminia identified and analyzed 21 studies on re-irradiation of gliomas (85). They opined that the incidence of toxicity, including radionecrosis, may be underreported, since only symptomatic necrosis is likely to be recorded. The major factor contributing to necrosis was the total dose received. There was no correlation between time to re-irradiation and its development, although the minimum time interval between treatments was 3 months. They concluded that the incidence of necrosis did not increase significantly until the total cumulative dose was 100 Gy. In younger patients with good PS, focal re-irradiation (stereotactic radiosurgery, SRS; hypofractionated stereotactic radiotherapy, HFSRT) for rGBM may improve outcomes compared to supportive care or systemic therapy alone. Tumor size and location should be taken in to account, when evaluating safety of re-irradiation.

STEREOTACTIC RADIOSURGERY AND HYPOFRACTIONATED STEREOTACTIC RADIOTHERAPY

Since most recurrences occur within brains previously irradiated with a high dose, re-irradiation with doses and margins used in the primary treatment of GBM could confer high toxicity risks. Thus, limited volume re-irradiation using SRS or HFSRT is often employed. Stereotactic methods offer optimal precision of target definition while sparing dose to the surrounding tissues. Both SRS and HFSRT deliver more than 2 Gy per fraction and typically have smaller margins and much shorter durations than conventionally fractionated radiotherapy (cfRT). RTOG 90-05, a phase I dose escalation study, established maximum tolerated doses and demonstrated that single-fraction SRS could be performed, in this setting, with acceptable morbidity (86). In the rare event that disease recurs in a portion of brain not previously irradiated, cfRT with chemotherapy should be considered, after surgery.

SRS and HFSRT appear to provide promising outcomes compared to chemotherapy alone for the treatment of rGBM. Shepherd et al. described 29 recurrent high-grade glioma patients treated with a diversity of HFSRT doses with a median OS of 11 months (87). This compared favorably to a matched cohort of patients treated with nitrosourea chemotherapy, with a median OS of 7 months. The studies were nearly all retrospective, however, lacking randomized control groups and with inherent selection bias limiting conclusions. Several of the early studies involving single-fraction SRS reported high rates of radiation necrosis requiring

reoperation (20–40%) (86, 88–90). Compared to SRS, the use of HFSRT may help to mitigate the risk of adverse radiation events. A series of 105 GBM patients treated with 35 Gy in 10 fractions had a median survival, from salvage HFSRT, of 11 months, without clinically significant acute morbidity and only one case of late grade 3 CNS toxicity (78). However, no direct comparison between salvage SRS and HFSRT is available. Defining target volumes for SRS and HFSRT is controversial and variable. A variety of dose-fractionation regimens, target volumes, and stereotactic systems have been used in the treatment of rGBM. These approaches have not been subjected to randomized comparison, so the optimum technique is yet to be established.

CONVENTIONALLY FRACTIONATED RADIATION

Despite most studies discussing re-irradiation with SRS or HFSRT focus, cfRT may theoretically allow more generous target volumes. A large retrospective series of 172 recurrent glioma patients included 59 patients with GBM, who attained a median survival of 8 months, with only one patient developing radiation necrosis (91). The median dose was 36 Gy (15–62 Gy; 2 Gy/day) and was delivered to the enhancing volume plus a 0.5–1 cm margin. There are not enough clinical data available to recommend cfRT for routine use in the recurrent setting. Practitioners using large-volume re-irradiation should take into account brain tolerance data to reduce the risk of radionecrosis (51).

BRACHYTHERAPY

Brachytherapy has also been evaluated for use in rGBM. Typically performed after resection of recurrent disease, brachytherapy features a sharp dose gradient. Strategies include permanent iodine 125 (I-125) seeds and a silicone balloon catheter system containing I-125 solution. Retrospective studies on I-125 have demonstrated median survivals, from the time of brachytherapy, ranging from 11 to 15 months (92). A review by Combs et al. reported high reoperation rates and radionecrosis incidence (93). It should be noted that patients that are selected for brachytherapy are normally those with resectable tumors, good PS, and small volume of disease. As given in the literature on SRS, selection bias confuses interpretation. Also, the patients receiving brachytherapy need to be healthy enough to undergo surgery and, generally, have localized rather than diffuse recurrences.

COMBINATION TREATMENT

Several studies have addressed the combination of chemotherapy with re-irradiation. A few studies have explored TMZ, given its efficacy at radiosensitization in the upfront treatment of GBM. TMZ plus re-irradiation has been found to be safe and effective. Other studies have explored the addition of bevacizumab, which may block hypoxia factor-mediated angiogenesis, which is upregulated by RT (94–96). Moreover, bevacizumab has been used to treat radionecrosis and may reduce its risk following re-irradiation (97–99). A few small studies have investigated concurrent TMZ and SRS or FSRT. Median OS ranged between 8 and 9.7 months. Regarding toxicity, it was mild in one study, while neurologic toxicity was reported

in two other studies (8–13%) (89, 100, 101). Several studies have investigated adding bevacizumab to SRS (72, 88, 102–105). A prospective trial at Memorial-Sloan Kettering Cancer Center, investigating the safety of SRS (30 Gy in 5 fractions) with bevacizumab, reported no radionecrosis among 25 recurrent malignant glioma patients, but three patients discontinued treatment because of bevacizumab grade 3 related toxicity. They documented a 50% RR in the GBM population and a median OS of 12.5 months (102, 106). Another prospective study, in 15 patients with recurrent malignant gliomas, reported one grade 3 and no grade 4–5 toxicities, while QoL and neurocognition were well maintained (88). Median OS from SRS was 14.4 months. A retrospective study from Duke University, in 63 recurrent malignant glioma patients, found that median survival was longer for those who received bevacizumab around the time of SRS, than those who did not (11 vs. 4 months for GBM patients, $P = 0.014$) (72). Several studies have reported relatively low rates of adverse radiation events in patients treated with bevacizumab and SRS/HFSRT (72). Minniti et al. combined HFSRT (25 Gy in five fractions) with bevacizumab or fotemustine and described significantly better OS and PFS in the bevacizumab cohort (107). These studies are nonrandomized, so selection bias remains a serious concern and additional data are required.

SECOND-LINE CHEMOTHERAPY

Several chemotherapy options are available for second-line treatment, but no standard of care has been established. Comparing results between the various studies, particularly the older ones, is difficult, given the heterogeneity of inclusion criteria, patient characteristics, and choice of endpoints and response criteria. Many trials included patients with anaplastic gliomas (WHO grade 3) and GBM (WHO grade 4). Trials conducted prior to the establishment of standard first-line TMZ chemoradiotherapy often included patients not pretreated with TMZ. In addition, most studies were noncomparative, or did not include an adequate control arm. Most considered the PFS6 and the median OS since recurrence as the primary end points. Although PFS6 is considered a reliable measure of tumor control and a strong predictor of survival, this is influenced by other rescue therapies (108). Regarding radiological response assessments, they were often incompletely reported, with most using the Macdonald criteria. The following sections will describe the most relevant trials performed to date with respect to the medical treatment of rGBM.

NITROSOUREA MONOTHERAPY AND COMBINATION REGIMENS

Nitrosoureas are DNA alkylating agents, namely carmustine (BCNU), lomustine (CCNU), nimustine (ACNU), and fotemustine. They are characterized by high lipophilicity and thus can cross the blood–brain barrier, making them useful in the treatment of brain tumors such as GBM (109). Table 2 summarizes nitrosourea-based trials in rGBM. Nitrosoureas, particularly BCNU, were the chemotherapeutic agents of choice for first-line treatment of GBM in the 1970s and 1980s. Based on two phase II trials, TMZ was approved for recurrent high-grade gliomas, and nitrosoureas were relocated into second-line therapy (126, 127).

TABLE 2
Retrospective studies and clinical trials with nitrosourea in recurrent GBM (nitrosourea + bevacizumab combination studies are described in Table 4)

Reference	Arm 1	Arm 2	Arm 3	Previous TMZ	Relapse	n	Phase	RR (%) Arm 1 vs. 2 vs. 3	PFS (months) Arm 1 vs. 2 vs. 3	PFS6 (%) Arm 1 vs. 2 vs. 3	OS (months) Arm 1 vs. 2 vs. 3
Single-arm monotherapy trials											
(110)	BCNU	–	–	No	1st	40	II	15	–	17.5	7.5
(111)	FOT	–	–	Yes	1st	27	II	30	5.7	48.2	9.1
(112)	FOT	–	–	Yes	1st	43	II	7	1.7	20.9	6.0
(113)	FOT	–	–	Yes	1st	50	II	18	6.1	52	8.1
(114)	FOT	–	–	Yes	1st	40	II	25	6.1	61	11.1
Single-arm combination therapy trials											
(115)	BCNU + IRI	–	–	Yes	1st	42	II	21.4	3.9	30.3	11.7
(116)	BCNU + TMZ	–	–	No	NA	38	II	5.6	2.5	21	7.8
(117)	FOT + TMZ	–	–	Yes	NA	20	Prospect.	NA	4.3	40	NA
Randomized trials											
(118)	BCNU or TMZ	ERL	–	Some (number of pts NA)	1st	106	II	10 vs. 4	2.4 vs. 1.8	24.1 vs. 11.4	7.3 vs. 7.7
(119)	CCNU	Enzastaurin	–	NA	1st, 2nd	265	III (2:1)	4 vs. 3	1.6 vs. 1.5	19 vs. 11	7.1 vs. 6.6
(120)	CCNU + P	CED	CCNU + CED	Yes	1st	325	III (1:2:2)	8 vs. 14 vs. 16	2.7 vs. 3.1 vs. 4.2	24.5 vs. 16 vs. 34.5	9.8 vs. 8.0 vs. 9.4
(121)	CCNU + Galun	Galun	CCNU + P	NA	NA	158	II (2:1:1)	1 vs. 5 vs. 0	1.8 vs. 1.8 vs. 1.9	–	6.7 vs. 8.0 vs. 7.5

TABLE 2

Retrospective studies and clinical trials with nitrosourea in recurrent GBM (nitrosourea + bevacizumab combination studies are described in Table 4) (Continued)

Reference	Arm 1	Arm 2	Arm 3	Previous TMZ	Relapse	n	Phase	RR (%) Arm 1 vs. 2 vs. 3	PFS (months) Arm 1 vs. 2 vs. 3	PFS6 (%) Arm 1 vs. 2 vs. 3	OS (months) Arm 1 vs. 2 vs. 3
Retrospective studies											
(122)	PCV	–	–	4 pts	NA	63	Retrosp.	17.5	NA	29	7.7
(123)	PCV	–	–	12 pts	1st	86	Retrosp.	3.5	4.0	38.4	7.8
(124)	ACNU ± combination ^a	–	–	Yes	≥1st	32	Retrosp.	6.3	2.7	20	6.7
(125)	BCNU	–	–	24 pts	1st, 2nd, 4th	35	Retrosp.	6.2	2.6	13	5.1

ACNU, nimustine; BCNU, carmustine; CCNU, lomustine; CED, cediranib; ERL, erlotinib; FOT, fotemustine; Galun, galunisertib; IRI, irinotecan; NA, not available; OS, median overall survival; P, placebo; PCV, procarbazine-lomustine-vincristine; PFS, median progression-free survival; PFS6, 6-month PFS; Pts, patients; Retrosp., retrospective; RR, response rate; TMZ, temozolomide.

^aCombination with teniposide (n = 17) or cytarabine (n = 1).

Two phase II trials and a retrospective study assessed the efficacy of BCNU monotherapy regimens in rGBM (110, 118, 125). They reported a PFS6 and a median OS of 13.0–17.5% and 5.1–7.5 months, respectively. RRs were limited and no complete remission was observed. The predominant side effects were hematologic and long-lasting hepatic and pulmonary toxicity. Although BCNU regimens have shown similar efficacy to other cytotoxic therapies, toxicity can be substantial, and the patient recovers slowly, such that the administration of other drugs in the case of further tumor progression can be infeasible (110). BCNU was also evaluated in combination with other agents, such as irinotecan and TMZ, in two phase II studies, with a median OS of 7.8–11.7 months (115, 116). These data demonstrate that BCNU is an effective agent in the treatment of rGBM, but at present its use in clinical practice is limited.

In a small retrospective study, with 32 patients pretreated with TMZ, ACNU was given alone ($n = 14$) or in combination with teniposide ($n = 17$) or cytarabine ($n = 1$), yielding a PFS6 of 20% and a median OS of 6.7 months (124). Hematological toxicity was substantial (grade 3 or 4 in 50% of patients). Three phase II–III randomized trials compared lomustine as monotherapy with investigational agents, namely enzastaurin, cediranib, or galunisertib (119–121). In all three trials, the results were comparable between arms, pointing toward relevant activity of the control arm or lack of efficacy of the investigational agent. PFS6 ranged from 11 to 34.5%, median OS from 6.6 to 9.8 months, and observed RRs were low (0–16%). Four prospective phase II trials, using different schedules of administration, evaluated fotemustine in TMZ pretreated patients at first recurrence/relapse of GBM (111–114). These four studies, encompassing 160 patients, showed a PFS6 of 20.9–61% and a median OS of 6 to 11 months. The best efficacy and toxicity profile was obtained with a low-dose induction regimen (fotemustine 80 mg/m² on days 1, 15, 30, 45, and 60, followed by a 4-week rest period) ensued by a maintenance therapy (80 mg/m² every 4 weeks) in nonprogressive patients (114). However, these data were derived from phase II trials with a small sample of patients. Phase III studies are required to determine the efficacy and safety of fotemustine, in the treatment of rGBM, after TMZ. The efficacy of PCV (procarbazine–lomustine–vincristine) was described in two retrospective studies (122, 123). They included 149 patients, of whom 16 received previous TMZ treatment. Similar results were described, with PFS6 of 29–38.4% and a median OS of 7.7–7.8 months. As expected, grade 3/4 hematologic toxicity was the most common (26%); pulmonary fibrosis was not reported (123). There is also suggestion that MGMT promoter methylation may be predictive of responsiveness to this class of agents (7, 128). In summary, different nitrosoureas show comparable efficacy in monotherapy, remaining an option in the treatment of rGBM. However, their toxicity profile, particularly hematological, limits the combination with other agents, as well as a more widespread use.

TEMOZOLOMIDE MONOTHERAPY AND COMBINATION REGIMENS

In both trials leading to the approval of TMZ, the sdTMZ schedule was used (126, 127). Four other prospective single-arm trials, all without previous TMZ treatment, used the same schedule and reached similar results with a PFS6 rate of 21–32% and a median OS of 7.0–9.9 months (129–132). Table 3 reviews

TABLE 3
Retrospective studies and clinical trials with temozolomide in recurrent GBM (temozolomide + nitrosourea combination studies are described in Table 2)

Reference	Arm 1	Arm 2	Arm 3	Previous TMZ	Relapse	n	Phase	RR (%) Arm 1 vs. 2 vs. 3	PFS (months) Arm 1 vs. 2 vs. 3	PFS6 (%) Arm 1 vs. 2 vs. 3	OS (months) Arm 1 vs. 2 vs. 3
Single-arm monotherapy trials											
(126)	TMZ 5/28	–	–	No	1st	126	II	8	2.1	18	5.4
(129)	TMZ 5/28	–	–	No	2nd	22	II	23	NA	32	7.6
(130)	TMZ 5/28	–	–	No	2nd	42	II	19	NA	24	7.0
(133)	TMZ 42/70	–	–	No	NA	28	II	0	2.3	19	7.7
(134)	TMZ 7/14	–	–	No	1st, 2nd, 3rd	21	II	10	4.9	48	NA
(131)	TMZ 5/28	–	–	No	1st	13	Prospect.	NA	NA	21	NA
(135)	TMZ 21/28	–	–	No	1st	33	II	9	3.7	30	9.2
(136)	TMZ cont.	–	–	Yes	NA	12	Prospect.	17	6	58.3	11
(132)	TMZ 5/28	–	–	No	NA	19	Prospect.	24	2.2	22	9.9
(137)	TMZ 7/14	–	–	9 pts	NA	64	II	NA	5.5	43.8	NA
(138)	TMZ q12h for 28 days	–	–	No	≥1st	68	II	31	4.2	35	8.8
(139)	TMZ 21/28	–	–	Yes	NA	27	II	7	NA	0	5.1 ^a

Table continued on following page

TABLE 3 Retrospective studies and clinical trials with temozolomide in recurrent GBM (temozolomide + nitrosourea combination studies are described in Table 2) (Continued)

Reference	Arm 1	Arm 2	Arm 3	Previous TMZ	Relapse	n	Phase	RR (%) Arm 1 vs. 2 vs. 3	PFS (months) Arm 1 vs. 2 vs. 3	PFS6 (%) Arm 1 vs. 2 vs. 3	OS (months) Arm 1 vs. 2 vs. 3
RESCUE study (140)	TMZ cont.	—	—	Yes	1st	91	II	NA	NA (all), 3.6 (early), 1.8 (extended), 3.7 (rechallenge)	23.9 (all), 27.3 (early), 7.4 (extended), 35.7 (rechallenge)	9.3 (all)
(141)	TMZ cont.	—	—	Yes	1st	38	II	5	3.9	32.5	9.4
(142)	TMZ 21/28	—	—	Yes	1st	47	II	12.8	2.3	23	13
(143)	TMZ 7/14	—	—	Yes	1st	27	II	11.1	4.2	33.3	6.9
(144)	TMZ 21/28	—	—	Yes	1st	58	II	13	1.8	11	11.7
(145)	TMZ 7/14	—	—	Yes	≥1st	40	II	NA	1.8	10	5
Single-arm combination therapy trials											
(146)	TMZ + CIS	—	—	No	NA	20	II	10	4.9	35	NA
(147)	TMZ + CIS	—	—	No	1st	50	II	20.4	4.2	34	11.2
(148)	TMZ + Lipo. DOX	—	—	No	1st	22	II	18	3.6	32	8.2
(149)	TMZ + IRI	—	—	No	NA	91	I	12	2.6	27.3	NA
(150)	TMZ + O ⁶ -BG	—	—	Yes	NA	34	II	3	1.7	9	4.5
(151)	TMZ + INF- α	TMZ + PEG-INF- α 2b	—	No	NA	63	II ^b	12 vs. 3	3.6 vs. 4.4	31 vs. 38	7.2 vs. 10

TABLE 3 Retrospective studies and clinical trials with temozolomide in recurrent GBM (temozolomide + nitrosourea combination studies are described in Table 2) (Continued)

Reference	Arm 1	Arm 2	Arm 3	Previous TMZ	Relapse	n	Phase	RR (%) Arm 1 vs. 2 vs. 3	PFS (months) Arm 1 vs. 2 vs. 3	PFS6 (%) Arm 1 vs. 2 vs. 3	OS (months) Arm 1 vs. 2 vs. 3
(152)	TMZ + BVZ	-	-	NA	2nd, 3rd	15	I-II	NA	2.4	6.7	3.6
(153)	TMZ + Sorafenib	-	-	Yes	1st to 6th	32	II	3	1.5	9.4	9.6
(154)	TMZ + BVZ	-	-	Yes	1st, 2nd, 3rd	32	II	28	3.7	18.8	8.6
(155)	TMZ + BVZ	-	-	Yes	1st	32	II	40.6	4.2	21.9	7.3
(156)	TMZ + ABT- 414	-	-	NA	NA	18	I	22.2	NA	NA	NA
Randomized trials											
(127)	TMZ	PCZ	-	No	1st	225	II	5 vs. 5	2.8 vs. 1.9	21 vs. 8	NA
(157)	TMZ 5/28	TMZ 21/28	PCV	No	1st	330 ^c	II	NA	5.0 vs. 4.2 vs. 3.6 ^c	NA	8.5 vs. 6.6 vs. 6.7 ^c
(158)	TMZ + BVZ	BVZ + ETOP	-	Yes	NA	23	II	0 vs. 0	1.0 vs. 1.9	0 vs. 7.7	2.9 vs. 4.4
(159)	TMZ 21/28	Afatimb	TMZ 21/28 + Afatimb	Yes	1st	119	II	19 vs. 2.4 vs. 5	1.9 vs. 1 vs. 1.5	2.3 vs. 3 vs. 10	10.6 vs. 9.8 vs. 8
DIRECTOR trial (160)	TMZ 7/14	TMZ 21/28	-	Yes	1st	105	II	8 vs. 16	NA	17.1 vs. 25	9.8 vs. 10.6

Table continued on following page

TABLE 3 Retrospective studies and clinical trials with temozolomide in recurrent GBM (temozolomide + nitrosourea combination studies are described in Table 2) (Continued)

Reference	Arm 1	Arm 2	Arm 3	Previous TMZ	Relapse	n	Phase	RR (%) Arm 1 vs. 2 vs. 3	PFS (months) Arm 1 vs. 2 vs. 3	PFS6 (%) Arm 1 vs. 2 vs. 3	OS (months) Arm 1 vs. 2 vs. 3
Retrospective studies											
(161)	TMZ	–	–	Yes	1st, 2nd	9	Retrosp.	44.4	7.0	NA	12
(162)	TMZ + resection + MITOX	TMZ + resection	TMZ	No	1st	276	Retrosp.	NA	70.7 vs. 64 vs. 39.3	NA	11 vs. 8 vs. 5
(163)	TMZ (PD during TMZ)	TMZ (SD during TMZ)	–	Yes	1st	47	Retrosp.	0.0 vs. 17.2	NA	26.3 vs. 28.6	6.6 vs. 5.3
(164)	TMZ + CEL	–	–	24 pts	1st, 2nd	28	Retrosp.	10.7	4.2	43	16.8

ACNU, nimustine; BCNU, carmustine; CCNU, lomustine; CED, cediranib; CIS, cisplatin; cont., continuous; DOX, doxorubicin; ERL, erlotinib; FOT, fotemustine; Galun, galunisertib; IFN, interferon; IRI, irinotecan; Lipo, liposomal; MITOX, mitoxantrone; NA, not available; O⁶-BG, O⁶-benzylguanine; OS, median overall survival; P, placebo; PCV, procarbazine-lomustine-vincristine; PCZ, procarbazine; PD, progression disease; PFS, median progression-free survival; PFS6, 6-month PFS; Pts, patients; Retrosp., retrospective; RR, response rate; SD, stable disease; TMZ, temozolomide.

^aOS from all patients; 27 patients with glioblastoma, 15 with anaplastic astrocytoma, and 5 with miscellaneous brain tumors; OS of glioblastoma patients was not reported separately.

^bTwo single-arm phase II studies: one with short-acting (IFN) and another with long-acting (pegylated) interferon $\alpha 2b$.

^cTwo hundred and seventy-seven patients with glioblastoma, 53 with anaplastic astrocytoma, and 20 with miscellaneous brain tumors; data of glioblastoma patients was not reported separately.

TMZ-based trials in rGBM. Different schedules of TMZ were experimented to increase dose intensity, aimed at overcoming TMZ resistance by cumulative depletion of MGMT (165). The main alternative schedules were continuous low dose (40–50 mg/m² daily), 3 weeks on/1 week off (75–100 mg/m² for 21 days every 28 days), 1 week on/1 week off (150 mg/m² for 7 days every 14 days), but other dose-dense schedules are described (133–145). The toxicity profile did not vary between the different schemes. Besides the fact that the studies did not have a comparator arm, the heterogeneity in the inclusion criteria, regarding the number of recurrences and previous treatments, limits the comparison of efficacy data. The RESCUE phase II trial examined the best timing for TMZ rechallenge, by prospectively dividing the 91 GBM patients into three groups, according to the “TMZ-free interval”: early group (progression during the first six cycles of adjuvant TMZ); extended group (progression while receiving extended adjuvant TMZ, beyond the standard six cycles, but before completion of adjuvant treatment); and rechallenge group (progression after completion of adjuvant treatment and a treatment-free interval greater than 2 months). The “early” and “rechallenge” groups, respectively, showed comparable PFS6 rates of 27.3% and 35.7%, with median PFS of 3.6 and 3.7 months, experiencing most benefit than the “extended group” (PFS6 of 7.4%, median PFS of 1.8 months). The authors considered the possibility that the PFS6 results in the “early” group could be attributable to pseudoprogression (140).

Four randomized phase II clinical trials were conducted using single-agent TMZ (127, 159, 166, 167). A randomized trial comparing sdTMZ with procarbazine, in TMZ-naïve patients, revealed a PFS6 of 21% versus 8%, with a median OS 1.5 months longer in the TMZ arm (127). Brada et al. compared two different TMZ schedules with PCV, before TMZ became first-line standard, in patients with recurrent high-grade glioma (no separate data for GBM patients were provided) (166). In this trial, TMZ (both arms combined) did not display a clear benefit compared with PCV. It also showed that TMZ dose-intense regimens do not provide a survival or PFS benefit compared with standard doses, in the treatment of TMZ-naïve patients. The DIRECTOR trial compared two dose-dense regimens of TMZ (120 mg/m²/day, 1 week on/1 week off versus 80 mg/m²/day, 3 weeks on/1 week off), in patients with GBM at first progression, after TMZ chemoradiotherapy and at least two maintenance TMZ cycles (160). The outcome was comparable between arms regarding efficacy, safety, and tolerability. The most important result of this trial was the strong prognostic role of the MGMT promoter methylation status in patients rechallenged with TMZ. PFS6 was increased by 5.8-fold (39.7% in patients with methylated MGMT versus 6.9% in unmethylated tumours), and OS at 12 months by 2.4-fold. Also, a significantly improved outcome was demonstrated in patients with an interval above 2 months from previous TMZ, and largely confined to patients with MGMT methylated promoter (160). Wick et al. conducted a retrospective review of 80 patients with recurrent glioma (45 with GBM) rechallenged with various TMZ schedules (163). Upon progression, those who had stable disease and a TMZ-free interval of at least 8 weeks were treated with the same or an alternative regimen of TMZ; the group progressing under TMZ received an alternative regimen. The efficacy results were comparable between groups and no clear evidence of cumulative toxicity has emerged (163). Considering the small numbers of patients in most studies and the wide range of TMZ regimens tested, there was no evidence that one

metronomic schedule was superior over the other in terms of efficacy or safety. Numerous other studies evaluated TMZ-based combination regimens in rGBM but have failed to deliver conclusive efficacy beyond single-agent activity of TMZ. Those combination partners prospectively evaluated in single-arm designs were bevacizumab, interferon- α 2b, sorafenib, O6-benzylguanine, irinotecan, cisplatin, liposomal doxorubicine, and ABT-414 (146–156, 158).

BEVACIZUMAB MONOTHERAPY AND COMBINATION REGIMENS

The first documented use of bevacizumab in GBM was a small series of patients with rGBM treated by Stark-Vance et al. (Table 4) (168). The authors used the combination of bevacizumab with irinotecan, which showed activity, with acceptable toxicity profile. Several prospective phase II studies were subsequently conducted. Two phase II studies, by Vredenborg et al., using the same combination, achieved a RR of 57–60.9%, PFS6 rate of 30–46%, and a median OS of 9 to 10 months (171, 172). Previous reports on salvage therapy for rGBM showed inferior efficacy results, with RR of 5–10%, PFS6 rate of 9–25%, and median OS of 5 to 6 months (108, 202, 203). In 2009, FDA approved bevacizumab for patients with rGBM, based on the results of two phase II prospective studies (64, 65). However, in Europe, bevacizumab was not approved because of lack of a bevacizumab-free control arm. The BRAIN study, a phase II noncomparative trial, randomized patients to bevacizumab plus irinotecan or bevacizumab monotherapy (64). RR was 37.8 and 28.2% for the combination and monotherapy arms, respectively, and PFS6 was similar between the groups (50.3 and 42.6%), which compared favorably with historical controls. Numerous other retrospective studies addressing the combination of bevacizumab plus irinotecan described similar results (191–193, 196, 199, 201). Several phase II trials evaluated the combination of irinotecan with bevacizumab, and two trials added a third combination partner, cetuximab or carboplatin (171–173, 176, 178, 179). RR ranged from 25 to 60.9%, PFS6 between 28 and 46.5%, and median OS between 6.7 and 9.7 months. A retrospective analysis by Nghiemphu et al. compared two groups: one with bevacizumab in combination with different chemotherapy agents, and the other, a control group, without bevacizumab. The authors found a significant improvement in PFS ($P = 0.01$) and OS ($P = 0.04$) in favor of the group treated with bevacizumab (195).

Numerous studies have assessed bevacizumab in combination with other agents, namely etoposide, TMZ, fotemustine, dasatinib, temsirolimus, erlotinib, sorafenib, panobinostat, or vorinostat (154, 158, 175, 177, 179–181, 183, 184, 187–189). In randomized trials involving two arms—one with bevacizumab in combination with experimental agents (irinotecan, carboplatin, vorinostat, or dasatinib) and the other with bevacizumab alone—it was found that both arms showed comparable efficacy, leading to the conclusion of poor efficacy of the experimental agent, without valid evidence regarding the single-agent activity of bevacizumab. A recent Dutch, open-label, three-group multicenter phase II trial (BELOB) reported promising results with bevacizumab combined with lomustine (128). Improved OS at 9 months (59% vs. 43% vs. 38%) and PFS6 (41% vs. 13% vs. 16%) were seen in the combination arm compared with single-agent lomustine and single-agent bevacizumab, respectively. Effectively, this was the first trial

TABLE 4 Retrospective studies and clinical trials with bevacizumab in recurrent GBM

Reference	Arm 1	Arm 2	Arm 3	Relapse	n	Phase	RR (%)		PFS (months)		OS (months)	
							Arm 1 vs. 2	vs. 3	Arm 1 vs. 2	vs. 3	Arm 1 vs. 2	vs. 3
Single-arm monotherapy trials												
(65)	BVZ	-	-	1st	48	II	35		3.7	29	7.2	
(169)	BVZ	-	-	≥1st	50	II	24.5		-	25	6.5	
(170)	BVZ	-	-	1st	29	II	27.6		3.3	33.9	10.5	
Single-arm combination therapy trials												
(171)	BVZ + IRI	-	-	NA	35	II	57.0		5.5	46.0	9.7	
(172)	BVZ + IRI	-	-	NA	23	II	60.9		4.6	30	9.2	
(173)	BVZ + IRI	-	-	NA	57	II	37		-	-	-	
(174)	BVZ + IRI	-	-	1st to 6th	37	Prospect.	63.9		5.0	44.3	9.0	
(175)	BVZ + ETOP	-	-	1st, 2nd, 3rd	27	II	23		-	44.4	10.7	
(176)	BVZ + IRI + CETUX	-	-	1st	32	II	26		-	33	6.7	
(177)	BVZ + Erlotinib	-	-	1st, 2nd, 3rd	25	II	50		-	29.2	10.5	
(178)	BVZ + IRI	-	-	NA	32	II	25		5.2	28	7.9	
(179)	BVZ + IRI + CARBO	-	-	1st, 2nd, 3rd	40	II	33		-	46.5	8.3	
(154)	BVZ + TMZ	-	-	1st, 2nd, 3rd	32	II	28		3.7	18.8	8.6	

Table continued on following page

TABLE 4 Retrospective studies and clinical trials with bevacizumab in recurrent GBM (Continued)

Reference	Arm 1	Arm 2	Arm 3	Relapse	n	Phase	RR (%)		PFS (months)		PFS6 (%)		OS (months)
							Arm 1 vs. 2	vs. 3	Arm 1 vs. 2	vs. 3	Arm 1 vs. 2	vs. 3	
(180)	BVZ + Tem	-	-	NA	13	II	0		1.8		-		3.5
(181)	BVZ + Sora	-	-	NA	54	II	18.5		2.9		20.4		5.6
(182)	BVZ + FOT	-	-	1st	54	II	52		5.2		42.6		9.1
(183)	BVZ + Pano	-	-	1st, 2nd	24	II	29.2		5.0		30.4		9.0
(184)	BVZ + VOR	-	-	NA	40	II	22.5		-		30		10.4
Randomized trials													
(64)	BVZ	BVZ + IRI	-	1st, 2nd	167	II	28.2 vs. 37.8		4.2 vs 5.6		42.6 vs. 50.3		9.2 vs. 8.7
(152)	BVZ + TMZ	-	-	2nd, 3rd	15	I-II	NA		2.4		6.7		3.6
(158)	BVZ + TMZ	BVZ + ETOP	-	NA	23	II	0 vs. 0		-		0 vs. 7.7		2.9 vs. 4.4
BELOB trial (128)	BVZ	CCNU	BVZ + CCNU 110/90	1st	148	II	38 vs. 5 vs. 63/34		3.0 vs. 1.0 vs. 11.0/4.0		16 vs. 13 vs. 50/41		8 vs. 8 vs. 16/11
(185)	BVZ	BVZ + CCNU	-	1st, 2nd, 3rd	68	II	-		4.1 vs. 4.3		-		Pts with 1st relapse: 8.8 vs. 13.1
(186)	BVZ	BVZ + CARBO	-	1st	110	II	6 vs. 14		3.5 vs. 3.5		18 vs. 15		7.5 vs. 6.9
(187)	BVZ	BVZ + VOR	-	1st	90	II	-		3.6 vs. 4.2		-		7.0 vs. 8.3
(188)	BVZ + P	BVZ + Dasa	-	NA	121	II (1:2)	26.5 vs. 18.3		-		18.4 vs. 27.2		7.9 vs. 7.2
(155)	BVZ + TMZ	-	-	1st	32	II	40.6		4.2		21.9		7.3
(189)	BVZ + CCNU	CCNU	-	1st	437	III (2:1)	-		4.2 vs. 1.5		-		9.1 vs. 8.6

TABLE 4
Retrospective studies and clinical trials with bevacizumab in recurrent GBM
 (Continued)

Reference	Arm 1	Arm 2	Arm 3	Relapse	n	Phase	RR (%)		PFS (months)		PFS6 (%)		OS (months)	
							Arm 1 vs. 2	vs. 3	Arm 1 vs. 2	vs. 3	Arm 1 vs. 2	vs. 3	Arm 1 vs. 2	vs. 3
Retrospective studies														
(168)	BVZ + IRI	-	-	NA	21	Retrosp.	42.9 ^b	-	-	-	-	-	-	-
(190)	BVZ + IRI or CARBO or ETOP	-	-	1st to 6th	14	Retrosp.	40 ^a	-	-	-	-	-	-	-
(191)	BVZ + IRI	-	-	1st to 5th	13	Retrosp.	77	-	-	-	-	-	6.3	-
(192)	BVZ + IRI	-	-	1st to 10th	27	Retrosp.	-	3.8	17	7.1	7.0 ^b	-	-	-
(193)	BVZ + IRI	-	-	≥1st	20	Retrosp.	47.4 ^b	4.2 ^b	25 ^b	42 ^a	-	-	-	-
(194)	BVZ + IRI or CARBO or CCNU or ETOP	-	-	1st to 7th	55	Retrosp.	34.1 ^b	-	-	-	-	-	-	-
(195)	BVZ + IRI or CARBO or CCNU or ETOP	Control group (various drugs with no BVZ)	-	1st to 3rd	20	Retrosp.	-	4.3 vs. 1.8 ^a	41 vs. 18 ^a	9.0 vs. 6.1 ^a	-	-	-	-
(196)	BVZ + IRI	-	-	≥1st	51	Retrosp.	67.6	7.6	63.7	11.5	-	-	-	-

Table continued on following page

TABLE 4
Retrospective studies and clinical trials with bevacizumab in recurrent GBM
 (Continued)

Reference	Arm 1	Arm 2	Arm 3	Relapse	n	Phase	RR (%)		PFS (months)		OS (months)
							Arm 1 vs. 2	vs. 3	Arm 1 vs. 2	vs. 3	
(171)	BVZ + CARBO or IRI or BCNU or CCNU or Erlotinib or ETOP	–	–	2nd (after BVZ)	54	Retrosp.	0 ^a	–	–	2 ^b	–
(172)	BVZ + CARBO + ETOP	–	–	1st to 5th	6	Retrosp.	83	–	–	22	7.0
(197)	BVZ	–	–	1st, 2nd	50	Retrosp.	42	–	–	42	8.5
(198)	BVZ	BVZ + IRI or CARBO or TMZ	–	2nd, 3rd	24	Retrosp.	50 vs. 19 ^a	–	–	0 vs. 14 ^a	1.5 vs. 5.2 ^a
(199)	BVZ + IRI	–	–	1st to 5th	93	Retrosp.	56	5.1	42	42	8.8
(200)	BVZ ± IRI or CARBO	–	–	2nd, 3rd	14	Retrosp.	29 ^a	4.0 ^a	29 ^a	29 ^a	7.8 ^a
(201)	BVZ + IRI	PCV	–	1st	60	Retrosp.	66.0 vs 11.0	5.0 vs. 3.0	–	–	9.0 vs. 5.0

BCNU, carmustine; BVZ, bevacizumab; CARBO, carboplatin; CETUX, cetuximab; CCNU, lomustine; Dasa, Dasatinib; EVE, everolimus; ETOP, etoposide; FOI, fotemustine; IRI, irinotecan; NA, not available; OS, median overall survival; P, placebo; Pano, Panobinostat; PCV, procarbazine-lomustine-vincristine; PFS, median progression-free survival; PFS6, 6-month PFS; Pts, patients; Retros., retrospective; RR, response rate; Sora, Sorafenib; Tem, temsirolimus; TMZ, temozolomide; VOR, vorinostat.

^aFor overall group. ^bIncludes patients with GBM and other high-grade gliomas.

with bevacizumab in rGBM to demonstrate an improvement in a primary OS endpoint, suggesting increased effectiveness with the combination of bevacizumab and lomustine versus each of these agents alone. Therefore, a randomized phase III trial was performed, comparing bevacizumab–lomustine with single-agent lomustine (189). Unfortunately, a benefit in OS was not observed, while the improvement in PFS for the combination arm was maintained. A crossover to bevacizumab occurred in 35.5% of patients, which may account for these results. To evaluate the efficacy of bevacizumab beyond the second-line treatment, Piccioni et al. performed a retrospective analysis of 468 GBM patients treated at different recurrences (first, second, third, or more), including 80 who were treated upfront. The authors found that PFS and OS were similar for all three recurrence groups (median 4.1 and 9.8 months, respectively) (204). These data suggest that bevacizumab could have a role in the treatment of GBM independent of the line of therapy, and that a deferred use of bevacizumab seems not to decrease effectiveness. When comparing the results of available phase II trials on bevacizumab, alone or in combination with irinotecan, with those of standard cytotoxic chemotherapy, in rGBM, several findings are clear: bevacizumab alone has activity and increases RR, PFS6, and median PFS; on the other hand, the impact on OS is less clear.

Tumor-Treating Electric Fields for Glioblastoma

CONCEPT

Tumor-Treating Fields (TTFields) has been called the “fourth cancer treatment modality,” after surgery, RT, and pharmacotherapy. It’s a locoregionally antimetabolic treatment that delivers low-intensity, intermediate-frequency (200 kHz), alternating electric fields, through four transducer arrays, consisting of nine insulated electrodes applied to the shaved scalp and connected to a portable device (11). *In vitro* studies have shown that TTFields arrests cell division and kills tumor cells through multiple mechanisms, namely, misalignment of microtubule subunits during division, aberrant chromosomal segregation, and cytoplasmic blebbing during anaphase.

CLINICAL TRIALS

Clinical effectiveness and feasibility of TTFields was first tested in 10 patients with rGBM, with PFS6 and median survival doubling that of historic controls (205).

Two pivotal randomized trials studied TTFields in rGBM (EF-11) and nGBM (EF-14).

In EF-11 trial, a total of 237 rGBM patients, after initial treatment with RT-TMZ, were randomized 1:1 to either the novel TTFields therapy (120 patients) or to treatment according to investigator’s choice (117 patients). Although EF-11 did not meet its primary endpoint of improving OS, similar median OS, and PFS in both arms, it established TTFields as noninferior to chemotherapy (206). In addition, the favorable QoL and toxicity profile led to FDA approval, in 2011, of TTFields as a therapeutic option for use in rGBM. The EF-14 trial, an open-label phase 3 study, enrolled 695 patients and evaluated the efficacy and safety of

TTFields in combination with TMZ maintenance treatment, after chemoradiation therapy for patients with nGBM. The trial was terminated based on the results of the preplanned interim analysis that evaluated the outcomes of the first 315 patients and showed a significant improvement in PFS and OS. The percentage of patients alive at 2 years was 43% in the TTFields/TMZ group and 29% in the TMZ alone group ($P = 0.006$) (207). In October 2015, the FDA approved TTFields for use in nGBM patients. National Comprehensive Cancer Network has further incorporated TTFields in their updated guidelines (208).

ISSUES

TTFields are particularly safe, since no additional systemic toxicity was observed with the addition of this technology. The most common side effects are mild to moderate skin reactions beneath the transducer arrays, observed in 44% of patients, and grade 3 skin reactions in 1–2 % of patients. Additional research is warranted, in order to identify which patients are most likely to be responsive to TTFields. Benefit was present across all subgroups studied (according to age, PS, MGMT methylation status, and EOR), but the follow-up remains short, and some subsets are rather small in number. Detailed subgroup analyses are to be performed on the final and validated dataset. Although approximately three-quarters of patients, in EF-14, had a treatment compliance of 75%, this is an important issue unique to this therapy, since it requires >18 h of usage per day. Another important point is the high cost of this therapeutic approach (about \$20,000 monthly). Strong price regulation by health authorities could make this technology more affordable and consequently accessible to patients (209). TTFields plus TMZ represents the first major advance in the field of GBM therapy in roughly a decade, and it should be considered for patients with nGBM and no contraindications.

Although showing significant improvements in survival, the results still underscore that the majority of patients did not survive beyond 2 years, highlighting the need for additional improvements in GBM therapeutic strategies. Due to its unique and localized mechanism of action, and general absence of systemic toxicity, TTFields is particularly well suited for combination therapies, such as immunotherapy and targeted therapies (210).

Glioblastoma in the Elderly

GBM is diagnosed at a median age of 64 years, and the incidence peaks between 75 and 84 years (15.24/100,000) (211). With aging population, this incidence is expected to increase. The poor survival rates associated with GBM (about 5% at 5 years) get even poorer in patients over 65 years (less than 2.1% at 5 years) (212). Age has long been recognized as the most important prognostic factor. Elderly patients tend to have more comorbidities and worse PS than their younger counterparts diagnosed with GBM. Similarly, their tumors seldom have favorable molecular features (IDH mutations occur in less than 2% of the tumors) (213). As a result, these patients have frequently been undertreated and underrepresented in clinical trials.

SURGERY

Several retrospective studies have shown an increase in OS, in elderly patients submitted to surgical resection (as opposed to biopsy) (206, 214–216). In the study by Keime-Guibert, and in the NOA-08 and the Nordic trials, the EOR was identified as an independent prognostic factor. As such, age alone should not preclude an attempt at complete resection (8, 206, 217).

RADIOTHERAPY

RT was associated with a statistically significant, although modest, gain in OS, when compared to best supportive care (BSC), in patients aged over 70 years (206). The study was interrupted after the first interim analysis due to superiority of RT. There was no difference between the two groups, regarding QoL and NCF. Roa et al. compared hypofractionated RT (HFRT; 40 Gy in 15 fractions over 3 weeks) with cfRT (60 Gy in 30 fractions over 6 weeks) in 100 patients aged 60 years or older (218). There was no difference in OS between the two groups and the patients treated with HFRT required less increment in post-therapy corticosteroid dose (23% vs. 49%; $P = 0.02$). Although the study could not show that the two treatments were equivalent, together these results led to the adoption of HFRT as a valid option in the treatment of elderly patients, particularly those with a poor PS.

CHEMOTHERAPY

In an ANOCEF phase II trial, 70 patients aged 70 years or older, with a KPS under 70%, received sdTMZ until disease progression (219). The 25 weeks median OS compared favorably with the 12–16 weeks expected with BSC alone. Furthermore, there was an improvement in functional status in 33% of patients. Patients with MGMT promoter methylation had longer PFS and OS. A previous study by Chinot and colleagues had shown similar survival results (220).

CHEMOTHERAPY AND RADIOTHERAPY

The 5-year analysis of the hallmark study by Stupp et al. (3) showed a survival benefit for the combination in all subgroups, including patients aged over 60 years, RPA class V, and unmethylated MGMT promoter (211). However, an analysis by age strata showed a diminishing benefit of TMZ association with increasing age, especially in patients older than 65 years (221). Caution should be made in interpreting these results as the group over the age of 65 years represented only 15% of the study population. The 2014 EANO guidelines reflected this concern by including the multimodality treatment as an option for fit elderly patients (9). A retrospective analysis of 293 patients over the age of 65 showed a benefit for the combined regimen (222). A retrospective survey of the National Cancer Database yielded similar results, with combined modality treatment showing superiority over both chemotherapy alone and RT alone, in a group of 16,717 patients, with nGBM, aged 65 years or older (223). Two prospective randomized studies addressed the question of which single modality treatment would be best for

elderly patients. In the Nordic trial, patients over the age of 60, with ECOG PS 0-3, were randomized between three treatment arms: sdTMZ (up to six cycles), HFRT (34.0 Gy administered in 3.4 Gy fractions over 2 weeks), and cfRT (217). Fewer patients completed the course of RT in the standard group (72%) compared to the hypofractionated one (95%), which may partly account for the poor results obtained in the former group. TMZ and HFRT yielded similar survival results and, particularly in patients over the age of 70, these were significantly better than the ones for cfRT. MGMT promoter methylation was predictive of response to TMZ. In the NOA-08 trial, patients older than 65 years, with a KPS >50%, were randomized to receive TMZ (100 mg/m², given on days 1–7 of 1 week on, 1 week off cycles) or cfRT (8). The trial showed noninferiority of TMZ and there were no differences regarding QoL either, between the treatment arms. MGMT promoter methylation was both prognostic and predictive of response to TMZ. Event-free survival was longer in patients with methylated MGMT promoter treated with TMZ than in those submitted to RT (8.4 vs. 4.6 months) and the opposite was true for the group of patients with an unmethylated promoter (3.3 vs. 4.6 months). Taken together, these results support the role of MGMT promoter methylation in the choice of single modality treatment, in elderly patients with nGBM.

The EORTC 26062-22061 trial was designed to assess whether the addition of TMZ to HFRT would translate into a survival benefit (224). A total of 562 patients, aged 65 years or older, were randomized, with the combined modality being associated with a longer median OS (9.3 vs. 7.6 months; $P < 0.001$) and PFS. Again, MGMT promoter methylation was predictive of response to TMZ (median OS: 13.5 months with RT-TMZ vs. 7.7 months with RT alone; $P < 0.001$). Although not reaching statistical significance, the combined therapy also offered a survival advantage to the group with an unmethylated MGMT status (median OS: 10.0 months vs. 7.9 months; $P = 0.055$). QoL was similar in both study groups. An unsolved question is which RT-TMZ scheme is better for fit elderly patients. Some retrospective studies have addressed this issue. Arvold and colleagues found no differences in OS, between cfRT-TMZ and HFRT-TMZ, after adjusting for selection bias (225). Minitti also found no differences in OS and PFS between the two groups (226). However, cfRT-TMZ was associated with more neurologic toxicity ($P = 0.01$), lowering of KPS scores over time ($P = 0.01$), and higher post-treatment dosing of corticosteroid ($P = 0.02$). There are numerous issues that make this a special and challenging group. The definition of elderly varies widely between studies limiting the extrapolation of results to our patients' population. Several trials lack NCF and QoL evaluations necessary for us to understand the real impact of the current available therapies in the elderly patient. The assessment of MGMT promoter methylation, although proven useful in this population, is not readily available to all. Furthermore, these patients are frequently only submitted to biopsy, which may render insufficient samples to MGMT promoter status determination.

Elderly patients with GBM have a worse prognosis than their younger counterparts. This relates to several factors, namely, poorer PS, comorbidities, delay in diagnosis (symptoms are often interpreted as signs of depression or dementia), and IDH wild-type tumors. These patients tend to be undertreated solely based on their biological age and because, they are underrepresented in clinical trials, there's a paucity of data guiding clinical decisions. Based on prospective trials, HFRT has

become standard in this population and proven equivalent to TMZ, and MGMT promoter methylation status has a paramount importance in the choice of single modality therapy. In addition, there's now evidence that the addition of TMZ to HFRT yields an increase in OS, representing an alternative to the Stupp regimen, in elderly patients with a good PS.

Supportive Care

The patient with GBM is, simultaneously, a patient with cancer and one with a progressive neurological disease. As such, there are certain specificities regarding not only the most frequent symptoms exhibited but also some end-of-life (EOL) care issues. Patients with primary brain tumors were found to have poorer PS, higher levels of nursing and social support, and more family overburden than other palliative care patients. Disorientation and confusion were also more frequent. Conversely, general EOL symptoms, such as dyspnoea, nausea, vomiting, anorexia, constipation, and pain, were experienced less frequently (227). Palliative care should aim at improving QoL, both for the patient and the caregiver, and is not limited to the EOL stage. The timing of its introduction, in the management of GBM patients, is an understudied issue. The experience with metastatic nonsmall cell lung cancer indicates improvements in QoL, mood, and symptom burden, as well as better EOL care and even extended survival, with early initiation of palliative care (228). Disease itself, along with GBM treatment side effects and symptomatic medication (namely antiepileptic drugs), affects cognition and impairs decision-making, very often early in the disease course (229, 230). As such, timely involvement of the patient in treatment decisions (including supportive measures ahead) is of paramount importance. Two systematic reviews of studies addressing the EOL phase, in high-grade gliomas, showed a high burden of symptoms, namely reduced consciousness (44–90%), dysphagia (10–85%), headache (36–62%), seizures (10–56%), focal neurological deficits (>50%), cognitive disturbances (>30%), confusion (15–51%), and poor communication (64–90%) (227, 231–236).

SEIZURES

Approximately 30% of glioma patients have a seizure during the last week of life, regardless of having or not having a history of seizures (235, 237). As mentioned earlier, prophylactic use of anticonvulsant drugs is not indicated in patients without history of seizures (12). Enzyme inducers antiepileptic drugs should be avoided as they interact with commonly used cytotoxic agents and dexamethasone, having the potential to reduce their efficacy (238). Valproic acid is an enzyme inhibitor that may increase therapeutic levels of antineoplastic agents. Several reports also suggest a direct antitumor effect, but this is yet to be proven (239). Levetiracetam is the most studied of the recent anticonvulsants in this setting. It appears safe without major interactions with the commonly used drugs (240). At the EOL, dysphagia and altered consciousness are common and impair the administration of oral medication. As a result, half of the patients taper antiepileptic drugs in the last week of life, with one-third experiencing seizures (237).

As the occurrence of seizures is associated with nonpeaceful death, it is important to maintain antiepileptic treatment throughout the EOL phase (231). This can be achieved by using alternative routes of administration. For patients in home care, rectal diazepam and buccal or intranasal midazolam are convenient alternatives (241).

DEPRESSION

Diagnosis can be difficult as all the symptoms of a major depressive disorder, with the exception of suicidal thoughts, can be attributed to the tumor, its treatment, or both (242). Selective serotonin reuptake inhibitors may be considered as first-line treatment of depression, as they have not shown increased toxicity in glioma patients and they are not associated with increased incidence of seizures in the general population (242, 243). The benefit and feasibility of psychotherapy in treating depression and anxiety in glioma patients is uncertain (242).

RAISED INTRACRANIAL PRESSURE

Raised intracranial pressure, as a result of tumor growth and cerebral edema, can cause headache, nausea, vomiting, somnolence, and visual disturbances. Corticosteroids are the treatment of choice. Dexamethasone is often used for its long half-life, anti-inflammatory activity, and absence of mineralocorticoid effect (244). Corticosteroids must be tapered as soon as possible and kept in the lowest dose capable of controlling symptoms. Attention must be given to the complications associated with prolonged steroid use.

CONFUSION

Confusion is a major cause of distress for the patient and his caregivers. It can arise from the tumor itself, or be caused by pain, infection, metabolic imbalances, symptomatic treatments, fecaloma, bladder retention, intracranial hemorrhage, or seizures (244). Neuroleptics, such as haloperidol, risperidone, and olanzapine, are often needed. Opioids and sedatives are also options if pain or sleep and behavioral disorders coexist.

ISSUES AT EOL CARE

During the EOL phase, dysphagia and altered consciousness will impair nutrition and hydration, and the administration of symptomatic medication, namely, corticosteroids and anticonvulsants. As mentioned before, these last ones should be kept, but steroids are often tapered and discontinued in the last days of life, when the patient is already unconscious, to avoid futile prolongation of life. Maintenance or withdrawal of artificial nutrition and hydration and symptomatic medications are EOL decisions common to all glioma patients. Another topic that can be discussed with the patient in advance is palliative sedation. Between 13 and 45% of patients were reported to have received it. Refractory seizures, agitation, and delirium are among the reasons that lead to its institution (245). The knowledge on palliative care in glioma patients is largely based on retrospective studies and

on extrapolations from studies performed on other cancer patients. Properly conducted prospective and interventional investigations, specifically designed for glioma patients, addressing the specificities of this population are needed.

Conclusion

Despite maximal safe surgical resection and combined chemotherapy and RT, GBM retains a poor prognostic value. To date, excluding TTFields, no new agents improve survival when added to standard therapy. Although MGMT promoter methylation is predictive of response to TMZ, its role in the choice of first-line therapy is currently limited to the elderly GMB patients. No standard of care is established in the recurrent setting. Bevacizumab clearly impacts PFS, although its role in OS is less certain. TMZ rechallenge is a treatment option, especially for MGMT promoter-methylated rGBM. All in all, while efforts are being put in strategies to prolong OS, enhancing QoL for these patients must be a priority.

Conflict of interest: The authors declare no potential conflicts of interest with respect to research, authorship, and/or publication of this manuscript.

Copyright and permission statement: We confirm that the materials included in this chapter do not violate copyright laws. Where relevant, appropriate permissions have been obtained from the original copyright holder(s). All original sources have been appropriately acknowledged and/or referenced.

References

1. Thakkar JP, Dolecek TA, Horbinski C, Ostrom QT, Lightner DD, Barnholtz-Sloan JS, et al. Epidemiologic and molecular prognostic review of glioblastoma. *Cancer Epidemiol Biomarkers Prev*. 2014;23(10):1985–96. <http://dx.doi.org/10.1158/1055-9965.EPI-14-0275>
2. Gilbert MR, Wang M, Aldape KD, Stupp R, Hegi ME, Jaeckle KA, et al. Dose-dense temozolomide for newly diagnosed glioblastoma: A randomized phase III clinical trial. *J Clin Oncol*. 2013;31(32):4085–91. <http://dx.doi.org/10.1200/JCO.2013.49.6968>
3. Stupp R, Mason WP, van den Bent MJ, Weller M, Fisher B, Taphoorn MJ, et al. Radiotherapy plus concomitant and adjuvant temozolomide for glioblastoma. *N Engl J Med*. 2005;352(10):987–96. <http://dx.doi.org/10.1056/NEJMoa043330>
4. Chinot OL, Wick W, Mason W, Henriksson R, Saran F, Nishikawa R, et al. Bevacizumab plus radiotherapy-temozolomide for newly diagnosed glioblastoma. *N Engl J Med*. 2014;370(8):709–22. <http://dx.doi.org/10.1056/NEJMoa1308345>
5. Gilbert MR, Dignam JJ, Armstrong TS, Wefel JS, Blumenthal DT, Vogelbaum MA, et al. A randomized trial of bevacizumab for newly diagnosed glioblastoma. *N Engl J Med*. 2014;370(8):699–708. <http://dx.doi.org/10.1056/NEJMoa1308573>
6. Esteller M, Gaidano G, Goodman SN, Zagonel V, Capello D, Botto B, et al. Hypermethylation of the DNA repair gene O(6)-methylguanine DNA methyltransferase and survival of patients with diffuse large B-cell lymphoma. *J Natl Cancer Inst*. 2002;94(1):26–32. <http://dx.doi.org/10.1093/jnci/94.1.26>
7. Esteller M, Garcia-Foncillas J, Andion E, Goodman SN, Hidalgo OF, Vanaclocha V, et al. Inactivation of the DNA-repair gene MGMT and the clinical response of gliomas to alkylating agents. *N Engl J Med*. 2000;343(19):1350–4. <http://dx.doi.org/10.1056/NEJM200011093431901>

8. Wick W, Platten M, Meisner C, Felsberg J, Tabatabai G, Simon M, et al. Temozolomide chemotherapy alone versus radiotherapy alone for malignant astrocytoma in the elderly: The NOA-08 randomised, phase 3 trial. *Lancet Oncol.* 2012;13(7):707–15. [http://dx.doi.org/10.1016/S1470-2045\(12\)70164-X](http://dx.doi.org/10.1016/S1470-2045(12)70164-X)
9. Weller M, van den Bent M, Hopkins K, Tonn JC, Stupp R, Falini A, et al. EANO guideline for the diagnosis and treatment of anaplastic gliomas and glioblastoma. *Lancet Oncol.* 2014;15(9):e395–403. [http://dx.doi.org/10.1016/S1470-2045\(14\)70011-7](http://dx.doi.org/10.1016/S1470-2045(14)70011-7)
10. Weller M, Cloughesy T, Perry JR, Wick W. Standards of care for treatment of recurrent glioblastoma—Are we there yet? *Neuro Oncol.* 2013;15(1):4–27. <http://dx.doi.org/10.1093/neuonc/nos273>
11. Hottinger AF, Pacheco P, Stupp R. Tumor treating fields: A novel treatment modality and its use in brain tumors. *Neuro Oncol.* 2016;18(10):1338–49. <http://dx.doi.org/10.1093/neuonc/now182>
12. Glantz MJ, Cole BF, Forsyth PA, Recht LD, Wen PY, Chamberlain MC, et al. Practice parameter: Anticonvulsant prophylaxis in patients with newly diagnosed brain tumors. Report of the Quality Standards Subcommittee of the American Academy of Neurology. *Neurology.* 2000;54(10):1886–93. <http://dx.doi.org/10.1212/WNL.54.10.1886>
13. Wolbers JG. Novel strategies in glioblastoma surgery aim at safe, supra-maximum resection in conjunction with local therapies. *Chin J Cancer.* 2014;33(1):8–15. <http://dx.doi.org/10.5732/cjc.013.10219>
14. Li YM, Suki D, Hess K, Sawaya R. The influence of maximum safe resection of glioblastoma on survival in 1229 patients: Can we do better than gross-total resection? *J Neurosurg.* 2016;124(4):977–88. <http://dx.doi.org/10.3171/2015.5.JNS142087>
15. Sanai N, Polley MY, McDermott MW, Parsa AT, Berger MS. An extent of resection threshold for newly diagnosed glioblastomas. *J Neurosurg.* 2011;115(1):3–8. <http://dx.doi.org/10.3171/2011.2.JNS10998>
16. Lacroix M, Abi-Said D, Fourney DR, Gokaslan ZL, Shi W, DeMonte F, et al. A multivariate analysis of 416 patients with glioblastoma multiforme: Prognosis, extent of resection, and survival. *J Neurosurg.* 2001;95(2):190–8. <http://dx.doi.org/10.3171/jns.2001.95.2.0190>
17. Sanai N, Berger MS. Intraoperative stimulation techniques for functional pathway preservation and glioma resection. *Neurosurg Focus.* 2010;28(2):E1. <http://dx.doi.org/10.3171/2009.12.FOCUS09266>
18. Chaichana KL, Jusue-Torres I, Navarro-Ramirez R, Raza SM, Pascual-Gallego M, Ibrahim A, et al. Establishing percent resection and residual volume thresholds affecting survival and recurrence for patients with newly diagnosed intracranial glioblastoma. *Neuro Oncol.* 2014;16(1):113–22. <http://dx.doi.org/10.1093/neuonc/not137>
19. Grabowski MM, Recinos PF, Nowacki AS, Schroeder JL, Angelov L, Barnett GH, et al. Residual tumor volume versus extent of resection: Predictors of survival after surgery for glioblastoma. *J Neurosurg.* 2014;121(5):1115–23. <http://dx.doi.org/10.3171/2014.7.JNS132449>
20. Pallud J, Rigaux-Viode O, Corns R, Muto J, Lopez Lopez C, Mellerio C, et al. Direct electrical bipolar electrostimulation for functional cortical and subcortical cerebral mapping in awake craniotomy. Practical considerations. *Neurochirurgie.* 2017 Jun;63(3):164–174. <http://dx.doi.org/10.1016/j.neuchi.2016.08.009>
21. Mueller WM, Yetkin FZ, Hammeke TA, Morris GL, 3rd, Swanson SJ, Reichert K, et al. Functional magnetic resonance imaging mapping of the motor cortex in patients with cerebral tumors. *Neurosurgery.* 1996;39(3):515–20; discussion 20–1. <http://dx.doi.org/10.1227/00006123-199609000-00015>
22. Szelenyi A, Bello L, Duffau H, Fava E, Feigl GC, Galanda M, et al. Intraoperative electrical stimulation in awake craniotomy: Methodological aspects of current practice. *Neurosurg Focus.* 2010;28(2):E7. <http://dx.doi.org/10.3171/2009.12.FOCUS09237>
23. De Witt Hamer PC, Robles SG, Zwinderman AH, Duffau H, Berger MS. Impact of intraoperative stimulation brain mapping on glioma surgery outcome: A meta-analysis. *J Clin Oncol.* 2012;30(20):2559–65. <http://dx.doi.org/10.1200/JCO.2011.38.4818>
24. Panciani PP, Fontanella M, Garbossa D, Agnoletti A, Ducati A, Lanotte M. 5-aminolevulinic acid and neuronavigation in high-grade glioma surgery: Results of a combined approach. *Neurocirugia (Astur).* 2012;23(1):23–8. <http://dx.doi.org/10.1016/j.neucir.2012.04.003>
25. Senders JT, Muskens IS, Schnoor R, Karhade AV, Cote DJ, Smith TR, et al. Agents for fluorescence-guided glioma surgery: A systematic review of preclinical and clinical results. *Acta Neurochir (Wien).* 2017;159(1):151–67. <http://dx.doi.org/10.1007/s00701-016-3028-5>

26. Stummer W, Pichlmeier U, Meinel T, Wiestler OD, Zanella F, Reulen HJ, et al. Fluorescence-guided surgery with 5-aminolevulinic acid for resection of malignant glioma: A randomised controlled multicentre phase III trial. *Lancet Oncol.* 2006;7(5):392–401. [http://dx.doi.org/10.1016/S1470-2045\(06\)70665-9](http://dx.doi.org/10.1016/S1470-2045(06)70665-9)
27. Eljamel MS, Goodman C, Moseley H. ALA and Photofrin fluorescence-guided resection and repetitive PDT in glioblastoma multiforme: A single centre Phase III randomised controlled trial. *Lasers Med Sci.* 2008;23(4):361–7. <http://dx.doi.org/10.1007/s10103-007-0494-2>
28. Stummer W, Tonn JC, Mehdorn HM, Nestler U, Franz K, Goetz C, et al. Counterbalancing risks and gains from extended resections in malignant glioma surgery: A supplemental analysis from the randomized 5-aminolevulinic acid glioma resection study. *Clinical article. J Neurosurg.* 2011;114(3):613–23. <http://dx.doi.org/10.3171/2010.3.JNS097>
29. Young RM, Jamshidi A, Davis G, Sherman JH. Current trends in the surgical management and treatment of adult glioblastoma. *Ann Transl Med.* 2015;3(9):121.
30. Athanassiou H, Synodinou M, Maragoudakis E, Paraskevaidis M, Verigos C, Misailidou D, et al. Randomized Phase II study of temozolomide and radiotherapy compared with radiotherapy alone in newly diagnosed glioblastoma multiforme. *J Clin Oncol.* 2005;23(10):2372–7. <http://dx.doi.org/10.1200/JCO.2005.00.331>
31. Karacetin D, Okten B, Yalcin B, Incekara O. Concomitant temozolomide and radiotherapy versus radiotherapy alone for treatment of newly diagnosed glioblastoma multiforme. *J BUON.* 2011;16(1):133–7.
32. Kocher M, Frommolt P, Borberg SK, Ruhl U, Steingraber M, Niewald M, et al. Randomized study of postoperative radiotherapy and simultaneous temozolomide without adjuvant chemotherapy for glioblastoma. *Strahlenther Onkol.* 2008;184(11):572–9. <http://dx.doi.org/10.1007/s00066-008-1897-0>
33. Szczepanek D, Marchel A, Moskala M, Krupa M, Kunert P, Trojanowski T. Efficacy of concomitant and adjuvant temozolomide in glioblastoma treatment. A multicentre randomized study. *Neurol Neurochir Pol.* 2013;47(2):101–8. <http://dx.doi.org/10.5114/ninp.2013.34398>
34. Feng E, Sui C, Wang T, Sun G. Temozolomide with or without radiotherapy in patients with newly diagnosed glioblastoma multiforme: A meta-analysis. *Eur Neurol.* 2017;77(3–4):201–10. <http://dx.doi.org/10.1159/000455842>
35. Gorlia T, van den Bent MJ, Hegi ME, Mirimanoff RO, Weller M, Cairncross JG, et al. Nomograms for predicting survival of patients with newly diagnosed glioblastoma: Prognostic factor analysis of EORTC and NCIC trial 26981-22981/CE.3. *Lancet Oncol.* 2008;9(1):29–38. [http://dx.doi.org/10.1016/S1470-2045\(07\)70384-4](http://dx.doi.org/10.1016/S1470-2045(07)70384-4)
36. Hegi ME, Liu L, Herman JG, Stupp R, Wick W, Weller M, et al. Correlation of O6-methylguanine methyltransferase (MGMT) promoter methylation with clinical outcomes in glioblastoma and clinical strategies to modulate MGMT activity. *J Clin Oncol.* 2008;26(25):4189–99. <http://dx.doi.org/10.1200/JCO.2007.11.5964>
37. Hegi ME, Diserens AC, Gorlia T, Hamou MF, de Tribolet N, Weller M, et al. MGMT gene silencing and benefit from temozolomide in glioblastoma. *N Engl J Med.* 2005;352(10):997–1003. <http://dx.doi.org/10.1056/NEJMoa043331>
38. Wick W, Platten M, Weller M. New (alternative) temozolomide regimens for the treatment of glioma. *Neuro Oncol.* 2009;11(1):69–79. <http://dx.doi.org/10.1215/15228517-2008-078>
39. Koukourakis GV, Kouloulas V, Zacharias G, Papadimitriou C, Pantelakos P, Maravelis G, et al. Temozolomide with radiation therapy in high grade brain gliomas: Pharmaceuticals considerations and efficacy; a review article. *Molecules.* 2009;14(4):1561–77. <http://dx.doi.org/10.3390/molecules14041561>
40. Hart MG, Garside R, Rogers G, Stein K, Grant R. Temozolomide for high grade glioma. *Cochrane Database Syst Rev.* 2013;(4):CD007415. <http://dx.doi.org/10.1002/14651858.cd007415.pub2>
41. Le Rhun E, Taillibert S, Chamberlain MC. The future of high-grade glioma: Where we are and where are we going. *Surg Neurol Int.* 2015;6(Suppl 1):S9–S44. <http://dx.doi.org/10.4103/2152-7806.151331>
42. Barbagallo GM, Paratore S, Caltabiano R, Palmucci S, Parra HS, Privitera G, et al. Long-term therapy with temozolomide is a feasible option for newly diagnosed glioblastoma: A single-institution

experience with as many as 101 temozolomide cycles. *Neurosurg Focus*. 2014;37(6):E4. <http://dx.doi.org/10.3171/2014.9.FOCUS14502>

43. Darlix A, Baumann C, Lorgis V, Ghiringhelli F, Blonski M, Chauffert B, et al. Prolonged administration of adjuvant temozolomide improves survival in adult patients with glioblastoma. *Anticancer Res*. 2013;33(8):3467–74.
44. Roldan Urgoiti GB, Singh AD, Easaw JC. Extended adjuvant temozolomide for treatment of newly diagnosed glioblastoma multiforme. *J Neurooncol*. 2012;108(1):173–7. <http://dx.doi.org/10.1007/s11060-012-0826-3>
45. Seiz M, Krafft U, Freyschlag CF, Weiss C, Schmieder K, Lohr F, et al. Long-term adjuvant administration of temozolomide in patients with glioblastoma multiforme: Experience of a single institution. *J Cancer Res Clin Oncol*. 2010;136(11):1691–5. <http://dx.doi.org/10.1007/s00432-010-0827-6>
46. Blumenthal DT, Gorlia T, Gilbert MR, Kim MM, Burt Nabors L, Mason WP, et al. Is more better? The impact of extended adjuvant temozolomide in newly diagnosed glioblastoma: A secondary analysis of EORTC and NRG Oncology/RTOG. *Neuro-Oncology*, Volume 19, Issue 8, 1 August 2017, Pages 1119–1126. <http://dx.doi.org/10.1093/neuonc/nox025>
47. Nabors LB, Fink KL, Mikkelsen T, Grujicic D, Tarnawski R, Nam DH, et al. Two cilengitide regimens in combination with standard treatment for patients with newly diagnosed glioblastoma and unmethylated MGMT gene promoter: Results of the open-label, controlled, randomized phase II CORE study. *Neuro Oncol*. 2015;17(5):708–17. <http://dx.doi.org/10.1093/neuonc/nou356>
48. Stupp R, Hegi ME, Gorlia T, Erridge SC, Perry J, Hong YK, et al. Cilengitide combined with standard treatment for patients with newly diagnosed glioblastoma with methylated MGMT promoter (CENTRIC EORTC 26071-22072 study): A multicentre, randomised, open-label, phase 3 trial. *Lancet Oncol*. 2014;15(10):1100–8. [http://dx.doi.org/10.1016/S1470-2045\(14\)70379-1](http://dx.doi.org/10.1016/S1470-2045(14)70379-1)
49. Gramatzki D, Kickingereder P, Hentschel B, Felsberg J, Herrlinger U, Schackert G, et al. Limited role for extended maintenance temozolomide for newly diagnosed glioblastoma. *Neurology*. 2017;88(15):1422–30. <http://dx.doi.org/10.1212/WNL.0000000000003809>
50. Bregy A, Shah AH, Diaz MV, Pierce HE, Ames PL, Diaz D, et al. The role of Gliadel wafers in the treatment of high-grade gliomas. *Expert Rev Anticancer Ther*. 2013;13(12):1453–61. <http://dx.doi.org/10.1586/14737140.2013.840090>
51. Lawrence YR, Li XA, el Naqa I, Hahn CA, Marks LB, Merchant TE, et al. Radiation dose-volume effects in the brain. *Int J Radiat Oncol Biol Phys*. 2010;76(3 Suppl):S20–7. <http://dx.doi.org/10.1016/j.ijrobp.2009.02.091>
52. Tosoni A, Franceschi E, Poggi R, Brandes AA. Relapsed glioblastoma: Treatment strategies for initial and subsequent recurrences. *Curr Treat Options Oncol*. 2016;17(9):49. <http://dx.doi.org/10.1007/s11864-016-0422-4>
53. Herrlinger U, Schaefer N, Steinbach JP, Weyerbrock A, Hau P, Goldbrunner R, et al. Survival and quality of life in the randomized, multicenter GLARIUS trial investigating bevacizumab/irinotecan versus standard temozolomide in newly diagnosed, MGMT-non-methylated glioblastoma patients. *J Clin Oncol*. 2014;32(15_suppl):2042.
54. Herrlinger U, Schafer N, Steinbach JP, Weyerbrock A, Hau P, Goldbrunner R, et al. Bevacizumab plus irinotecan versus temozolomide in newly diagnosed O6-methylguanine-DNA methyltransferase non-methylated glioblastoma: The randomized GLARIUS trial. *J Clin Oncol*. 2016;34(14):1611–19. <http://dx.doi.org/10.1200/JCO.2015.63.4691>
55. Carlson JA, Reddy K, Gaspar LE, Ney D, Kavanagh BD, Damek D, et al. Hypofractionated-intensity modulated radiotherapy (hypo-IMRT) and temozolomide (TMZ) with or without bevacizumab (BEV) for newly diagnosed glioblastoma multiforme (GBM): A comparison of two prospective phase II trials. *J Neurooncol*. 2015;123(2):251–7. <http://dx.doi.org/10.1007/s11060-015-1791-4>
56. Omuro A, Beal K, Gutin P, Karimi S, Correa DD, Kaley TJ, et al. Phase II study of bevacizumab, temozolomide, and hypofractionated stereotactic radiotherapy for newly diagnosed glioblastoma. *Clin Cancer Res*. 2014;20(19):5023–31. <http://dx.doi.org/10.1158/1078-0432.CCR-14-0822>
57. Nicholas MK, Lukas RV, Amidei C, Vick N, Paleologos N, Malkin MG, et al. Final results of a single-arm phase II study of bevacizumab and temozolomide following radiochemotherapy in newly diagnosed adult glioblastoma patients. *J Clin Oncol*. 2013;31(15_suppl):2076.
58. Raizer JJ, Giglio P, Hu JL, Groves MD, Merrell R, Conrad CA, et al. BTTC08-01: A phase II study of bevacizumab and erlotinib after radiation therapy and temozolomide in patients with

- newly diagnosed glioblastoma (GBM) without MGMT promoter methylation. *J Clin Oncol.* 2013;31(15_suppl):2019.
59. Narayana A, Gruber D, Kunnakkat S, Golfinos JG, Parker E, Raza S, et al. A clinical trial of bevacizumab, temozolomide, and radiation for newly diagnosed glioblastoma. *J Neurosurg.* 2012;116(2):341–5. <http://dx.doi.org/10.3171/2011.9.JNS11656>
 60. Hainsworth JD, Shih KC, Shepard GC, Tillinghast GW, Brinker BT, Spigel DR. Phase II study of concurrent radiation therapy, temozolomide, and bevacizumab followed by bevacizumab/everolimus as first-line treatment for patients with glioblastoma. *Clin Adv Hematol Oncol.* 2012;10(4):240–6.
 61. Friedman HS, Desjardins A, Peters KB, Reardon DA, Kirkpatrick J, Herndon JE, et al. The addition of bevacizumab to temozolomide and radiation therapy followed by bevacizumab, temozolomide, and oral topotecan for newly diagnosed glioblastoma multiforme (GBM). *J Clin Oncol.* 2012;30(15_suppl):2090.
 62. Vredenburgh JJ, Desjardins A, Reardon DA, Peters KB, Herndon JE, 2nd, Marcello J, et al. The addition of bevacizumab to standard radiation therapy and temozolomide followed by bevacizumab, temozolomide, and irinotecan for newly diagnosed glioblastoma. *Clin Cancer Res.* 2011;17(12):4119–24. <http://dx.doi.org/10.1158/1078-0432.CCR-11-0120>
 63. Lai A, Tran A, Nghiemphu PL, Pope WB, Solis OE, Selch M, et al. Phase II study of bevacizumab plus temozolomide during and after radiation therapy for patients with newly diagnosed glioblastoma multiforme. *J Clin Oncol.* 2011;29(2):142–8. <http://dx.doi.org/10.1200/JCO.2010.30.2729>
 64. Friedman HS, Prados MD, Wen PY, Mikkelsen T, Schiff D, Abrey LE, et al. Bevacizumab alone and in combination with irinotecan in recurrent glioblastoma. *J Clin Oncol.* 2009;27(28):4733–40. <http://dx.doi.org/10.1200/JCO.2008.19.8721>
 65. Kreisl TN, Kim L, Moore K, Ducic P, Royce C, Stroud I, et al. Phase II trial of single-agent bevacizumab followed by bevacizumab plus irinotecan at tumor progression in recurrent glioblastoma. *J Clin Oncol.* 2009;27(5):740–5. <http://dx.doi.org/10.1200/JCO.2008.16.3055>
 66. Nabors LB, Mikkelsen T, Hegi ME, Ye X, Batchelor T, Lesser G, et al. A safety run-in and randomized phase 2 study of cilengitide combined with chemoradiation for newly diagnosed glioblastoma (NABTT 0306). *Cancer.* 2012;118(22):5601–7. <http://dx.doi.org/10.1002/cncr.27585>
 67. Reardon DA, Fink KL, Mikkelsen T, Cloughesy TF, O'Neill A, Plotkin S, et al. Randomized phase II study of cilengitide, an integrin-targeting arginine-glycine-aspartic acid peptide, in recurrent glioblastoma multiforme. *J Clin Oncol.* 2008;26(34):5610–17. <http://dx.doi.org/10.1200/JCO.2008.16.7510>
 68. Stupp R, Hegi ME, Neyns B, Goldbrunner R, Schlegel U, Clement PM, et al. Phase I/IIa study of cilengitide and temozolomide with concomitant radiotherapy followed by cilengitide and temozolomide maintenance therapy in patients with newly diagnosed glioblastoma. *J Clin Oncol.* 2010;28(16):2712–18. <http://dx.doi.org/10.1200/JCO.2009.26.6650>
 69. Montemurro N, Perrini P, Blanco MO, Vannozzi R. Second surgery for recurrent glioblastoma: A concise overview of the current literature. *Clin Neurol Neurosurg.* 2016;142:60–4. <http://dx.doi.org/10.1016/j.clineuro.2016.01.010>
 70. Carson KA, Grossman SA, Fisher JD, Shaw EG. Prognostic factors for survival in adult patients with recurrent glioma enrolled onto the new approaches to brain tumor therapy CNS consortium phase I and II clinical trials. *J Clin Oncol.* 2007;25(18):2601–6. <http://dx.doi.org/10.1200/JCO.2006.08.1661>
 71. Chan TA, Weingart JD, Parisi M, Hughes MA, Olivi A, Borzillary S, et al. Treatment of recurrent glioblastoma multiforme with GliaSite brachytherapy. *Int J Radiat Oncol Biol Phys.* 2005;62(4):1133–9. <http://dx.doi.org/10.1016/j.ijrobp.2004.12.032>
 72. Cuneo KC, Vredenburgh JJ, Sampson JH, Reardon DA, Desjardins A, Peters KB, et al. Safety and efficacy of stereotactic radiosurgery and adjuvant bevacizumab in patients with recurrent malignant gliomas. *Int J Radiat Oncol Biol Phys.* 2012;82(5):2018–24. <http://dx.doi.org/10.1016/j.ijrobp.2010.12.074>
 73. Gabayan AJ, Green SB, Sanan A, Jenrette J, Schultz C, Papagikos M, et al. GliaSite brachytherapy for treatment of recurrent malignant gliomas: A retrospective multi-institutional analysis. *Neurosurgery.* 2006;58(4):701–9; discussion 701–9.
 74. Gorlia T, Stupp R, Brandes AA, Rampling RR, Fumoleau P, Ditttrich C, et al. New prognostic factors and calculators for outcome prediction in patients with recurrent glioblastoma: A pooled analysis of

- EORTC Brain Tumour Group phase I and II clinical trials. *Eur J Cancer*. 2012;48(8):1176–84. <http://dx.doi.org/10.1016/j.ejca.2012.02.004>
75. Minniti G, Scaringi C, De Sanctis V, Lanzetta G, Falco T, Di Stefano D, et al. Hypofractionated stereotactic radiotherapy and continuous low-dose temozolomide in patients with recurrent or progressive malignant gliomas. *J Neurooncol*. 2013;111(2):187–94. <http://dx.doi.org/10.1007/s11060-012-0999-9>
 76. Park JK, Hodges T, Arko L, Shen M, Dello Iacono D, McNabb A, et al. Scale to predict survival after surgery for recurrent glioblastoma multiforme. *J Clin Oncol*. 2010;28(24):3838–43. <http://dx.doi.org/10.1200/JCO.2010.30.0582>
 77. Combs SE, Edler L, Rausch R, Welzel T, Wick W, Debus J. Generation and validation of a prognostic score to predict outcome after re-irradiation of recurrent glioma. *Acta Oncol*. 2013;52(1):147–52. <http://dx.doi.org/10.3109/0284186X.2012.692882>
 78. Fogh SE, Andrews DW, Glass J, Curran W, Glass C, Champ C, et al. Hypofractionated stereotactic radiation therapy: An effective therapy for recurrent high-grade gliomas. *J Clin Oncol*. 2010;28(18):3048–53. <http://dx.doi.org/10.1200/JCO.2009.25.6941>
 79. Park CK, Kim JH, Nam DH, Kim CY, Chung SB, Kim YH, et al. A practical scoring system to determine whether to proceed with surgical resection in recurrent glioblastoma. *Neuro Oncol*. 2013;15(8):1096–101. <http://dx.doi.org/10.1093/neuonc/not069>
 80. Chang SM, Parney IF, McDermott M, Barker FG, 2nd, Schmidt MH, Huang W, et al. Perioperative complications and neurological outcomes of first and second craniotomies among patients enrolled in the Glioma Outcome Project. *J Neurosurg*. 2003;98(6):1175–81. <http://dx.doi.org/10.3171/jns.2003.98.6.1175>
 81. Brandes AA, Franceschi E, Tosoni A, Bartolini S, Bacci A, Agati R, et al. O(6)-methylguanine DNA-methyltransferase methylation status can change between first surgery for newly diagnosed glioblastoma and second surgery for recurrence: Clinical implications. *Neuro Oncol*. 2010;12(3):283–8. <http://dx.doi.org/10.1093/neuonc/nop050>
 82. Suchorska B, Weller M, Tabatabai G, Senft C, Hau P, Sabel MC, et al. Complete resection of contrast-enhancing tumor volume is associated with improved survival in recurrent glioblastoma—results from the DIRECTOR trial. *Neuro Oncol*. 2016;18(4):549–56. <http://dx.doi.org/10.1093/neuonc/nov326>
 83. Ringel F, Pape H, Sabel M, Krex D, Bock HC, Misch M, et al. Clinical benefit from resection of recurrent glioblastomas: Results of a multicenter study including 503 patients with recurrent glioblastomas undergoing surgical resection. *Neuro Oncol*. 2016;18(1):96–104. <http://dx.doi.org/10.1093/neuonc/nov145>
 84. Nieder C, Adam M, Molls M, Grosu AL. Therapeutic options for recurrent high-grade glioma in adult patients: Recent advances. *Crit Rev Oncol Hematol*. 2006;60(3):181–93. <http://dx.doi.org/10.1016/j.critrevonc.2006.06.007>
 85. Mayer R, Sminia P. Reirradiation tolerance of the human brain. *Int J Radiat Oncol Biol Phys*. 2008;70(5):1350–60. <http://dx.doi.org/10.1016/j.ijrobp.2007.08.015>
 86. Shaw E, Scott C, Souhami L, Dinapoli R, Kline R, Loeffler J, et al. Single dose radiosurgical treatment of recurrent previously irradiated primary brain tumors and brain metastases: Final report of RTOG protocol 90-05. *Int J Radiat Oncol Biol Phys*. 2000;47(2):291–8. [http://dx.doi.org/10.1016/S0360-3016\(99\)00507-6](http://dx.doi.org/10.1016/S0360-3016(99)00507-6)
 87. Shepherd SF, Laing RW, Cosgrove VP, Warrington AP, Hines F, Ashley SE, et al. Hypofractionated stereotactic radiotherapy in the management of recurrent glioma. *Int J Radiat Oncol Biol Phys*. 1997;37(2):393–8. [http://dx.doi.org/10.1016/S0360-3016\(96\)00455-5](http://dx.doi.org/10.1016/S0360-3016(96)00455-5)
 88. Cabrera AR, Cuneo KC, Desjardins A, Sampson JH, McSherry F, Herndon JE, 2nd, et al. Concurrent stereotactic radiosurgery and bevacizumab in recurrent malignant gliomas: A prospective trial. *Int J Radiat Oncol Biol Phys*. 2013;86(5):873–9. <http://dx.doi.org/10.1016/j.ijrobp.2013.04.029>
 89. Minniti G, Armosini V, Salvati M, Lanzetta G, Caporello P, Mei M, et al. Fractionated stereotactic reirradiation and concurrent temozolomide in patients with recurrent glioblastoma. *J Neurooncol*. 2011;103(3):683–91. <http://dx.doi.org/10.1007/s11060-010-0446-8>
 90. Niyazi M, Ganswindt U, Schwarz SB, Kreth FW, Tonn JC, Geisler J, et al. Irradiation and bevacizumab in high-grade glioma retreatment settings. *Int J Radiat Oncol Biol Phys*. 2012;82(1):67–76. <http://dx.doi.org/10.1016/j.ijrobp.2010.09.022>

91. Combs SE, Thilmann C, Edler L, Debus J, Schulz-Ertner D. Efficacy of fractionated stereotactic reirradiation in recurrent gliomas: Long-term results in 172 patients treated in a single institution. *J Clin Oncol.* 2005;23(34):8863–9. <http://dx.doi.org/10.1200/JCO.2005.03.4157>
92. Darakchiev BJ, Albright RE, Breneman JC, Warnick RE. Safety and efficacy of permanent iodine-125 seed implants and carmustine wafers in patients with recurrent glioblastoma multiforme. *J Neurosurg.* 2008;108(2):236–42. <http://dx.doi.org/10.3171/JNS/2008/108/2/0236>
93. Combs SE, Debus J, Schulz-Ertner D. Radiotherapeutic alternatives for previously irradiated recurrent gliomas. *BMC Cancer.* 2007;7:167. <http://dx.doi.org/10.1186/1471-2407-7-167>
94. Moeller BJ, Cao Y, Li CY, Dewhirst MW. Radiation activates HIF-1 to regulate vascular radiosensitivity in tumors: Role of reoxygenation, free radicals, and stress granules. *Cancer Cell.* 2004;5(5):429–41. [http://dx.doi.org/10.1016/S1535-6108\(04\)00115-1](http://dx.doi.org/10.1016/S1535-6108(04)00115-1)
95. Moeller BJ, Dewhirst MW. Raising the bar: How HIF-1 helps determine tumor radiosensitivity. *Cell Cycle.* 2004;3(9):1107–10. <http://dx.doi.org/10.4161/cc.3.9.1099>
96. Moeller BJ, Dreher MR, Rabbani ZN, Schroeder T, Cao Y, Li CY, et al. Pleiotropic effects of HIF-1 blockade on tumor radiosensitivity. *Cancer Cell.* 2005;8(2):99–110. <http://dx.doi.org/10.1016/j.ccr.2005.06.016>
97. Boothe D, Young R, Yamada Y, Prager A, Chan T, Beal K. Bevacizumab as a treatment for radiation necrosis of brain metastases post stereotactic radiosurgery. *Neuro Oncol.* 2013;15(9):1257–63. <http://dx.doi.org/10.1093/neuonc/not085>
98. Levin VA, Bidaut L, Hou P, Kumar AJ, Wefel JS, Bekele BN, et al. Randomized double-blind placebo-controlled trial of bevacizumab therapy for radiation necrosis of the central nervous system. *Int J Radiat Oncol Biol Phys.* 2011;79(5):1487–95. <http://dx.doi.org/10.1016/j.ijrobp.2009.12.061>
99. Torcuator R, Zuniga R, Mohan YS, Rock J, Doyle T, Anderson J, et al. Initial experience with bevacizumab treatment for biopsy confirmed cerebral radiation necrosis. *J Neurooncol.* 2009;94(1):63–8. <http://dx.doi.org/10.1007/s11060-009-9801-z>
100. Greenspoon JN, Sharieff W, Hirte H, Overholt A, Devillers R, Gunnarsson T, et al. Fractionated stereotactic radiosurgery with concurrent temozolomide chemotherapy for locally recurrent glioblastoma multiforme: A prospective cohort study. *Onco Targets Ther.* 2014;7:485–90. <http://dx.doi.org/10.2147/OTT.S60358>
101. Grosu AL, Weber WA, Franz M, Stark S, Piert M, Thamm R, et al. Reirradiation of recurrent high-grade gliomas using amino acid PET (SPECT)/CT/MRI image fusion to determine gross tumor volume for stereotactic fractionated radiotherapy. *Int J Radiat Oncol Biol Phys.* 2005;63(2):511–19. <http://dx.doi.org/10.1016/j.ijrobp.2005.01.056>
102. Gutin PH, Iwamoto FM, Beal K, Mohile NA, Karimi S, Hou BL, et al. Safety and efficacy of bevacizumab with hypofractionated stereotactic irradiation for recurrent malignant gliomas. *Int J Radiat Oncol Biol Phys.* 2009;75(1):156–63. <http://dx.doi.org/10.1016/j.ijrobp.2008.10.043>
103. Hundsberger T, Brugge D, Putora PM, Weder P, Weber J, Plasswilm L. Re-irradiation with and without bevacizumab as salvage therapy for recurrent or progressive high-grade gliomas. *J Neurooncol.* 2013;112(1):133–9. <http://dx.doi.org/10.1007/s11060-013-1044-3>
104. Park KJ, Kano H, Iyer A, Liu X, Niranjana A, Flickinger JC, et al. Salvage gamma knife stereotactic radiosurgery followed by bevacizumab for recurrent glioblastoma multiforme: A case-control study. *J Neurooncol.* 2012;107(2):323–33. <http://dx.doi.org/10.1007/s11060-011-0744-9>
105. Torcuator RG, Thind R, Patel M, Mohan YS, Anderson J, Doyle T, et al. The role of salvage reirradiation for malignant gliomas that progress on bevacizumab. *J Neurooncol.* 2010;97(3):401–7. <http://dx.doi.org/10.1007/s11060-009-0034-y>
106. Shapiro LQ, Beal K, Goenka A, Karimi S, Iwamoto FM, Yamada Y, et al. Patterns of failure after concurrent bevacizumab and hypofractionated stereotactic radiation therapy for recurrent high-grade glioma. *Int J Radiat Oncol Biol Phys.* 2013;85(3):636–42. <http://dx.doi.org/10.1016/j.ijrobp.2012.05.031>
107. Minniti G, Agolli L, Falco T, Scaringi C, Lanzetta G, Caporello P, et al. Hypofractionated stereotactic radiotherapy in combination with bevacizumab or fotemustine for patients with progressive malignant gliomas. *J Neurooncol.* 2015;122(3):559–66. <http://dx.doi.org/10.1007/s11060-015-1745-x>
108. Lamborn KR, Yung WK, Chang SM, Wen PY, Cloughesy TF, DeAngelis LM, et al. Progression-free survival: An important end point in evaluating therapy for recurrent high-grade gliomas. *Neuro Oncol.* 2008;10(2):162–70. <http://dx.doi.org/10.1215/15228517-2007-062>

109. Takimoto CH, Calvo E. Principles of oncologic pharmacotherapy. In: Cancer management: A multi-disciplinary approach. 11th ed. 2007. Available from: <http://www.cancernetwork.com/articles/principles-oncologic-pharmacotherapy-0>.
110. Brandes AA, Tosoni A, Amista P, Nicolardi L, Grosso D, Berti F, et al. How effective is BCNU in recurrent glioblastoma in the modern era? A phase II trial. *Neurology*. 2004;63(7):1281–4. <http://dx.doi.org/10.1212/01.WNL.0000140495.33615.CA>
111. Scoccianti S, Detti B, Sardaro A, Iannalfi A, Meattini I, Leonulli BG, et al. Second-line chemotherapy with fotemustine in temozolomide-pretreated patients with relapsing glioblastoma: A single institution experience. *Anticancer Drugs*. 2008;19(6):613–20. <http://dx.doi.org/10.1097/CAD.0b013e3283005075>
112. Brandes AA, Tosoni A, Franceschi E, Blatt V, Santoro A, Faedi M, et al. Fotemustine as second-line treatment for recurrent or progressive glioblastoma after concomitant and/or adjuvant temozolomide: A phase II trial of Gruppo Italiano Cooperativo di Neuro-Oncologia (GICNO). *Cancer Chemother Pharmacol*. 2009;64(4):769–75. <http://dx.doi.org/10.1007/s00280-009-0926-8>
113. Fabrini MG, Silvano G, Lolli I, Perrone F, Marsella A, Scotti V, et al. A multi-institutional phase II study on second-line Fotemustine chemotherapy in recurrent glioblastoma. *J Neurooncol*. 2009;92(1):79–86. <http://dx.doi.org/10.1007/s11060-008-9739-6>
114. Addeo R, Caraglia M, De Santi MS, Montella L, Abbruzzese A, Parlato C, et al. A new schedule of fotemustine in temozolomide-pretreated patients with relapsing glioblastoma. *J Neurooncol*. 2011;102(3):417–24. <http://dx.doi.org/10.1007/s11060-010-0329-z>
115. Brandes AA, Tosoni A, Basso U, Reni M, Valduga F, Monfardini S, et al. Second-line chemotherapy with irinotecan plus carmustine in glioblastoma recurrent or progressive after first-line temozolomide chemotherapy: A phase II study of the Gruppo Italiano Cooperativo di Neuro-Oncologia (GICNO). *J Clin Oncol*. 2004;22(23):4779–86. <http://dx.doi.org/10.1200/JCO.2004.06.181>
116. Prados MD, Yung WK, Fine HA, Greenberg HS, Junck L, Chang SM, et al. Phase 2 study of BCNU and temozolomide for recurrent glioblastoma multiforme: North American Brain Tumor Consortium study. *Neuro Oncol*. 2004;6(1):33–7. <http://dx.doi.org/10.1215/S1152851703000309>
117. Gaviani P, Salmaggi A, Silvani A. Combined chemotherapy with temozolomide and fotemustine in recurrent glioblastoma patients. *J Neurooncol*. 2011;104(2):617–18. <http://dx.doi.org/10.1007/s11060-010-0515-z>
118. van den Bent MJ, Brandes AA, Rampling R, Kouwenhoven MC, Kros JM, Carpentier AF, et al. Randomized phase II trial of erlotinib versus temozolomide or carmustine in recurrent glioblastoma: EORTC brain tumor group study 26034. *J Clin Oncol*. 2009;27(8):1268–74. <http://dx.doi.org/10.1200/JCO.2008.17.5984>
119. Wick W, Puduvalli VK, Chamberlain MC, van den Bent MJ, Carpentier AF, Cher LM, et al. Phase III study of enzastaurin compared with lomustine in the treatment of recurrent intracranial glioblastoma. *J Clin Oncol*. 2010;28(7):1168–74. <http://dx.doi.org/10.1200/JCO.2009.23.2595>
120. Batchelor TT, Mulholland P, Neyns B, Nabors LB, Campone M, Wick A, et al. Phase III randomized trial comparing the efficacy of cediranib as monotherapy, and in combination with lomustine, versus lomustine alone in patients with recurrent glioblastoma. *J Clin Oncol*. 2013;31(26):3212–18. <http://dx.doi.org/10.1200/JCO.2012.47.2464>
121. Brandes AA, Carpentier AF, Kesari S, Sepulveda-Sanchez JM, Wheeler HR, Chinot O, et al. A Phase II randomized study of galunisertib monotherapy or galunisertib plus lomustine compared with lomustine monotherapy in patients with recurrent glioblastoma. *Neuro Oncol*. 2016;18(8):1146–56. <http://dx.doi.org/10.1093/neuonc/now009>
122. Kappelle AC, Postma TJ, Taphoorn MJ, Groeneveld GJ, van den Bent MJ, van Groeningen CJ, et al. PCV chemotherapy for recurrent glioblastoma multiforme. *Neurology*. 2001;56(1):118–20. <http://dx.doi.org/10.1212/WNL.56.1.118>
123. Schmidt F, Fischer J, Herrlinger U, Dietz K, Dichgans J, Weller M. PCV chemotherapy for recurrent glioblastoma. *Neurology*. 2006;66(4):587–9. <http://dx.doi.org/10.1212/01.wnl.0000197792.73656.c2>
124. Happold C, Roth P, Wick W, Steinbach JP, Linnebank M, Weller M, et al. ACNU-based chemotherapy for recurrent glioma in the temozolomide era. *J Neurooncol*. 2009;92(1):45–8. <http://dx.doi.org/10.1007/s11060-008-9728-9>

125. Reithmeier T, Graf E, Piroth T, Trippel M, Pinsker MO, Nikkhah G. BCNU for recurrent glioblastoma multiforme: Efficacy, toxicity and prognostic factors. *BMC Cancer*. 2010;10:30. <http://dx.doi.org/10.1186/1471-2407-10-30>
126. Brada M, Hoang-Xuan K, Rampling R, Dietrich PY, Dirix LY, Macdonald D, et al. Multicenter phase II trial of temozolomide in patients with glioblastoma multiforme at first relapse. *Ann Oncol*. 2001;12(2):259–66. <http://dx.doi.org/10.1023/A:1008382516636>
127. Yung WK, Albright RE, Olson J, Fredericks R, Fink K, Prados MD, et al. A phase II study of temozolomide vs. procarbazine in patients with glioblastoma multiforme at first relapse. *Br J Cancer*. 2000;83(5):588–93. <http://dx.doi.org/10.1054/bjoc.2000.1316>
128. Taal W, Oosterkamp HM, Walenkamp AM, Dubbink HJ, Beerepoot LV, Hanse MC, et al. Single-agent bevacizumab or lomustine versus a combination of bevacizumab plus lomustine in patients with recurrent glioblastoma (BELOB trial): A randomised controlled phase 2 trial. *Lancet Oncol*. 2014;15(9):943–53. [http://dx.doi.org/10.1016/S1470-2045\(14\)70314-6](http://dx.doi.org/10.1016/S1470-2045(14)70314-6)
129. Brandes AA, Ermani M, Basso U, Amista P, Berti F, Scienza R, et al. Temozolomide as a second-line systemic regimen in recurrent high-grade glioma: A phase II study. *Ann Oncol*. 2001;12(2):255–7. <http://dx.doi.org/10.1023/A:1008336732273>
130. Brandes AA, Ermani M, Basso U, Paris MK, Lumachi F, Berti F, et al. Temozolomide in patients with glioblastoma at second relapse after first line nitrosourea-procarbazine failure: A phase II study. *Oncology*. 2002;63(1):38–41. <http://dx.doi.org/10.1159/000065718>
131. Chan DT, Poon WS, Chan YL, Ng HK. Temozolomide in the treatment of recurrent malignant glioma in Chinese patients. *Hong Kong Med J*. 2005;11(6):452–6.
132. Nagane M, Kobayashi K, Ohnishi A, Shimizu S, Shiokawa Y. Prognostic significance of O6-methylguanine-DNA methyltransferase protein expression in patients with recurrent glioblastoma treated with temozolomide. *Jpn J Clin Oncol*. 2007;37(12):897–906. <http://dx.doi.org/10.1093/jcco/hym132>
133. Khan RB, Raizer JJ, Malkin MG, Bazylewicz KA, Abrey LE. A phase II study of extended low-dose temozolomide in recurrent malignant gliomas. *Neuro Oncol*. 2002;4(1):39–43. <http://dx.doi.org/10.1215/15228517-4-1-39>
134. Wick W, Steinbach JP, Kuker WM, Dichgans J, Bamberg M, Weller M. One week on/one week off: A novel active regimen of temozolomide for recurrent glioblastoma. *Neurology*. 2004;62(11):2113–15. <http://dx.doi.org/10.1212/01.WNL.0000127617.89363.84>
135. Brandes AA, Tosoni A, Cavallo G, Bertorelle R, Gioia V, Franceschi E, et al. Temozolomide 3 weeks on and 1 week off as first-line therapy for recurrent glioblastoma: Phase II study from gruppo italiano cooperativo di neuro-oncologia (GICNO). *Br J Cancer*. 2006;95(9):1155–60. <http://dx.doi.org/10.1038/sj.bjc.6603376>
136. Kong DS, Lee JI, Kim WS, Son MJ, Lim DH, Kim ST, et al. A pilot study of metronomic temozolomide treatment in patients with recurrent temozolomide-refractory glioblastoma. *Oncol Rep*. 2006;16(5):1117–21. <http://dx.doi.org/10.3892/or.16.5.1117>
137. Wick A, Felsberg J, Steinbach JP, Herrlinger U, Platten M, Blaschke B, et al. Efficacy and tolerability of temozolomide in an alternating weekly regimen in patients with recurrent glioma. *J Clin Oncol*. 2007;25(22):3357–61. <http://dx.doi.org/10.1200/JCO.2007.10.7722>
138. Balmaceda C, Peereboom D, Pannullo S, Cheung YK, Fisher PG, Alavi J, et al. Multi-institutional phase II study of temozolomide administered twice daily in the treatment of recurrent high-grade gliomas. *Cancer*. 2008;112(5):1139–46. <http://dx.doi.org/10.1002/cncr.23167>
139. Berrocal A, Perez Segura P, Gil M, Balana C, Garcia Lopez J, Yaya R, et al. Extended-schedule dose-dense temozolomide in refractory gliomas. *J Neurooncol*. 2010;96(3):417–22. <http://dx.doi.org/10.1007/s11060-009-9980-7>
140. Perry JR, Belanger K, Mason WP, Fulton D, Kavan P, Easaw J, et al. Phase II trial of continuous dose-intense temozolomide in recurrent malignant glioma: RESCUE study. *J Clin Oncol*. 2010;28(12):2051–7. <http://dx.doi.org/10.1200/JCO.2009.26.5520>
141. Kong DS, Lee JI, Kim JH, Kim ST, Kim WS, Suh YL, et al. Phase II trial of low-dose continuous (metronomic) treatment of temozolomide for recurrent glioblastoma. *Neuro Oncol*. 2010;12(3):289–96. <http://dx.doi.org/10.1093/neuonc/nop030>

142. Hammond S, Norden AD, Lesser GJ, Drappatz J, Fadul CE, Batchelor T, et al. Phase II study of dose-intense temozolomide in recurrent glioblastoma. *J Clin Oncol*. 2011;29(Suppl 15):2038. http://dx.doi.org/10.1200/jco.2011.29.15_suppl.2038
143. Santoni M, Paccapelo A, Burattini L, Bianconi M, Cardinali M, Fabbietti L, et al. Protracted low doses of temozolomide for the treatment of patients with recurrent glioblastoma: A phase II study. *Oncol Lett*. 2012;4(4):799–801. <http://dx.doi.org/10.3892/ol.2012.788>
144. Norden AD, Lesser GJ, Drappatz J, Ligon KL, Hammond SN, Lee EQ, et al. Phase 2 study of dose-intense temozolomide in recurrent glioblastoma. *Neuro Oncol*. 2013;15(7):930–5. <http://dx.doi.org/10.1093/neuonc/not040>
145. Han SJ, Rolston JD, Molinaro AM, Clarke JL, Prados MD, Chang SM, et al. Phase II trial of 7 days on/7 days off temozolomide for recurrent high-grade glioma. *Neuro Oncol*. 2014;16(9):1255–62. <http://dx.doi.org/10.1093/neuonc/nou044>
146. Silvani A, Eoli M, Salmaggi A, Lamperti E, Maccagnano E, Broggi G, et al. Phase II trial of cisplatin plus temozolomide, in recurrent and progressive malignant glioma patients. *J Neurooncol*. 2004;66(1–2):203–8. <http://dx.doi.org/10.1023/B:NEON.0000013479.64348.69>
147. Brandes AA, Basso U, Reni M, Vastola F, Tosoni A, Cavallo G, et al. First-line chemotherapy with cisplatin plus fractionated temozolomide in recurrent glioblastoma multiforme: A phase II study of the Gruppo Italiano Cooperativo di Neuro-Oncologia. *J Clin Oncol*. 2004;22(9):1598–604. <http://dx.doi.org/10.1200/JCO.2004.11.019>
148. Chua SL, Rosenthal MA, Wong SS, Ashley DM, Woods AM, Dowling A, et al. Phase 2 study of temozolomide and Caelyx in patients with recurrent glioblastoma multiforme. *Neuro Oncol*. 2004;6(1):38–43. <http://dx.doi.org/10.1215/S1152851703000188>
149. Reardon DA, Quinn JA, Rich JN, Desjardins A, Vredenburgh J, Gururangan S, et al. Phase I trial of irinotecan plus temozolomide in adults with recurrent malignant glioma. *Cancer*. 2005;104(7):1478–86. <http://dx.doi.org/10.1002/cncr.21316>
150. Quinn JA, Jiang SX, Reardon DA, Desjardins A, Vredenburgh JJ, Rich JN, et al. Phase II trial of temozolomide plus o6-benzylguanine in adults with recurrent, temozolomide-resistant malignant glioma. *J Clin Oncol*. 2009;27(8):1262–7. <http://dx.doi.org/10.1200/JCO.2008.18.8417>
151. Groves MD, Pudukall VK, Gilbert MR, Levin VA, Conrad CA, Liu VH, et al. Two phase II trials of temozolomide with interferon-alpha2b (pegylated and non-pegylated) in patients with recurrent glioblastoma multiforme. *Br J Cancer*. 2009;101(4):615–20. <http://dx.doi.org/10.1038/sj.bjc.6605189>
152. Verhoeff JJ, Lavini C, van Linde ME, Stalpers LJ, Majoie CB, Reijneveld JC, et al. Bevacizumab and dose-intense temozolomide in recurrent high-grade glioma. *Ann Oncol*. 2010;21(8):1723–7. <http://dx.doi.org/10.1093/annonc/mdp591>
153. Reardon DA, Vredenburgh JJ, Desjardins A, Peters K, Gururangan S, Sampson JH, et al. Effect of CYP3A-inducing anti-epileptics on sorafenib exposure: Results of a phase II study of sorafenib plus daily temozolomide in adults with recurrent glioblastoma. *J Neurooncol*. 2011;101(1):57–66. <http://dx.doi.org/10.1007/s11060-010-0217-6>
154. Desjardins A, Reardon DA, Coan A, Marcello J, Herndon JE, 2nd, Bailey L, et al. Bevacizumab and daily temozolomide for recurrent glioblastoma. *Cancer*. 2012;118(5):1302–12. <http://dx.doi.org/10.1002/cncr.26381>
155. Sepulveda JM, Belda-Iñiesta C, Gil-Gil M, Perez-Segura P, Berrocal A, Reynes G, et al. A phase II study of feasibility and toxicity of bevacizumab in combination with temozolomide in patients with recurrent glioblastoma. *Clin Transl Oncol*. 2015;17(9):743–50. <http://dx.doi.org/10.1007/s12094-015-1304-0>
156. Gan HK, Fichtel L, Lassman AB, Merrell R, van den Bent MJ, Kumthekar P, et al. A phase I study evaluating ABT-414 in combination with temozolomide (TMZ) for subjects with recurrent or unresectable glioblastoma (GBM). *J Clin Oncol*. 2014;32(15_suppl):2021.
157. Bower M, Newlands ES, Bleehen NM, Brada M, Begent RJ, Calvert H, et al. Multicentre CRC phase II trial of temozolomide in recurrent or progressive high-grade glioma. *Cancer Chemother Pharmacol*. 1997;40(6):484–8. <http://dx.doi.org/10.1007/s002800050691>
158. Reardon DA, Desjardins A, Peters K, Gururangan S, Sampson J, Rich JN, et al. Phase II study of metronomic chemotherapy with bevacizumab for recurrent glioblastoma after progression on bevacizumab therapy. *J Neurooncol*. 2011;103(2):371–9. <http://dx.doi.org/10.1007/s11060-010-0403-6>

159. Reardon DA, Nabors LB, Mason WP, Perry JR, Shapiro W, Kavan P, et al. Phase I/randomized phase II study of afatinib, an irreversible ErbB family blocker, with or without protracted temozolomide in adults with recurrent glioblastoma. *Neuro Oncol.* 2015;17(3):430–9.
160. Weller M, Tabatabai G, Kastner B, Felsberg J, Steinbach JP, Wick A, et al. MGMT promoter methylation is a strong prognostic biomarker for benefit from dose-intensified temozolomide rechallenge in progressive glioblastoma: The DIRECTOR trial. *Clin Cancer Res.* 2015;21(9):2057–64. <http://dx.doi.org/10.1158/1078-0432.CCR-14-2737>
161. Franceschi E, Omuro AM, Lassman AB, Demopoulos A, Nolan C, Abrey LE. Salvage temozolomide for prior temozolomide responders. *Cancer.* 2005;104(11):2473–6. <http://dx.doi.org/10.1002/cncr.21564>
162. Boiardi A, Silvani A, Eoli M, Lamperti E, Salmaggi A, Gaviani P, et al. Treatment of recurrent glioblastoma: Can local delivery of mitoxantrone improve survival? *J Neurooncol.* 2008;88(1):105–13. <http://dx.doi.org/10.1007/s11060-008-9540-6>
163. Wick A, Pascher C, Wick W, Jauch T, Weller M, Bogdahn U, et al. Rechallenge with temozolomide in patients with recurrent gliomas. *J Neurol.* 2009;256(5):734–41. <http://dx.doi.org/10.1007/s00415-009-5006-9>
164. Stockhammer F, Misch M, Koch A, Czabanka M, Plotkin M, Blechschmidt C, et al. Continuous low-dose temozolomide and celecoxib in recurrent glioblastoma. *J Neurooncol.* 2010;100(3):407–15. <http://dx.doi.org/10.1007/s11060-010-0192-y>
165. van den Bent MJ, Taal W. Are we done with dose-intense temozolomide in recurrent glioblastoma? *Neuro Oncol.* 2014;16(9):1161–3. <http://dx.doi.org/10.1093/neuonc/nou157>
166. Brada M, Stenning S, Gabe R, Thompson LC, Levy D, Rampling R, et al. Temozolomide versus procarbazine, lomustine, and vincristine in recurrent high-grade glioma. *J Clin Oncol.* 2010;28(30):4601–8. <http://dx.doi.org/10.1200/JCO.2009.27.1932>
167. Weller M, Tabatabai G, Reifenberger G, Herrlinger U, Pichler J, Schnell O, et al. Dose-intensified rechallenge with temozolomide: One week on/one week off versus 3 weeks on/one week off in patients with progressive or recurrent glioblastoma (DIRECTOR). *J Clin Oncol.* 2010;28(Suppl. 15):TPS154. http://dx.doi.org/10.1200/jco.2010.28.15_suppl.tps154
168. Stark-Vance V. Bevacizumab and CPT-11 in the treatment of relapsed malignant glioma. *Neuro Oncology.* 2005;7(3):369.
169. Raizer JJ, Grimm S, Chamberlain MC, Nicholas MK, Chandler JP, Muro K, et al. A phase 2 trial of single-agent bevacizumab given in an every-3-week schedule for patients with recurrent high-grade gliomas. *Cancer.* 2010;116(22):5297–305. <http://dx.doi.org/10.1002/cncr.25462>
170. Nagane M, Nishikawa R, Narita Y, Kobayashi H, Takano S, Shinoura N, et al. Phase II study of single-agent bevacizumab in Japanese patients with recurrent malignant glioma. *Jpn J Clin Oncol.* 2012;42(10):887–95. <http://dx.doi.org/10.1093/jjco/hys121>
171. Vredenburgh JJ, Desjardins A, Herndon JE, 2nd, Marcello J, Reardon DA, Quinn JA, et al. Bevacizumab plus irinotecan in recurrent glioblastoma multiforme. *J Clin Oncol.* 2007;25(30):4722–9. <http://dx.doi.org/10.1200/JCO.2007.12.2440>
172. Vredenburgh JJ, Desjardins A, Herndon JE, 2nd, Dowell JM, Reardon DA, Quinn JA, et al. Phase II trial of bevacizumab and irinotecan in recurrent malignant glioma. *Clin Cancer Res.* 2007;13(4):1253–9. <http://dx.doi.org/10.1158/1078-0432.CCR-06-2309>
173. Gilbert MR, Wang M, Aldape K, Lassman A, Sorensen AG, Mikkelsen T, et al. RTOG 0625: A phase II study of bevacizumab with irinotecan in recurrent glioblastoma (GBM). *J Clin Oncol.* 2009;27(15_suppl):89s.
174. Narayana A, Kelly P, Golfinos J, Parker E, Johnson G, Knopp E, et al. Antiangiogenic therapy using bevacizumab in recurrent high-grade glioma: Impact on local control and patient survival. *J Neurosurg.* 2009;110(1):173–80. <http://dx.doi.org/10.3171/2008.4.17492>
175. Reardon DA, Desjardins A, Vredenburgh JJ, Gururangan S, Sampson JH, Sathornsumetee S, et al. Metronomic chemotherapy with daily, oral etoposide plus bevacizumab for recurrent malignant glioma: A phase II study. *Br J Cancer.* 2009;101(12):1986–94. <http://dx.doi.org/10.1038/sj.bjc.6605412>
176. Hasselbalch B, Lassen U, Hansen S, Holmberg M, Sorensen M, Kosteljanetz M, et al. Cetuximab, bevacizumab, and irinotecan for patients with primary glioblastoma and progression after radiation therapy and temozolomide: A phase II trial. *Neuro Oncol.* 2010;12(5):508–16.

177. Sathornsumetee S, Desjardins A, Vredenburgh JJ, McLendon RE, Marcello J, Herndon JE, et al. Phase II trial of bevacizumab and erlotinib in patients with recurrent malignant glioma. *Neuro Oncol.* 2010;12(12):1300–10. <http://dx.doi.org/10.1093/neuonc/nuq099>
178. Moller S, Grunnet K, Hansen S, Schultz H, Holmberg M, Sorensen M, et al. A phase II trial with bevacizumab and irinotecan for patients with primary brain tumors and progression after standard therapy. *Acta Oncol.* 2012;51(6):797–804. <http://dx.doi.org/10.3109/0284186X.2012.681063>
179. Reardon DA, Desjardins A, Peters KB, Gururangan S, Sampson JH, McLendon RE, et al. Phase II study of carboplatin, irinotecan, and bevacizumab for bevacizumab naive, recurrent glioblastoma. *J Neurooncol.* 2012;107(1):155–64. <http://dx.doi.org/10.1007/s11060-011-0722-2>
180. Lassen U, Sorensen M, Gaziel TB, Hasselbalch B, Poulsen HS. Phase II study of bevacizumab and temsirolimus combination therapy for recurrent glioblastoma multiforme. *Anticancer Res.* 2013;33(4):1657–60.
181. Galanis E, Anderson SK, Lafky JM, Uhm JH, Giannini C, Kumar SK, et al. Phase II study of bevacizumab in combination with sorafenib in recurrent glioblastoma (N0776): A north central cancer treatment group trial. *Clin Cancer Res.* 2013;19(17):4816–23. <http://dx.doi.org/10.1158/1078-0432.CCR-13-0708>
182. Soffietti R, Trevisan E, Bertero L, Cassoni P, Morra I, Fabrini MG, et al. Bevacizumab and fotemustine for recurrent glioblastoma: A phase II study of AINO (Italian Association of Neuro-Oncology). *J Neurooncol.* 2014;116(3):533–41. <http://dx.doi.org/10.1007/s11060-013-1317-x>
183. Lee EQ, Reardon DA, Schiff D, Drappatz J, Muzikansky A, Grimm SA, et al. Phase II study of panobinostat in combination with bevacizumab for recurrent glioblastoma and anaplastic glioma. *Neuro Oncol.* 2015;17(6):862–7. <http://dx.doi.org/10.1093/neuonc/nou350>
184. Ghiaeseddin A, Reardon DA, Massey W, Mannerino A, Lipp ES, Herndon JE, et al. Phase II study of bevacizumab and vorinostat for recurrent glioblastoma. *J Clin Oncol.* 2015;33(15_suppl):2034.
185. Weathers SP, Han X, Liu DD, Conrad CA, Gilbert MR, Loghin ME, et al. A randomized phase II trial of standard dose bevacizumab versus low dose bevacizumab plus lomustine (CCNU) in adults with recurrent glioblastoma. *J Neurooncol.* 2016;129(3):487–94. <http://dx.doi.org/10.1007/s11060-016-2195-9>
186. Field KM, Simes J, Nowak AK, Cher L, Wheeler H, Hovey EJ, et al. Randomized phase 2 study of carboplatin and bevacizumab in recurrent glioblastoma. *Neuro Oncol.* 2015;17(11):1504–13. <http://dx.doi.org/10.1093/neuonc/nov104>
187. Puduvalli VK, Wu J, Yuan Y, Armstrong TS, Groves MD, Raizer JJ, et al. Brain tumor trials collaborative Bayesian adaptive randomized phase II trial of bevacizumab plus vorinostat versus bevacizumab alone in adults with recurrent glioblastoma (BTTC-1102). *J Clin Oncol.* 2015;33(15_suppl):2012.
188. Galanis E, Anderson SK, Anastasiadis P, Tran DD, Jeyapalan SA, Anderson DM, et al. NCCTG N0872 (Alliance): A randomized placebo-controlled phase II trial of bevacizumab plus dasatinib in patients with recurrent glioblastoma (GBM). *J Clin Oncol.* 2015;33(15_suppl):2004.
189. Wick W, Brandes AA, Gorlia T, Bendszus M, Sahm F, Taal W, et al. Phase III trial exploring the combination of bevacizumab and lomustine in patients with first recurrence of a glioblastoma: The EORTC 26101 trial. *Neuro Oncol.* 2015;17(suppl_5):v1.
190. Pope WB, Lai A, Nghiemphu P, Mischel P, Cloughesy TF. MRI in patients with high-grade gliomas treated with bevacizumab and chemotherapy. *Neurology.* 2006;66(8):1258–60. <http://dx.doi.org/10.1212/01.wnl.0000208958.29600.87>
191. Ali SA, McHayleh WM, Ahmad A, Sehgal R, Braffet M, Rahman M, et al. Bevacizumab and irinotecan therapy in glioblastoma multiforme: A series of 13 cases. *J Neurosurg.* 2008;109(2):268–72. <http://dx.doi.org/10.3171/JNS/2008/109/8/0268>
192. Kang TY, Jin T, Elinzano H, Peereboom D. Irinotecan and bevacizumab in progressive primary brain tumors, an evaluation of efficacy and safety. *J Neurooncol.* 2008;89(1):113–18. <http://dx.doi.org/10.1007/s11060-008-9599-0>
193. Bokstein F, Shpigel S, Blumenthal DT. Treatment with bevacizumab and irinotecan for recurrent high-grade glioma tumors. *Cancer.* 2008;112(10):2267–73. <http://dx.doi.org/10.1002/cncr.23401>
194. Norden AD, Young GS, Setayesh K, Muzikansky A, Klufas R, Ross GL, et al. Bevacizumab for recurrent malignant gliomas: Efficacy, toxicity, and patterns of recurrence. *Neurology.* 2008;70(10):779–87. <http://dx.doi.org/10.1212/01.wnl.0000304121.57857.38>

195. Nghiemphu PL, Liu W, Lee Y, Than T, Graham C, Lai A, et al. Bevacizumab and chemotherapy for recurrent glioblastoma: A single-institution experience. *Neurology*. 2009;72(14):1217–22. <http://dx.doi.org/10.1212/01.wnl.0000345668.03039.90>
196. Zuniga RM, Torcuator R, Jain R, Anderson J, Doyle T, Elicka S, et al. Efficacy, safety and patterns of response and recurrence in patients with recurrent high-grade gliomas treated with bevacizumab plus irinotecan. *J Neurooncol*. 2009;91(3):329–36. <http://dx.doi.org/10.1007/s11060-008-9718-y>
197. Chamberlain MC, Johnston SK. Salvage therapy with single agent bevacizumab for recurrent glioblastoma. *J Neurooncol*. 2010;96(2):259–69. <http://dx.doi.org/10.1007/s11060-009-9957-6>
198. Scott BJ, Quant EC, McNamara MB, Ryg PA, Batchelor TT, Wen PY. Bevacizumab salvage therapy following progression in high-grade glioma patients treated with VEGF receptor tyrosine kinase inhibitors. *Neuro Oncol*. 2010;12(6):603–7. <http://dx.doi.org/10.1093/neuonc/nop073>
199. Gil MJ, de Las Penas R, Reynes G, Balana C, Perez-Segura P, Garcia-Velasco A, et al. Bevacizumab plus irinotecan in recurrent malignant glioma shows high overall survival in a multicenter retrospective pooled series of the Spanish Neuro-Oncology Research Group (GEINO). *Anticancer Drugs*. 2012;23(6):659–65. <http://dx.doi.org/10.1097/CAD.0b013e3283534d3e>
200. Goldlust SA, Cavaliere R, Newton HB, Hsu M, Deangelis LM, Batchelor TT, et al. Bevacizumab for glioblastoma refractory to vascular endothelial growth factor receptor inhibitors. *J Neurooncol*. 2012;107(2):407–11. <http://dx.doi.org/10.1007/s11060-011-0768-1>
201. Carvalho BF, Fernandes AC, Almeida DS, Sampaio LV, Costa A, Caeiro C, et al. Second-line chemotherapy in recurrent glioblastoma: A 2-cohort study. *Oncol Res Treat*. 2015;38(7–8):348–54. <http://dx.doi.org/10.1159/000431236>
202. Ballman KV, Buckner JC, Brown PD, Giannini C, Flynn PJ, LaPlant BR, et al. The relationship between six-month progression-free survival and 12-month overall survival end points for phase II trials in patients with glioblastoma multiforme. *Neuro Oncol*. 2007;9(1):29–38. <http://dx.doi.org/10.1215/15228517-2006-025>
203. Wong ET, Hess KR, Gleason MJ, Jaeckle KA, Kyrtsis AP, Prados MD, et al. Outcomes and prognostic factors in recurrent glioma patients enrolled onto phase II clinical trials. *J Clin Oncol*. 1999;17(8):2572–8. <http://dx.doi.org/10.1200/JCO.1999.17.8.2572>
204. Piccioni DE, Lai A. Deferred use of bevacizumab for recurrent glioblastoma is not associated with diminished efficacy. *Neuro Oncol*. 2014;16(10):1427–8. <http://dx.doi.org/10.1093/neuonc/nou214>
205. Kirson ED, Dbaly V, Tovarys F, Vymazal J, Soustiel JF, Itzhaki A, et al. Alternating electric fields arrest cell proliferation in animal tumor models and human brain tumors. *Proc Natl Acad Sci U S A*. 2007;104(24):10152–7. <http://dx.doi.org/10.1073/pnas.0702916104>
206. Keime-Guibert F, Chinot O, Taillandier L, Cartalat-Carel S, Frenay M, Kantor G, et al. Radiotherapy for glioblastoma in the elderly. *N Engl J Med*. 2007;356(15):1527–35. <http://dx.doi.org/10.1056/NEJMoa065901>
207. Stupp R, Taillibert S, Kanner AA, Kesari S, Steinberg DM, Toms SA, et al. Maintenance therapy with tumor-treating fields plus temozolomide vs temozolomide alone for glioblastoma: A randomized clinical trial. *JAMA*. 2015;314(23):2535–43. <http://dx.doi.org/10.1001/jama.2015.16669>
208. Nabors LB, Portnow J, Ammirati M, Baehring J, Brem H, Brown P, et al. National comprehensive cancer network clinical practice guidelines in oncology, Central Nervous System cancers. Version 1. 2016. Available from: http://www.nccn.org/professionals/physician_gls/f_guidelines.asp.
209. Bernard-Arnoux F, Lamure M, Ducray F, Aulagner G, Honnorat J, Armoiry X. The cost-effectiveness of tumor-treating fields therapy in patients with newly diagnosed glioblastoma. *Neuro Oncol*. 2016;18(8):1129–36. <http://dx.doi.org/10.1093/neuonc/now102>
210. Mehta M, Wen P, Nishikawa R, Reardon D, Peters K. Critical review of the addition of tumor treating fields (TTFields) to the existing standard of care for newly diagnosed glioblastoma patients. *Crit Rev Oncol Hematol*. 2017;111:60–5. <http://dx.doi.org/10.1016/j.critrevonc.2017.01.005>
211. Stupp R, Hegi ME, Mason WP, van den Bent MJ, Taphoorn MJ, Janzer RC, et al. Effects of radiotherapy with concomitant and adjuvant temozolomide versus radiotherapy alone on survival in glioblastoma in a randomised phase III study: 5-year analysis of the EORTC-NCIC trial. *Lancet Oncol*. 2009;10(5):459–66. [http://dx.doi.org/10.1016/S1470-2045\(09\)70025-7](http://dx.doi.org/10.1016/S1470-2045(09)70025-7)

212. Ostrom QT, Gittleman H, Fulop J, Liu M, Blanda R, Kromer C, et al. CBRUS statistical report: Primary brain and Central Nervous System tumors diagnosed in the United States in 2008–2012. *Neuro Oncol*. 2015;17(Suppl 4):iv1–iv62. <http://dx.doi.org/10.1093/neuonc/nov189>
213. Holdhoff M, Ye X, Blakeley JO, Blair L, Burger PC, Grossman SA, et al. Use of personalized molecular biomarkers in the clinical care of adults with glioblastomas. *J Neurooncol*. 2012;110(2):279–85. <http://dx.doi.org/10.1007/s11060-012-0968-3>
214. Chaichana KL, Garzon-Muvdi T, Parker S, Weingart JD, Olivi A, Bennett R, et al. Supratentorial glioblastoma multiforme: The role of surgical resection versus biopsy among older patients. *Ann Surg Oncol*. 2011;18(1):239–45. <http://dx.doi.org/10.1245/s10434-010-1242-6>
215. Ewelt C, Goepfert M, Rapp M, Steiger HJ, Stummer W, Sabel M. Glioblastoma multiforme of the elderly: The prognostic effect of resection on survival. *J Neurooncol*. 2011;103(3):611–18. <http://dx.doi.org/10.1007/s11060-010-0429-9>
216. Stark AM, Hedderich J, Held-Feindt J, Mehdorn HM. Glioblastoma—The consequences of advanced patient age on treatment and survival. *Neurosurg Rev*. 2007;30(1):56–61; discussion 61–2.
217. Malmstrom A, Gronberg BH, Marosi C, Stupp R, Frappaz D, Schultz H, et al. Temozolomide versus standard 6-week radiotherapy versus hypofractionated radiotherapy in patients older than 60 years with glioblastoma: The Nordic randomised, phase 3 trial. *Lancet Oncol*. 2012;13(9):916–26. [http://dx.doi.org/10.1016/S1470-2045\(12\)70265-6](http://dx.doi.org/10.1016/S1470-2045(12)70265-6)
218. Roa W, Brasher PM, Bauman G, Anthes M, Bruera E, Chan A, et al. Abbreviated course of radiation therapy in older patients with glioblastoma multiforme: A prospective randomized clinical trial. *J Clin Oncol*. 2004;22(9):1583–8. <http://dx.doi.org/10.1200/JCO.2004.06.082>
219. Gallego Perez-Larraya J, Ducray F, Chinot O, Catry-Thomas I, Taillandier L, Guillamo JS, et al. Temozolomide in elderly patients with newly diagnosed glioblastoma and poor performance status: An ANOCEF phase II trial. *J Clin Oncol*. 2011;29(22):3050–5. <http://dx.doi.org/10.1200/JCO.2011.34.8086>
220. Chinot OL, Barrie M, Frauger E, Dufour H, Figarella-Branger D, Palmari J, et al. Phase II study of temozolomide without radiotherapy in newly diagnosed glioblastoma multiforme in an elderly populations. *Cancer*. 2004;100(10):2208–14. <http://dx.doi.org/10.1002/cncr.20224>
221. Laperriere N, Weller M, Stupp R, Perry JR, Brandes AA, Wick W, et al. Optimal management of elderly patients with glioblastoma. *Cancer Treat Rev*. 2013;39(4):350–7. <http://dx.doi.org/10.1016/j.ctrv.2012.05.008>
222. Behm T, Horowski A, Schneider S, Bock HC, Mielke D, Rohde V, et al. Concomitant and adjuvant temozolomide of newly diagnosed glioblastoma in elderly patients. *Clin Neurol Neurosurg*. 2013;115(10):2142–6. <http://dx.doi.org/10.1016/j.clineuro.2013.08.002>
223. Rusthoven CG, Koshy M, Sher DJ, Ney DE, Gaspar LE, Jones BL, et al. Combined-modality therapy with radiation and chemotherapy for elderly patients with glioblastoma in the temozolomide era: A national cancer database analysis. *JAMA Neurol*. 2016;73(7):821–8. <http://dx.doi.org/10.1001/jamaneuro.2016.0839>
224. Perry JR, Laperriere N, O’Callaghan CJ, Brandes AA, Menten J, Phillips C, et al. Short-course radiation plus temozolomide in elderly patients with glioblastoma. *N Engl J Med*. 2017;376(11):1027–37. <http://dx.doi.org/10.1056/NEJMoa1611977>
225. Arvold ND, Tanguturi SK, Aizer AA, Wen PY, Reardon DA, Lee EQ, et al. Hypofractionated versus standard radiation therapy with or without temozolomide for older glioblastoma patients. *Int J Radiat Oncol Biol Phys*. 2015;92(2):384–9. <http://dx.doi.org/10.1016/j.ijrobp.2015.01.017>
226. Minniti G, Scaringi C, Lanzetta G, Terrenato I, Esposito V, Arcella A, et al. Standard (60 Gy) or short-course (40 Gy) irradiation plus concomitant and adjuvant temozolomide for elderly patients with glioblastoma: A propensity-matched analysis. *Int J Radiat Oncol Biol Phys*. 2015;91(1):109–15. <http://dx.doi.org/10.1016/j.ijrobp.2014.09.013>
227. Ostgathe C, Gaertner J, Kotterba M, Klein S, Lindena G, Nauck F, et al. Differential palliative care issues in patients with primary and secondary brain tumours. *Support Care Cancer*. 2010;18(9):1157–63. <http://dx.doi.org/10.1007/s00520-009-0735-y>
228. Temel JS, Greer JA, Muzikansky A, Gallagher ER, Admane S, Jackson VA, et al. Early palliative care for patients with metastatic non-small-cell lung cancer. *N Engl J Med*. 2010;363(8):733–42. <http://dx.doi.org/10.1056/NEJMoa1000678>

229. Sizoo EM, Pasman HR, Buttolo J, Heimans JJ, Klein M, Deliëns L, et al. Decision-making in the end-of-life phase of high-grade glioma patients. *Eur J Cancer*. 2012;48(2):226–32. <http://dx.doi.org/10.1016/j.ejca.2011.11.010>
230. Triebel KL, Martin RC, Nabors LB, Marson DC. Medical decision-making capacity in patients with malignant glioma. *Neurology*. 2009;73(24):2086–92. <http://dx.doi.org/10.1212/WNL.0b013e3181c67bce>
231. Bausewein C, Hau P, Borasio GD, Voltz R. How do patients with primary brain tumours die? *Palliat Med*. 2003;17(6):558–9. <http://dx.doi.org/10.1177/026921630301700615>
232. Faithfull S, Cook K, Lucas C. Palliative care of patients with a primary malignant brain tumour: Case review of service use and support provided. *Palliat Med*. 2005;19(7):545–50. <http://dx.doi.org/10.1191/0269216305pm1068oa>
233. Oberndorfer S, Lindeck-Pozza E, Lahrmann H, Struhlar W, Hitzenberger P, Grisold W. The end-of-life hospital setting in patients with glioblastoma. *J Palliat Med*. 2008;11(1):26–30. <http://dx.doi.org/10.1089/jpm.2007.0137>
234. Pace A, Di Lorenzo C, Guariglia L, Jandolo B, Carapella CM, Pompili A. End of life issues in brain tumor patients. *J Neurooncol*. 2009;91(1):39–43. <http://dx.doi.org/10.1007/s11060-008-9670-x>
235. Sizoo EM, Braam L, Postma TJ, Pasman HR, Heimans JJ, Klein M, et al. Symptoms and problems in the end-of-life phase of high-grade glioma patients. *Neuro Oncol*. 2010;12(11):1162–6. <http://dx.doi.org/10.1093/neuonc/nop045>
236. Sizoo EM, Pasman HR, Dirven L, Marosi C, Grisold W, Stockhammer G, et al. The end-of-life phase of high-grade glioma patients: A systematic review. *Support Care Cancer*. 2014;22(3):847–57. <http://dx.doi.org/10.1007/s00520-013-2088-9>
237. Sizoo EM, Koekkoek JA, Postma TJ, Heimans JJ, Pasman HR, Deliëns L, et al. Seizures in patients with high-grade glioma: A serious challenge in the end-of-life phase. *BMJ Support Palliat Care*. 2014;4(1):77–80. <http://dx.doi.org/10.1136/bmjspcare-2013-000456>
238. Vecht CJ, Wagner GL, Wilms EB. Treating seizures in patients with brain tumors: Drug interactions between antiepileptic and chemotherapeutic agents. *Semin Oncol*. 2003;30(6 Suppl 19):49–52. <http://dx.doi.org/10.1053/j.seminoncol.2003.11.030>
239. Weller M, Gorlia T, Cairncross JG, van den Bent MJ, Mason W, Belanger K, et al. Prolonged survival with valproic acid use in the EORTC/NCIC temozolomide trial for glioblastoma. *Neurology*. 2011;77(12):1156–64. <http://dx.doi.org/10.1212/WNL.0b013e31822f02e1>
240. Usery JB, Michael LM, Sills AK, Finch CK. A prospective evaluation and literature review of levetiracetam use in patients with brain tumors and seizures. *J Neurooncol*. 2010;99(2):251–60. <http://dx.doi.org/10.1007/s11060-010-0126-8>
241. Koekkoek JA, Postma TJ, Heimans JJ, Reijneveld JC, Taphoorn MJ. Antiepileptic drug treatment in the end-of-life phase of glioma patients: A feasibility study. *Support Care Cancer*. 2016;24(4):1633–8. <http://dx.doi.org/10.1007/s00520-015-2930-3>
242. Rooney AG, Brown PD, Reijneveld JC, Grant R. Depression in glioma: A primer for clinicians and researchers. *J Neurol Neurosurg Psychiatry*. 2014;85(2):230–5. <http://dx.doi.org/10.1136/jnnp-2013-306497>
243. Alper K, Schwartz KA, Kolts RL, Khan A. Seizure incidence in psychopharmacological clinical trials: An analysis of Food and Drug Administration (FDA) summary basis of approval reports. *Biol Psychiatry*. 2007;62(4):345–54. <http://dx.doi.org/10.1016/j.biopsych.2006.09.023>
244. Taillandier L, Blonski M, Darlix A, Hoang Xuan K, Taillibert S, Cartalat Carel S, et al. Supportive care in neurooncology. *Rev Neurol (Paris)*. 2011;167(10):762–72. <http://dx.doi.org/10.1016/j.neurol.2011.08.008>
245. Walbert T, Khan M. End-of-life symptoms and care in patients with primary malignant brain tumors: A systematic literature review. *J Neurooncol*. 2014;117(2):217–24. <http://dx.doi.org/10.1007/s11060-014-1393-6>

12

Surgical Management of Glioblastoma

SALVADOR MANRIQUE-GUZMÁN • TENOCH HERRADA-PINEDA • FRANCISCO REVILLA-PACHECO

ABC Neurological Center, Neurosurgery Department, Mexico City, Mexico

Author for correspondence: Salvador Manrique-Guzman, ABC Neurological Center, Neurosurgery Department, Calle Sur 136-116 Office 2-B, Col. Las Américas, 01120 Mexico City, México. E-mail: manriquemd@yahoo.com

Doi: <http://dx.doi.org/10.15586/codon.glioblastoma.2017.ch12>

Abstract: Malignant gliomas are characterized by their propensity to invade surrounding brain parenchyma. The median survival of patients is less than 2 years with maximal surgical resection, chemotherapy, and radiotherapy. Although there have been controversial arguments about the role of surgical resection, there is increasing evidence that a safe and radical removal of malignant glioma is associated with a better survival outcome. Surgery is still essential to obtain brain tissue for pathological analysis, and reduce mass effect. Intraoperative magnetic resonance imaging, neuronavigation, ultrasonography, and fluorescence-guided surgery are the most used tools worldwide. 5-Aminolevulinic acid surgery, combined with Stupp protocol, produces a median survival of 15 months. The objectives of perioperative positioning are to enhance optimal exposure, prevent injury related to position, and maintain normal body alignment without excess flexion, extension, or rotation. Advances in surgical techniques have contributed to enhanced recovery after tumor resection, improved postoperative functional status, and decreased length of stay in the hospital. This chapter presents the current literature related to the surgical management of high-grade gliomas.

Key words: Extent of resection; Fluorescence-guided surgery; High-grade glioma

In: *Glioblastoma*. Steven De Vleeschouwer (Editor), Codon Publications, Brisbane, Australia ISBN: 978-0-9944381-2-6; Doi: <http://dx.doi.org/10.15586/codon.glioblastoma.2017>

Copyright: The Authors.

Licence: This open access article is licenced under Creative Commons Attribution 4.0 International (CC BY 4.0). <https://creativecommons.org/licenses/by-nc/4.0/>

Introduction

The annual incidence of malignant glioma is about 5.26 cases per 100,000 people (1, 2). Malignant astrocytomas are the most common malignant primary central nervous system tumors in adults (3). Glioblastoma accounts for approximately 60–70% of malignant glioma (1, 3, 4). The number of patients is expected to increase with the aging of population, the peak incidence being within the fifth and sixth decades of life (2, 4). The most common symptoms of glioblastoma include headache, focal neurologic deficits, and other nonspecific changes such as altered mental state or gait alteration (5). The classification of brain tumors has been based largely on concepts of histogenesis that label tumors according to their microscopic similarities with putative cells of origin, their presumed differentiation level, and the degree of tumor as a prognostic factor (6, 7). According to clinical characteristics, glioblastomas can be divided into primary and secondary subtypes. Primary glioblastomas emerge from *de novo* process whereas secondary glioblastomas develop progressively from low-grade astrocytoma, over a period of 5–10 years (8). Recently, the Cancer Genome Atlas Network classified glioblastoma into proneural, neural, classical, and mesenchymal, and established an integrated multidimensional genomic data based on patterns of somatic mutations and DNA copy number (9) (Table 1).

Adult neural stem cells, in the subventricular zone and on the walls of the lateral ventricle (LV), generate young neurons and oligodendrocytes under non-pathologic conditions (10). This unique region, which harbors neural stem cells, appears to be more susceptible to tumorigenesis (10). Tumors bordering the LV and patients with subependymal-spreading tumor may be associated with decreased survival. Chaichana et al. reported that the median survival time of patients with LV tumors is less than those with non-LV tumors (8 months vs. 11 months; $P = 0.02$) (11). Glioblastoma progression is thought to be driven by a subpopulation of cancer stem cells, and *in vitro* studies show that these cells are chemoresistant and radioresistant (12). However, Nestler et al. were not able to support the theory of malignant glioma developing in the periventricular stem cell region (13). Most tumors (89%) were in contact with brain cortical regions,

TABLE 1
Comparative Table of the Molecular Classification of Glioblastoma

Phillips et al. (14)	Proneural	Proliferative		Mesenchyme
Verhaak et al. (9)	Proneural	Neural	Classic	Mesenchyme
Genetic signature	Olig2/DLL#/SOX2	MBP/MAL	EGFR/AKT2	YKL40/CD44
Mutation	TP53 PI3K PDGFRA		crom7 (gain) crom10 (lost) PDGFRA	NFkB NF1
Clinical characteristic	Little response to chemotherapy		Favorable prognostic to TMZ and RT	Favorable prognostic to TMZ and RT

whereas only half of glioblastomas (52%) involved the ventricular wall (13). Older age, poor performance status, motor or language deficit, and periventricular tumor location independently predict poor survival in patients with glioblastoma (15). Infiltration and invasion of malignant astrocytoma often involve eloquent areas (4). Historically, surgery has been the initial therapeutic approach for tumor debulking (decompressing mass effect) as well as for obtaining tissues for diagnosis (16, 17). Walter Dandy, in 1928, studied a series of patients undergoing hemispherectomy for invasive high-grade glioma (17, 18). The case series included a patient surviving three and a half years following surgical resection. High doses of corticosteroids (usually dexamethasone 8–16 mg/day) allowed fast decrease of tumor-associated edema and improved clinical symptoms, which were rapidly tapered according to individual needs (4, 19, 20). This chapter provides an overview of surgical management of high-grade gliomas.

PREOPERATIVE EVALUATION

Signed informed consent is mandatory for all surgical candidates in Mexico and in most surgical centers worldwide before going into the operating room (OR). Abstinence from both alcohol and cigarette for 1 month is recommended when appropriate and feasible (21). Preoperative intracranial tumor evaluation should include the assessment of neurological and general status. Current treatments such as steroids and osmotic diuretics must be considered. Assessing status of intracranial pressure (ICP) is the primary aim of evaluating neurological status. Seizures secondary to direct mass effect can also occur in about 60% of cases (22). Antiepileptic drug for seizure prophylaxis is decided by assessment of individual risk factors and careful discussion with patients (22). Preoperative administration of steroids helps to control ICP by reducing peritumoral edema. Patients with symptomatic high-grade tumors (HGTs) or with poor life expectancy can be maintained on dexamethasone 0.5–1 mg daily. The side effects of steroids are common, and their frequency and severity increase with higher dose and therapy duration. Patients must be monitored for endocrine, muscular, skeletal, gastrointestinal, psychiatric, and hematological complications (19). Brain relaxation can be achieved using either hypertonic saline (HS) or mannitol. A recent meta-analysis pointed out that HS could increase the odds of satisfactory intraoperative brain relaxation (OR: 2.25, 95% CI: 1.32–3.81; $P = 0.003$) (22).

INTRAVENOUS ANESTHETICS

Barbiturates have four main actions in the brain: (i) hypnosis, (ii) depression of cerebral metabolic rate (CMR), (iii) reduction in cerebral blood flow (CBF) by increasing cerebral vascular resistance (CVR), and (iv) anticonvulsant activity. All of these actions are able to produce significant hypotension. Propofol has a relative short half-life (1–2 h) but causes hypotension with marked reduction in cerebral perfusion pressure (CPP) (24). Opioids (synthetic opioids: fentanyl, sufentanil, alfentanil, and remifentanil) attenuate ventilator response to hypercarbia and enable the ventilator response to hypoxia, increasing CBF through an increase in PaCO_2 . Most opioids (except meperidine) are vasotonic, so they can lead to bradycardia; in patients with brain tumors, it is important to distinguish this effect from Cushing's reflex (25). Dexmedetomidine is a highly selective alpha-2 adrenergic receptor agonist.

Clinical effects are both sedative-hypnotic and analgesic by activating alpha-2 adrenergic receptors in the locus coeruleus and the spinal cord. This sedation is useful for awake craniotomy because of the mild increase in PaCO₂ (26, 27).

MUSCLE RELAXANTS

Neuromuscular blocking agents (NMBAs) do not have direct effect on CMR, ICP, or CBF. Pancuronium can increase heart rate and mean arterial pressure (MAP). Succinylcholine can increase ICP in brain tumor patients, secondary to the cerebral activation associated with fasciculation and enhanced muscle spindle activity; however, when coadministered with the intravenous agent propofol, ICP can be alleviated (28).

EXTENT OF RESECTION

Cytoreductive surgery for malignant glioma has been performed for decades, from lobectomies to hemispherectomies (17, 29). The purpose of resection is to remove as much tumor as possible to alleviate mass effect and to obtain brain tissue for pathological analysis (class I evidence) (30). Tumor recurrence occurs within a 2-cm margin of the primary site in 90% of the cases (31–33). Evidence to promote brain tumor resections in the current literature are as follows: Ia: 0(0%), Ib: 0(0%), IIa: 1(0.8%), IIb: 7(5.8%), IIc: 0(0%), IIIa: 16 (13.3%), IIIb: 63 (52.5%), IV: 13 (10.8%), and V: 20 (16.8%) (31). Post hoc analysis of 243 patients, randomized for extent of resection in a trial of 5-Aminolevulinic acid (5-ALA) versus white light in newly diagnosed HGG, suggested a positive correlation between complete resection and survival benefit (HR 0.54, 95% CI 0.41 to 0.71) (5). Once the diagnosis for malignant glioma is established, fractionated focal radiotherapy (60 Gys) and chemotherapy are continued. The first-line of choice for chemotherapy is temozolomide (TMZ 75 mg/m²), administered daily around 1 and 1.5 h prior to radiotherapy during the initial phase. For the maintenance phase, the dosage increases to 150–200 mg/m², 5 days a week, every 28 days (29).

Intraoperative Technologies

Emerging imaging technologies facilitate the extent of resection while minimizing the associated morbidity profile (16). Novel assisting technologies require expensive equipment along with prolonged surgical time; more evidence is necessary to justify such adjuncts (34).

FLUORESCENCE-GUIDED SURGERY

5-ALA is a natural amino acid biosynthesized from glycine and succinyl-CoA in the mitochondria. Following systemic administration, ALA in tumor cells is metabolized into protoporphyrin IX (PpIX), a photosensitizing porphyrin (35). The reason for the selective PpIX accumulation in malignant glioma is not fully understood. It is highly specific (98%) in areas of infiltrating tumor, and

TABLE 2

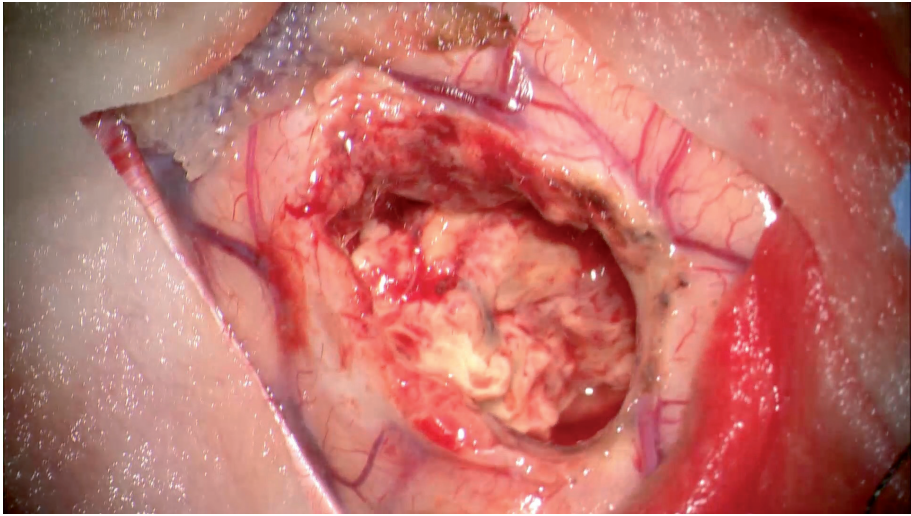
Commercially Available Fluorophores for Fluorescence-Guided Surgery

	5-ALA	Fluorescein	ICG
Fluorophores	Protoporphyrin IX (PpIX)	Sodium Fluorescein	ICG tricarbo-cyanine
Localization	Intracellular	Extracellular/ Intravascular (43)	Intravascular
Range of photo-stimulation	409 ± 10 nm	540–690 nm	790–835 nm
Sensitivity & specificity	0.87 (IC 95%, 0.81–0.92) 0.89 (IC 95%, 0.79–0.94) (44)	NA	Correlation >90% Digital Angiographic Subtraction
Dose	20 mg/kg	8–10 mg/kg 20 mg/kg	0.3 mg/kg
Administration route	Orally	Intravenous	Intravenous (45)
Adverse reactions	Photosensitivity, nausea, hypertension	Nausea and vomit, anaphylaxis, death (7, 46)	None
Auto fluorescence	Yes	No	No (45)
Contraindications	Porphyria	NR	Iodine allergy, pregnancy, liver disease, uremia, and history of anaphylaxis

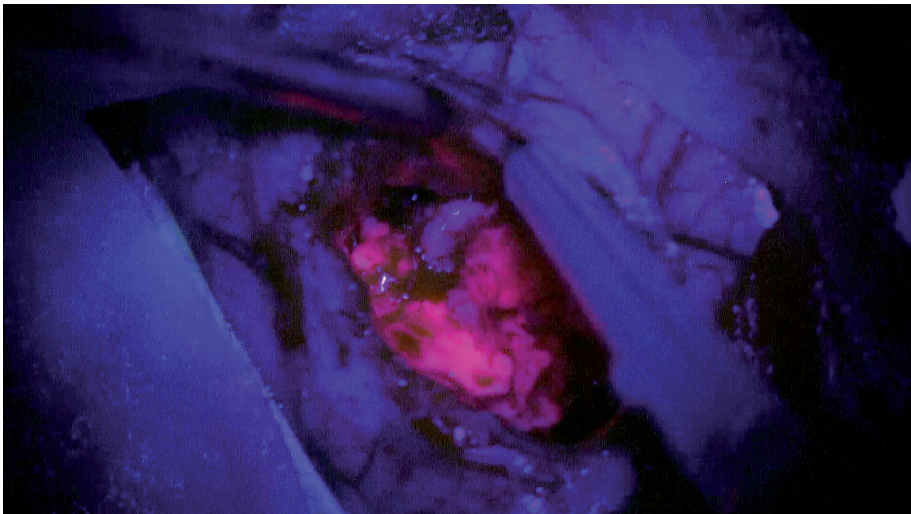
PpIX-levels in tumor tissue are highest at 6 h after administration (36) (Table 2). 5-ALA is an orally administered product used for visualization of high-grade glioma tissue during surgery, allowing a safer and more extensive tumor resection. Under blue light excitation (400–410 nm), the tumor tissue appears red, whereas normal tissue (including edema) does not show fluorescence (37) (Figure 1). Another fluorophore is fluorescein sodium; the major disadvantage is that the fluorescence depends on blood–brain barrier integrity, making it less specific. Fluorescein concentration will be high in all perfused tissues and vessels. If tissue is perturbed by surgery, there is unspecific extravasation of fluorescein unrelated to tumor (38). After patient intubation and before skin incision, patients receive 5–10 mg/kg of a 20% solution of sodium fluorescein, administered intravenously using a modified microscope with wavelength range of 560 nm (39) (Figure 2).

INDOCYANINE GREEN

Angiography with indocyanine green (ICG) was first developed for ophthalmology purposes in 1956 to evaluate choroidal microcirculation; other uses are to assess hepatic function, live blood flow, and cardiac output (40). Near-infrared ICG videoangiography was introduced in the neurosurgical field to visualize cerebral vessels for aneurysm clipping, bypasses, and vascular malformations. Superficial avascular areas in HGT have been seen during pre-resection



(a)



(b)

Figure 1 (a) Brain tumor resection using regular white light and (b) blue excitation light (400–410 nm) using 5-ALA; the tumor tissue appears red, whereas normal tissue shows no fluorescence. (Courtesy of Prof. Walter Stummer.)

ICG videoangiography (41). Neovascular architecture; alterations of the caliber, morphology, and course of vessels; and the hemodynamic patterns can be observed. The dye does not penetrate the membrane and therefore is unable to define the margins of the tumors (42). ICG helps to avoid injury by preserving small caliber vessels during brain tumor surgery (Figure 3).



Figure 2 Brain tumor resection using fluorescein. The whole brain parenchyma and tumor tissues were colored and fixed; the blood–brain barrier had been damaged, making it less specific. (Courtesy of Prof. Walter Stummer.)

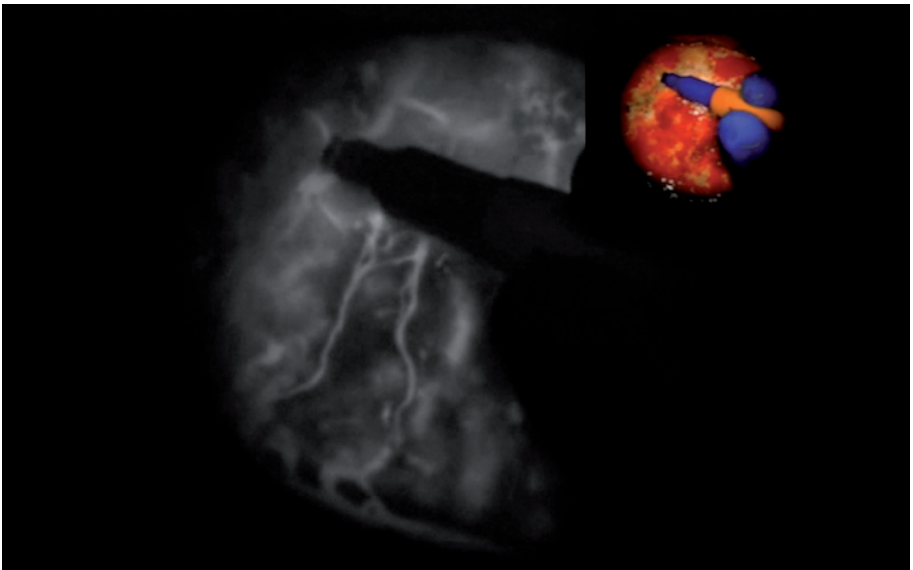


Figure 3 Intraoperative videoangiography in the arterial phase with combined white-light visualization to localize major vasculature and avoid medium and small vessel injury. (Courtesy of Prof. Alfredo Quiñones-Hinojosa.)

NEURONAVIGATION

Neuronavigation systems have been developed for image-guided neurosurgery to aid accurate lesion localization in the brain. Before craniotomy, the patient's head is secured to a head holder with head pins; this fixation might cause skin displacement (skin shift) and reduce accuracy which could be corrected using intraoperative imaging systems (CT and/or magnetic resonance imaging, MRI) (43). The most-widely used tracking systems utilize dual infrared camera that tracks the position of a probe relative to a fixed reference frame. Electromagnetic tracking systems are the major commercially available alternatives to optical tracking systems. Electromagnetic navigation relies on the tracking probe within an electromagnetic field, created by a field generator in a fixed location. Using MRI, the positional accuracy is within 2–3 mm during surgery. Clinical factors that cause shift of the brain or a lesion, such as cerebrospinal fluid loss, cyst decompression, and cerebral edema, may diminish navigational accuracy (44). Neuronavigation is most useful as an adjunct to other brain-mapping techniques such as awake mapping and electrocorticography in the resection of lesions within eloquent motor and language areas (45). Intraoperative MRI has become more widespread and the evidence supporting the use of intraoperative MRI to maximize resection has also grown. A systematic review of existing data on the use of intraoperative MRI for glioma surgery revealed 12 high-quality studies providing level II evidence for the use of intraoperative MRI to improve the extent of resection, quality of life, and survival in glioma patients (46).

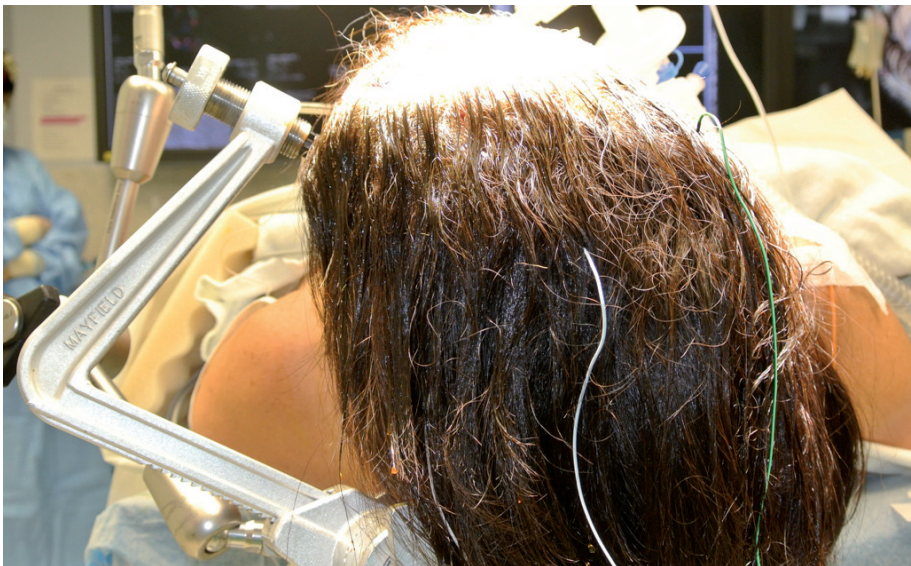
Patient Position

Patient positioning is an essential element before the surgical procedure. Patient's safety is the responsibility of all team members. The objectives of perioperative positioning are the following: optimal surgical exposure; preventing injury; and maintaining normal body alignment without too much flexion, extension, or rotation (47). The operating table is situated in the central area of the OR. Control consoles (monopolar and bipolar coagulation, suction, and drills) are located at the foot of the operating table. An electrophysiological technician is involved when neurophysiological monitoring is indicated. The surgical microscope should be used carefully in accordance with the manufacturer's recommendations. All hardware (optic attachments, eyepieces, mouthpiece, and video-recording device) must be checked before the surgical procedure and adjusted to the surgeon's specifications. When possible, neuronavigation systems can be synchronized to the microscope with the focal point of the surgeon's microscopic view (48). Maintaining normothermia is essential; peripheral vasoconstriction following anesthesia is often common and can result in peripheral hypoperfusion and cell hypoxia (47, 49). Other measures include minimizing skin exposure, using a temperature-regulating blanket or forced-air warming device, and controlling the OR ambient temperature. Neurosurgical procedures are known for extended surgical time, thus increasing the risk of pressure ulcers. Tissue hypoperfusion, ischemia, and necrosis can occur. Soft devices (i.e., gel pad, cotton roll) have to be placed between the patient and any hard surface. The use of graduate compression

stocking and intermittent pneumatic compression is recommended in craniotomy patients to prevent venous thromboembolism (50, 51). Routine use of anticoagulants is not recommended (20, 51). Burn prevention, from electrosurgical tools, can be achieved by ensuring that the patient's skin does not rub against any metal surface (47). *Staphylococcus aureus* is responsible for 32% of the surgical site infections after craniotomy (52). Proper head position allows optimal exposure for surgical access. The use of the three-pin skull clamp can firmly fixate the head in the desired position. Pins should be placed in a band-like distribution on the head. They are often coated with antibiotic ointment before pinning the head. Thin bones, for example, the temporal bone squamous portion, frontal sinus, and mastoid sinus should be avoided. Prior placed shunt, cranial defects, and thick temporalis muscle may cause unstable fixation (53). The practice of shaving before surgery has not proven to reduce surgical site infection. Most surgeons choose to perform a small (<1 cm) strip parallel to the skin incision (21).

SUPRATENTORIAL APPROACHES: SUPINE POSITION

Supine position is often used in neurosurgery because it offers good exposure to (i) anterior and middle fossae of the cranium, (ii) anterior aspect of the neck, and (iii) anterior, medial, and lateral aspects of the upper and lower extremities. Patients' arms should be flexed less than 90° from the long axis to avoid intravenous drop obstruction, injury to the brachial plexus, and compression or occlusion of the subclavian and axillary arteries (54) (Figure 4). Preoperative MRI is obtained with skin markers (fiducials when needed), and a surgical trajectory is planned,

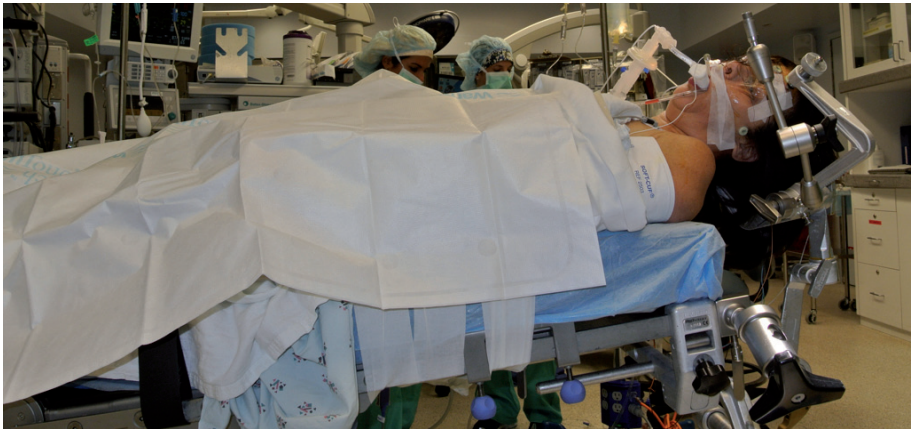


(a)

Figure continued on following page



(b)



(c)

Figure 4 Head-fixation system is recommended when the neuronavigation system is used. The head clamp must be firmly secured to the skull. Special attention is required when awake craniotomy is performed (a). Head rotation should be limited to the patient's cervical spine condition and to avoid reducing venous return (b). The head must be maintained above the heart level to reduce bleeding (c). (Courtesy of Prof. Alfredo Quiñones-Hinojosa.)

avoiding corticospinal tracts or any other eloquent area. After head fixation, the tumor plane is aligned perpendicular to the floor. The head is kept above the level of the heart. The skin incision is planned based on the location of the lesion. Eyebrow or eyelid incisions can be selected in patients with anterior lesions (55, 56). The craniotomy entry point depends on tumor location; one burr hole is often

sufficient for small craniotomies using a high-speed drill. Dural opening is adjusted to specific needs using either a cruciate or a C-shaped fashion. Trans-sulcal approach can be used for intra-axial lesions in the subcortical space underlying an evident sulcus. For deep tumors in the subcortical space (>1 cm), it may allow an easy access for resection while minimizing disruption of the overlying cortical tissue. The arachnoid overlying the sulcus is incised sharply and is usually opened where the subarachnoid space is the largest. Arteries and veins running within the sulci that supply and provide venous drainage to surrounding gyri must be preserved and bipolar cautery should be used only if bleeding occurs. Use of brain retraction system must be carefully evaluated to avoid pressure-related iatrogenic injury to the surrounding cortical tissue. Once the tumor is identified, it can be resected en bloc or by piecemeal fashion. The tumor can be debulked in such a way that edges are moved inward and removed. Transcortical approaches could be used for subcortical tumors that neither underlie an obvious sulcus nor involve eloquent cortical regions. Corticectomy should be performed in a linear fashion for small tumors. For larger tumors, circumferential corticectomy is preferred (57). For deep intra-axial lesion, tubular retractor system could be useful, as it creates a controlled surgical corridor with minimal brain retraction and damage to the surrounding brain tissue, to reach lesion in the basal ganglia, insular cortex, lateral and/or third ventricle, pineal region, and the thalamus (58). The craniotomy must be large enough to fit the tubular retractor. The initial approach might be transcortical or trans-sulcal. The navigation probe is conducted through the brain parenchyma and the tubular retractor is gently pushed down into the white matter. The retractor is opened to create the surgical corridor to access the lesion (59).

INFRATENTORIAL APPROACHES

Infratentorial approaches have been used since the 1990s for posterior fossa lesions using either craniotomy or craniectomy, usually using the asterion as a constant bone landmark, extending the resection down into the foramen magnum (60). Numerous approaches including anterior petrosectomy, posterior petrosectomy, translabyrinthine, and transcochlear have been developed. A key element to reduce surgical complications is the correct position of the patient, as it will provide a good surgical corridor minimizing brain tissue retraction. Lesions of the cerebellar-pontine angle, whether emerging extra-axially or intra-axially, are challenging due to surrounding vascular and eloquent neural structures. Furthermore, bone anatomy limits access to the ventral surface of the brain stem. Most surgeons begin with the surgical exposure of Dandy's point for potential intraoperative intraventricular catheter placement (61).

PRONE POSITION

Prone position provides good exposure to the dorsal surface of the body. It allows access to the posterior head, neck, and spinal column. For occipital and suboccipital lesions, chest rolls are required. Areas on the patient's body with excess pressure or traction are to be protected using a thick foam pad. The suboccipital craniotomy is used for most lesions in the posterior fossa, for example, tumors (meningiomas, ependymomas, gliomas, medulloblastomas, acoustic neuromas, and metastatic lesions), vascular lesions (aneurysm, cavernous malformations, arteriovenous

malformations, and intraparenchymal hemorrhages), and development anomalies (Chiari malformations). Patients with cervical spine disease with limited flexion and rotation movements should be excluded from this position (62).

SITTING POSITION

In 1931, De Martel introduced the sitting position for patients undergoing neurosurgical procedures (63). Posterior fossa tumors can be reached with good exposure using the sitting position. Although it has lost its popularity, it is still used in some surgical centers. Major disadvantages of this approach include venous air emboli (6–76%), pneumocephalus, and bradycardia (63). Preoperative cardiology evaluation, cardiac Doppler ultrasound, and intraoperative neurophysiology monitoring are essential. Intraoperative transesophageal echo or precordial Doppler monitoring can be used to track any air embolism, while a right atrial central venous pressure line can be placed to aspirate the air embolism. Patients with patent foramen ovale are in higher morbidity risk, so an alternative surgical position should be considered. Anesthesiological monitoring also includes a central venous catheter placed in the right atrium, continuous invasive blood pressure measurement with an arterial catheter (radial artery most of the times), electrocardiogram, pulse oximetry, and capnography with end-tidal CO₂ (64) (Figure 5).



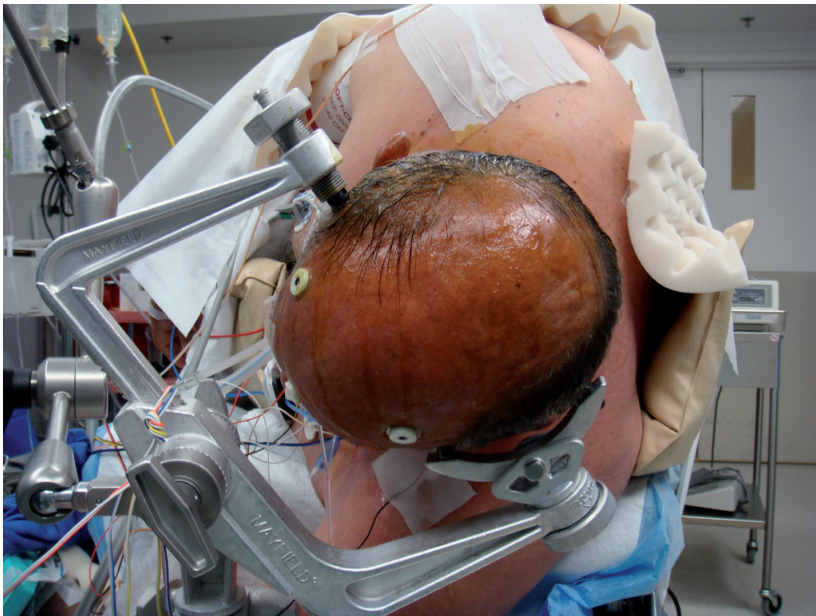
Figure 5 Although it has lost its popularity, sitting position is still used in some surgical centers. Attention must be paid to avoid pressure points (red arrows). The head is partially flexed and the neck turned to lesion side. All care must be taken to prevent neural injury of the spinal cord or the brachial plexus with continuous neurophysiological monitoring. Air embolism detection is essential to avoid complications. Used with permission from the original copyright holder, Elsevier.

PARK BENCH POSITION

Park bench position is the modification of the lateral position and is very commonly used for more laterally positioned lesions, including the lateral cerebellar hemisphere and cerebellopontine angle. The head is flexed and the vertex of the head is tilted toward the floor. Excessive neck flexion and/or side bending may prevent venous return. Patient is well padded to avoid pressure injuries, especially to the ulnar nerve, brachial plexus, and popliteal fossa (Table 3; Figure 6).

TABLE 3
Advantages and Disadvantages of Prone and Sitting Positions for Posterior Fossa Approaches

	Prone position	Sitting position
Air embolism	Less likely	Highly likely
Brain tissue retraction	Highly likely	Less likely
Cervical spine traction	Less likely	Highly likely
Venous sinus thrombosis	Equally likely	Equally likely
Pneumoencephalus	Less likely	Highly likely
Anatomic orientation	Less likely	Highly likely
Cranial nerve preservation (65)	Highly likely	Less likely



(a)

Figure continued on following page



(b)



(c)

Figure 6 The park bench position. (a) The face should be facing the floor. Shoulder retractor will allow a more comfortable working area for the surgeon. (b) Cushion paths are placed under the axilla to prevent brachial plexus injury. (c) The incision is planned from above the pinna down to the mastoid process, 2 cm behind the ear. (Courtesy of Prof. Alfredo Quinones-Hinojosa.)

TABLE 4**Preoperative and Operative Predictors of Extended Length of Hospital Stay Following Craniotomy for Tumor (8 Days)**

Variable	OR	95%CI	P
Age over 70 years	1.67	1.41–1.99	<0.001
African American	1.79	1.48–2.17	<0.001
Hispanic	1.54	1.25–1.89	<0.001
Infratentorial	1.42	1.26–1.61	<0.001
ASA class 3	1.59	1.40–1.79	<0.001
ASA class 4 & 5	2.41	2.03–2.86	<0.001
Diabetes mellitus with insulin treatment	1.50	1.20–1.87	<0.001
Class I obesity	0.84	0.72–0.97	0.02
Preop sodium (mEq/L) <135	1.26	1.08–1.47	0.003
Impaired sensorium	1.69	1.24–2.31	0.001
Hemiplegia	2.40	1.84–3.13	<0.001
Steroid use	0.67	0.58–0.76	<0.001
Anesthesia time >300 min	2.28	1.96–2.65	<0.001
Mechanical ventilation >48 h	11.07	6.56–18.70	<0.001 ^a

Source: Adapted from Ref. (66).

ASA = American Society of Anesthesiologists.

^aAll predictors model.

POSTOPERATIVE CARE

Incidence of postoperative complications within 30 days of tumor resection is as follows: stroke (2.1%), myocardial infarction (1.3%), death (2.7%), infection (2.4%), and the need for revision surgery (6.6%). Aiding early hospital discharge for cancer patients expedites chemotherapy and/or radiation therapy and other treatments, potentially improving patient outcomes by decreasing the time period between surgery and resumption of daily activities (20). Bladder catheters are to be removed on postoperative day 1 or as early as possible. Postoperative artificial nutrition is not typically needed for these patients, unless patients are in a prolonged comatose state (>7 days). Early mobilization of patients is encouraged (20) (Table 4). Venous thromboembolic events, pneumonia, and respiratory complications are preventable comorbidities. Urinary tract infections are independently associated with longer hospitalization (67%).

Conclusion

Surgery plays an essential role in the management of glioblastoma. A combination of techniques including intraoperative MRI, neuronavigation, ultrasonography,

and fluorescence-guided surgery has enabled safe and maximal surgical resection, leading to a better survival outcome, and postoperative functional recovery. Despite maximal surgical resection and adjuvant chemoradiation, tumor recurrence occurs within 10 months in many cases, thought to be mediated by resident cancer stem cells. It is imperative that more effective treatment strategies are developed for glioblastoma.

Conflict of interest: The authors declare no potential conflicts of interest with respect to research, authorship, and/or publication of this manuscript.

Copyright and permission statement: To the best of our knowledge, the materials included in this chapter do not violate copyright laws. All original sources have been appropriately acknowledged and/or referenced. Where relevant, appropriate permissions have been obtained from the original copyright holder(s). Figures 1 and 2 are courtesy of Prof. Walter Stummer. Figure 5 has copyright statement, and it has not been modified from its original version.

References

1. Wen PY, Kesari S. Malignant gliomas in adults. *N Engl J Med*. 2008;359(5):492–507. <http://dx.doi.org/10.1056/NEJMra0708126>
2. Omuro A, DeAngelis LM. Glioblastoma and other malignant gliomas: A clinical review. *JAMA*. 2013;310(17):1842–50. <http://dx.doi.org/10.1001/jama.2013.280319>
3. McGirt MJ, Chaichana KL, Gathinji M, Attenello FJ, Than K, Olivi A, et al. Independent association of extent of resection with survival in patients with malignant brain astrocytoma. *J Neurosurg*. 2009;110(1):156–62. <http://dx.doi.org/10.3171/2008.4.17536>
4. Stupp R, Tonn JC, Brada M, Pentheroudakis G, Group EGW. High-grade malignant glioma: ESMO clinical practice guidelines for diagnosis, treatment and follow-up. *Ann Oncol*. 2010;21(Suppl 5):v190–3. <http://dx.doi.org/10.1093/annonc/mdq187>
5. Metcalfe SE. Biopsy versus resection for malignant glioma. *Cochrane Database Syst Rev*. 2000;(2):CD002034.
6. Louis DN, Ohgaki H, Wiestler OD, Cavenee WK, Burger PC, Jouvet A, et al. The 2007 WHO classification of tumours of the central nervous system. *Acta Neuropathol*. 2007;114(2):97–109. <http://dx.doi.org/10.1007/s00401-007-0243-4>
7. Louis DN, Perry A, Reifenberger G, von Deimling A, Figarella-Branger D, Cavenee WK, et al. The 2016 World Health Organization classification of tumors of the central nervous system: A summary. *Acta Neuropathol*. 2016;131(6):803–20. <http://dx.doi.org/10.1007/s00401-016-1545-1>
8. Zhu Y, Parada LF. The molecular and genetic basis of neurological tumours. *Nat Rev Cancer*. 2002;2(8):616–26. <http://dx.doi.org/10.1038/nrc866>
9. Verhaak RG, Hoadley KA, Purdom E, Wang V, Qi Y, Wilkerson MD, et al. Integrated genomic analysis identifies clinically relevant subtypes of glioblastoma characterized by abnormalities in PDGFRA, IDH1, EGFR, and NF1. *Cancer Cell*. 2010;17(1):98–110. <http://dx.doi.org/10.1016/j.ccr.2009.12.020>
10. Gonzalez-Perez O, Quinones-Hinojosa A. Dose-dependent effect of EGF on migration and differentiation of adult subventricular zone astrocytes. *Glia*. 2010;58(8):975–83. <http://dx.doi.org/10.1002/glia.20979>
11. Chaichana KL, McGirt MJ, Frazier J, Attenello F, Guerrero-Cazares H, Quinones-Hinojosa A. Relationship of glioblastoma multiforme to the lateral ventricles predicts survival following tumor resection. *J Neurooncol*. 2008;89(2):219–24. <http://dx.doi.org/10.1007/s11060-008-9609-2>
12. Chen L, Chaichana KL, Kleinberg L, Ye X, Quinones-Hinojosa A, Redmond K. Glioblastoma recurrence patterns near neural stem cell regions. *Radiother Oncol*. 2015;116(2):294–300. <http://dx.doi.org/10.1016/j.radonc.2015.07.032>

13. Nestler U, Lutz K, Pichlmeier U, Stummer W, Franz K, Reulen HJ, et al. Anatomic features of glioblastoma and their potential impact on survival. *Acta Neurochir (Wien)*. 2015;157(2):179–86. <http://dx.doi.org/10.1007/s00701-014-2271-x>
14. Phillips HS, Kharbanda S, Chen R, Forrest WF, Soriano RH, Wu TD, et al. Molecular subclasses of high-grade glioma predict prognosis, delineate a pattern of disease progression, and resemble stages in neurogenesis. *Cancer Cell*. 2006;9(3):157–73. <http://dx.doi.org/10.1016/j.ccr.2006.02.019>
15. Chaichana KL, Jusue-Torres I, Navarro-Ramirez R, Raza SM, Pascual-Gallego M, Ibrahim A, et al. Establishing percent resection and residual volume thresholds affecting survival and recurrence for patients with newly diagnosed intracranial glioblastoma. *Neuro Oncol*. 2014;16(1):113–22. <http://dx.doi.org/10.1093/neuonc/not137>
16. Sanai N, Berger MS. Operative techniques for gliomas and the value of extent of resection. *Neurotherapeutics*. 2009;6(3):478–86. <http://dx.doi.org/10.1016/j.nurt.2009.04.005>
17. Dandy WE. Removal of right cerebral hemisphere for certain tumors with hemiplegia: Preliminary report. *J Am Med Assoc*. 1928;90(11):823–5. <http://dx.doi.org/10.1001/jama.1928.02690380007003>
18. Mukherjee D, Quinones-Hinojosa A. Impact of extent of resection on outcomes in patients with high-grade gliomas. In: Hayat MA, editor. *Tumors of the central nervous system, volume 2: Gliomas: Glioblastoma (Part 2)*. Dordrecht: Springer Netherlands; 2011. p. 173–9.
19. Kostaras X, Cusano F, Kline GA, Roa W, Easaw J. Use of dexamethasone in patients with high-grade glioma: A clinical practice guideline. *Curr Oncol*. 2014;21(3):e493–503. <http://dx.doi.org/10.3747/co.21.1769>
20. Kotsarini C, Griffiths PD, Wilkinson ID, Hoggard N. A systematic review of the literature on the effects of dexamethasone on the brain from in vivo human-based studies: Implications for physiological brain imaging of patients with intracranial tumors. *Neurosurgery*. 2010;67(6):1799–815; discussion 815.
21. Hagan KB, Bhavsar S, Raza SM, Arnold B, Arunkumar R, Dang A, et al. Enhanced recovery after surgery for oncological craniotomies. *J Clin Neurosci*. 2016;24:10–16. <http://dx.doi.org/10.1016/j.jocn.2015.08.013>
22. Tremont-Lukats IW, Ratilal BO, Armstrong T, Gilbert MR. Antiepileptic drugs for preventing seizures in people with brain tumors. *Cochrane Database Syst Rev*. 2008;(2):CD004424. <http://dx.doi.org/10.1002/14651858.CD004424.pub2>
23. Shao L, Hong F, Zou Y, Hao X, Hou H, Tian M. Hypertonic saline for brain relaxation and intracranial pressure in patients undergoing neurosurgical procedures: A meta-analysis of randomized controlled trials. *PLoS One*. 2015;10(1):e0117314. <http://dx.doi.org/10.1371/journal.pone.0117314>
24. Sneyd JR, Andrews CJ, Tsubokawa T. Comparison of propofol/remifentanyl and sevoflurane/remifentanyl for maintenance of anaesthesia for elective intracranial surgery. *Br J Anaesth*. 2005;94(6):778–83. <http://dx.doi.org/10.1093/bja/aei141>
25. Balakrishnan G, Raudzens P, Samra SK, Song K, Boening JA, Bosek V, et al. A comparison of remifentanyl and fentanyl in patients undergoing surgery for intracranial mass lesions. *Anesth Analg*. 2000;91(1):163–9. <http://dx.doi.org/10.1213/00005539-200007000-00030>
26. Aryan HE, Box KW, Ibrahim D, Desiraju U, Ames CP. Safety and efficacy of dexmedetomidine in neurosurgical patients. *Brain Inj*. 2006;20(8):791–8. <http://dx.doi.org/10.1080/02699050600789447>
27. Bekker A, Sturaitis MK. Dexmedetomidine for neurological surgery. *Neurosurgery*. 2005;57(1 Suppl):1–10; discussion 1–10. <http://dx.doi.org/10.1227/01.NEU.0000163476.42034.A1>
28. Martyn JA, Richtsfeld M. Succinylcholine-induced hyperkalemia in acquired pathologic states: Etiologic factors and molecular mechanisms. *Anesthesiology*. 2006;104(1):158–69. <http://dx.doi.org/10.1097/0000542-200601000-00022>
29. Manrique-Guzman S, Castillo-Rueda L, Wolfsberger S, Herrada-Pineda T, Revilla-Pacheco Francisco, Torres-Corzo J, Loyo-Varela M, Stummer W. Fluorescence guided brain tumor surgery: Case report. *Int J Neurol Res*. 2015;1(2):1–7. <http://dx.doi.org/10.17554/j.issn.2313-5611.2015.01.21>
30. Metcalfe SE, Grant R. Biopsy versus resection for malignant glioma. *Cochrane Database Syst Rev*. 2001;(3):CD002034.
31. Proescholdt MA, Macher C, Woertgen C, Brawanski A. Level of evidence in the literature concerning brain tumor resection. *Clin Neurol Neurosurg*. 2005;107(2):95–8. <http://dx.doi.org/10.1016/j.clineuro.2004.02.025>

32. Stummer W, van den Bent MJ, Westphal M. Cytoreductive surgery of glioblastoma as the key to successful adjuvant therapies: New arguments in an old discussion. *Acta Neurochir (Wien)*. 2011;153(6):1211–18. <http://dx.doi.org/10.1007/s00701-011-1001-x>
33. Hung AL, Garzon-Muvdi T, Lim M. Biomarkers and immunotherapeutic targets in glioblastoma. *World Neurosurg*. 2017;102:494–506. <http://dx.doi.org/10.1016/j.wneu.2017.03.011>
34. Barbosa BJ, Dimostheni A, Teixeira MJ, Tatagiba M, Lepski G. Insular gliomas and the role of intraoperative assistive technologies: Results from a volumetry-based retrospective cohort. *Clin Neurol Neurosurg*. 2016;149:104–10. <http://dx.doi.org/10.1016/j.clineuro.2016.08.001>
35. Ishizuka M, Abe F, Sano Y, Takahashi K, Inoue K, Nakajima M, et al. Novel development of 5-aminolevulinic acid (ALA) in cancer diagnoses and therapy. *Int Immunopharmacol*. 2011;11(3):358–65. <http://dx.doi.org/10.1016/j.intimp.2010.11.029>
36. Novotny A, Stummer W. 5-Aminolevulinic acid and the blood-brain barrier – A review. *Med Laser Appl*. 2003;18(1):36–40. <http://dx.doi.org/10.1078/1615-1615-00085>
37. Esteves S, Alves M, Castel-Branco M, Stummer W. A pilot cost-effectiveness analysis of treatments in newly diagnosed high-grade gliomas: The example of 5-aminolevulinic acid compared with white-light surgery. *Neurosurgery*. 2015;76(5):552–62; discussion 62. <http://dx.doi.org/10.1227/NEU.0000000000000673>
38. Stummer W. Factors confounding fluorescein-guided malignant glioma resections: Edema bulk flow, dose, timing, and now: Imaging hardware? *Acta Neurochir (Wien)*. 2016;158(2):327–8. <http://dx.doi.org/10.1007/s00701-015-2655-6>
39. Acerbi F, Broggi M, Eoli M, Anghileri E, Cavallo C, Boffano C, et al. Is fluorescein-guided technique able to help in resection of high-grade gliomas? *Neurosurgical Focus*. 2014;36(2):E5. <http://dx.doi.org/10.3171/2013.11.FOCUS13487>
40. Hope-Ross M, Yannuzzi LA, Gragoudas ES, Guyer DR, Slakter JS, Sorenson JA, et al. Adverse reactions due to indocyanine green. *Ophthalmology*. 1994;101(3):529–33. [http://dx.doi.org/10.1016/S0161-6420\(94\)31303-0](http://dx.doi.org/10.1016/S0161-6420(94)31303-0)
41. Kim EH, Cho JM, Chang JH, Kim SH, Lee KS. Application of intraoperative indocyanine green video-angiography to brain tumor surgery. *Acta Neurochir (Wien)*. 2011;153(7):1487–95; discussion 94–5. <http://dx.doi.org/10.1007/s00701-011-1046-x>
42. Ferroli P, Acerbi F, Albanese E, Tringali G, Broggi M, Franzini A, et al. Application of intraoperative indocyanine green angiography for CNS tumors: Results on the first 100 cases. *Acta Neurochir Suppl*. 2011;109:251–7. http://dx.doi.org/10.1007/978-3-211-99651-5_40
43. Mitsui T, Fujii M, Tsuzaka M, Hayashi Y, Asahina Y, Wakabayashi T. Skin shift and its effect on navigation accuracy in image-guided neurosurgery. *Radiol Phys Technol*. 2011;4(1):37–42. <http://dx.doi.org/10.1007/s12194-010-0103-0>
44. Orringer DA, Golby A, Jolesz F. Neuronavigation in the surgical management of brain tumors: Current and future trends. *Expert Rev Med Devices*. 2012;9(5):491–500. <http://dx.doi.org/10.1586/erd.12.42>
45. Walter J, Kuhn SA, Waschke A, Kalf R, Ewald C. Operative treatment of subcortical metastatic tumours in the central region. *J Neurooncol*. 2011;103(3):567–73. <http://dx.doi.org/10.1007/s11060-010-0420-5>
46. Kubben PL, ter Meulen KJ, Schijns OE, ter Laak-Poort MP, van Overbeeke JJ, van Santbrink H. Intraoperative MRI-guided resection of glioblastoma multiforme: A systematic review. *Lancet Oncol*. 2011;12(11):1062–70. [http://dx.doi.org/10.1016/S1470-2045\(11\)70130-9](http://dx.doi.org/10.1016/S1470-2045(11)70130-9)
47. St-Arnaud D, Paquin MJ. Safe positioning for neurosurgical patients. *AORN J*. 2008;87(6):1156–68; quiz 69–72. <http://dx.doi.org/10.1016/j.aorn.2008.03.004>
48. Eseonu CI, Rincon-Torroella J, Refaey K, Quiñones-Hinojosa A. Operating room requirements for brain tumor surgery. In: Quiñones Hinojosa A, editor. *Video atlas of neurosurgery contemporary tumor and skull base surgery*. 1st ed. Oxford: Elsevier; 2017. p. xxv–xxx.
49. O'Connell MP. Positioning impact on the surgical patient. *Nurs Clin North Am*. 2006;41(2):173–92, v. <http://dx.doi.org/10.1016/j.cnur.2006.01.010>
50. Auguste KI, Quiñones-Hinojosa A, Berger MS. Efficacy of mechanical prophylaxis for venous thromboembolism in patients with brain tumors. *Neurosurg Focus*. 2004;17(4):E3. <http://dx.doi.org/10.3171/foc.2004.17.4.3>
51. Danish SF, Burnett MG, Stein SC. Prophylaxis for deep venous thrombosis in patients with craniotomies: A review. *Neurosurg Focus*. 2004;17(4):E2. <http://dx.doi.org/10.3171/foc.2004.17.4.2>

52. Chiang HY, Kamath AS, Pottinger JM, Greenlee JD, Howard MA, 3rd, Cavanaugh JE, et al. Risk factors and outcomes associated with surgical site infections after craniotomy or craniectomy. *J Neurosurg*. 2014;120(2):509–21. <http://dx.doi.org/10.3171/2013.9.JNS13843>
53. Kobayashi S, Sugita K, Matsuo K. An improved neurosurgical system: New operating table, chair, microscope and other instrumentation. *Neurosurg Rev*. 1984;7(2–3):75–80. <http://dx.doi.org/10.1007/BF01780687>
54. Practice advisory for the prevention of perioperative peripheral neuropathies: A report by the American Society of Anesthesiologists Task Force on Prevention of Perioperative Peripheral Neuropathies. *Anesthesiology*. 2000;92(4):1168–82. <http://dx.doi.org/10.1097/00000542-200004000-00036>
55. Raza SM, Quinones-Hinojosa A, Lim M, Boahene KD. The transconjunctival transorbital approach: A keyhole approach to the midline anterior skull base. *World Neurosurg*. 2013;80(6):864–71. <http://dx.doi.org/10.1016/j.wneu.2012.06.027>
56. Raza SM, Garzon-Muvdi T, Boahene K, Olivi A, Gallia G, Lim M, et al. The supraorbital craniotomy for access to the skull base and intraaxial lesions: A technique in evolution. *Minim Invasive Neurosurg*. 2010;53(1):1–8. <http://dx.doi.org/10.1055/s-0030-1247504>
57. Chaichana KL, Rincon-Torroella J, Acharya SY, Quiñones-Hinojosa A. Trans-sulcal versus transcortical resection of subcortical metastases. In: Quiñones Hinojosa A, editor. *Video atlas of neurosurgery contemporary tumor and skull base surgery*. Oxford: Elsevier; 2017. p. 17–21.
58. Raza SM, Recinos PF, Avendano J, Adams H, Jallo GI, Quinones-Hinojosa A. Minimally invasive transportal resection of deep intracranial lesions. *Minim Invasive Neurosurg*. 2011;54(1):5–11. <http://dx.doi.org/10.1055/s-0031-1273734>
59. Rincon-Torroella J, Chaichana KL, Manrique-Guzmán S, Quiñones-Hinojosa A. Deep intra-axial tumors. In: Quiñones Hinojosa A, editor. *Video atlas of neurosurgery contemporary tumor and skull base surgery*. 1st ed. Oxford: Elsevier; 2017. p. 22–4.
60. Dandy WE. An operation for the cure of tic douloureux: Partial section of the sensory root at the pons. *Arch Surg*. 1929;18(2):687–734. <http://dx.doi.org/10.1001/archsurg.1929.04420030081005>
61. Raza SM, Quinones-Hinojosa A. The extended retrosigmoid approach for neoplastic lesions in the posterior fossa: Technique modification. *Neurosurg Rev*. 2011;34(1):123–9. <http://dx.doi.org/10.1007/s10143-010-0284-3>
62. Chaichana KL Rincon-Torroella J, Manrique-Guzmán S, Quiñones-Hinojosa A. Cerebellar tumors. In: Quiñones Hinojosa A, editor. *Video atlas of neurosurgery contemporary tumor and skull base surgery*. 1st ed. Oxford: Elsevier; 2017. p. 32–5.
63. Feigl GC, Decker K, Wurms M, Krischek B, Ritz R, Unertl K, et al. Neurosurgical procedures in the semisitting position: Evaluation of the risk of paradoxical venous air embolism in patients with a patent foramen ovale. *World Neurosurg*. 2014;81(1):159–64. <http://dx.doi.org/10.1016/j.wneu.2013.01.003>
64. Dobrowolski S, Ebner F, Lepski G, Tatagiba M. Foramen magnum meningioma: The midline suboccipital subtonsillar approach. *Clin Neurol Neurosurg*. 2016;145:28–34. <http://dx.doi.org/10.1016/j.clineuro.2016.02.027>
65. Black S, Ockert DB, Oliver WC Jr, Cucchiara RF. Outcome following posterior fossa craniectomy in patients in the sitting or horizontal positions. *Anesthesiology*. 1988;69(1):49–56.
66. Black S, Ockert DB, Oliver WC, Jr., Cucchiara RF. Outcome following posterior fossa craniectomy in patients in the sitting or horizontal positions. *Anesthesiology*. 1988;69(1):49–56. <http://dx.doi.org/10.1097/00000542-198807000-00008>

13

Cortical Mapping in the Resection of Malignant Cerebral Gliomas

JEHAD ZAKARIA • VIKRAM C. PRABHU

Department of Neurological Surgery, Loyola University Medical Center/Stritch School of Medicine, Maywood, IL, USA

Author for Correspondence: Vikram C. Prabhu, Department of Neurological Surgery, Loyola University Medical Center/Stritch School of Medicine, 2160 S 1st Avenue, Maguire 1900, Maywood, IL 60153, USA. E-mail: vprabhu@lumc.edu

Doi: <http://dx.doi.org/10.15586/codon.glioblastoma.2017.ch13>

Abstract: Cerebral gliomas are diffuse intrinsic primary brain tumors that are most commonly encountered in the frontal, temporal, and parietal lobes, and that can present with an array of symptoms including alterations in mental status, speech and language difficulties, motor or sensory abnormalities, and seizures. Maximal safe surgical debulking of the tumor reduces mass effect, provides a precise histological diagnosis, and facilitates genetic analysis that may shed light on the response to therapies and prognosis, reduces the oncological burden of the tumor facilitating the effectiveness of adjuvant treatments such as radiation and chemotherapy, and may reduce seizures. Preoperative and intraoperative cortical mapping strategies are used to delineate the relationship of the tumor with adjacent eloquent and association cortical areas to provide a maximal functionally safe surgical resection. This chapter describes the protocols used at our institution for the surgical management of patients with malignant gliomas in proximity to or involving eloquent cortical areas.

Key words: Cortical mapping; Eloquent cortex; Functional mapping; Glioma

In: *Glioblastoma*. Steven De Vleeschouwer (Editor), Codon Publications, Brisbane, Australia ISBN: 978-0-9944381-2-6; Doi: <http://dx.doi.org/10.15586/codon.glioblastoma.2017>

Copyright: The Authors.

Licence: This open access article is licenced under Creative Commons Attribution 4.0 International (CC BY 4.0). <https://creativecommons.org/licenses/by-nc/4.0/>

Introduction

Cerebral gliomas are diffuse intrinsic primary brain tumors that are most commonly encountered in the frontal, temporal, and parietal lobes. They can present with an array of symptoms including alterations in mental status, speech and language difficulties, motor or sensory abnormalities, and seizures. Maximal safe surgical debulking of the tumor reduces mass effect, provides a precise histological diagnosis, and facilitates genetic analysis that may shed light on the response to therapies and prognosis, reduces the oncological burden of the tumor facilitating the effectiveness of adjuvant treatments such as radiation and chemotherapy, and may reduce seizures. Retrospective reviews suggest that the extent of resection is a critical prognostic factor for all grades of glioma (1). However, functional deficits from tumor resection are assiduously avoided as they have a strong negative prognostic effect both on the patient's quality of life and on the overall outcome related to the primary tumor. Hence, a strong emphasis remains on maximal safe resection with preservation of neurological function particularly in critical areas of the brain. Preoperative and intraoperative cortical mapping strategies are used to delineate the relationship of the tumor with adjacent eloquent and association cortical areas to provide a maximal functionally safe surgical resection. A protocol that encompasses anatomical, functional, and metabolic imaging provides a comprehensive view of the location and nature of the tumor and its relationship with the adjacent cortex (1–3). Preoperative and postoperative neuropsychological testing further identifies areas of subtle cognitive, motor, and language deficit. This facilitates more effective preoperative patient counseling and maximal safe resection.

Preoperative Planning

MAGNETIC RESONANCE IMAGING

Cranial computed tomography (CT) has utility in presenting bone detail and the presence of calcification within a tumor bed. However, the anatomic detail provided by magnetic resonance imaging (MRI) is exquisite and provides cortical anatomical landmarks that are useful in preoperative planning. Relatively predictable patterns of sulci and gyri allow for identification of the primary sensory/motor cortices and speech centers. The concordance between MRI images and gross anatomical specimens has revealed “keys” for cortical landmark identification (4, 5). The first key is the Sylvian fissure and its five major rami. The posterior horizontal ramus (PHR) forms the main fissure that is visible on the convexity of the brain; it extends rostrally into the posterior ascending (PAR) and descending rami (PDR). The PAR is “capped” by the supramarginal gyrus (SMG). Anteriorly along the PHR, the Sylvian fissure extends into two sulci, the anterior horizontal and anterior ascending rami. These rami extend into the inferior frontal gyrus (IFG) dividing it into the pars orbitalis, pars triangularis, and pars opercularis. The pars triangularis (Brodmann's areas 45) and pars opercularis (Brodmann's area 44) represent the primary motor or expressive speech area (Broca's area).

The frontal lobe contains three gyri (superior, middle, inferior) separated by the superior and inferior frontal sulci. The superior frontal gyrus is appreciated on both axial and sagittal images (Figure 1). The middle frontal gyrus (MFG) extends posteriorly and fuses with the vertically oriented precentral gyrus. The precentral sulcus starts at midline and extends anteriorly and laterally in an oblique direction. The next key finding is the merging of the inferior frontal sulcus with the inferior ramus of the precentral sulcus, forming a “T” shape (4, 5). More posteriorly, the central sulcus is identified over the convexity on axial or sagittal images. It is oriented obliquely from posterior to anterior and does not extend all the way into the Sylvian fissure. Inferiorly, the precentral gyrus and postcentral gyrus merge under the central sulcus through a “U”-shaped gyrus (the subcentral gyrus). The postcentral gyrus is characteristically narrower than the precentral gyrus (4, 5). Posteriorly, the Sylvian fissure is capped by the SMG, which is the anterior most portion of the inferior parietal lobule. Inferiorly, within the temporal lobe, coursing in parallel with the Sylvian fissure, is the superior temporal sulcus, which is capped posteriorly by the angular gyrus, the posterior limit of the inferior parietal lobule. The angular gyrus (Brodmann’s area 39) and posterior aspect of the superior temporal gyrus (STG) (Brodmann’s area 22) represent the primary receptive speech area (Wernicke’s area). The SMG (Brodmann’s area 40) contains fibers from the arcuate fasciculus that connect Wernicke’s and Broca’s areas (4, 5). The cingulate sulcus separates the cingulate gyrus from the medial aspect of the superior frontal gyrus. If followed posteriorly, the cingulate sulcus angles superiorly to form the pars marginalis, marking the posterior aspect of the paracentral lobule. The paracentral lobule houses the central sulcus, Brodmann Areas 3,1,2 and 4,6. On axial images, the pars marginalis may be appreciated as a “bracket” (pars bracket) extending symmetrically from midline left and right. Anterior to

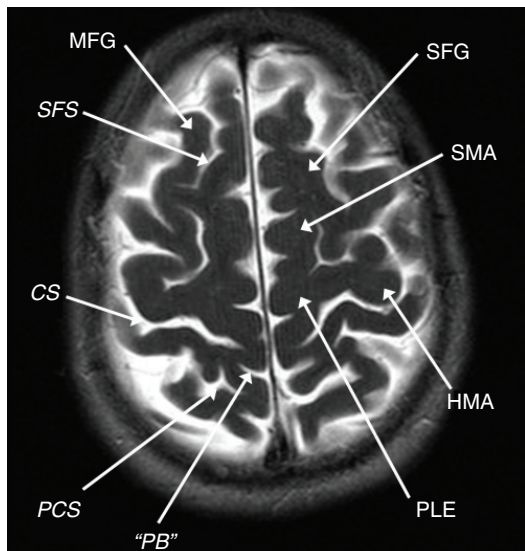


Figure 1 Axial T2-weighted MRI showing the middle frontal gyrus (MFG), superior frontal gyrus (SFG), superior frontal sulcus (SFS), central sulcus (CS), supplementary motor area (SMA), postcentral sulcus (PCS), pars bracket (PB), hand motor area (HMA), and proximal leg area (PLE).



Figure 2 Figure 2 Midline sagittal T1-weighted MRI scan showing the callosal sulcus (CalloS); cingulate sulcus (CinS); cingulate gyrus (CinG); supplementary motor area (SMA); paracentral lobule (PCL); pars marginalis (PM); precuneus (PreC); parietal-occipital sulcus (POS); cuneus (Cun), calcarine sulcus (CalcS), lingula (Lin).

this are the primary motor cortex and the postcentral sulcus. Areas 3,1,2 relate to the primary sensory cortex, and areas 4,6 include primary motor and supplemental motor areas (4, 5) (Figures 1 and 2).

FUNCTIONAL MRI

Functional MRI (fMRI) is a noninvasive imaging procedure that allows one to localize speech, language, and motor centers through blood oxygenation-level-dependent (BOLD) contrast imaging (6, 7). It relies on two principles: local tissue magnetic fields and blood flow. With task-related activation, cerebral cortical tissue will augment its own blood flow via autoregulation, increasing local oxyhemoglobin relative to deoxyhemoglobin. Deoxyhemoglobin is paramagnetic; therefore, its relative decrease locally causes less distortion of the local tissue magnetic field, thereby increasing the strength of the MRI signal. A statistical significance is ascribed to this change in signal and color coded and is superimposed on standard anatomical MRI images allowing localization of critical and eloquent areas. Several sensory, motor, and language paradigms may be used to identify eloquent

cortex (6, 7). For identification of sensory areas, the subject's fingers are stimulated with a coarse plastic surface. A checkerboard pattern is used to activate the visual cortices. For motor testing, finger-thumb tapping is an excellent task to activate the precentral gyrus and supplementary motor areas (SMAs). Active and passive (silent) speech allow for identification of Broca's and Wernicke's areas. These paradigms have excellent sensitivities for the ascribed tasks and localizations can be confirmed with intraoperative cortical stimulation, and/or WADA testing.

While fMRI is useful in delineating functional cortical anatomy, subcortical white matter tracts can be outlined using diffusion tensor imaging, which can be used for preoperative planning. Diffusion tensor imaging is based on the anisotropic diffusion of water molecules in white matter tracts; color codes depict the directionality of the tract. It is a robust modality that provides useful information as to the deformation and displacement of a subcortical pathway or infiltration of that pathway. Particularly in the latter case, surgical removal is purposely restrained to avoid a permanent neurological deficit. The combination of preoperative structural imaging, fMRI, and DTI allows the surgeon to create a plan and counsel a patient and his/her family regarding the surgical approach and the goal and risks of surgery (8).

Magnetoencephalography

Synchronized neuronal currents induce weak magnetic fields that can be detected with multichannel sensors placed over the patient's scalp (9–11). Superconducting quantum inference devices (SQUIDS) allow detection of small cortical field differences and large shielded rooms cooled by liquid helium and are used to minimize distortion of signal from outside magnetic fields. Mathematical models infer the location of signal generators on the cortex, overlaying them on synchronized MR images. Magnetoencephalography (MEG) has been utilized in localization of seizure foci, language centers, and primary somatosensory cortices (9–11). One technique involves placement of standard fiducial markers on the patient's scalp, completion of an MRI, and integration of MRI and MEG studies, yielding a magnetic source image (MSI), that can be integrated with standard intraoperative navigation systems.

Transcortical Magnetic Stimulation

Transcortical magnetic stimulation (Tms) is a modality that allows preoperative definition of the primary motor cortex and subcortical pathways. A high precision stimulation coil held to the patient's head delivers biphasic magnetic stimulation to spots on the motor cortex eliciting motor-evoked potentials in the contralateral limb that may be recorded and analyzed. When combined with fMRI and structural MRI navigation, there is a reasonably high degree of accuracy of localization of the primary motor cortex, particularly in the region of the hand representation in the precentral gyrus. The magnetic coil stimulation is typically performed on both hemispheres and recording electrodes are attached to the key muscles such as the abductor pollicis brevis, first digital interosseous, adductor digiti minimi, and the tibialis anterior muscles. This is a reliable preoperative, noninvasive method of

establishing the primary motor cortex in glioma resection, with a good concordance with intraoperative direct cortical stimulation mapping responses (12).

Positron Emission Tomography

This modality depends on the detection of gamma rays (photons) emitted through the collision of positrons and electrons following injection of a radioactive tracer. Cerebral blood flow, volume, oxygen use, glucose transport, protein metabolism, and other characteristics can be detected and localized. For cerebral functional localization, the isotope ^{15}O is injected intravenously; as local blood flow increases to an activated region of cortex, higher concentrations of tracer will be detected (13). Baseline gamma emission levels are compared to those during stimulation and statistical analysis determines if regional activation is significant ($P > 0.05$).

Neuropsychological Assessment

Neuropsychological evaluation is the use of standardized tests for cognitive, perceptual, motor, and psychological functions in order to characterize brain systems according to the American Academy of Neurology (1). These tests measure general intellectual ability, skills pertaining to school or job performance, and psychological adjustment. Preoperative neuropsychological evaluation in awake craniotomy cases helps select patients who have the necessary cognitive skills and behavioral control necessary for cooperating with the functional assessment during surgery. Second, preoperative testing establishes a baseline for quantifying treatment outcome. Third, it helps inform the surgical plan. In the case of a dominant hemisphere lesion, testing will quantify the degree, if any, of preoperative language or sensorimotor impairment. Findings referable to the regional effects of the brain lesion serve either to corroborate or contradict expected functional neuroanatomy. Findings may also supplement functional imaging by demonstrating more narrow or more diffuse involvement of critical skills than suggested by fMRI. Following surgery, repeat neuropsychological evaluation allows sensitive tracking of recovery and is a measure of treatment outcome; it can characterize residual deficits, identify behavioral changes, and guide services for the patient and family. The assessment focuses on domains relevant to the location of the tumor and subsequent surgery and the impact on functions relevant to the patient's resumption of his or her premorbid role.

Surgical Considerations

Patients with gliomas located in eloquent parts of the brain essential for language or motor function are candidates for intraoperative cortical mapping (3, 14–16). Commonly, these eloquent zones include the posterior frontal or anterior parietal lobe in either hemisphere; or the insula, inferior frontal; or superior temporal gyri in the dominant hemisphere. Occasionally, preoperative functional imaging may

suggest eloquent areas beyond these confines, indicating the need for surgical mapping. Motor mapping may be done with the patient awake or asleep, while language mapping is always done awake, which requires a patient to be calm and cooperative (3, 14–16). Apprehensive or uncooperative patients, or those with airway or chronic pulmonary problems, may not tolerate being awake during surgery (2, 17). Coagulopathy, bleeding diathesis, or severe systemic illness is the general contraindication to elective cranial operations. Morbid obesity is also a relative contraindication while systemic illness such as cardiac or pulmonary problems may also be a significant factor. A patient who cannot identify simple objects or read simple phrases is also not a candidate for intraoperative speech mapping. In these individuals or in children, cortical mapping may be done with surgically implanted subdural grids with stimulation performed extraoperatively in a video-monitored electroencephalographic (EEG) suite over several days. The presence of functioning or mature neurons that respond to electrical stimulation is essential. Patients with a fixed or profound neurological deficit such as hemiplegia, or receptive or expressive aphasia, are not candidates for cortical mapping. Similarly, children under 7 years of age may have cortical sites not mature enough to respond to electric stimulation.

Surface Anatomical Landmarks

Knowledge of scalp and cranial landmarks allows determination of the relationship of the lesion with the motor strip, language areas, ventricles, thalamus, basal ganglia, and their projecting fibers (1, 3, 18–21). Surface landmarks easily identified are the glabella, nasion, frontozygomatic (FZ) point, root of the zygoma, mastoid process,inion, and midline, indicating location of the sagittal suture. The FZ suture marks the FZ point situated on the upper part of the lateral orbital rim just below the junction of the frontal and zygomatic bones. The coronal suture may be palpable; if not, the upper end of the coronal suture is just anterior to the tragus of the ear and the lower end is in line with the midpoint of the zygomatic arch. The central sulcus lies 4–6 cm behind the coronal suture and at 45° to the orbitomeatal plane sloping anteriorly and inferiorly. The squamosal suture turns inferiorly just past the central sulcus; the central sulcus may also be approximated by joining the upper and lower rolandic points. The upper rolandic point lies approximately 2 cm behind the midpoint of a line extending from the nasion to theinion (N-I line) or straight up in line with the external auditory meatus (EAM). The lower rolandic point lies 2–3 cm behind the pterion, or about 5 cm above the EAM. The upper end of the precentral gyrus lies almost straight up from the EAM near the midline (1, 3, 19).

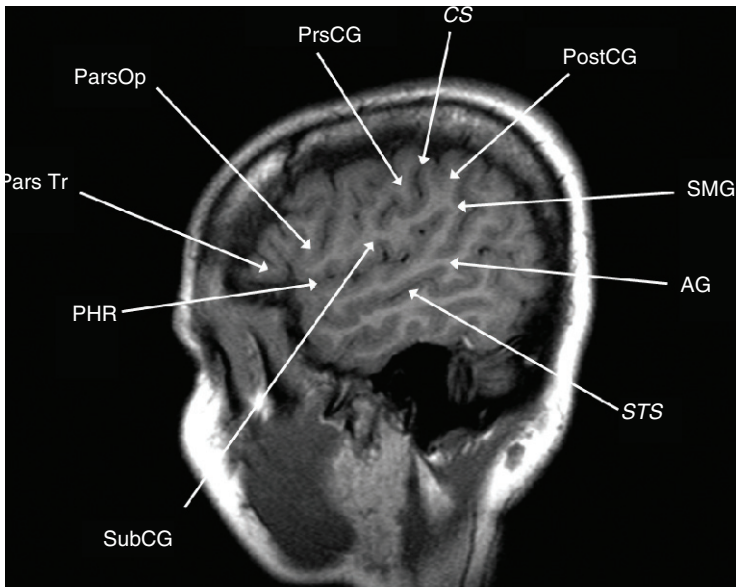
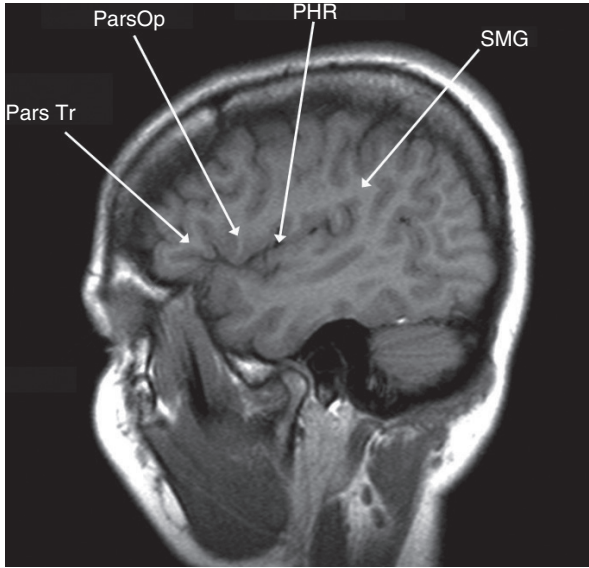
The pterion is about 2–3 cm behind the FZ point along the stem of the Sylvian fissure and 3 cm above the zygomatic arch. The Sylvian fissure lies along a line extending from the FZ point toward the junction of the anterior 3/4ths and posterior 1/4ths of the N-I line. The central sulcus and sylvian fissure meet at an obtuse angle of approximately 120°. The pars triangularis of the frontal lobe lies just above the anterior part of the Sylvian fissure, 2–3 cm behind the FZ point, or behind the pterion. The AG or inferior part of the inferior parietal lobule lies just above the pinna of the ear. Theinion lies over the torcular herophili and the

attachment of the tentorium to the inner table of the skull. The transverse sinus lies beneath a line connecting the root of the zygoma and theinion, and the asterion approximates the junction of the transverse and sigmoid sinuses. The superior parietal lobule lies approximately 6–7 cm above theinion and 2–3 cm lateral to the midline. The interparietal sulcus is oriented anteroposteriorly and lies 3–4 cm lateral and parallel to the midline (1, 3, 19).

Eloquent Cortex

Anatomical and functional variability is reported between individuals, and between the two hemispheres in the same individual. Such human genetic polymorphisms are most evident in frontal and parieto-occipital areas and may involve the perisylvian cortex, sylvian fissure, and planum temporale. Despite this, essential sites may be predicted by structural or functional imaging modalities, and clinical findings. This may then be used to guide surgical decision-making, and these established anatomical landmarks are of critical importance in the preoperative diagnosis, workup, and surgical treatment of cerebral gliomas (3). Notwithstanding that, and more recently with the aid of sophisticated neuroimaging modalities, a more holistic interpretation of cerebral function and the localization of various eloquent brain regions have gained popularity. The concept that the human brain is a highly sophisticated and intricately connected network that functions as a whole rather than being driven from a few select eloquent areas is supported by functional imaging studies. This concept of the human “connectome” adds another layer of complexity that goes beyond basic anatomical landmarks and is highly individual. Nonetheless, for the purpose of surgical removal of intrinsic cerebral gliomas, one has to rely on the standard concepts of *essential* eloquent cortex and strive for the goal of maximal safe removal of the tumor while preserving these areas.

Eloquent cortex generally implies speech, sensorimotor, and visual areas. Broca’s area lies in the pars opercularis and triangularis of the IFG Brodman’s area 44 (Figure 3). It controls the complex orofacial movements required to articulate speech and lies just anterior to motor cortex for lip, tongue, face, and larynx movements. Additional essential language sites in the dominant hemisphere can extend into the MFG, STG, middle temporal gyrus (MTG), or the insula. Expressive aphasia results from injury to Broca’s area, while receptive aphasia results from injury to Wernicke’s area (Figure 3). Injury to the arcuate fasciculus or white matter tracts connecting these speech areas results in conduction aphasias with impaired repetition. Injury to association cortex around the speech areas results in transcortical aphasias in which the primary function is impaired but repetition is preserved. The fusiform gyrus may also participate in speech, “basal temporal language area,” although deficits from surgical resections in this area typically recover. Auditory functions are bilaterally represented and resections involving the transverse temporal gyri in one hemisphere are well tolerated. Optic radiations, representing the inferior half of the contralateral retina, loop forward over the temporal horn before arching back toward the striate cortex in the banks of the calcarine fissure. Temporal resections that encroach upon these fibers cause a



Figures 3 Lateral sagittal T1-weighted MRI scans. Pars triangularis (Pars Tr), pars opercularis (Pars Op), posterior horizontal ramus of the sylvian fissure (PHR), and supramarginal gyrus (SMG). Subcentral gyrus (SCG), precentral gyrus (PCG), central sulcus (CS), postcentral gyrus (PoCG), supramarginal gyrus (SMG), angular gyrus (AG), and superior temporal sulcus (STS).

contralateral upper outer quadrantonopsia, a “pie-in-the-sky” defect, which is also well tolerated (3, 18–21).

Primary motor and sensory function reside in the precentral and postcentral gyri, respectively, and variability in sensorimotor cortex is less common. Awake mapping is an option in these cases; motor sites can be mapped with the patient asleep under nonparalytic general anesthesia. Injury to the primary motor cortex will result in paresis involving the face, upper extremity, or lower extremity. The nondominant face motor cortex has bilateral cortical representation, and resections in this area may be better tolerated. The SMA on the medial aspect of the frontal lobe lies anterior to the primary leg motor cortex and extends down to the cingulate gyrus; it has a role in planning, initiation, and execution of movements, and in the dominant hemisphere it participates in expressive speech function. Resections involving the SMA in either hemisphere may cause contralateral hemiparesis or plegia but this generally improves over 4–8 weeks, although some residual deficits such as apraxia, hesitancy, and difficulty initiating movements may persist. Tumor resections from the dominant or left SMA may be complicated by expressive aphasia; this also reportedly recovers 1–2 weeks after surgery, but some deficits such as hesitations, word-finding difficulties, perseveration, dysnomia, and dysgraphia may persist. Exner’s area lies lateral to the SMA and superior to Broca’s area; it integrates functions essential for writing and that may be affected by resections in this area. The frontal eye fields responsible for saccadic and voluntary eye movements to the opposite side are located just in front of the precentral sulcus, anterior to the SMA. The prefrontal cortex serves intellectual and social functions bilaterally; deficits from resections in these areas are better tolerated than speech and motor impairments (3, 18–21).

The parietal lobe is marked by the central sulcus anteriorly and the Sylvian fissure inferiorly. Over the convexity, the parietal lobe blends imperceptibly into the occipital lobe. The inferior parietal lobule contains the SMG and AG that constitute the receptive speech area of Wernicke on the dominant side. The occipital lobe has a roughly pyramidal shape. The occipital pole lies at the junction of the posterior end of the falx cerebri and tentorium; the visual cortex is close to the occipital pole in the banks of the calcarine fissure. A contralateral, congruent, visual field deficit such as a homonymous hemianopsia follows surgery in this location. The AG lies 3–4 cm lateral and anterior while the preoccipital notch lies 6–7 cm lateral to the occipital pole and midline just behind the vein of Labbe. Speech comprehension problems may result from resections that stray into these areas. Surgery involving the somatosensory cortex may result in contralateral parietal sensory loss with astereognosis, graphesthesia, and impaired two-point discrimination. Further posterior, the parietal lobe has an important heteromodal association capacity, integrating visual, auditory, and perceptual modalities and providing an awareness of the body and extrapersonal space, particularly on the nondominant side. Damage to the dominant inferior parietal lobule causes Gerstmann’s syndrome (finger agnosia, right–left confusion, acalculia, and agraphia without alexia) (3, 18–21).

The insula lies buried under the frontal, parietal, and temporal opercula (22). The circular sulcus forms an incompletely defined peripheral insular margin. The central sulcus of the insula divides it into anterior and posterior components with numerous short and long gyri and sulci interspersed within. The insula is

supplied by small arteriolar branches of the M2 segment of the middle cerebral artery (MCA), which lies draped over it. Deep to it are the extreme capsule, claustrum, external capsule, and basal ganglia. At surgery, the superior and deep margins of the insula are hard to define. Gliomas may be confined to the insula or extend into the adjacent opercula and deeper structures. With dominant hemisphere lesions, speech or motor problems may be noted as a result of opercular injury. Vascular injury or vasospasm, or injury to deep white matter tracts at the superior and medial aspects of the tumor, will also contribute to these problems. Nondominant hemisphere resections may have motor weakness through similar mechanisms even though motor function may not be consistently elicited by insula stimulation.

Memory depends on the integrity of the mesial temporal structures of the dominant hemisphere, in particular the hippocampus. Chemical inactivation of the hemisphere harboring the lesion with intracarotid sodium amytal injection (WADA test) can determine its role in language and memory function, and also determine whether the contralateral hemisphere can support these functions following surgery. Limitations of the WADA test are inadequate perfusion of mesial temporal structures, underestimation of the contribution of lateral temporal neocortical structures to memory, and possible vascular complications from angiographic studies. Alternative noninvasive tests for memory function include fMRI and neuropsychological testing, but the WADA test remains the gold standard (1, 3).

Surgical Technique

The best surgical corridor to a lesion is the shortest and the most direct route through noneloquent cortex (3). Cortical draining veins and arterial structures are preserved when possible. Trans-sulcal or trans-gyral approaches are used as needed and with careful attention to deeper structures. The deep end of cerebral sulci is usually directed toward the lateral ventricle; the collateral sulcus, for example, is an excellent path to the temporal horn. The sylvian and interhemispheric fissures are also safe corridors to deep lesions. Retraction injury to the gyral banks of the sulcus may occur and one may encounter arteries that require sacrifice without knowledge of the cortical territory supplied with resultant unexpected deficits; hence, this approach is not without risks. Trans-gyral approaches sacrifice cortical tissue but are undertaken through the crest of a gyrus that is stimulated and determined not to contain essential eloquent tissue. The SFG, MFG, MTG, ITG, and SPL are safe corridors. Knowledge of the ventricular anatomy is also useful to access deep lesions. The outer margin of the lateral ventricle in a nonhydrocephalic adult or child over 7 years of age lies 4–5 cm deep to the convex pial surface. The frontal horn extends 1–2 cm anterior to the coronal suture in the mid-pupillary line and lies deep to the IFG. A pre-coronal route at least 2–3 cm lateral to the midline through the SFG or MFG is safe. The temporal horn is deep to the MTG and the atrium lies deep to the SMG. Keen's point, 3 cm above and 3 cm behind the pinna of the ear, is used to approach a lesion in or around the atrium of the ventricle (3).

Frontal lobe resections stay 1–2 cm away from positive speech or motor response sites. The rolandic and other large cortical draining veins are preserved

and injury to the pericallosal vessels is avoided. Nondominant hemisphere temporal tumor resections extend 6 cm behind the temporal pole; on the dominant side, the resection is limited to the anterior 4–5 cm. The posterior limit is just anterior to the vein of Labbé and speech sites are similarly respected with a 1–2 cm margin. In the absence of temporal speech sites, the resection can extend all the way to the pial bank of the sylvian fissure, protecting the MCA and its branches. Neuropsychological and functional testing for memory localization is done before undertaking dominant hemisphere temporal lobe lesion resections; mesial temporal structures posterior to the amygdala are not removed unless the contralateral hemisphere can unequivocally support memory function. A postoperative contralateral superior quadrantanopia may follow temporal lesion resections that extend to the temporal horn of the lateral ventricle. The superior parietal lobule, 6–7 cm above theinion and 3 cm lateral to the midline, is a safe access route, with care to avoid injury to the vein of Trolard. Resection of occipital tumors can safely extend 3 cm away from the occipital pole with a resultant contralateral congruous homonymous hemianopia. Beyond that, resections may encroach on the posterior reaches of Wernicke's area and may affect comprehension of language on the dominant side and of prosody on the nondominant side (3).

Awake language and motor mapping help reduce morbidity with insular tumor resections, especially on the dominant side (22). The Sylvian fissure is split and the superior and inferior peri-insular sulci provide dissection planes above and below the tumor, respectively. The lateral lenticulostriates define the medial resection plane but are sometimes hard to clearly identify or are obscured by the tumor bulk (22). The safe posterior border is the posterior limb of the internal capsule which may be identified by subcortical stimulation. On the dominant side, resection should not be taken posterior to any language sites. The tumor is resected piece-meal between the MCA perforators in a subpial fashion with sacrifice of small arteries supplying the tumor and insula. Subtle perturbations in motor or speech function truncate the resection at that point. With dominant hemisphere lesions, speech or motor problems may result from frontal or temporal opercular retraction, manipulation spasm of the MCA or interruption of the lateral lenticulostriate or opercular MCA branches, or injury to deep white matter tracts at the superior and medial aspects of the tumor (Figure 4). Nondominant hemisphere resections may have motor weakness through similar mechanisms even though motor function may not be consistently elicited by insula stimulation. With tumors involving the frontal or temporal opercula, a transopercular approach to the insula is a reasonable option (3).

Surgical Navigation

Frameless stereotactic localization is a standard with accuracy within 2–3 mm and is cross-checked against anatomical landmarks. Contrast-enhanced T1-weighted images are used, but with nonenhancing lesions T2-weighted images are used for navigation. Brain shift with cranial opening, CSF egress, and lesion resection places limitations on the accuracy of intraoperative neuronavigation systems. The use of intraoperative ultrasound (e.g., 7.5Hz, SSD-1700 Dynaview, Aloka Co., Tokyo, Japan) helps overcome some of these problems, but the resolution and spatial localization with ultrasound is not optimal.

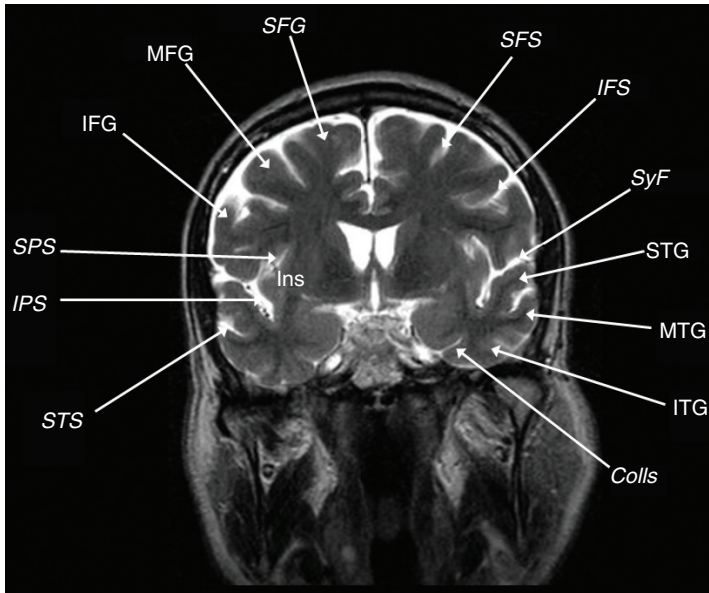


Figure 4 Coronal T2-weighted MRI scan showing the superior frontal gyrus (SFG), middle frontal gyrus (MFG), inferior frontal gyrus (IFG), superior peri-insular sulcus (SPS), inferior peri-insular sulcus (IPS), superior frontal sulcus (SFS), inferior frontal sulcus (IFS), sylvian fissure (SyF), superior temporal gyrus (STG), superior temporal sulcus (STS), middle temporal gyrus (MTG), inferior temporal gyrus (ITG), and collateral sulcus (Colls).

Malignant gliomas have a relative bold echogenicity, allowing distinction from the adjacent cortex. However, low-grade gliomas may be hard to distinguish from the adjacent cortex with similar echogenic properties. Co-registration of ultrasound and preoperatively obtained MRI images is feasible but not universally available or routinely employed. Intraoperative MRI (iMRI) is an option at some institutions; however, the special setup required to operate with the patient awake may not be compatible with the iMRI environment. Ancillary equipment utilized in mapping procedures, such as electrodes and EEG machines, also preclude the use of iMRI. Cavitron ultrasonic aspiration (CUSA) provides rapid debulking with minimal trauma to adjacent tissues; we usually obtain samples for frozen and permanent sections before using the CUSA.

Electric Stimulation Mapping

SOMATOSENSORY EVOKED POTENTIALS

Direct measurement of cortical activity is done with an eight-contact surface platinum-electrode strip which samples the quasi-random electric potentials of the superficial layers of the cerebral cortex (3, 23–25). The somatosensory evoked potential (SSEP) is generated by giving a timed sensory stimulus at the level of the wrist using 20 mm diameter silver/silver-chloride electrodes. Stimulation is

delivered at intensities ranging from 5 to 15mA, with a stimulation duration of 2 msec at frequencies ranging from 4 to 7 Hz, averaging up to 1000 trials per response. This stimulus elicits a depolarization wave that travels to the sensory cortex and elicits a localized electrical response that is filtered, amplified, and computer averaged to generate a standardized response which stands out from background electrical activity. Stimulation of the median or ulnar nerve in an adult will generate a cortical response with negative polarity 20 ms later; this response is termed the N20 with a maximal localized response recorded over the hand area in the postcentral gyrus. The electrodes in the platinum-electrode strip traversing the central sulcus are connected in series. Thus, a signature switch in polarity of the N20 response is recorded and indicates the presumed location of the central sulcus.

While reasonably accurate, SSEP localization of the central sulcus may be compromised by the presence of a tumor or peritumoral edema. Phase reversal may occur up to 10 mm or one sulcus away from the central sulcus. fMRI, MEG, or positron emission tomography may show activation at sites that participate in a particular behavior, rather than purely essential sites. These preoperative imaging data sets are also susceptible to inaccuracies related to the nature of functional task and the patient's ability to carry it out. When translated into the operative environment, spatial errors may result from brain shift with cranial bone opening, cerebrospinal fluid egress, and tumor resection. SSEP accuracy may also be affected by the type of anesthesia utilized and the temperature of the patient; high-dose inhalational anesthetic techniques may produce a dose-related decrease in amplitude and increased waveform latency. Opioids alter cortical SSEPs but changes are much less marked than with inhalational agents. Body temperature will also change waveform characteristics with lower temperatures, producing changes in waveform latency. Maintenance of normothermia is a key consideration when using SSEP to localize the central sulcus (23–25).

DIRECT CORTICAL STIMULATION

Direct cortical stimulation (DCS) interrupts local cortical activity, identifying areas whose function is essential for a particular behavior at that point in time. Application of an epicortical electric current activates excitatory and inhibitory neurons and associated pathways. In some instances, the stimulus may induce a depolarization neuronal blockade. Constraints for stimulation include limited cortical sampling and current spread to nonessential sites. Despite this, DCS is the most accurate way to map essential eloquent sites and is used to confirm location of sensory, motor, and language cortex (3, 23–25). The Ojemann bipolar electrode is used, which consists of 1 mm round tips which are 5 mm apart. Stimuli are delivered as a biphasic square wave in 1 msec pulses at a frequency of 60 Hz, with amplitudes ranging from 2 to 12 mA, although stimuli up to 18 mA have been described (2). Higher stimulation thresholds have a greater chance of eliciting motor responses or inducing speech arrest but run the risk of also inciting seizure activity or producing significant cortical depolarization which then decreases the possibility of response to the next stimulus. It thus is a fine art to pick the best stimulation threshold that can achieve the objective of cortical mapping without the risk of eliciting seizures or prolonged depolarization.

Optical imaging studies indicate that the stimulated zone is confined to the area between the electrode tips with no significant histopathological sequelae reported. The eight-point platinum-electrode strip used for SSEP is also used to monitor continuous EEG activity for stimulation-induced epileptiform after-discharges. This phenomenon of clinically evident seizure activity may occur in 5–20% of cases, generally during stimulation of the face and hand motor cortex. It manifests as a focal motor seizure involving the contralateral face and extremities. In most instances, the seizure subsides spontaneously with cessation of stimulation. If persistent, ice-cold Ringer's lactate solution is dripped onto the stimulated area which is effective in 5–10 s without compromising subsequent mapping or clouding the patient's sensorium. Stimulation is resumed at a lower current after normal EEG activity is noted. All sites are repeatedly stimulated at currents effective in obtaining a motor response or altering speech function but not eliciting after-discharges. Subcortical stimulation is performed using a similar technique to ascertain the integrity of the descending motor pathways. Most essential sites have a surface area of 2 cm² or less with relatively sharp boundaries although 2–3 noncontiguous essential sites may exist for the same function (3).

In children, immaturity of the cerebral cortex may cause difficulty in obtaining stimulation responses due to the lack of myelination of major tracts. This may be overcome by increasing the stimulus intensity, but this may predispose to after-discharges or clinical seizures, and hence SSEP localization is preferred. In patients not suitable for intraoperative mapping, electrode grids or strips may be implanted and stimulation performed. Standard grids are 9 cm long and 7 cm wide; hence, the cortical exposure should be large enough to accommodate these dimensions. Smaller grids may be used for basal temporal or interhemispheric recordings. These electrode arrays have multiple contact points, 12 mm² in size, 1 mm apart, and can be arranged in various configurations. Individual electrodes may be stimulated in an extraoperative setting in a special video-EEG equipped suite in 1–3 h sessions, 1–2 times a day, testing for language, motor, and sensory function (3).

Language tasks are multiple items of approximately equal difficulty that the patient is comfortable handling in the absence of stimulation and require only a few seconds to answer or complete. Object naming is disrupted in all aphasic syndromes; other tasks include counting, comprehension, and repetition. Speech errors include hesitation, slurring, anomia, problems with comprehension, repetition, or arrest. Stimulation of the primary motor and sensory cortex results in localized movements or dysesthetic sensation, respectively, in the contralateral extremity. Stimulation-associated seizures are more common with motor cortex stimulation in the vicinity of the face motor cortex, while stimulation of the primary visual cortex causes localized flashes or phosphenes in the contralateral visual field. Stimulation of association cortex may not result in such positive phenomena but instead may disrupt performance of a task, such as speech arrest, with IFG stimulation. Stimulation of the SMA causes somewhat unpredictable effects; it may not only result in contralateral extremity movements or sensory phenomena but may also paradoxically result in the arrest of movement or speech. Tonic, rather than clonic, movements occur with premotor cortex activation.

Voluntary or induced cortical activation may be analyzed at surgery using an optical imaging technique that reflects vascular and metabolic changes coupled with neuronal activity. Optical imaging of intrinsic signals (OIS) depicts changes

in blood volume, oxygenated hemoglobin, cellular swelling, and cytochrome activity within an activated gyrus, using a charge-coupled device camera mounted via a custom adapter to the video monitor port of a standard surgical microscope (26). This promising technique relies on complex vascular and metabolic parameters but discordance with preoperative fMRI and to a lesser extent intraoperative SSEP has been reported. Subcortical pathways may be visualized using anisotropic diffusion-weighted imaging that relies on the direction of water molecule diffusion in white matter. Craniocaudally oriented white matter pathways, such as the corticospinal tract, are depicted and this information is integrated into the intraoperative neuronavigation system.

Conclusion

Cortical mapping techniques for the maximal safe resection of gliomas of all grades are valuable in minimizing surgical morbidity and maximizing resection of neoplastic elements that have an impact on the progression-free survival and overall survival of these patients. They have been repeatedly validated and refined and continue to improve particularly with expanding neurological, functional, and metabolic imaging capabilities and improved resolution. It is hence essential that practicing neurosurgeons involved in the care of these patients are familiar with these techniques and are capable of deploying them when necessary.

Conflict of interest: The authors declare no potential conflicts of interest with respect to research, authorship, and/or publication of the article.

Copyright and permission statement: To the best of our knowledge, the materials included in this chapter do not violate copyright laws. All original sources have been appropriately acknowledged and/or referenced. Where relevant, appropriate permissions have been obtained from the original copyright holder(s).

References

1. Benedict W, Primeau M, Blodgett-Dycus C, Thulborn KR, Prabhu VC. Cortical mapping in the resection of cerebral gliomas – Preoperative planning. *Contemp Neurosurg.* 2006;28(26):1–6. <http://dx.doi.org/10.1097/00029679-200612310-00001>
2. Prabhu VC, Benedict W, Primeau M, Blodgett-Dycus C, Macken M, Haccin-Bey L, et al. Cortical mapping in the resection of cerebral gliomas – Surgical considerations. *Contemp Neurosurg.* 2007;30(2):1–6.
3. Prabhu VC, Vargas C, Benedict W, Owen K, Jellish WS. Cortical mapping in the resection of cerebral gliomas – Anesthetic considerations. *Contemp Neurosurg.* 2007;29(1):1–6. <http://dx.doi.org/10.1097/00029679-200701150-00001>
4. Naidich TP, Valavanis AG, Kubik S. Anatomic relationships along the low-middle convexity: Part I – Normal specimens and magnetic resonance imaging. *Neurosurgery.* 1995;36(3):517–32. <http://dx.doi.org/10.1227/00006123-199503000-00011>
5. Naidich TP, Brightbill TC. The Pars Marginalis: Part I A “bracket” sign for the central sulcus in axial plane CT and MRI. *Int J Neuroradiol.* 1996;2:3–19.

6. Ogawa S, Tank DW, Menon R, Ellermann JM, Kim SG, Merkle H, et al. Intrinsic signal changes accompanying sensory stimulation: Functional brain mapping with magnetic resonance imaging. *Proc Natl Acad Sci U S A*. 1992;89(13):5951–5. <http://dx.doi.org/10.1073/pnas.89.13.5951>
7. Hirsch J, Ruge ML, Kim KH, Correa DD, Victor JD, Relkin NR, et al. An integrated functional magnetic resonance imaging procedure for preoperative mapping of cortical areas associated with tactile, motor, language, and visual functions. *Neurosurgery*. 2000;47(3):711–21; discussion 721–2.
8. Duffau H, Capelle L, Denvil D, Sichez N, Gatignol P, Taillandier L, et al. Usefulness of intraoperative electrical subcortical mapping during surgery for low-grade gliomas located within eloquent brain regions: Functional results in a consecutive series of 103 patients. *Neurosurg*. 2003;98(4):764–78. <http://dx.doi.org/10.3171/jns.2003.98.4.0764>
9. Pataraja E, Baumgartner C, Lindinger G, Deecke L. Magnetoencephalography in presurgical epilepsy evaluation. *Neurosurg Rev*. 2002;25(3):141–59; discussion 160–1. <http://dx.doi.org/10.1007/s10143-001-0197-2>
10. Gallen CC, Schwartz BJ, Bucholz RD, Malik G, Barkley GL, Smith J, et al. Presurgical localization of functional cortex using magnetic source imaging. *J Neurosurg*. 1995;82(6):988–94. <http://dx.doi.org/10.3171/jns.1995.82.6.0988>
11. Martin NA, Beatty J, Johnson RA, Collaer ML, Vinuela F, Becker DP, et al. Magnetoencephalographic localization of a language processing cortical area adjacent to a cerebral arteriovenous malformation. Case report. *J Neurosurg*. 1993;79(4):584–8. <http://dx.doi.org/10.3171/jns.1993.79.4.0584>
12. Frey D, Schilt S, Strack V, Zdunczyk A, Rösler J, Niraula B, et al. Navigated transcranial magnetic stimulation improves the treatment outcome in patients with brain tumors in motor eloquent locations. *Neuro Oncol*. 2014;16(10):1365–72. <http://dx.doi.org/10.1093/neuonc/nou110>
13. Bittar RG, Olivier A, Sadikot AF, Andermann F, Comeau RM, Cyr M, et al. Localization of somatosensory function by using positron emission tomography scanning: A comparison with intraoperative cortical stimulation. *J Neurosurg*. 1999;90(3):478–83. <http://dx.doi.org/10.3171/jns.1999.90.3.0478>
14. Berger MS, Ojemann GA. Techniques for functional brain mapping during glioma surgery. In: Berger M, Weller M, editors. *The Gliomas*. Amsterdam: Elsevier; 2016. p. 334–78.
15. Berger MS, Kincaid J, Ojemann GA, Lettich E. Brain mapping techniques to maximize resection, safety, and seizure control in children with brain tumors. *Neurosurgery*. 1989;25:786–92. <http://dx.doi.org/10.1227/00006123-198911000-00015>
16. Toga AW, Ojemann GA, Ojemann JG, Cannestra AF. Intraoperative brain mapping. In: Mazziotta JC, Toga AW, Frackowiak RSJ, editors. *Brain mapping: The disorders*. San Diego, CA: Academic Press; 2000. p. 77–105.
17. Kamada K, Todo T, Masutani Y, Aoki S, Ino K, Takano T, et al. Combined use of tractography-integrated functional neuronavigation and direct fiber stimulation. *J Neurosurg*. 2005;102:664–72. <http://dx.doi.org/10.3171/jns.2005.102.4.0664>
18. Peterson DO, Drummond JC, Todd MM. Effects of halothane enflurane, isoflurane and nitrous oxide on somatosensory evoked potentials in humans. *Anesthesiology*. 1986;65:35–40. <http://dx.doi.org/10.1097/0000542-198607000-00006>
19. Greenberg M. Surface anatomy of the cranium. In: Greenberg Publishing, editor. *Handbook of neurosurgery*. 3rd ed. Lakeland, FL: Greenberg Graphics; 1994. p. 99–101.
20. Peuskens D, van Loon J, Van Calenbergh F, van den Bergh R, Goffin J, Plets C. Anatomy of the anterior temporal lobe and the frontotemporal region demonstrated by fiber dissection. *Neurosurgery*. 2004;55:1174–84. <http://dx.doi.org/10.1227/01.NEU.0000140843.62311.24>
21. Barker FG II, Gutin PH. Surgical approaches to gliomas. In: Berger MS, Wilson CB, editors. *The Gliomas*. Philadelphia, PA: WB Saunders Co.; 1999. p. 796.
22. Lang FF, Olansen NE, DeMonte F, Gokaslan ZL, Holland EC, Kalhorn C, Sawaya R. Surgical resection of intrinsic insular tumors: Complication avoidance. *J Neurosurg*. 2001;95:638–50. <http://dx.doi.org/10.3171/jns.2001.95.4.0638>
23. Sartorius CJ, Berger MS. Rapid termination of intraoperative stimulation-evoked seizures with application of cold Ringer's lactate to the cortex. Technical note. *J Neurosurg*. 1998;88:349–51. <http://dx.doi.org/10.3171/jns.1998.88.2.0349>

24. Rostomily RC, Berger MS, Ojemann GA, Lettich E. Postoperative deficits and functional recovery following removal of tumors involving the dominant hemisphere supplementary motor area. *J Neurosurg.* 1991;75:62–8. <http://dx.doi.org/10.3171/jns.1991.75.1.0062>
25. Petrovich N, Holodny AI, Tabar V, Correa DD, Hirsch J, Gutin PH, Brennan CW. Discordance between functional magnetic resonance imaging during silent speech tasks and intraoperative speech arrest. *J Neurosurg.* 2005;103:267–74. <http://dx.doi.org/10.3171/jns.2005.103.2.0267>
26. Nariai T, Sato K, Hirakawa K, Ohta Y, Tanaka Y, Ishiwata K, et al. Imaging of somatotopic representation of sensory cortex with intrinsic optical signals as guides for brain tumor surgery. *J Neurosurg.* 2005;103:414–23. <http://dx.doi.org/10.3171/jns.2005.103.3.0414>

14

Recurring Glioblastoma: A Case for Reoperation?

JOOST DEJAEGHER • STEVEN DE VLEESCHOUWER

Department of Neurosurgery, University Hospitals Leuven, Leuven, Belgium

Author for correspondence: Steven De Vleeschouwer, Department of Neurosurgery, University Hospitals Leuven, Belgium. E-mail: steven.devleeschouwer@uzleuven.be

Doi: <http://dx.doi.org/10.15586/codon.glioblastoma.2017.ch14>

Abstract: Unlike newly diagnosed glioblastoma, no clear or widely accepted standard of care is available for patients with a recurrence. A purely radiological diagnosis of recurrence or progression can be hampered by flaws induced by pseudoprogression, pseudoresponse, or radionecrosis. Based on parameters like tumor location and volume, patient's performance status, time from initial diagnosis, and availability of alternative salvage therapies, reoperation can be considered as a treatment option to extend the overall survival and quality of life of the patient. The achieved extent of resection of the relapsed tumor—especially with the intention of having a safe, complete resection of the enhancing tumor—most likely plays a crucial role in the ultimate outcome and prognosis of the patient, regardless of other modes of treatment. Validated scores to predict the prognosis after reoperation of a patient with a recurrent glioblastoma can help to select suitable candidates for surgery. Safety issues and complication avoidance are pivotal to maximally preserve the patient's quality of life. Besides a possible direct oncological effect, resampling of the recurrent tumor with detailed pathological and molecular analysis might have an impact on the development, testing, and validation of new salvage therapies.

Key words: Prognosis; Recurrence; Relapse; Reoperation; Resampling

In: *Glioblastoma*. Steven De Vleeschouwer (Editor), Codon Publications, Brisbane, Australia ISBN: 978-0-9944381-2-6; Doi: <http://dx.doi.org/10.15586/codon.glioblastoma.2017>

Copyright: The Authors.

Licence: This open access article is licenced under Creative Commons Attribution 4.0 International (CC BY 4.0). <https://creativecommons.org/licenses/by-nc/4.0/>

Introduction

Maximal safe debulking surgery is well accepted as the mainstay treatment for newly diagnosed glioblastoma (GBM), and postoperative radiochemotherapy was determined in 2005 as the standard of care (SOC) by a pivotal phase 3 randomized trial by the European Organisation for the Research and Treatment of Cancer (EORTC) and National Cancer Institute of Canada Clinical Trials Group (NCIC) (1, 2). According to this trial, adult patients, up to the age of 70, with newly diagnosed GBM are being treated with 6 weeks of radiotherapy with concomitant temozolomide chemotherapy, followed by six adjuvant cycles of adjuvant temozolomide. However, despite multimodal therapy, prognosis for GBM patients remains poor with a median progression-free survival (PFS) of only 6.9 months, median overall survival (OS) of 14.6 months, and a 5-year survival rate of 9.8%. The low PFS is also reflected in the fact that less than 50% of patients completed the six cycles of adjuvant temozolomide in the EORTC–NCIC trial.

Notwithstanding intense preclinical research and clinical trials, standard therapy has not changed over the past decade. New agents with promising results in Phase 1 and/or Phase 2 trials, for example, the Vascular Endothelial Growth Factor-A (VEGF-A) Inhibitor bevacizumab or the integrin inhibitor Cilengitide, failed to improve survival in randomized phase 3 trials (3, 4). Moreover, in an effort to optimize the current chemotherapy, a dose-dense schedule of adjuvant temozolomide did not lead to improved survival (5). Recurrence, regrowth of tumor after a period of complete remission or stable disease, is universal. Unlike the well-defined treatment schedule in the newly diagnosed setting, no standard therapy exists for recurrent GBM. Treatment options in the recurrent setting include reoperation, re-irradiation, rechallenge temozolomide, or nitrosourea chemotherapy (e.g., lomustin [CCNU]), bevacizumab, or combinations of therapies (6). Given the absence of SOC, inclusion in clinical trials is optional upon recurrence. Whichever therapy is given, prognosis at recurrence is grim, with median survival in recent years estimated to be about 9 months and only one-third of patients alive after 1 year (7). Eventually, GBM will recur and lead to progressive neurological deterioration and death. Preserving quality of life (QoL) for as long as possible, therefore, becomes a priority in this palliative oncological setting.

Radiological Diagnosis of a Recurrence in Clinical Practice

During follow-up of GBM patients, most oncologists will perform an MRI scan every 2–3 months, or earlier upon clinical deterioration (8). This regular MRI scan will detect many recurrences in the early phase, often in asymptomatic patients. However, interpretation of these follow-up MRI scans can be challenging in the context of possible appearance of contrast enhancement due to radionecrosis or pseudoprogression in patients treated with radiotherapy and chemotherapy. Pseudoprogression is thought to occur in up to 50% of patients during the first 3–6 months after radiotherapy, whereas radionecrosis can occur up to several years after treatment and does not spontaneously regress without treatment (9).

As much as 15% of samples after reoperation showed only radionecrosis but no viable tumor in a series by Azoulay et al. (10). Moreover, bevacizumab, which is often used to treat recurrent GBM, compromises interpretation of follow-up MRIs as it normalizes leaky tumor vasculature and hence decreases T1 gadolinium enhancement and peritumoral edema (11, 12), sometimes resulting in only a pseudoresponse. To assess progressive disease, it is therefore recommended to use the recent Response Assessment in Neuro-Oncology (RANO) criteria that include evaluation of corticosteroid use, T2/FLAIR images, and restricted parameters to determine progressive disease during the first 3 months after radiochemotherapy, instead of the classical MacDonald criteria (13).

When there is a clear relapse or high suspicion of a (symptomatic) recurrence for which new treatment has to be initiated, a neurosurgeon should always be consulted to assess whether the patient is suitable for a repeat surgery. In general, it is estimated that only about 25% of patients can be considered for repeat surgery (6). Certainly, in the case in which clinical symptoms are due to mass effect, surgery remains the only treatment strategy that can drastically and rapidly decrease tumor load and possible symptoms. This can alleviate symptoms such as headache and (more rapidly) reduce the need for steroids to decrease peritumoral edema (14, 15). On the other hand a reoperation exposes patients to a risk of new temporary or permanent neurological deficits, general surgical and/or anesthesiological risks, and, at least temporarily, exclusion from other second-line treatments. Moreover, the oncological effect remains controversial (16).

Most recurrences appear locally in or close to the resection cavity of the first surgery (14). In a study by Brandes et al. on 79 patients with a recurrent GBM after initial treatment with standard therapy, almost 80% of recurrences occurred inside or at the margin of the radiotherapy field, where radiotherapy was administered at the contrast-enhancing mass with a margin of 2–3 cm (17). Rapp et al. reported on 97 recurrent GBM patients and found pure local recurrences in 79.3%, and combined local and distant recurrences in another 10.3% of patients (18). Obviously, diffuse, multifocal recurrences or deep infiltrative lesions are not surgical indications, contrary to a local well-circumscribed lesion. However, many patients will present with a local but poorly delineated lesion, for which a surgical indication cannot be advocated based on radiology alone.

Clinical Outcome after Surgery for Recurrent GBM

INHERENT SELECTION BIAS LEADS TO BETTER OUTCOME IN SURGICALLY TREATED RECURRENT PATIENTS

No randomized trials exist that randomize patients for surgery in the relapse setting, and most reported surgical series in recurrent GBM are retrospective (15). An overview of selected surgical outcome series is given in Table 1. Several authors have reported better outcome after surgery for recurrent GBM, compared to control nonsurgical populations. However, we have to take into account that these reports inherently suffer from selection bias, as patients who are selected for reoperation usually tend to be younger and have a better Karnofsky Performance Scale (KPS), and hence belong to a more favorable prognostic group (19). Azoulay et al. compared 68 reoperated patients with a matched

TABLE 1 Selected Surgical Series Reporting Outcomes after Reoperation for Recurrent GBM

Ref.	Number of reoperated patients (only GBM)	Age at reoperation (median, unless otherwise specified)	Adjuvant therapy after reoperation	Median OS total	Median OS after reoperation	Control group
(25)	39	45.5 years	Chemotherapy (not further specified)	82 weeks	36 weeks	AA: median OS after reoperation: 88 weeks
(24)	35 (20 AA)	48 years (grades 3 + 4, not given for GBM separately)	55%: CT 13%: CT and radiotherapy 7%: Radiotherapy (grades 3 + 4, not given for GBM separately)	76.4 weeks (GBM only)	29 weeks (GBM only)	AA: median OS after reoperation: 61.1 weeks
(40)	60	48 years (mean)	22%: CT 22%: Radiotherapy and CT 8%: Radiotherapy	72.5 weeks	18.5 weeks	AA: median OS after reoperation: 55 weeks
(41)	20	51 years (only reoperation) 52 years (reoperation and CT/SRS)	45%: Only reoperation 45%: CT 10%: SRS	Not given	13 weeks (only reoperation) 34 weeks (reoperation and CT/SRS)	Nonsurgical recurrent GBM patients: median OS after reoperation: 28 weeks

TABLE 1
Selected Surgical Series Reporting Outcomes after Reoperation for Recurrent GBM (Continued)

Ref.	Number of patients reoperated (only GBM)	Age at reoperation (median, unless otherwise specified)	Adjuvant therapy after reoperation	Median OS total	Median OS after reoperation	Control group
(22)	168: 1 reoperation 41: 2 reoperations 15: 3 reoperations	51 years (mean) (1 reoperation) 46 years (mean) (2 reoperations) 40 years (mean) (3 reoperations)	Not given	15.5 months (1 reoperation) 22.4 months: (2 reoperations) 26.6 months: (3 reoperations)	Not given	None (only case control between patients with 1, 2, or 3 reoperations matched for other prognostic variables)
(27)	33	59 years (mean) (whole group, also nonsurgical patients)	48%: Adjuvant therapy (not further specified)	Not given	6 months: (only reoperation) 14 months: (reoperation and adjuvant therapy)	Nonsurgical recurrent GBM patients that received CT alone (24 patients): median OS after recurrence: 8 months Group that received palliative treatment (19 patients): median OS after recurrence: 5 months
(52)	40	58 years	7.5%: Radiotherapy 48%: CT 7.5%: CT and radiotherapy	21.7 months	13.0 months	None
(20)	20	53.5 years (mean)	40%: CT 10%: Radiotherapy 20%: CT and radiotherapy 30%: Palliative treatment	25.4 months (reoperation) 11.6 months (nonsurgical group)	13.5 months (reoperation) 5.8 months (nonsurgical group)	Nonsurgical recurrent GBM patients (45) Median OS after recurrence: 5.8 months

Table continued on following page

TABLE 1
Selected Surgical Series Reporting Outcomes after Reoperation for Recurrent GBM (Continued)

Ref.	Number of patients reoperated (only GBM)	Age at reoperation (median, unless otherwise specified)	Adjuvant therapy after reoperation	Median OS total	Median OS after reoperation	Control group
(21)	49	59 years	Not given	20.1 months	7.6 months	Nonsurgical recurrent GBM patients (155); median OS 13.4 months
(26)	48	Not given	81.3% additional systemic therapy of which: 71.8% chemotherapy 23.1% fotemustine and bevacizumab 5.1% re-irradiation and temozolomide	21 months	7 months	None
(30)	503	58 years	57.1%: CT 25.5%: Palliative treatment 14.4%: CT and radiotherapy 3.1%: Radiotherapy	25 months	11.9 months	None
(10)	69	56 years	59.4% radio and/or CT	Not given	9.8 months	Matched nonsurgical group of 68 patients; median OS 5.3 months versus 9.6 months in matched reoperated patients

AA, Anaplastic Astrocytoma; CT, Chemotherapy; GBM, Glioblastoma; SRS, stereotactic radiosurgery.

cohort of nonsurgically treated recurrent GBM patients, based on initial extent of resection (EOR) and subventricular zone involvement (10). Median OS in the surgical subgroup was 9.6 months versus 5.3 months in the nonsurgical group, which was statistically significant. They concluded that reoperation, combined with additional rescue therapies, can induce prolonged survival in recurrent GBM. Chen et al. described 65 recurrent GBM patients, of whom 20 were reoperated. Median OS after recurrence in the surgical group was statistically higher with 13.5 months versus 5.8 months in the nonsurgical group (20). However, KPS at recurrence was also significantly higher in the surgical group, and 77.8% of the nonsurgical group received only palliative therapy. Tully et al. described 204 GBM patients of whom 24% were reoperated at recurrence, and they found a significantly improved survival of 20.1 months in reoperated patients compared to 9.0 months in recurrent patients who were treated nonsurgically (21). In their series, reoperated patients were younger, had a smaller initial tumor diameter, and were more likely to have an initial EOR of $\geq 50\%$ at first resection. Moreover, reoperated patients had a significantly higher percentage of completion of adjuvant therapy (79.6% vs. 35.9%). To compensate for this selection bias, patients that were *a priori* unlikely to be selected for reoperation based on age or performance scale were excluded in a subgroup analysis. A much less significant, though still present, advantage for the surgical group was found at first recurrence, but not anymore at second recurrence. Moreover, reoperation was no longer an independent predictor of OS in a multivariate analysis. The authors suggested that the improved OS in the surgical group might be more of a reflection of favorable patient characteristics than surgery itself. Chaichana et al. showed a survival benefit resulting from repeat resections using a multivariate analysis and case control evaluation to correct for selection bias (22). In their series, median survival was 6.8 months for patients that had one resection versus 26.6 months for patients that underwent four resections. Very often, a more favorable course of disease and pattern of recurrence render these patients eligible for reoperation rather than vice versa (Figure 1).

On the other hand several authors did not find a survival advantage for surgery. Franceschi et al. reported outcomes of a retrospective study on 232 recurrent GBM patients of whom 102 were treated with reoperation and chemotherapy, and compared these patients with 130 recurrent patients who were treated only with chemotherapy. They did not find a survival advantage in the reoperation group (23). In a large prospective registry database, including >1000 patients treated from 1997 to 2010, Nava et al. did not find better survival after recurrence in patients that underwent a reoperation. However, this study did not provide data on patient stratification at recurrence or EOR (7).

KARNOFSKY PERFORMANCE SCALE AND AGE AT RECURRENCE

The importance of patient characteristics at recurrence cannot be overestimated. Several older surgical outcome series have identified preoperative KPS as an important factor related to survival (24) or prolonged high QoL survival after recurrence (25). Also, KPS at recurrence in many studies turned out to be associated with better OS (19, 26–30). Patients with a poor performance scale are generally not proposed to undergo repeat surgery. A KPS of ≥ 70 , which means the patient is able to take care of himself or herself but cannot perform normal

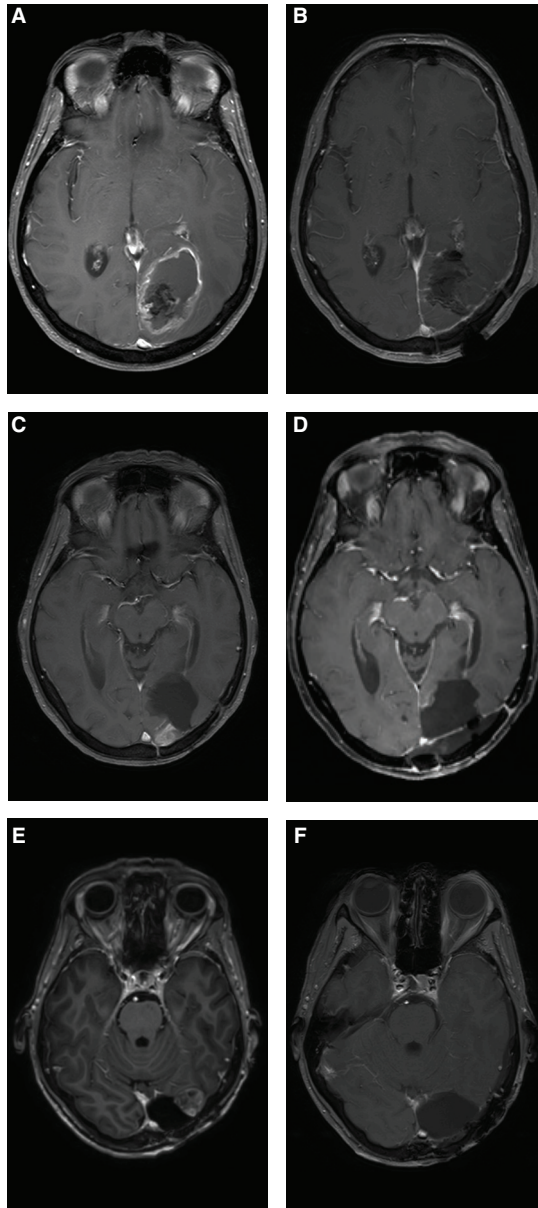


Figure 1 A 57-year-old lady was diagnosed with a left occipital glioblastoma (A), for which a total resection was performed (B). She was treated with standard radiotherapy, temozolomide chemotherapy, and experimental dendritic cell vaccination. An asymptomatic recurrence in the medial wall of the resection cavity was seen in a routine follow-up scan 16 months after the first surgery (C). A second total resection was performed (D), after which combined CCNU and bevacizumab was given in the EORTC 26101 study. A second asymptomatic local recurrence at the lateral side of the resection cavity was seen 14 months later (E), and again a total resection was performed (F). Nine months later she developed a multifocal progression, resistant to temozolomide. She died 42 months after the first surgery.

daily work, is generally accepted as a cut-off to select patients fit for surgery. The influence of age *per se* seems to be less pronounced in the absence of a good KPS, and reoperations in selected elderly patients were reported to be still feasible (31).

SCALES TO PREDICT SURVIVAL AFTER SURGERY FOR RECURRENT GBM

Two helpful prognostic scales to select patients for recurrent surgery are available. In 2010, Park et al. published a scale based on factors significantly associated with poor postoperative survival: involvement of ≥ 2 eloquent/critical brain regions, KPS ≤ 80 , and tumor volume of ≥ 50 cm³ (32). An additive scale based on these three variables stratified patients into good, intermediate, and poor postoperative survival groups. The authors were able to validate their score in a cohort of 109 recurrent GBM patients with a median survival of 9.2, 6.3, and 1.9 months in the three respective predictive groups. Patients with a poor prognosis as defined by this scale do not seem to have a benefit from reoperations. The applicability of this scale has been questioned, as the estimation of eloquent brain regions (referred to as MSM-score after involvement of motor or speech areas or involvement of middle cerebral artery areas) is somewhat subjective, and tumor volume is not always easy to measure. In 2013, Park et al. introduced a simpler prognostic scale (33) that combined one clinical parameter with one radiological parameter. A 0–2 points score was given based on KPS (≥ 70 or < 70) and the presence or absence of ependymal involvement in contrast MRI. This score distinguished patients with good, intermediate, and poor prognosis with median OS of 18.0, 10.0, and 4.0 months, respectively. For patients with a poor prognosis, surgery was not recommended.

Extent of Resection in the Recurrent Glioblastoma

EXTENT OF RESECTION: EQUALLY IMPORTANT AT RECURRENCE?

In a newly diagnosed GBM, it is generally accepted that an improved EOR is an independent prognostic factor for better outcome. A significant benefit on OS was present when EOR was at least 78%, with a further stepwise improvement with an EOR in the 95–100% range (34). The survival benefit for complete versus incomplete resection was estimated to be almost 5 months in a post hoc analysis on patients initially included in the 5-ALA trial by Stummer et al. (35).

In recurrent GBM patients, the importance of improving EOR is less universally accepted with highly variable survival rates in the literature. However, in recent years, several authors have reported a better OS when a higher EOR was achieved in the recurrent setting. McGirt et al. described a significantly improved OS after gross total (GTR) or near resection (NTR) compared to a subtotal resection (STR) in a study on 294 reoperated patients. Median survival for GTR and NTR were 11 and 9 months, respectively, versus 5 months for STR (28). Also, Bloch et al. showed in a series of 107 patients undergoing reoperation for recurrent GBM that EOR at reoperation was a significant predictor of OS. Interestingly, EOR at first resection was not a statistically significant factor when EOR at reoperation was included in a Cox proportional hazards model, suggesting that a

complete resection at reoperation could overcome an initial STR (19). A large retrospective study by Ringel et al. described outcomes in 503 reoperated patients (30). In this series, EOR at reoperation was also found to be significantly associated with better outcome. Also, these authors concluded that a complete resection at first recurrence could compensate for an incomplete resection at the initial surgery. The authors of the two last mentioned studies favored an aggressive surgical resection in recurrent GBM, as the improved survival with higher EOR suggested a real oncological effect, not a reflection of the selection of younger patients with higher KPS for recurrence surgery. Oppenlander et al. reported on 170 patients reoperated for recurrent GBM. They also found EOR to be significantly associated with OS following repeat resection. A threshold of at minimum 80% EOR was calculated to offer a significant survival benefit, suggesting usefulness of repeat surgery even if only a STR can be achieved (36). Also, Perrini et al. found EOR at reoperation to be associated with longer OS in a multivariate analysis of 48 reoperated patients (26).

In a smaller series, however, De Bonis et al. did not find a survival advantage for patients who received a GTR (11 patients) versus partial resection (22 patients) (27). Suchorska et al. analyzed post hoc the influence of reoperation in patients of the DIRECTOR trial, originally designed to test different dosing schemes of temozolomide administered at recurrence. Patients who were reoperated before entry into the study had similar prognostic factors (age, KPS, MGMT promotor methylation) than patients who were not reoperated. OS was not different between the two groups. However, the subgroup of patients that had a complete resection had a significantly better OS than nonsurgical patients, and patients with an incomplete resection showed a trend toward a worse prognosis than nonsurgical patients. The authors concluded that reoperation improved survival if complete resection of contrast-enhancing tumor (CRET) could be achieved (37).

IMPROVING RESECTION IN THE RECURRENT SETTING

Surgery for recurrent GBM can be technically more demanding, as the tumor is usually more invasive, and anatomical margins are less-defined than initially due to post-treatment gliosis (14). Given the growing evidence to obtain a maximal resection in the recurrent setting, surgical adjuncts such as intraoperative navigation, functional mapping, intraoperative ultrasound, and/or intraoperative MRI can be useful. To maximize EOR, the use of 5-aminolevulinic acid has been shown to lead to more complete resection and improved PFS in newly diagnosed GBM (38). In surgery for recurrent GBM, the use of 5-ALA has also been shown to have a high predictive value for detection of tumor cells and, importantly, did not seem to be affected by prior radiotherapy and/or chemotherapy (39).

Surgical Risks and Complications at Reoperation

In 1987, Ammirati et al. reported an early mortality rate of 1.4% and surgical morbidity of 16% per procedure. In their series on reoperated malignant glioma patients, they found that 46% of patients improved on performance scale

after surgery but also found worsening in 25% of patients. Harsh et al. had a 5.1% mortality and 7.7% morbidity (25). Sipos and Afra found a 3.4% mortality rate in 60 reoperated GBM patients (40). In their series, patients with a lower preoperative KPs were more likely to deteriorate postoperatively. In a series of 20 reoperated GBM patients, Mandl et al. found a mortality of 15%, and permanent neurological morbidity of 15% (41). Moreover, 40% of patients had a worse KPS postoperatively. More recently, in a series of 503 reoperated patients, Ringel et al. found a nonneurological complication rate of 7.4% (30). New neurological deficits appeared in 16.8% of patients, of which 9.2% were transient and 7.6% were permanent. The authors concluded that complications in reoperations are higher than in primary surgery, but the increase is rather small, and the overall complication rate stayed fairly small. D'Amico et al. published a retrospective study of 28 patients aged ≥ 65 years operated for recurrent GBM (31). In their study, no postoperative mortality was seen after reoperation, and the overall complication rate in reoperated patients was 17.9% at first surgery and 25.8% at reoperation. This difference was not statistically significant, and the authors concluded that age itself should not exclude patients from repeat surgeries. In summary, combined mortality and morbidity rates of repeat surgery can be estimated to be around 12–30%. This should always be taken into account, as the goal of surgery in recurrent GBM is essentially prolonging survival with good QoL.

Beyond Cyto-reduction: Additional Benefits of Surgery

TISSUE DIAGNOSIS AND SUBCLASSIFICATION

Surgery has the advantage over other treatment strategies by providing clinicians with a new tissue diagnosis. This can be important when radiology remains uncertain about possible pseudoprogression, real progression, or radionecrosis. If the diagnosis of a recurrence based on radiology, supplemented with nuclear imaging techniques, remains uncertain, surgery provides a unique opportunity for tissue confirmation of tumor regrowth or presence of viable tumor tissue (42), although no wide consensus exists about resampling pathology as the gold standard to confirm or definitively exclude pseudoprogression. Although currently not part of clinical practice, there is growing interest in the molecular subclassification of GBM to propel (personalized) experimental salvage treatments. Several subtypes of GBM have been described based on gene-expression profiles (43) and DNA methylation patterns (44). These subclassifications are already used to stratify and/or select patients in early clinical trials evaluating new anti-tumoral agents. For example, it has been shown that the mesenchymal subtype correlates with poor radiation response and shorter survival (45) but may be more immunogenic and respond better to immunotherapy (46). Moreover, Phillips et al. showed that upon recurrence, a class switch toward the mesenchymal subclass is frequently seen, showing that initial molecular diagnosis might not be easily extrapolated in the recurrence setting (47). As it is believed that these molecular genetic data will become part of clinical trials, the possibility of obtaining new tissue at recurrence will be of interest for researchers and neurooncologists.

SURGERY TO OBTAIN A STATE OF MINIMAL RESIDUAL DISEASE

Surgery is unique due to the fact that it rapidly leads to at least a substantial reduction of the tumor mass. This can result in a (macroscopically) state of *minimal residual disease*, which can be of benefit for other therapies. Keles et al. published a study on 119 GBM patients who were treated with temozolomide upon recurrence. They showed that the residual tumor volume was a significant predictor for “time to progression” and “survival,” even when adjusted for age, KPS, and time from initial diagnosis. They dichotomized between residual tumor volume of $<10\text{ cm}^3$, $10\text{--}15\text{ cm}^3$, and $>15\text{ cm}^3$; this was correlated with 6 and 12 months of PFS and OS, respectively. Although only three patients (3%) were reoperated before the start of chemotherapy in this series, the authors suggest that debulking surgery with the intent to reduce tumor volume to less than 10 cm^3 could be considered before chemotherapy is commenced (48). Stummer et al. described that a complete resection not only improves survival by itself but also may enhance the efficacy of adjuvant therapies such as radiochemotherapy and BCNU wafers, based on post hoc analyses on data from three separate randomized phase 3 trials in newly diagnosed GBM (49).

SURGERY TO START LOCAL CHEMOTHERAPY

After resection of a recurrent GBM, the resection cavity can be implanted with carmustine wafers (Gliadel). The effects were evaluated in a randomized trial. Patients with recurrent GBM had a 50% increased survival (56% vs. 36%), without increased complications or toxicity (50). However, in a retrospective study comparing recurrent GBM patients treated with Gliadel with a matched cohort group, Subach et al. did report on increased complications without survival benefit (51). Currently, Gliadel is rarely being used in Europe (52), although Quick et al reported in their recent publication that some form of chemotherapy was used after reoperation in more than 50% of cases all together (52) (table 1).

Conclusion

No prospective randomized trials directly evaluating the effect of reoperation for recurrent GBM have been published, and almost all available outcome data in surgical series are blurred by the inherent selection bias of patients with a high performance score and local recurrences. However, literature provides some evidence for an oncological advantage when a high EOR (or a CRET) can be obtained. This judgment needs to be made by a multidisciplinary oncological team with oncological neurosurgeons. Besides a cytoreductive effect, surgery can have an important role in obtaining tissue. Given the future expected importance of subclassification of glioblastoma and/or detection of specific druggable mutations, surgery probably will remain an important treatment strategy in the recurrent setting.

Conflict of interest: Dr. S. De Vleeschouwer organizes Gliolan (5-ALA) training sessions for neurosurgeons, for which a fee is received from Medac GmbH.

Copyright and permission statement: To the best of our knowledge, the materials included in this chapter do not violate copyright laws. All original

sources have been appropriately acknowledged and/or referenced. Where relevant, appropriate permissions have been obtained from the original copyright holder(s).

References

1. Stupp R, Mason WP, van den Bent MJ, Weller M, Fisher B, Taphoorn MJB, et al. Radiotherapy plus concomitant and adjuvant temozolomide for glioblastoma. *N Engl J Med.* 2005;352(10):987–96. <http://dx.doi.org/10.1056/NEJMoa043330>
2. Stupp R, Hegi ME, Mason WP, van den Bent MJ, Taphoorn MJB, Janzer RC, et al. Effects of radiotherapy with concomitant and adjuvant temozolomide versus radiotherapy alone on survival in glioblastoma in a randomised phase III study: 5-year analysis of the EORTC-NCIC trial. *Lancet Oncol.* 2009;10(5):459–66. [http://dx.doi.org/10.1016/S1470-2045\(09\)70025-7](http://dx.doi.org/10.1016/S1470-2045(09)70025-7)
3. Gilbert MR, Dignam JJ, Armstrong TS, Wefel JS, Blumenthal DT, Vogelbaum MA, et al. A randomized trial of bevacizumab for newly diagnosed glioblastoma. *N Engl J Med.* 2014;370(8):699–708. <http://dx.doi.org/10.1056/NEJMoa1308573>
4. Stupp R, Hegi ME, Gorlia T, Erridge SC, Perry J, Hong Y-K, et al. Cilengitide combined with standard treatment for patients with newly diagnosed glioblastoma with methylated MGMT promoter (CENTRIC EORTC 26071-22072 study): A multicentre, randomised, open-label, phase 3 trial. *Lancet Oncol.* 2014;15(10):1100–8. [http://dx.doi.org/10.1016/S1470-2045\(14\)70379-1](http://dx.doi.org/10.1016/S1470-2045(14)70379-1)
5. Gilbert MR, Wang M, Aldape KD, Stupp R, Hegi ME, Jaeckle KA, et al. Dose-dense temozolomide for newly diagnosed glioblastoma: A randomized phase III clinical trial. *J Clin Oncol.* 2013;31(32):4085–91. <http://dx.doi.org/10.1200/JCO.2013.49.6968>
6. Weller M, Cloughesy T, Perry JR, Wick W. Standards of care for treatment of recurrent glioblastoma—Are we there yet? *Neuro Oncol.* 2013;15(1):4–27. <http://dx.doi.org/10.1093/neuonc/nos273>
7. Nava F, Tramacere I, Fittipaldo A, Bruzzone MG, Dimeco F, Fariselli L, et al. Survival effect of first- and second-line treatments for patients with primary glioblastoma: A cohort study from a prospective registry, 1997–2010. *Neuro Oncol.* 2014;16(5):719–27.
8. Seystahl K, Wick W, Weller M. Therapeutic options in recurrent glioblastoma—An update. *Crit Rev Oncol Hematol.* 2016;99:389–408. <http://dx.doi.org/10.1016/j.critrevonc.2016.01.018>
9. Ellingson BM, Chung C, Pope WB, Boxerman JL, Kaufmann TJ. Pseudoprogression, radionecrosis, inflammation or true tumor progression? Challenges associated with glioblastoma response assessment in an evolving therapeutic landscape. *J Neurooncol.* 2017 Apr 5 (Epub ahead of print). <http://dx.doi.org/10.1007/s11060-017-2375-2>
10. Azoulay M, Santos F, Shenouda G, Petrecca K, Oweida A, Guiot MC, et al. Benefit of re-operation and salvage therapies for recurrent glioblastoma multiforme: Results from a single institution. *J Neurooncol.* 2017 Apr 3;132(3):419–26. <http://dx.doi.org/10.1007/s11060-017-2383-2>
11. Cohen MH, Shen YL, Keegan P, Pazdur R. FDA Drug approval summary: Bevacizumab (Avastin(R)) as treatment of recurrent glioblastoma multiforme. *Oncologist.* 2009;14(11):1131–8. <http://dx.doi.org/10.1634/theoncologist.2009-0121>
12. Ananthnarayan S, Bahng J, Roring J, Nghiemphu P, Lai A, Cloughesy T, et al. Time course of imaging changes of GBM during extended bevacizumab treatment. *J Neurooncol.* 2008;88(3):339–47. <http://dx.doi.org/10.1007/s11060-008-9573-x>
13. Wen PY, Macdonald DR, Reardon DA, Cloughesy TF, Sorensen AG, Galanis E, et al. Updated response criteria for high-grade gliomas: Response assessment in neuro-oncology working group. *J Clin Oncol.* 2010 Apr 10;28(11):1963–72.
14. Barbagallo GMV, Jenkinson MD, Brodbelt AR. “Recurrent” glioblastoma multiforme, when should we reoperate? *Br J Neurosurg.* 2008;22(3):452–5. <http://dx.doi.org/10.1080/02688690802182256>
15. Ryken TC, Kalkanis SN, Buatti JM, Olson JJ. The role of cytoreductive surgery in the management of progressive glioblastoma: A systematic review and evidence-based clinical practice guideline. *J Neurooncol.* 2014;118(3):479–88. <http://dx.doi.org/10.1007/s11060-013-1336-7>

16. Tosoni A, Franceschi E, Poggi R, Brandes AA. Relapsed glioblastoma: Treatment strategies for initial and subsequent recurrences. *Curr Treat Options Oncol.* 2016;17(9):49. <http://dx.doi.org/10.1007/s11864-016-0422-4>
17. Brandes AA, Tosoni A, Franceschi E, Sotti G, Frezza G, Amistà P, et al. Recurrence pattern after temozolomide concomitant with and adjuvant to radiotherapy in newly diagnosed patients with glioblastoma: Correlation with MGMT promoter methylation status. *J Clin Oncol.* 2009;27(8):1275–9. <http://dx.doi.org/10.1200/JCO.2008.19.4969>
18. Rapp M, Baernreuther J, Turowski B, Steiger H-J, Sabel M, Kamp MA. Recurrence pattern analysis of primary glioblastoma. *World Neurosurg.* 2017 Apr 18 (Epub ahead of print). <http://dx.doi.org/10.1016/j.wneu.2017.04.053>
19. Bloch O, Han S, Cha S, Zun M, Aghi M, McDermott MW, et al. Impact of extent of resection for recurrent glioblastoma on overall survival. *J Neurosurg.* 2012;117:1032–8. <http://dx.doi.org/10.3171/2012.9.JNS12504>
20. Chen MW, Morsy AA, Liang S, Ng WH. Re-do craniotomy for recurrent grade IV glioblastomas: Impact and outcomes from the National Neuroscience Institute Singapore. *World Neurosurg.* 2016;87:439–45. <http://dx.doi.org/10.1016/j.wneu.2015.10.051>
21. Tully PA, Gogos AJ, Love C, Liew D, Drummond KJ, Morokoff AP. Reoperation for recurrent glioblastoma and its association with survival benefit. *Neurosurgery.* 2016;79(5):678–89. <http://dx.doi.org/10.1227/NEU.0000000000001338>
22. Chaichana KL, Zadnik P, Weingart JD, Olivi A, Gallia GL, Blakeley J, et al. Multiple resections for patients with glioblastoma: Prolonging survival. *J Neurosurg.* 2013;118(4):812–20. <http://dx.doi.org/10.3171/2012.9.JNS1277>
23. Franceschi E, Bartolotti M, Tosoni A, Bartolini S, Sturiale C, Fioravanti A, et al. The effect of re-operation on survival in patients with recurrent glioblastoma. *Anticancer Res.* 2015;35(3):1743–8.
24. Ammirati M, Galichich J, Arbit E, Liao Y. Reoperation in the treatment of recurrent intracranial malignant gliomas. *Neurosurgery.* 1987;21(5):607–14. <http://dx.doi.org/10.1227/00006123-198711000-00001>
25. Harsh G, Levin V, Gutin P, Seager M, Silver P, Wilson CB. Reoperation for recurrent glioblastoma and anaplastic astrocytoma. *Neurosurgery.* 1987;21(5):615–21. <http://dx.doi.org/10.1227/00006123-198711000-00002>
26. Perrini P, Gambacciani C, Weiss A, Pasqualetti F, Delishaj D, Paia F, et al. Survival outcomes following repeat surgery for recurrent glioblastoma: A single-center retrospective analysis. *J Neurooncol.* 2017;131(3):585–91. <http://dx.doi.org/10.1007/s11060-016-2330-7>
27. De Bonis P, Fiorentino A, Anile C, Balducci M, Pompucci A, Chiesa S, et al. The impact of repeated surgery and adjuvant therapy on survival for patients with recurrent glioblastoma. *Clin Neurol Neurosurg.* 2013;115(7):883–6. <http://dx.doi.org/10.1016/j.clineuro.2012.08.030>
28. McGirt MJ, Chaichana KL, Gathinji M, Attenello FJ, Than K, Olivi A, et al. Independent association of extent of resection with survival in patients with malignant brain astrocytoma. *J Neurosurg.* 2009;110(1):156–62. <http://dx.doi.org/10.3171/2008.4.17536>
29. Garber ST, Hashimoto Y, Weathers S-P, Xiu J, Gatalica Z, Verhaak RGW, et al. Immune checkpoint blockade as a potential therapeutic target: Surveying CNS malignancies. *Neuro Oncol.* 2016;18(10):1357–660. <http://dx.doi.org/10.1093/neuonc/nov145>
30. Ringel F, Pape H, Sabel M, Krex D, Bock HC, Misch M, et al. Clinical benefit from resection of recurrent glioblastomas: Results of a multicenter study including 503 patients with recurrent glioblastomas undergoing surgical resection. *Neuro Oncol.* 2016;18(1):96–104. <http://dx.doi.org/10.1093/neuonc/nov145>
31. D'Amico RS, Cloney MB, Sonabend AM, Zacharia B, Nazarian MN, Iwamoto FM, et al. The safety of surgery in elderly patients with primary and recurrent glioblastoma. *World Neurosurg.* 2015;84(4):913–19. <http://dx.doi.org/10.1016/j.wneu.2015.05.072>
32. Park JK, Hodges T, Arko L, Shen M, Dello Iacono D, McNabb A, et al. Scale to predict survival after surgery for recurrent glioblastoma multiforme. *J Clin Oncol.* 2010;28(24):3838–43. <http://dx.doi.org/10.1200/JCO.2010.30.0582>
33. Park C, Kim J, Nam D, Kim C, Chung S, Kim Y, et al. A practical scoring system to determine whether to proceed with surgical resection in recurrent glioblastoma. *Neuro Oncol.* 2013;15(8):1096–101. <http://dx.doi.org/10.1093/neuonc/not069>

34. Sanai N, Polley M-Y, McDermott MW, Parsa AT, Berger MS. An extent of resection threshold for newly diagnosed glioblastomas. *J Neurosurg.* 2011 Jul;115(1):3–8. <http://dx.doi.org/10.3171/2011.2.JNS10998>
35. Stummer W, Reulen H-J, Meinel T, Pichlmeier U, Schumacher W, Tonn J-C, et al. Extent of resection and survival in glioblastoma multiforme: Identification of and adjustment for bias. *Neurosurgery.* 2008;62(3):564–76. <http://dx.doi.org/10.1227/01.neu.0000317304.31579.17>
36. Oppenlander ME, Wolf AB, Snyder LA, Bina R, Wilson JR, Coons SW, et al. An extent of resection threshold for recurrent glioblastoma and its risk for neurological morbidity. *J Neurosurg.* 2014;120(4):846–53. <http://dx.doi.org/10.3171/2013.12.JNS13184>
37. Suchorska B, Weller M, Tabatabai G, Senft C, Hau P, Sabel MC, et al. Complete resection of contrast-enhancing tumor volume is associated with improved survival in recurrent glioblastoma—Results from the DIRECTOR trial. *Neuro Oncol.* 2016;18(4):549–56. <http://dx.doi.org/10.1093/neuonc/nov326>
38. Stummer W, Pichlmeier U, Meinel T, Wiestler OD, Zanella F, Reulen H-J. Fluorescence-guided surgery with 5-aminolevulinic acid for resection of malignant glioma: A randomised controlled multicentre phase III trial. *Lancet Oncol.* 2006 May;7(5):392–401. [http://dx.doi.org/10.1016/S1470-2045\(06\)70665-9](http://dx.doi.org/10.1016/S1470-2045(06)70665-9)
39. Nabavi A, Thurm H, Zountsas B, Pietsch T, Lanfermann H, Pichlmeier U, et al. Five-aminolevulinic acid for fluorescence-guided resection of recurrent malignant gliomas: A phase II study. *Neurosurgery.* 2009;65(6):1070–6. <http://dx.doi.org/10.1227/01.NEU.0000360128.03597.C7>
40. Sipos L, Afra D. Re-operations of supratentorial anaplastic astrocytomas. *Acta Neurochir (Wien).* 1997;139(2):99–104. <http://dx.doi.org/10.1007/BF02747187>
41. Mandl ES, Dirven CMF, Buis DR, Postma TJ, Vandertop WP. Repeated surgery for glioblastoma multiforme: Only in combination with other salvage therapy. *Surg Neurol.* 2008;69(5):506–9. <http://dx.doi.org/10.1016/j.surneu.2007.03.043>
42. Butowski NA, Sneed PK, Chang SM. Diagnosis and treatment of recurrent high-grade astrocytoma. *J Clin Oncol.* 2006;24(8):1273–80. <http://dx.doi.org/10.1200/JCO.2005.04.7522>
43. Verhaak RGW, Hoadley KA, Purdom E, Wang V, Qi Y, Wilkerson MD, et al. Integrated genomic analysis identifies clinically relevant subtypes of glioblastoma characterized by abnormalities in PDGFRA, IDH1, EGFR, and NF1. *Cancer Cell.* 2010;17(1):98–110. <http://dx.doi.org/10.1016/j.ccr.2009.12.020>
44. Sturm D, Witt H, Hovestadt V, Khuong-Quang D-A, Jones DTW, Konermann C, et al. Hotspot mutations in H3F3A and IDH1 define distinct epigenetic and biological subgroups of glioblastoma. *Cancer Cell.* 2012;22(4):425–37. <http://dx.doi.org/10.1016/j.ccr.2012.08.024>
45. Bhat KPL, Balasubramaniyan V, Vaillant B, Ezhilarasan R, Hummelink K, Hollingsworth F, et al. Mesenchymal differentiation mediated by NF- κ B promotes radiation resistance in glioblastoma. *Cancer Cell.* 2013;24(3):331–46. <http://dx.doi.org/10.1016/j.ccr.2013.08.001>
46. Prins RM, Soto H, Konkankit V, Odesa SK, Eskin A, Yong WH, et al. Gene expression profile correlates with T-cell infiltration and relative survival in glioblastoma patients vaccinated with dendritic cell immunotherapy. *Clin Cancer Res.* 2011;17(6):1603–15. <http://dx.doi.org/10.1158/1078-0432.CCR-10-2563>
47. Phillips HS, Kharbanda S, Chen R, Forrest WF, Soriano RH, Wu TD, et al. Molecular subclasses of high-grade glioma predict prognosis, delineate a pattern of disease progression, and resemble stages in neurogenesis. *Cancer Cell.* 2006;9(3):157–73. <http://dx.doi.org/10.1016/j.ccr.2006.02.019>
48. Keles GE, Lamborn KR, Chang SM, Prados MD, Berger MS. Volume of residual disease as a predictor of outcome in adult patients with recurrent supratentorial glioblastomas multiforme who are undergoing chemotherapy. *J Neurosurg.* 2004;100(1):41–6. <http://dx.doi.org/10.3171/jns.2004.100.1.0041>
49. Stummer W, Van Den Bent MJ, Westphal M. Cytoreductive surgery of glioblastoma as the key to successful adjuvant therapies: New arguments in an old discussion. *Acta Neurochir (Wien).* 2011;153(6):1211–18. <http://dx.doi.org/10.1007/s00701-011-1001-x>
50. Brem H, Piantadosi S, Burger PC, Walker M, Selker R, Vick NA, et al. Placebo-controlled trial of safety and efficacy of intraoperative controlled delivery by biodegradable polymers of chemotherapy for recurrent gliomas. *Lancet.* 1995;345:1008–11. [http://dx.doi.org/10.1016/S0140-6736\(95\)90755-6](http://dx.doi.org/10.1016/S0140-6736(95)90755-6)

51. Subach, BR, Witham, TF, Kondziolka D, Lunsford LD, Bozik M, Schiff D. Morbidity and survival after 1,3-bis(2-chloroethyl)-1-nitrosourea wafer implantation for recurrent glioblastoma: A retrospective case-matched cohort series. *Neurosurgery*. 1999;36(2):17–22. <http://dx.doi.org/10.1227/00006123-199907000-00004>
52. Quick J, Gessler F, Dützmann S, Hattingen E, Harter PN, Weise LM, et al. Benefit of tumor resection for recurrent glioblastoma. *J Neurooncol*. 2014;117(2):365–72. <http://dx.doi.org/10.1007/s11060-014-1397-2>

15

Pediatric Glioblastoma

KUNTAL KANTI DAS • RAJ KUMAR

Department of Neurosurgery, Sanjay Gandhi Postgraduate Institute of Medical Sciences, Lucknow, UP, India

Author for correspondence: Dr. Raj Kumar, Department of Neurosurgery, Sanjay Gandhi Postgraduate Institute of Medical Sciences, Lucknow, UP, India, 226014. E-mail: rajkumar1959@gmail.com

Doi: <http://dx.doi.org/10.15586/codon.glioblastoma.2017.ch15>

Abstract: Glioblastoma in children, when compared with adults, is relatively rare. Despite this rarity, it is apparent from the limited number of publications that pediatric glioblastoma is quite distinct from their adult counterparts. The differences pertain to the molecular genetics, effectiveness of the adjuvant therapies, and possibly the prognosis after treatment. With a plethora of path-breaking translational research coming through in recent times, a host of new information is now available on pediatric glioblastomas that holds great promise as far as the future treatment options are concerned. This chapter is an attempt to highlight the key clinical aspects of pediatric glioblastoma in the light of the emerging clinical and laboratory evidence.

Key words: High-grade glioma; Neuroimaging; Pediatric glioblastoma; Radiotherapy; Supratentorial

In: *Glioblastoma*. Steven De Vleeschouwer (Editor), Codon Publications, Brisbane, Australia
ISBN: 978-0-9944381-2-6; Doi: <http://dx.doi.org/10.15586/codon.glioblastoma.2017>

Copyright: The Authors.

Licence: This open access article is licenced under Creative Commons Attribution 4.0 International (CC BY 4.0). <https://creativecommons.org/licenses/by-nc/4.0/>

Introduction

Glioblastoma (GBM) is the commonest and the most lethal primary brain tumor in adults (1). In contrast, GBM accounts for no more than 3–15% of primary central nervous system (CNS) tumors in children (2–7). This is despite the fact that CNS tumors are the most common solid tumors of childhood, and 40–50% of these tumors are constituted by the astrocytomas (8). Naturally, this relative rarity has been a great hurdle in properly deciphering the enigma of pediatric glioblastomas (p-GBM). Nevertheless, GBM remains an equally devastating disease in children with substantial morbidity and mortality. The reported median survival in p-GBM ranges from 13 to 73 months with a 5-year survival of less than 20% (2, 4, 6, 9–13). A few reports, however, reveal a relatively better prognosis and long-term survival figures in p-GBM as compared with adults (4, 9–11).

Maximal safe tumor resection followed by concurrent and adjuvant chemoradiation using oral temozolomide (TMZ) is the current standard of care in adult GBM (12). In fact, no such standard exists in children although a similar management policy is employed by most neurosurgeons across the globe. While there is sufficient evidence for the prognostic impact of maximal surgical excision of the visible tumor mass (4, 9, 10, 14), the concerns of irradiation on the developing brain and contradictory results of various chemotherapy regimens in p-GBM make the treatment decisions rather complicated and difficult in children.

A number of key clinical and laboratory investigations have led to a far better understanding of tumor biology of p-GBM today. Unlike in the past, these tumors are now considered to be distinctly different biological diseases compared with the adults. Numerous novel targeted drug therapies are emerging for the postoperative management of these tumors and hold great promise in times to come. However, it has to be agreed that the translation of the laboratory research into clinical patient management and patient outcomes have been relatively disappointing.

Epidemiology

Tumors of the CNS are the second most common childhood tumors after leukemia and are the commonest solid tumors in childhood (15). The overall incidence of primary CNS tumors in childhood is estimated to be approximately 30 per million (16). While astrocytic tumors account for 40–50% of the CNS tumors in children, high-grade gliomas are relatively rare. Estimation of the true incidence of p-GBM is often hampered by the fact that most studies tend to analyze GBMs (WHO grade IV) and anaplastic astrocytomas (WHO grade III) together, probably to derive a larger sample size for analysis. There is also a lack of consensus regarding the definition of pediatric age group. While the majority of studies consider 18 years as the cutoff, some studies consider 16 years or even 21 years for the same. On the contrary, many researchers also include adolescents in their analysis, thereby adding a lot of heterogeneity in the literature that hampers their holistic analysis.

As per the Central Brain Tumor Registry of the United States (CBTRUS) 2012 data, the incidence of pediatric high-grade glioma is approximately 0.85 per

100,000 (17). Most studies estimate the incidence of pediatric high-grade gliomas to be between 8 and 12% (18, 19). When only the GBM is considered, its incidence in the pediatric age group varies from 3 to 15% (2–7).

p-GBMs are most commonly reported in the second decade of life although their occurrence have been reported even *in utero* (2, 4, 5, 9, 20, 21). The highest incidence of p-GBM is seen between ages 15 and 19. This probably reflects the cumulative effects of different genetic insults in the eventual tumorigenesis. As far as gender predilection is concerned, most studies point towards a male predilection, the reasons for which are rather unknown. While it is unclear whether the patients' gender has any effect on the disease outcome, GBM in very young patients (<5 years) may have a slightly better prognosis compared to the older children.

As far as location is concerned, p-GBM is most commonly seen in the supratentorial brain, when the brainstem is excluded (12, 15, 20). Primary spinal cord high-grade gliomas constitute only 3% of the pediatric high-grade gliomas (22). In the supratentorial compartment, cerebral hemispheres are affected in nearly 50% of the cases. The incidence of deeper midline structure involvement, for example, thalamus, corpus callosum, hypothalamus, etc., is fortunately low (4, 23). In the infratentorial compartment, cerebellum is an extremely uncommon site with 1–2% of the GBMs in children affecting this site (24). Brainstem high-grade gliomas constitute nearly 20% of the intrinsic tumors in this area (25). Interestingly, when the nonbrainstem high-grade gliomas are analyzed, younger children are particularly susceptible compared with the older children and adolescents (26).

p-GBM remains a multifactorial disease similar to the malignancies at other age groups and systems. Prior history of ionizing radiations, particularly for hematologic malignancies like leukemia, is a proven factor in tumorigenesis (27, 28). Certain syndromes like Neurofibromatosis-1, Li-Fraumeni syndrome (characterized by inactivation of the tumor suppressor gene p53), and Turcot syndrome are also known to be associated with high-grade gliomas in children (23). We studied the association of matrix metalloproteinase (MMP)-1 gene of 110 patients with adult GBM and found a very high prevalence of 2G allele in these patients. A very strong association between 2G/2G genotype and GBM was detected in our study which indicated likely susceptibility for GBM in patients harboring this particular variant of MMP-1 (29). We also noted, in a separate study, that MMP-2 gene was not responsible for an increased susceptibility to high-grade gliomas in our population, unlike MMP-1 (30). These factors are discussed in detail below. However, it has to be agreed that the genetic syndromes constitute only a minuscule part of the entire spectrum of pediatric high-grade gliomas, the majority of which are sporadic without any clearly known predisposition. A number of genetic factors are now known to be associated with GBM in general and p-GBM in particular. These include p53 mutation, PDGFR mutation, H3K27M, etc., to name a few.

Pathology and Molecular Biology

GROSS AND MICROSCOPIC FEATURES

GBMs originate from the astrocytes, the chief glial constituent of the CNS. The gross and microscopic features of p-GBM are no different from the adults (5).

They are diffusely infiltrative despite their often apparent well-demarcated nature on imaging or even at surgery. These are usually dusky red or yellowish pink, friable, and vascularized tumors. Presence of thrombosed vessels inside the tumor mass is very much characteristic. There may be foci of hemorrhage or necrosis inside the lesion. Calcific components are rare but can be seen particularly in secondary GBMs. The usual sites of affections are supratentorial cerebral lobes like the frontal/temporal lobe. As mentioned before, deeper midline location, infratentorial compartment, and spinal cord locations are relatively uncommon (12, 15, 20). Although extracranial distant metastasis is rare, secondary dissemination inside the brain or the leptomeninges does occur in nearly 17% of patients (31).

Microscopically, these tumors are typically characterized by four histopathological hallmarks, namely, hypercellularity, nuclear atypia, pseudopalisading necrosis, and vascular endothelial cell proliferation. Multinucleated cells, bizarre nuclei, and neovascularization with glomeruloid formation are often detected. There are abundant mitotic figures with a high MIB labeling index, indicating a highly aggressive growth potential of the tumor. Satellite lesions are frequently seen. In one of the studies from our center, nearly 11% of GBMs were found to be multiple, the majority of the patients in that study being adults. Although these figures may not necessarily apply in pediatric population, our study showed that a high mitotic index (>40%), satellitosis, and a higher proportion of small cells correlate with tumor multiplicity in GBM (32).

PATHOLOGICAL VARIANTS/PATTERNS

WHO recognizes three variants of GBMs: giant-cell GBM, gliosarcoma, and, most recently, the epithelioid GBM. While the former two variants are relatively rare in children, epithelioid GBM, characterized by large eosinophilic cells, prominent melanoma-like nuclei, and often rhabdoid cells, is more common in children. These tumors tend to occur in the midline and are typically characterized by positive immunoreactivity for BRAF V600E, indicating their origin from a pre-existing low-grade precursor (33). GBM with primitive neuroectodermal components, small-cell GBM, and granular cell GBM are not true variants but specific patterns recognized by WHO. While the former is associated with a high risk of CSF spread, the latter two patterns portend poor outcomes despite the lack of necrosis inside the tumor (33).

MOLECULAR BIOLOGY

Incorporating the latest evidence emanating from laboratory research all over the world, WHO has updated its classification of brain tumors in 2016 (33). GBM is now classified as per the Isocitrate Dehydrogenase (IDH) gene mutation status. As a result, GBM can be either IDH mutation positive or IDH wild type. While the former group represents the secondary GBMs, the latter represents *de novo* lesions occurring mostly in elderly patients. But studies on pediatric high-grade gliomas, including GBMs, have noted a very low incidence of IDH mutation, particularly in younger children (34). Thus, for all practical purposes, p-GBM is almost always IDH wild type, although as Pollack et al. showed, the incidence of secondary GBM

(IDH mutated) may be higher in adolescents and younger adults (35). Lack of IDH mutation negatively impacts the outcome to therapy.

As far as the underlying genetic alterations are concerned, it is now well-known that p-GBMs have a higher incidence of p53 mutation/overexpression than mutation of epithelial growth factor receptor (EGFR) or deletion of phosphatase and tensin homologue (PTEN), the signatures of adult GBM. P53 mutation is particularly common in young children (<3 years). Interestingly, there may be overexpression of p53 in p-GBM even in the face of absent TP53 mutation (5, 36). Although, traditionally it was believed that PTEN mutation (with inactivation of its tumor suppressive effect on the downstream AKT pathway) played little role in p-GBM, certain recent studies have questioned the traditional belief and have noted activation of the AKT pathway, a feature that may negatively affect the patient outcomes (37). ATRX mutations have been reported in a fraction of p-GBMs, usually in the presence of p-53 mutation. Such tumors affect older children and are usually associated with better prognosis (38).

Recent studies have identified histone mutations (H3.3) in the DNA of pediatric high-grade glioma patients (39, 40). In fact, the H3K27M variant, wherein lysine is replaced by methionine at 27 positions, has been identified as an exclusive finding in pediatric high-grade gliomas. In addition, in slightly older children, replacement of glycine by valine or arginine at amino acid 34 of the H3.3 nucleic acid (G34V/R) is also frequently identified. While H3K27M variant is associated with poor prognosis, the outcome in patients with G34V/R is thought to be relatively better. Hemizygous deletions of ODZ3 have been described in the epithelioid variant of p-GBM. This particular variant, as already stated, shows BRAF V600E mutation, indicating its origin from low-grade pilomyxoid astrocytomas.

Vascular endothelial growth factor (VEGF) is commonly expressed by adult GBM cells. It is responsible for increased vascularity, tumor progression, and infiltration capacity of GBMs. As a result, anti-VEGF (bevacizumab) therapy is frequently employed in adult GBMs. The expression of VEGF is, however, relatively low in p-GBM, and it may be responsible for comparative ineffectiveness of anti-VEGF therapy in children (41). Somatic mutations of *PDGFRA* have also been recently reported in pediatric HGGs. This is in contrast to *EGFRA* mutations seen in adults. This has prompted anti-*PDGFRA* therapy in the form of receptor tyrosine kinase inhibitor imatinib (42, 43).

Apart from these clearly defined molecular aberrations, the pediatric HGGs seem to possess a significantly higher incidence of gains at 1q and losses at 16q and 4q. The 1p19q co-deletions are characteristic of oligodendroglial lineage. Some GBMs, particularly the secondary GBM, may have partial deletion of either 1p or more commonly 19q arms, and this may potentially confer a better prognosis (44). These GBMs are rare and were previously classified as GBM with oligodendroglial component (2007, WHO). As far as the O6-Methylguanine-DNA Methyltransferase (MGMT) promoter methylation status is concerned, it assumes an important prognostic significance in GBMs. Inactivation of MGMT generally correlates with chemoresponsiveness of these tumors. Studies on the expression of MGMT in p-GBM have revealed little difference in the promoter methylation status in children, with some studies noting even an overexpression of MGMT in tumors in children (45). It may be one of the reasons for reduced efficacy of TMZ in children compared with the adults. Whenever present,

the prognostic significance of the inactivating hypermethylation of MGMT confers a survival benefit to the affected children. Thus, a number of key molecular signatures of GBMs are now available for diagnosis and prognostication of high-grade gliomas in general.

Clinical Features

Symptoms of GBM are protean and are largely nonspecific. The duration of symptoms is usually short, often spanning a few months (2, 4, 20). The most common presentations are headache, vomiting, diplopia, and altered sensorium, indicating raised intracranial tension. It is reported as an initial symptom in 80–100% of patients (4, 20, 46). Children with GBM may present with acute neurological deterioration, usually from intratumoral hemorrhage, although an episode of seizure may also bring about such a dramatic presentation. The incidence of seizures as a clinical feature is estimated to be around 30%, being more common when frontotemporal lobes are affected or in the setting of secondary GBMs (4, 20, 46). Some authors have noted a relatively higher incidence of seizures in p-GBM, unlike in adults. Focal symptoms like neurological deficits, cranial nerve dysfunction, cerebellar symptoms, etc., depend on the location of the lesion. Neurological deficits, when present preoperatively, are known to affect postoperative prognosis negatively (47). Compared to the older children, infants and young children often present with nonspecific complaints, such as failure to thrive, lethargy, nausea/emesis, and macrocephaly, which, at times, can be difficult to diagnose. Assessment of the functional status is critically important in a disease like GBM. A number of scales are available to determine the functional status of children with brain tumors that are used preoperatively as well as during the posttreatment period. Karnofsky performance scale (KPS) is one such commonly utilized scale (4). A cutoff score of 80 generally differentiates good performance status from the poorly performing patients. In addition, neurological function scale (NFS) is another similar assessment tool in children (10). In our own study, the prognostic significance of preoperative performance status of these patients on the postoperative outcome was clearly demonstrated (4).

Neuroimaging

Neuroimaging plays an important part in the diagnosis, management, and prognostication of GBMs. Computed tomography (CT) and magnetic resonance imaging (MRI) form the backbones as far as the radiological assessment of these tumors is concerned. On CT and conventional sequences of MRI, these tumors appear as irregular, heterogeneously contrast-enhancing masses with significant perilesional edema. Although, some of the anaplastic astrocytomas may not enhance, GBMs almost always enhance. Necrosis, hemorrhage, and a garland pattern of enhancement are often characteristic of GBMs. The common differential diagnosis includes metastasis, lymphoma, brain abscess, etc. Although contrast-enhanced computed

tomogram is usually characteristic, MRI provides finer details needed for surgical as well as radiotherapy (RT) planning. Magnetic resonance spectroscopy typically displays choline peak with reduced N-acetyl aspartate in the region of the tumor although no such peaks may be seen in areas of necrosis. Diffusion-weighted images may show restricted diffusion with low apparent diffusion coefficient in the cellular parts of the tumor. While contrast images delineate the portions of the tumor with blood–brain barrier disruption, T2 fluid-attenuated inversion recovery (FLAIR) images clearly demonstrate the nonenhancing and edematous portions. Figure 1 shows the different radiological characteristics of GBM. Apart from the above diagnostic information, recent MRI techniques like functional MRI, tractography, etc., help in planning tumor resections, especially in eloquent locations. Perfusion-weighted MRI, although not routinely used, shows increased vascularity inside the tumor, a characteristic feature in high-grade gliomas. It can be performed by utilizing one of the three techniques, namely, magnetic resonance perfusion imaging, dynamic susceptibility contrast-MRI, and dynamic contrast-enhanced MRI (48).

An important role of neuroimaging is to assess response to therapy. Volumetric MRI is able to provide the extent of tumor excision, an important prognostic variable in GBMs. Moreover, the response assessment criteria like McDonald's criteria and RANO criteria rely on the posttreatment neuroimaging. In this regard, neuroimaging plays an important role in deciphering the true nature of two interesting radiological phenomena in high-grade gliomas, namely, “pseudoprogression” and “pseudoresponse” (48, 49). The former typically occurs after 3 months of chemoradiation when an erroneous observation of tumor progression is made when, in actuality, there is none. Different neuroimaging modalities

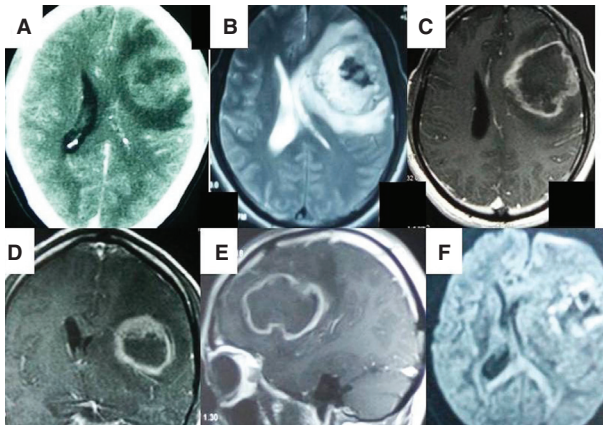


Figure 1 (A). Post-contrast computed tomography of the head shows a left frontal irregularly enhancing intraaxial mass of size approximately 4.5×4.5 cm with perilesional edema. The mass is causing effacement of the adjacent lateral ventricle. The mass is heterogeneously hyperintense on T2-weighted image with central necrosis (B). The peritumoral edema and ventricular compression is well made out on T2 images (B). The mass shows peripheral and ring-like contrast enhancement (C, D, E). The peripheral enhancing part shows hyperintensity on diffusion-weighted films suggestive of diffusion restriction (F). (The image was taken in 3T MRI scanner, GE, USA.)

like MR spectroscopy, diffusion-weighted MRI, positron emission tomography (PET), and perfusion-weighted MRI, etc., usually reveal the true nature of this spurious radiological finding. In true tumor progression, the typical metabolite profile of elevated choline, choline: creatinine >2 , and reduced N-acetyl aspartate peaks would be seen in MRS while there will be diffusion restriction on DWI. PET and perfusion-weighted MRI usually shows hypermetabolism and increased blood flow inside the enhancing area if there is true tumor progression, while the findings will be contradictory in pseudoprogression. Pseudo response, on the contrary, occurs as early as 24 h of anti-VEGF (Bevacizumab) therapy and is characterized by the lack of enhancement on contrast images even though the tumor is still there. Such pseudo responses are detected using T2 flair and diffusion-weighted MRI. While T2 flair shows the nonenhancing tumor as a hyperintense area, persistent diffusion restriction in the suspected area is usually diagnostic of residual tumor tissue. Neuroimaging has prognostic significance as well. In a recent study, Wangaryattawanich et al. (49) from MD Anderson Cancer Hospital showed that preoperative eloquent tumor location ($P = 0.007$), deep white matter invasion ($P = 0.006$), tumor volume (measured on contrast T1) $>35,000 \text{ cm}^3$ ($P = 0.08$), and volume of nonenhancing tumor/brain edema volume (measured in T2 flair) $>85,000 \text{ mm}^3$ ($P = 0.003$) were associated with poor survival in GBM.

Management

SURGERY

Maximal surgical resection followed by chemoradiotherapy remains the best current treatment in adult GBMs. Numerous studies have reiterated the utility of maximal tumor removal on both progression free as well as overall survival (OS) in p-GBM (4, 9, 10, 13, 14, 51). The Children's Cancer Group (CCG) study-945 showed that children with HGG who underwent a surgical resection of 90% or greater had a progression-free survival (PFS) of $35 \pm 7\%$ as compared with a 5-year PFS of $17 \pm 4\%$ in patients who did not (50, 51). Reporting on probably the largest single-center experience of p-GBM, we have also shown that the extent of tumor excision was a strong predictor of long progression-free survival as well as OS (4). The utility of maximal surgical excision has been proven in a recent multiple propensity analysis, the scientific value of which is as good as a randomized clinical trial (14). The extent of resection is, however, dependent on the location as well as extensions of the tumor (4). Brainstem location, midline supratentorial tumors, tumors affecting eloquent area, etc., are often difficult to excise completely without incurring significant neurological deficits. Apart from providing tissue for diagnosis, surgical debulking relieves tumor-related mass effect and potentiates the effect of the adjuvant therapy. Different intraoperative imaging techniques may allow larger extents of tumor excision which in turn translates into better survival outcomes. These advanced techniques include intraoperative neuronavigation, intraoperative ultrasound, intraoperative MRI, intraoperative cortical mapping, etc. Recent technological advances utilizing microfluidic chips allow for rapid analysis of the operative specimen for molecular signatures like IDH mutation within no time (51, 52). Therefore, it is possible now to make a molecular diagnosis

even intraoperatively. Such advances have the potential of facilitating intraoperative decision-making regarding the radicalism of the surgical excision in the future.

RADIATION THERAPY

Radiotherapy is an integral part of the comprehensive management basket of p-GBM. This is more so as the role of chemotherapy is not yet clear in these patients unlike their adult counterparts. Usually, the radiotherapy dose ranges from 50 to 60 Gy fractionated over 5–6 weeks (52, 53). Trials on hypo/hyper fractionation of the total dose have not shown any better results (54). It is routinely used in children aged more than 3 years. The primary reason why it should not be used before 3 years of age is that RT may lead to adverse neurocognitive complications due to its damaging effects on the developing brain. Moreover, it is believed that the tumors in the early years of life are rather indolent, responding less completely to irradiation (55, 56). The various long-term sequels of childhood cranial irradiation include endocrine dysfunctions, neurocognitive impairments, psychosocial and behavioral abnormalities, ototoxicity, growth abnormalities, and heightened chances of secondary malignancies (57). There has been a change in the way RT is administered in these patients. Previously, RT protocols encompassed the whole brain RT with additional boost at the site of the tumor with a 2-cm margin. However, with improvements in technology and accurate delineation of tumor margins, made possible by newer generation MRI scanners, currently RT is delivered using 3-dimensional conformal techniques. Thus, many of the earlier concerns with radiation treatment are no longer there. The conformal radiation treatment technologies include intensity-modulated RT, stereotactic RT, and proton beam RT (57). The latter techniques employ head fixation using rigid frames to enable precisely localized radiation. Therefore, recent advances have made RT in pediatric high-grade gliomas rather safe and effective.

CHEMOTHERAPY

Chemotherapy forms an important and integral part of the comprehensive treatment regime in adult GBMs. The same, however, cannot be said about the pediatric patients. Sposto et al. (CCG 943 trial) were the first to prove the effectiveness of chemotherapy (concomitant vincristine and adjuvant eight cycles of PCV regimen comprising procarbazine, CCNU, and vincristine) in high-grade gliomas (57). This regimen demonstrated a statistically significant improvement in the outcome of patients with GBM treated with chemotherapy compared with RT-alone group (5-year PFS: 42% vs. 18%). However, the regimen never reproduced similar results thereafter and hence failed to become a standard regime. It was later found that many of the patients included in that trial actually had low-grade gliomas. A subsequent trial looked at eight-drug chemotherapeutic regimen consisting of vincristine, carmustine, procarbazine, hydroxyurea, cisplatin, cytosine arabinoside, prednisone, and dimethyl-triazenoimidazole-carboxamide (DTIC) in children younger than 2 years (50, 58). This trial did not show any benefit in p-GBM. Moreover, the regimen failed to show any effectiveness in older children as well. Intensive chemotherapy after surgical excision has shown promising results in children, provided the tumor excision was

complete. The treatment using HIT-GBM-C protocol showed 5-year OS rate for these patients, with total resections of 63% versus 17% for historical controls. The OS was 19% at 60 months from diagnosis (50, 59). Some trials have also looked into the high-dose chemotherapy with bone marrow rescue in p-GBM, but these trials are mainly applicable for recurrent cases and their results have not been consistently proven. Unacceptable drug toxicity is usually the major handicap in these trials (60).

The landmark trial by Stupp et al. showed that the addition of concomitant and adjuvant TMZ improved progression-free survival and OS in adult GBMs (12). Five years' OS in this study for the TMZ arm was 9.8% versus 1.9% for the radiation alone arm. This trial has established the current therapeutic standard of concurrent and adjuvant TMZ in adult GBM. The Stupp trial, however, did not include p-GBMs. Thus, despite its landmark findings, the Stupp trial has not really helped matters as far as the p-GBM are concerned. Most studies indicate that TMZ chemotherapy does not affect survival figures in children, although a recent study has shown otherwise. A trial similar to the Stupp trial involving the pediatric patients did not show any benefit of TMZ in children (61). MGMT promoter methylation, whenever present, potentiates the activity of TMZ even in children. Thus, the ambiguity of the results of these studies has put a question mark on the routine use of chemotherapy in p-GBM vis-à-vis adult GBM, at least as of now. The PCV regimen is still used at many centers, often as a salvage therapy after disease recurrence.

ANTIANGIOGENESIS INHIBITORS

p-GBMs express VEGF similar to the adults. The clinical trials with anti-VEGF therapy (bevacizumab), however, have been rather disappointing in children (62). In a study of 10 patients with supratentorial HGGs and two studies with diffuse intrinsic pontine glioma (DIPG), clinical responses to bevacizumab were inferior to those in adult patients (62). Trials of combining chemotherapeutic agent (irinotecan) with bevacizumab has not improved the outcome either (63). Thalidomide, another antiangiogenic agent, has also failed to prove its efficacy in clinical trials when combined with RT. In particular, this combination led to rather high and unacceptable toxicities (64).

MOLECULAR TARGETED THERAPY

Recent insights into the molecular biology of gliomas in general and pediatric high-grade glioma in particular have led to the development of a number of agents directed specifically against these molecular targets. These include monoclonal antibodies like imatinib (anti-PDGFR) (65); erlotinib; gefitinib (anti-EGFR) (66, 67); and tipifarnib, a farnesyltransferase inhibitor (68). Most of these agents are in Stage I/II trials and have not really lived up to the expectations. One of the primary reasons for lack of expected success could be the fact that a number of tumorigenic pathways act simultaneously in these tumors, thereby negating the effect of blockade of a particular pathway. Similar to the above agents, lobaradimil, a bradykinin agonist, was tried with chemotherapy in a Phase II trial involving pediatric high-grade glioma, with a view to

enhance the drug permeability of the chemotherapeutic agents. The fate was unfortunately no different (68).

EMERGING NEWER DRUGS AND THERAPEUTIC MODALITIES

A number of other drugs and therapeutic modalities are being tested currently in the laboratories that hold great promise in the days to come. These include integrin inhibitors (cilengitide), EGFR inhibitors (cetuximab, nimotuzumab), novel antiangiogenic agents (enzastaurin, cediranib), histone deacetylase inhibitors (vorinostat, valproic acid), and dendritic cell vaccines. These agents have been tested in children with HGG and have shown good response in the clinical trials. Some agents are in the pre-trial recruitment phase and are likely to enter clinical trials in days to come. These include boron neutron capture therapy, cytomegalovirus-specific cytotoxic T cells, IL-13-PE38QR (an enzymatically active portion of pseudomonas exotoxin A conjugated with human interleukin-13), smoothed inhibitor LDE225, telomerase inhibitors, gamma secretase inhibitors, poly(ADP-ribose) polymerase inhibitor, etc., to name a few. Details of these advances are beyond the scope of this chapter and can be found in other articles (69).

Factors Affecting Outcome

The OS in p-GBM varies from 10 to 73 months (2, 4, 6, 9–12). Majority of the studies emphasize on improved survival figures in p-GBM compared with the adults (4, 9–11). There are studies on the long-term outcomes in p-GBM, defined as survival beyond 3 years of diagnosis. Although the factors determining the outcomes are still being studied, a number of factors are already known to predict survival in p-GBM in particular (Table 1). Of all the reported factors, the extent of surgical tumor excision probably remains the strongest predictor of outcome in p-GBM as of today.

TABLE 1

Factors Predicting a Longer Survival in p-GBM

Demographic factors	<ul style="list-style-type: none"> • Age <5 years of age • Female sex
Clinical factors	<ul style="list-style-type: none"> • Longer duration of symptoms • Presentation with seizures • Lack of preoperative neurological deficits • Good preoperative performance status
Radiologic factors	<ul style="list-style-type: none"> • Superficial, well-circumscribed tumor • Lack of extensive edema or intense contrast enhancement
Pathologic factors	<ul style="list-style-type: none"> • Lack of necrosis • Epithelioid/giant-cell variants • Low-MIB-1-labeling index

Table continued on following page

TABLE 1

Factors Predicting a Longer Survival in p-GBM (Continued)

Molecular genetics factors	<ul style="list-style-type: none"> • IDH mutation • MGMT promoter methylation • P53 over expression • PTEN deletion • Bcl underexpression • Expression of the tissue inhibitor of matrix metalloproteinase-1 and coexpression of the extracellular matrix metalloproteinase inducer and matrix metalloproteinase-2 • Lack of self-renewal genes like HOXA9/HOXA10 • Presence of BRAF/ATRX/G34V/R mutations
Treatment-related factors	<ul style="list-style-type: none"> • Gross total tumor excision • Chemoradiotherapy • Completion of entire treatment regime

Conclusion

p-GBM is a rare but distinctly different biological disease compared with the adults. Specific sets of genetic aberrations characterize p-GBMs. In the absence of concrete evidence for adjuvant chemotherapy, maximal surgical excision followed by adjuvant RT (in children >3 years of age) remains the current best treatment strategy for these tumors. Prognosis in the majority of children is better than the adults which in turn may be explained by a different biological make up of these tumors. With rapid scientific advances being made in this field, newer targeted molecular and other treatment strategies are likely to emerge and change the future course as well as the prognosis of p-GBM.

Conflict of interest: The authors declare no potential conflicts of interest with respect to research, authorship, and/or publication of this manuscript.

Copyright and permission statement: To the best of our knowledge, the materials included in this chapter do not violate copyright laws. All original sources have been appropriately acknowledged and/or referenced. Where relevant, appropriate permissions have been obtained from the original copyright holder(s).

References

1. Adamson C, Kanu OO, Mehta AI, Di C, Lin N, Mattox AK, et al. Glioblastoma multiforme: A review of where we have been and where we are going. *Expert Opin Investig Drugs*. 2009 Aug; 18(8):1061–83. <http://dx.doi.org/10.1517/13543780903052764>
2. Perkins SM, Rubin JB, Leonard JR, Smyth MD, El Naqa I, Michalski JM, et al. Glioblastoma in children: A single-institution experience. *Int J Radiat Oncol Biol Phys*. 2011 July;80(4):1117–21. <http://dx.doi.org/10.1016/j.ijrobp.2010.03.013>

3. Sánchez-Herrera F, Castro-Sierra E, Gordillo-Domínguez LF, Vaca-Ruiz MA, Santana-Montero B, Perezpeña-Diazconti M, et al. Glioblastoma multiforme in children: Experience at Hospital Infantil de Mexico Federico Gomez. *Childs Nerv Syst.* 2010 May;25(5):551–7. <http://dx.doi.org/10.1007/s00381-008-0780-8>
4. Das KK, Mehrotra A, Nair AP, Kumar S, Srivastava AK, Sahu RN et al. Pediatric glioblastoma: Clinico-radiological features and factors affecting the outcome. *Childs Nerv Syst.* 2012 Dec;28(12):2055–62. <http://dx.doi.org/10.1007/s00381-012-1890-x>
5. Suri V, Das P, Pathak P, Jain A, Sharma MC, Borkar SA, et al. Pediatric glioblastomas: A histopathological and molecular genetic study. *Neuro Oncol.* 2009 Jun;11(3):274–80. <http://dx.doi.org/10.1215/15228517-2008-092>
6. Faury D, Nantel A, Dunn SE, Guiot MC, Haque T, Hauser P, et al. Molecular profiling identifies prognostic subgroups of pediatric glioblastoma and shows increased YB-1 expression in tumors. *J Clin Oncol.* 2007;25:1196–208. <http://dx.doi.org/10.1200/JCO.2006.07.8626>
7. Dohrmann GJ, Farwell JR, Flannery JT Astrocytomas in childhood: A population-based study. *Surg Neurol.* 1985 Jan;23(1):64–8. [http://dx.doi.org/10.1016/0090-3019\(85\)90162-4](http://dx.doi.org/10.1016/0090-3019(85)90162-4)
8. Song KS, Phi JH, Cho BK, Wang KC, Lee JY, Kim DG, et al. Long-term outcomes in children with glioblastoma. *J Neurosurg Pediatr.* 2010 Aug;6(2):145–9. <http://dx.doi.org/10.3171/2010.5.PEDS09558>
9. Nikitović M, Stanić D, Pekmezović T, Gazibara MS, Bokun J, Paripović L. Pediatric glioblastoma: A single institution experience. *Childs Nerv Syst.* 2016 Jan;32(1):97–103. <http://dx.doi.org/10.1007/s00381-015-2945-6>
10. Mahvash M, Hugo H-H, Maslehaty H, Mehdorn HM, Stark AM. Glioblastoma multiforme in children: Report of 13 cases and review of the literature. *Pediatr Neurol.* 2011 Sep;45(3):178–80. <http://dx.doi.org/10.1016/j.pediatrneurol.2011.05.004>
11. Broniscer A, Gajjar A. Supratentorial high-grade astrocytoma and diffuse brainstem glioma: Two challenges for the pediatric oncologist. *Oncologist.* 2004;9(2):197–206. <http://dx.doi.org/10.1634/theoncologist.9-2-197>
12. Stupp R, Mason WP, van den Bent MJ, Weller M, Fisher B, Taphoorn MJ, et al. Radiotherapy plus concomitant and adjuvant temozolomide for glioblastoma. *N Engl J Med.* 2005 Mar;352(10):987–96. <http://dx.doi.org/10.1056/NEJMoa043330>
13. Adams H, Adams HH, Jackson C, Rincon-Torroella J, Jallo GI, Quiñones-Hinojosa A. Evaluating extent of resection in pediatric glioblastoma: A multiple propensity score-adjusted population-based analysis. *Childs Nerv Syst.* 2016 Mar;32(3):493–503. <http://dx.doi.org/10.1007/s00381-015-3006-x>
14. Packer J. Diagnosis and treatment of pediatric brain tumors. *Curr Opin Neurol.* 1994 Dec;7(6):484–91. <http://dx.doi.org/10.1097/00019052-199412000-00003>
15. Staneczek W, Jänisch W. Epidemiology of primary tumors of the central nervous system in children and adolescents. A population-based study. *Pathologe.* 1994 Aug;15(4):207–15. <http://dx.doi.org/10.1007/s002920050047>
16. CBTRUS statistical report: Primary brain and central nervous system tumors diagnosed in the United States in 2004–2008. Hinsdale, IL: CBTRUS; 2012. http://www.cbtrus.org/2012-NPCR-SEER/CBTRUS_Report_2004-2008_3-23-2012
17. Broniscer A. Past, present, and future strategies in the treatment of high-grade glioma in children. *Cancer Invest.* 2006 Feb;24(1):77–81. <http://dx.doi.org/10.1080/07357900500449702>
18. Finlay JL, Zacharoulis S. The treatment of high grade gliomas and diffuse intrinsic pontine tumors of childhood and adolescence: A historical—And futuristic—Perspective. *J. Neurooncol.* 2005 Dec;75(3):253–66. <http://dx.doi.org/10.1007/s11060-005-6747-7>
19. Artico M, Cervoni L, Celli P, Salvati M, Palma L. Supra-tentorial glioblastoma in children: A series of 27 surgically treated cases. *Childs Nerv Syst.* 1993 Feb;9(1):7–9. <http://dx.doi.org/10.1007/BF00301926>
20. Milano GM, Cerri C, Ferruzzi V, Capolsini I, Mastrodicasa E, Genitori LL, et al. Congenital glioblastoma. *Pediatr. Blood Cancer.* 2009 Jul;53(1):124–6. <http://dx.doi.org/10.1002/pbc.22008>
21. Wolff B, Ng A, Roth D, Parthey K, Warmuth-Metz M, Eyrich M, et al. Pediatric high grade glioma of the spinal cord: Results of the HIT- GBM database. *J. Neurooncol.* 2012 Mar;107(1):139–46. <http://dx.doi.org/10.1007/s11060-011-0718-y>

22. Fangusaro J. Pediatric high grade glioma: A review and update on tumor clinical characteristics and biology. *Front Oncol*. 2012 Aug;2:105. <http://dx.doi.org/10.3389/fonc.2012.00105>
23. Sgouros S, Fineron PW, Hockley AD. Cerebellar astrocytoma of childhood: Long-term follow-up. *Childs Nerv Syst*. 1995 Feb;11(2):89–96. <http://dx.doi.org/10.1007/BF00303812>
24. Epstein F, Wisoff J. Intra-axial tumors of the cervicomedullary junction. *J Neurosurg*. 1987 Oct;67(4):483–87. <http://dx.doi.org/10.3171/jns.1987.67.4.0483>
25. Fangusaro J. Pediatric high- grade gliomas and diffuse intrinsic pontine gliomas. *J Child Neurol*. 2009 Nov;24(11):1409–17. <http://dx.doi.org/10.1177/0883073809338960>
26. Neglia JP, Robison LL, Stovall M, Liu Y, Packer RJ, Hammond S, et al. New primary neoplasms of the central nervous system in survivors of childhood cancer: A report from the Childhood Cancer Survivor Study. *J Natl Cancer Inst*. 2006 Nov;98(21):1528–37. <http://dx.doi.org/10.1093/jnci/djj411>
27. Walter AW, Hancock ML, Pui CH, Hudson MM, Ochs JS, Rivera GK, et al. Secondary brain tumors in children treated for acute lymphoblastic leukemia at St Jude Children's Research Hospital. *J Clin Oncol*. 1998 Dec;16(12):3761–7. <http://dx.doi.org/10.1200/JCO.1998.16.12.3761>
28. Malik N, Kumar R, Prasad KN, Kawal P, Srivastava A, Mahapatra AK. Association of matrix metalloproteinase-1 gene polymorphism with glioblastoma multiforme in a northern Indian population. *J Neurooncol*. 2011 May;102(3):347–52. <http://dx.doi.org/10.1007/s11060-010-0337-z>
29. Kumar R, Malik N, Tungaria A, Kawal P. Matrix metalloproteinase-2 gene polymorphism is not associated with increased glioblastoma multiforme susceptibility: An Indian institutional experience. *Neurol India*. 2011 Mar–Apr;59(2):236–40. <http://dx.doi.org/10.4103/0028-3886.79131>
30. Wagner S, Benesch M, Berthold F, Gnekow AK, Rutkowski S, Sträter R, et al. Secondary dissemination in children with high-grade malignant gliomas and diffuse intrinsic pontine gliomas. *Br J Cancer*. 2006 Oct;95(8):991–7. <http://dx.doi.org/10.1038/sj.bjc.6603402>
31. Singh G, Mehrotra A, Sardhara J, Das KK, Jamdar J, Pal L, et al. Multiple glioblastomas: Are they different from their solitary counterparts? *Asian J Neurosurg*. 2015 Oct–Dec;10(4):266–71. <http://dx.doi.org/10.4103/1793-5482.162685>
32. Louis DN, Perry A, Reifenberger G, von Deimling A, Figarella-Branger D, Cavenee WK, et al. The 2016 World Health Organization classification of tumors of the central nervous system: A summary. *Acta Neuropathol*. 2016 Jun;131(6):803–20. <http://dx.doi.org/10.1007/s00401-016-1545-1>
33. Yan H, Parsons DW, Jin G, McLendon R, Rasheed BA, Yuan W, et al. IDH1 and IDH2 mutations in gliomas. *N Engl J Med*. 2009 Feb;360(8):765–73. <http://dx.doi.org/10.1056/NEJMoa0808710>
34. Pollack IF, Hamilton RL, Sobol RW, Nikiforova MN, Lyons-Weiler MA, LaFramboise WA, et al. IDH1 mutations are common in malignant gliomas arising in adolescents: A report from the Children's Oncology Group. *Childs Nerv Syst*. 2011 Jan;27(1):87–94. <http://dx.doi.org/10.1007/s00381-010-1264-1>
35. Pollack IF, Finkelstein SD, Woods J, Burnham J, Holmes EJ, Hamilton RL, et al. Expression of p53 and prognosis in children with malignant gliomas. *N Engl J Med*. 2002 Feb;346(6):420–7. <http://dx.doi.org/10.1056/NEJMoa12224>
36. Pollack IF, Hamilton RL, Burger PC, Brat DJ, Rosenblum MK, Murdoch GH, et al. Akt activation is a common event in pediatric malignant gliomas and a potential adverse prognostic marker: A report from the Children's Oncology Group. *J Neurooncol*. 2010 Sep;99(2):155–63. <http://dx.doi.org/10.1007/s11060-010-0297-3>
37. Heaphy CM, de Wilde RF, Jiao Y, Klein AP, Edil BH, Shi C, et al. Altered telomeres in tumors with ATRX and DAXX mutations. *Science*. 2011 Jul;333(6041):425. <http://dx.doi.org/10.1126/science.1207313>
38. Simon JA, Kingston RE. Mechanisms of polycomb gene silencing: Knowns and unknowns. *Nat Rev Mol Cell Biol*. 2009 Oct;10(10):697–708. <http://dx.doi.org/10.1038/nrm2763>
39. Wu G, Broniscer A, McEachron TA, Lu C, Paugh BS, Becksfors J, et al. Somatic histone H3 alterations in pediatric diffuse intrinsic pontine gliomas and non-brainstem glioblastomas. *Nat Genet*. 2012 Jan;44(3):251–3. <http://dx.doi.org/10.1038/ng.1102>
40. Lai A, Filka E, McGibbon B, Nghiemphu PL, Graham C, Yong WH, et al. Phase II pilot study of bevacizumab in combination with temozolomide and regional radiation therapy for up-front treatment of

- patients with newly diagnosed glioblastoma multiforme: Interim analysis of safety and tolerability. *Int J Radiat Oncol Biol Phys*. 2008 Aug;71(5):1372–80. <http://dx.doi.org/10.1016/j.ijrobp.2007.11.068>
41. Paugh BS, Zhu X, Qu C, Endersby R, Diaz AK, Zhang J, et al. Novel oncogenic PDGFRA mutations in pediatric high-grade gliomas. *Cancer Res*. 2013 Oct;73(20):6219–29. <http://dx.doi.org/10.1158/0008-5472.CAN-13-1491>
 42. Raymond E, Brandes AA, Dittrich C, Fumoleau P, Coudert B, Clement PM, et al. Phase II study of imatinib in patients with recurrent gliomas of various histologies: A European Organisation for Research and Treatment of Cancer Brain Tumor Group study. *J Clin Oncol*. 2008 Oct;26(28):4659–65. <http://dx.doi.org/10.1200/JCO.2008.16.9235>
 43. Nakamura M, Yang F, Fujisawa H, Yonekawa Y, Kleihues P, Ohgaki H. Loss of heterozygosity on chromosome 19 in secondary glioblastomas. *J Neuropathol Exp Neurol*. 2000 Jun;59(6):539–43. <http://dx.doi.org/10.1093/jnen/59.6.539>
 44. Lee JY, Park CK, Park SH, Wang KC, Cho BK, Kim SK. MGMT promoter gene methylation in pediatric glioblastoma: Analysis using MS-MLPA. *Childs Nerv Syst*. 2011 Nov;27(11):1877–83. <http://dx.doi.org/10.1007/s00381-011-1252-7>
 45. Ceroni L, Celli P, Salvati M, Palma L. Supratentorial glioblastoma in children: A series of 27 surgically treated cases. *Childs Nerv Syst*. 1993 Feb;9(1):7–9. <http://dx.doi.org/10.1007/BF00301926>
 46. Chaichana K, Parker S, Olivi A, Quiñones-Hinojosa A. A proposed classification system that projects outcomes based on preoperative variables for adult patients with glioblastoma multiforme. *J Neurosurg*. 2010 May;112(5):997–1004. <http://dx.doi.org/10.3171/2009.9.JNS09805>
 47. Huang RY, Neagu MR, Reardon DA, Wen PY. Pitfalls in the neuroimaging of glioblastoma in the era of antiangiogenic and immuno/targeted therapy—Detecting illusive disease, defining response. *Front Neurol*. 2015 Feb;6:33. <http://dx.doi.org/10.3389/fneur.2015.00033>
 48. Wen PY, Macdonald DR, Reardon DA, Cloughesy TF, Sorensen AG, Galanis E, et al. Updated response assessment criteria for high-grade gliomas: Response assessment in neuro-oncology working group. *J Clin Oncol*. 2010 Apr;28(11):1963–72. <http://dx.doi.org/10.1200/JCO.2009.26.3541>
 49. Wangaryattawanich P, Hatami M, Wang J, Thomas G, Flanders A, Kirby J, et al. Multicenter imaging outcomes study of The Cancer Genome Atlas glioblastoma patient cohort: Imaging predictors of overall and progression-free survival. *Neuro Oncol*. 2015 Nov;17(11):1525–37. <http://dx.doi.org/10.1093/neuonc/nov117>
 50. Finlay JL, Boyett JM, Yates AJ, Wisoff JH, Milstein JM, Geyer JR, et al. Randomized phase III trial in childhood high-grade astrocytoma comparing vincristine, lomustine, and prednisone with the eight-drugs-in-1-day regimen. *Childrens Cancer Group*. *J Clin Oncol*. 1995 Jan;13(1):112–23. <http://dx.doi.org/10.1200/JCO.1995.13.1.112>
 51. Aibaidula A, Zhao W, Wu JS, Chen H, Shi ZF, Zheng LL, et al. Microfluidics for rapid detection of isocitrate dehydrogenase 1 mutation for intraoperative application. *J Neurosurg*. 2016 Jun;124(6):1611–18. <http://dx.doi.org/10.3171/2015.4.JNS141833>
 52. Mallick S, Gandhi AK, Joshi NP, Kumar A, Puri T, Sharma DN, et al. Outcomes of pediatric glioblastoma treated with adjuvant chemoradiation with temozolomide and correlation with prognostic factors. *Indian J Med Paediatr Oncol*. 2015 Apr–Jun;36(2):99–104. <http://dx.doi.org/10.4103/0971-5851.158838>
 53. Fallai C, Olmi P. Hyper-fractionated and accelerated radiation therapy in central nervous system tumors (malignant gliomas, pediatric tumors, and brain metastases). *Radiother. Oncol*. 1997 Jun;43(3):235–46. [http://dx.doi.org/10.1016/S0167-8140\(96\)01897-X](http://dx.doi.org/10.1016/S0167-8140(96)01897-X)
 54. Geyer JR, Finlay JL, Boyett JM, Wisoff J, Yates A, Mao L, et al. Survival of infants with malignant astrocytomas. A Report from the Childrens Cancer Group. *Cancer*. 1995 Feb;75(4):1045–50. [http://dx.doi.org/10.1002/1097-0142\(19950215\)75:4%3C1045::AID-CNCR2820750422%3E3.0.CO;2-K](http://dx.doi.org/10.1002/1097-0142(19950215)75:4%3C1045::AID-CNCR2820750422%3E3.0.CO;2-K)
 55. Sanders RP, Kocak M, Burger PC, Merchant TE, Gajjar A, Broniscer A. High-grade astrocytoma in very young children. *Pediatr Blood Cancer*. 2007 Dec;49(7):888–93.
 56. Knab B, Connell PP. Radiotherapy for pediatric brain tumors: When and how. *Expert Rev Anticancer Ther*. 2007 Dec;7(12 Suppl):69–77. <http://dx.doi.org/10.1002/pcb.21272>
 57. Sposto R, Ertel IJ, Jenkin RD, Boesel CP, Venes JL, Ortega JA, et al. The effectiveness of chemotherapy for treatment of high grade astrocytoma in children: Results of a randomized trial. A report from

- the Children's Cancer Study Group. *J Neurooncol.* 1989 Jul;7(2):165–77. <http://dx.doi.org/10.1007/BF00165101>
58. Wolff JE, Driever PH, Erdlenbruch B, Kortmann RD, Rutkowski S, Pietsch T, et al. Intensive chemotherapy improves survival in pediatric high-grade glioma after gross total resection: Results of the HIT-GBM-C protocol. *Cancer.* 2010 Feb;116(3):705–12. <http://dx.doi.org/10.1002/cncr.24730>
59. Finlay JL, Dhall G, Boyett JM, Dunkel IJ, Gardner SL, Goldman S, et al. Myeloablative chemotherapy with autologous bone marrow rescue in children and adolescents with recurrent malignant astrocytoma: Outcome compared with conventional chemotherapy: A report from the Children's Oncology Group. *Pediatr Blood Cancer.* 2008 Dec;51(6):806–11. <http://dx.doi.org/10.1002/pcb.21732>
60. Cohen KJ, Pollack IF, Zhou T, Buxton A, Holmes EJ, Burger PC, et al. Temozolomide in the treatment of high-grade gliomas in children: A report from the Children's Oncology Group. *Neuro Oncol.* 2011 Mar;13(3):317–23. <http://dx.doi.org/10.1093/neuonc/noq191>
61. Narayana A, Kunnakkat S, Chacko-Mathew J, Gardner S, Karajannis M, Raza S, et al. Bevacizumab in recurrent high-grade pediatric gliomas. *Neuro Oncol.* 2010 Sep;12(9):985–90. <http://dx.doi.org/10.1093/neuonc/noq033>
62. Gururangan S, Chi SN, Young Poussaint T, Onar-Thomas A, Gilbertson RJ, Vajapeyam S, et al. Lack of efficacy of bevacizumab plus irinotecan in children with recurrent malignant glioma and diffuse brainstem glioma: A Pediatric Brain Tumor Consortium study. *J Clin Oncol.* 2010 Jun;28(18):3069–75. <http://dx.doi.org/10.1200/JCO.2009.26.8789>
63. Turner CD, Chi S, Marcus KJ, MacDonald T, Packer RJ, Poussaint TY, et al. Phase II study of thalidomide and radiation in children with newly diagnosed brain stem gliomas and glioblastoma multiforme. *J Neurooncol.* 2007 Mar;82(1):95–101. <http://dx.doi.org/10.1007/s11060-006-9251-9>
64. Pollack IF, Jakacki RI, Blaney SM, Hancock ML, Kieran MW, Phillips P, et al. Phase I trial of imatinib in children with newly diagnosed brainstem and recurrent malignant gliomas: A Pediatric Brain Tumor Consortium report. *Neuro Oncol.* 2007;9:145–60. <http://dx.doi.org/10.1215/15228517-2006-031>
65. Broniscer A, Baker SJ, Stewart CF, Merchant TE, Laningham FH, Schaiquevich P, et al. Phase I and pharmacokinetic studies of erlotinib administered concurrently with radiotherapy for children, adolescents, and young adults with high-grade glioma. *Clin Cancer Res.* 2009 Jan;15(2):701–7. <http://dx.doi.org/10.1158/1078-0432.CCR-08-1923>
66. Geyer JR, Stewart CF, Kocak M, Broniscer A, Phillips P, Douglas JG, et al. A phase I and biology study of gefitinib and radiation in children with newly diagnosed brain stem gliomas or supratentorial malignant gliomas. *Eur J Cancer.* 2010 Dec;46(18):3287–93. <http://dx.doi.org/10.1016/j.ejca.2010.07.005>
67. Fouladi M, Nicholson HS, Zhou T, Laningham F, Helton KJ, Holmes E, et al. A phase II study of the farnesyl transferase inhibitor, tipifarnib, in children with recurrent or progressive high-grade glioma, medulloblastoma/primitive neuroectodermal tumor, or brainstem glioma: A Children's Oncology Group study. *Cancer.* 2007 Dec;110(11):2535–41. <http://dx.doi.org/10.1002/cncr.23078>
68. Warren K, Jakacki R, Widemann B, Aikin A, Libucha M, Packer R, et al. Phase II trial of intravenous lobradimil and carboplatin in childhood brain tumors: A report from the Children's Oncology Group. *Cancer Chemother Pharmacol.* 2006 Sep;58(3):343–47. <http://dx.doi.org/10.1007/s00280-005-0172-7>
69. MacDonald TJ, Aguilera D, Kramm CM. Treatment of high-grade glioma in children and adolescents. *Neuro Oncol.* 2011 Oct;13(10):1049–58. <http://dx.doi.org/10.1093/neuonc/nor092>

Section III

**Upcoming Cutting-Edge
Innovations**

16 Glioblastoma: To Target the Tumor Cell or the Microenvironment?

STEVEN DE VLEESCHOUWER¹ • GABRIELE BERGERS²

¹Department of Neurosurgery, University Hospitals Leuven, Leuven, Belgium;

²VIB-KU Leuven Center for Cancer Biology, Campus Gasthuisberg, Leuven, Belgium

Author for correspondence: Steven De Vleeschouwer, Department of Neurosurgery, University Hospitals Leuven, Belgium.

E-mail: Steven.devleeschouwer@uzleuven.be

Doi: <http://dx.doi.org/10.15586/codon.glioblastoma.2017.ch16>

Abstract: Solid cancers develop in dynamically modified microenvironments in which they seem to hijack resident and infiltrating nontumor cells, and exploit existing extracellular matrices and interstitial fluids for their own benefit. Glioblastoma (GBM), the most malignant intrinsic glial brain tumor, hardly colonizes niches outside the central nervous system (CNS). It seems to need the unique composition of cranial microenvironment for growth and invasion as the incidence of extracranial metastasis of GBM is as low as 0.5%. Different nontumor cells (both infiltrating and resident), structures and substances constitute a semi-protected environment, partially behind the well-known blood–brain barrier, benefiting from the relatively immune privileged state of the CNS. This imposes a particular challenge on researchers and clinicians who try to tackle this disease and desire to penetrate efficiently into this shielded environment to weaken the GBM cells and cut them off from the Hinterland they are addicted to. In this chapter, we focus on how GBM interacts with the different components of its tumor microenvironment (TME), how we can target this TME as a useful contribution to the existing treatments, how we could make further progress in our understanding

In: *Glioblastoma*. Steven De Vleeschouwer (Editor), Codon Publications, Brisbane, Australia
ISBN: 978-0-9944381-2-6; Doi: <http://dx.doi.org/10.15586/codon.glioblastoma.2017>

Copyright: The Authors.

Licence: This open access article is licenced under Creative Commons Attribution 4.0 International (CC BY 4.0). <https://creativecommons.org/licenses/by-nc/4.0/>

and interaction with this environment as a crucial step toward a better disease control in the future, and what efforts have already been taken thus far.

Key words: Immune cell infiltration; Tissue matrix; Tumor heterogeneity; Tumor microenvironment; Vascularization

Introduction

For many decades, cancer has been regarded and therapeutically approached as a chaotic aggregate of uncontrolled cancer cells, escaping any type of internal cell cycle control due to driving and bystander (passenger) genetic alterations as elegantly summarized by Vogelstein et al. (1). Referring to the often used, illustrative metaphor of a cancer cell as an encyclopedia in which variable amounts and types of information have been incorrectly copied and translated, any given cancer cell can be described based on the number of pages missing (deletions), the number of double pages (amplifications), or the typos in the body of the encyclopedia's text (mutations). This abnormal genetic information leads to “druggable” protein modifications in the cell in conventional chemotherapy (2) or more recently in the logic of the emerging immunotherapies, to “neoantigens” (neoepitopes) in case of nonsynonymous mutations (3, 4). Although undisputable on the cancer cell level, this one-dimensional interpretation of cancer strongly neglected the complex interplay of the cancer cell with its environment in the cancerous organ. Especially, this tumor microenvironment (TME) starts to become crucial for a better understanding of pivotal concepts like intratumor heterogeneity (5), organ specificity of a cancer and its metastases (6), or its hostility against conventional and emerging treatments, causing chemoresistance and radioresistance (7) or immune escape, (8). Glioblastoma (GBM), the most common and aggressive brain tumor arising from glial cells in the central nervous system (CNS), either *de novo* as primary GBM, or from preexisting low-grade astrocytomas as secondary GBM (9), thrives in a highly specific and poorly accessible microenvironment rendering this fatal tumor notoriously hard to treat. Tackling this, TME is increasingly being recognized as a promising, novel asset in the anticancer armamentarium to diminish or overcome therapy resistance and (selectively) break down the different layers of protection the tumor creates to escape from its ultimate destruction. In this regard, therapies aiming to interfere with the protective TME might be ideally designed to combine conventional and upcoming cytotoxic agents and treatments in general. This chapter presents an overview of the TME composition and interactions in GBM, the ways to interrogate, study, and mimic, or ultimately even modulate this environment in order to improve the chances for tumor control and destruction.

The Heterogeneous Nature of Glioblastoma Cells

GBM cells are considered to be of glial, astrocytic origin (9). Although the stochastic tumor model, which states that all tumor cells have comparable proliferative, migrating, and infiltrating properties, and arise at random from

genetically impaired glial cells, is increasingly being challenged by the hierarchical tumor model in which cancer stem cells (CSCs) are the only ones with true self-renewal and multipotent differentiating properties (10), it remains very hard to define uniform CSC markers - in GBM. Based on gene cluster analysis of abnormalities in PDGFRA, IDH1, EGFR, and NF1, four molecular subtypes of GBM have been characterized; theoretically, every GBM can be stratified into proneural/neural-classical-mesenchymal subtypes (11). Using global DNA methylation profiling techniques like the Illumina 450k methylation array, Sturm et al. introduced an epigenetic classifier of six pediatric and adult GBM subtypes with distinct mutational patterns (12). Again, it should be stressed that even this meticulous and elegant molecular dissection of the GBM cancer cell holds a substantial risk of underestimating the true heterogeneity of this tumor, as already in 2013, Sottoriva et al. demonstrated that more than one molecular subtype can be found in one individual tumor depending on the tumor quadrant the sample had been harvested from (13). Particularly because of the highly invasive nature of GBM, we should realize that interrogating cells harvested from the tumor bulk might neglect the increasing genetic difference between founder cells in the tumor and infiltrating cells in the surrounding brain as spatially adjacent cells in the tumor are more likely to be closely related in terms of number and type of genetic alterations as compared to mutually distant cells within the same tumor (14). Needless to say that, without a more generalizable concept behind this heterogeneity, any attempt for personalized medicine against a validated target within a given subtype will result in only partially hitting the tumor with inevitable recurrence or outgrowth as a direct consequence. In this regard, more conventional treatments like temozolomide (TMZ) and radiotherapy have already proven to modify the predominant genetic signature of the surviving tumor cells (15), as well as the TME (16).

Glioblastoma Needs a Supportive Environment to Develop and Grow

GBM is the most malignant variant of a spectrum of intrinsic brain tumors called gliomas; it is, unfortunately, also the most frequent variant, occurring with an age-adjusted incidence of 0.59 to 3.69 per 10^5 persons per year (17). The standard-of-care (SOC) treatment consists of maximal safe surgery, followed by a combination of radiotherapy and chemotherapy (with TMZ), and results in a median overall survival (OS) of less than 15 months and a 5-year OS of less than 10% (18). To date, the disease is incurable and because of the high case fatality rate and the occurrence in also young and adolescent patients, GBM has the highest number of years of life lost (YLL) in several rankings over the last 10 years, representing a major socioeconomic burden and unmet medical need (19, 20).

Although GBM is rightfully considered as a highly aggressive neoplasm, with a median OS of less than 15 months after full therapy, it virtually only affects the CNS and only very rarely metastasizes toward distant organs (21). It generally exerts its detrimental activity locally at the site of origin, although hematogenous spreading of glial fibrillary acidic protein (GFAP-) positive GBM cells has been reported by Müller et al. (22). Moreover, up to 80% of local recurrences after

contemporary SOC therapy of maximal safe surgery followed by radiochemotherapy with fractionated, limited field, external beam radiation and TMZ occur within a 2.5 cm margin of the initial resection cavity, although infiltrating GBM cells can easily spread further away throughout the supratentorial CNS (23). This preferential anchoring of the tumor toward its original site of origin somehow contradicts its intrinsic biological aggressiveness but could partially be explained by degressive concentration of infiltrated cells in the periphery, its exclusive homing properties, and the hypothesized systemic immunity preventing it from colonizing extracranial tissues (24). The preferential route of infiltration seems to follow axonal tracks or to a lesser extent perivascular spaces (25), again pointing to a well-organized interaction with its direct TME rather than random growth or expansion.

The GBM TME is constituted not only by highly proliferative malignant astrocytoma cells and probably CSCs (26), but sometimes also by impressive quantities of immune cells, both residing and infiltrating, stromal cells, and vascular endothelial cells and pericytes, all creating separate niches within the tumor (27). All these cells are able to interact with each other within the frame of the extracellular matrix (ECM) in which fluids and macromolecules compose the noncellular substrates. Although intratumor heterogeneity as a concept is often restricted to the varying presence of different genetic alterations present in the different tumor cells (1), the true heterogeneity probably far exceeds this level, as many intratumoral niches can be defined based on the relative composition of contributing cell (sub-) types and ECM substances. There is growing evidence that in these niches, different tumor cell types (proliferating, infiltrating, CSC like) and different noncancerous cells (microglia, macrophages, dendritic cells (DCs), lymphocytes) dynamically reshape different parts of the tumor without exactly knowing which cell is the playmaker in which context and background (Figure 1). Microscopically, this results in different microenvironments within the tumor varying from solid tumor cores with densely packed proliferating tumor cells, to necrotic and perinecrotic areas, perivascular areas around vessels with endothelial proliferation, and hypoxic and perihypoxic regions (27). All these regions are ruled by microclimates of cells and molecules, thereby underpinning the need to unmask the tumor as a true organ rather than as a tissue.

Constituents of the Tumor Microenvironment in Glioblastoma

THE GBM VASCULATURE

GBMs are one of the most vascularized tumors with extensive neo-angiogenesis and an abnormal vasculature depicting hyperdilated and leaky vessels as well as vascular glomerular structures in which endothelial cells and pericytes form poorly organized vascular structures, a common hallmark of GBM (28). The presence of various angiogenic factors and chemokines have been reported in gliomas that are mainly expressed by tumor cells or infiltrating immune cells. The vascular abnormalities in GBM are however predominantly attributed to the highly elevated levels of vascular endothelial growth factor (VEGF) which subsequently cause the disruption of the blood–brain barrier (BBB). The BBB is comprised of endothelial cells, pericytes, and astrocytes, forming a neurovascular unit that tightly regulates

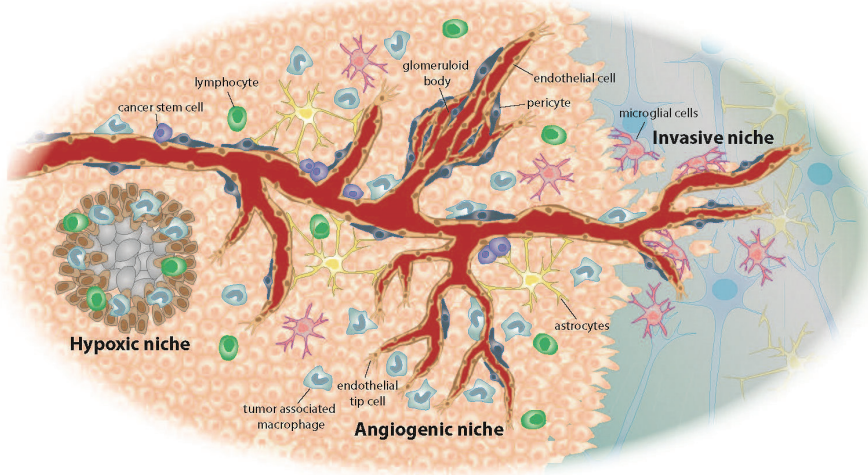


Figure 1 GBM TME niches. Glioblastoma (GBM) and glioma stem cells (GSCs) are embedded in a heterogeneous tumor microenvironment (TME) which not only is composed of diverse stromal cells, including vascular cells, the various infiltrating and resident immune cells, and other nonneoplastic glial cell types, but it is also compartmentalized in anatomically distinct regions, coined tumor niches. These niches can be composed of different cell constituents and look morphologically distinct from each other while the vasculature remains a central part. These niches regulate metabolic needs, immune surveillance, survival, invasion, as well as glioma stem cell maintenance. In the *angiogenic tumor niche* tumor (stem) cells nestle in close juxtaposition with the abnormal angiogenic vasculature while in the *vascular-invasive tumor niche* tumor cells co-opt normal blood vessels to migrate deep into the brain parenchyma. In the *hypoxic tumor niche*, there is either nonfunctional or regressed leading to necrotic areas that are surrounded by a row of hypoxic palisading tumor cells.

the transfer of ions and molecules between the blood and the brain (29, 30). A failure in these barrier properties induces vessel permeability with plasma and fluid leaking into the tumor tissue and thereby inducing cerebral edema and interstitial pressure. These changes also compromise vascular function and lead to sluggish blood flow and inconsistent oxygen delivery within GBM. In turn, local hypoxic areas develop that can turn into pseudopalisading necrosis, another hallmark of GBM, when tumor vessels become obstructed. These conditions also attract innate immune cells such as macrophages which elicit proangiogenic and immunosuppressive properties, thereby helping to expand the tumor vasculature to these poorly perfused areas.

Although the GBM vasculature expands mostly by angiogenesis, the proliferation of existing endothelial cells in tumor vessels, and bone marrow-derived vascular progenitors, can also promote neovascularization, albeit to a modest degree (31, 32). More recently, lineage-tracing experiments in mouse GBM models, and genetic mutational analysis of endothelial cells in patient-derived GBM, elicited glioma stem cells (GSCs) as another source of vascular constituents by their ability to transdifferentiate into endothelial cells or pericytes in GBM (33–36). The heterogeneous nature of the GBM vasculature not only affects its

important role as a gatekeeper for potential medicinal products and drugs against the tumor but also changes its adhesive properties affecting cellular adhesion and diapedesis of immune cells. In this respect, it is important to note that VEGF elevation besides generating an abnormal and angiogenic vasculature also thwarts the extravasation of tumor-reactive T cells and fosters an immune-suppressive microenvironment that enables tumors, including GBM to evade host immunosurveillance (37). VEGF reduces ICAM1 and VCAM1 adhesion molecules in angiogenic vessels and thereby hinders infiltration of immune T-effector cells into the tumor; it also directly inhibits the maturation of DCs and activates antigen-specific regulatory T cells (Tregs). This collectively contributes to the severely immunosuppressive nature of GBM and subsequent rather low CTL infiltration.

THE GLIAL CELL COMPARTMENT

The vast majority of GBMs arise in the supratentorial cerebral hemispheres. There, the tumor cells intermingle with (and overgrow) the local astrocyte, oligodendrocyte, and neuronal population. To this end, neither much is known about the ultimate fate of these original cell populations at the tumor site, nor do we have a clear view of the interactions between normal stromal cells, neurons, and cancer cells within the tumor and its immediate periphery. The remnants of oligodendrocyte-like cells and/or (reactive) astrocytes have been identified in many pathological specimens of resected GBM (38).

Astrocytes, which regulate metabolic and fluid homeostasis as well as vascular blood flow, contact endothelial cells and pericytes with their astrocytic endfeet, covering more than 99% of the cerebrovascular surface in the brain. During gliomagenesis, astrocytoma cells displace normal astrocytes from vessels, thereby disrupting the astrocyte–vascular interactions and regulation of the vascular tone which is sufficient to rupture the BBB (39). In addition, astrocytes surrounding GBM undergo reactive astrogliosis similar to that observed during CNS injury, by which they become proliferative and migratory and produce growth factors, metabolites, and cytokines that promote gliomagenesis. Several paracrine interactions have been described between astrocytes and glioma cell; for example, reactive astrocytes produce connective tissue growth factor (CTGF) that binds to tyrosine kinase receptor type A (TrkA) and integrin beta 1 on CSCs, thereby activating nuclear factor kappa B (NF- κ B) and inducing zinc finger E-box binding homeobox 1 (ZEB1), an epithelial–mesenchymal transition (EMT) transcription factor that facilitated tumor cell infiltration (40). To which extent astrocytes and oligodendrocytes contribute to tumor growth is still an ongoing issue of debate, but there appears to be a metabolic symbiosis between stromal and tumor cells based on the differing glycolytic and oxidative (glucose) metabolic flux of the respective cell populations (41, 42).

Although neurons have not been considered as active contributors to tumor propagation or bodily defense, tumor cells like to migrate along axonal trajectories and perivascular spaces. On the molecular level, some enigmatic correlations seem to exist between a higher PDL-1 expression on neurons in the peritumoral adjacent normal brain and a better patient outcome as opposed to the correlation between a higher PDL-1 expression in the tumor and a poor prognosis (43). These observations point to the importance of the precise context depending on which the same biomarkers can predict different biological evolutions. In pediatric GBM

and diffuse intrinsic pontine glioma (DIPG), Venkatesh et al. (44) were able to show that excitatory neuronal activity, through neuroligin-3 synaptic secretion, promotes glioma progression.

INFILTRATING AND RESIDING IMMUNE CELLS

A major part of the GBM tumor volume, up to 30 or 40% of the mass, can be made up by immune cells, especially myeloid-derived cells like infiltrating macrophages (45). Although in nonpathological conditions, no substantial amounts of immune cells infiltrate the brain parenchyma, and many of them never trespass the perivascular Virchow Robin spaces where they are held by the glia limitans/BBB, this can rapidly shift in several brain disorders in which inflammation plays a certain role (46). This clearly underscores that the brain and CNS is not absolutely immune privileged as once believed, but that quantity and quality of the immune reaction in the brain is highly contextual (47). Recently, another remarkable anatomical dogma has been challenged since Louveau et al. demonstrated the presence of lymphatics in the wall of (major) dural sinuses thereby providing evidence for a second gateway to (and from) the brain for immune cells (and interstitial fluids), apart from the vascular route (48, 49). In the context of malignant gliomas, making the difference between residing and infiltrating immune cells is difficult; microglia (CD11b+, CD45-) and residing (nonmigratory) DC, are believed to make up only a small minority of immune cells as compared with their infiltrated counterparts, classically called tumor-associated macrophages (TAMs) (50). Traditionally split up as M1 (pro-inflammatory, anti-tumoral) and M2 (anti-inflammatory, pro-tumoral) subtypes, the full spectrum of TAM is much more diverse (51) and highly dynamic. In an orthotopic mouse model, at early stages of tumor development, M1 TAM infiltrate the microenvironment but a rapid and massive differentiation toward M2 takes place in a more advanced stage of tumorigenesis, possibly corresponding to differences found in human low-grade versus high-grade glioma samples (unpublished own work). Remarkably, these macrophage populations seem to drive stromal and blood vessel architecture in the TME which can be offset (or partially corrected) by knocking down galectin-1 in the TME (52). Chemotactic gradients of substances like GM-CSF, M-CSF, MCP-1, and HGF are responsible for attraction (and retention) of these macrophages. Moreover, the CSF-1 pathway has been elucidated as crucial for M2 macrophage polarization in the TME, culminating in the possibility to re-educate M2 macrophages by the use of CSF1-R inhibition in gliomas (53, 54). The most enigmatic myeloid cell population in the TME and the blood of patients with malignancies, including GBM, are the myeloid-derived suppressor cells (55). To date, no uniform definition based on (lineage-)markers is universally used; this highly versatile cell population might play a key role in the mutual communication between the local immune cell population in the TME and the systemic immunity in the blood and extracranial organs. Recently, Chae et al. (56) elegantly showed that green fluorescent protein (GFP)-labeled monocytes, after undergoing intratumoral immunosuppressive education, can be precursors of MDSC both intratumoral and systemic in the context of glioma bearing mice. This does not only demonstrate the close familiarity of the different myeloid cell populations involved, but also the capacity of the TME to act as a local immune-suppressive factory of immune suppressor cells that can spread back to the systemic immunity after education in the TME.

Tumor-infiltrating lymphocytes (TIL), constitute the smaller, adaptive immunity counterpart of TAM in the TME. Although often outnumbered by TAM, TIL possibly have a more contextual importance for tumor progression, promotion, and ultimate patient prognosis (57). Although conventional CD8+ cytotoxic T cells (CTL) can mediate tumor regression and rejection in several experimental conditions, Tregs seem to infiltrate GBM in untreated conditions. Most of these Tregs are believed to be natural Tregs, thymus-dependent, and active through cellular contact via the so-called checkpoint inhibitors like CTLA-4 and PD-1 (58). Inducible Treg (iTreg), on the contrary, interfere with the local immune reaction predominantly by secreting IL-10 and TGF β , often called immunosuppressive cytokines (59). Several reports elaborated that TAM may play a role in the induction/attraction of the local Treg compartment in the TME, mainly via CCL22 and to a lesser extent through CCL2 (MCP-1) (60).

THE ECM AND TISSUE MECHANICS IN GB

The ECM is the noncellular component present within all tissues that not only provides essential physical scaffolding for all the cellular constituents but also initiates crucial biochemical and biomechanical cues that are pivotal for tissue morphogenesis, migration, differentiation, and homeostasis. The adult brain consists to about 20% of a uniquely composed ECM that is very distinct and different from the network of fibrous proteins normally found in many peripheral tissues. The brain ECM is almost entirely constituted of a mesh-like scaffold (i.e., perineuronal net [PNN]) of glycosaminoglycans (GAGs), including hyaluronic acid (HA), proteoglycans (e.g., lecticans), and glycoproteins (e.g., tenascins) (61–66). Thereby, long chains of HA project perpendicularly from the neuronal cell membrane at sites where hyaluronan synthases are located (HAS1–HAS3 in mammals) to form the bulk of the matrix. HA chains are bound along their axis by one end of a lectican (a member of the chondroitin sulfate proteoglycan family, including aggrecan, brevican, neurocan, and versican), which are cross-linked to neighboring lecticans at their other end through the glycoprotein tenascin (61, 63, 67, 68). Due to the unique brain properties, neuronal cells of all types contribute to ECM production, maturation, and structure while ECM proteins in many tissues are rather synthesized and deposited by fibroblasts and other mesenchymal cells. For cells, the ECM can provide guidance for preferred migration, invasion of infiltration depending on their nature or an active labyrinth to trap infiltrating immune cells.

During glioma progression, the ECM undergoes deposition and remodeling changing its composition and architecture in part due to the increased and altered production of some of the ECM components in glioma such as tenascin-C (TNC) and HA. Interestingly, in line with these observations, recent studies revealed that lower-grade gliomas (LGGs) and GBMs are progressively stiffer when compared with nontumor gliotic brain tissue (69). This is in agreement with the long-known fact that peripheral tumors are characteristically stiffer than the surrounding normal tissue.

Besides ECM stiffening, there are additional physical changes in the TME that facilitate glioma stiffness, specifically elevated fluid pressure (subsequent to edema), cell compression, and increased tumor cellular contractility. Such PNN alterations have been shown to promote tumor progression through sustained

activation of pro-tumorigenic mechanosignaling pathways, or by providing new “tracks” on which tumor cells can migrate. In addition, these changes obstruct blood vessel integrity, which in turn can influence both the recruitment of inflammatory cells and the permeability of macromolecules, including therapeutic compounds (70–72).

For interstitial fluid components, several substances in the ECM can modify the free diffusion and as such create environmental niches predisposing to the attraction of different types of infiltrating immune cells based on established gradients (73). In GBM and other malignancies, galectins (74) act as binders (scavengers) of glycosylated cytokines (IFN γ) and hamper an efficient anti-tumor immune rejection/response. GBM and their host cells interact with several of these ECM components through abundant secretion of enzymes like hyaluronidase or matrix metalloproteinases. These mechanisms are key for migration and invasion, the preferential way of spreading throughout the brain for GBM tumor cells (75). Some of these ECM components (or the relative lack of it) like fibronectin, have been connected to the low incidence of metastasis of GBM cells outside the CNS (76). Others like tenascin-C have been considered as targets for older monoclonal antibody approaches, some of which had been linked to radioactive OR cytotoxic components (77).

INTERSTITIAL FLUIDS AND SOLUBLE FACTORS

Within the TME, numerous soluble factors, secreted by tumor or stromal cells or extravasated from the intravascular compartments build a dynamic interstitial fluid compartment in which cells and ECM are bathing. Metabolites like lactate, as a result of the typical Warburg effect in tumor metabolism, and adenosine cumulate in hypoxic areas and have a strong impact both on tumor cells and immune cells (78). For the latter, they exert predominantly suppressive effects, for the former they mediate neo-angiogenesis or tumor progression. In spite of their frequently abundant presence in the TME, many of them are unequally distributed throughout the tissue, thereby contributing to the enormous intratumoral heterogeneity in tumors in general and GBM in particular: often this coincides with geographical differences of cell composition in the tumor like has been shown for galectin-1 and TAM (79). These variations in concentrations of soluble factors cause dynamic changes in chemotactic gradients, constantly reshaping the cellular composition of most tumor areas. Many cytokines have been documented in the TME of GBM, with a vast predominance of those especially known to have immunosuppressive effects. Transforming growth factor beta, (TGF β), originally demonstrated in GBM (80) and interleukin-10, classically depicted as immunosuppressive Th0 cytokine (81) are well-documented examples. The former has been the target of the first-in-kind trabedersen trial in which an antisense oligonucleotide was used to knock down the TGF β in the GBM TME (82). The latter is a more enigmatic cytokine rather fulfilling a multifaceted mode of action (83) than the purely immunosuppressive effect that is mostly attributed to it. More recently, our group looked at the importance of galectin-1, a key hub molecule in the GBM TME (84) and described a novel approach to selectively modulate it in the TME (85). Galectin-1 (Gal-1) is an evolutionary conserved, β -galactoside-binding lectin of 14.5 kDa, first isolated more than 30 years ago (86). It is a member of the galectin

family, consisting of 15 distinct galectins and characterized by a carbohydrate recognition domain (CRD), responsible for binding glycoproteins and glycolipids (87). Galectin-1 can be found both intra- and extracellularly, as well as at the cell membranes, and exerts its diverse functions through its presence in these different compartments.

Quantitative analysis from computer-assisted immunohistochemical (IHC) assessment revealed that Galectin-1 is being expressed by all subtypes of glial tumors and found a significant higher Gal-1 expression in poor-prognosis high-grade astrocytomas when compared to the clearly lower expression in high-grade glioma patients with better prognosis (88). Moreover, galectin-1 has been identified as a key hub molecule in glioma growth, invasion, and therapy resistance (89) as well as immune escape and suppression (84). Through promotion of the unfolded protein response in glioma cells, Galectin-1 was shown to contribute to the resistance of TMZ (90), an oral alkylating chemotherapeutic drug used in the SOC postoperative treatment of GBM, together with ionizing radiation (18). The latter seems to even increase the levels of galectin-1 expression in GBM rendering a Galectin-1 silencing strategy in GBM even more attractive to restore susceptibility to chemotherapy. In terms of tumor angiogenesis, Thijssen et al. (91) elegantly showed that tumor endothelial cell proliferation and migration relied on the presence of Galectin-1 in the TME and targeted inhibition of Gal-1 expression in Hs683 GBM cells resulted in a decreased VEGF secretion in the culture medium (92). Brain invasion, a problematic hallmark of GBM cells is being promoted by Galectin-1 that is expressed preferentially in tumor cells at the tumor periphery rather than in the core (93). This is perfectly consistent with earlier findings by Rorive et al. (94) and Camby et al. (95), both linking Gal-1 to cell motility and migration. In 2013, we were able to conclude that serum levels of Gal-1 of newly diagnosed GBM patients and recurrent high-grade glioma patients were significantly higher than those in age- and sex-matched healthy volunteers (96), based on the analysis of a prospective data set of 43 healthy controls and 125 patients. This indirectly indicates the important impact of GBM-related production of Gal-1 in the TME, on the systemic level outside the brain.

Apart from a direct promotion of tumor growth, angiogenesis, invasion, and therapy resistance, galectin-1 also indirectly stimulates GBM tumor promotion through impairment of the patient's immune system. Multiple modes of interaction, both with the innate and adaptive arms of immunity have been described and extensively been reviewed (84). These mechanisms include, but are not restricted to: the apoptosis induction of activated T cells, promotion of Th2 type of immune responses while blunting Th1 and Th17 responses, modulation of T-cell proliferation, modulation of T-cell receptor signaling, modulation of the cytokine balance, regulation of T-cell adhesion and trafficking, control of Treg function, modulation of DC tolerogenicity, and macrophage function. All of these lead to a state of immune suppression and immune evasion. As a direct consequence of all these abundant, galectin-1-mediated mechanisms, it was a logical step to investigate the immunological potentials and benefits of a targeted inhibition of galectin-1 gene expression in tumors. Rubinstein et al. (97) were the first to illustrate an increased T-cell-mediated tumor rejection after silencing galectin-1 expression in mouse melanoma cells. In 2014, for malignant gliomas residing in the CNS, we (79) demonstrated the huge impact of a tumor-derived Gal-1

knockdown (Gal-1-KD) in an orthotopic, syngeneic GL261 brain tumor model, on the local brain tumor immune microenvironment and its beneficial consequences for retarded tumor progression. The observed modifications included a decrease of myeloid cell accumulation and phenotype in the tumor after Gal-1 KD, an altered CCL2 and VEGF mRNA expression in brain infiltrating immune cells, a boost in IFN- γ producing tumor-infiltrating CD8 $^{+}$ T cells, an immune-mediated survival benefit of mice, and an impaired tumor angiogenesis. Therefore, an improved outcome with DC-based vaccination could be seen after silencing brain tumor-derived (but not systemic, nontumor derived) Galectin-1 in this mouse model.

Treatment Routes to Reach the Glioblastoma Microenvironment

The hematogenous route appears to be the most accessible path for drugs to the GBM TME but as described above, several restrictions apply to the chemical structure and nature of the compounds to overcome the BBB and egress from the intravascular compartment to the TME to exert its function in a brain tumor (98). Although the BBB does impose evident limitations to drug design, it has been shown that this barrier is not fully intact in GBM, due to the generation of leaky vessels in GBM that can be visualized by conventional MRI imaging in form of strong gadolinium enhancement (99). This, nevertheless, does not detract from the problematic vascular shunting effect that exists in GBM, leading to a poor parenchymal perfusion in the brain tumor in spite of the highly vascularized nature of a GBM (100). As a consequence, many parenterally administered drugs fail to reach the appropriate intratumoral drug concentration for an efficient biological effect.

For several decades, the intraventricular route has been used as an attractive way to administer medicinal compounds directly into the cerebrospinal fluid (CSF) where it can be distributed further throughout the CNS. Although several examples exist to date, many refrain from a universal adoption of this technique given its dose-limiting toxicity and its highly invasive nature with concerns about the reported high rates of infectious complications (101). A comparable approach with one or more catheters directly into the TME or the surrounding brain parenchyma has been coined convection-enhanced delivery (CED). Thereby, a small but active pressure gradient drives the active substance in a soluble form through a microcatheter into the TME. Although perfectly possible and applied for many different types of substances, similar concerns about its invasive nature and side effects limits its full implementation in the clinical arena (102). Moreover, it remains problematic to get a reliable measurement of the isodistribution volumes of a specific drug in the fluid phase throughout the TME and the brain (103).

A more recent approach of drug delivery that gains increasing interest is the nose-to-brain delivery route. Using a transnasal pathway to the CNS, especially the brain, has been studied for more than 30 years with the aspects of anatomical and pharmacodynamic challenges (104). The olfactory region of the nasal mucosa is directly connected to the intracranial forebrain regions and entorhinal circuits via the olfactory receptor neurons, the olfactory filia, nerves, and bulbus (105). To a lesser extent, the same goes for the trigeminal pathway via sensory nerve ends of

the first and second branch of the trigeminal nerve (V1 and V2) in the endonasal respiratory mucosa (106). The presumed predominant mode of transport is paracellular and, as such, it is capable to bypass the BBB, which still is a major issue in the design of new therapies and the development of new pharmaceutical agents (107–109). Transcellular intraneural transport, however, has been described too, mainly for larger molecules (110). Moreover, the nose-to-brain route provides a beneficial biodistribution in which drug concentrations in the brain could largely outnumber systemic availability of the administered active substances. Its theoretical consequence of less frequent and less serious adverse systemic events should translate in a beneficial shift of the therapeutic window. From a patient's perspective, the nose-to-brain route for drug delivery is likely to be much more appealing when compared to other local delivery technology like the invasive CED systems through insertion of brain catheters (111, 112). The noninvasive nature of drug administration and the possibility for repetitive self-administration will lead to a high patient compliance and therapy comfort. The noninvasive character of intranasal delivery avoiding important drawbacks of CED like infections, inflammation, brain edema, wound healing problems, local hemorrhages, and seizures, together with the rapid availability of the drug in the brain environment and the presumed reduced systemic side effects might turn this route into a preferred delivery for the treating physicians too.

The majority of the research regarding the opportunities and pitfalls of nose-to-brain drug delivery has been performed in (small) animal models. Both for non-oncological brain disease (109, 113) and for GBM (85), comprehensive reviews are available in the literature. For neuro-oncological diseases like GBM and CNS lymphoma, mainly the intranasal delivery of several chemotherapeutic agents like methotrexate (114), 5-fluorouracil (115), and the related molecule raltitrexed (116) has been explored in rodent models. A remarkable, common finding in all these studies has been the indication for a preferential drug delivery to the brain (in different grading concentrations at different brain locations) rather than to the systemic circulation. Moreover, in each study, the drug concentrations in the CSF were higher for the intranasal group as compared to the systemic administration. To target Gal-1 in the TME of a malignant intrinsic brain tumor, we aimed to be both selective and inclusive: interference with other galectins should be avoided and reduction of both intracellular and extracellular Gal-1 is mandatory to tackle the full biological repertoire of this key hub molecule in GBM. Therefore, rather than opting for monoclonal antibodies (with a notorious problem to cross the intact BBB), small molecules like Davanat (117) or polypeptides like Anginex (118), we chose to develop an anti-Gal-1 siRNA molecule (siGal-1)-based formulation that could reach the GBM microenvironment upon intranasal delivery to exert its selective biological activity locally at the brain tumor site. Small interfering (si) RNA molecules are double-stranded RNA molecules of 21–25 base pairs that can initiate a sequence-specific mRNA degradation of the target RNA through cytoplasmic interactions with RNAi-induced silencing complex (RISC), resulting in a temporary (reversible) decrease of the protein of interest as nicely reviewed by Agrawal et al. (119). Hashizume et al. (120) reported the results of a study with GRN163, an antisense oligonucleotide targeting telomerase in GBM, which had been delivered intranasally in rats. They reported a rapid distribution in the brainstem through the trigeminal nerve pathway, a significant survival benefit in animals with an established brain tumor and a remarkable tumor tropism within

the brain. As fragile siRNA molecules are easily and rapidly degraded in an extracellular environment, it is mandatory to load this siRNA in specific (nano-)formulations that can protect and transport it until it reaches its intracellular target. The formulations has several capabilities of which the most important are (i) protecting siRNA from rapid degradation during its journey to the brain, (ii) influencing the mucoadhesive properties (in the nasal mucosa), (iii) facilitating transport through the mucosal and epithelial nasal barriers, (iv) stimulating the perineural (and/or transcellular) transport to the brain parenchyma, (v) promoting tumor tropism, (vi) transfecting the cells and finally, and (vii) getting released from the formulation once it reaches the tumor cell cytoplasm to exert its specific biological activity through interaction with the RISC. Moreover, the excipients used need to be well tolerated and biodegradable. Until now, rather few of the theoretical possibilities have been tested in preclinical animal models of different brain diseases (121–123). To date, we have been able to show a convincing nose-to-brain transport of both siGal-1 formulations based on naïve-chitosan and pegylated-chitosan nanoparticles (NNP and PNP, respectively) in the orthotopic, syngeneic, GL261 brain tumor model, leading to a selective and sequence-specific degradation of Gal-1 in the brain TME (124). This Gal-1 knockdown in the tumor dramatically increased the chemosensitivity to TMZ and showed a promising synergy with anti-PD-1 blocking monoclonal antibodies in the same model (52).

Is It Possible to Capture the Complexity of the Microenvironment in Glioblastoma Models?

Interrogating the TME and respecting all the layers of information (see Table 1) involved, as well as the highly interactive nature of all its constituents, remains a major challenge. Obviously, no *in vitro* cell culture model, whether monolayer, specially designed (125) or neurospheres (126), will faithfully reflect the highly complex interactions of all TME components. Three-dimensional *in vitro* culture models, built on special scaffolds (before being grafted in animals) might be able to mimic key histologic characteristics of GBM (127, 128) but to what extent they also accurately represent the TME remains unknown. The same goes for almost all conventional animal models (129). Heterotopic brain tumor models with GBM cells growing in subcutaneous tissues can never mimic the particular CNS environment of the brain and therefore, orthotopic brain tumor models should be preferred for this type of research. In that regard, xenograft models, even patient-derived (130), are being created in immune-compromised animals, thereby fully neglecting the impact of the immune system, which accounts for the major supplier of nontumoral cells constructing the GBM TME. Garcia et al. reported in 2014 about an orthotopic xenotransplant model successfully recapitulating the GBM microenvironment (131). Syngeneic orthotopic brain tumor animal models (132) can correct for that shortcoming, although tumor cell biology and immunity differ considerably between species. The ideal model is yet to be built, but will have to combine human tumor cell biology interacting with a human(-ized) immune system (133). Direct on-site interrogation and quick mapping of the GBM TME, for example, during surgery, might be another future track to considerably improve our understanding of its complexity.

TABLE 1
Selected Overview of Components of the Glioblastoma Tumor Microenvironment Targeted by Different Types of Compounds in Varying Phases of Preclinical and Clinical Development

TME Component	Target	Type of Compound	Authors and Reference	Year	Phase of Development in GB
Blood vessel components					
VEGF	VEGF-A	mAb (bevacizumab)	Chinot et al. (144), Gilbert et al. (137)	2014	Phase III trial, clinical
VEGF receptor	VEGFR2	Small molecule, TK inhibitor (axitinib)	Duerinck et al. (145)	2016	Randomized, open-label, Phase II, clinical
Pericytes	PDGF	Radioimmunotherapeutic	Behling et al. (146)	2016	Preclinical target validation
Glia limitans	AQP5	siRNA	Yang et al. (147)	2017	Preclinical target validation
Stromal cells					
Microglia	CXCR4	Peptide, ligand-based antagonist	Mercurio et al. (148)	2016	Preclinical PoC
Macrophages	CSF1-R	Small molecule (PLX3397)	Butowski et al. (54)	2016	Phase II trial, clinical
Lymphocytes	PD1	mAb (nivolumab)	Blumenthal (149)	2017	Clinical cohort study
	IL13aR	CAR T-cell	Brown et al. (150, 151)	2017	Phase I + case report, clinical
ECM					
Tenascin and neuropilin 1		Peptide	Kang et al. (152)	2016	Preclinical xenograft model
Hyaluronic acid (HA)	CD44	HA-conjugated liposome nanoparticle	ayward et al. (153)	2016	Preclinical target validation
Fibronectin	neuropilin 1	mAb	Chen et al. (154)	2014	Preclinical target validation
Chondroitin		Humanized bacterial enzyme (chondroitinase ABC)	Jaime-Ramirez et al. (155)	2017	Preclinical xenograft model

Table continued on following page

TABLE 1
Selected Overview of Components of the Glioblastoma Tumor Microenvironment Targeted by Different Types of Compounds in Varying Phases of Preclinical and Clinical Development (Continued)

TME Component	Target	Type of Compound	Authors and Reference	Year	Phase of Development in GB
Soluble factors					
TGFβ		Oligonucleotide (Trabedersen)	Bogdahn et al. (82)	2011	Open-label, randomized phase I/II, clinical
Galectin 1		siRNA formulation	Van Woensel et al. (52)	2017	Preclinical rodent model
CCL2/MCP-1		Minocycline, telmisartan and zoledronic acid (drug repurposing)	Salacz et al. (156)	2016	Theoretical concept
Osteopontin		shRNA	Lamour et al. (157)	2015	Preclinical xenograft model

CAR, chimeric antigen receptor; ECM, extracellular matrix; mAb, monoclonal antibody; PoC, proof-of-concept; shRNA, short hairpin RNA; siRNA, small interference RNA; TME, tumor microenvironment.

Therapeutic Targeting of the Glioblastoma Microenvironment Components

TARGETING THE VASCULATURE

Due to the substantial inter- and intratumor heterogeneity of GBM cells, an attractive and potentially more effective tactic to overcome the plasticity that is associated with therapeutic GBM resistance may be to target the TME, specifically nonneoplastic components or the molecules they release to support tumor cell growth (Table 1). The first promising TME treatment strategy has been based on abrogating tumor vessel growth by blocking VEGF/VEGFR signaling in GBM. VEGF inhibition with bevacizumab, a humanized monoclonal antibody directed against VEGF-A, resulted in improvements in radiographic response, progression-free survival (PFS), and quality of life of GBM patients which subsequently became the third drug approved by the United States Food and Drug Administration (FDA) for use in recurrent GBM in 2009 (134).

Bevacizumab reduces vasogenic brain edema, and enhances vessel perfusion and subsequent oxygenation concomitant with a decrease in immune suppression which creates conditions for better drug delivery and efficacy (135). Nevertheless, anti-VEGF therapy has benefitted only a subset of GBM patients with transitory improvements in PFS but without improving OS. Interestingly, recent trials revealed that the effects of anti-VEGF therapy maybe dependent on the GBM subtype and thus genetic backbone of these tumors. Two randomized placebo-controlled Phase III trials in newly diagnosed GBM AVAglio (136) and RTOG-0825 (137) reported prolonged PFS, but not OS, with the addition of bevacizumab to radiotherapy plus TMZ. A multivariable analysis, however, revealed that bevacizumab conferred a significant OS advantage versus placebo for patients with proneural isocitrate dehydrogenase 1 (IDH1) wild-type tumors (138). These results, together with the observation that patients who experience enhanced tumor blood perfusion with bevacizumab have a longer survival benefit than those without vascular changes, suggest that subtype stratification of GBM patients with early imaging perfusion markers could help to stratify patients who will benefit the most from bevacizumab (135).

In order to understand the transient improvements of this therapy, it is important to note the inability to finely tune anti-VEGF/VEGFR therapy to create persistent normalization without further vessel pruning. This in turn results in enhanced hypoxic areas and hypoxia-dependent resistance mechanisms which lead to GBM relapse (139). Hypoxia promotes EMT and stem-like properties of tumor cells, upregulates pro-angiogenic and invasive factors, and drives the infiltration and polarization of angiogenic and immune-suppressive myeloid cells (reviewed in (140, 141)).

Indeed, radiographic and tissue studies from a subset of patients with recurrent GBM who were treated with bevacizumab or the angiokinase inhibitor cediranib support the results of enhanced tumor invasiveness and immune cell infiltration of TAMs and other CD11b+ myeloid cells observed in GBM mouse model systems (135, 142). Infiltrating innate immune cells including macrophages and neutrophils, have been shown to facilitate resistance to antiangiogenic therapy in various tumor types by rendering tumors nonresponsive to VEGF blockade (139).

TARGETING IMMUNE CELLS

The observation that 30–40% of the cells in gliomas consist of microglia or macrophages has raised the question whether targeting these innate immune cells would provide better efficacy and potentially be useful in combination with other therapies. Indeed, inhibition of the CSF-1 receptor that targets macrophages and microglia, resulted in increased survival and tumor shrinkage in a proneural murine GBM model (53). Intriguingly, the beneficial effects were caused by reeducation of TAMs, rather than their deletion. In contrast to the promising effects in this preclinical GBM model, a recent Phase 2 study of the CSF1-receptor inhibitor PLX3397 in patients with recurrent GBM tissue did not identify any significant improvements, not even in PFS (54). Whether the differing results may be a reflection of GBM subtype-specific responses to blocking CSF1R + myeloid cells,—as observed in recent anti-angiogenic trials—, or a matter of the animal model, remains to be determined. At least, further support for the impact of macrophages and microglia in glioma stems from a recent study in which naïve human macrophages and microglial cells alleviated sphere-forming capacity of glioma-patient-derived stem cells by inducing cell cycle arrest and differentiation while glioma-associated myeloid cells were unable to do so (143). Amphotericin B, a common anti-fungal medication, was able to reprogram myeloid cells and induce an immune-stimulating phenotype that sufficed to impede growth of GSCs *in vitro* and tumor growth *in vivo* (143). Using a different approach with similar effects, therapeutic galectin 1 knockdown in glioma by intranasal delivery of siGal1 RNA enhanced an immunostimulatory environment by reducing Tregs and MDSC and enhancing Th1 properties of macrophages and CTL infiltration (52). Targeting immune cells as part of the TME represents only one approach of all that have been identified in the past and present (144–157) (Table 1)

The studies summarized above highlight some new developments to target signaling cues of host cell constituents in GBM. They also underscore the importance of therapies that promote an immune-stimulatory milieu to enhance the infiltration of cytotoxic T cells into glioma. As some of the drugs targeting those pathways have already been approved for other diseases, this approach may yield an attractive and more effective strategy in combination with standard chemotherapy to sensitize as well as re-sensitize GBM.

Conclusion

Table 1 presents an overview of several approaches to target the GBM TME in their different preclinical or clinical stages of development. Some of the approaches are quite recent and still reside in a phase of early exploratory findings or proof-of-concept in cell cultures or well-defined animal models. Other approaches transcended this stage and have shown preclinical evidence for useful exploitation in upcoming early phase clinical trials. A few substances targeting elements of the microenvironment already passed clinical testing even in randomized controlled trials which up to date have not been able to deliver clinical proof of efficacy in actual GBM treatment strategies. According to the actual state of science and knowledge, it can be anticipated that most, if not all, of these approaches will only

show their full, durable potential if they are used in a rational combination with more conventional surgical, radiotherapeutic, or cytotoxic (chemo-)therapies, especially those that are able to mount an immunogenic cell death in an immune-receptive environment.

Acknowledgment: We would like to thank Rindert Missiaen for creating Figure 1 in this text. This work has been supported by the funding of NIH/NCI R01CA188404-03 granted to Gabriele Bergers.

Conflict of interest: Steven De Vleeschouwer is co-patent holder of a transnasal siGal-1 formulation (International Patent Classification: A61K9/51 (2006.01)).

Copyright and permissions statement: To the best of our knowledge, the materials included in this chapter do not violate copyright laws. All original sources have been appropriately acknowledged and/or referenced. Where relevant, appropriate permissions have been obtained from the original copyright holder(s).

References

1. Vogelstein B, Papadopoulos N, Velculescu VE, Zhou S, Diaz LA, Kinzler KW. Cancer genome landscapes. *Science*. 2013;339(6127):1546–58. <http://dx.doi.org/10.1126/science.1235122>
2. Yoshihara K, Wang Q, Torres-Garcia W, Zheng S, Vegesna R, Kim H, et al. The landscape and therapeutic relevance of cancer-associated transcript fusions. *Oncogene*. 2015;34(37):4845–54. <http://dx.doi.org/10.1038/onc.2014.406>
3. Lawrence MS, Stojanov P, Polak P, Kryukov GV, Cibulskis K, Sivachenko A, et al. Mutational heterogeneity in cancer and the search for new cancer-associated genes. *Nature*. 2013;499(7457):214–18. <http://dx.doi.org/10.1038/nature12213>
4. Snyder A, Makarov V, Merghoub T, Yuan J, Zaretsky JM, Desrichard A, et al. Genetic basis for clinical response to CTLA-4 blockade in melanoma. *N Engl J Med*. 2014;371(23):2189–99. <http://dx.doi.org/10.1056/NEJMoa1406498>
5. Eason K, Sadanandam A. Molecular or metabolic reprogramming: What triggers tumor subtypes? *Cancer Res*. 2016;76(18):5195–200. <http://dx.doi.org/10.1158/0008-5472.CAN-16-0141>
6. Massagué J, Obenauf AC. Metastatic colonization by circulating tumour cells. *Nature*. 2016;529(7586):298–306. <http://dx.doi.org/10.1038/nature17038>
7. Dauer P, Nomura A, Saluja A, Banerjee S. Microenvironment in determining chemo-resistance in pancreatic cancer: Neighborhood matters. *Pancreatology*. 2017;17(1):7–12. <http://dx.doi.org/10.1016/j.pan.2016.12.010>
8. Pitt JM, Marabelle A, Eggermont A, Soria JC, Kroemer G, Zitvogel L. Targeting the tumor microenvironment: Removing obstruction to anticancer immune responses and immunotherapy. *Ann Oncol*. 2016;27(8):1482–92. <http://dx.doi.org/10.1093/annonc/mdw168>
9. Louis DN, Perry A, Reifenberger G, von Deimling A, Figarella-Branger D, Cavenee WK, et al. The 2016 World Health Organization classification of tumors of the central nervous system: A summary. *Acta Neuropathol*. 2016;131(6):803–20. <http://dx.doi.org/10.1007/s00401-016-1545-1>
10. Vescovi AL, Galli R, Reynolds BA. Brain tumour stem cells. *Nat Rev Cancer*. 2006;6(6):425–36. <http://dx.doi.org/10.1038/nrc1889>
11. Verhaak RG, Hoadley KA, Purdom E, Wang V, Qi Y, Wilkerson MD, et al. Integrated genomic analysis identifies clinically relevant subtypes of glioblastoma characterized by abnormalities in PDGFRA, IDH1, EGFR, and NF1. *Cancer Cell*. 2010;17(1):98–110. <http://dx.doi.org/10.1016/j.ccr.2009.12.020>

12. Sturm D, Witt H, Hovestadt V, Khuong-Quang DA, Jones DT, Konermann C, et al. Hotspot mutations in H3F3A and IDH1 define distinct epigenetic and biological subgroups of glioblastoma. *Cancer Cell*. 2012;22(4):425–37. <http://dx.doi.org/10.1016/j.ccr.2012.08.024>
13. Sottoriva A, Spiteri I, Piccirillo SG, Touloumis A, Collins VP, Marioni JC, et al. Intratumor heterogeneity in human glioblastoma reflects cancer evolutionary dynamics. *Proc Natl Acad Sci USA*. 2013; 110(10):4009–14. <http://dx.doi.org/10.1073/pnas.1219747110>
14. Yachida S, Jones S, Bozic I, Antal T, Leary R, Fu B, et al. Distant metastasis occurs late during the genetic evolution of pancreatic cancer. *Nature*. 2010;467(7319):1114–17. <http://dx.doi.org/10.1038/nature09515>
15. Johnson BE, Mazar T, Hong C, Barnes M, Aihara K, McLean CY, et al. Mutational analysis reveals the origin and therapy-driven evolution of recurrent glioma. *Science*. 2014;343(6167):189–93. <http://dx.doi.org/10.1126/science.1239947>
16. Weiss T, Weller M, Roth P. Immunological effects of chemotherapy and radiotherapy against brain tumors. *Expert Rev Anticancer Ther*. 2016;16(10):1087–94. <http://dx.doi.org/10.1080/14737140.2016.1229600>
17. Ostrom QT, Bauchet L, Davis FG, Deltour I, Fisher JL, Langer CE, et al. The epidemiology of glioma in adults: A “state of the science” review. *Neuro Oncol*. 2014;16(7):896–913. <http://dx.doi.org/10.1093/neuonc/nou087>
18. Stupp R, Hegi ME, Mason WP, van den Bent MJ, Taphoorn MJ, Janzer RC, et al. Effects of radiotherapy with concomitant and adjuvant temozolomide versus radiotherapy alone on survival in glioblastoma in a randomised phase III study: 5-year analysis of the EORTC-NCIC trial. *Lancet Oncol*. 2009;10:459–66.
19. Burnet NG, Jefferies SJ, Benson RJ, Hunt DP, Treasure FP. Years of life lost (YLL) from cancer is an important measure of population burden—And should be considered when allocating research funds. *Br J Cancer*. 2005;92(2):241–5. <http://dx.doi.org/10.1038/sj.bjc.6602321>
20. Rouse C, Gittleman H, Ostrom QT, Kruchko C, Barnholtz-Sloan JS. Years of potential life lost for brain and CNS tumors relative to other cancers in adults in the United States, 2010. *Neuro Oncol*. 2016;18(1):70–7. <http://dx.doi.org/10.1093/neuonc/nov249>
21. Lun M, Lok E, Gautam S, Wu E, Wong ET. The natural history of extracranial metastasis from glioblastoma multiforme. *J Neurooncol*. 2011;105(2):261–73. <http://dx.doi.org/10.1007/s11060-011-0575-8>
22. Müller C, Holtschmidt J, Auer M, Heitzer E, Lamszus K, Schulte A, et al. Hematogenous dissemination of glioblastoma multiforme. *Sci Transl Med*. 2014;6(247):247ra101. <http://dx.doi.org/10.1126/scitranslmed.3009095>
23. Wernicke AG, Smith AW, Taube S, Mehta MP. Glioblastoma: Radiation treatment margins, how small is large enough? *Pract Radiat Oncol*. 2016;6(5):298–305. <http://dx.doi.org/10.1016/j.prro.2015.12.002>
24. Volovitz I, Marmor Y, Azulay M, Machlenkin A, Goldberger O, Mor F, et al. Split immunity: Immune inhibition of rat gliomas by subcutaneous exposure to unmodified live tumor cells. *J Immunol*. 2011;187(10):5452–62. <http://dx.doi.org/10.4049/jimmunol.1003946>
25. Guillamo JS, Lisovski F, Christov C, Le Guérinel C, Defer GL, Peschanski M, et al. Migration pathways of human glioblastoma cells xenografted into the immunosuppressed rat brain. *J Neurooncol*. 2001;52(3):205–15. <http://dx.doi.org/10.1023/A:1010620420241>
26. Gilbertson RJ, Rich JN. Making a tumour's bed: Glioblastoma stem cells and the vascular niche. *Nat Rev Cancer*. 2007;7(10):733–6. <http://dx.doi.org/10.1038/nrc2246>
27. Hambardzumyan D, Bergers G. Glioblastoma: Defining tumor niches. *Trends Cancer*. 2015;1(4): 252–65. <http://dx.doi.org/10.1016/j.trecan.2015.10.009>
28. Wesseling P, Ruiter DJ, Burger PC. Angiogenesis in brain tumors; pathobiological and clinical aspects. *J Neurooncol*. 1997;32(3):253–65. <http://dx.doi.org/10.1023/A:1005746320099>
29. Daneman R, Prat A. The blood-brain barrier. *Cold Spring Harb Perspect Biol*. 2015;7(1):a020412. <http://dx.doi.org/10.1101/cshperspect.a020412>
30. Zlokovic BV. Neurovascular pathways to neurodegeneration in Alzheimer's disease and other disorders. *Nat Rev Neurosci*. 2011;12(12):723–38. <http://dx.doi.org/10.1038/nrn3114>
31. Du R, Lu KV, Petritsch C, Liu P, Ganss R, Passegué E, et al. HIF1 α induces the recruitment of bone marrow-derived vascular modulatory cells to regulate tumor angiogenesis and invasion. *Cancer Cell*. 2008;13(3):206–20. <http://dx.doi.org/10.1016/j.ccr.2008.01.034>

32. Gabriele B. Bone marrow-derived cells in GBM neovascularization. In: Van Meir EG, editor. *CNS Cancer* (Part 3). Dordrecht: Humana Press, part of Springer Science+Business Media, LLC; 2009. p. 749–73.
33. Wang R, Chadalavada K, Wilshire J, Kowalik U, Hovinga KE, Geber A, et al. Glioblastoma stem-like cells give rise to tumour endothelium. *Nature*. 2010;468(7325):829–33. <http://dx.doi.org/10.1038/nature09624>
34. Soda Y, Marumoto T, Friedmann-Morvinski D, Soda M, Liu F, Michiue H, et al. Transdifferentiation of glioblastoma cells into vascular endothelial cells. *Proc Natl Acad Sci U S A*. 2011;108(11):4274–80. <http://dx.doi.org/10.1073/pnas.1016030108>
35. Ricci-Vitiani L, Pallini R, Biffoni M, Todaro M, Iavernici G, Cenci T, et al. Tumour vascularization via endothelial differentiation of glioblastoma stem-like cells. *Nature*. 2010;468(7325):824–8. <http://dx.doi.org/10.1038/nature09557>
36. Cheng L, Huang Z, Zhou W, Wu Q, Donnola S, Liu JK, et al. Glioblastoma stem cells generate vascular pericytes to support vessel function and tumor growth. *Cell*. 2013;153(1):139–52. <http://dx.doi.org/10.1016/j.cell.2013.02.021>
37. Motz GT, Coukos G. Deciphering and reversing tumor immune suppression. *Immunity*. 2013;39(1):61–73. <http://dx.doi.org/10.1016/j.immuni.2013.07.005>
38. Charles NA, Holland EC, Gilbertson R, Glass R, Kettenmann H. The brain tumor microenvironment. *Glia*. 2012;60(3):502–14. <http://dx.doi.org/10.1002/glia.12164>
39. Watkins S, Robel S, Kimbrough IF, Robert SM, Ellis-Davies G, Sontheimer H. Disruption of astrocyte-vascular coupling and the blood-brain barrier by invading glioma cells. *Nat Commun*. 2014;5:4196. <http://dx.doi.org/10.1038/ncomms5196>
40. Edwards LA, Woolard K, Son MJ, Li A, Lee J, Ene C, et al. Effect of brain- and tumor-derived connective tissue growth factor on glioma invasion. *J Natl Cancer Inst*. 2011;103(15):1162–78. <http://dx.doi.org/10.1093/jnci/djr224>
41. Seyfried TN, Flores R, Poff AM, D'Agostino DP, Mukherjee P. Metabolic therapy: A new paradigm for managing malignant brain cancer. *Cancer Lett*. 2015;356(2 Pt A):289–300. <http://dx.doi.org/10.1016/j.canlet.2014.07.015>
42. Martinez-Outschoorn UE, Peiris-Pagés M, Pestell RG, Sotgia F, Lisanti MP. Cancer metabolism: A therapeutic perspective. *Nat Rev Clin Oncol*. 2017;14(2):113. <http://dx.doi.org/10.1038/nrclinonc.2017.1>
43. Liu Y, Carlsson R, Ambjørn M, Hasan M, Badn W, Darabi A, et al. PD-L1 expression by neurons nearby tumors indicates better prognosis in glioblastoma patients. *J Neurosci*. 2013;33(35):14231–45. <http://dx.doi.org/10.1523/JNEUROSCI.5812-12.2013>
44. Venkatesh HS, Johung TB, Caretti V, Noll A, Tang Y, Nagaraja S, et al. Neuronal activity promotes glioma growth through neuropilin-3 secretion. *Cell*. 2015;161(4):803–16. <http://dx.doi.org/10.1016/j.cell.2015.04.012>
45. Glass R, Synowitz M. CNS macrophages and peripheral myeloid cells in brain tumours. *Acta Neuropathol*. 2014;128(3):347–62. <http://dx.doi.org/10.1007/s00401-014-1274-2>
46. Sasaki A. Microglia and brain macrophages: An update. *Neuropathology*. 2016. Epub ahead of print. <http://dx.doi.org/10.1111/neup.12354>
47. Carare RO, Hawkes CA, Weller RO. Afferent and efferent immunological pathways of the brain. *Anatomy, function and failure*. *Brain Behav Immun*. 2014;36:9–14. <http://dx.doi.org/10.1016/j.bbi.2013.10.012>
48. Louveau A, Smirnov I, Keyes TJ, Eccles JD, Rouhani SJ, Peske JD, et al. Structural and functional features of central nervous system lymphatic vessels. *Nature*. 2015;523(7560):337–41. <http://dx.doi.org/10.1038/nature14432>
49. Louveau A, Harris TH, Kipnis J. Revisiting the mechanisms of CNS immune privilege. *Trends Immunol*. 2015;36(10):569–77. <http://dx.doi.org/10.1016/j.it.2015.08.006>
50. Gierzyng A, Psczolkowska D, Walentyowicz KA, Rajan WD, Kaminska B. Immune microenvironment of gliomas. *Lab Invest*. 2017;97(5):498–518. <http://dx.doi.org/10.1038/labinvest.2017.19>
51. Gabrusiewicz K, Rodriguez B, Wei J, Hashimoto Y, Healy LM, Maiti SN, et al. Glioblastoma-infiltrated innate immune cells resemble M0 macrophage phenotype. *JCI Insight*. 2016;1(2):1–19. <http://dx.doi.org/10.1172/jci.insight.85841>
52. Van Woensel M, Mathivet T, Wauthoz N, Rosière R, Garg AD, Agostinis P, et al. Sensitization of glioblastoma tumor micro-environment to chemo- and immunotherapy by Galectin-1 intranasal knock-down strategy. *Sci Rep*. 2017;7(1):1217. <http://dx.doi.org/10.1038/s41598-017-01279-1>

53. Pyonteck SM, Akkari L, Schuhmacher AJ, Bowman RL, Sevenich L, Quail DF, et al. CSF-1R inhibition alters macrophage polarization and blocks glioma progression. *Nat Med.* 2013;19(10):1264–72. <http://dx.doi.org/10.1038/nm.3337>
54. Butowski N, Colman H, De Groot JF, Omuro AM, Nayak L, Wen PY, et al. Orally administered colony stimulating factor 1 receptor inhibitor PLX3397 in recurrent glioblastoma: An Ivy Foundation Early Phase Clinical Trials Consortium phase II study. *Neuro Oncol.* 2016;18(4):557–64. <http://dx.doi.org/10.1093/neuonc/nov245>
55. Giering A, Kaminska B. Myeloid-derived suppressor cells in gliomas. *Contemp Oncol (Pozn).* 2016;20(5):345–51. <http://dx.doi.org/10.5114/wo.2016.64592>
56. Chae M, Peterson TE, Balgeman A, Chen S, Zhang L, Renner DN, et al. Increasing glioma-associated monocytes leads to increased intratumoral and systemic myeloid-derived suppressor cells in a murine model. *Neuro Oncol.* 2015;17(7):978–91. <http://dx.doi.org/10.1093/neuonc/nou343>
57. Dunn GP, Dunn IF, Curry WT. Focus on TILs: Prognostic significance of tumor infiltrating lymphocytes in human glioma. *Cancer Immun.* 2007;7:12.
58. Wainwright DA, Dey M, Chang A, Lesniak MS. Targeting tregs in Malignant brain cancer: Overcoming IDO. *Front Immunol.* 2013;4:116. <http://dx.doi.org/10.3389/fimmu.2013.00116>
59. Li Z, Liu X, Guo R, Wang P. CD4(+)Foxp3(-) type 1 regulatory T cells in glioblastoma multiforme suppress T cell responses through multiple pathways and are regulated by tumor-associated macrophages. *Int J Biochem Cell Biol.* 2016;81(Pt A):1–9.
60. Chang AL, Miska J, Wainwright DA, Dey M, Rivetta CV, Yu D, et al. CCL2 Produced by the glioma microenvironment is essential for the recruitment of regulatory T cells and myeloid-derived suppressor cells. *Cancer Res.* 2016;76(19):5671–82. <http://dx.doi.org/10.1158/0008-5472.CAN-16-0144>
61. Barnes JM, Przybyla L, Weaver VM. Tissue mechanics regulate brain development, homeostasis and disease. *J Cell Sci.* 2017;130(1):71–82. <http://dx.doi.org/10.1242/jcs.191742>
62. Ruoslahti E. Brain extracellular matrix. *Glycobiology.* 1996;6(5):489–92. <http://dx.doi.org/10.1093/glycob/6.5.489>
63. Zimmermann DR, Dours-Zimmermann MT. Extracellular matrix of the central nervous system: From neglect to challenge. *Histochem Cell Biol.* 2008;130(4):635–53. <http://dx.doi.org/10.1007/s00418-008-0485-9>
64. Soleman S, Filipov MA, Dityatev A, Fawcett JW. Targeting the neural extracellular matrix in neurological disorders. *Neuroscience.* 2013;253:194–213. <http://dx.doi.org/10.1016/j.neuroscience.2013.08.050>
65. Mouw JK, Ou G, Weaver VM. Extracellular matrix assembly: A multiscale deconstruction. *Nat Rev Mol Cell Biol.* 2014;15(12):771–85. <http://dx.doi.org/10.1038/nrm3902>
66. Kwok JC, Dick G, Wang D, Fawcett JW. Extracellular matrix and perineuronal nets in CNS repair. *Dev Neurobiol.* 2011;71(11):1073–89. <http://dx.doi.org/10.1002/dneu.20974>
67. Carulli D, Rhodes KE, Brown DJ, Bonnert TP, Pollack SJ, Oliver K, et al. Composition of perineuronal nets in the adult rat cerebellum and the cellular origin of their components. *J Comp Neurol.* 2006;494(4):559–77. <http://dx.doi.org/10.1002/cne.20822>
68. Spicer AP, Joo A, Bowling RA. A hyaluronan binding link protein gene family whose members are physically linked adjacent to chondroitin sulfate proteoglycan core protein genes: The missing links. *J Biol Chem.* 2003;278(23):21083–91. <http://dx.doi.org/10.1074/jbc.M213100200>
69. Miroshnikova YA, Mouw JK, Barnes JM, Pickup MW, Lakins JN, Kim Y, et al. Tissue mechanics promote IDH1-dependent HIF1 α -tenascin C feedback to regulate glioblastoma aggression. *Nat Cell Biol.* 2016;18(12):1336–45. <http://dx.doi.org/10.1038/ncb3429>
70. Netti PA, Berk DA, Swartz MA, Grodzinsky AJ, Jain RK. Role of extracellular matrix assembly in interstitial transport in solid tumors. *Cancer Res.* 2000;60(9):2497–503.
71. Pickup MW, Mouw JK, Weaver VM. The extracellular matrix modulates the hallmarks of cancer. *EMBO Rep.* 2014;15(12):1243–53. <http://dx.doi.org/10.15252/embr.201439246>
72. Padera TP, Stoll BR, Tooredman JB, Capen D, di Tomaso E, Jain RK. Pathology: Cancer cells compress intratumour vessels. *Nature.* 2004;427(6976):695. <http://dx.doi.org/10.1038/427695a>
73. Thakur R, Mishra DP. Matrix reloaded: CCN, tenascin and SIBLING group of matricellular proteins in orchestrating cancer hallmark capabilities. *Pharmacol Ther.* 2016;168:61–74. <http://dx.doi.org/10.1016/j.pharmthera.2016.09.002>

74. Rabinovich GA, Conejo-García JR. Shaping the immune landscape in cancer by galectin-driven regulatory pathways. *J Mol Biol.* 2016;428(16):3266–81. <http://dx.doi.org/10.1016/j.jmb.2016.03.021>
75. Payne LS, Huang PH. The pathobiology of collagens in glioma. *Mol Cancer Res.* 2013;11(10):1129–40. <http://dx.doi.org/10.1158/1541-7786.MCR-13-0236>
76. Bernstein JJ, Woodard CA. Glioblastoma cells do not intravasate into blood vessels. *Neurosurgery.* 1995;36(1):124–32; discussion 32. <http://dx.doi.org/10.1227/00006123-199501000-00016>
77. Reardon DA, Zalutsky MR, Bigner DD. Antitenascin-C monoclonal antibody radioimmunotherapy for malignant glioma patients. *Expert Rev Anticancer Ther.* 2007;7(5):675–87. <http://dx.doi.org/10.1586/14737140.7.5.675>
78. Liberti MV, Locasale JW. The warburg effect: How does it denefit cancer cells? *Trends Biochem Sci.* 2016;41(3):211–18. <http://dx.doi.org/10.1016/j.tibs.2015.12.001>
79. Verschuere T, Toelen J, Maes W, Poirier F, Boon L, Tousseyn T, et al. Glioma-derived galectin-1 regulates innate and adaptive antitumor immunity. *Int J Cancer.* 2014;134(4):873–84. <http://dx.doi.org/10.1002/ijc.28426>
80. Fontana A, Bodmer S, Frei K, Malipiero U, Siepl C. Expression of TGF-beta 2 in human glioblastoma: A role in resistance to immune rejection? *Ciba Found Symp.* 1991;157:232–8; discussion 8–41.
81. Dix AR, Brooks WH, Roszman TL, Morford LA. Immune defects observed in patients with primary malignant brain tumors. *J Neuroimmunol.* 1999;100(1–2):216–32. [http://dx.doi.org/10.1016/S0165-5728\(99\)00203-9](http://dx.doi.org/10.1016/S0165-5728(99)00203-9)
82. Bogdahn U, Hau P, Stockhammer G, Venkataramana NK, Mahapatra AK, Suri A, et al. Targeted therapy for high-grade glioma with the TGF-β2 inhibitor trabedersen: Results of a randomized and controlled phase IIb study. *Neuro Oncol.* 2011;13(1):132–42. <http://dx.doi.org/10.1093/neuonc/nq142>
83. De Vleeschouwer S, Spencer Lopes I, Ceuppens JL, Van Gool SW. Persistent IL-10 production is required for glioma growth suppressive activity by Th1-directed effector cells after stimulation with tumor lysate-loaded dendritic cells. *J Neurooncol.* 2007;84(2):131–40. <http://dx.doi.org/10.1007/s11060-007-9362-y>
84. Verschuere T, De Vleeschouwer S, Lefranc F, Kiss R, Van Gool SW. Galectin-1 and immunotherapy for brain cancer. *Expert Rev Neurother.* 2011;11(4):533–43. <http://dx.doi.org/10.1586/ern.11.40>
85. van Woensel M, Wauthoz N, Rosière R, Amighi K, Mathieu V, Lefranc F, et al. Formulations for intranasal delivery of pharmacological agents to combat brain disease: A new opportunity to tackle GBM? *Cancers (Basel).* 2013;5(3):1020–48. <http://dx.doi.org/10.3390/cancers5031020>
86. Levi G, Teichberg VI. Isolation and physicochemical characterization of electrolectin, a beta-D-galactoside binding lectin from the electric organ of *Electrophorus electricus*. *J Biol Chem.* 1981;256(11):5735–40.
87. Camby I, Le Mercier M, Lefranc F, Kiss R. Galectin-1: A small protein with major functions. *Glycobiology.* 2006;16(11):137R–57R. <http://dx.doi.org/10.1093/glycob/cwl025>
88. Camby I, Belot N, Rorive S, Lefranc F, Maurage CA, Lahm H, et al. Galectins are differentially expressed in supratentorial pilocytic astrocytomas, astrocytomas, anaplastic astrocytomas and glioblastomas, and significantly modulate tumor astrocyte migration. *Brain Pathol.* 2001;11(1):12–26. <http://dx.doi.org/10.1111/j.1750-3639.2001.tb00377.x>
89. Le Mercier M, Fortin S, Mathieu V, Kiss R, Lefranc F. Galectins and gliomas. *Brain Pathol.* 2010;20(1):17–27. <http://dx.doi.org/10.1111/j.1750-3639.2009.00270.x>
90. Le Mercier M, Lefranc F, Mijatovic T, Debeir O, Haibe-Kains B, Bontempi G, et al. Evidence of galectin-1 involvement in glioma chemoresistance. *Toxicol Appl Pharmacol.* 2008;229(2):172–83. <http://dx.doi.org/10.1016/j.taap.2008.01.009>
91. Thijssen VL, Barkan B, Shoji H, Aries IM, Mathieu V, Deltour L, et al. Tumor cells secrete galectin-1 to enhance endothelial cell activity. *Cancer Res.* 2010;70(15):6216–24. <http://dx.doi.org/10.1158/0008-5472.CAN-09-4150>
92. Le Mercier M, Mathieu V, Haibe-Kains B, Bontempi G, Mijatovic T, Decaestecker C, et al. Knocking down galectin 1 in human hs683 glioblastoma cells impairs both angiogenesis and endoplasmic reticulum stress responses. *J Neuropathol Exp Neurol.* 2008;67(5):456–69. <http://dx.doi.org/10.1097/NEN.0b013e318170f892>

93. Toussaint LG, Nilson AE, Goble JM, Ballman KV, James CD, Lefranc F, et al. Galectin-1, a gene preferentially expressed at the tumor margin, promotes glioblastoma cell invasion. *Mol Cancer*. 2012;11:32. <http://dx.doi.org/10.1186/1476-4598-11-32>
94. Rorive S, Belot N, Decaestecker C, Lefranc F, Gordower L, Micic S, et al. Galectin-1 is highly expressed in human gliomas with relevance for modulation of invasion of tumor astrocytes into the brain parenchyma. *Glia*. 2001;33(3):241–55. [http://dx.doi.org/10.1002/1098-1136\(200103\)33:3%3C241::AID-GLIA1023%3E3.0.CO;2-1](http://dx.doi.org/10.1002/1098-1136(200103)33:3%3C241::AID-GLIA1023%3E3.0.CO;2-1)
95. Camby I, Belot N, Lefranc F, Sadeghi N, de Launoit Y, Kaltner H, et al. Galectin-1 modulates human glioblastoma cell migration into the brain through modifications to the actin cytoskeleton and levels of expression of small GTPases. *J Neuropathol Exp Neurol*. 2002;61(7):585–96. <http://dx.doi.org/10.1093/jnen/61.7.585>
96. Verschuere T, Van Woensel M, Fieuwis S, Lefranc F, Mathieu V, Kiss R, et al. Altered galectin-1 serum levels in patients diagnosed with high-grade glioma. *J Neurooncol*. 2013;115(1):9–17. <http://dx.doi.org/10.1007/s11060-013-1201-8>
97. Rubinstein N, Alvarez M, Zwirner NW, Toscano MA, Ilarregui JM, Bravo A, et al. Targeted inhibition of galectin-1 gene expression in tumor cells results in heightened T cell-mediated rejection; A potential mechanism of tumor-immune privilege. *Cancer Cell*. 2004;5(3):241–51. [http://dx.doi.org/10.1016/S1535-6108\(04\)00024-8](http://dx.doi.org/10.1016/S1535-6108(04)00024-8)
98. de Vries NA, Beijnen JH, Boogerd W, van Tellingen O. Blood-brain barrier and chemotherapeutic treatment of brain tumors. *Expert Rev Neurother*. 2006;6(8):1199–209. <http://dx.doi.org/10.1586/14737175.6.8.1199>
99. Upadhyay N, Waldman AD. Conventional MRI evaluation of gliomas. *Br J Radiol*. 2011;84 Spec No 2: S107–11. <http://dx.doi.org/10.1259/bjr/65711810>
100. Jain RK. Normalizing tumor microenvironment to treat cancer: Bench to bedside to biomarkers. *J Clin Oncol*. 2013;31(17):2205–18. <http://dx.doi.org/10.1200/JCO.2012.46.3653>
101. Gabay MP, Thakkar JP, Stachnik JM, Woelich SK, Villano JL. Intra-CSF administration of chemotherapy medications. *Cancer Chemother Pharmacol*. 2012;70(1):1–15. <http://dx.doi.org/10.1007/s00280-012-1893-z>
102. Ung TH, Malone H, Canoll P, Bruce JN. Convection-enhanced delivery for glioblastoma: Targeted delivery of antitumor therapeutics. *CNS Oncol*. 2015;4(4):225–34. <http://dx.doi.org/10.2217/cns.15.12>
103. Saucier-Sawyer JK, Seo YE, Gaudin A, Quijano E, Song E, Sawyer AJ, et al. Distribution of polymer nanoparticles by convection-enhanced delivery to brain tumors. *J Control Release*. 2016;232:103–12. <http://dx.doi.org/10.1016/j.jconrel.2016.04.006>
104. Shipley MT. Transport of molecules from nose to brain: Transneuronal anterograde and retrograde labeling in the rat olfactory system by wheat germ agglutinin-horseradish peroxidase applied to the nasal epithelium. *Brain Res Bull*. 1985;15(2):129–42. [http://dx.doi.org/10.1016/0361-9230\(85\)90129-7](http://dx.doi.org/10.1016/0361-9230(85)90129-7)
105. Thorne RG, Emory CR, Ala TA, Frey WH. Quantitative analysis of the olfactory pathway for drug delivery to the brain. *Brain Res*. 1995;692(1–2):278–82. [http://dx.doi.org/10.1016/0006-8993\(95\)00637-6](http://dx.doi.org/10.1016/0006-8993(95)00637-6)
106. Johnson NJ, Hanson LR, Frey WH. Trigeminal pathways deliver a low molecular weight drug from the nose to the brain and orofacial structures. *Mol Pharm*. 2010;7(3):884–93. <http://dx.doi.org/10.1021/mp100029t>
107. Illum L. Transport of drugs from the nasal cavity to the central nervous system. *Eur J Pharm Sci*. 2000;11(1):1–18. [http://dx.doi.org/10.1016/S0928-0987\(00\)00087-7](http://dx.doi.org/10.1016/S0928-0987(00)00087-7)
108. Dhuria SV, Hanson LR, Frey WH. Intranasal delivery to the central nervous system: Mechanisms and experimental considerations. *J Pharm Sci*. 2010;99(4):1654–73. <http://dx.doi.org/10.1002/jps.21924>
109. Lochhead JJ, Thorne RG. Intranasal delivery of biologics to the central nervous system. *Adv Drug Deliv Rev*. 2012;64(7):614–28. <http://dx.doi.org/10.1016/j.addr.2011.11.002>
110. Baker H, Spencer RF. Transneuronal transport of peroxidase-conjugated wheat germ agglutinin (WGA-HRP) from the olfactory epithelium to the brain of the adult rat. *Exp Brain Res*. 1986;63(3):461–73. <http://dx.doi.org/10.1007/BF00237470>

111. Bobo RH, Laske DW, Akbasak A, Morrison PF, Dedrick RL, Oldfield EH. Convection-enhanced delivery of macromolecules in the brain. *Proc Natl Acad Sci U S A*. 1994;91(6):2076–80. <http://dx.doi.org/10.1073/pnas.91.6.2076>
112. Groothuis DR. The blood-brain and blood-tumor barriers: A review of strategies for increasing drug delivery. *Neuro Oncol*. 2000;2(1):45–59. <http://dx.doi.org/10.1215/15228517-2-1-45>
113. Mistry A, Stolnik S, Illum L. Nanoparticles for direct nose-to-brain delivery of drugs. *Int J Pharm*. 2009;379(1):146–57. <http://dx.doi.org/10.1016/j.ijpharm.2009.06.019>
114. Shingaki T, Inoue D, Furubayashi T, Sakane T, Katsumi H, Yamamoto A, et al. Transnasal delivery of methotrexate to brain tumors in rats: A new strategy for brain tumor chemotherapy. *Mol Pharm*. 2010;7(5):1561–8. <http://dx.doi.org/10.1021/mp900275s>
115. Sakane T, Yamashita S, Yata N, Sezaki H. Transnasal delivery of 5-fluorouracil to the brain in the rat. *J Drug Target*. 1999;7(3):233–40. <http://dx.doi.org/10.3109/10611869909085506>
116. Wang D, Gao Y, Yun L. Study on brain targeting of raltitrexed following intranasal administration in rats. *Cancer Chemother Pharmacol*. 2006;57(1):97–104. <http://dx.doi.org/10.1007/s00280-005-0018-3>
117. Miller MC, Klyosov A, Mayo KH. The alpha-galactomannan Davanat binds galectin-1 at a site different from the conventional galectin carbohydrate binding domain. *Glycobiology*. 2009;19(9):1034–45. <http://dx.doi.org/10.1093/glycob/cwp084>
118. Salomonsson E, Thijssen VL, Griffioen AW, Nilsson UJ, Leffler H. The anti-angiogenic peptide anginex greatly enhances galectin-1 binding affinity for glycoproteins. *J Biol Chem*. 2011;286(16):13801–4. <http://dx.doi.org/10.1074/jbc.C111.229096>
119. Agrawal N, Dasaradhi PV, Mohammed A, Malhotra P, Bhatnagar RK, Mukherjee SK. RNA interference: Biology, mechanism, and applications. *Microbiol Mol Biol Rev*. 2003;67(4):657–85. <http://dx.doi.org/10.1128/MMBR.67.4.657-685.2003>
120. Hashizume R, Ozawa T, Gryaznov SM, Bollen AW, Lamborn KR, Frey WH, et al. New therapeutic approach for brain tumors: Intranasal delivery of telomerase inhibitor GRN163. *Neuro Oncol*. 2008;10(2):112–20. <http://dx.doi.org/10.1215/15228517-2007-052>
121. Perez AP, Mundiña-Weilenmann C, Romero EL, Morilla MJ. Increased brain radioactivity by intranasal P-labeled siRNA dendriplexes within in situ-forming mucoadhesive gels. *Int J Nanomedicine*. 2012;7:1373–85.
122. Kanazawa T, Akiyama F, Kakizaki S, Takashima Y, Seta Y. Delivery of siRNA to the brain using a combination of nose-to-brain delivery and cell-penetrating peptide-modified nano-micelles. *Biomaterials*. 2013;34(36):9220–6. <http://dx.doi.org/10.1016/j.biomaterials.2013.08.036>
123. Kanazawa T, Morisaki K, Suzuki S, Takashima Y. Prolongation of life in rats with malignant glioma by intranasal siRNA/drug codelivery to the brain with cell-penetrating peptide-modified micelles. *Mol Pharm*. 2014;11(5):1471–8. <http://dx.doi.org/10.1021/mp400644e>
124. Van Woensel M, Wauthoz N, Rosière R, Mathieu V, Kiss R, Lefranc F, et al. Development of siRNA-loaded chitosan nanoparticles targeting Galectin-1 for the treatment of glioblastoma multiforme via intranasal administration. *J Control Release*. 2016;227:71–81. <http://dx.doi.org/10.1016/j.jconrel.2016.02.032>
125. Goldbrunner RH, Wagner S, Roosen K, Tonn JC. Models for assessment of angiogenesis in gliomas. *J Neurooncol*. 2000;50(1–2):53–62. <http://dx.doi.org/10.1023/A:1006462504447>
126. Hardee ME, Marciscano AE, Medina-Ramirez CM, Zagzag D, Narayana A, Lonning SM, et al. Resistance of glioblastoma-initiating cells to radiation mediated by the tumor microenvironment can be abolished by inhibiting transforming growth factor- β . *Cancer Res*. 2012;72(16):4119–29. <http://dx.doi.org/10.1158/0008-5472.CAN-12-0546>
127. Gomez-Roman N, Stevenson K, Gilmour L, Hamilton G, Chalmers AJ. A novel 3D human glioblastoma cell culture system for modeling drug and radiation responses. *Neuro Oncol*. 2017;19(2):229–41.
128. Rape A, Ananthanarayanan B, Kumar S. Engineering strategies to mimic the glioblastoma microenvironment. *Adv Drug Deliv Rev*. 2014;79–80:172–83. <http://dx.doi.org/10.1016/j.addr.2014.08.012>
129. Stylli SS, Luwor RB, Ware TM, Tan F, Kaye AH. Mouse models of glioma. *J Clin Neurosci*. 2015;22(4):619–26. <http://dx.doi.org/10.1016/j.jocn.2014.10.013>
130. Lee HW, Lee K, Kim DG, Yang H, Nam DH. Facilitating tailored therapeutic strategies for glioblastoma through an orthotopic patient-derived xenograft platform. *Histol Histopathol*. 2016;31(3):269–83.

131. Garcia C, Dubois LG, Xavier AL, Geraldo LH, da Fonseca AC, Correia AH, et al. The orthotopic xenotransplant of human glioblastoma successfully recapitulates glioblastoma-microenvironment interactions in a non-immunosuppressed mouse model. *BMC Cancer*. 2014;14:923. <http://dx.doi.org/10.1186/1471-2407-14-923>
132. Maes W, Van Gool SW. Experimental immunotherapy for malignant glioma: Lessons from two decades of research in the GL261 model. *Cancer Immunol Immunother*. 2011;60(2):153–60. <http://dx.doi.org/10.1007/s00262-010-0946-6>
133. Morton JJ, Bird G, Refaeli Y, Jimeno A. Humanized mouse xenograft models: Narrowing the tumor-microenvironment gap. *Cancer Res*. 2016;76(21):6153–8. <http://dx.doi.org/10.1158/0008-5472.CAN-16-1260>
134. Cohen MH, Shen YL, Keegan P, Pazdur R. FDA drug approval summary: Bevacizumab (Avastin) as treatment of recurrent glioblastoma multiforme. *Oncologist*. 2009;14(11):1131–8. <http://dx.doi.org/10.1634/theoncologist.2009-0121>
135. Lu-Emerson C, Duda DG, Emblem KE, Taylor JW, Gerstner ER, Loeffler JS, et al. Lessons from anti-vascular endothelial growth factor and anti-vascular endothelial growth factor receptor trials in patients with glioblastoma. *J Clin Oncol*. 2015;33(10):1197–213. <http://dx.doi.org/10.1200/JCO.2014.55.9575>
136. LaViolette PS, Cohen AD, Prah MA, Rand SD, Connelly J, Malkin MG, et al. Vascular change measured with independent component analysis of dynamic susceptibility contrast MRI predicts bevacizumab response in high-grade glioma. *Neuro Oncol*. 2013;15(4):442–50. <http://dx.doi.org/10.1093/neuonc/nos323>
137. Gilbert MR, Dignam JJ, Armstrong TS, Wefel JS, Blumenthal DT, Vogelbaum MA, et al. A randomized trial of bevacizumab for newly diagnosed glioblastoma. *N Engl J Med*. 2014;370(8):699–708. <http://dx.doi.org/10.1056/NEJMoa1308573>
138. Sandmann T, Bourgon R, Garcia J, Li C, Cloughesy T, Chinot OL, et al. Patients with proneural glioblastoma may derive overall survival benefit from the addition of bevacizumab to first-line radiotherapy and temozolomide: Retrospective analysis of the AVAglio trial. *J Clin Oncol*. 2015;33(25):2735–44. <http://dx.doi.org/10.1200/JCO.2015.61.5005>
139. Rivera LB, Bergers G. Intertwined regulation of angiogenesis and immunity by myeloid cells. *Trends Immunol*. 2015;36(4):240–9. <http://dx.doi.org/10.1016/j.it.2015.02.005>
140. Lu KV, Bergers G. Mechanisms of evasive resistance to anti-VEGF therapy in glioblastoma. *CNS Oncol*. 2013;2(1):49–65. <http://dx.doi.org/10.2217/cns.12.36>
141. Bergers G, Hanahan D. Modes of resistance to anti-angiogenic therapy. *Nat Rev Cancer*. 2008;8(8):592–603. <http://dx.doi.org/10.1038/nrc2442>
142. Piao Y, Liang J, Holmes L, Zurita AJ, Henry V, Heymach JV, et al. Glioblastoma resistance to anti-VEGF therapy is associated with myeloid cell infiltration, stem cell accumulation, and a mesenchymal phenotype. *Neuro Oncol*. 2012;14(11):1379–92. <http://dx.doi.org/10.1093/neuonc/nos158>
143. Sarkar S, Döring A, Zemp FJ, Silva C, Lun X, Wang X, et al. Therapeutic activation of macrophages and microglia to suppress brain tumor-initiating cells. *Nat Neurosci*. 2014;17(1):46–55. <http://dx.doi.org/10.1038/nn.3597>
144. Chinot OL, Wick W, Mason W, Henriksson R, Saran F, Nishikawa R, et al. Bevacizumab plus radiotherapy-temozolomide for newly diagnosed glioblastoma. *N Engl J Med*. 2014;370(8):709–22. <http://dx.doi.org/10.1056/NEJMoa1308345>
145. Duerinck J, Du Four S, Vandervorst F, D'Haene N, Le Mercier M, Michotte A, et al. Randomized phase II study of axitinib versus physicians best alternative choice of therapy in patients with recurrent glioblastoma. *J Neurooncol*. 2016;128(1):147–55. <http://dx.doi.org/10.1007/s11060-016-2092-2>
146. Behling K, Maguire WF, Di Galleonardo V, Heeb LE, Hassan IF, Veach DR, et al. Remodeling the vascular microenvironment of glioblastoma with α -particles. *J Nucl Med*. 2016;57(11):1771–7. <http://dx.doi.org/10.2967/jnumed.116.173559>
147. Yang J, Zhang JN, Chen WL, Wang GS, Mao Q, Li SQ, et al. Effects of AQP5 gene silencing on proliferation, migration and apoptosis of human glioma cells through regulating EGFR/ERK/p38 MAPK signaling pathway. *Oncotarget*. 2017;8(24):38444–55. <http://dx.doi.org/10.18632/oncotarget.16461>

148. Mercurio L, Ajmone-Cat MA, Cecchetti S, Ricci A, Bozzuto G, Molinari A, et al. Targeting CXCR4 by a selective peptide antagonist modulates tumor microenvironment and microglia reactivity in a human glioblastoma model. *J Exp Clin Cancer Res*. 2016;35:55. <http://dx.doi.org/10.1186/s13046-016-0326-y>
149. Blumenthal DT, Yalon M, Vainer GW, Lossos A, Yust S, Tzach L, et al. Pembrolizumab: First experience with recurrent primary central nervous system (CNS) tumors. *J Neurooncol*. 2016;129(3):453–60. <http://dx.doi.org/10.1007/s11060-016-2190-1>
150. Brown CE, Badie B, Barish ME, Weng L, Ostberg JR, Chang WC, et al. Bioactivity and safety of IL13R α 2-redirected chimeric antigen receptor CD8+ T cells in patients with recurrent glioblastoma. *Clin Cancer Res*. 2015;21(18):4062–72. <http://dx.doi.org/10.1158/1078-0432.CCR-15-0428>
151. Brown CE, Alizadeh D, Starr R, Weng L, Wagner JR, Naranjo A, et al. Regression of glioblastoma after chimeric antigen receptor T-cell therapy. *N Engl J Med*. 2016;375(26):2561–9. <http://dx.doi.org/10.1056/NEJMoa1610497>
152. Kang T, Zhu Q, Jiang D, Feng X, Feng J, Jiang T, et al. Synergistic targeting tenascin C and neuropilin-1 for specific penetration of nanoparticles for anti-glioblastoma treatment. *Biomaterials*. 2016;101:60–75. <http://dx.doi.org/10.1016/j.biomaterials.2016.05.037>
153. Hayward SL, Wilson CL, Kidambi S. Hyaluronic acid-conjugated liposome nanoparticles for targeted delivery to CD44 overexpressing glioblastoma cells. *Oncotarget*. 2016;7(23):34158–71.
154. Chen L, Miao W, Zhang H, Zeng F, Cao C, Qiu R, et al. The inhibitory effects of a monoclonal antibody targeting neuropilin-1 on adhesion of glioma cells to fibronectin. *J Biomed Nanotechnol*. 2014;10(11):3373–80. <http://dx.doi.org/10.1166/jbn.2014.1867>
155. Jaime-Ramirez AC, Dmitrieva N, Yoo JY, Banasavadi-Siddegowda Y, Zhang J, Relation T, et al. Humanized chondroitinase ABC sensitizes glioblastoma cells to temozolomide. *J Gene Med*. 2017;19(3):e2942. <http://dx.doi.org/10.1002/jgm.2942>
156. Salacz ME, Kast RE, Saki N, Brüning A, Karpel-Massler G, Halatsch ME. Toward a noncytotoxic glioblastoma therapy: Blocking MCP-1 with the MTZ Regimen. *Onco Targets Ther*. 2016;9:2535–45. <http://dx.doi.org/10.2147/OTT.S100407>
157. Lamour V, Henry A, Kroonen J, Nokin MJ, von Marschall Z, Fisher LW, et al. Targeting osteopontin suppresses glioblastoma stem-like cell character and tumorigenicity *in vivo*. *Int J Cancer*. 2015;137(5):1047–57. <http://dx.doi.org/10.1002/ijc.29454>

17

Maximizing Local Access to Therapeutic Deliveries in Glioblastoma. Part I: Targeted Cytotoxic Therapy

WALDEMAR DEBINSKI¹ • WALDEMAR PRIEBE² • STEPHEN B. TATTER^{1,3}

¹Brain Tumor Center of Excellence, Wake Forest Baptist Medical Center Comprehensive Cancer Center, Winston Salem, NC, USA; ²Department of Experimental Therapeutics, Division of Cancer Medicine, University of Texas MD Anderson Cancer Center, Houston, TX, USA; ³Department of Neurosurgery, Wake Forest Baptist Medical Center, Winston Salem, NC, USA

Author for correspondence: Waldemar Debinski, Brain Tumor Center of Excellence, Wake Forest Baptist Medical Center, NRC/Commons Rm 210A, 1 Medical Center Boulevard, Winston Salem, NC 27157, USA.
E-mail: debinski@wakehealth.edu

Doi: <http://dx.doi.org/10.15586/codon.glioblastoma.2017.ch17>

Abstract: Glioblastoma (GBM), a primary brain tumor, remains an unmet medical need. One of the major obstacles to GBM treatment is the adequate properties of drugs. Complex pathobiology of GBM, including local invasion and intratumoral heterogeneity, represent major challenges to generating effective therapies. We discuss here the design of targeted cytotoxic drugs with an increased access to tumors and pathophysiologically important tumor compartments. Our research and others' have shown that interleukin 13 receptor alpha 2 (IL-13RA2), EphA2, and EphA3 receptors are overexpressed in most patients with GBM, but not in normal brain, and also in spontaneous canine high-grade gliomas like GBM, an excellent translational model of GBM. These receptors and also the EphB2 receptor are overexpressed and are functional in several GBM compartments involved

In: *Glioblastoma*. Steven De Vleeschouwer (Editor), Codon Publications, Brisbane, Australia
ISBN: 978-0-9944381-2-6; Doi: <http://dx.doi.org/10.15586/codon.glioblastoma.2017>

Copyright: The Authors.

Licence: This open access article is licenced under Creative Commons Attribution 4.0 International (CC BY 4.0). <https://creativecommons.org/licenses/by-nc/4.0/>

in tumor progression and/or resistance to therapies. We pursue the novel idea of targeting all four receptors with one targeted cytotoxic compound (QUAD-CTX). We are constructing a molecularly targeted anti-GBM drug that (i) may not require patient prescreening, (ii) will attack most tumor compartments known to be pathobiologically important, and (iii) performs these functions in one pharmaceutical entity, so it will be suitable for monotherapy. We thus wish to take advantage of a unique opportunity to produce an off-the-shelf, highly specific, molecularly targeted drug candidate suitable to treat perhaps even all patients with GBM. We envision that this “molecular resection” will translate into clear-cut durable responses in patients suffering from this dreadful disease.

Key words: Convection-enhanced delivery; Glioblastoma; IL-13RA2; Receptors; Targeted cytotoxins

Introduction

Effective therapy of glioblastoma (GBM) remains an elusive goal. Despite nearly 80 years of effort, only 1 month per decade has been added to the mean survival rate of GBM patients, and the 2-year survival rate remains below 25% with practically no cures (1). Recently, several highly anticipated efficacy trials including antiangiogenic therapies all failed in patients with GBM (2–5). Similarly, inhibiting a vital signaling pathway in a single compartment of GBM, namely, glioma stem-like cells (GSCs), conferred no clinical benefit (6, 7). Many small-molecule inhibitors have not progressed beyond early-phase trials based on little objective benefit (8, 9). On the other hand, immunotherapy trials showed promising results, including dendritic cell vaccination against IL-13RA2 (10), among other targets, and peptide vaccination against EGFRvIII (11). Although the vaccination against EGFRvIII in recently finished efficacy trial reproduced results from Phase I and II, the control group unexpectedly showed an increase in overall survival by 40% from previously observed (12). This is reminiscent of a similar happening when an IL-13-based cytotoxin was used in Phase III PRECISE trial (13, 14). Of interest, a medical device called Optune (Novocure) generating electric fields demonstrated clinical efficacy (15, 16). In short, GBM remains refractory to standard and experimental treatments. Predictions about translational potential of virtually all therapeutic approaches have not been realized thus far.

High mortality in GBM is often attributed to its complex pathobiology, including high cellularity, neovascularization, hypoxia/necrosis, immune cell infiltration, and local invasion (17). Moreover, GSCs may play an important role in GBM progression/recurrence and resistance to therapies like chemotherapy or radiation (18, 19). Recently, four genomic subtypes of GBM were delineated: proneural, neural, mesenchymal, and classical (20, 21), supportive of the complex pathobiological nature of GBM. Common treatment approaches involve surgery (22), radiation therapy (23), and various chemotherapeutic regimens (24, 25).

Other major obstacles to GBM treatment is the presence of barriers like blood–brain barrier (BBB) and blood–brain tumor barrier (BBTB), limiting or outrightly preventing any diffusion of drugs into tumors when given systemically (Figure 1). We believe that we can improve treatment of GBM by addressing crucial issues in

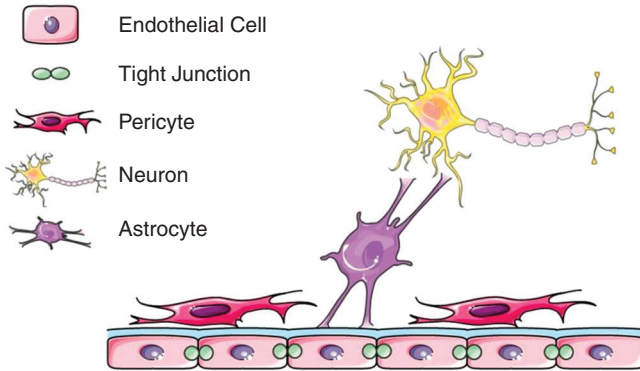


Figure 1 Schematic drawing of the blood-brain barrier. The blood–brain barrier is comprised of neurovascular units. Endothelial cells are connected by tight junctions and share a basement lamina with pericytes. Astrocytic end-feet are also at the basement lamina interface and these cells interact with neurons (This figure was developed using Servier Medical Art (<http://www.servier.com/Powerpointimage-bank>) under a Creative Commons attribution 3.0 Unported License). (Adapted from *Pharmaceutics* 2015;7(3):175–187.)

drug design and their delivery by maximizing drugs access to tumors and their targets. This can be achieved by generating anti-GBM drugs that attack concomitantly multiple GBM compartments that are responsible for tumor progression and resistance to the existing therapies and experimental therapies. For example, we can aim at four molecular targets like IL-13RA2, EphA2, EphA3, and EphB2 receptors that are specifically overexpressed on GBM tumor cells.

Targeted Cytotoxic Therapy of GBM

GBM is the most common primary brain tumor in adults, and the median survival is only ~14.5 months (1, 26). We discovered that interleukin 13 receptor alpha 2 (IL-13RA2) and EphA2 receptor are overexpressed in most patients with GBM, but not in normal brain (27–31), and also in spontaneous canine GBM, an excellent translational model of GBM (32–35). Expression of IL-13RA2 and EphA2 is partially overlapping; hence, the combined overexpression is ~90% in patients with GBM (31). IL-13RA2 and EphA2 are targets for multiple therapeutic approaches currently in the clinic or under preclinical evaluation (36–52). The first generation of an IL-13-based cytotoxin produced in our laboratory, which nonspecifically targeted IL-13RA2, demonstrated clinical efficacy in patients with recurrent GBM (13, 53–55). We developed a protocol for a Phase I clinical trial in dogs with gliomas (see also chapter 21, page 405) and began the trial using a cocktail of cytotoxins targeting IL-13RA2 (using a variant of IL-13 as a specific targeting ligand) and EphA2 receptor (based on ephrin A1, a ligand for the EphA2 receptor). The drugs are given locoregionally through convection-enhanced delivery (CED) using anti-reflux catheters (Figure 2 in Chapter 21). We have already seen significant antitumor responses in this dose-finding trial.

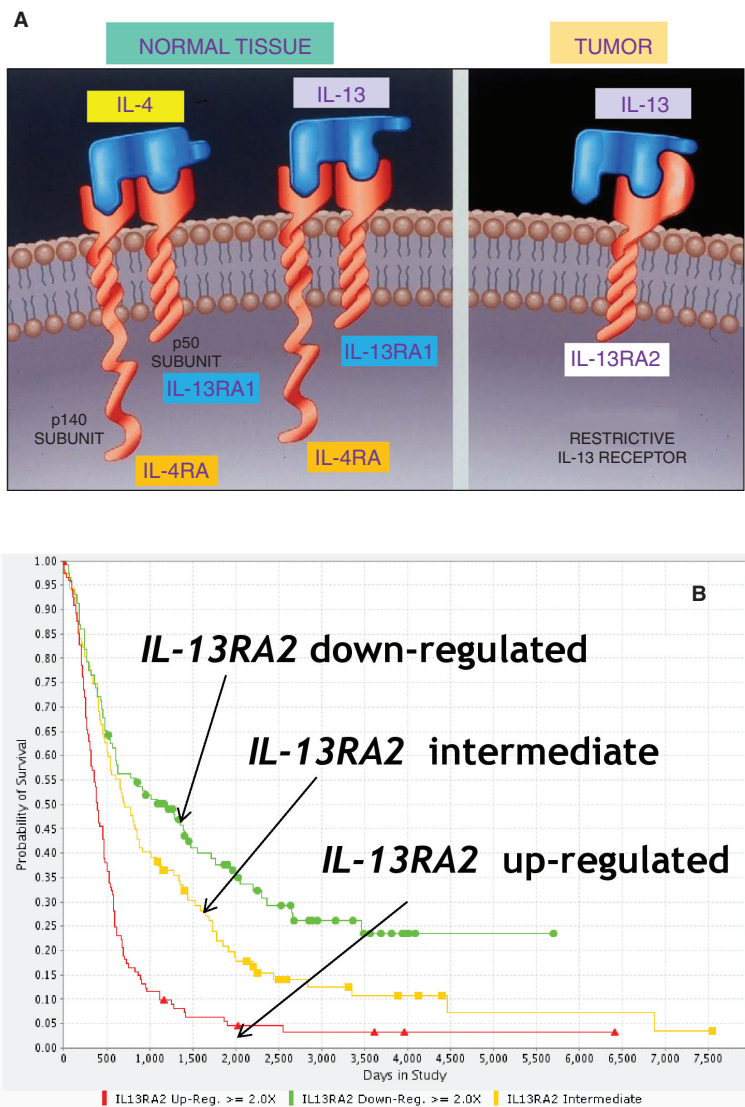


Figure 2 IL-13RA2 and EphA2 in cancer. (A) Schemata of normal tissue, IL-13RA1/IL-4A, and tumor-associated receptor, IL-13RA2 for IL-13 (adapted from Sci Med 1998;5:36–42). (B) Kaplan–Meier survival plots with differential *IL-13RA2* gene expression. REMBRANDT database of human gliomas was used for calculations (<https://caintegrator.nci.nih.gov/rembrandt/>). All differences were statistically significant. (C, D) Schemata of Eph receptors and their ligands, ephrinAs, respectively. (E) Kaplan–Meier survival plots with differential *EphA2* gene expression. REMBRANDT database of human gliomas was used for calculations as in B. All differences were statistically significant.

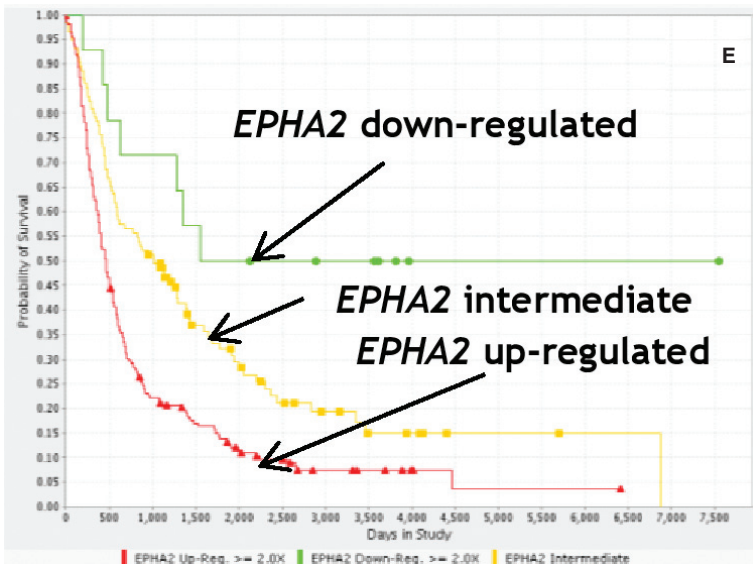
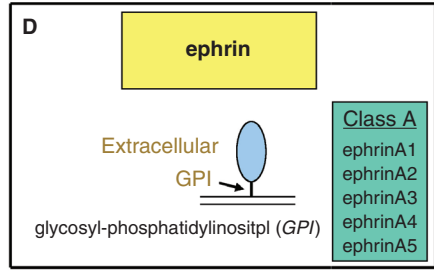
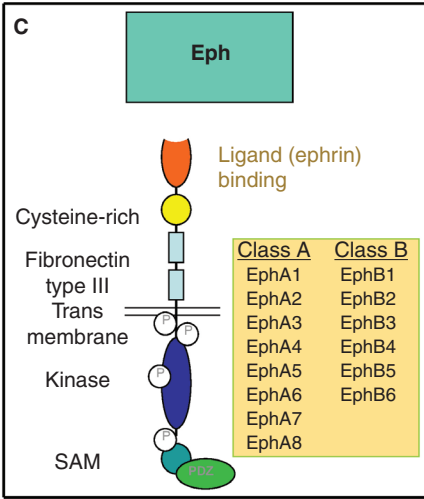


Figure 2 (Continued). IL-13RA2 and EphA2 in cancer. (A) Schemata of normal tissue, IL-13RA1/IL-4A, and tumor-associated receptor, IL-13RA2 for IL-13 (adapted from Sci Med 1998;5:36–42). (B) Kaplan–Meier survival plots with differential *IL-13RA2* gene expression. REMBRANDT database of human gliomas was used for calculations (<https://cainTEGRATOR.nci.nih.gov/rembrandt/>). All differences were statistically significant. (C, D) Schemata of Eph receptors and their ligands, ephrinAs, respectively. (E) Kaplan–Meier survival plots with differential *EphA2* gene expression. REMBRANDT database of human gliomas was used for calculations as in B. All differences were statistically significant.

Our research and others' have shown that IL-13RA2, EphA2, and also EphA3 (Figure 2) are widely present in various compartments of GBM tumors. For example, all three receptors are expressed in tumor cells of the core of GBM tumors. Importantly, IL-13RA2, EphA2, and EphA3 are present on tumor-infiltrating cells, while EphA2 is also overexpressed in tumor neovasculature (56, 57). Interestingly, IL-13RA2, EphA2, and EphA3 were associated with, and play crucial roles in, the pathobiology of GSCs. IL-13RA2 is abundant in cells isolated as GSCs from GBM (58–60) and contributes to their cell stem properties (61). EphA2 and EphA3 drive self-renewal and tumorigenicity of GSCs (62–64). Finally, the EphA3 receptor can be readily detected in GBM-infiltrating cells of monocytic origin, tumor-associated macrophages (TAM) (Figure 3). Thus, collectively, IL-13RA2, EphA2, and EphA3 are expressed in several GBM compartments documented to be involved in tumor progression and/or resistance to therapies (18, 19). Of importance, ephrin-A5 (eA5) binds EphA2 and EphA3 receptors and also the EphB2 (17, 65, 66) receptor, all present in abundance in

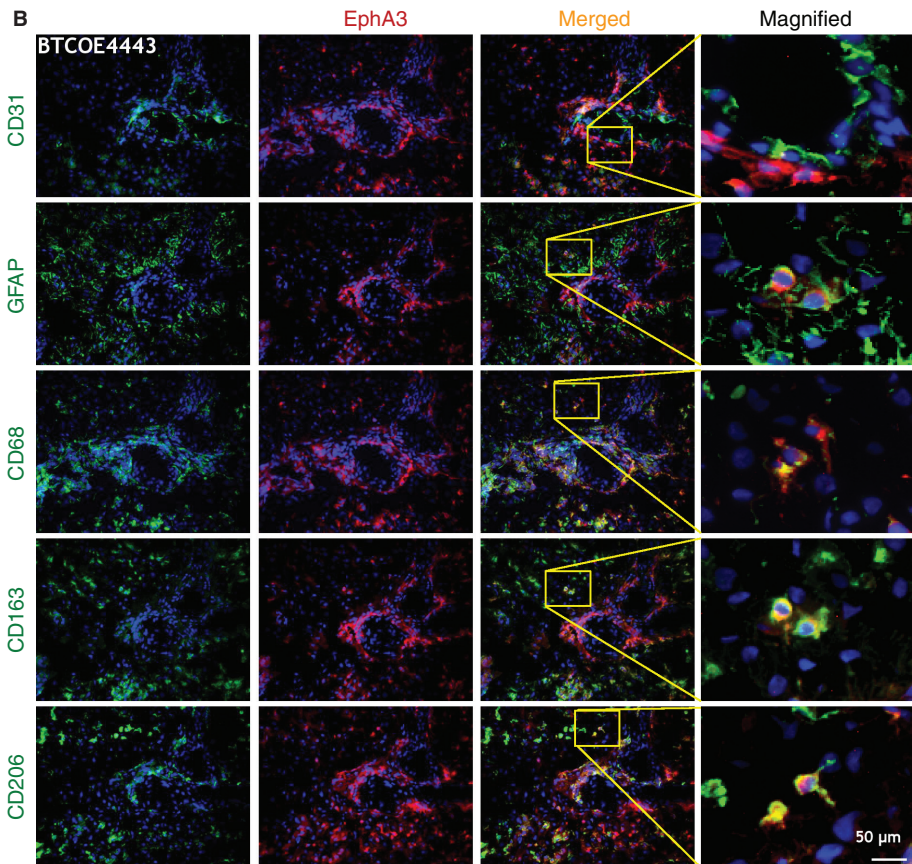


Figure 3 EphA3 receptor in GBM. Immunofluorescent staining of EphA3 (red) and CD31, GFAP, CD68, CD163 and CD206 (green) on consecutive sections of the same GBM specimen. Nuclei were stained with DAPI (blue). (Adapted from *Oncotarget* 2016;7(37):59860–59876.)

GBM tumors, but not in normal brain. Here, we discuss the novel idea of targeting all four receptors with one pharmaceutical compound. We are exploiting the favorable properties of our previously generated IL-13 variants and those of engineered eA5, to construct a human IgG₁ scaffold-based single pharmaceutical compound. The multivalent compound will bind IL-13RA2, EphA2, EphA3, and EphB2 and deliver a catalyst(s) to GBM tumors, specifically killing tumor cells and abnormal cells of the tumor environment. Such an approach offers a unique opportunity to gain an increased access to tumor compartments of high resistance, or poor availability, to current treatment modalities.

ATTRACTIVE MOLECULAR TARGETS IN GBM

We discovered the first receptor target overexpressed in most GBM patients, but not in normal brain: IL-13RA2 (29). IL-13RA2 is a monomeric receptor to which only IL-13 binds, unlike its normal tissue counterpart, IL-13RA1/IL-4A, which binds IL-13 and IL-4 (5) (Figure 2A). *IL-13RA2* is (i) associated with GBM patients' survival, (ii) expressed preferentially in a GBM mesenchymal subtype, and (iii) its gene, based on TCGA data, is overexpressed in 58% of patients (58; Figure 2B) and in the protein in up to 75% of GBM cases (35). IL-13RA2 was readily detected in cells isolated as GSC (59, 60) and appears to contribute to GBM cell stemness. For example, GBM cells selected for lack of IL-13RA2 have a significantly lower stem cell-like forming and tumorigenic potential (61). This observation provides strong rationale for treatments eliminating IL-13RA2 positive cells. IL-13RA2 may influence intracellular signaling (67) and may be a signaling molecule (68).

Our continuous efforts to find pharmaceutically tractable molecular targets led to discovery of the EphA2 receptor in GBM (31, 69–71). EphA2 belongs to the largest protein tyrosine kinase receptor family in eukaryotes (72–75) (Figure 2C); these receptors are bound by natural ligands called ephrins (Figure 2D). EphA2 is over-expressed in ~60% of patients with GBM (31, 76), but jointly with IL-13RA2 it is over-expressed in ~90% of all GBM, while absent in normal brain (31). Expression of *EphA2* and EphA2 correlates with glioma patients' survival (75) (see also Figure 2E) (77, 78). IL-13RA2 and EphA2 exist in a significant proportion of locally infiltrating GBM cells, and EphA2 is overexpressed on abnormal endothelium of tumor-associated vessels (52, 79). EphA2 activation by its preferred ligand, ephrin-A1 (eA1), induces prominent, dose-dependent inhibitory effects on anchorage-independent growth and invasiveness of GBM cells (79, 80). The EphA2/eA1 system function in GBM is complex; the receptor is oncogenic when ligand unactivated, but tumor suppressing when activated by eA1 (68, 69). EphA2 is also important for the self-renewing and tumorigenic potential of GSCs (62, 63). Thus, IL-13RA2 and EphA2 are attractive molecular targets for urgently needed targeted combinatorial therapy (31, 80, 81).

Most recently, we found that another receptor of the EphA subfamily, the EphA3 receptor, is overexpressed in GBM (Figure 3). The gene for *EphA3* was highly upregulated in G48a GBM cell tumorspheres (56) and even more so in nonpassaged GBM cells. Others found the EphA3 receptor is important for the self-renewing potential and tumorigenicity of GSCs (64). Interestingly, the distribution of EphA2 and EphA3 receptors only partially overlaps. For example, EphA3 receptors are found in cells of monocytic origin infiltrating GBM (82) like TAMs (Figure 3). The difference in

these receptors' distribution also agrees with the existence of multiple phenotypic types of GSCs (83). EphA3 often co-localized with a GSC marker Nestin *in situ*, in accordance with a recent report (64). EphA3 did not co-localize with the endothelial cell marker CD31 (Figure 3). Microglia/macrophages variably infiltrate gliomas and contribute to the total tumor mass (82). Three markers of monocyte/macrophage lineage (CD68, CD163, and CD206) co-stained with EphA3 on a subpopulation of cells within the tumor and surrounding the tumor neovasculature (64). This novel finding widens the spectrum of GBM compartments that can be exploited as targets in molecular anti-GBM therapies using Eph receptors.

PROMISING TREATMENT BYPASSING THE BBB

We and others have continued to optimize CED as a minimally invasive approach (33–35, 84–97). This way of drugs delivery is discussed in Part II of the chapter (page 347). A critical therapeutic advantage in using cytotoxins *via* CED is that they cause death of targeted cells (70). Even though the GBM tumor environment is highly immunosuppressive (98, 99) and patients with GBM are immunosuppressed (100, 101), a large number of killed tumor cells provides a “danger signal” and evokes effective antitumor immune responses. Our published (41) and unpublished observations suggested, and another study demonstrated directly (102), the existence of effective immune responses in preclinical studies with cytotoxic proteins. Importantly, the “*in situ* vaccine” effect of a treatment causing cell death is also the principal mechanism of antitumor action when using oncolytic viruses delivered directly to tumors using CED (6, 103). In this approach, the virus is delivered only to a portion of GBM tumors through a single catheter, but cell death at the site and near the virus injection appears sufficient to produce readily measurable immune responses in patients and subsequent antitumor effects (6, 103). Therefore, if one cannot distribute cytotoxins perfectly throughout the whole tumor and its vicinity in all patients at all times, the death of most cells in tumors during each treatment will result in an antitumor vaccination effect meaning new influx of immune cells responsible for the whole mechanism of response. This principle is tested in other cancers like melanoma; the viral gene therapy drug, Imlygic, has been approved by the FDA (104). Conceivably, the addition of immune checkpoint inhibitors should result in potentiation of such responses (105, 106).

INCREASING DRUGS ACCESS TO TUMOR COMPARTMENTS AND OPTIMIZING CED FOR EFFECTIVE GBM TREATMENT

The clinical results obtained with the first generation of IL-13-based cytotoxin, huIL-13-PE38QQR, which is a fusion protein between a wild type IL-13 and a modified pseudomonas exotoxin A (PE) represent promising translational starting point to improve treatment of patients with GBM. Early-phase trials with huIL-13-PE38QQR showed up to 56 weeks of median survival and a number of long-lasting responses (107). Importantly, the efficacy trial extended the lives of patients with recurrent GBM by almost 50%, but the control arm had extended from previously observed survivals and the favorable difference did not achieve statistical significance (13). The ways to improve the CED are described in further detail in chapter 18 (page 359) and chapter 21 (Page 405).

TARGETING EPH RECEPTORS SIMULTANEOUSLY

As pointed out above, IL-13RA2, EphA2, EphA3, and EphB2 are overexpressed, functionally important, and linked to survival in patients with GBM. They are all pharmaceutically targetable as demonstrated in preclinical and clinical studies. These receptors are distributed among several tumor compartments important for progression of GBM. Debinski's group has long been advocating attacking GBM with a combinatorial approach (31, 80, 81). Given that only two modified ligands may be needed to generate a drug delivery system targeting all four receptors, we have a completely new opportunity for combinatorial therapy and highly increased drug access in a complex disease of dismal prognosis, with just one pharmaceutical agent.

eA5 can bind and induce internalization of the Eph receptors A2, A3, and EphB2. Hence, we produced a dimeric form of eA5 in a fusion with an Fc fragment of human IgG₁, eA5-Fc (Figure 4A) (56). We also made an eA5-Fc-PE38QQR cytotoxin chemical conjugate (Figure 4A). eA5-Fc-PE38QQR killed U-251 MG, U-373 MG, and G48a GBM cells very efficiently and specifically (Figure 4B). The IC₅₀ of eA5-Fc-PE38QQR was in the range of 10⁻¹¹ M. To confirm the specificity of the cytotoxin in targeting EphA2 and EphA3, the three GBM cell lines were pretreated with either eA1-Fc or eA5-Fc at 10 μg/mL for 1 h. As expected, the cytotoxin was less active on the three cell lines tested when pretreated with eA1-Fc, which binds only the EphA2 receptor, and completely lost its activity when cells were pretreated with eA5-Fc, which binds EphA2, EphA3, and EphB2 (Figure 4B). Even though the readings in colorimetric cell viability assay were not reaching 100% kill, the live/dead assay (Life Technologies) demonstrated that vast majority of GBM cells were dead at

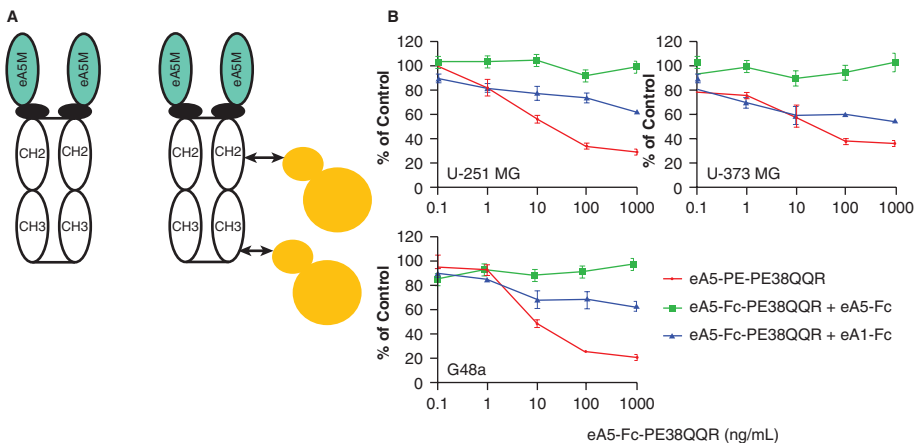


Figure 4 EA5-Fc-PE38QQR kills GBM tumor cells, specifically targeting both EphA3 and EphA2 receptors. (A) The structure of an eA5-Fc and eA5-Fc chemically conjugated to PE38QQR (right). Opposite arrows represent chemical conjugation. Closed small ovals represent hinge regions; thin straight lines represent disulfide bonds. Orange circles are the domains of PE: smaller = D2 and larger = Domain III. (B) Cell viability assay on GBM cell lines treated with eA5-Fc-PE38QQR for 48 h or pretreated with either eA1-Fc or eA5-Fc. (Adapted from *Oncotarget* 2016;7(37):59860–59876.)

10 ng/ml of conjugate concentration and almost all were dead at 100 ng/ml of conjugate (56).

TARGETING EPH RECEPTORS AND IL-13RA2 SIMULTANEOUSLY

eA5-Fc interacts with EphA2, EphA3, and EphB2 receptors. To further widen the reach of a targeting agent, we are incorporating mutated IL-13 (IL-13M), which has dramatically altered reactivity toward the normal tissue receptor, IL-13RA1/IL-4RA, but not toward the tumor-associated receptor, IL-13RA2 (41, 108–111) into the eA5-Fc construct (Figures 2A and 5A). The very first construct retained an ability to bind to the EphA2 receptor and IL-13RA2. Next, we will produce a chemical conjugate between eA5M-Fc-IL-13M and PE38QQR to demonstrate feasibility of the QUAD-CTX approach in a direct way similarly to eA5-Fc-PE38QQR. We will also make conjugates of eA5-Fc-IL-13M with chemotherapeutics like WP936 (112). This will eliminate several potential problems related to possible systemic delivery of toxin-based therapeutics.

QUAD-CTX BASED ON SCFV RECEPTOR TARGETING

We are generating another type of QUAD-CTX drug candidate in which we will use single-chain (sc) Fv fragments of antibodies (scFv) directed individually against the three Eph receptors: A2, A3, and B2. It will be also based on a human IgG₁ scaffold similarly to eA5M-Fc-IL-13M. We have already made the first step in generating a quadrivalent scFv(EphA2)-scFv(EphA3)-scFv(EphB2)-Fc-IL-13M. We have produced a bivalent scFv(EphA2)-Fc-IL-13M (Figure 6A). We will stepwise introduce scFvs for EphA3 and EphB2 receptors (Figure 6B) with various placement configuration and test for the exhibition of expected binding properties. Once it is made, the quadrivalent ligand will be conjugated to either modified toxins or a chemotherapeutic like WP936 (Figure 6C).

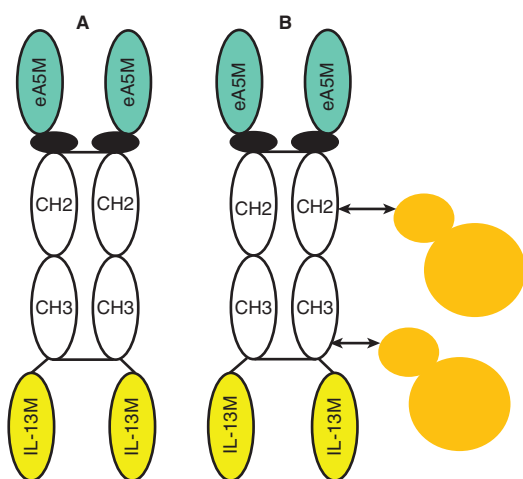


Figure 5 Design of a QUAD-CTX. (A) Schemata of eA5M-Fc-IL-13M in which the moieties of eA5M and IL-13M are targeting ligands. (B) Schemata of eA5M-Fc-IL-13M conjugated to PE38QQR. Closed small ovals represent hinge regions. Opposite arrows represent chemical conjugation. Closed small blue ovals represent chemotherapeutic. Filled triangles represent chemotherapeutic. Orange circles are the domains of PE: smaller = D2, and larger = Domain III.

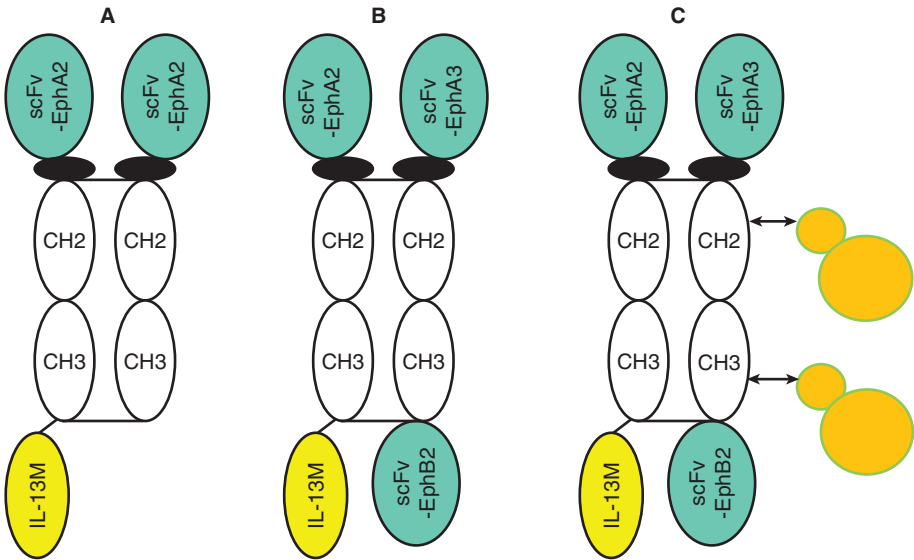


Figure 6 Construction of a QUAD-CTX based on scFvs. (A) Bivalent scFv(EphA2)-Fc-IL-13M construct. (B) Schemata of a quadrivalent scFv(EphA2)-scFv(EphA3)-scFv(EphB2)-Fc-IL-13M construct. (C) Schemata of a quadrivalent scFv(EphA2)-scFv(EphA3)-scFv(EphB2)-Fc-IL-13M chemical conjugate with toxic load. Closed small ovals represent hinge regions; thin straight lines represent disulfide bonds. Opposite arrows represent chemical conjugation. Closed small blue ovals represent either toxins or chemotherapeutic.

Conclusion

We have discussed our idea to target the three molecular targets that we identified in GBM: IL-13RA2, EphA2, and EphA3, and yet another receptor, EphB2 that are specifically overexpressed on GBM tumor cells as well. We are developing a cytotoxic drug of highly unique properties that can recognize four receptors, QUAD-CTX. Also, because virtually all GBM patients have these receptors in abundance, prescreening patients for this treatment may not be necessary. Thus, our new design will increase drug access to hard-to-target GBM compartments believed to be responsible for dismal prognosis of the disease. Thus, despite significant obstacles in drug delivery to GBM and the high complexity and heterogeneity of GBM, an off-the-shelf drug used as monotherapy can represent an effective combinatorial therapy approach using both passive and active immunotherapy.

Acknowledgment: This work was supported by NCI R01 CA74145, R01 CA139099, P01 CA 207206 and Thomas K. Hearn, Pratto, Dallas Ray Swing, and JS Farmer III Family Funds for Brain Tumor Research.

Conflict of Interest: Dr. Waldemar Debinski is an inventor on the patent applications filed or patents issued on the subject of this chapter. He is also a Scientific Advisor to Targeptics, Inc. and holds equity in the company.

Copyright and permission statement: To the best of our knowledge, the materials included in this chapter do not violate copyright laws. All original sources have been appropriately acknowledged and/or referenced. Where relevant, appropriate permissions have been obtained from the original copyright holder(s).

References

1. Stupp R, Mason WP, van den Bent MJ, Weller M, Fisher B, Taphoorn MJ, et al. Radiotherapy plus concomitant and adjuvant temozolomide for glioblastoma. *N Engl J Med*. 2005;352:987–96. <http://dx.doi.org/10.1056/NEJMoa043330>
2. Friedman HS, Prados MD, Wen PY, Mikkelsen T, Schiff D, Abrey LE, et al. Bevacizumab alone and in combination with irinotecan in recurrent glioblastoma. *J Clin Oncol*. 2009;27:4733–40. <http://dx.doi.org/10.1200/JCO.2008.19.8721>
3. Gilbert MR, Dignam JJ, Armstrong TS, Wefel JS, Blumenthal DT, Vogelbaum MA, et al. A randomized trial of bevacizumab for newly diagnosed glioblastoma. *N Engl J Med*. 2014 Feb 20;370(8):699–708. <http://dx.doi.org/10.1056/NEJMoa1308573>
4. Chinot OL, Wick W, Mason W, Henriksson R, Saran F, Nishikawa R, et al. Bevacizumab plus radiotherapy-temozolomide for newly diagnosed glioblastoma. *N Engl J Med*. 2014 Feb 20;370(8):709–22. <http://dx.doi.org/10.1056/NEJMoa1308345>
5. Stupp R, Hegi ME, Gorlia T, Erridge SC, Perry J, Hong YK, et al. Cilengitide combined with standard treatment for patients with newly diagnosed glioblastoma with methylated MGMT promoter (CENTRIC EORTC 26071-22072 study): A multicentre, randomised, open-label, phase 3 trial. *Lancet Oncol*. 2014 Sep;15(10):1100–8. [http://dx.doi.org/10.1016/S1470-2045\(14\)70379-1](http://dx.doi.org/10.1016/S1470-2045(14)70379-1)
6. Desjardins A, Vlahovic G, Friedman HS. Vaccine therapy, oncolytic viruses, and gliomas. *Oncology (Williston Park)*. 2016 Mar;30(3):211–18.
7. Sloan AE, Nock CJ, Kerstetter A, Supko J, Ye X, Barnholtz-Sloan JS, et al. Targeting glioma stem cells (GSC): A biomarker and Phase II study of GDC-0449 in patients with recurrent glioblastoma multiforme. *Neuro Oncol*. 2012 Oct;14(Suppl 6):vi101–vi105.
8. Wick W, Weller M, Weiler M, Batchelor T, Yung AW, Platten M. Pathway inhibition: Emerging molecular targets for treating glioblastoma. *Neuro Oncol*. 2011 Jun;13(6):566–79. <http://dx.doi.org/10.1093/neuonc/nor039>
9. Nathanson DA, Gini B, Mottahedeh J, Visnyei K, Koga T, Gomez G, et al. Targeted therapy resistance mediated by dynamic regulation of extrachromosomal mutant EGFR DNA. *Science*. 2014; 343(6166):72–6. <http://dx.doi.org/10.1126/science.1241328>
10. ImmunoCellular therapeutics phase II study demonstrates that glioblastoma patients live longer without disease progression when treated with ICT-107. <http://investors.imuc.com/releasedetail.cfm?ReleaseID=813442>.
11. Reardon D, Schuster J, Tran D, Fink K, Nabors L, Li G, et al. IT-30. ReACT: A phase II study of rindopepimut vaccine (CDX-110) plus bevacizumab in relapsed glioblastoma. *Neuro Oncol*. 2014;16(Suppl 5):v116.
12. Malkki H. Glioblastoma vaccine therapy disappointment in Phase III trial. *Nature Rev Neurol*. 2016;12:190. <http://dx.doi.org/10.1038/nrneurol.2016.38>
13. Sampson JH, Archer G, Pedain C, Wembacher-Schröder E, Westphal M, Kunwar S, et al. Poor drug distribution as a possible explanation for the results of the PRECISE trial. *J Neurosurgery*. 2010;113:301–309. <http://dx.doi.org/10.3171/2009.11.JNS091052>

14. Kunwar S, Chang S, Westphal M, Vogelbaum M, Sampson J, Barnett G, et al. Phase III randomized trial of CED of IL13-PE38QQR vs Gliadel wafers for recurrent glioblastoma. PRECISE Study Group. *Neuro Oncol*. 2010 Aug;12(8):871–881. <http://dx.doi.org/10.1093/neuonc/nop054>
15. Stupp R, Wong ET, Kanner AA, Steinberg D, Engelhard H, Heidecke V, et al. NovoTTF-100A versus physician's choice chemotherapy in recurrent glioblastoma: A randomised phase III trial of a novel treatment modality. *Eur J Cancer*. 2012;48(14):2192–202. <http://dx.doi.org/10.1016/j.ejca.2012.04.011>
16. Stupp R, Taillibert S, Kanner AA, Kesari S, Steinberg DM, Toms SA, et al. Maintenance therapy with tumor-treating fields plus temozolomide vs temozolomide alone for glioblastoma: A randomized clinical trial. *JAMA*. 2015 Dec 15;314(23):2535–43. <http://dx.doi.org/10.1001/jama.2015.16669>
17. Vartanian A, Singh SK, Agnihotri S, Jalali S, Burrell K, Aldape KD, et al. GBMs multifaceted landscape: highlighting regional and microenvironmental heterogeneity. *Neuro Oncol*. 2014 Aug;16(8):1025–6. <http://dx.doi.org/10.1093/neuonc/nou121>
18. McLendon RE, Rich JN. Glioblastoma stem cells: A neuropathologist's view. *J Oncol*. 2011;2011:397195. <http://dx.doi.org/10.1155/2011/397195>
19. Singh SK, Hawkins C, Clarke ID, Squire JA, Bayani J, Hide T, et al. Identification of human brain tumor initiating cells. *Nature*. 2004;432(7015):396–401. <http://dx.doi.org/10.1038/nature03128>
20. Verhaak RG, Hoadley KA, Purdom E, Wang V, Qi Y, Wilkerson MD, et al. Cancer Genome Atlas Research Network. Integrated genomic analysis identifies clinically relevant subtypes of glioblastoma characterized by abnormalities in PDGFRA, IDH1, EGFR, and NF1. *Cancer Cell*. 2010 Jan 19;17(1):98–110. <http://dx.doi.org/10.1016/j.ccr.2009.12.020>
21. Brennan CW, Verhaak RG, McKenna A, Campos B, Noushmehr H, Salama SR, et al. TCGA Research Network. The somatic genomic landscape of glioblastoma. *Cell*. 2013 Oct 10;155(2):462–77. <http://dx.doi.org/10.1016/j.cell.2013.09.034>
22. Sanai N, Berger MS. Recent surgical management of gliomas. *Adv Exp Med Biol*. 2012;746:12–25. http://dx.doi.org/10.1007/978-1-4614-3146-6_2
23. Chan MD, Tatter SB, Lesser G, Shaw EG. Radiation oncology in brain tumors: Current approaches and clinical trials in progress. *Neuroimaging Clin N Am*. 2010;20(3):401–8. <http://dx.doi.org/10.1016/j.nic.2010.04.005>
24. Blakeley J, Grossman SA. Chemotherapy with cytotoxic and cytostatic agents in brain cancer. *Handb Clin Neurol*. 2012;104:229–54. <http://dx.doi.org/10.1016/B978-0-444-52138-5.00017-7>
25. Reardon DA, Perry JR, Brandes AA, Jalali R, Wick W. Advances in malignant glioma drug discovery. *Expert Opin Drug Discov*. 2011 Jul;6(7):739–53. <http://dx.doi.org/10.1517/17460441.2011.584530>
26. Louis DN, Perry A, Reifenberger G, von Deimling A, Figarella-Branger D, Cavenee WK, et al. The 2016 World Health Organization classification of tumors of the central nervous system: A summary. *Acta Neuropathol*. 2016 Jun;131(6):803–20. <http://dx.doi.org/10.1007/s00401-016-1545-1>
27. Debinski W, Gibo DM, Hulet SW, Connor JR, Gillespie GY. Receptor for interleukin 13 is a marker and therapeutic target for human high grade gliomas. *Clin Cancer Res*. 1999;5:985–90.
28. Mintz A, Gibo DM, Webb (Slagle) B, Christensen AD, Debinski W. IL13R α 2 is a glioma-restricted receptor for IL13. *Neoplasia*. 2002;4:388–99. <http://dx.doi.org/10.1038/sj.neo.7900234>
29. Debinski W. An immune regulatory cytokine receptor and glioblastoma multiforme: An unexpected link. *Crit Rev Oncog*. 1998;9:255–68.
30. Debinski W, Gibo DM. Molecular expression analysis of restrictive receptor for interleukin 13, a brain tumor-associated cancer/testis antigen. *Mol Med*. 2000;6:440–9.
31. Wykosky J, Gibo DM, Stanton C, Debinski W. IL-13 Receptor alpha-2, EphA2, and Fra-1 as molecular denominators of high-grade astrocytomas and specific targets for combinatorial therapy. *Clin Cancer Res*. 2008;14:199–208. <http://dx.doi.org/10.1158/1078-0432.CCR-07-1990>
32. Debinski W, Dickinson P, Rossmeisl JH, Robertson J, Gibo DM. New agents for targeting of IL-13RA2 expressed in primary human and canine brain tumors. *PLoS One*. 2013 Oct 16;8(10):e77719. <http://dx.doi.org/10.1371/journal.pone.0077719>
33. Candolfi M, Curtin JF, Nichols W, Muhammad AG, King GD, Pluhar GE, et al. Intracranial glioblastoma models in preclinical neuro-oncology: Neuropathological characterization and tumor progression. *J Neurooncol*. 2007 Nov;85(2):133–48. <http://dx.doi.org/10.1007/s11060-007-9400-9>

34. Dickinson PJ, LeCouteur RA, Higgins RJ, Bringas JR, Larson RF, Yamashita Y, et al. Canine spontaneous glioma: A translational model system for convection-enhanced delivery. *Neuro Oncol.* 2010;12:928–40. <http://dx.doi.org/10.1093/neuonc/noq046>
35. Dickinson PJ, LeCouteur RA, Higgins RJ, Bringas JR, Roberts B, Larson RF, et al. Canine model of convection-enhanced delivery of liposomes containing CPT-11 monitored with real-time magnetic resonance imaging: Laboratory investigation. *J Neurosurgery.* 2008;108:989–98. <http://dx.doi.org/10.3171/JNS.2008.108.5.0989>
36. Okano F, Storkus WJ, Chambers WH, Pollack IF, Okada H. Identification of a novel HLA-A*0201-restricted, cytotoxic T lymphocyte epitope in a human glioma-associated antigen, interleukin 13 receptor alpha 2 chain. *Clin Cancer Res.* 2002;8:2851–5.
37. Mintz A, Gibo DM, Madhankumar AB, Cladel NM, Christensen ND, Debinski W. Protein and DNA-based active immunotherapy targeting interleukin 13 receptor alpha 2. *Cancer Biother Radiopharm.* 2008;23:581–9. <http://dx.doi.org/10.1089/cbr.2008.0462>
38. Zhou G, Ye G-J, Debinski W, Roizman B. Genetic engineering of a herpes virus 1 vector dependent on the IL-13R-2 receptor for entry into cells: Interaction of glycoprotein D with its receptors is independent of the fusion of the envelope and the plasma membrane. *Proc Natl Acad Sci.* 2002;99:15124–15129. <http://dx.doi.org/10.1073/pnas.232588699>
39. Kahlon KS, Brown C, Cooper LJJ, Raubitschek A, Forman SJ, Jensen MC. Specific recognition and killing of glioblastoma multiforme by interleukin 13-zetakine redirected cytolytic T cells. *Cancer Res.* 2004;64:9160–7. <http://dx.doi.org/10.1158/0008-5472.CAN-04-0454>
40. Chunbin L, Hall WA, Jin N, Todhunter DA, Panoskaltis-Mortari A, Vallera DA. Targeting glioblastoma multiforme with an IL-13/diphtheria toxin fusion protein *in vitro* and *in vivo* in nude mice. *Prot Engin.* 2002;15:419–427.
41. Debinski W, Gibo DM, Kealisher A, Puri RK. Novel anti-brain tumor cytotoxins specific for cancer cells. *Nature Biotech.* 1998;16:449–53. <http://dx.doi.org/10.1038/nbt0598-449>
42. Mintz A, Gibo DM, Madhankumar AB, Debinski W. Molecular targeting with recombinant cytotoxins of interleukin-13 receptor alpha-2-expressing glioma. *J Neuro-Oncol.* 2003;64:117–23. <http://dx.doi.org/10.1007/BF02700026>
43. Ulasov IV, Tyler MA, Han Y, Glasgow JN, Lesniak MS. Novel recombinant adenoviral vector that targets the interleukin-13 receptor alpha2 chain permits effective gene transfer to malignant glioma. *Hum Gene Ther.* 2007;18:118–29. <http://dx.doi.org/10.1089/hum.2006.146>
44. Brown CE, Alizadeh D, Starr R, Weng L, Wagner JR, Naranjo A, et al. Regression of glioblastoma after chimeric antigen receptor T-cell therapy. *N Engl J Med.* 2016 Dec 29;375(26):2561–9. <http://dx.doi.org/10.1056/NEJMoa1610497>
45. Balyasnikova IV, Wainwright DA, Solomaha E, Lee G, Han Y, Thaci B, Lesniak MS. Characterization and immunotherapeutic implications for a novel antibody targeting interleukin (IL)-13 receptor $\alpha 2$. *J Biol Chem.* 2012;287(36):30215–27. <http://dx.doi.org/10.1074/jbc.M112.370015>
46. Kong S, Sengupta S, Tyler B, Bais AJ, Ma Q, Doucette S, et al. Suppression of human glioma xenografts with second-generation IL13R-specific chimeric antigen receptor-modified T cells. *Clin Cancer Res.* 2012 Nov 1;18(21):5949–60. <http://dx.doi.org/10.1158/1078-0432.CCR-12-0319>
47. Okada H, Kalinski P, Ueda R, Hoji A, Kohanbash G, Donegan TE, et al. Induction of CD8+ T-cell responses against novel glioma-associated antigen peptides and clinical activity by vaccinations with $\{\alpha\}$ -type 1 polarized dendritic cells and polyinosinic-polycytidylic acid stabilized by lysine and carboxymethylcellulose in patients with recurrent malignant glioma. *J Clin Oncol.* 2011 Jan 20;29(3):330–6. <http://dx.doi.org/10.1200/JCO.2010.30.7744>
48. Okada H, Kalinski P, Ueda R, Hoji A, Kohanbash G, Donegan TE, et al. Antigenic profiling of glioma cells to generate allogeneic vaccines or dendritic cell-based therapeutics. *Clin Cancer Res.* 2007;13:566–75. <http://dx.doi.org/10.1158/1078-0432.CCR-06-1576>
49. Turtle CJ, Hudecek M, Jensen MC, Riddell SR. Engineered T cells for anti-cancer therapy. *Curr Opin Immunol.* 2012 Oct;24(5):633–9. <http://dx.doi.org/10.1016/j.coi.2012.06.004>
50. Allen C, Paraskevovou G, Iankov I, Giannini C, Schroeder M, Sarkaria J, et al. Interleukin-13 displaying retargeted oncolytic measles virus strains have significant activity against gliomas with improved specificity. *Mol Ther.* 2008 Sep;16(9):1556–64. <http://dx.doi.org/10.1038/mt.2008.152>

51. Wykosky J, Debinski W. The EphA2 receptor and ephrinA1 ligand in solid tumors: Function and therapeutic targeting. *Mol Cancer Res.* 2008;6:1795–806. <http://dx.doi.org/10.1158/1541-7786.MCR-08-0244>
52. Hatano M, Eguchi J, Tatsumi T, Kuwashima N, Dusak JE, Kinch MS, et al. EphA2 as a glioma-associated antigen: A novel target for glioma vaccines. *Neoplasia.* 2005 Aug;7(8):717–22. <http://dx.doi.org/10.1593/neo.05277>
53. Debinski W, Obiri NI, Pastan I, Puri RK. A novel chimeric protein composed of interleukin 13 and *Pseudomonas* exotoxin is highly cytotoxic to human carcinoma cells expressing receptors for interleukin 13 and interleukin 4. *J Biol Chem.* 1995;270:16775–80. <http://dx.doi.org/10.1074/jbc.270.28.16775>
54. Debinski W, Obiri NI, Powers SK, Pastan I, Puri RK. Human glioma cells overexpress receptor for interleukin 13 and are extremely sensitive to a novel chimeric protein composed of interleukin 13 and *Pseudomonas* exotoxin. *Clin Cancer Res.* 1995;1:1253–8.
55. Debinski W, Tatter SB. Convection-enhanced delivery for the treatment of brain tumors. *Expert Rev Neurother.* 2009;9:1519–27. <http://dx.doi.org/10.1586/ern.09.99>
56. Ferluga S, Tomé CM, Herpai DM, D'Agostino R, Debinski W. Simultaneous targeting of Eph receptors in glioblastoma. *Oncotarget.* 2016 Sep 13;7(37):59860–76. <http://dx.doi.org/10.18632/oncotarget.10978>
57. Hatano M, Kuwashima N, Tatsumi T, Dusak JE, Nishimura F, Reilly KM, et al. Vaccination with EphA2-derived T cell-epitopes promotes immunity against both EphA2-expressing and EphA2-negative tumors. *J Transl Med.* 2004 Nov 24;2(1):40. <http://dx.doi.org/10.1186/1479-5876-2-40>
58. Brown CE, Warden CD, Starr R, Deng X, Badie B, Yuan YC, et al. Glioma IL13R α 2 is associated with mesenchymal signature gene expression and poor patient prognosis. *PLoS One.* 2013 Oct 18;8(10):e77769. <http://dx.doi.org/10.1371/journal.pone.0077769>
59. Brown CE, Starr R, Aguilar B, Shami AF, Martinez C, D'Apuzzo M, et al. Stem-like tumor-initiating cells isolated from IL-13R α 2 expressing gliomas are targeted and killed by IL13-zetakine-redirected T Cells. *Clin Cancer Res.* 2012;18:2199–209. <http://dx.doi.org/10.1158/1078-0432.CCR-11-1669>
60. Brown CE, Starr R, Martinez C, Aguilar B, D'Apuzzo M, Todorov I, et al. Recognition and killing of brain tumor stem-like initiating cells by CD8+ cytolytic T cells. *Cancer Res.* 2009;69(23):8886–93. <http://dx.doi.org/10.1158/0008-5472.CAN-09-2687>
61. Nguyen V, Conyers JM, Zhu D, Gibo DM, Dorsey JF, Debinski W, et al. IL-13R α 2-targeted therapy escapees: Biologic and therapeutic implications. *Transl Oncol.* 2011;4:390–400. <http://dx.doi.org/10.1593/tlo.111175>
62. Binda E, Visioli A, Giani F, Lamorte G, Copetti M, Pitter KL, et al. The EphA2 receptor drives self-renewal and tumorigenicity in stem-like tumor-propagating cells from human glioblastomas. *Cancer Cell.* 2012;22(6):765–80. <http://dx.doi.org/10.1016/j.ccr.2012.11.005>
63. Miao H, Gale NW, Guo H, Qian J, Petty A, Kaspar J, et al. EphA2 promotes infiltrative invasion of glioma stem cells *in vivo* through cross-talk with Akt and regulates stem cell properties. *Oncogene.* 2015 Jan 29;34(5):558–67. <http://dx.doi.org/10.1038/onc.2013.590>
64. Day BW, Stringer BW, Al-Ejeh F, Ting MJ, Wilson J, Ensbey KS, et al. EphA3 maintains tumorigenicity and is a therapeutic target in glioblastoma multiforme. *Cancer Cell.* 2013;23(2):238–48. <http://dx.doi.org/10.1016/j.ccr.2013.01.007>
65. Himanen JP, Chumley MJ, Lackmann M, Li C, Barton WA, Jeffrey PD, et al. Repelling class discrimination: Ephrin-A5 binds to and activates EphB2 receptor signaling. *Nat Neurosci.* 2004 May;7(5):501–509. <http://dx.doi.org/10.1038/nm1237>
66. Nakada M, Niska JA, Miyamori H, McDonough WS, Wu J, Sato H, Berens ME. The phosphorylation of EphB2 receptor regulates migration and invasion of human glioma cells. *Cancer Res.* 2004 May 1;64(9):3179–3185. <http://dx.doi.org/10.1158/0008-5472.CAN-03-3667>
67. Hsi LC, Kundu S, Palomo J, Xu B, Ficco R, Vogelbaum MA, Cathcart MK. Silencing IL-13R α 2 promotes glioblastoma cell death via endogenous signaling. *Mol Cancer Ther.* 2011 Jul;10(7):1149–60. <http://dx.doi.org/10.1158/1535-7163.MCT-10-1064>
68. Tu M, Wange W, Cai L, Zhu P, Gao Z, Zheng W. IL-13 receptor α 2 stimulates human glioma cell growth and metastasis through the Src/PI3K/Akt/mTOR signaling pathway. *Tumour Biol.* 2016 Nov;37(11):14701–9. <http://dx.doi.org/10.1007/s13277-016-5346-x>

69. Wykosky J, Gibo DM, Stanton C, Debinski W. EphA2 as a novel molecular marker and target in glioblastoma multiforme. *Mol Cancer Res*. 2005;3(10):541–51. <http://dx.doi.org/10.1158/1541-7786.MCR-05-0056>
70. Wykosky J, Palma E, Gibo DM, Ringer S, Turner CP, Debinski W. Soluble monomeric ephrinA1 is released from tumor cells and is a functional ligand for the EphA2 receptor. *Oncogene*. 2008;27:7260–73. <http://dx.doi.org/10.1038/onc.2008.328>
71. Wykosky J, Gibo DM, Debinski W. A novel, potent, and specific ephrinA1-based cytotoxin against EphA2 receptor-expressing tumor cells. *Mol Cancer Ther*. 2007;6:3208–18. <http://dx.doi.org/10.1158/1535-7163.MCT-07-0200>
72. Beckmann MP, Cerretti DP, Baum P, Vanden Bos T, James L, Farrah T, et al. Molecular characterization of a family of ligands for eph-related tyrosine kinase receptors. *EMBO J*. 1994;13:3757–62.
73. Xu Q, Wilkinson DG. Eph-related receptors and their ligands: Mediators of contact dependent cell interactions. *J Mol Med*. 1997;75:576–86. <http://dx.doi.org/10.1007/s001090050142>
74. Kullander K, Klein R. Mechanisms and functions of Eph and ephrin signalling. *Nat Rev Mol Cell Biol*. 2002;3:475–86. <http://dx.doi.org/10.1038/nrm856>
75. Pasquale EB. Eph receptor signalling casts a wide net on cell behaviour. *Nat Rev Mol Cell Biol*. 2005;6:462–75. <http://dx.doi.org/10.1038/nrm1662>
76. Liu F, Park PJ, Lai W, Maher E, Chakravarti A, Durso L, et al. A genome-wide screen reveals functional gene clusters in the cancer genome and identifies EphA2 as a mitogen in glioblastoma. *Cancer Res*. 2006;66:10815–23. <http://dx.doi.org/10.1158/0008-5472.CAN-06-1408>
77. Li X, Wang Y, Wang Y, Zhen H, Yang H, Fei Z, et al. *Tumour Biol*. 2007;28:165–72. <http://dx.doi.org/10.1159/000103010>
78. Wang LF, Fokas E, Bieker M, Rose F, Rexin P, Zhu Y, et al. Increased expression of EphA2 correlates with adverse outcome in primary and recurrent glioblastoma multiforme patients. *Oncol Rep*. 2008;19:151–6. <http://dx.doi.org/10.3892/or.19.1.151>
79. Beauchamp A, Debinski W. Ephs and ephrins in cancer: Ephrin-A1 signalling. *Semin Cell Dev Biol*. 2012 Feb;23(1):109–15. <http://dx.doi.org/10.1016/j.semdb.2011.10.019>
80. Debinski W, Wykosky J. Molecular targeting of IL-13R-2 and EphA2 receptor in GBM. In: van Meir E, editor. *CNS cancer: Models, prognostic factors and targets*. New York: Springer; 2009. p. 841–858.
81. Debinski W. Drug cocktails for effective treatment of glioblastoma multiforme. *Expert Rev Neurother*. 2008;8(4):515–517. <http://dx.doi.org/10.1586/14737175.8.4.515>
82. Li W, Graeber MB. The molecular profile of microglia under the influence of glioma. *Neuro Oncol*. 2012;14(8):958–78. <http://dx.doi.org/10.1093/neuonc/nos116>
83. Chen R, Nishimura MC, Bumbaca SM, Kharbanda S, Forrest WF, Kasman IM, et al. A hierarchy of self-renewing tumor-initiating cell types in glioblastoma. *Cancer Cell*. 2010 Apr 13;17(4):362–75. <http://dx.doi.org/10.1016/j.ccr.2009.12.049>
84. Laske DW, Youle RJ, Oldfield EH. Tumor regression with regional distribution of the targeted toxin TF-CRM107 in patients with malignant brain tumors. *Nature Med*. 1997;3:1362–8. <http://dx.doi.org/10.1038/nm1297-1362>
85. Debinski W. Molecular targeting of brain tumors with cytotoxins. In: Lorberboum-Galski H, Lazarovici P, editors. *Chimeric toxins*. Reading, UK: Harwood Academic Publishers Reading, UK; 2002. p. 222–246.
86. Debinski W. Local treatment of brain tumors with targeted chimera cytotoxic proteins. *Cancer Invest*. 2002;20:801–9. <http://dx.doi.org/10.1081/CNV-120003545>
87. Wersall P, Ohlsson I, Biberfeld P, Collins V, von Krusenstjerna Larsson S, Mellstedt H, et al. Intratumoral infusion of the monoclonal antibody, mAb 425, against the epidermal-growth-factor receptor in patients with advanced malignant glioma. *Cancer Immunol Immunother*. 1997;44:157–64. <http://dx.doi.org/10.1007/s002620050368>
88. Raghavan R, Brady ML, Rodriguez-Ponce MI, Hartlep A, Pedain C, Sampson JH. Convection-enhanced delivery of therapeutics for brain disease, and its optimization. *Neurosurg Focus*. 2006 Apr 15;20(4):E12. <http://dx.doi.org/10.3171/foc.2006.20.4.7>
89. Yun J, Rothrock RJ, Canoll P, Bruce JN. Convection-enhanced delivery for targeted delivery of anti-glioma agents: The translational experience. *J Drug Deliv*. 2013;2013:107573.
90. Vogelbaum MA, Iannotti CA. Convection-enhanced delivery of therapeutic agents into the brain. *Handb Clin Neurol*. 2012;104:355–62. <http://dx.doi.org/10.1016/B978-0-444-52138-5.00023-2>

91. Chen PY, Ozawa T, Drummond DC, Kalra A, Fitzgerald JB, Kirpotin DB, et al. Comparing routes of delivery for nanoliposomal irinotecan shows superior anti-tumor activity of local administration in treating intracranial glioblastoma xenografts. *Neuro Oncol.* 2013 Feb;15(2):189–97. <http://dx.doi.org/10.1093/neuonc/nos305>
92. Richardson RM, Kells AP, Martin AJ, Larson PS, Starr PA, Piferi PG, et al. Novel platform for MRI-guided convection-enhanced delivery of therapeutics: Preclinical validation in nonhuman primate brain. *Stereotact Funct Neurosurg.* 2011;89(3):141–51. <http://dx.doi.org/10.1159/000323544>
93. Mehta AI, Choi BD, Raghavan R, Brady M, Friedman AH, Bigner DD, et al. Imaging of convection enhanced delivery of toxins in humans. *Toxins (Basel).* 2011 Mar;3(3):201–206. <http://dx.doi.org/10.3390/toxins3030201>
94. Sampson JH, Brady M, Raghavan R, Mehta AI, Friedman AH, Reardon DA, et al. Colocalization of gadolinium-diethylene triamine pentaacetic acid with high-molecular-weight molecules after intracerebral convection-enhanced delivery in humans. *Neurosurgery.* 2011 Sep;69(3):668–76. <http://dx.doi.org/10.1227/NEU.0b013e3182181ba8>
95. Debinski W, Tatter SB. Convection-enhanced delivery to achieve widespread distribution of viral vectors: Predicting clinical implementation. *Curr Opin Mol Ther.* 2010 Dec;12(6):647–53.
96. Vogelbaum MA, Aghi MK. Convection-enhanced delivery for the treatment of glioblastoma. *Neuro Oncol.* 2015 Mar;17(Suppl 2):ii3–ii8. <http://dx.doi.org/10.1093/neuonc/nou354>
97. Chen TC, Napolitano GR, Adell F, Schönthal AH, Shachar Y. Development of the metronomic biofeedback pump for leptomeningeal carcinomatosis: Technical note. *J Neurosurg.* 2015 Aug;123(2):362–72. <http://dx.doi.org/10.3171/2014.10.JNS14343>
98. Wainwright DA, Nigam P, Thaci B, Dey M, Lesniak MS. Recent developments on immunotherapy for brain cancer. *Expert Opin Emerg Drugs.* 2012 Jun;17(2):181–202. <http://dx.doi.org/10.1517/14728214.2012.679929>
99. Wu A, Wei J, Kong LY, Wang Y, Priebe W, Qiao W, et al. Glioma cancer stem cells induce immunosuppressive macrophages/microglia. *Neuro Oncol.* 2010 Nov;12(11):1113–25. <http://dx.doi.org/10.1093/neuonc/noq082>
100. Wainwright DA, Dey M, Chang A, Lesniak MS. Targeting tregs in malignant brain cancer: Overcoming IDO. *Front Immunol.* 2013 May 15;4:116. <http://dx.doi.org/10.3389/fimmu.2013.00116>
101. Avril T, Vauleon E, Tanguy-Royer S, Mosser J, Quillien V. Mechanisms of immunomodulation in human glioblastoma. *Immunotherapy.* 2011 Apr;3(4 Suppl):42–4. <http://dx.doi.org/10.2217/imt.11.39>
102. Ochiai H, Archer GE, Herndon JE 2nd, Kuan CT, Mitchell DA, Bigner DD, et al. EGFRvIII-targeted immunotoxin induces antitumor immunity that is inhibited in the absence of CD4+ and CD8+ T cells. *Cancer Immunol Immunother.* 2008 Jan;57(1):115–21. <http://dx.doi.org/10.1007/s00262-007-0363-7>
103. Lang FF, Conrad C, Gomez-Manzano C, Tufaro F, Yung WKA, Sawaya R, et al. First-in-human Phase I clinical trial of oncolytic delta-24-RGD (DNX-2401) with biological endpoints: Implications for viro-immunotherapy. *Neuro Oncol.* 2014;16(Suppl 3):iii39. <http://dx.doi.org/10.1093/neuonc/nou208.61>
104. Harrington KJ, Andtbacka RH, Collichio F, Downey G, Chen L, Szabo Z, et al. Efficacy and safety of talimogene laherparepvec versus granulocyte-macrophage colony-stimulating factor in patients with stage IIIB/C and IVM1a melanoma: Subanalysis of the Phase III OPTiM trial. *Oncotargets Ther.* 2016 Nov 16;9:7081–7093.
105. Couzin-Frankel J. Breakthrough of the year 2013. *Cancer immunotherapy. Science.* 2013 Dec 20;342(6165):1432–3. <http://dx.doi.org/10.1126/science.342.6165.1432>
106. Hu-Lieskovan S, Robert L, Homet Moreno B, Ribas A. Combining targeted therapy with immunotherapy in BRAF-mutant melanoma: Promise and challenges. *J Clin Oncol.* 2014 Jul 20;32(21):2248–54. <http://dx.doi.org/10.1200/JCO.2013.52.1377>
107. Kunwar S, Prados MD, Chang SM, Berger MS, Lang FF, Piepmeier JM, et al. Direct intracerebral delivery of cintredekin besudotox (IL13-PE38QQR) in recurrent malignant glioma: A report by the Cintredekin Besudotox Intracranial Study Group. *J Clin Oncol.* 2007 Mar 1;25(7):837–44. <http://dx.doi.org/10.1200/JCO.2006.08.1117>
108. Candolfi M, Xiong W, Yazig K, Liu C, Muhammad AK, Puntel M, et al. Gene therapy-mediated delivery of targeted cytotoxins for glioma therapeutics. *Proc Natl Acad Sci.* 2010;107:20021–6. <http://dx.doi.org/10.1073/pnas.1008261107>

109. Thompson J, Debinski W. Mutants of interleukin 13 with altered reactivity toward IL13 receptors. *J Biol Chem.* 1999;274:29944–50. <http://dx.doi.org/10.1074/jbc.274.42.29944>
110. Madhankumar AB, Mintz A, Debinski W. Alanine scanning mutagenesis of a-helix D segment of interleukin-13 reveals new functionally important residues of the cytokine. *J Biol Chem.* 2002;277:43194–205. <http://dx.doi.org/10.1074/jbc.M205047200>
111. Madhankumar AB, Mintz A, Debinski W. Interleukin 13 mutants of enhanced avidity toward the glioma-associated receptor, IL13Ralpha2. *Neoplasia.* 2004 Jan–Feb;6(1):15–22. [http://dx.doi.org/10.1016/S1476-5586\(04\)80049-6](http://dx.doi.org/10.1016/S1476-5586(04)80049-6)
112. Sonawane P, Choi YA, Pandya H, Herpai DM, Fokt I, Priebe W, et al. Novel molecular multilevel targeted antitumor agents. *Cancer Transl Med.* 2017;3(3):69–79.

18 Maximizing Local Access to Therapeutic Deliveries in Glioblastoma. Part II: Arborizing Catheter for Convection-Enhanced Delivery in Tissue Phantoms

EGLEIDE Y. ELENES¹ • CHRISTOPHER G. RYLANDER^{1,2}

¹Department of Biomedical Engineering, The University of Texas at Austin, TX, USA; ²Department of Mechanical Engineering, The University of Texas at Austin, TX, USA

Author for correspondence: Christopher Rylander, Department of Mechanical Engineering, The University of Texas at Austin, 204 E. Dean Keeton Street, Stop C2200, Austin, TX 78712-1591, USA. E-mail: cgr@austin.utexas.edu

Doi: <http://dx.doi.org/10.15586/codon.glioblastoma.2017.ch18>

Abstract: Convection-enhanced delivery (CED) is the process of local, pressure-driven flow of drugs into brain parenchyma containing tumor tissue, resulting in greater distribution of the infused drugs compared to diffusion-dependent therapies. Nevertheless, even with the advantage of CED over simple diffusion, the large volumes necessary to target entire tumors and peritumor volumes have been previously unachievable with currently available catheters. We present a novel, multiport, arborizing catheter designed specifically for improving drug distribution into the brain. We evaluated the performance of the arborizing catheter by quantifying volume dispersed (V_d) and mean distribution ratios ($V_d:V_i$) in infusion studies

In: *Glioblastoma*. Steven De Vleeschouwer (Editor), Codon Publications, Brisbane, Australia ISBN: 978-0-9944381-2-6; Doi: <http://dx.doi.org/10.15586/codon.glioblastoma.2017>

Copyright: The Authors.

Licence: This open access article is licenced under Creative Commons Attribution 4.0 International (CC BY 4.0). <https://creativecommons.org/licenses/by-nc/4.0/>

using agarose brain phantoms and compared results to a single-port catheter. Three experimental groups were evaluated: (i) single-port infusions at 1 $\mu\text{L}/\text{min}$; (ii) single-port infusions at 7 $\mu\text{L}/\text{min}$; and (iii) seven-port arborizing catheter infusions at 1 $\mu\text{L}/\text{min}/\text{port}$. Significantly greater V_d was calculated for the arborizing catheter group ($10.47 \pm 1.07 \text{ cm}^3$) compared with the single-port catheter groups at the low- and high-flow rates ($2.36 \pm 0.21 \text{ cm}^3$ and $5.14 \pm 0.56 \text{ cm}^3$), respectively. $V_d:V_i$ for the arborizing catheter was 37% lower than the single-port catheter at 1 $\mu\text{L}/\text{min}$, but 100% greater than the single-port catheter at 7 $\mu\text{L}/\text{min}$. The multiport, arborizing catheter produced the greatest distribution of the infusate, which would be advantageous for CED; however, it did not exhibit the greatest distribution ratio, likely due to overlapping distribution volumes from the multiple individual ports.

Key words: Blood–brain barrier; Catheters; Convection-enhanced delivery; Glioblastoma; Infusate

Introduction

Distribution of therapeutic agents within the central nervous system (CNS) is limited and challenging with existing drug delivery techniques. Systemic delivery of drugs is nontargeted and has been associated with systemic toxicity. Furthermore, the blood–brain barrier (BBB) hinders drugs from reaching the CNS in sufficient quantities (1). Technologies such as catheters and pumps, intrathecal injections, and drug-impregnated polymers are challenged by interstitial fluid pressure and are limited to the diffusivity and molecular weight of the therapeutic. In an effort to address the challenges of current drug-delivery methods, convection-enhanced delivery (CED) was pioneered at the National Institute of Neurological Disorders and Stroke, as an alternate approach to deliver large concentrations of macromolecules directly into the brain parenchyma, effectively circumventing the BBB (2, 3). CED permits local delivery of high-molecular weight molecules via a small-caliber catheter inserted through a burr hole created in the skull and dura. This technique relies on pressure-driven bulk flow of the fluid that is pushed primarily through the interstitial space, achieving high concentrations of the infusate, distributed centimeters into the tissue, an order of magnitude greater than with diffusion alone (2, 4). Moreover, CED per se does not lead to cerebral edema and is unaffected by capillary loss or metabolism of the macromolecule (5). With these initial studies, CED was established as a viable method for providing regional distribution of large molecules, such as proteins and some conventional chemotherapeutic agents, in the brain (6–9). Compared with other therapies, CED minimizes systemic and CNS toxicity by local delivery of high concentrations of therapeutics directly to the brain tissue and has led to treatment applications in several cerebral disorders, including Parkinson's (10, 11), epilepsy (12), Alzheimer's (13, 14), and malignant gliomas (4, 5, 15–21).

Although distribution of macromolecules is more effective with CED than with diffusion-based therapies and positive results in pre-clinical and early clinical trials for malignant gliomas (7, 8, 18, 22–24) showed promise of this technique,

progress toward clinical translation has been challenged by inadequate results in high-profile, Phase III clinical trials (16). The PRECISE trial was a study of the experimental drug IL13-PE38QQR, a tumor-targeting agent made by combining the human protein IL13 with a portion of the bacterial toxin *Pseudomonas* exotoxin, which was continuously infused directly into the brain for treatment in adult patients with glioblastoma at first recurrence. Retrospective investigations of the study's results have revealed that overly ambitious study endpoints, inaccurate catheter positioning, and poor drug distribution are likely explanations behind the PRECISE trial's failure to meet clinical endpoints (25). Sampson et al. estimated that, on average, only approximately 20% of the 2-cm tumor margins surrounding the resection cavity were covered with the therapeutic (25). The inability of CED to perfuse drugs over large volumes, including margins beyond the primary enhancing tumor detected by magnetic resonance imaging, is highly problematic as these margins contain infiltrative malignant cells that may be responsible for regrowth of the tumor.

Arborizing Catheter for CED in Tissue Phantoms

OPTIMIZATION OF CATHETERS USED FOR CED

In light of the results of various clinical trials, researchers have turned to examine whether the available technology used to perform CED is suited to overcome the unique challenges hindering drug distribution in the brain. The anatomical heterogeneity of the brain and tumor tissue, differences in permeability between white and gray matter, and issues arising from low-pressure “sinks,” such as cerebrospinal fluid spaces, can all inhibit drug distribution with CED. Specifically, the design of the catheters used to perform the infusions has undergone scrutiny (26–29). In the PRECISE trial, investigators performed the treatment using commercially available catheters designed for different medical applications. Similarly, various other CED studies have been limited by the “off-label-use” of various commercial catheters that may not possess the capability to effectively perfuse drugs over large tissue volumes (Table 1). In order to achieve targeted delivery and infuse greater tumor volumes, CED often requires insertions of multiple catheters, thus increasing the risk of trauma to healthy neurological tissue and increasing the probability of seeding malignant cells in healthy tissue along the needle tract. Thus, researchers have begun to investigate using catheters that offer multiple ports of infusion originating from a single insertion tract (Cleveland Multiport Catheter™, Infuseon Therapeutics, Inc.) (30). Others have opted for a different approach and are investigating chronic delivery of therapeutics using catheters that are permanently implanted, and accessed via a port on the side of the cranium (31). Another common drawback of CED is reflux of drug along the insertion tract, which results in ineffective drug distribution and premature termination of the CED therapy. Reflux-arresting properties have been investigated and incorporated in the design of catheters such as a “step change,” in which the diameter of the catheter changes drastically along the distal tip of the catheter, which has shown to mitigate reflux during CED (26, 27, 32–34).

It is our hypothesis that addressing the challenge of poor drug distribution can potentially improve the success of CED. Here, we present the design and

TABLE 1

Catheters Used in CED Studies

Catheter	Company	Study
Barium-impregnated one-port infusion catheter	Medtronic® PS Medical (Goleta, CA, USA)	Phase I/II (35)
Barium-impregnated one-port infusion catheter	Vygon US LLC (Valley Forge, PA, USA)	Phase III (PRECISE) (36)
Reflux-preventing neuro-ventricular cannula	SmartFlow® MRI Interventions (Irvine, CA, USA)	Phase I (37)
Cleveland Multiport Catheter™	Infuseon Therapeutics, Inc (Cleveland, OH, USA)	Early Phase I (30)

evaluation of an arborizing catheter that enhances dispersal of the infusate. Once the arborizing catheter is inserted into the skull, individual microneedles can be deployed, arborizing from a single cannula, providing multiple infusion ports per one primary cannula insertion tract. These individual microneedles can be positioned independently, at various insertion depths, to control the location of infusion. Upon completion of the therapy, the microneedles can be fully retracted back into the cannula; thus, the tumor-contacting surfaces of needles would remain completely shielded within the primary cannula, reducing the probability of tumor cell-seeding in healthy brain tissue and preventing mechanical damage to surrounding tissue when extracting the catheter. Furthermore, the arborizing catheter has an inherent step change at the interface between the microneedles and the primary cannula to help reduce the occurrence of reflux during the infusion. We hypothesize that with multiple, separated infusion ports, the arborizing catheter will achieve greater volumetric dispersal of the infusate and greater mean distribution ratio (volume dispersed to the total volume infused), compared to a single-port catheter.

ARBORIZING CATHETER DESIGN AND MANUFACTURING

Early-stage prototypes for the arborizing catheter (Figure 1A, B) consisted of a primary cannula with an outer diameter of 3 mm (38). The cannula was manufactured by bonding seven aligned biocompatible polyether ether ketone (PEEK) tubes (41568-L4, Analytical Sales & Services; OD 794 μm \times ID 381 μm) with a light-cured medical grade adhesive (3972, Loctite®). At the distal end of the cannula, the PEEK tubes were twisted using a custom-designed fixture. The twist at the end of the cannula caused the microneedles to branch out at an angle of up to 20° (angle of peripheral needles from cannula axis) when they were deployed. Once the adhesive was cured, the distal end of the cannula was polished to a smooth conical tip (Figure 1B). The cannula was made to house seven microneedles made from flexible, hollow silica optical fibers (TSP180375, General Separation Technologies) (OD 375 μm \times ID 180 μm) polished to a smooth bevel tip (Figure 1C). The distal end of each microneedle was attached

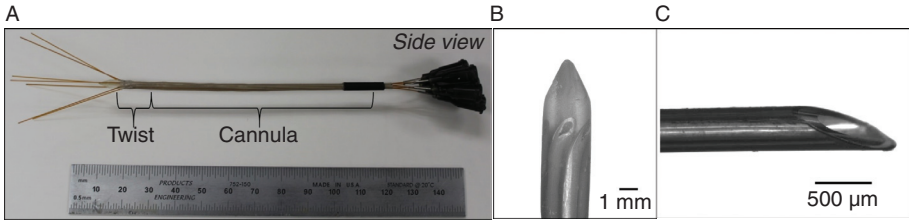


Figure 1 Images of the arborizing catheter prototype. (A) Side view of the arborizing catheter with deployed microneedles at the distal end of the cannula (left) where the twisted PEEK tubing is labeled. At the proximal end of the cannula (right), the proximal end of the microneedles is shown with attached Luer lock adapters. (B) Magnified image showing twisted PEEK tubing at distal end of the cannula, which allowed microneedle deflection. (C) Magnified image of a polished, bevel-tipped microneedle.

to a 22G hypodermic needle with a Luer lock adapter to allow for easy connection to small bore extension tubing. When deploying the microneedles, the small diameter of the needles compared to the primary cannula created a step change that helped arrest reflux as demonstrated in other catheters with an incorporated step change (32, 34).

MANUFACTURING OF SINGLE-PORT MICRONEEDLE CATHETER

We manufactured single-port catheters in order to test our hypothesis and compare the performance of the single-port catheter versus the arborizing catheter prototypes in infusion studies. The single-port catheter consisted of a single microneedle (OD 375 μm × ID 180 μm), 3 cm in length, attached to a 22 G hypodermic needle (0.75 in. length) with a Luer lock. The distal end of the single-port catheter was polished to a smooth bevel tip.

EVALUATION OF ARBORIZING CATHETER PROTOTYPE IN TISSUE PHANTOMS

Agarose tissue phantoms were prepared for infusion studies. An agarose solution was mixed at 0.6% (w/w) by reconstituting agarose powder in deionized water. The solution was heated to a low boil and continuously stirred until all the agarose powder was completely mixed. The agarose was allowed to cool at room temperature and then poured into transparent molds. For all experiments, the agarose solution was decanted into the mold, and the device of interest (single or arborizing catheter) was inserted in the solution while still liquid (approximately at 50°C). This casting method allowed a tight seal around the device and helped mitigate reflux. The agarose was allowed to set at room temperature and infusion began when the temperature of the agarose reached $23 \pm 2^\circ\text{C}$. For infusions using a single microneedle, a polystyrene mold (1.7 cm × 8.1 cm × 3.9 cm) with an open top was used, and for infusions using an arborizing catheter, a 10-cm cubic glass mold was used.

The goal of this study was to compare the volume dispersed and mean distribution ratio for a given infusion using a single-port catheter versus the arborizing

catheter, which is a multiport catheter consisting of seven microneedles. Using a programmable pump (PHD ULTRA™ Syringe Pump, Harvard Apparatus) to control volumetric flow rate, 5% (w/w) indigo carmine dye was infused in the agarose gel. As a baseline, the V_d and $V_d:V_i$ for a single-port catheter was determined at a flow rate of 1 $\mu\text{L}/\text{min}$ for 100 min. The mean distribution ratio ($V_d:V_i$) was calculated by dividing the V_d by the total infused volume (V_i) that was programmed in the syringe pump. A similar infusion was performed using the arborizing catheter. The flow rate for each microneedle was kept at 1 $\mu\text{L}/\text{min}/\text{needle}$. Finally, because the arborizing catheter consists of seven microneedles, each a delivery port, a third set of infusions was performed using a single-port catheter with seven times higher flow rate in order to compare V_d and $V_d:V_i$ when equal volumes of infusate were delivered to the tissue phantom (i.e., equivalent to the V_i for the arborizing catheter). To summarize, the three experimental groups were: (i) single-port infusions ($n = 5$) at a flow rate of 1 $\mu\text{L}/\text{min}$ for a total V_i of 100 μL ; (ii) single-port infusions ($n = 5$) at a flow rate of 7 $\mu\text{L}/\text{min}$ for a total V_i of 700 μL , and (iii) infusion with the arborizing catheter ($n = 5$) performed at 1 $\mu\text{L}/\text{min}/\text{needle}$ for a total V_i of 700 μL .

To evaluate the prototypes, a shadowgraphy experimental setup was used consisting of a clear stage with reflecting mirrors on the left side and bottom (Figure 2). For each infusion, the sample was placed on the stage and backlit

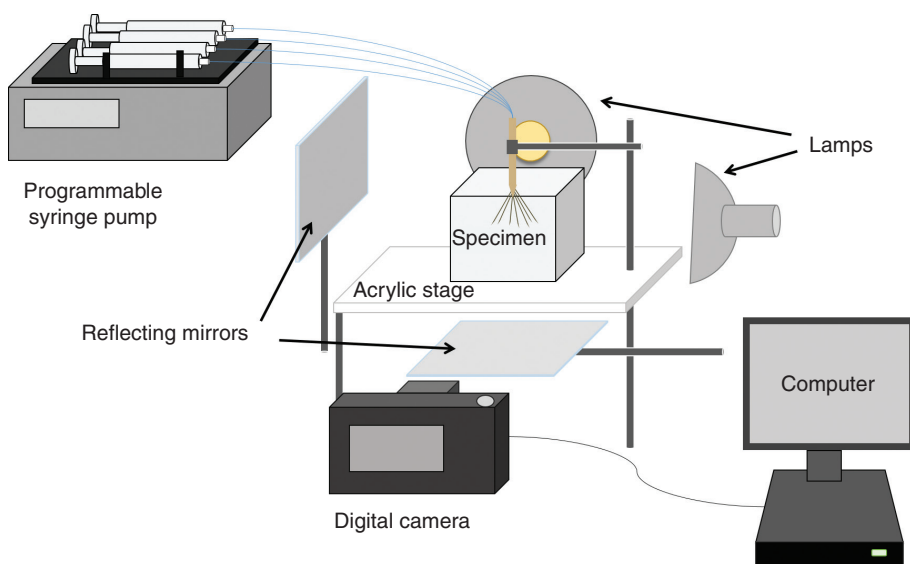


Figure 2 Shadowgraphy experimental setup. A programmable syringe pump is used to control the infusion of indigo carmine dye into agarose tissue phantoms placed on a clear acrylic stage backlit by lamps placed behind a light-diffusing sheet (not shown) to minimize variations in light intensity in each of the three views. A DSLR camera controlled by a desktop computer captures images of all three views (front view captured directly by the camera, and side and bottom views reflected to the camera by the angled mirrors) at a rate of one frame per minute.

with various lamps placed behind a light-diffusing sheet. A DSLR camera (Rebel T1i, Cannon), mounted in front of the stage, simultaneously captured images containing three views of the sample (front, side, and bottom), within the same frame, which were used to estimate the volume dispersed of the infused dye. Images were captured at a rate of one frame per minute for a total of 100 min. Metric scale bars were included in each image.

The images were then processed using an algorithm coded in Matlab (Mathworks, Natick, MA). Original images were cropped into three separate view frames: front, side, and bottom. Each cropped frame was then subtracted from the first image in the series to remove the background and thus only show the infusion volume. The differential images were converted to grayscale and then to binary images using image processing functions on Matlab that compute a global threshold value using Otsu's method (39). Pixels with intensity values below the threshold value were assigned black and pixels with intensity values greater than the threshold value were assigned white.

The volume dispersed for each cropped view frame was quantified using an image processing method previously described (40). Briefly, the method assumes that V_d is axisymmetric about the axis of single-port catheter or primary cannula of the arborizing catheter. The volume is discretized into elementary frustums of right circular cones. The algorithm counts the number of black pixels in each discretized section to calculate the bottom and top diameters of each frustum. A scale factor, extracted from the original image, was used to scale the pixel sizes of each binary image. The final volume was calculated by summing the volume of all the individual frustums. The final V_d for an infusion was reported as the average of the three views (front, side, and bottom) of each image. The mean distribution ratio was calculated by dividing the V_d by the total volume (V_i) that was programmed in the syringe pump. For infusions using the single-port catheter, the volume was observed to be relatively spherical. Therefore, only the front view of the images was used to calculate V_d .

Using the statistical software R (R Foundation for Statistical Computing, Vienna, Austria), one-way ANOVA tests were performed to analyze differences in V_d and $V_d:V_i$ for the three experimental groups assuming a significance level of 0.05. A Tukey–Kramer test was performed for pairwise comparisons among the three experimental groups.

ADVANTAGE OF SEVEN PORTS VERSUS SINGLE PORT

Results for volume dispersed and mean distribution ratio using a single-port catheter at 1 $\mu\text{L}/\text{min}$ for 100 min were 2.36 cm^3 and 23.61, respectively (Figure 3). When the flow rate for the single-port catheter was increased sevenfold, the V_d increased by only approximately 117.7% to 5.14 cm^3 , and $V_d:V_i$ decreased by approximately 69% to 7.34. However, comparisons of V_d and $V_d:V_i$ using the arborizing catheter show that we can achieve a V_d of 10.47 cm^3 and $V_d:V_i$ of 14.95 with our current catheter prototype. Compared to the single-port catheter at 7 $\mu\text{L}/\text{min}$, the values for V_d and $V_d:V_i$ achieved with the arborizing catheter were two times greater. It is important to note that the total V_i , across all microneedles in the arborizing catheter, was the same for the arborizing catheter and the single-port catheter at a 7 $\mu\text{L}/\text{min}$ flow rate experimental groups. This suggests that the

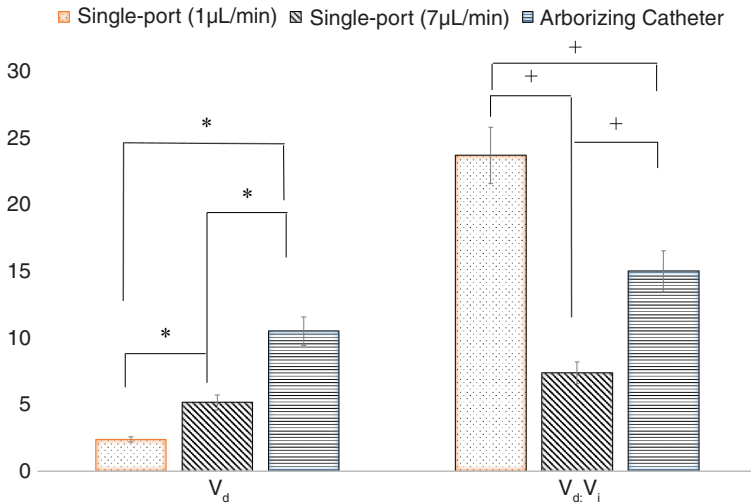


Figure 3 Statistical comparisons of average volume dispersed and mean distribution ratio results. A one-way ANOVA test was performed to analyze differences in average volume dispersed (V_d in cm³) and average mean distribution ratios ($V_d:V_i$) after 100 min of continuous infusion in agarose tissue phantoms for the three experimental groups: (i) single-port catheter at a flow rate of 1 μ L/min; (ii) single-port infusions at a flow rate of 7 μ L/min; (iii) arborizing catheter. A Tukey–Kramer test was performed for pairwise comparisons. Values for V_d were significantly different when each group was compared ($*P < 0.001$). Similarly, values for $V_d:V_i$ were significantly different from each other among the three groups (+ $P < 0.0001$).

arborizing catheter can achieve significantly ($P < 0.001$) greater volumetric dispersal of the infusate, when it is distributed among seven microneedles instead of coming out of a single port. This would be beneficial in CED because it is desirable to distribute the therapeutic agent throughout the entire tumor volume, including the surrounding tumor margins, in order to completely target any infiltrative malignant cells.

A visual representation of V_d for the three groups can be seen in Figure 4. In these binary images taken at the final time point of the infusion for each experimental group, the greater V_d achieved with the arborizing catheter can be appreciated. For this sample, the V_d of 12.13 cm³ obtained after 100 min is equivalent to coverage of a spherical volume with a 2.8-cm radius. The single-port catheter at the slower flow rate (1 μ L/min) resulted in the lowest V_d value. This is expected because the overall V_i for that group was seven times lower than for the single-port catheter at the higher flow rate (7 μ L/min) and for the arborizing catheter groups. However, it can be appreciated that even though the total infused volume for the single-port group at the highest flow rate (7 μ L/min) and the arborizing catheter were the same, the resultant volume dispersed was greater for the arborizing catheter.

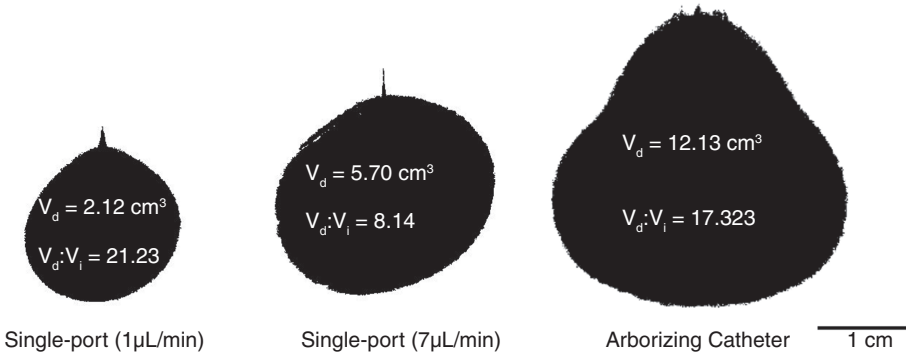


Figure 4 Representative volume dispersed for each experimental group after 100 min of continuous infusion. All images are of the front view captured directly by the DSLR camera. The volume dispersed (V_d) and mean distribution ratios ($V_d:V_i$) were calculated using an algorithm that discretizes the volume into elementary frustums of right circular cones (40). The final volume is calculated by summing the volumes of all the frustums.

$V_d:V_i$ VERSUS TIME INDICATES OVERLAP IN THE INFUSION DISTRIBUTION

Although the single-port catheter (1 $\mu\text{L}/\text{min}$) group showed the lowest V_d , it resulted in the highest $V_d:V_i$ of the three groups. In comparison to the arborizing catheter group, the catheter is composed of seven microneedles, with each individual microneedle representing a single port (each at a flow rate of 1 $\mu\text{L}/\text{min}$). However, at the end of the 100-min-long infusion, the overall $V_d:V_i$ for all the microneedles of the arborizing catheter resulted in an approximately 37% lower mean distribution ratio compared to single-port catheter at the slower flow rate (1 $\mu\text{L}/\text{min}$). The $V_d:V_i$ over time is shown in Figure 5 for the three experimental groups. The $V_d:V_i$ for the arborizing catheter group is similar to that of the single port at the slower infusion rate of 1 $\mu\text{L}/\text{min}$; however, it begins to decline and eventually becomes lower than the single-port (1 $\mu\text{L}/\text{min}$) group by 60 min of continuous infusion. This could be explained by the likely overlap in the local infusions from individual microneedles as they become larger with time. It is likely that at the beginning of the infusion, the overlap of the individual volume provided by each needle is less pronounced, therefore the $V_d:V_i$ is similar to that of the single-port catheter. However, as the volumes dispersed from individual needles become bigger and merge with one another into one large volume, the benefit gained from the multiple ports in the arborizing catheter is reduced until eventually the $V_d:V_i$ becomes less than that of a single-port catheter. The single-port (7 $\mu\text{L}/\text{min}$) group, which has the lowest $V_d:V_i$, further supports the concept of overlap. The infused dye, concentrated in a smaller volume, resulted in mean distribution ratios that plateau quickly during the infusion and stayed relatively constant after approximately 20 min of continuous infusion. We observed that, once deployed, the separation distance of the individual microneedles of the arborizing catheter affects the amount of overlap between the local infusions of

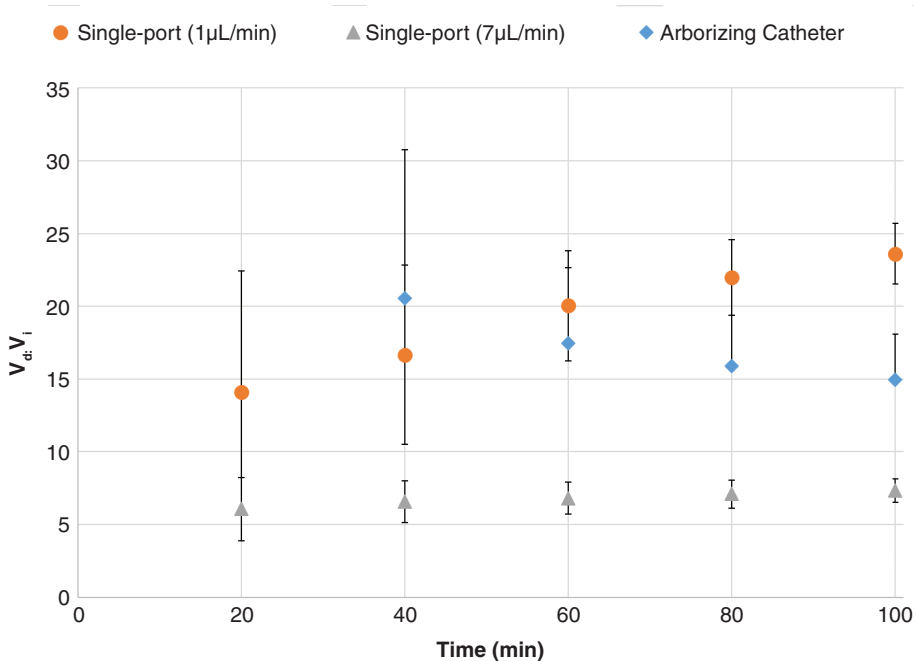


Figure 5 Mean distribution ratios ($V_d:V_i$) versus time of infusions for the three experimental groups. The average $V_d:V_i$ for each group was calculated every 20 min. However, the image processing algorithm was limited to calculating volume of solid, axisymmetric shapes and could not reliably calculate the volume of infusion shapes with gaps or holes. Therefore, infusions in the arborizing catheter group were calculated at 40 min and beyond, after the infusion shapes of individual microneedles had overlapped sufficiently to form a solid shape.

each microneedle and influences the measured V_d . In future iterations of the arborizing catheter prototype, we will optimize the catheter design to increase the angle of deflection of the microneedles, so that we can minimize the amount of overlap in the V_d of individual needles and maximize $V_d:V_i$ for the arborizing catheter.

It is important to note that our image processing algorithm was not able to reliably calculate V_d for the arborizing catheter at time points less than 40 min. This is because we assumed that the infusion volume was axisymmetric about the axis of the primary cannula of the arborizing catheter and thus, it was not able to account for any amorphous shapes or holes in the infusion volume. Figure 6 shows binary images of three representative time points in the infusion of an arborizing catheter. After 10 min of continuous infusion, the dispersed volume from individual microneedles is clearly discernible. At 20 min, there are still gaps present in the volume dispersed. However, after 40 min, most gaps in the volume dispersed had been filled and a reliable calculation for V_d could be obtained.

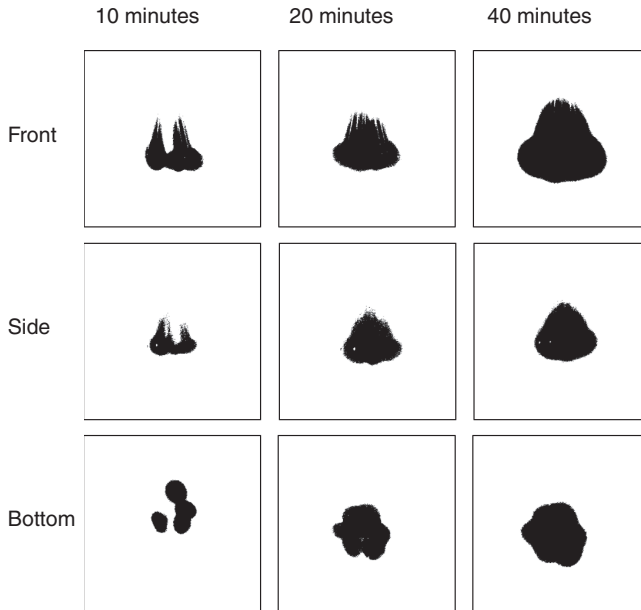


Figure 6 Representative binary images of volume dispersed for the arborizing catheter at three time points during the infusion for three view frames. The images show that at time points below 40 min, there were gaps in the dispersed volume due to branching out of the microneedles in the arborizing catheter. As the individual infusion volumes from each microneedle grew and began overlapping each other, the gaps were filled.

Conclusion

Results indicate that the multiport, arborizing catheter can significantly enhance volumetric dispersal of the infusate over a single port. By separating the volume infused, the arborizing catheter achieved a twofold greater volumetric dispersal and mean distribution volume compared to a single-port catheter for the same total infused volume. When comparing infusions of the arborizing catheter to that of a single-port catheter at the same flow rate per microneedle, the mean distribution ratio for the arborizing catheter drops to approximately 37% less than the single-port, perhaps due to overlap in the individual volume dispersed in the seven microneedles of the catheter. In the next design iteration, separation of individual microneedles within the arborizing catheter will be optimized to minimize overlap in the infusion volumes of individual microneedles (but, with no gaps in between them), while maximizing volumetric dispersal.

Acknowledgment: Portions of this chapter were supported by grants from the Wallace H. Coulter Foundation, National Science Foundation NSF/CBET 0933571, National Institutes of Health NIH/NCI R21CA156078, and the Virginia Center for Innovative Technology Commonwealth Research Commercialization Fund.

The author would like to thank the following institutions and collaborators for their contributions to the generation of data and material support of experiments presented in this section:

- Wake Forest University Comprehensive Cancer Center and Brain Tumor Center of Excellence: Dr. Waldemar Debinski and Dr. Stephen Tatter
- Virginia Tech-Wake Forest University School of Biomedical Engineering and Sciences: Dr. John Rossmeisl, Dr. John Robertson, and Dr. David Grant

Conflict of Interest: Arborizing catheter and fiberoptic microneedle device fabrication methods and applications are described in US Patent 8,798,722, issued on August 5, 2014, and US Application 14/002,058, both of which are managed by the Virginia Tech Intellectual Properties (VTIP) Group.

Copyright and permission statement: To the best of our knowledge, the materials included in this chapter do not violate copyright laws. All original sources have been appropriately acknowledged and/or referenced. Where relevant, appropriate permissions have been obtained from the original copyright holder(s).

References

1. Patel MM, Goyal BR, Bhadada SV, Bhatt JS, Amin AF. Getting into the brain: Approaches to enhance brain drug delivery. *CNS Drugs*. 2009 Feb;23(1):35–58. <https://doi.org/10.2165/0023210-200923010-00003>
2. Bobo RH, Laske DW, Akbasak A, Morrison PF, Dedrick RL, Oldfield EH. Convection-enhanced delivery of macromolecules in the brain. *Proc Natl Acad Sci U S A*. 1994 March;91:2076–80. <https://doi.org/10.1073/pnas.91.6.2076>
3. Morrison PF, Laske DW, Bobo H, Oldfield EH, Dedrick RL. High-flow microinfusion: Tissue penetration and pharmacodynamics. *Am J Physiol*. 1994 Jan;266(1 Pt 2):R292–305. https://doi.org/10.1007/978-3-7091-8592-6_58
4. Bosch DA, Hindmarch T, Larsson S, Backlund EO. Intraneoplastic administration of bleomycin in intracerebral gliomas: A pilot study. In: Gillingham F, Gybels J, Hitchcock E, Rossi G, Szikla G, editors. *Advances in stereotactic and functional neurosurgery 4*. Acta Neurochirurgica Supplementum. 30. Vienna: Springer; 1980. p. 441–4.
5. Vandergrift WA, Patel SJ, Nicholas JS, Varma AK. Convection-enhanced delivery of immunotoxins and radioisotopes for treatment of malignant gliomas. *Neurosurg Focus*. 2006 April;20(4):E13. <https://doi.org/10.3171/foc.2006.20.4.8>
6. Degen JW, Walbridge S, Vortmeyer AO, Oldfield EH, Lonser RR. Safety and efficacy of convection-enhanced delivery of gemcitabine or carboplatin in a malignant glioma model in rats. *J Neurosurg*. 2003 Nov;99(5):893–8. <https://doi.org/10.3171/jns.2003.99.5.0893>
7. Kunwar S. Convection enhanced delivery of IL13-PE38QQR for treatment of recurrent malignant glioma: Presentation of interim findings from ongoing phase 1 studies. *Acta Neurochir Suppl*. 2003 Feb;88:105–11. https://doi.org/10.1007/978-3-7091-6090-9_16
8. Laske DW, Youle RJ, Oldfield EH. Tumor regression with regional distribution of the targeted toxin TF-CRM107 in patients with malignant brain tumors. *Nat Med*. 1997 Dec;3:1362–8. <https://doi.org/10.1038/nm1297-1362>
9. Lieberman DM, Laske DW, Morrison PF, Bankiewicz KS, Oldfield EH. Convection-enhanced distribution of large molecules in gray matter during interstitial drug infusion. *J Neurosurg*. 1995 Jun;82:1021–9. <https://doi.org/10.3171/jns.1995.82.6.1021>

10. Gill SS, Patel NK, Hotton GR, O'Sullivan K, McCarter R, Bunnage M, et al. Direct brain infusion of glial cell line-derived neurotrophic factor in Parkinson disease. *Nat Med.* 2003 May;9(5):589–95. <https://doi.org/10.1038/nm850>
11. Slevin JT, Gerhardt GA, Smith CD, Gash DM, Kryscio R, Young B. Improvement of bilateral motor functions in patients with Parkinson disease through the unilateral intraputamina infusion of glial cell line-derived neurotrophic factor. *J Neurosurg.* 2005 Feb;102:216–22. <https://doi.org/10.3171/jns.2005.102.2.0216>
12. Rogawski MA. Convection-enhanced delivery in the treatment of epilepsy. *Neurotherapeutics.* 2009 Apr;6(2):344–51.
13. Barua NU, Miners JS, Bienemann AS, Wyatt MJ, Welser K, Tabor AB, et al. Convection-enhanced delivery of neprilysin: A novel amyloid- β -degrading therapeutic strategy. *J Alzheimers Dis.* 2012;32(1):43–56. <https://doi.org/10.3233/JAD-2012-120658>
14. Miners JS, Barua N, Kehoe PG, Gill S, Love S. AB-degrading enzymes: Potential for treatment of Alzheimer disease. *J Neuropathol Exp Neurol.* 2011 Nov;70(11):944–59. <https://doi.org/10.1097/NEN.0b013e3182345e46>
15. Sampson JH, Brady ML, Petry NA, Croteau D, Friedman AH, Friedman HS, et al. Intracerebral infusate distribution by convection-enhanced delivery in humans with malignant gliomas: Descriptive effects of target anatomy and catheter positioning. *Neurosurgery.* 2007 Feb;90(2):89–99. <https://doi.org/10.1227/01.NEU.0000249256.09289.5F>
16. Kunwar S, Chang S, Westphal M, Vogelbaum M, Sampson J, Barnett G, et al. Phase III randomized trial of CED of IL13-PE38QQR vs gliadel wafers for recurrent glioblastoma. *Neuro Oncol.* 2010 Aug;12(8):871–81. <https://doi.org/10.1093/neuonc/nop054>
17. Debinski W, Tatter SB. Convection-enhanced delivery for the treatment of brain tumors. *Expert Rev Neurother.* 2009 Oct;9(10):1519–27. <https://doi.org/10.1586/ern.09.99>
18. Lidar Z, Mardor Y, Jonas T, Pfeffer R, Faibel M, Nass D, et al. Convection-enhanced delivery of paclitaxel for the treatment of recurrent malignant glioma: A phase I/II clinical study. *J Neurosurg.* 2004 Mar;100(3):472–9. <https://doi.org/10.3171/jns.2004.100.3.0472>
19. Yang W, Huo T, Barth RF, Gupta N, Weldon M, Grecula JC, et al. Convection enhanced delivery of carboplatin in combination with radiotherapy for the treatment of brain tumors. *J Neurooncol.* 2011 Feb;101(3):379–90. <https://doi.org/10.1007/s11060-010-0272-z>
20. Vogelbaum MA, Aghi MK. Convection-enhanced delivery for the treatment of glioblastoma. *Neuro Oncol.* 2015 Mar;17 Suppl 2:ii3–ii8. <https://doi.org/10.1093/neuonc/nou354>
21. Patchell RA, Regine WF, Ashton P, Tibbs PA, Wilson D, Shapley D, et al. A phase I trial of continuously infused intratumoral bleomycin for the treatment of recurrent glioblastoma multiforme. *J Neurooncol.* 2002 Oct;60(1):37–42. <https://doi.org/10.1023/A:1020291229317>
22. Patel SJ, Shapiro WR, Laske DW, Jensen RL, Asher AL, Wessels BW, et al. Safety and feasibility of convection-enhanced delivery of cotara for the treatment of malignant glioma: Initial experience in 51 patients. *Neurosurgery.* 2005 June;56(6):1243–53. <https://doi.org/10.1227/01.NEU.0000159649.71890.30>
23. Rand RW, Kreitman RJ, Patronas N, Varricchio F, Pastan I, Puri RK. Intratumoral administration of recombinant circularly permuted interleukin-4-pseudomonas exotoxin in patients with high-grade glioma. *Clin Cancer Res.* 2010 Jun;6:2157–65.
24. Sampson JH, Akabani G, Archer GE, Bigner DD, Berger MS, Friedman AH, et al. Progress report of a phase I study of the intracerebral microinfusion of a recombinant chimeric protein composed of transforming growth factor (TGF)- α and a mutated form of the Pseudomonas exotoxin termed PE-38 (TP-38) for the treatment of malignant brain tumors. *J Neurooncol.* 2003 Nov;65(1):27–35. <https://doi.org/10.1023/A:1026290315809>
25. Sampson JH, Archer G, Pedain C, Wembacher-Schroder E, Westphal M, Kunwar S, et al. Poor drug distribution as a possible explanation for the results of the PRECISE trial. *J Neurosurg.* 2010 Aug;113(2):301–9. <https://doi.org/10.3171/2009.11.JNS091052>
26. Brady ML, Raghavan R, Singh D, Anand PJ, Fleisher AS, Mata J, et al. In vivo performance of a micro-fabricated catheter for intraparenchymal delivery. *J Neurosci Meth.* 2014 May 30;229:76–83. <https://doi.org/10.1016/j.jneumeth.2014.03.016>

27. Gill T, Barua NU, Woolley M, Bienemann AS, Johnson DE, Sullivan SO, et al. In vitro and in vivo testing of a novel recessed-step catheter for reflux-free convection-enhanced drug delivery to the brain. *J Neurosci Meth*. 2013 Sep 30;219(1):1–9. <https://doi.org/10.1016/j.jneumeth.2013.06.008>
28. Seunguk O, Odland R, Wilson SR, Kroeger KM, Liu C, Lowenstein PR, et al. Improved distribution of small molecules and viral vectors in the murine brain using a hollow fiber catheter. *J Neurosurg*. 2007 Sep;107(3):568–77. <https://doi.org/10.3171/JNS-07/09/0568>
29. Olson JJ, Zhang Z, Dillehay D, Stubbs J. Assessment of a balloon-tipped catheter modified for intracerebral convection-enhanced delivery. *J Neurooncol*. 2008 Sep;89(2):159–68. <https://doi.org/10.1007/s11060-008-9612-7>
30. Vogelbaum M. A pilot trial of intraparenchymally-administered topotecan using Convection-Enhanced Delivery (CED) in patients with suspected recurrent/progressive WHO grade III or IV (High Grade) glioma requiring stereotactic biopsy. In: *ClinicalTrials.gov*. Bethesda, MD: National Library of Medicine (US). NLM Identifier: NCT02278510; 2014.
31. Barua NU, Hopkins K, Woolley M, O'Sullivan K, Harrison R, Edwards RJ, et al. A novel implantable catheter system with transcatheter port for intermittent convection-enhanced delivery of carboplatin for recurrent glioblastoma. *Drug Delivery*. 2016;23(1):17–173. <https://doi.org/10.3109/10717544.2014.908248>
32. Krauze MT, Saito R, Noble C, Tamas M, Bringas J, Park JW, et al. Reflux-free cannula for convection-enhanced high-speed delivery of therapeutic agents. *J Neurosurg*. 2005 Nov;103(5):923–9. <https://doi.org/10.3171/jns.2005.103.5.0923>
33. Vazquez LC, Hagel E, Willenberg BJ, Dai W, Casanova F, Batich CD, et al. Polymer-coated cannulas for the reduction of backflow during intraparenchymal infusions. *J Mater Sci Mater Med*. 2012 Aug;23(8):2037–46. <https://doi.org/10.1007/s10856-012-4652-0>
34. Yin D, Forsayeth J, Bankiewicz KS. Optimized cannula design and placement for convection-enhanced delivery in rat striatum. *J Neurosci Meth*. 2010 Mar 15;187(1):46–51. <https://doi.org/10.1016/j.jneumeth.2009.12.008>
35. Andriani RT. Design and validation of medical devices for photothermally augmented treatments [MS Thesis]. Blacksburg, VA: Virginia Tech; 2014.
36. Otsu N. A threshold selection method from gray-level histograms. *IEEE Trans Syst Man Cyb*. 1975 Jun;9(1):62–6. <https://doi.org/10.1109/TSMC.1979.4310076>
37. Sabliov CM, Boldor D, Keener KM, Farkas BE. Image processing method to determine surface area and volume of axi-symmetric agricultural products. *Int J Food Prop*. 2002 Jan;5(3):641–53. <https://doi.org/10.1081/JFP-120015498>
38. Mut M, Sherman JH, Shaffrey ME, Schiff D. Cintredekin besudotox in treatment of malignant glioma. *Expert Opin Biol Ther*. 2008;8(6):805–12.
39. Mueller S, Polley MY, Lee B, Kunwar S, Pedain C, Wembacher-Schroder E, et al. Effect of imaging and catheter characteristics on clinical outcome for patients in the PRECISE study. *J Neurooncol*. 2011 Jan;101(2):267–77. <https://doi.org/10.1007/s11060-010-0255-0>
40. Tocagen. A phase 1 ascending dose trial of the safety and tolerability of toca 511 in patients with recurrent high grade glioma. In: *ClinicalTrials.gov* [Internet]. Bethesda, MD: National Library of Medicine (US). NLM Identifier: NCT01156584; 2010.

19 Maximizing Local Access to Therapeutic Deliveries in Glioblastoma. Part III: Irreversible Electroporation and High-Frequency Irreversible Electroporation for the Eradication of Glioblastoma

MELVIN F. LORENZO¹ • CHRISTOPHER B. ARENA^{1,2} • RAFAEL V. DAVALOS¹

¹School of Biomedical Engineering and Sciences, Virginia Tech-Wake Forest University, Blacksburg, VA, USA; ²Laboratory for Therapeutic Directed Energy, Department of Physics, Elon University, Elon, NC, USA

Author for correspondence: Rafael V. Davalos, School of Biomedical Engineering and Sciences, Virginia Tech-Wake Forest University, 325 Kelly Hall, Stanger Street, Blacksburg, VA 24061, USA. E-mail: davalos@vt.edu

Doi: <http://dx.doi.org/10.15586/codon.glioblastoma.2017.ch19>

Abstract: Glioblastoma (GBM) is the most common and aggressive primary brain tumor in adults. Approximately 9180 primary GBM tumors are diagnosed in the United States each year, in which median survival is up to 16 months. GBM eludes and resists typical cancer treatments due to the presence of infiltrative cells beyond the solid tumor margin, heterogeneity within the tumor microenvironment, and protection from the blood–brain barrier. Conventional treatments for GBM, such as surgical resection, radiotherapy, and chemotherapy, have shown limited efficacy;

In: *Glioblastoma*. Steven De Vleeschouwer (Editor), Codon Publications, Brisbane, Australia
ISBN: 978-0-9944381-2-6; Doi: <http://dx.doi.org/10.15586/codon.glioblastoma.2017>

Copyright: The Authors.

Licence: This open access article is licenced under Creative Commons Attribution 4.0 International (CC BY 4.0). <https://creativecommons.org/licenses/by-nc/4.0/>

therefore, alternate treatments are needed. Tumor chemoresistance and its proximity to critical structures make GBM a prime theoretical candidate for nonthermal ablation with irreversible electroporation (IRE) and high-frequency IRE (H-FIRE). IRE and H-FIRE are treatment modalities that utilize pulsed electric fields to permeabilize the cell membrane. Once the electric field magnitude exceeds a tissue-specific lethal threshold, cell death occurs. Benefits of IRE and H-FIRE therapy include, but are not limited to, the elimination of cytotoxic effects, sharp delineation from treated tissue and spared tissue, a nonthermal mechanism of ablation, and sparing of nerves and major blood vessels. Preclinical studies have confirmed the safety and efficacy of IRE and H-FIRE within their experimental scope. In this chapter, studies will be collected and information extrapolated to provide possible treatment regimens for use in high-grade gliomas, specifically in GBM.

Keywords: Blood–brain barrier disruption; Glioblastoma; High-frequency irreversible electroporation; Irreversible electroporation; Treatment planning

Introduction

Glioblastoma (GBM) is the most recurrent, aggressive brain tumor representing ~50% of all primary brain gliomas. Ninety percent of GBM tumors are diagnosed *de novo* as primary tumors, and 10% are diagnosed as secondary tumors, where primary tumors correlate to lower survival rates (1). Approximately 9180 primary GBM tumors are diagnosed in the United States each year, in which median survival is up to 16 months. Current standard of care for malignant gliomas (MGs) include, if feasible, tumor resection followed by radiotherapy (RT) and chemotherapy (CT). Difficulties in treatment of GBM are due to infiltrative cells beyond the solid tumor margin, heterogeneity within tumor microenvironment, and protection from the blood–brain barrier (BBB) (1). Due to dismal prognosis of patients with GBM, quality of life (QoF) post-treatment is an important factor when considering treatment options. Aside from temozolomide (TMZ), cytotoxic chemotherapeutic agents do not significantly alter prognosis outcomes (2). Therefore, new aims in therapy for MGs include reducing morbidity, maintaining and improving QoF, and preserving neurologic function.

Recent advancements in the treatment of GBM have marginally extended median survival rates. These improvements seem to be dependent on GBM cellular morphology rather than improvement of holistic treatment regimes. In a study conducted by Glas et al., the overall 5-year survival rate in a cohort of 39 patients was reported to be 15.8%, which is much higher than the usually reported rate between 4 and 5% (3). This study utilized a combination of tumor resection and RT, followed by delivery of CT agents, lomustine (CCNU) and TMZ. Significant findings include increased dosage of CCNU and TMZ resulted in greater survival rates with comparable toxicities among standard doses, as well as a link between long-term survival and the O-methylguanine-DNA methyltransferase (MGMT) gene (3). Nonetheless, GBM remains a lethal and aggressive tumor that evades standard treatment; therefore, alternative approaches are discussed.

Irreversible Electroporation and High-Frequency Irreversible Electroporation for the Eradication of GBM

REVERSIBLE ELECTROPORATION

The cell membrane acts as a selectively permeable barrier that regulates the transport of ions and molecules. It is composed of a phospholipid bilayer and protein channels that together maintain homeostasis. Therapies dependent on the transport of molecules across the membrane rely heavily on cell permeabilization without causing damage to the cell, which can be achieved, for example, with focused ultrasound (4–6). In this chapter, we present the use of electroporation as a means of accomplishing cell permeabilization. Electroporation is a phenomenon in which the cell membrane undergoes a physiological transformation caused by pulsed electric fields (PEFs). Following the application of PEFs, naturally occurring hydrophobic pores, or defects, in the membrane transition to lipid-lined hydrophilic pores through which polar molecules can pass (7). This transition occurs as an energy minimization with pore radius, and increasing the transmembrane potential (TMP) by applying PEFs further decreases pore energy and increases hydrophilic pore creation rate. Once created, the hydrophilic pores can expand or reseal depending on the pulse parameters. The net effect of PEFs on tissue is transient permeabilization of the phospholipid bilayers of individual cells, as well as heat generation. Generally, a TMP of ~0.5 V is needed to induce reversible electroporation (RE), a process marked by rapid depolarization of the cell membrane and delayed resealing of transient, nanoscale defects (8, 9). Figure 1 depicts pore formation using molecular dynamics simulations after 50 ns as performed by Böchman et al. (10).

During RE, the cell membrane exhibits a tremendous increase in molecular transport. This phenomenon has been exploited in electrochemotherapy (ECT) to improve cellular uptake of cytotoxic drugs, such as bleomycin or cisplatin, and increase drug cytotoxicity (11). It has also been used to deliver genetic material, plasmid DNA, into cells to correct genetic disorders, in a process known as DNA electrotransfer or electrogene therapy (12).

Clinically, RE is administered through two or more electrodes placed into or around the target tissue, as depicted in Figure 2A. Using custom electrodes, Gehl et al. inoculated mice with N32 glioma-derived cells and treated them with ECT using bleomycin as the chemotherapeutic agent. Nine of 13 mice showed tumor regression and elimination, while 4 mice showed tumor progression. Of the four mice that showed tumor progression, three mice were identified to have the largest tumor volumes of the study. Lack of eradication was attributed to incomplete electroporation and envelopment of the tumor within electric field thresholds needed to induce RE and increase cytotoxicity (13). ECT has also been used in the treatment of metastases from melanoma, breast, and head and neck cancer (14). Recently, Gehl et al. performed ECT using calcium as a substitute for cytotoxic drugs. This process, known as calcium electroporation, demonstrated its ability to induce ATP depletion-associated cellular death with NaCl and CaCl₂ (15, 16).

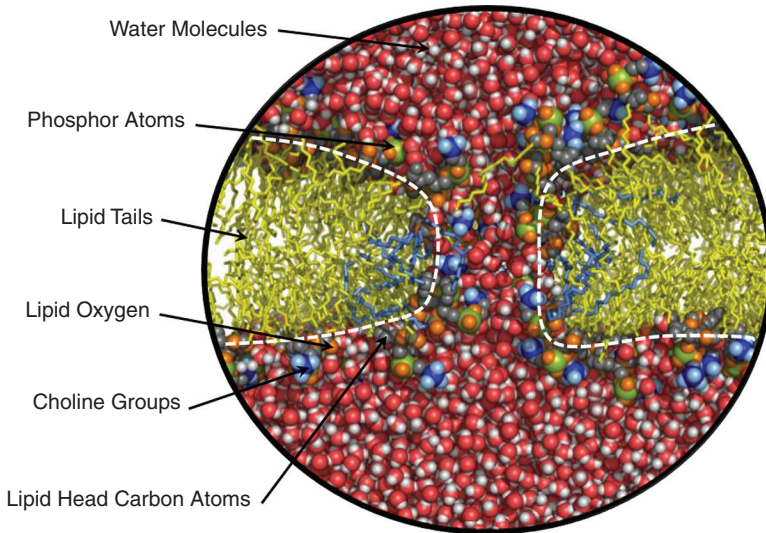


Figure 1 Pore formation as modeled by Böckmann et al. Molecular dynamics simulation of pore formation after 50 ns shown as a section through the lipid bilayer membrane. The outline of the hydrophilic pore is shown by the white dashed lines. The pore starts off in an impermeable hydrophobic state, transitions into a hydrophobic pore intermediate, and finishes off as a stable hydrophilic pore. (Adapted from *Biophys J* 2008;95(4):1837–1850.)

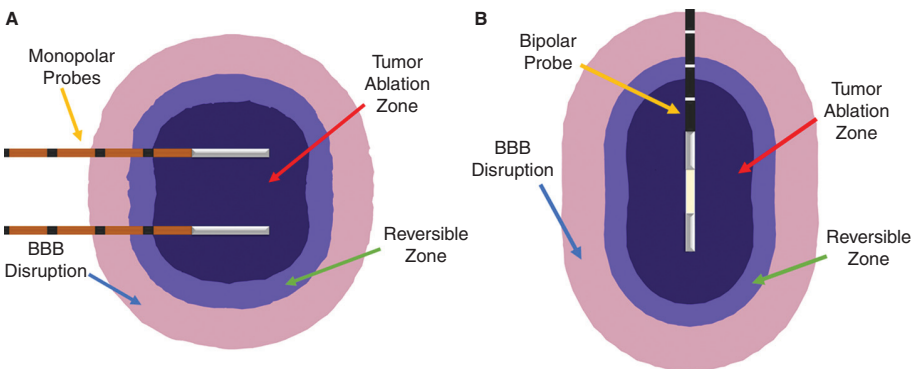


Figure 2 Monopolar probe and bipolar probe insertion. Clinical application of electroporation is achieved by inserting either (A) two monopolar probes or (B) a single bipolar probe. One electrode is set to ground while the other is energized and pulsed to produce PEFs. Three zones of interest include the ablation zone, the RE (reversible) zone, as well as the BBB disruption zone. It is debatable whether the BBB disruption zone and the RE zone are separate regions; for illustrative purposes they are modeled individually.

IRREVERSIBLE ELECTROPORATION

More recently, IRE has been developed to directly ablate unwanted tissue by further increasing the TMP through higher electric field magnitudes or by applying additional sets of pulses to prolong pore lifetime. Davalos et al. demonstrated that electric pulses could be applied to raise the TMP past a threshold associated with permanent cell damage, without causing significant thermal damage (17). It is considered that IRE effects occur when the TMP reaches $\sim 1.0V$ (18). On a cellular level, this increase in TMP also induces nanoscale defects on the cell membrane, resulting in irrevocable disruption in homeostasis ultimately leading to cell death. A typical IRE pulse is presented in Figure 3A, in which the energized electrode would experience an applied voltage 100 μs in duration, repeating once every second.

Unlike thermal ablation techniques, such as radiofrequency ablation and cryoablation, IRE is not thermally driven. As will be discussed later in this chapter, numerical models are used for treatment planning purposes, in which IRE volumes and temperature changes are calculated. A study conducted by Garcia et al. demonstrated numerically that applying ninety 100 μs pulses produces minimal thermal damage. In this study, a statistical model that incorporated dynamic electrical conductivity was used to simulate cell kill due to IRE as well as thermal damage. Results suggested that for tissues with lower electrical conductivities, ranging between 0.067 and 0.241 S/m, necrotic tissue volume produced via Joule heating was only 1.3% of the total ablation volume produced by IRE. Using higher electrical conductivity values, 1.75 times greater, resulted in a percentage of 6.1%, in which the thermally induced necrotic tissue was located at the electrode/tissue interface (19, 20).

In addition to the treatment of brain tumors, IRE has been implemented to treat human patients with prostate (21, 22), pancreatic (23–25), liver (26–28), and kidney (29, 30) tumors. Benefits of IRE therapy include elimination of cytotoxic effects, sharp delineation between treated and spared tissue, a nonthermal mechanism of ablation, treatment planning abilities, sparing of nerves and major blood vessels (31, 32), and, if desired, it can be used as a combinatorial treatment with CT and/or RT. Although effective, RE and IRE are known to cause

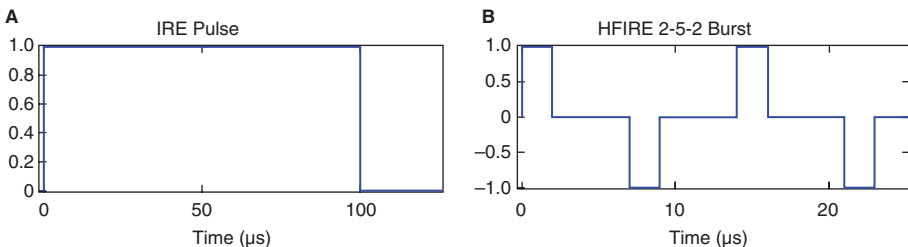


Figure 3 IRE and H-FIRE pulse waveforms. (A) IRE and RE treatments typically utilize 100 μs pulses to achieve cell permeabilization while maintaining relatively low thermal damage. (B) H-FIRE waveforms are given in positive-rest-negative burst schemes and achieve similar effects to IRE. Comparison between IRE and H-FIRE waveforms is usually done by counting the on-time per pulse period. In this case, the 2-5-2 burst would be repeated until 100 μs of on-time has elapsed.

muscle contractions during treatment, necessitating the use of neuroparalytic agents (33). This poses additional concerns for anesthesiologists, as the dosage of neuroparalytics must be continually monitored to ensure adequate muscle relaxation and proper respiratory function (34). Also, due to changes in electrical conductivity of the tissue during IRE and the heterogeneous nature of tissue on a microscale, treatment planning for IRE can be challenging. Studies have confirmed possible “electric field sink” effects which distort electric field distributions near blood vessels and may lead to undertreatment of tumor tissue (35, 36). Infusing the blood vessels with lower conductivity fluids helps to alleviate the sharp transition from lower conductivity to higher conductivity tissues, but this may be cumbersome and impractical in a clinical setting. To address these challenges associated with RE and IRE, our group developed a novel method of electroporation that utilizes high-frequency bursts to induce electroporation effects.

HIGH-FREQUENCY IRREVERSIBLE ELECTROPORATION

Pulse generators capable of delivering new IRE waveforms have been developed to alleviate the concerns associated with neuroparalytic agents and to simplify treatment planning (37). Namely, these high-frequency IRE (H-FIRE) systems split the $\sim 100 \mu\text{s}$ unipolar pulse into a series of shorter duration $\sim 1 \mu\text{s}$ pulses of alternating polarity (Figure 3B). According to classic literature on electrical stimulation, a bipolar pulse has a higher current threshold for action potential excitation as compared to a unipolar pulse of equivalent phase duration (38). This effect is enhanced as pulse duration is reduced. When a microsecond order pulse is applied, there is a latency period between the offset of the pulse and the rising phase of the action potential. A rapid reversal of polarity falling within this latency period can accelerate passive repolarization and inhibit action potential generation (39). An example of this phenomenon is shown in Figure 4, which was derived based on the Hodgkin–Huxley set of partial differential equations for modeling nerve stimulation (40).

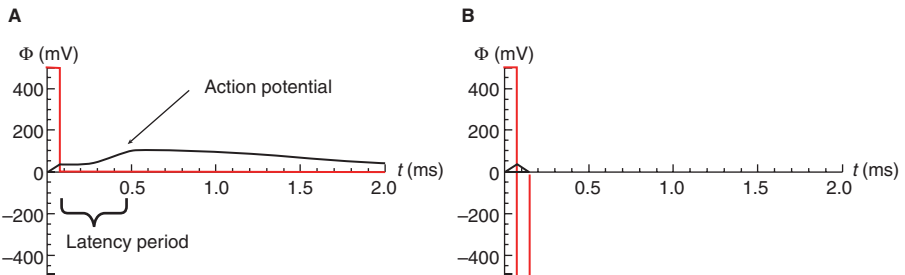


Figure 4 Illustration of action potential inhibition by polarity reversal. (A) Unipolar pulse with an amplitude of 500 mV and duration of 75 μs . (B) Bipolar pulse with an amplitude of 500 mV and duration of single polarity of 75 μs . This simulation of the Hodgkin–Huxley model was performed in Mathematica 9.0 using parameter values. (Adapted from Bull Math Biol 1952;52(1–2):25–71.)

Following membrane charging, pore formation occurs in the order of ~ 10 ns (10) and with no latency period. Therefore, it is possible to first induce electroporation and subsequently inhibit muscle contractions by reversing pulse polarity. The first *in vivo* study on H-FIRE was conducted in healthy rat brain (37). Muscle contractions were monitored by placing an acceleromoter at the cervicothoracic junction and inserting electrodes into the center of the forelimb area of the sensorimotor cortex. A total of 180 bursts with a total on-time of 200 μ s were delivered, and the individual pulse duration comprising each burst varied between 1, 2, and 200 μ s for the IRE control. No visual or tactile evidence of muscle contraction was seen during H-FIRE with 1 μ s or 2 μ s pulses, while the IRE protocol resulted in detectable movement. In addition, H-FIRE produced ablative lesions in brain tissue that were characteristic of IRE treatments, with complete uniformity of tissue death and a sharp transition zone between lesioned and normal brain.

The cell-killing effects of H-FIRE were later explored using 3D *in vitro* tumor constructs and *in vivo* subcutaneous murine tumors over a wide range of pulse durations (250 ns–100 μ s) (41). The *in vitro* tumor constructs were assembled by mixing murine pancreatic tumor cells with collagen I hydrogel, injecting into cylindrical molds, and polymerizing at 37°C (42); the *in vivo* subcutaneous tumors were produced by injecting human GBM cells (DBTRG-05MG) into the dorsolateral flank region of athymic nude-Foxn1^{nu} mice. The *in vitro* tests revealed electric field thresholds for cell death of 2022, 1687, 1070, 755, 640, 629, and 531 V/cm for 80 bursts containing 0.25, 0.5, 1, 2, 5, 10, and 50 μ s pulses, respectively. *In vivo*, tumor growth was significantly inhibited and all protocols tested (1, 2, and 5 μ s pulses) were able to achieve complete regressions. Localized muscle twitching in the treated limb was evident in mice, due to their relatively small size and mass. When similar treatments (5 μ s pulses) were applied to spontaneous tumors in equine patients, no movement was observed.

As compared to IRE, H-FIRE waveforms are capable of producing more predictable ablation volumes. The theoretical basis for this argument is twofold. First, the electrical properties of various tissue types converge at high frequencies, and H-FIRE waveforms are comprised of predominately high-frequency components. For example, in a skin-fold geometry, the ratio between the electrical conductivity of fat and skin is 2.25 at 1 MHz (0.027 S/m divided by 0.012 S/m) and 83 at 100 Hz (0.015 S/m divided by 0.00018 S/m) (43). Numerical models have shown that an H-FIRE burst with 500 ns pulses (1 MHz carrier frequency) produces a nearly homogenous electric field distribution across a skin fold (44). This logic can be extended to other heterogeneous tissues, such as the pancreas and brain. Second, electroporation is an active process and the electric conductivity of the tissue increases as pores form and expand. When performing IRE treatments, this step-like change in conductivity must be known *a priori* (45), or measured in real time (46), in order to accurately predict the ablation volume. For H-FIRE waveforms, there is a smaller difference between the pre-treatment and post-treatment conductivities due to capacitive coupling. Bhonsle et al. has shown that the electric field distribution during H-FIRE resembles a theoretical approximation based on the Laplace equation, and the ablation volume can be predicated without additional knowledge of dynamic tissue properties. To demonstrate this phenomenon, IRE and H-FIRE ablations were induced in potato tuber, a proven alternate for studying bioelectric effects of electroporation, and results are shown in Figure 5 (47, 48).



Figure 5 IRE versus H-FIRE ablations in potato tuber. A qualitative comparison between an IRE ablation and an H-FIRE ablation created using a single bipolar probe. (A) IRE was induced with 80 pulses energized for 100 μ s at 1000 V. (B) Laplace solution for the electric field distribution at an arbitrary electric field magnitude, assuming static electrical conductivity. (C) H-FIRE was induced with 140 bursts, using a burst scheme of 2-5-2 μ s at 1300 V. Typical H-FIRE protocols require higher voltages and more bursts to produce lesion volumes comparable to IRE.

While studying the time course of membrane charging during H-FIRE, Sano et al. recognized that the inter-pulse delay can be tuned to maximize the TMP across the nuclear envelope. Specifically, a delay of 140 ns or less causes the nuclear TMP to double due to compounding effects from pulse falling edges and rising edges (49). In addition, metastatic cells with a larger nucleus-to-cytoplasm ratio can achieve even greater nuclear TMP. In terms of overall cell killing, Pakhomov et al. demonstrated that using bipolar nanosecond electric pulses with sub-microsecond inter-pulse delays induces somewhat of a cancellation effect, resulting in higher lethal thresholds (50). However, a greater inter-pulse delay can lower the threshold for cell death. At 3.7 kV/cm, cell viability was similar when comparing a 300 ns monopulse and a 300–300 ns bipolar pulse with a 10 μ s interpulse delay. This illustrates a trade-off between potential selectivity and the overall field threshold required for cell death.

Using the 3D *in vitro* tumor constructs, Ivey and Latouche et al. experimentally validated the selectivity claim (51). In this study, U-87 human GBM cells, DBTRG human GBM cells, C6 rat GBM cells, normal human astrocytes (NHA), normal rat astrocytes D1TNC1, and undifferentiated rat neurons PC12 were cultured in collagen hydrogels and H-FIRE therapy was delivered using a 1-5-1 μ s burst scheme. Using numerical models, individual lethal thresholds were determined by overlaying appropriate contours over the lesion. Experimental results showed statistically lower lethal threshold for malignant cells as opposed to healthy cells. Lethal thresholds for U-87, DBTRG, C6, NHA, D1TNC1, and PC 12 were 601, 720, 752, 1006, 1107, and 1076 V/cm, respectively. H-FIRE treatment on hydrogel cocultures of healthy and malignant cells also demonstrated selectivity through partial sparing of healthy tissue. Upon clinical translation, H-FIRE has the potential to kill infiltrative cells beyond the tumor margin while minimizing damage to healthy cells.

BLOOD–BRAIN BARRIER DISRUPTION WITH IRE AND H-FIRE

Difficulties arising from treating MGs with conventional chemotherapy are partly due to protection from the BBB, where the BBB prevents the delivery of these drugs. The BBB is a network of tight junctions that mitigates the transport of large molecules, thereby not only protecting the brain from infections but also hindering the efficacy of chemotherapeutic drugs (52). Garcia et al. demonstrated that

IRE can be applied to the brain not only to ablate tissue but also to cause a transient focal disruption of the BBB, thereby providing a pathway for chemotherapeutics to penetrate (53). For this study, 21 mice received IRE therapy from two monopolar caliper electrodes, measuring 0.45 mm in diameter and 1 mm in exposure with spacing of 4 mm. BBB permeabilization was visualized using Evan's Blue (EB) dye for histological examinations and Gadolinium (Gd) for MR imaging, where EB would represent increased uptake of higher molecular weight compounds, such as proteins, and Gd would represent increased uptake of ions. Results demonstrated that permeability of EB and Gd increased linearly as a function of electric field magnitude, in which 400 V/cm served as a lower threshold, signifying a difference between inducing BBB disruption and IRE ablation. This difference in threshold manifests as having a larger volume of BBB disruption than IRE ablation, as depicted in Figure 2. It was also concluded that BBB disruption is transient due to decreased uptake of both EB and Gd if these agents are administered 30 min after IRE treatment, as opposed to administration within 5 min of treatment.

Alternatively, Arena et al. investigated BBB disruption using H-FIRE waveforms (54). The experimental methods, in terms of electrode design and detection of BBB disruption using EB and Gd, were similar to the study mentioned above. High-frequency PEFs were applied to the superficial cerebral cortex of 18 male rats outfitted with a 3-axis accelerometer, as shown in Figure 6. It was discovered that electric field magnitudes of 250 and 2000 V/cm did not induce any muscle

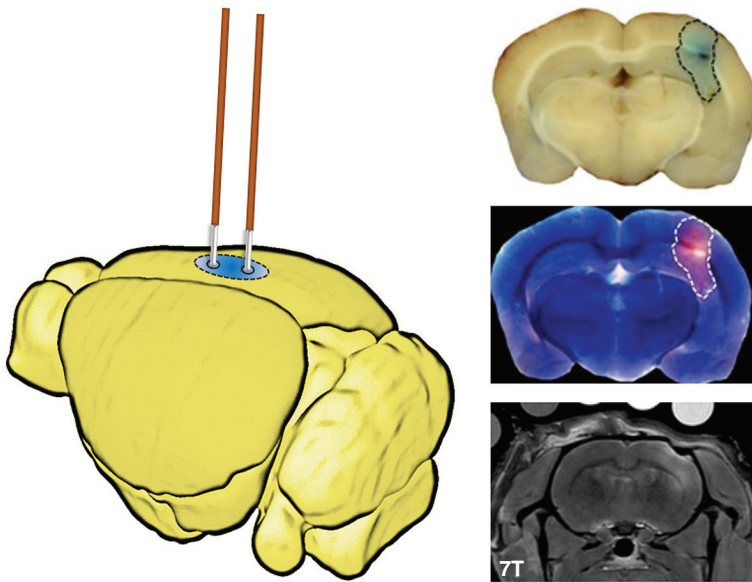


Figure 6 BBB disruption using H-FIRE waveforms. Schematic of BBB disruption using high-frequency PEFs (left), and pathology and MRI evidence of BBB disruption (right). The results are shown for 300 bursts of 0.5 μ s bipolar pulses at an applied field of 250 V/cm. The dashed lines depict the limits of BBB disruption. (Adapted from Technology 2014;2(3):206.)

contractions for pulse widths of 0.5 and 2 μs , although visual inspections determined lack of muscle contraction for the 2000 V/cm group because of electrical interference with the accelerometer. Using the lowest energy setting, consisting of 300 bursts and an electric magnitude of 250 V/cm, a BBB disruption zone of 0.51 cm^3 was induced. More importantly, there was no evidence of tissue damage from the high-frequency PEFs, except the physical damage due to electrode insertion. However, if the number of bursts is increased to 600, there is significant cell death with no increase in BBB disruption zone, indicating a maximum energy threshold to disrupting BBB while not sustaining damage by high-frequency PEFs. The total charge delivered with IRE pulses and H-FIRE bursts is typically compared to the charge delivered during electroconvulsive therapy (33) due to the ultrashort duration of these pulses/bursts.

The data presented indicate that both IRE and H-FIRE can be optimized to promote cell death via ablation mechanism and simultaneously disrupt the BBB, allowing adjuvant therapies to reach the infiltrative cell region in GBM. Most notably, H-FIRE has been shown to extend BBB disruption without causing cell death. Additional benefits of H-FIRE include no induced muscle contractions, targeted malignant cellular ablation, and more predictable ablation geometries. Although not discussed, investigations for permeabilization of the BBB have also been performed *in vitro* (55).

IRE AND H-FIRE TREATMENT PLANNING

Treatment planning for IRE and H-FIRE can be accomplished using a finite element package, for example, COMSOL Multiphysics 5.2a (Stockholm, Sweden). The degree of electroporation is dependent on the electrical impedance distribution, electric field distribution, electrode and tissue geometries, and pulsing parameters such as pulse width, number of pulses, and inter-pulse delay. Maxwell's equations are a set of partial differential equations that form the foundation of electromagnetism. The fundamental equations for solving the electric field distribution of IRE and H-FIRE include Faraday's Law and Ampere's Law:

$$\nabla \times \vec{E} = -\frac{\partial \vec{B}}{\partial t} \quad [1]$$

$$\nabla \times \vec{H} = \vec{J} + \frac{\partial \vec{D}}{\partial t} \quad [2]$$

where \vec{E} is the electric field, \vec{B} is the magnetic field, \vec{H} is the auxiliary magnetic field, \vec{J} is the total current density, and \vec{D} is the displacement current density. By taking the divergence of Ampere's Law, equation 2, and substituting constitutive equations, we obtain the following:

$$\nabla \cdot (\sigma \vec{E}) + \frac{\partial}{\partial t} (\nabla \cdot (\epsilon \vec{E})) = 0 \quad [3]$$

where σ is the electrical conductivity and ϵ is the dielectric permittivity. Using the electroquasistatic approximation for Faraday's Law, equation 1, in which the magnetic field can be considered negligible in contributing to the displacement of electrical charge, we can describe the electric field in terms of an electric potential, ϕ :

$$\nabla \times \vec{E} = 0 \quad [4]$$

$$\vec{E} = -\nabla \phi \quad [5]$$

Thus, by combining equations 3 and 4 and assuming steady state, we can rewrite this equation as:

$$-\nabla \cdot (\sigma \cdot \nabla \phi) = 0 \quad [6]$$

$$\sigma = f(\vec{E}) \quad [7]$$

For IRE, boundary conditions are applied to the electrode/tissue interface in which one electrode is energized at a voltage V_0 and the other is grounded, while in the case of H-FIRE, the boundary conditions would need to be alternated between each electrode due to the rapid reversal of polarity. The remaining boundaries are treated as electrically insulating. For the thermal boundary and initial conditions, we assume an adiabatic boundary to calculate the maximum possible temperature increase and an initial temperature of T_0 .

Using these equations, it is possible to map the electric field distribution and predict volumes of electroporated heterogeneous dynamic tissue for use in clinical application. It has been largely accepted that changes in electrical conductivity due to electroporation is a dynamic phenomenon (18–20, 25, 56). Accounting for dynamic conductivity allows for more accurate representation of lesions created by IRE (57), and potentially H-FIRE. Incorporating changes in tissue conductivity can be achieved using a fitted Gompertz function (58). Alternatively, a sigmoid function can mimic changes in electrical conductivity due to electric field magnitude as well as temperature. Garcia et al. incorporated the following equation for analysis of IRE ablations in intracranial tissue (20):

$$\sigma(E, T(t)) = \sigma_0 \cdot \left[1 + 2 \cdot flc2hs(E_{norm} - E_{Delta}, E_{range}) + \alpha \cdot (T(t) - T_0) \right] \quad [8]$$

where σ_0 represents the initial electrical conductivity, $flc2hs$ is a Heaviside function, α is the temperature coefficient, E_{norm} represents the norm of the electric field, and E_{delta} and E_{range} are coefficients pertaining to the electric field thresholds required for conductivity changes.

Temperature changes due to resistive heating from pulsing, Joule heating, can also be incorporated into numerical models. Joule heating and blood perfusion are modeled through a modified Pennes' Bioheat equation:

$$\nabla \cdot (k \nabla T) - \omega_b C_b \rho_b (T - T_a) + q''' + \sigma |\nabla \phi|^2 = \rho C_p \frac{\partial T}{\partial t} \quad [9]$$

where $\sigma|\nabla\phi|^2$ is the Joule heating term, k is the thermal conductivity, ω_b is the blood perfusion rate, C_b is the blood-specific heat capacity, ρ_b is the density of blood, T_a is the arterial blood temperature, q''' is the metabolic heat generation, ρ is the density of the tissue, and C_p is the specific heat capacity of the tissue. Rather than simulating hundreds of IRE or H-FIRE pulses, a modified duty cycle approach is applied to ease the computational burden (20). We can rewrite this modified Bioheat equation as:

$$\nabla \cdot (k\nabla T) - \omega_b C_b \rho_b (T - T_a) + q''' + \frac{\tau(\sigma|\bar{E}|^2)}{P} = \rho C_p \frac{\partial T}{\partial t} \quad [10]$$

where τ represents the on-time per pulse and P is the period per pulse. For example, if a 50 μ s pulse was repeated every 0.5 s, the ratio would equal to 100 μ s. This simplification has proven effective in representing the energy associated with intra-pulse heating, as a constant heat source acting over the period of one pulse.

In addition, thermal damage analysis can be incorporated by adding a thermal damage equation:

$$\Omega(t) = \int_0^{\tau} \zeta e^{-\frac{E_a}{R^*T(t)}} dt \quad [11]$$

where ζ represents the frequency factor, E_a the activation energy, R the universal gas constant, and τ the total time of heating (59). For the values in Table 1, an Ω value of 1 correlates to tissue coagulation.

As an example, the results of Garcia et al. were replicated using monopolar electrodes inserted into a homogeneous medium. A human brain and tumor were segmented using 3D Slicer 4.6 (Boston, United States) (60–64), and imported into COMSOL. The dynamic conductivity function was applied in COMSOL with $\sigma_0 = 0.256$ S/m, $\sigma_{\max} = 0.768$ S/m, $E_{\text{delta}} = 580$ V/cm, and $E_{\text{range}} = \pm 120$ V/cm. However, in the thermal damage calculations, a zeta of 7.39×10^{39} was used for protein coagulation. The value of α was set to zero because of the relatively low increase in temperature. The spacing and electrode exposure were set to 2.5 cm and a voltage of 2500 V was applied to maintain a 1000 V/cm electric field magnitude. It is important to note that more accurate models will incorporate the separation of white and gray matter, as well as account for the anisotropy in white matter. Nonetheless, even simple numerical models such as this one can provide clinicians with valuable information regarding heat generation during pulsing as well as estimates for ablation volumes before performing the procedure *in vivo*. The results show the tumor mostly engulfed within lethal IRE thresholds, while causing minimum temperature changes at the midpoint between the electrodes (Table 2). Due to the abnormally large tumor size, 18.81 cm³, two sets of pulses were simulated in which the electrode depth was moved vertically 2 cm to allow sufficient treatment. Although the entire tumor is not within the ablation zone, adjuvant chemotherapy can be utilized in the BBB disruption zone as discussed previously. For large, irregular tumors, it is not unusual to use more than two electrode pairs, while for smaller tumors, the bipolar probe, as shown in Figure 2B,

TABLE 1

Material Properties and Parameters

Material	Property	Symbol	Value	Units	Reference
Brain	Thermal conductivity	k	0.565	$W \cdot m^{-1} \cdot K^{-1}$	(70)
	Heat capacity	C_p	3680	$J \cdot kg^{-1} \cdot K^{-1}$	(70)
	Density	ρ	1039	$kg \cdot m^{-3}$	(70)
	Temperature coefficient	α	0.032	$^{\circ}C^{-1}$	(70)
	Metabolic heat generation	q'''	10,437	$W \cdot m^{-3}$	(20)
Blood	Heat capacity	C_b	3840	$J \cdot kg^{-1} \cdot K^{-1}$	(20)
	Density	ρ	1060	$kg \cdot m^{-3}$	(20)
	Blood perfusion rate	ω_b	7.15×10^{-3}	S^{-1}	(20)
Insulation	Electrical conductivity	σ	1.0×10^{-5}	$S \cdot m^{-1}$	(71)
	Thermal conductivity	k	0.01	$W \cdot m^{-1} \cdot K^{-1}$	(71)
	Heat capacity	C_p	3400	$J \cdot kg^{-1} \cdot K^{-1}$	(71)
	Density	ρ	800	$kg \cdot m^{-3}$	(71)
Stainless steel	Electrical conductivity	σ	2.22×10^6	$S \cdot m^{-1}$	(20)
	Thermal conductivity	k	15	$W \cdot m^{-1} \cdot K^{-1}$	(71)
	Heat capacity	C_p	500	$J \cdot kg^{-1} \cdot K^{-1}$	(71)
	Density	ρ	7900	$kg \cdot m^{-3}$	(71)

TABLE 2

Temperature Profile at Various Time Points

Time [s]	T_{mid} [K]	$T_{electrode}$ [K]
0	310.15	310.15
10	310.53	315.23
20	310.87	317.51
30	311.18	319.08
40	311.47	320.15
50	311.73	320.99
60	311.97	321.66
70	312.19	322.18
80	312.40	322.60
90	312.59	322.95
100	312.42	318.31
130	312.01	314.15
160	311.70	312.58

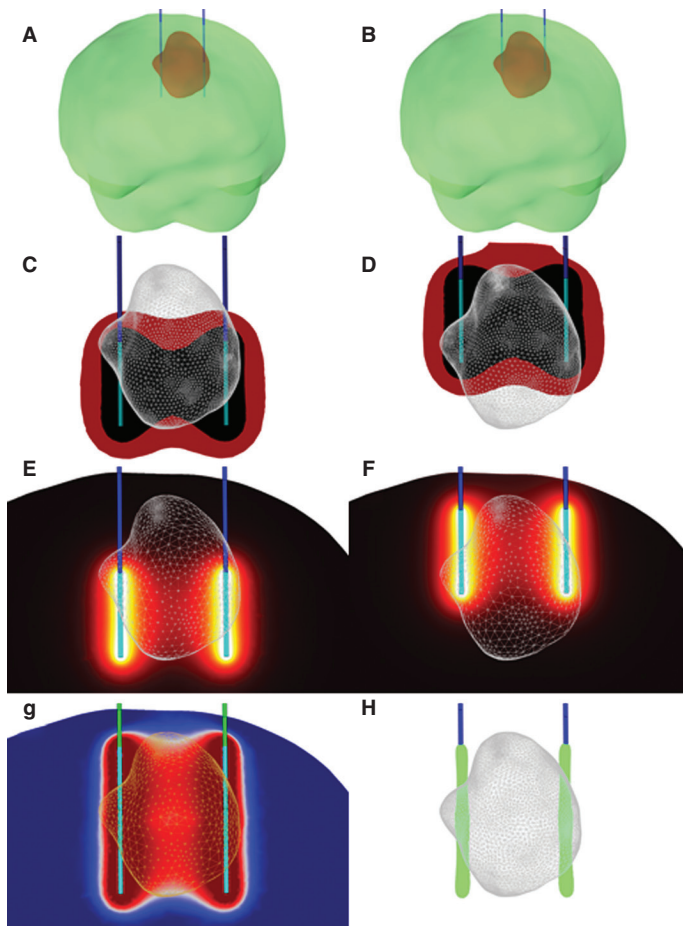


Figure 7 Results of IRE therapy in 3D reconstruction of a human brain. Results from IRE therapy with monopolar electrodes (1 mm diameter, 2.5 cm exposure, 2.5 cm spacing) in a segmented brain and tumor (A, B) showing the electric field (C, D), temperature (E, F), and the effective electrical conductivity distribution (G), as well as the thermal damage (H). Ninety 50 μ s pulses were delivered at voltage-to-distance ratio of 1000 V/cm (applied voltage of 2500 V). A damage integral of $\Omega(t)=1$ corresponds to a 63% probability of cell death. The simulation parameters were identical to those used by Garcia et al. (20), except that the frequency factor of $7.39 \times 1039 \text{ S}^{-1}$ was used for thermal damage associated with protein coagulation. Maximum temperature during treatment was 322.95 K.

has proven to be effective (24). The results of this simulation, Figure 7, demonstrate a maximum temperature change of about 12°C at the electrode surface, and 2°C in between the electrodes.

Treatment planning for both IRE and H-FIRE can be accomplished using the method described previously. Adapting to either IRE or H-FIRE would mean that the conductivity values would change depending on which method is being employed. As mentioned earlier, the ratio of conductivities between different

tissues converges when using higher frequency waveforms; thus, H-FIRE will produce lesions that are more closely approximated by electric fields in static conductivity mediums.

IRE/H-FIRE PRECLINICAL ANIMAL TRIALS

When applying IRE to the liver, kidney, prostate, and pancreas, it is important to maintain a high IRE to thermal ablation ratio. For example, a temperature increase between 10°C and 15°C at the electrode/tissue interface is considered not to cause significant thermal damage to the surrounding tissue. As calculated previously, a 12°C increase at the electrode/tissue interface correlated to a 2°C increase at the midpoint of the electrodes, indicating the tissue exposed to higher temperatures is localized at this interface. Like other organs, the brain is also susceptible to fluctuations in temperature, thus preliminary studies aimed to numerically validate the use of nonthermal IRE (N-TIRE), where pulse parameters are tuned to eliminate most thermal effects.

Studies were conducted to elucidate the lethal threshold for dog GBM cell line J3T (65). As opposed to using 100 μ s pulses, Neal et al. utilized 50 μ s pulses to minimize the energy delivered while still maintaining electroporation effects. 96-well electroporation plates seeded with J3T cells were electroporated using combinations of 1000 and 1500 V/cm electric fields and 10, 30, 50, and 70 pulses. A WST-1 reagent was used to quantify cell viability, where an absorbance of 0.2 would indicate 100% cell death. It was concluded that IRE can be achieved by applying 50 pulses at 1000 V/cm, absorbance of 0.229, without incurring significant thermal damage.

Rossmesl and Garcia et al. aimed to verify *in vitro* studies by performing IRE therapy in seven canines with spontaneous brain tumors (66). Canines are preferred translational models because they develop brain cancers three times more often than their human counterparts. Canine gliomas also show similar biologic, pathologic, and molecular properties as human gliomas do, thus making them an acceptable translational model (see Part V, page xxx) (67). Prior to the application of IRE, pre-treatment planning models were developed and used to determine pulse parameters and electrode configurations. From these models, total ablation protocols were created for tumors smaller than 2.5 cm³ and volume reduction protocols were created for those larger than 2.5 cm³. A craniectomy defect is introduced to allow placement of blunt tip electrodes into the gray matter. Prior to procedure, atracurium, a neuromuscular blockade, is administered to suppress muscle contraction during the onset of pulses. A range of pulses between 90 and 270 were delivered at electric field magnitudes ranging between 1000 and 2000 V/cm in sets consisting of 10 and 20 pulses. After each set of pulses, the polarity was reversed to minimize charge build up, which has become customary when doing these procedures. Brain edema was noticed in one dog during IRE treatment but was resolved by administering corticosteroids and diuretics. MRI confirmed a sharp delineation between treated and healthy tissue, as well as signs of BBB disruption. Common adverse events occurring after IRE treatment included seizure, vomiting, and diarrhea, although one dog developed fatal aspiration pneumonia. In the six canines that survived, the median Karnofsky Performance Scale score increased from 70 to 80, 14 days post-IRE treatment.

Ellis et al. performed IRE in four canines, of which one dog served to find an upper safety limit when applying higher voltages (68). Nine sets of ten 50 μ s pulses were delivered at a rate of 4 Hz. Like before, polarities were alternated after the completion of each set which were delivered at electric field magnitudes of 1000 and 2000 V/cm. Similar results were achieved as in the previous study, except in the case of the canine undergoing higher voltage treatment. Higher voltage pulses resulted in coagulative necrosis of tissue located within the treatment zone, which led to arterial thrombosis and lacunar infarction. Canines that received treatment at 1600 V produced lesion volumes of ~ 1.655 cm³ while maintaining a thermal isoeffective dose of 5.6 min. The canine that received higher voltage treatment experienced an isothermal dose over 60 min, where doses over 60 min correlate to neuronal damage. Based on *in vivo* data from this study, Garcia et al. backed out lethal thresholds using numerical models which incorporated dynamic electrical conductivity dependent on electroporation and temperature effects (33). It was concluded that lethal thresholds for healthy canine brain tissue are 495 and 510 V/cm for applied voltages of 500 and 1000 V, respectively.

Studies have also confirmed nonthermal ablation in deep-seated tumors (33). This ablation was performed primarily in white matter, which, using *in vivo* measurements, was calculated to have higher conductivity, $\sigma = 0.35$ S/m, than what has been determined for gray matter. Numerical simulations which incorporated dynamic conductivity predicted lethal thresholds for white matter to be 630–875 V/cm. In the clinic, this translates to having to apply slightly higher voltages to treat deep-seated tumors.

Combinatorial IRE treatments have also been studied. Garcia et al. applied IRE therapy and adjuvant RT to a 12-year-old mixed breed dog with an 8-week history of partial seizures and behavioral changes (69). Numerical treatment planning for IRE incorporated dynamic conductivity changes, and from these simulations, it was determined that two groups of pulses would be delivered. The first group consisted of four sets of twenty 50 μ s pulses and the second group of two sets of twenty 50 μ s pulses, with an applied voltage of 650 and 500 V, respectively. No adverse clinical effects were observed, and 48 h after treatment, the size of the neoplasm was reduced 75% in size. It was concluded that the lethal threshold for malignant tissue is much lower than that of healthy tissue, implying some sort of selectivity in the brain. Five days after N-TIRE treatment, the patient's neurologic status improved and the previously noted aggression improved. Sixteen days postoperation, the canine received 50 Gy of fractionated RT delivered in 20 treatment sessions, each consisting of 2.5 Gy. Upon completion of radiotherapy, the patient showed evidence of cognitive dysfunction, disturbed sleep–wake cycle, and lack of awareness of familiar people. At 4.5 months post-IRE, the patient showed acute deterioration in mentation and circling to the left. Clinical and MRI results suggested early delayed radiation encephalopathy. At the owner's request, the patient was euthanized. The patient had an overall survival of 149 days after N-TIRE therapy. Postmortem exam showed no evidence of recurrent MG. H-FIRE was also shown to be safe when applied without the use of neuroparalytics and was capable of destroying brain tumors, although these exploratory treat and resect studies are currently ongoing.

Conclusion

The use of IRE and H-FIRE in treating unresectable tumors has been supported by *in vivo*, *ex vivo*, and *in vitro* studies. These therapies have demonstrated their effectiveness in eradicating tumors of the kidney, prostate, pancreas, liver, and, most importantly, the brain in animal models. Benefits of utilizing H-FIRE for treating GBM include sparing of major blood vessels and nerves, focal BBB disruption, selectivity toward malignant cells, more predictable ablation geometries due to mitigation of impedance changes, lack of muscle contractions, and nonthermal ablation.

Acknowledgment: The authors would like to thank Temple Douglas, Maltish Lorenzo, Natalie White, Philip Graybill, Suyashree Bhonsle, Dan Sweeney and Elisa Wasson for their help in editing and providing feedback for writing this chapter. The authors also thank the NIH (R01CA213423 High-Frequency IRE for combinatorial GBM treatment) for funding and general support of this research.

Conflict of Interest: Dr. Davalos and Dr. Arena have patents in the fields of irreversible electroporation and high-frequency irreversible electroporation.

Copyright and permission statement: To the best of our knowledge, the materials included in this chapter do not violate copyright laws. All original sources have been appropriately acknowledged and/or referenced. Where relevant, appropriate permissions have been obtained from the original copyright holder(s).

References

1. Zhang X, Zhang W, Cao W-D, Cheng G, Zhang Y-Q. Glioblastoma multiforme: Molecular characterization and current treatment strategy (Review). *Exp Ther Med*. 2012;3(1):9–14.
2. Henriksson R, Asklund T, Poulsen HS. Impact of therapy on quality of life, neurocognitive function and their correlates in glioblastoma multiforme: A review. *J Neurooncol*. 2011;104(3):639–46. <http://dx.doi.org/10.1007/s11060-011-0565-x>
3. Glas M, Happold C, Rieger J, Wiewrodt D, Bixhr O, Steinbach JP, et al. Long-term survival of patients with glioblastoma treated with radiotherapy and lomustine plus temozolomide. *J Clin Oncol*. 2009;27(8):1257–61. <http://dx.doi.org/10.1200/JCO.2008.19.2195>
4. Mitragotri S. Healing sound: The use of ultrasound in drug delivery and other therapeutic applications. *Nat Rev Drug Discov*. 2005 4(3):255–60. <http://dx.doi.org/10.1038/nrd1662>
5. Mehier-Humbert S, Bettinger T, Yan F, Guy RH. Plasma membrane poration induced by ultrasound exposure: Implication for drug delivery. *J Control Release*. 2005;104(1):213–22. <http://dx.doi.org/10.1016/j.jconrel.2005.01.007>
6. Liu J, Lewis TN, Prausnitz MR. Non invasive assessment and control of ultrasound-mediated membrane permeabilization. *Pharmaceut Res*. 1998;15:918–24. <http://dx.doi.org/10.1023/A:1011984817567>
7. Neu W, Neu J. Theory of electroporation. In: Efimov IR, Kroll MW, Tchou PJ, editors. *Cardiac bioelectric therapy mechanisms*. NY: Springer; 2015. p. 133–61.
8. Weaver JC. Electroporation: A general phenomenon for manipulating cells and tissues. *J Cell Biochem*. 1993;51(4):426–35. <http://dx.doi.org/10.1002/jcb.2400510407>

9. Sweeney DC, Reberšek M, Dermol J, Rems L, Miklavčič D, Davalos RV. Quantification of cell membrane permeability induced by monopolar and high-frequency bipolar bursts of electrical pulses. *Biochim Biophys Acta Biomembr*. 2016;1858(11):2689–98.
10. Böckmann RA, de Groot BL, Kakorin S, Neumann E, Grubmüller H. Kinetics, statistics, and energetics of lipid membrane electroporation studied by molecular dynamics simulations. *Biophys J*. 2008;95(4):1837–50. <http://dx.doi.org/10.1529/biophysj.108.129437>
11. Miklavčič D, Mali B, Kos B, Heller R, Serša G. Electrochemotherapy: From the drawing board into medical practice. *Biomed Eng Online*. 2014;13(1):29. <http://dx.doi.org/10.1186/1475-925X-13-29>
12. André F, Mir LM. DNA electrotransfer: Its principles and an updated review of its therapeutic applications. *Gene Ther*. 2004;11(Suppl 1):S33–42. <http://dx.doi.org/10.1038/sj.gt.3302367>
13. Agerholm-Larsen B, Iversen HK, Ibsen P, Moller JM, Mahmood F, Jensen KS, et al. Preclinical validation of electrochemotherapy as an effective treatment for brain tumors. *Cancer Res*. 2011;71(11):3753–62. <http://dx.doi.org/10.1158/0008-5472.CAN-11-0451>
14. Gothelf A, Mir LM, Gehl J. Electrochemotherapy: Results of cancer treatment using enhanced delivery of bleomycin by electroporation. *Cancer Treat Rev*. 2003;29(5):371–87. [http://dx.doi.org/10.1016/S0305-7372\(03\)00073-2](http://dx.doi.org/10.1016/S0305-7372(03)00073-2)
15. Frandsen SK, Gissel H, Hojman P, Eriksen J, Gehl J. Calcium electroporation in three cell lines: A comparison of bleomycin and calcium, calcium compounds, and pulsing conditions. *Biochim Biophys Acta Gen Subj*. 2014;1840(3):1204–8. <http://dx.doi.org/10.1016/j.bbagen.2013.12.003>
16. Frandsen SK, Gissel H, Hojman P, Tramm T, Eriksen J, Gehl J. Direct therapeutic applications of calcium electroporation to effectively induce tumor necrosis. *Cancer Res*. 2012;72(6):1336–41. <http://dx.doi.org/10.1158/0008-5472.CAN-11-3782>
17. Davalos RV, Mir LM, Rubinsky B. Tissue ablation with irreversible electroporation. *Ann Biomed Eng*. 2005;33(2):223–31. <http://dx.doi.org/10.1007/s10439-005-8981-8>
18. Edd JF, Davalos R V. Mathematical modeling of irreversible electroporation for treatment planning. *Technol Cancer Res Treat*. 2007;6(4):275–86. <http://dx.doi.org/10.1177/153303460700600403>
19. Garcia PA, Davalos RV, Miklavcic D. A numerical investigation of the electric and thermal cell kill distributions in electroporation-based therapies in tissue. *PLoS One*. 2014;9(8):e103083. <http://dx.doi.org/10.1371/journal.pone.0103083>
20. Garcia PA, Rossmeisl JH, Neal RE, Ellis TL, Davalos RV, Rossmeisl JH, Jr., et al. A parametric study delineating irreversible electroporation from thermal damage based on a minimally invasive intracranial procedure. *Biomed Eng Online*. 2011;10(1):34. <http://dx.doi.org/10.1186/1475-925X-10-34>
21. Valerio M, Dickinson L, Ali A, Ramachandran N, Donaldson I, Freeman A, et al. A prospective development study investigating focal irreversible electroporation in men with localised prostate cancer: Nanoknife electroporation ablation trial (NEAT). *Contemp Clin Trials*. 2014;39(1):57–65. <http://dx.doi.org/10.1016/j.cct.2014.07.006>
22. Neal RE, Millar JL, Kavnoudias H, Royce P, Rosenfeldt F, Pham A, et al. In vivo characterization and numerical simulation of prostate properties for non-thermal irreversible electroporation ablation. *Prostate*. 2014;74(5):458–68. <http://dx.doi.org/10.1002/pros.22760>
23. Martin RCG, McFarland K, Ellis S, Velanovich V. Irreversible electroporation in locally advanced pancreatic cancer: Potential improved overall survival. *Ann Surg Oncol*. 2013 Nov;20(Suppl 3):443–9.
24. Martin RCG, McFarland K, Ellis S, Velanovich V. Irreversible electroporation therapy in the management of locally advanced pancreatic adenocarcinoma. *J Am Coll Surg*. 2012;215(3):361–9. <http://dx.doi.org/10.1016/j.jamcollsurg.2012.05.021>
25. Latouche EL, Sano MB, Lorenzo MF, Davalos RV, Martin RCG. Irreversible electroporation for the ablation of pancreatic malignancies: A patient-specific methodology. *J Surg Oncol*. 2017 Jan:1–7. <http://dx.doi.org/10.1002/jso.24566>
26. Cannon R, Ellis S, Hayes D, Narayanan G, Martin RCG. Safety and early efficacy of irreversible electroporation for hepatic tumors in proximity to vital structures. *J Surg Oncol*. 2013;107(5):544–9. <http://dx.doi.org/10.1002/jso.23280>
27. Kingham TP, Karkar AM, D'Angelica MI, Allen PJ, Dematteo RP, Getrajdman GI, et al. Ablation of perivascular hepatic malignant tumors with irreversible electroporation. *J Am Coll Surg*. 2012;215(3):379–87. <http://dx.doi.org/10.1016/j.jamcollsurg.2012.04.029>

28. Scheffer HJ, Nielsen K, De Jong MC, Van Tilborg AAJM, Vieveen JM, Bouwman A, et al. Irreversible electroporation for nonthermal tumor ablation in the clinical setting: A systematic review of safety and efficacy. *J Vasc Interv Radiol*. 2014;25(7):997–1011. <http://dx.doi.org/10.1016/j.jvir.2014.01.028>
29. Pech M, Janitzky A, Wendler JJ, Strang C, Blaschke S, Dudeck O, et al. Irreversible electroporation of renal cell carcinoma: A first-in-man phase I clinical study. *Cardiovasc Intervent Radiol*. 2011;34(1):132–8. <http://dx.doi.org/10.1007/s00270-010-9964-1>
30. Thomson KR, Cheung W, Ellis SJ, Federman D, Kavnoudias H, Loader-Oliver D, et al. Investigation of the safety of irreversible electroporation in humans. *J Vasc Interv Radiol*. 2011 22(5):611–21. <http://dx.doi.org/10.1016/j.jvir.2010.12.014>
31. Li W, Fan Q, Ji Z, Qiu X, Li Z. The effects of irreversible electroporation (IRE) on nerves. *PLoS One*. 2011;6(4):e18831. <http://dx.doi.org/10.1371/journal.pone.0018831>
32. Maor E, Ivorra A, Leor J, Rubinsky B. The effect of irreversible electroporation on blood vessels. *Technol Cancer Res Treat*. 2007;6(4):307–12. <http://dx.doi.org/10.1177/153303460700600407>
33. Garcia PA, Rossmeisl JH, Neal RE, Ellis TL, Olson JD, Henao-Guerrero N, et al. Intracranial nonthermal irreversible electroporation: In vivo analysis. *J Membr Biol*. 2010;236(1):127–36. <http://dx.doi.org/10.1007/s00232-010-9284-z>
34. Eikermann M, Groeben H, Hüsing J, Peters J. Accelerometry of adductor pollicis muscle predicts recovery of respiratory function from neuromuscular blockade. *Anesthesiology*. 2003;98(6):1333–7. <http://dx.doi.org/10.1097/0000542-200306000-00006>
35. Golberg A, Bruinsma BG, Uygun BE, Yarmush ML. Tissue heterogeneity in structure and conductivity contribute to cell survival during irreversible electroporation ablation by “electric field sinks.” *Sci Rep*. 2015;5:8485. <http://dx.doi.org/10.1038/srep08485>
36. Qasrawi R, Silve L, Burdío F, Abdeen Z, Ivorra A. Anatomically realistic simulations of liver ablation by irreversible electroporation. *Technol Cancer Res Treat*. 2017;153303461668747. <http://dx.doi.org/10.1177/1533034616687477>
37. Arena CB, Sano MB, Rossmeisl JH, Caldwell JL, Garcia PA, Rylander MN, et al. High-frequency irreversible electroporation (H-FIRE) for non-thermal ablation without muscle contraction. *Biomed Eng Online*. 2011;10(1):102. <http://dx.doi.org/10.1186/1475-925X-10-102>
38. Patrick Reilly J, Freeman VT, Larkin WD. Sensory effects of transient electrical stimulation—Evaluation with a neuroelectric model. *IEEE Trans Biomed Eng*. 1985;BME-32(12):1001–11. <http://dx.doi.org/10.1109/TBME.1985.325509>
39. van den Honert C, Mortimer JT. The response of the myelinated nerve fiber to short duration. *Ann Biomed Eng*. 1979;7:117–25. <http://dx.doi.org/10.1007/BF022363130>
40. Hodgkin AL, Huxley AF. A quantitative description of membrane current and its application to conduction and excitation in nerve. *Bull Math Biol*. 1952;52(1–2):25–71. <http://dx.doi.org/10.1113/jphysiol.1952.sp004764>
41. Sano MB, Arena CB, Bittleman KR, DeWitt MR, Cho HJ, Szot CS, et al. Bursts of bipolar microsecond pulses inhibit tumor growth. *Sci Rep*. 2015;5:14999. <http://dx.doi.org/10.1038/srep14999>
42. Arena CB, Szot CS, Garcia PA, Rylander MN, Davalos RV. A three-dimensional in vitro tumor platform for modeling therapeutic irreversible electroporation. *Biophys J*. 2012;103(9):2033–42. <http://dx.doi.org/10.1016/j.bpj.2012.09.017>
43. Andreuccetti D, Fossi R, Petrucci C. An Internet resource for the calculation of the dielectric properties of body tissues in the frequency range 10Hz–100GHz. Institute for Applied Physics, Italian National Research Council. Available from: <http://niremf.ifac.cnr.it/tissprop/> (Accessed February 8, 2017).
44. Arena CB, Sano MB, Rylander MN, Davalos RV. Theoretical considerations of tissue electroporation with high-frequency bipolar pulses. *IEEE Trans Biomed Eng*. 2011;58(5):1474–82. <http://dx.doi.org/10.1109/TBME.2010.2102021>
45. Davalos RV, Otten DM, Mir LM, Rubinsky B. Electrical impedance tomography for imaging tissue electroporation. *IEEE Trans Biomed Eng*. 2004;51(5):761–7.
46. Bonakdar M, Latouche EL, Mahajan RL, Davalos RV. The feasibility of a smart surgical probe for verification of IRE treatments using electrical impedance spectroscopy. *IEEE Trans Biomed Eng*. 2015;62(11):2674–84.

47. Bhonsle SP, Arena CB, Sweeney DC, Davalos RV. Mitigation of impedance changes due to electroporation therapy using bursts of high-frequency bipolar pulses. *Biomed Eng Online*. 2015;14(Suppl 3):S3.
48. Ivorra A, Mir LM, Rubinsky B. Electric field redistribution due to conductivity changes during tissue electroporation: Experiments with a simple vegetal model. In: Dössel O, Schlegel WC, editors. *World Congress on Medical Physics and Biomedical Engineering, September 7–12, 2009, Munich, Germany. IFMBE Proceedings*, vol. 25/13. Berlin: Springer.
49. Sano MB, Arena CB, DeWitt MR, Saur D, Davalos RV. In-vitro bipolar nano- and microsecond electro-pulse bursts for irreversible electroporation therapies. *Bioelectrochemistry*. 2014;100:69–79. <http://dx.doi.org/10.1016/j.bioelechem.2014.07.010>
50. Pakhomov AG, Semenov I, Xiao S, Pakhomova ON, Gregory B, Schoenbach KH, et al. Cancellation of cellular responses to nanoelectroporation by reversing the stimulus polarity. *Cell Mol Life Sci*. 2014;71(22):4431–41. <http://dx.doi.org/10.1007/s00018-014-1626-z>
51. Ivey JW, Latoche EL, Sano MB, Rossmeisl JH, Davalos RV, Verbridge SS. Targeted cellular ablation based on the morphology of malignant cells. *Sci Rep*. 2015;5:17157. <http://dx.doi.org/10.1038/srep17157>
52. Janzer RC, Raff MC. Astrocytes induce blood-brain barrier properties in endothelial cells. *Nature*. 1987;325:253–7. <http://dx.doi.org/10.1038/325253a0>
53. Garcia PA, Rossmeisl JH, Robertson JL, Olson JD, Johnson AJ, Ellis TL, et al. 7.0-T Magnetic resonance imaging characterization of acute blood-brain-barrier disruption achieved with intracranial irreversible electroporation. *PLoS One*. 2012;7(11):1–8. <http://dx.doi.org/10.1371/journal.pone.0050482>
54. Arena CB, Garcia PA., Sano MB, Olson JD, Rogers-Cotrone T, Rossmeisl JH, et al. Focal blood-brain-barrier disruption with high-frequency pulsed electric fields. *Technology*. 2014;2(3):1–8. <http://dx.doi.org/10.1142/S2339547814500186>
55. Bonakdar M, Wasson EM, Lee YW, Davalos RV. Electroporation of brain endothelial cells on chip toward permeabilizing the blood-brain barrier. *Biophys J*. 2016;110(2):503–13. <http://dx.doi.org/10.1016/j.bpj.2015.11.3517>
56. Langus J, Kranjc M, Kos B, Šuštar T, Miklavčič D. Dynamic finite-element model for efficient modelling of electric currents in electroporated tissue. *Sci Rep*. 2016 May;6:26409. <http://dx.doi.org/10.1038/srep26409>
57. Corovic S, Lackovic I, Sustaric P, Sustar T, Rodic T, Miklavcic D. Modeling of electric field distribution in tissues during electroporation. *Biomed Eng Online*. 2013;12(1):16. <http://dx.doi.org/10.1186/1475-925X-12-16>
58. Neal RE, Garcia PA, Robertson JL, Davalos RV. Experimental characterization and numerical modeling of tissue electrical conductivity during pulsed electric fields for irreversible electroporation treatment planning. *IEEE Trans Biomed Eng*. 201259(4):1076–85. <http://dx.doi.org/10.1109/TBME.2012.2182994>
59. Tropea BI, Lee RC. Thermal injury kinetics in electrical trauma. *J Biomech Eng*. 1992;114(2):241–50. <http://dx.doi.org/10.1115/1.2891378>
60. Brigham and Women's Hospital, 3D Slicer Contributors. *3D Slicer*. 2015:1–4. Available from: <http://www.slicer.org> (Accessed January 16, 2017).
61. Fedorov A, Beichel R, Kalpathy-Cramer J, Finet J, Fillion-Robin JC, Pujol S, et al. 3D Slicer as an image computing platform for the Quantitative Imaging Network. *Magn Reson Imaging*. 2012;30(9):1323–41. <http://dx.doi.org/10.1016/j.mri.2012.05.001>
62. Gering DT, Nabavi A, Kikinis R, Hata N, O'Donnell LJ, Grimson WE, et al. An integrated visualization system for surgical planning and guidance using image fusion and an open MR. *J Magn Reson Imaging*. 2001;13(6):967–75. <http://dx.doi.org/10.1002/jmri.1139>
63. Gering DT, Nabavi A, Kikinis R, Grimson WEL, Hata N, Everett P, et al. An integrated visualization system for surgical planning and guidance using image fusion and interventional imaging. In: *International Conference on Medical Image Computing and Computer-Assisted Intervention*, September 1999. *Med Image Comput Assist Interv. MICCAI*. 1999. p. 809–19.
64. Pieper S, Lorenzen B, Schroeder W, Kikinis R. The NA-MIC Kit: ITK, VTK, pipelines, grids and 3D Slicer as an open platform for the medical image computing community. In: *IEEE 3rd International Symposium on Biomedical Imaging: Macro to Nano*, April 2006, *Proc IEEE Intl Symp on Biomedical Imaging ISBI*. 2006. p. 698–701.

65. Neal RE, Rossmeisl JH, D'Alfonso V, Robertson JL, Garcia PA, Elankumaran S, et al. In vitro and numerical support for combinatorial irreversible electroporation and electrochemotherapy glioma treatment. *Ann Biomed Eng.* 2014;42(3):475–87. <http://dx.doi.org/10.1007/s10439-013-0923-2>
66. Rossmeisl JH, Garcia PA, Pancotto TE, Robertson JL, Henao-Guerrero, Neal RE, et al. Safety and feasibility of the NanoKnife system for irreversible electroporation ablative treatment of canine spontaneous intracranial gliomas. *J Neurosurg.* 2015;123(4):1008–25. <http://dx.doi.org/10.3171/2014.12.JNS141768>
67. Rossmeisl JH, Duncant RB, Huckle WR, Troy GC. Expression of vascular endothelial growth factor in tumors and plasma from dogs with primary intracranial neoplasms. *Am J Vet Res.* 68(11):1239–45. <http://dx.doi.org/10.2460/ajvr.68.11.1239>
68. Ellis TL, Garcia PA, Rossmeisl JH, Henao-Guerrero N, Robertson J, Davalos RV. Nonthermal irreversible electroporation for intracranial surgical applications. Laboratory investigation. *J Neurosurg.* 2011;114(3):681–8. <http://dx.doi.org/10.3171/2010.5.JNS091448>
69. Garcia PA, Pancotto T, Rossmeisl JH, Henao-Guerrero N, Gustafson NR, Daniel GB, et al. Non-thermal irreversible electroporation (N-TIRE) and adjuvant fractionated radiotherapeutic multimodal therapy for intracranial malignant glioma in a canine patient. *Technol Cancer Res Treat.* 2011;10(1):73–83. <http://dx.doi.org/10.7785/tcrt.2012.500181>
70. Duck F. *Physical properties of tissues: A comprehensive reference book.* San Diego, CA: Academic Press; 1990.
71. Cosman ER, Jr., Cosman ER, Sr. Electric and thermal field effects in tissue around. *Am Acad Pain Med.* 2005;6(6):405–24.

Maximizing Local Access to Therapeutic Deliveries in Glioblastoma. Part IV: Image-Guided, Remote-Controlled Opening of the Blood–Brain Barrier for Systemic Brain Tumor Therapy

ANIRUDH SATTIRAJU¹ • YAO SUN¹ • KIRAN KUMAR SOLINGAPURAM SAI¹ • KING C.P. LI² • AKIVA MINTZ¹

¹Department of Radiology, Brain Tumor Center of Excellence, Wake Forest Baptist Medical Center Comprehensive Cancer Center, Winston Salem, NC, USA; ²Carle Illinois College of Medicine, Urbana, IL, USA

Author for correspondence: Akiva Mintz, Department of Radiology, Columbia University Medical Center. Columbia University College of Physicians and Surgeons Radiology Administrative Office, 1st Floor, Room PH1-333 New York, NY 10032, USA. E-mail: am4754@cumc.columbia.edu

Doi: <http://dx.doi.org/10.15586/codon.glioblastoma.2017.ch20>

Abstract: Disease in the central nervous system (CNS) is a challenge to treat with systemic therapies due to the presence of the blood–brain barrier (BBB), which excludes common and novel therapeutics. For example, glioblastoma (GBM) is the most common and aggressive primary brain tumor, with an extremely poor prognosis due to infiltrating tumor cells in areas of normal brain. A primary

In: *Glioblastoma*. Steven De Vleeschouwer (Editor), Codon Publications, Brisbane, Australia ISBN: 978-0-9944381-2-6; Doi: <http://dx.doi.org/10.15586/codon.glioblastoma.2017>

Copyright: The Authors.

Licence: This open access article is licenced under Creative Commons Attribution 4.0 International (CC BY 4.0). <https://creativecommons.org/licenses/by-nc/4.0/>

challenge of treating this devastating disease is the exclusion of systemic therapies from the CNS. While efforts are being made to develop strategies for designing drugs that can pass through the BBB, there are also efforts to use novel engineering techniques to safely allow any systemic therapy into the CNS and areas of disease. In this chapter, we focus on using high-intensity focused ultrasound (HIFU) to circumvent the BBB.

Key words: Blood–brain barrier; Glioblastoma; High-intensity ultrasound; Stem cells

Introduction

Glioblastoma (GBM) is the most common and aggressive primary brain tumor, with an extremely poor prognosis (1). The dismal prognosis is a direct result of the fact that standard therapies fail to eradicate residual or infiltrating cells that reside adjacent to and infiltrate normal brain tissue. This failure is mostly due to the unique physiology of the blood–brain barrier (BBB), which is designed not only to protect the brain from exogenous and endogenous toxins but also to prevent the full cytotoxic effects of most therapeutics on intracranial tumors. Thus, many groups are developing novel methods of permeabilizing the BBB to treat infiltrating tumor cells that are in regions of normal brain. One focus of these efforts to circumvent the BBB is using novel ultrasound technology that is emerging as a noninvasive and translational approach to safely allow systemic therapies to access GBM.

Image-Guided, Remote-Controlled Opening of the BBB for Systemic Brain Tumor Therapy

HIGH-INTENSITY FOCUSED ULTRASOUND IN REMOTELY OVERCOMING OF THE BBB FOR DRUG DELIVERY

High-intensity focused ultrasound (HIFU) is a therapeutic ultrasound technique that delivers high-intensity acoustic energy to a localized area in the body. These ultrasound waves are significantly higher than what is commonly used in imaging or diagnostic ultrasound. HIFU can thus be used to ablate tissue from the resulting high temperature without affecting the surrounding tissues. This is accomplished by focusing an ultrasound beam via acoustic lens, a curved transducer or a phased array (2–4). Since ultrasound waves pass through skin and other intervening tissues at relative low intensities, they produce no effect or damage outside the area of focus, where they typically provide intensities up to three to four orders of magnitude higher compared to the unfocused beam (3).

When used for therapeutic purposes, the focused ultrasound energy from HIFU induces a temperature rise or intensive mechanical force to alter tissue structure and functions, resulting in a large variety of localized bioeffects through

either mechanical or thermal activity (5). Depending on the energy level, the generated bioeffects can be mild and nondestructive, such as those for hyperthermia or physical therapy, or more extreme and destructive, such as thermal ablation of tumors in prostate, uterus, brain, etc. (6–12). Although destructive ultrasound exposures for ablation of a variety of tumors are currently the best-known application of HIFU technology, there is increasing interest in using nondestructive HIFU to induce BBB opening to allow the delivery of therapeutic agents to the brain.

HIFU has been studied to treat brain diseases as far back as the 1940s (4, 13, 14). Localized and reversible BBB disruption created by direct sub-lethal HIFU exposure with or without pre-injection of microbubbles has been reported extensively in recent decades (5, 15, 16). Direct HIFU exposure without any ultrasound contrast agent may in itself induce BBB disruption, but tissue necrosis due to the high energy makes this technique suboptimal. By introducing microbubbles, which are typically used in diagnostic ultrasound as a contrast agent, at the time of sub-lethal HIFU exposure, researchers have demonstrated the potential of permeabilizing the BBB without producing any apparent neuronal damage (5, 17). The mechanism of this disruption is thought to be from the mechanical forces created by the oscillation of circulating microbubbles driven by focused ultrasound. This phenomenon may change the array of endothelial cells in the blood vessel wall, thus transiently increasing the permeability of the BBB without any lethal effects (18).

Although different imaging modalities have been used to guide the targeting of HIFU exposures in the body, MRI presents the standard modality in the studies for HIFU-induced BBB opening. Compared to other imaging modalities such as diagnostic ultrasound, MRI enables more accurate placement of the HIFU beam in the brain, and the delivery of gadolinium-based MR contrast agents can be used as a reliable surrogate marker for successful permeability enhancement and optimization. Thus, it is hopeful that nondestructive HIFU technologies can permeabilize the BBB to systemic therapeutics that cannot be currently used against brain cancer due to exclusion by the BBB.

CONTROLLABLE DRUG DELIVERY USING STEM CELLS IN CONJUNCTION WITH HIFU

One of the primary reasons of GBM recurrence is the presence of infiltrating tumor cells that can be found at distances far away from the primary tumor. These cells do not permeabilize the BBB to standard gadolinium contrast and are thus not visible on MRI. Using HIFU with microbubbles to permeabilize the BBB requires visualization of the target, which may be insufficient in regions of undetectable invasive cells at a far distance from the tumor (Figure 1A). Xiong et al. have developed a HIFU technique used in conjunction with therapeutic stem cells to access these infiltrating tumor cells using the tumor-homing biological properties of stem cells to locate the invisible invasive tumor cells.

Due to their tumor-tropic capacity, stem cells are emerging as feasible delivery vehicles to therapeutically target primary and invasive tumor cells (Figure 1B). Investigators have demonstrated the *in vivo* migratory capacity of stem cells toward primary GBM tumors as well as invasive tumor cells that intermingle with normal brain tissue (19–28). Various stem cells such as embryonic stem cells,

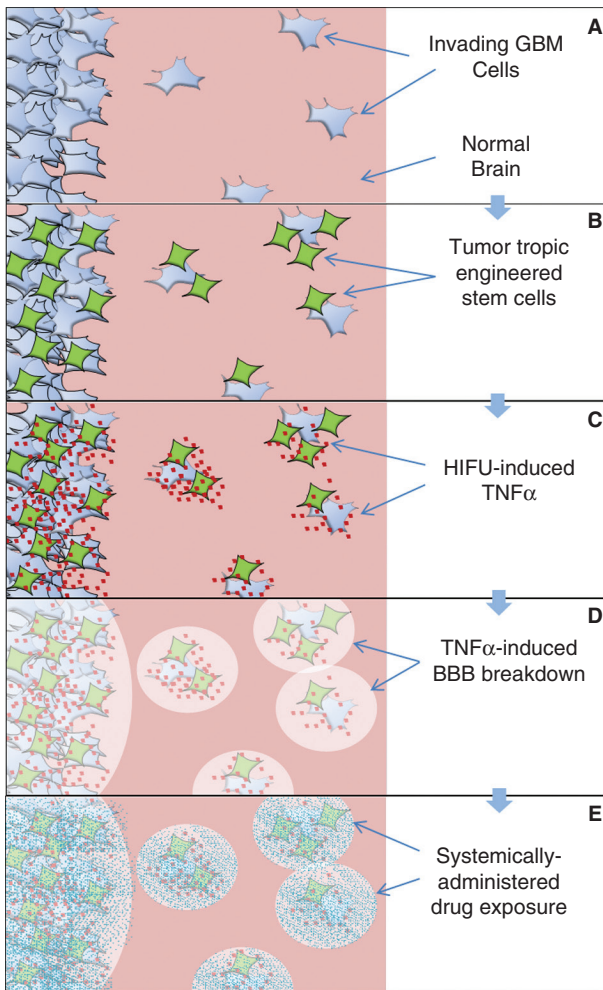


Figure 1 Schemata of invasive GBM cells and how they can be targeted by a combination of stem cells and HIFU. (A) Invasive GBM cells migrating away from the primary tumor mass. (B) These cells have been shown to be targeted by engineered stem cells capable of secreting therapeutics, including TNF α . (C) Mild heating by HIFU can induce stem cells that express TNF α , which is engineered to be under the control of the HSP70 promoter. (D) TNF α causes local BBB breakdown, allowing for systemically injected therapeutics to precisely target areas of tumor invasion but not areas that are not targeted by engineered stem cells (E).

mesenchymal stem cells, neural stem cells, induced pluripotent stem cells (iPSCs), and neural stem cells derived from iPSCs have been shown to migrate to intracranially established GBMs when implanted loco-regionally within the brain, and their ability to secrete anti-GBM therapies after genetic modification has been investigated (29). The reason for the migration of stem cells toward sites of GBM and the molecular pathways involved in this process are under further investigation. Evidence suggests that the tumor tropism of stem cells is due to their affinity to the tumor microenvironment which often mimics aspects of the stem cell niches, such as by releasing various cytokines, the presence of severe hypoxia, and extensive vascularization (30, 31). Even though various chemokine receptors and their ligands have been attributed to play a role in tumor-tropic migration of stem cells, the stromal derived factor-1 (SDF-1) CXC-chemokine receptor 4 (CXCR4)

signaling axis is the most studied, and is implicated to play an important role in migration of various stem cells towards tumors (32, 33). In addition to SDF-1/CXCR4 axis, other signaling pathways such as urokinase-type plasminogen activator (uPA)/uPA receptor, PI3K, vascular endothelial growth factor receptor 2 (VEGF2), and matrix metalloproteinase 1 (MMP1)/protease-activated receptor 1 (PAR1) signaling pathways have been implicated in migration of stem cells to sites of tumors (29). SDF-1 has been reported to play a vital role in NSC maintenance and regulates NSC homing during neurogenesis (34). SDF-1 is reported to be expressed and secreted by GBM stem cells and endothelial cells which implicate its role in GBM stem cell migration and recruitment of other components of the tumor microenvironment as well. SDF-1 is also highly expressed in regions of hypoxia within GBMs and is thought to promote survival through activation of NF- κ B (33, 35).

Various tumor-tropic stem cells have previously been reported to deliver anti-GBM therapies using different strategies. Stem cells genetically modified to express tumor necrosis factor–related apoptosis inducing ligand (TRAIL) have been used previously in preclinical studies to induce apoptosis in tumor cells. Tumor-tropic stem cells that express ligands that inhibit tumor specific receptors such as EGFRvIII and stem cells that express “decoy” receptors that sequester essential paracrine factors within the tumor microenvironment have been shown to reduce GBM cell proliferation in preclinical studies (36). Another strategy of inducing secretion of cytokines is to increase recruitment of cytotoxic T cells and anti-tumor immunity within GBM microenvironment. This strategy could also be used to in combination with immune checkpoint inhibitors to enhance tumor-directed cytotoxicity. In addition, tumor-tropic stem cells have also been shown to deliver nanoparticles loaded with chemotherapy and oncolytic viruses. The accumulation of effective concentrations of nanoparticles within GBM tissue could be increased using a stem cell–based strategy to bypass the BBB (37, 38). The efficiency and safety of delivering GBM-targeted oncolytic viruses have also been enhanced using tumor-tropic stem cells (39, 40). Thus, it has been established that using engineered stem cells to secrete therapeutics after migrating to tumor sites has strong therapeutic potential.

The biologic targeting of stem cells along with the spatial targeting of HIFU can be combined to create a remote-controlled expression platform has been leveraged to assist in locally opening up the BBB for facilitated drug delivery of systemically administered agents (41). This can be accomplished by remotely triggering expression of effector cytokines, such as TNF α , from engineered tumor-homing stem cells in response to noninvasive image-guided HIFU (Figure 1C). Recently, such an application of nondestructive HIFU has been used to heat tissue to nonlethal temperatures (~42°C) to locally activate the upregulation of a number of genes including heat shock protein (HSP) (42, 43). This biology has enabled investigators to *in vivo* regulate genes of their choice by engineering them to be expressed under the control of the HSP70 promoter and activating expression *in vivo* using sub-lethal HIFU (44). By combining stem cell delivery, heat-inducible gene expression and mild heating with HIFU, Xiong et al. demonstrated that HIFU can be used to remotely control the expression of pro-inflammatory factors engineered in stem cells under the control of the HSP70 promoter (Figure 1C). This targeted expression led to the permeabilization of the BBB with high-spatiotemporal precision and biologic selectivity, allowing for penetration of

systemically administered small molecular MRI contrast agent and 300-nm-sized nanoparticles into the brain (Figure 1D, E) (41). This opening of the BBB was limited to where selected factors were secreted secondary to HIFU activation, near the engineered stem cells and consequently the infiltrating tumor cells. A major advantage of this process over using focused ultrasound and microbubbles for BBB opening is the fact that this process relies on the combination of physical energy deposition and a biologic response (stem cell tumor tropism). Thus, although a much larger volume would need to be heated by HIFU to nonlethal temperatures (42–43°C), the BBB opening will be much more focused and enhanced only where the heated engineered stem cells are located, which has been demonstrated to be adjacent to primary and invasive GBM cells (Figure 1D, E) (2–4, 16–20). Although there is an added component of therapeutic stem cells, this technique can potentially be performed in a noninvasive manner, as the engineered stem cells can be placed directly into a GBM resection cavity during standard-of-care surgery using an encapsulation technique. This approach was developed by Kauer et al. who demonstrated that encapsulating therapeutic stem cells in biodegradable, synthetic extracellular matrix (sECM) significantly increased their retention time in the GBM resection cavity, permitted strong tumor-selective migration and allowed secretion of anti-tumor proteins from sECM-encapsulated stem cells *in vivo* (45). Seven to fourteen days post stem cell implantation/tumor resection, HIFU can be used to noninvasively mildly heat (42–43°C) the resection cavity and surrounding brain to activate stem cell TNF α production and selectively permeabilize the BBB where the stem cells migrate, including the infiltrating tumor cells. Of translational relevance, there is already a clinical HIFU system (InSightec) that is being used to transcranially treat brain disorders and is in clinical trials for brain cancer (46–48). This MRI-compatible helmet-like device houses a multi-channel-phased array system and can cover large volumes. Since one only needs to heat the brain and tumor to 42–43°C for gene activation under the HSP70 promoter, this technique is not constrained to only treating focal areas, a restriction that may limit the treating volume for reaching ablation temperatures (55°C). Heating to 42–43°C only requires a fraction of the energy needed for ablation and is feasible over large volumes in preclinical and clinical settings and does not result in overheating of the skull seen with conventional ablative HIFU. For example, an early clinical trial in using HIFU for brain tumors reported “The skull area that the acoustic beam was distributed over was calculated by the treatment planning workstation to be 284, 327, and 354 cm², for patients 1–3” (48). Importantly, all patients received heat treatment to at least 42°C, indicating the translational potential of gently heating large areas of the brain to nonablation temperatures.

One enabling technology to controlled sub-lethal HIFU activation is MR thermometry, which incorporates automated, real-time feedback control of a pre-defined temperature, allowing for stably controlling HIFU to heat the brain tissue to around 42–43°C for successful gene activation to open the BBB (41). Indeed, transcranial magnetic resonance-guided focused ultrasound (tsMRgFUS), which employs a phase array comprised of hundreds of transducer elements, has been used in clinical trial to precisely heat or ablate target areas in the brain (49). A commercially available clinical tsMRgFUS system (inSightec Inc. Tirat Carmel, Israel) that is being used to transcranially treat various brain disorders including essential tremors, Parkinson’s disease, and brain cancer. The availability of clinical

tsMRgFUS system that can deliver HIFU energy through the human skull to a focal spot in the brain may further facilitate the translational and clinic application of using nondestructive HIFU to induce BBB opening to allow the delivery of therapeutic agents to the brain.

Conclusion

In order to better treat GBM, it will be crucial to develop novel techniques to deliver chemotherapies and novel molecular-targeted therapies to invasive GBM cells. HIFU provides a remote-controlled platform to permeabilize the BBB using mechanical forces via microbubbles or by mildly heating areas to induce engineered stem cells to secrete select cytokines. Translating these and other novel delivery approaches have the potential to enable significantly improved outcomes that have eluded patients receiving traditional systemic therapies.

Acknowledgment: This work was supported by the National Institutes of Health grants 1R01CA179072-01A1 (to Mintz), the American Cancer Society Mentored Research Scholar grant 124443-MRSG-13-121-01-CDD (to Mintz) and P30 CA012197 (to Pasche, Comprehensive Cancer Center of Wake Forest University (CCCWFU)).

Conflict of Interest: The authors declare no potential conflicts of interest with respect to research, authorship, and/or publication of this manuscript.

Copyright and permission statement: To the best of our knowledge, the materials included in this chapter do not violate copyright laws. All original sources have been appropriately acknowledged and/or referenced. Where relevant, appropriate permissions have been obtained from the original copyright holder(s).

References

1. Wen PY, Kesari S. Malignant gliomas in adults. *N Engl J Med*. 2008;359(5):492–507. <http://dx.doi.org/10.1056/NEJMra0708126>
2. Kennedy JE. High-intensity focused ultrasound in the treatment of solid tumours. *Nat Rev Cancer*. 2005;5(4):321–7. <http://dx.doi.org/10.1038/nrc1591>
3. Clement GT. Perspectives in clinical uses of high-intensity focused ultrasound. *Ultrasonics*. 2004;42(10):1087–93. <http://dx.doi.org/10.1016/j.ultras.2004.04.003>
4. Lynn JG, Zwemer RL, Chick AJ, Miller AE. A new method for the generation and use of focused ultrasound in experimental biology. *J Gen Physiol*. 1942;26(2):179. <http://dx.doi.org/10.1085/jgp.26.2.179>
5. Mesiwala AH, Farrell L, Wenzel HJ, Silbergeld DL, Crum LA, Winn HR, et al. High-intensity focused ultrasound selectively disrupts the blood-brain barrier *in vivo*. *Ultrasound Med Biol*. 2002;28(3):389–400. [http://dx.doi.org/10.1016/S0301-5629\(01\)00521-X](http://dx.doi.org/10.1016/S0301-5629(01)00521-X)
6. Vaezy S, Fujimoto VY, Walker C, Martin RW, Chi EY, Crum LA. Treatment of uterine fibroid tumors in a nude mouse model using high-intensity focused ultrasound. *Am J Obstet Gynecol*. 2000;183(1):6–11.

7. Stewart EA, Rabinovici J, Tempany C, Inbar Y, Regan L, Gastout B, et al. Clinical outcomes of focused ultrasound surgery for the treatment of uterine fibroids. *Fertil Steril.* 2006;85(1):22–9. <http://dx.doi.org/10.1016/j.fertnstert.2005.04.072>
8. Wu F, Wang ZB, Cao YD, Chen W, Bai J, Zou J, et al. A randomised clinical trial of high-intensity focused ultrasound ablation for the treatment of patients with localised breast cancer. *Br J Cancer.* 2003;89(12):2227–33. <http://dx.doi.org/10.1038/sj.bjc.6601411>
9. Kennedy J, Wu F, Ter Haar G, Gleeson F, Phillips R, Middleton M, et al. High-intensity focused ultrasound for the treatment of liver tumours. *Ultrasonics.* 2004;42(1):931–5. <http://dx.doi.org/10.1016/j.ultras.2004.01.089>
10. Iling R, Kennedy J, Wu F, Ter Haar G, Protheroe A, Friend P, et al. The safety and feasibility of extracorporeal high-intensity focused ultrasound (HIFU) for the treatment of liver and kidney tumours in a Western population. *Br J Cancer.* 2005;93(8):890–5. <http://dx.doi.org/10.1038/sj.bjc.6602803>
11. Thüroff S, Chaussy C, Vallancien G, Wieland W, Kiel HJ, Le Duc A, et al. High-intensity focused ultrasound and localized prostate cancer: Efficacy results from the European multicentric study. *J Endourol.* 2003;17(8):673–7. <http://dx.doi.org/10.1089/089277903322518699>
12. Blana A, Walter B, Rogenhofer S, Wieland WF. High-intensity focused ultrasound for the treatment of localized prostate cancer: 5-year experience. *Urology.* 2004;63(2):297–300. <http://dx.doi.org/10.1016/j.urology.2003.09.020>
13. Fry WJ. Intense ultrasound in investigations of the central nervous system. *Adv Biol Med Phys.* 1958;6:281–348. <http://dx.doi.org/10.1016/B978-1-4832-3112-9.50012-8>
14. Fry F. Production of reversible changes in the central nervous system by ultrasound. *Science.* 1958;127:83–4.
15. Kinoshita M, McDannold N, Jolesz FA, Hynynen K. Noninvasive localized delivery of Herceptin to the mouse brain by MRI-guided focused ultrasound-induced blood–brain barrier disruption. *Proc Natl Acad Sci.* 2006;103(31):11719–23. <http://dx.doi.org/10.1073/pnas.0604318103>
16. McDannold N, Vykhodtseva N, Raymond S, Jolesz FA, Hynynen K. MRI-guided targeted blood-brain barrier disruption with focused ultrasound: Histological findings in rabbits. *Ultrasound Med Biol.* 2005;31(11):1527–37. <http://dx.doi.org/10.1016/j.ultrasmedbio.2005.07.010>
17. Hynynen K, McDannold N, Vykhodtseva N, Jolesz FA. Noninvasive MR Imaging–guided focal opening of the blood-brain barrier in rabbits I. *Radiology.* 2001;220(3):640–6. <http://dx.doi.org/10.1148/radiol.2202001804>
18. Sheikov N, McDannold N, Vykhodtseva N, Jolesz F, Hynynen K. Cellular mechanisms of the blood-brain barrier opening induced by ultrasound in presence of microbubbles. *Ultrasound Med Biol.* 2004;30(7):979–89. <http://dx.doi.org/10.1016/j.ultrasmedbio.2004.04.010>
19. Bitsika V, Roubelakis MG, Zagoura D, Trohatou O, Makridakis M, Pappa KI, et al. Human amniotic fluid-derived mesenchymal stem cells as therapeutic vehicles: A novel approach for the treatment of bladder cancer. *Stem Cells Dev.* 2012;21(7):1097–111.
20. Dembinski JL, Wilson SM, Spaeth EL, Studeny M, Zompetta C, Samudio I, et al. Tumor stroma engraftment of gene-modified mesenchymal stem cells as anti-tumor therapy against ovarian cancer. *Cytotherapy.* 2013;15(1):20–32. <http://dx.doi.org/10.1016/j.jcjt.2012.10.003>
21. Kidd S, Spaeth E, Dembinski JL, Dietrich M, Watson K, Klopp A, et al. Direct evidence of mesenchymal stem cell tropism for tumor and wounding microenvironments using *in vivo* bioluminescent imaging. *Stem Cells.* 2009;27(10):2614–23. <http://dx.doi.org/10.1002/stem.187>
22. Klopp AH, Spaeth EL, Dembinski JL, Woodward WA, Munshi A, Meyn RE, et al. Tumor irradiation increases the recruitment of circulating mesenchymal stem cells into the tumor microenvironment. *Cancer Res.* 2007;67(24):11687–95. <http://dx.doi.org/10.1158/0008-5472.CAN-07-1406>
23. Marini FC, Shayakhmetov D, Gharwan H, Lieber A, Andreeff M. Advances in gene transfer into haematopoietic stem cells by adenoviral vectors. *Expert Opin Biol Ther.* 2002;2(8):847–56. <http://dx.doi.org/10.1517/14712598.2.8.847>
24. Nakamizo A, Marini F, Amano T, Khan A, Studeny M, Gumin J, et al. Human bone marrow-derived mesenchymal stem cells in the treatment of gliomas. *Cancer Res.* 2005;65(8):3307–18.
25. Spaeth EL, Marini FC. Dissecting mesenchymal stem cell movement: Migration assays for tracing and deducing cell migration. *Methods Mol Biol.* 2011;750:241–59. http://dx.doi.org/10.1007/978-1-61779-145-1_17

26. Studeny M, Marini FC, Champlin RE, Zompetta C, Fidler IJ, Andreeff M. Bone marrow-derived mesenchymal stem cells as vehicles for interferon-beta delivery into tumors. *Cancer Res.* 2002; 62(13):3603–8.
27. Studeny M, Marini FC, Dembinski JL, Zompetta C, Cabreira-Hansen M, Bekele BN, et al. Mesenchymal stem cells: Potential precursors for tumor stroma and targeted-delivery vehicles for anticancer agents. *J Natl Cancer Inst.* 2004;96(21):1593–603. <http://dx.doi.org/10.1093/jnci/djh299>
28. Yong RL, Shinjima N, Fueyo J, Gumin J, Vecil GG, Marini FC, et al. Human bone marrow-derived mesenchymal stem cells for intravascular delivery of oncolytic adenovirus Delta24-RGD to human gliomas. *Cancer Res.* 2009;69(23):8932–40. <http://dx.doi.org/10.1158/0008-5472.CAN-08-3873>
29. Stuckey DW, Shah K. Stem cell-based therapies for cancer treatment: Separating hope from hype. *Nat Rev Cancer.* 2014;14(10):683–91. <http://dx.doi.org/10.1038/nrc3798>
30. Sohni A, Verfaillie CM. Mesenchymal stem cells migration homing and tracking. *Stem Cells Int.* 2013;2013:8.
31. Wels J, Kaplan RN, Rafii S, Lyden D. Migratory neighbors and distant invaders: Tumor-associated niche cells. *Genes Dev.* 2008;22(5):559–74. <http://dx.doi.org/10.1101/gad.1636908>
32. Lapidot T, Dar A, Kollet O. How do stem cells find their way home? *Blood.* 2005;106(6):1901–10. <http://dx.doi.org/10.1182/blood-2005-04-1417>
33. Duda DG, Kozin SV, Kirkpatrick ND, Xu L, Fukumura D, Jain RK. CXCL12 (SDF1alpha)-CXCR4/CXCR7 pathway inhibition: An emerging sensitizer for anticancer therapies? *Clin Cancer Res.* 2011;17(8):2074–80. <http://dx.doi.org/10.1158/1078-0432.CCR-10-2636>
34. Kokovay E, Goderie S, Wang Y, Lotz S, Lin G, Sun Y, et al. Adult SVZ lineage cells home to and leave the vascular niche via differential responses to SDF1/CXCR4 signaling. *Cell Stem Cell.* 2010;7(2): 163–73. <http://dx.doi.org/10.1016/j.stem.2010.05.019>
35. Helbig G, Christopherson KW, 2nd, Bhat-Nakshatri P, Kumar S, Kishimoto H, Miller KD, et al. NF-kappaB promotes breast cancer cell migration and metastasis by inducing the expression of the chemokine receptor CXCR4. *J Biol Chem.* 2003;278(24):21631–8. <http://dx.doi.org/10.1074/jbc.M300609200>
36. Balyasnikova IV, Ferguson SD, Sengupta S, Han Y, Lesniak MS. Mesenchymal stem cells modified with a single-chain antibody against EGFRvIII successfully inhibit the growth of human xenograft malignant glioma. *PLoS One.* 2010;5(3):e9750. <http://dx.doi.org/10.1371/journal.pone.0009750>
37. Gao Z, Zhang L, Hu J, Sun Y. Mesenchymal stem cells: A potential targeted-delivery vehicle for anti-cancer drug, loaded nanoparticles. *Nanomedicine.* 2013;9(2):174–84. <http://dx.doi.org/10.1016/j.nano.2012.06.003>
38. McMillan J, Batrakova E, Gendelman HE. Cell delivery of therapeutic nanoparticles. *Prog Mol Biol Transl Sci.* 2011;104:563–601. <http://dx.doi.org/10.1016/B978-0-12-416020-0.00014-0>
39. Power AT, Bell JC. Cell-based delivery of oncolytic viruses: A new strategic alliance for a biological strike against cancer. *Mol Ther.* 2007;15(4):660–5. <http://dx.doi.org/10.1038/sj.mt.6300098>
40. Ferguson MS, Lemoine NR, Wang Y. Systemic delivery of oncolytic viruses: Hopes and hurdles. *Adv Virol.* 2012;2012:14.
41. Xiong X, Sun Y, Sattiraju A, Jung Y, Mintz A, Hayasaka S, et al. Remote spatiotemporally controlled and biologically selective permeabilization of blood-brain barrier. *J Control Release.* 2015;217: 113–20. <http://dx.doi.org/10.1016/j.jconrel.2015.08.044>
42. Kramer G, Steiner GE, Grobl M, Hrachowitz K, Reithmayr F, Paucz L, et al. Response to sub-lethal heat treatment of prostatic tumor cells and of prostatic tumor infiltrating T-cells. *Prostate.* 2004;58(2):109–20.
43. Rome C, Couillaud F, Moonen CT. Spatial and temporal control of expression of therapeutic genes using heat shock protein promoters. *Methods.* 2005;35(2):188–98. <http://dx.doi.org/10.1016/j.ymeth.2004.08.011>
44. Madio DP, van Gelderen P, DesPres D, Olson AW, de Zwart JA, Fawcett TW, et al. On the feasibility of MRI-guided focused ultrasound for local induction of gene expression. *J Magn Reson Imaging.* 1998;8(1):101–4. <http://dx.doi.org/10.1002/jmri.1880080120>
45. Kauer TM, Figureueiredo JL, Hingtgen S, Shah K. Encapsulated therapeutic stem cells implanted in the tumor resection cavity induce cell death in gliomas. *Nat Neurosci.* 2012;15(2):197–204. <http://dx.doi.org/10.1038/nn.3019>

46. Bauer R, Martin E, Haegele-Link S, Kaegi G, von Specht M, Werner B. Noninvasive functional neurosurgery using transcranial MR imaging-guided focused ultrasound. *Parkinsonism Relat Disord.* 2014;20(Suppl 1):S197–9. [http://dx.doi.org/10.1016/S1353-8020\(13\)70046-4](http://dx.doi.org/10.1016/S1353-8020(13)70046-4)
47. Medel R, Monteith SJ, Elias WJ, Eames M, Snell J, Sheehan JP, et al. Magnetic resonance-guided focused ultrasound surgery: Part 2: A review of current and future applications. *Neurosurgery.* 2012;71(4):755–63. <http://dx.doi.org/10.1227/NEU.0b013e3182672ac9>
48. McDannold N, Clement GT, Black P, Jolesz F, Hynynen K. Transcranial magnetic resonance imaging-guided focused ultrasound surgery of brain tumors: Initial findings in 3 patients. *Neurosurgery.* 2010;66(2):323–32; discussion 32. <http://dx.doi.org/10.1227/01.NEU.0000360379.95800.2F>
49. Ram Z, Cohen ZR, Harnof S, Tal S, Faibel M, Nass D, et al. Magnetic resonance imaging-guided, high-intensity focused ultrasound for brain tumor therapy. *Neurosurgery.* 2006;59(5):949–55.

21

Maximizing Local Access to Therapeutic Deliveries in Glioblastoma. Part V: Clinically Relevant Model for Testing New Therapeutic Approaches

JOHN ROSSMEISL^{1,2,3}

¹Brain Tumor Center of Excellence, Wake Forest Baptist Medical Center Comprehensive Cancer Center, Winston Salem, NC, USA; ²School of Biomedical Engineering and Sciences, Virginia Tech-Wake Forest University, Blacksburg, VA, USA; ³Department of Small Animal Clinical Sciences, Virginia-Maryland Regional College of Veterinary Medicine; Blacksburg, VA, USA

Author for correspondence: John H. Rossmeisl, Jr., Veterinary and Comparative Neuro-oncology Laboratory, Virginia-Maryland College of Veterinary Medicine, 215 Duckpond Drive, Virginia Tech Blacksburg, VA 24061, USA. E-mail: jrossmei@vt.edu

Doi: <http://dx.doi.org/10.15586/codon.glioblastoma.2017.ch21>

Abstract: A significant obstacle to the development of new brain tumor therapeutics remains the lack of rodent models that faithfully reproduce the *in vivo* complexities of human glioblastoma. Dogs and humans are the only species that frequently develop spontaneous brain tumors. Remarkable clinical, phenotypic, and molecular similarities exist between human and canine malignant glioma. Our research has focused on the development of pharmacologically tractable molecular targets common to human and canine gliomas, as well as the discovery

In: *Glioblastoma*. Steven De Vleeschouwer (Editor), Codon Publications, Brisbane, Australia ISBN: 978-0-9944381-2-6; Doi: <http://dx.doi.org/10.15586/codon.glioblastoma.2017>

Copyright: The Authors.

Licence: This open access article is licenced under Creative Commons Attribution 4.0 International (CC BY 4.0). <https://creativecommons.org/licenses/by-nc/4.0/>

and refinement of novel methods of drug delivery to the brain, such as convection-enhanced delivery (CED), irreversible electroporation (IRE), and focused ultrasound, that can overcome the limitations imposed by the blood–brain and blood–tumor barriers. Through the conduct of early phase clinical trials in dogs, we demonstrate the safety, feasibility, and preliminary efficacies of IL-13RA2- and EphA2-targeted bacterial cytotoxins and IRE for the treatment of spontaneous malignant glioma, illustrate the clinical utility of real-time imaging monitored CED as a robust drug delivery platform, and describe the use of the tumor-bearing dog in transcranial-focused ultrasound applications related to neuro-oncology. The dog brain cancer model offers unique opportunities to expedite the clinical translation of cancer therapeutics through the design of preclinical investigations that ask and answer drug and medical device development questions that cannot be sufficiently addressed in rodent models.

Key words: Convection-enhanced delivery; Dog; Electroporation; Focused ultrasound; Glioma

Introduction

Although significant advancements in the understanding of the biology of human cancers have been made in the past two decades, clinical translation of new drugs that improve the survival and quality of life of patients with many aggressive malignancies continues to be challenging. The unmet clinical need for beneficial cancer therapeutics is highlighted by the fact that in the United States, approximately one in four deaths is attributed to cancer annually (1). Malignant primary brain tumors, and in particular malignant gliomas (MGs), represent some of the most treatment-refractory human cancers, and are leading causes of cancer-related death in adults and children (1). The median survival of adults with glioblastoma (GBM), the most aggressive and common MG variant, treated with the current standards of care is ~16 months, and the 2-year survival rate is approximately 25% (2, 3). The MG landscape also poignantly illustrates the current obstacles to the development of novel therapeutics, as only two new drugs and two medical devices have been approved for the treatment of these tumors in the last 20 years (2, 4).

The majority of preclinical studies aimed at the development of new therapies for gliomas have been conducted in small animal rodent models. While chemically induced, xenograft and genetically engineered murine glioma models have contributed significantly to the current body of knowledge regarding the pathobiology and treatment of MG, none of these modeling systems is capable of recapitulating the complex *in vivo* environment that characterizes human MG (5). As far back as 2002, a report from the National Institute of Neurological Disorders and Stroke (NINDS) and National Cancer Institute (NCI) stated, “...currently available cellular, tissue, and animal models do not accurately represent the biology of human brain tumors...” (6). Recognizing the benefits and limitations of rodent models of human brain tumors, it would be desirable to have animal models that could fill the gaps presented by current model systems, and thus better predict the therapeutic outcome in humans.

In this context, the identification and use of novel preclinical models that allow for the study of fundamental cancer drug and device development questions would meet a critical and shared need among stakeholders in the cancer research and global health care communities. The potential of companion animals, and particularly dogs, with naturally occurring cancers to provide answers to these questions is being increasingly recognized and realized (7–10). A growing body of evidence indicates that several spontaneous canine cancers are clinically, phenotypically, and molecularly similar to their human analogs, thus providing unique avenues for preclinical discovery and testing (7, 8, 10). Translational studies of investigational agents in, for example, tumor-bearing dogs can provide a variety of pharmacokinetic, mechanistic, toxicity, and anti-tumor activity data in an immunocompetent host, and thus offer numerous opportunities to more accurately guide the drug development process (8–10). It has been suggested that inclusion of preclinical canine studies in the drug development pathway could result in billions of dollars of research savings, principally by improving the design of Phase II human clinical trials and thus potential avoidance of the historically high late-stage failure and attrition rates of new cancer agents (9, 11). Dogs with spontaneous brain tumors have been assimilated into several comparative neuro-oncology research programs in an effort to accelerate the development and translation of cancer drugs to the clinic, and to mutually improve the lives of dogs and humans with brain tumors (5, 10, 12–15).

Clinically Relevant Model for Testing New Therapeutic Approaches in Gliomas

SPONTANEOUS CANINE GLIOMAS AS A FAITHFUL MODEL OF HUMAN DISEASE

Canines and humans are the only mammalian species in which spontaneous primary central nervous system (CNS) tumors are common. Estimated incidences of canine nervous system tumors range from 14.5 to 20/100,000 dogs (16, 17), which closely approximates epidemiological data indicating a primary CNS tumor incidence of 20.5/10,000 people (18). Postmortem surveys indicate that intracranial tumors are found in 2–4.5% of all dogs in which necropsy is performed (19–21), a frequency comparable to a study reporting brain tumors in 2% of humans undergoing autopsy (22). Gliomas account for 35% of all primary brain tumors in dogs, and collectively represent the second most frequently diagnosed primary tumor type after meningiomas (19, 20, 23). The median age of dogs diagnosed with glioma is 8.5 years, corresponding to the fifth and sixth decades of life in humans (21, 23). In both people and dogs, the risk for developing glioma increases with age (16, 18, 21, 24). Gliomas are significantly overrepresented in certain brachycephalic breeds of dogs, namely, Boston terriers, Boxers, and Bulldogs, which strongly suggests a genetic contribution to tumor development, and a glioma susceptibility locus has been identified on canine chromosome 26 (19, 21, 23, 25). The existence of a predisposition to gliomas in these select and highly related dog breeds with relatively limited genetic variation provides unique

opportunities to probe the canine genome for glioma-associated genetic aberrations that may not be as easily discernible amidst the much more diverse genetic background that exists in humans (25).

Considerable similarities exist between human and canine anatomy and physiology, and the physical size of the canine brain is amenable to the testing and optimization of diagnostics and therapeutics developed for human patients, without a need to rescale instrumentation. Dogs with brain tumors present with significant clinical signs, including seizures, alterations in consciousness, and motor and sensory dysfunction that can be objectively characterized and annotated using instruments comparable to those used in humans including the neurological examination, modified Glasgow Coma Scale, canine Karnofsky performance score, Engel seizure classification, and Modified Rankin Scale (26–28). As two-thirds of canine gliomas occur in the forebrain, seizures and behavior changes are the most commonly reported clinical signs (23, 28, 29). In addition, health-related quality of life surveys for use in the assessment of clinical disability in dogs with cancer do exist, although the current iterations have not been specifically developed for or validated in dogs with brain tumors (30). The prognosis for dogs with gliomas is also poor, with death occurring weeks to months following diagnosis in the absence of treatment.

The histopathological and diagnostic imaging features of canine gliomas (Figure 1) are also remarkable similar to their human counterparts (31–35). These shared morphologic features facilitate comparative classification and grading of tumors using World Health Organization criteria (36) and performing objective imaging-based therapeutic response assessments using the Response Assessment in Neuro-Oncology (RANO) system criteria (28, 37). However, the frequency of glioma subtypes encountered in dogs differs from that seen in humans (Table 1), with oligodendrogliomas accounting for a significantly higher proportion of all canine gliomas compared to humans (19–21, 23, 37).

Molecular and genetic profiling of brain tumors is becoming a routine procedure in human neuro-oncology (38, 39). These analyses have led to evolutions in the classification and prognostic stratification of human brain tumors, and are fundamental to the rational translational application of molecularly targeted therapies (38–40). The characterization of the molecular and genomic landscapes of canine brain tumors has been facilitated by the increasing availability of canine-specific reagents and advancements in high-throughput sequencing platforms (25). To date, studies in dogs have demonstrated that hallmark alterations in proteins involved in cellular proliferation, apoptosis, and cell-cycle regulation, such as the RTK, p53, and RB1 pathways that participate in tumorigenesis, parallel those seen in human gliomas (31, 38, 40–42). Also similar to humans, overexpression of alpha3-beta1 integrin, c-Met, EGFR, EphA2, IGFBP2, IL-13RA2, MMP-2, and -9, PDGFRa, uPAR, and VEGF/VEGFR1/2 have been observed in canine gliomas (43–51). Homologous overexpression of cell surface receptors in canine and human gliomas, such as EGFR, EphA2, and IL-13RA2, have driven the preclinical investigation of molecularly targeted therapeutics in glioma-bearing dogs (48, 52).

Continuing the global genetic characterization of canine gliomas, as well as the confirmation of the molecular signatures of individual canine patient tumors are paramount to the rational design of preclinical investigations, especially in

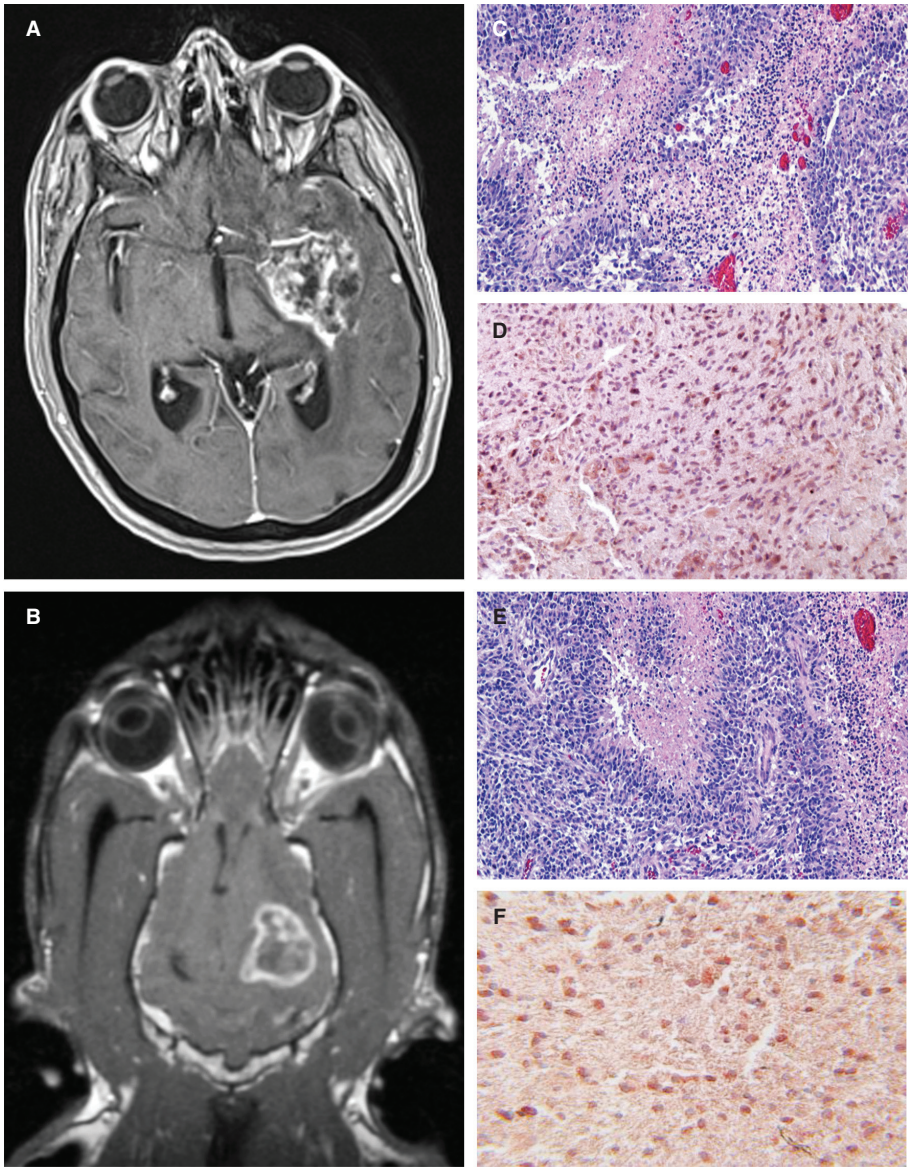


Figure 1 Comparative morphological and immunophenotypic features of human and canine glioblastoma (GBM). Post-contrast T1-weighted magnetic resonance images from a human (A) and dog (B) demonstrating ring-enhancing cerebral GBM. Classic microscopic features of hypercellularity and pseudopalisading necrosis in a human (C) and canine (E) GBM (H&E stain, bar = 150 μ m). GBM from both species demonstrate intense immunoreactivity to IL-13RA2 (D, F).

TABLE 1

Comparative Frequencies of Glioma Subtypes and Grades in Dogs and Humans

Tumor type	Grade	Grade distribution within tumor type	
		Canine (%) [†]	Human (%)
Astrocytoma (1, 18, 19, 21, 23)	I (Pilocytic)	<1	5
• 30–60% of all canine neuroepithelial tumors	II (Diffuse)	~40	10–15
• 60–70% of all human neuroepithelial tumors	III (Anaplastic)	~20	10–20
	IV (Glioblastoma)	~30	60–75
Oligodendroglioma (1, 18, 19, 21, 23)	II (Oligodendroglioma)	70	70
• 30–50% of all canine neuroepithelial tumors	III (Anaplastic)	30	30
• 10–15% of all human neuroepithelial tumors			

[†]Grade distribution data obtained from archived specimens in Veterinary and Comparative Neuro-oncology Laboratory tissue biorepository.

the context of the rapidly growing library of targeted agents available for cancer diagnostics and treatment (53). Although the discovery of additional common denominators shared among canine and human tumors is likely with the use of more robust whole genomic sequencing and single-nucleotide polymorphism platforms, it is also probable that aberrations in key gliomagenesis pathways that are unique to the dog will also be revealed, as some fundamental species-specific differences have already been documented. For example, the favorable prognostic hallmark in human oligodendroglioma of co-deletion of chromosome 1p/19q has not been identified in canine gliomas, nor have the classical genetic mutations in TP53 or IDH1 that define human astrocytomas (41, 54, 55).

The value of dogs with spontaneous brain tumors as faithful preclinical models of human disease has been demonstrated in several additional areas of neuro-oncology. A study investigating dendritic cell vaccination of glioma-bearing dogs with tumor cell lysates containing a toll-like receptor ligand adjuvant in combination with *in situ* adenoviral interferon-gamma gene transfer demonstrated sufficient safety and promise to result in rapid translation of this immunogenetic therapy to a human clinical trial (56, 57), and promising active immunotherapeutic approaches using dogs with intracranial meningiomas have recently been published (58). Pioneering work in dogs with gliomas illustrated the feasibility and importance of real-time MR imaging monitoring of convection-enhanced delivery (CED) for confirmation of target coverage, as well as providing an opportunity to detect and remedy any local adverse effects of CED treatment, including reflux of the infusate along the catheter (59–61).

PRECLINICAL TESTING OF VARIOUS THERAPEUTIC METHODS (CONVECTION-ENHANCED DELIVERY, IRREVERSIBLE ELECTROPORATION, TRANSCRANIAL-FOCUSED ULTRASOUND) IN DOGS WITH SPONTANEOUS TUMORS OF THE BRAIN

Recognizing the translational relevance of and collaborative opportunities offered by the spontaneous canine brain tumor model, our laboratory's research focuses on the multi-scale, comparative targeting of brain tumors. Our efforts include the identification of pharmacologically tractable molecular targets common to human and canine brain tumors, as well as the development of novel macroscopic methods of CNS drug delivery that overcome the limitations imposed by the blood-brain barrier (BBB) and blood brain tumor barrier (BBTB) (13, 14). The design and conduct of clinical trials in dogs with naturally occurring brain tumors is a major mechanism by which we assess our drug and device discoveries (10, 13).

CONVECTION-ENHANCED DELIVERY

The CED technique involves the pressurized infusion of therapeutic agents directly into tumor or other target tissues using specialized catheters (13, 62–64). By bypassing the BBB, CED allows for delivery of high concentrations of macromolecular drugs directly to the tumor with negligible or no systemic drug exposure, and CED is capable of achieving clinically relevant drug distribution volumes by bulk fluid flow without significantly increasing intracranial pressure when infusions are administered at low pressures over several hours or days (60, 62–64). CED can increase drug distribution volumes in the brain by at least an order of magnitude relative to simple diffusion, and it can be performed safely throughout the CNS in humans and animals (65). It has been demonstrated that liposomal CPT-11 and EGFRvIII-antibody conjugated to iron oxide nanoparticles can be safely delivered via CED to canine gliomas, and these studies have provided evidence of the efficacies of these approaches in this model (52, 60).

Historically, major technical impediments to the widespread adoption of CED for the treatment of human glioma has been an inability of the technique to distribute drugs to the entire heterogeneous tumor volume and margin (60, 61, 66), as well as inherent limitations of catheters adopted for use in CED. To overcome these obstacles, advancements in CED have included the incorporation of predictive computational imaging analyses into therapeutic planning, real-time MR imaging of infusions to facilitate and confirm target coverage, and the design and utilization of novel catheters appropriate for CED (59–61, 64).

Building upon these advancements and cognizant of the lessons learned from prior CED clinical trials, we are investigating the use of CED to deliver high-molecular weight-targeted therapeutics to canine gliomas. Given the potential efficacy of first generation of IL-13RA2 conjugated pseudomonas exotoxins in human GBM (67), and common overexpression of IL-13RA2 and EphA2 in canine and human gliomas (Figure 1), potent IL-13 and ephrin-A1-based cytotoxins containing modified *Pseudomonas* exotoxin A or *Diphtheria* toxin targeted to IL-13RA2 and EphA2 receptors were generated, respectively (47, 48, 68, 69).

We are actively conducting a clinical trial in dogs with gliomas to evaluate the tolerability and preliminary efficacy of this targeted bacterial cytotoxic cocktail administered by delivered using MRI-monitored CED.

Canine subjects enrolled in the trial have mild-to-moderate clinical signs of brain dysfunction and histopathologically confirmed gliomas demonstrating immunoreactivity to IL-13RA2 and/or EphA2. The trial is designed using a 3+3 dose-escalation scheme, with cohorts administered 0.05, 0.1, 0.2, or 0.4 μg of each cytotoxin/ml of infusate. To optimize the CED procedure, an inverse therapeutic planning method, using a spherical shape-fitting algorithm generated from patient-specific, segmented MRI/CT images, is used to simulate ideal cannula placement and target coverage prior to treatment (69, 70). CED is performed in the anesthetized dog using reflux-preventing cannulae to co-administer the cytotoxins with a gadolinium tracer (Figure 2) to allow for intraoperative MRI visualization of infusate distribution. Tolerability is defined as the absence of dose-limiting toxicities (DLT) within 28 days of infusion. DLT are considered the development of Grades 3, 4, or 5 adverse events, as defined by the Cancer Therapy Evaluation Program CTCAE standards (71). Serial clinical, laboratory, and brain MRI examinations are performed for 6 months following CED treatment, and the

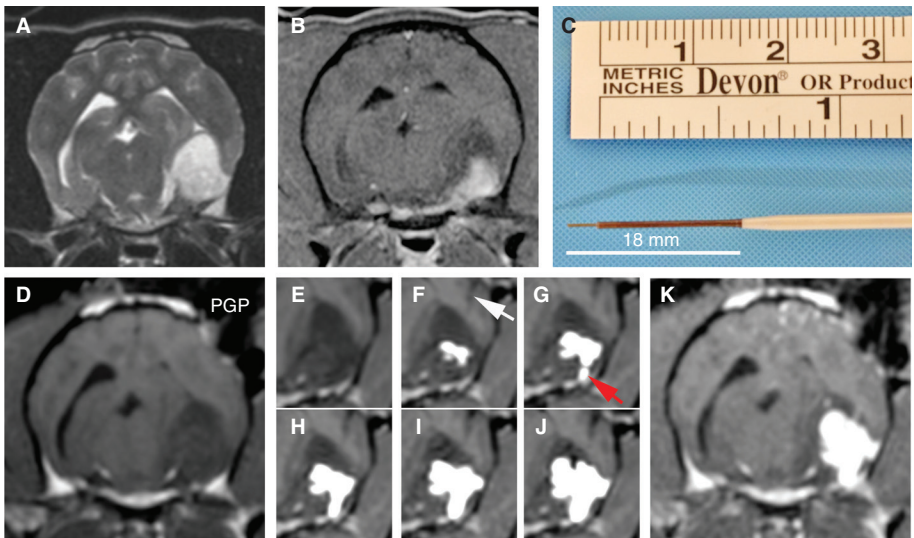


Figure 2 Intratumoral convection-enhanced delivery (CED) of molecularly targeted therapeutics into a canine astrocytoma. Pre-treatment transverse T2-weighted (A) and post-contrast T1-weighted (B) images demonstrating the tumor in the temporal-piriform lobes of the brain. (C) Fused silica and ceramic reflux-preventing cannula (RPC) with multistep tip design used for CED. (D) Intraoperative, transverse T1-weighted images obtained immediate prior to infusion, showing probe guide pedestal (PGP) implanted in the skull, through which RPC (F, white arrow) will be stereotactically placed into the tumor. (E–J) Time-lapsed 3DT1-weighted images taken over approximately 2 h of MR-monitored infusion showing progressively increasing volume of distribution of the infusate co-delivered with gadolinium (white) within the tumor. An additional RPC has been inserted (G, red arrow) to facilitate tumor coverage. (K) Immediate post-infusion T1-weighted image demonstrating tumor coverage and infusate containment achieved at completion of CED.

CED infusions can be repeated in the event of tumor progression or suboptimal target coverage is achieved during the initial infusion. Efficacy is determined by characterizing objective tumor responses using RANO and volumetric criteria modified for use in canine patients (72).

Using this approach, we have achieved robust and clinically relevant volumes of infusate distribution in unresected canine MGs (Figure 2). In addition, inclusion of real-time MR-monitoring-facilitated intraoperative cannulae revisions that allowed continued target coverage after observation of ventricular leakage or infusate reflux in some procedures. Clinical and partial tumor volumetric responses ($\geq 50\%$ volumetric tumor reductions) have been observed in 55% (5/9) of the dogs treated to date. Necropsy examinations performed in four dogs with progressive disease have revealed tumor necrosis in infused regions. In the first three dosing cohorts, significant DLT have not been observed. Results from this trial indicate that improvements in CED cannula design, therapeutic planning, and MRI monitoring allow for safe and effective intratumoral delivery of IL-13RA2- and EphA2-targeted cytotoxins. This ongoing study also provides preliminary evidence of the efficacy of these cytotoxins when used as a monotherapy in a spontaneous animal glioma model.

In our continuing effort to more precisely and specifically target gliomas with locally delivered therapies, we have clinical trials planned that will incorporate infusion our next generation multivalent cytotoxin, QUAD-CTX, that simultaneously targets the IL-13RA2, EphA2, EphA3, and EphB2 receptors into canine gliomas (see Part I, page xxx). Similar to humans, we have also demonstrated that canine gliomas overexpress EphA3. To further increase the efficiency and utility of CED, we will administer the QUAD-CTX using our innovative convection-enhanced arborizing catheter (see Part III, page xxx).

IRREVERSIBLE ELECTROPORATION

Electroporation is a technique in which electrical pulses are used to permeabilize tissue through formation of nanoscale pores in cellular membranes (73). When the applied electric field strength exceeds a critical value, irreversible electroporation (IRE) is achieved, which creates permanent defects in cellular membranes resulting in cell death (73, 74). IRE is a novel, minimally invasive, rapid, and non-thermal method of tissue ablation that has been demonstrated to be safe and effective for the treatment of solid tumors in animals and humans (75–78). It has been shown that IRE therapy has also been shown to have sparing effects on the vasculature, ductal networks, and extracellular matrix, which facilitates posttreatment healing (73, 74, 79).

We have developed a novel technology, coined high-frequency irreversible electroporation (H-FIRE) that represents a significant advancement in IRE therapy, the specifics of which have been covered in Part III of this chapter (80). Briefly, the treatment of patients with high-amplitude IRE pulses (1–3 kv, $\sim 100 \mu\text{s}$) requires administration of neuromuscular agents in order to abolish muscle contractions associated with pulse delivery (79). The requirements for general anesthesia and neuromusculars may complicate or exclude IRE treatment of some tumors in some debilitated patients. The H-FIRE generator is capable of delivering bipolar bursts of pulses with individual pulse durations two orders of

magnitude shorter than in IRE ($\sim 1 \mu\text{s}$). This allows H-FIRE to non-thermally ablate tissue without causing muscle contractions, which negates the need for neuroparalytic use during treatment, achieves more predictable zone of treatment by mitigating tissue heterogeneities (80, 81), and may allow for selective tumor cell ablation based on altered cellular morphology (82).

In addition, we and others have demonstrated that IRE and H-FIRE pulses are capable of transiently disrupting the BBB outside the region of irreversible tissue ablation in a voltage-dependent manner (83–85). This provides an opportunity for the delivery of otherwise impermeable macromolecules to a penumbra of tissue surrounding the macroscopic tumor volume exposed to the electrical field, which could be exploited for delivery of therapeutics to microscopic tumor infiltrates extending beyond the gross tumor margins, which account for the majority of local treatment failures in MG (83, 85). We believe that these unique features of IRE and H-FIRE make them particularly attractive for use in intracranial surgery, and have been developing these platforms for the treatment of brain cancer.

We have evaluated the safety and preliminary efficacy both IRE (Figure 3) and H-FIRE (Figure 4) in dogs with spontaneous brain tumors (77, 79, 86).

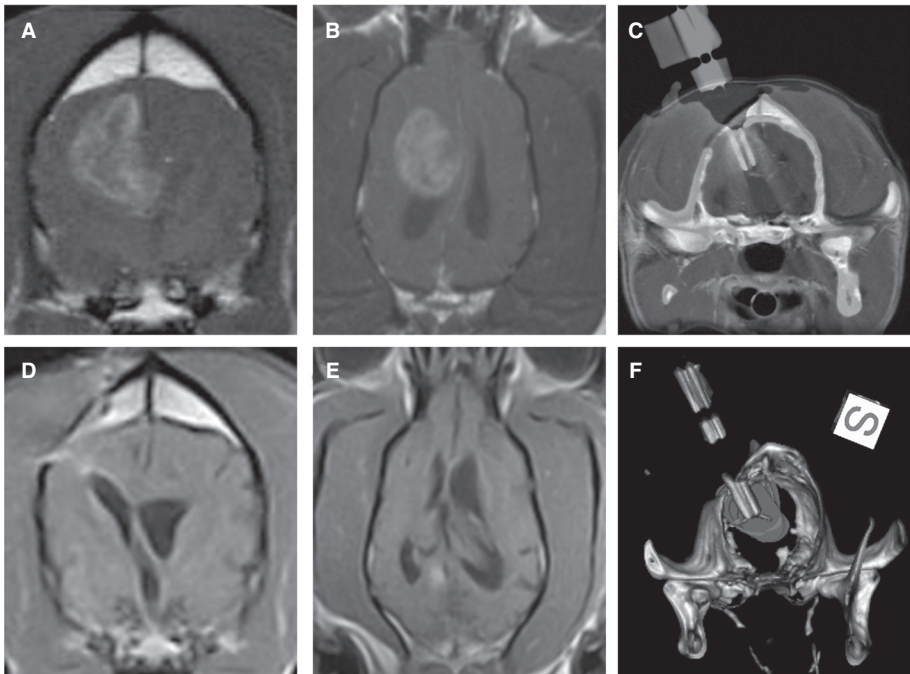


Figure 3 Stereotactic glioblastoma ablation with irreversible electroporation (IRE). Pre-treatment transverse (A) and dorsal planar (B) post-contrast T1-weighted MR demonstrating ring-enhancing glioblastoma in the frontoparietal lobe of the cerebrum. Co-registered intraoperative CT and pre-treatment MR images (C) and three-dimensional reconstructed CT (F) with IRE electrodes in situ within the tumor in preparation for ablation. Three-month post-IRE treatment transverse (D) and dorsal planar (E) post-contrast T1-weighted MR illustrating 95% reduction in tumor burden.

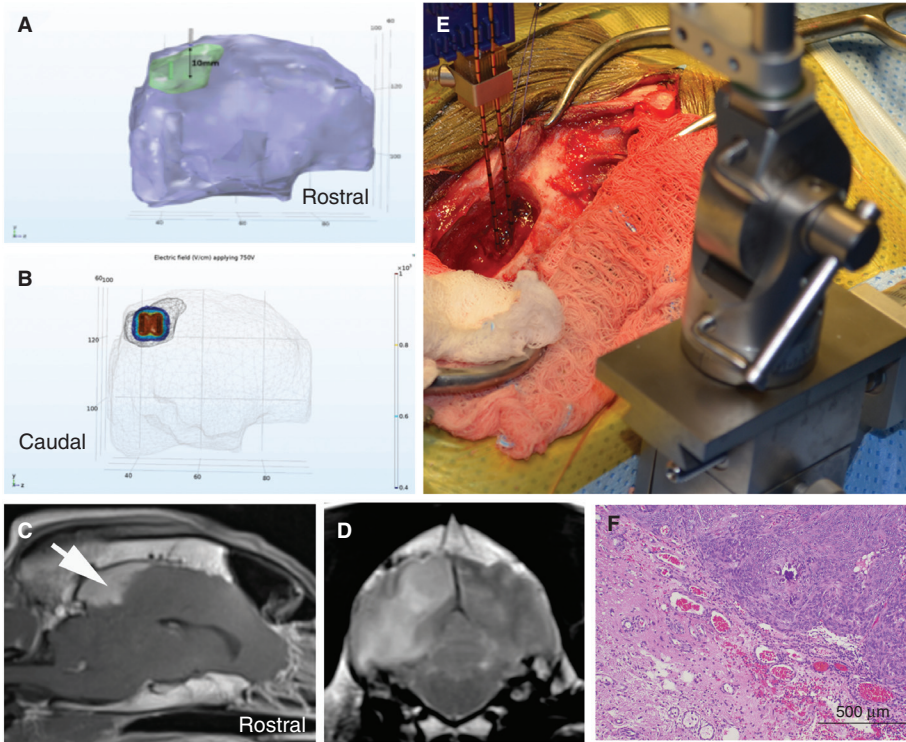


Figure 4 High-frequency irreversible electroporation (H-FIRE) treatment of a canine Type I parasagittal meningioma. Treatment planning (A, B) involves segmentation of the tumor (green) and brain (purple) from the patient's MR images (C, D), and determination of the electrode placement trajectory (A). The resulting electric field distributions are then simulated (B) using finite element analysis software (B). The H-FIRE electrodes are placed using intraoperative stereotaxy (E) according to the treatment plan, and the pulses delivered. After-HFIRE treatment, the tumor was resected and serially sectioned to correlate the predicted with actual ablation volume. Photomicrograph of the treatment margin (F), illustrating a sharp line of demarcation between H-FIRE ablated (lower left) and viable tumor (upper right); H&E stain.

An integral component of the preclinical evaluation of IRE and H-FIRE was the development of anatomically accurate numerical treatment planning models that maximize tumor coverage while minimizing damage to surrounding healthy tissue and also account for the increase in tissue conductivity that occurs during pulse delivery (86–88). Incorporating therapeutic plans developed from patient-specific, segmented medical images imported into finite element analysis modeling software, we have confirmed the ability of IRE and H-FIRE to safely and precisely ablate normal and neoplastic canine brain tissues with a submillimeter line of demarcation between ablated and non-treated tissues (79, 86, 89). IRE treatment of canine gliomas resulted in significant objective tumor responses in 4/5 dogs with quantifiable target lesions (Figure 3), and these radiographic responses were accompanied by improvements in Karnofsky

performance scores and posttreatment seizure control (72, 86). Similarly, using a treat and resect treatment paradigm, we have confirmed the ability of H-FIRE to safely and precisely ablate clinically relevant volumes of canine brain tumors without the induction of muscular contractions during pulse delivery (Figure 4).

To overcome previously recognized barriers to the translation IRE and H-FIRE therapies to the clinic, such as the inability to incorporate MR image-guidance into treatments and need to use multiple software programs for therapeutic planning, we have been developing a comprehensive solution that combines all of the necessary components of the workflow in a user-friendly platform that can be incorporated into contemporary neurosurgical theaters (86, 90, 91). The foundation for this platform is an open-source, online interface that uses a treatment planning approach similar to that employed in radiotherapeutic applications. The software allows for tissue-specific segmentation, determination of the tumor dimensions, and formulation of virtual electrode insertion approaches that can be used in surgery (91). These volumetric representations are then used to perform computational simulations of the electric field distribution surrounding the active electrodes during pulse delivery to determine tumor coverage (Figure 4) and cell kill probabilities (90, 92). Validation of the predicted therapeutic outcomes generated with this platform is currently underway using clinical data from IRE-treated dogs with intracranial gliomas (90).

Another fundamental step which we have undertaken to clinically implement this technology is the development MR compatible electrodes for use in IRE and H-FIRE procedures. This provides for coupling of the imaging-based computational predictive models to near real-time imaging-derived feedback with regard to the electrode location and electrical properties of the tumor through the use of magnetic resonance electrical impedance tomography, which allows for intraoperative monitoring of the electrical field distribution during electroporation-based treatments (93). Using this anatomical and biophysical imaging-guided approach, the expected outcome of the treatment can be confirmed after pulse delivery is completed, and the treatment can be revised, if necessary, to accommodate any suboptimally treated areas that are identified.

TRANSCRANIAL MR-GUIDED-FOCUSED ULTRASOUND SURGERY

The use of acoustic energy for therapeutic applications in the CNS was first described more than a half century ago in seminal studies performed in a feline model by Fry and colleagues (94–96). Ultrasound transducers are capable of focusing acoustic waves on targets located deep within tissues. By manipulating the sonication parameters, focused ultrasound is capable of thermal tissue ablation, mechanical tissue ablation (histotripsy), neuromodulation, and BBB disruption, and thus has many potential applications in the treatment of brain disease (97–105). Although early studies showed the promise of focused ultrasound for the treatment of intracranial disorders, obstacles associated with the control and monitoring of the procedure coupled with the limitations associated with application of acoustic waves through the skull have, until recently, impeded the widespread application of this technology in neuro-oncology.

The skull has been a major challenge to the clinical adoption of focused ultrasound in the brain. The attenuation of acoustic waves that occurs in bone is approximately 50 times higher than that of soft tissue, and this causes rapid heating of the skull which limits the safe energy exposures that can be delivered (101). The skull also has a significant effect on the propagation of acoustic waves, as variations in skull shape and thickness make it difficult to reliably focus the ultrasound beam. In early focused ultrasound trials, the barriers posed by the calvarium required delivery of ultrasound through a craniectomy defect, which negated the benefits of a noninvasive transcranial procedure (98, 99, 106).

Vast improvements in technology have resulted in the development of several focused ultrasound systems which incorporate MR imaging and allow for the precision targeting and control of the procedure with real-time feedback obtained from quantitative MR thermometric imaging (103, 107, 108). The precision offered by MR-guidance, coupled with the incorporation of active tissue cooling measures, the design of large geometric phased transducer arrays, application-specific tuning of the ultrasound frequency, and computational phase offset beam correction, have allowed the successful mitigation of the heating and beam focusing problems traditionally posed by the skull, and ushered in the era of noninvasive transcranial MR-guided-focused ultrasound (TcFUS).

In parallel with advancements made in humans, non-human primates, and other animal models, we have been working toward the use of TcFUS for thermal ablation of canine tumors and focused disruption of the blood–brain barrier to facilitate drug delivery to the canine brain (109). The preclinical evaluation of TcFUS in dogs has posed additional and unique challenges. The tremendous inherent variations in skull size, conformation, and thickness within and among dog breeds has required expanding and refining engineering solutions developed to reliably achieve transcranial beam focusing. Although beam focusing aberrations associated with skull variability can be corrected using large arrays of individually controllable transducing elements, the geometry of existing FUS hemispheric arrays and the size and conformation variability, as well as positioning constraints of the canine cranium within these arrays complicates treatment delivery in the dog (Figure 5). Using computed tomographic scans of the head obtained prior to treatment co-registered with diagnostic MR data sets and a customized multi-element elliptical array, we are in the process of optimizing patient and canine species-specific phase offset simulations to correct for differences in acoustic wave propagation associated with skull heterogeneity, and to allow for electronic steering of the focal position.

We have also attempted transcranial BBB opening in the normal canine brain using existing FUS systems (Figure 5). In our preliminary studies in dogs, we observed that the assessment of BBB opening using passive cavitation detection (PCD) resulted in considerable variability that was poorly associated with other measures of BBB opening, such as the opening volume (110). This is in contrast to findings indicating that PCD is an acceptable surrogate of BBB permeability in rodent models. We believe that these differences may be attributable to the gyrencephalic structure and increased white/gray matter, vascular, and ventricular heterogeneity of the canine brain compared with rodents, as other investigators have demonstrated similar PCD variability when using a non-human primate model (100). Optimization of PCD monitoring remains a focus of our current canine TcFUS work, and will be paramount to answering questions associated

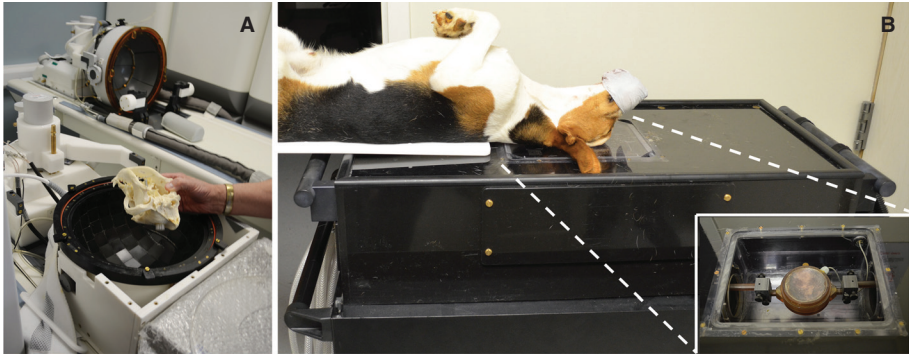


Figure 5 Evaluation of TcFUS instrumentation in the canine model. Canine skull (A) positioned in the Exablate platform (InSightec Ltd., Dallas, TX, USA) hemispheric transducer array. In the background, an additional Exablate hemispheric transducer and couch are visible illustrating the equipment configuration that would be used to treat a human brain. Canine positioned on the RK-100 couch (FUS Instruments, Toronto, Ontario, Canada) system in preparation for transport into the MR suite for TcFUS BBB opening. Note the size difference in the transducers between the two systems (B, inset).

with quantifying drug delivery and efficiency that are fundamental to assessment of TcFUS in the canine brain tumor model, and translation of these drugs and technologies to humans.

Conclusion

Dogs with spontaneous brain tumors represent an immunocompetent model that recapitulates many key clinical and pathobiological features of human tumors, and thus provide a unique avenue for the assessment of novel therapeutics. Integration of the canine brain tumor model into neuro-oncology research programs offers an opportunity to accelerate the development of effective treatments that will mutually benefit humans and dogs. The potential translational impacts of clinical trials in dogs with spontaneous brain tumors on neuro-oncologic technologies and techniques have been demonstrated in investigations focused on CED and immunotherapy. Continued critical analyses of the natural biology and molecular genetics of canine brain tumors will be paramount to defining standards of care for specific canine tumor types, the expansion and validation of canine-specific reagents and techniques necessary for quantitative and reproducible end-point evaluations, and ultimately, the optimal design of investigational clinical trials that incorporate brain tumor-bearing dogs that attempt to evaluate therapeutic outcomes.

Acknowledgment: Portions of this section were supported by grants from the Wallace H. Coulter Foundation, National Science Foundation CAREER Award, NIH/NCI R01CA139099, NIH/NCI R01CA213423, Wake Forest University Translational Sciences Institute, and the Virginia Biosciences Health Research Corporation.

The author would like to thank the following institutions and collaborators for their contributions to the generation of data and material support of experiments presented in this section:

- Wake Forest University Comprehensive Cancer Center and Brain Tumor Center of Excellence: Drs. Waldemar Debinski, Stephen Tatter, Thomas Ellis, Constance Stanton, John Olson, and Mrs. Denise Herpai;
- Virginia Tech-Wake Forest University School of Biomedical Engineering and Sciences: Drs. Rafael Davalos, John Robertson, Scott Verbridge, Paulo Garcia, Michael Sano, Chris Arena, Robert Neal, Mr. Eduardo Latouche, Mr. Rudy Andriani, and Ms. Jill Ivey;
- University of Texas, Austin, Department of Mechanical Engineering: Drs. Chris Rylander and Robert Hood, Ms. Egleide Elenes, Mr. Jason Mehta;
- University of California, Davis, School of Veterinary Medicine: Dr. Peter Dickinson;
- University of Virginia Department of Biomedical Engineering and Focused Ultrasound Center: Drs. Richard Price and Yuval Gruber;
- University of Ljubljana, Faculty of Electrical Engineering, Laboratory of Biocybernetics, Slovenia: Drs. Damijan Miklavcic, Bor Kos, and Denis Pavliha;
- Sheikh Zayed Institute for Pediatric Surgical Innovation, Children's National Health System: Dr. Pavel Yarmolenko.

The author recognizes the following investigators at the Virginia–Maryland College of Veterinary Medicine for clinical care and patient professional services provided to dogs enrolled in clinical trials described here: Drs. Theresa Pancotto, John Robertson, Jeffery Ruth, Kemba Clapp, Gregory Daniel, Samatha Emch, Kelli Kopf, Thomas Cecere, Jamie King, Tanya LeRoith, Philip Sponenberg, Natalia Henao-Guerrero, Noah Pavlisko, Joao Soares, Rachel Carpenter, Kevin Lahmers, Ms. Mindy Quigley, Ms. Barbara Wheeler, Ms. Maureen Sroufe, and Ms. Kelli Hall-Manning.

Conflict of Interest: Dr. Rossmeisl holds patents and has patents pending in the use of irreversible electroporation (IRE) for the treatment of cancer, IRE for blood–brain barrier disruption, and fiberoptic microneedle convection-enhanced delivery catheter systems.

Copyright and permission statement: To the best of my knowledge, the materials included in this chapter do not violate copyright laws. All original sources have been appropriately acknowledged and/or referenced. Where relevant, appropriate permissions have been obtained from the original copyright holder(s).

References

1. Cancer Facts & Figures 2015. Available from: www.cancer.org (accessed March 12, 2016).
2. Omuro A, DeAngelis DM. Glioblastoma and other malignant gliomas: A clinical review. *JAMA*. 2013;310(17):1842–50. <http://dx.doi.org/10.1001/jama.2013.280319>
3. Stupp R, Mason WP, van den Bent MJ, Weller M, Fisher B, Taphoorn MJB, et al. Radiotherapy plus concomitant and adjuvant temozolomide for glioblastoma. *N Engl J Med*. 2005;352(10):987–96. <http://dx.doi.org/10.1056/NEJMoa043330>

4. Kang JH, Adamson C. Novel chemotherapeutics and other therapies for treating high-grade glioma. *Expert Opin Investig Drugs*. 2015;24(10):1361–79. <http://dx.doi.org/10.1517/13543784.2015.1048332>
5. Candolfi M, Curtin J, Nichols W, Muhammad AKM, King G, Pluhar G, et al. Intracranial glioblastoma models in preclinical neuro-oncology: Neuropathological characterization and tumor progression. *J Neurooncol*. 2007;85(2):133–48. <http://dx.doi.org/10.1007/s11060-007-9400-9>
6. Brain Tumor Progress Review Group. Strategic plan for addressing the recommendations of the Brain Tumor Progress Review Group. Washington, DC: NINDS/NCI; 2002.
7. Vail DG, MacEwen EG. Spontaneously occurring tumors of companion animals as models for human cancer. *Cancer Invest*. 2000;18(8):781–92. <http://dx.doi.org/10.3109/07357900009012210>
8. Schiffman JD, Breen M. Comparative oncology: What dogs and other species can teach us about humans with cancer. *Philos Trans R Soc Lond B Biol Sci*. 2015;370:1673. <http://dx.doi.org/10.1098/rstb.2014.0231>
9. Khanna C, London C, Vail D, Mazcko C, Hirschfield S. Guiding the optimal translation of new cancer treatments from canine to human cancer patients. *Clin Cancer Res*. 2009;15:5671–7. <http://dx.doi.org/10.1158/1078-0432.CCR-09-0719>
10. LeBlanc AK, Mazcko C, Brown DE, Koehler JW, Miller AD, Miller R, et al. Creation of an NCI comparative brain tumor consortium: Informing the translation of new knowledge from canine to human brain tumor patients. *Neuro Oncol*. 2016;18(9):1209–18. <http://dx.doi.org/10.1093/neuonc/nov051>
11. Gordon I, Khanna C. Modeling opportunities in comparative oncology for drug development. *ILAR J*. 2010;51:214–20. <http://dx.doi.org/10.1093/ilar.51.3.214>
12. Hicks J, Platt S, Kent M, Haley A. Canine brain tumours: A model for the human disease? *Vet Comp Oncol*. 2017;15(1):252–72. <http://dx.doi.org/10.1111/vco.12152>
13. Rossmel JH. New treatment modalities for brain tumors in dogs and cats. *Vet Clin North Am Small Anim Pract*. 2014;44(6):1013–38. <http://dx.doi.org/10.1016/j.cvsm.2014.07.003>
14. Dickinson PJ. Advances in diagnostic and treatment modalities for intracranial tumors. *J Vet Int Med* 2014;28(4):1165–85. <http://dx.doi.org/10.1111/jvim.12370>
15. Bentley RT, Ahmed AU, Yanke AB, Cohen-Gadol AA, Dey M. Dogs are man's best friend: In sickness and in health. *Neuro Oncol*. 2017;19(3):312–22. <http://dx.doi.org/10.1093/neuonc/nov109>
16. Dorn CR, Taylor DO, Frye FL, Hibbard HH. Survey of animal neoplasms in Alameda and Contra Costa Counties, California. I. Methodology and description of cases. *J Natl Cancer Inst*. 1968;40:295–305.
17. Dobson JM, Samuel S, Milstein H, Rogers K, Wood JL. Canine neoplasia in the UK: Estimates of incidence rates from a population of insured dogs. *J Sm Anim Pract*. 2002;43:240–6. <http://dx.doi.org/10.1111/j.1748-5827.2002.tb00066.x>
18. Dolecek TA, Propp JM, Stroup NE, Kruchko C. CBTRUS statistical report: Primary brain and central nervous system tumors diagnosed in the United States in 2005–2009. *Neuro Oncol*. 2012;14(Suppl 5):v1–v49. <http://dx.doi.org/10.1093/neuonc/nos218>
19. McGrath JT. Intracranial pathology of the dog. *Acta Neuropathol (Berl)*. 1962;Suppl I:3–4. http://dx.doi.org/10.1007/978-3-642-92847-5_2
20. Priester WA, Mantel N. Occurrence of tumors in domestic animals. Data from 12 United States and Canadian colleges of veterinary medicine. *J Natl Cancer Inst*. 1971;47:1333–1344.
21. Song RB, Vite CH, Bradley CW, Cross JR. Postmortem evaluation of 435 cases of intracranial neoplasia in dogs and relationship of neoplasm with breed, age, and body weight. *J Vet Intern Med*. 2013;27:1143–52. <http://dx.doi.org/10.1111/jvim.12136>
22. Klotz M. Incidence of brain tumors in patients hospitalized for chronic mental disorders. *Psychiatr Q*. 1957;31:669–80. <http://dx.doi.org/10.1007/BF01568758>
23. Snyder JM, Shofer FS, Van Winkle TJ, Massicotte C. Canine intracranial primary neoplasia: 173 cases (1986–2003). *J Vet Intern Med*. 2006;20:669–75.
24. Hayes HM, Priester WA, Pendergrass TW. Occurrence of nervous-tissue tumors in cattle, horses, cats and dogs. *Int J Cancer*. 1975;15:39–47. <http://dx.doi.org/10.1002/ijc.2910150106>
25. Truve K, Dickinson P, Xiong A, York D, Jayashankar K, Peilberg G, et al. Utilizing the dog genome in the search for novel candidate genes involved in glioma development—Genome wide association mapping followed by targeted massive parallel sequencing identifies a strongly associated locus. *PLoS Genet*. 2016;12(5):e1006000. <http://dx.doi.org/10.1371/journal.pgen.1006000>

26. Platt SR, Radaelli ST, McDonnell JJ. The prognostic value of the modified Glasgow Coma Scale in head trauma in dogs. *J Vet Int Med.* 2001;15(6):581–584. <http://dx.doi.org/10.1111/j.1939-1676.2001.tb01594.x>
27. Valladao ML, Scarpelli KC, Metze K. Clinical utility of a life quality score in dogs with canine transmissible venereal tumor treated by vincristine chemotherapy. *Arq Bras Med Vet Zootec.* 2010;62(5):1086–1093. <http://dx.doi.org/10.1590/S0102-09352010000500010>
28. Rossmeisl JH, Garcia PA, Pancotto TE, Robertson JL, Henaó-Guerrero N, Neal RE, et al. Safety and feasibility of the NanoKnife system for irreversible electroporation ablative treatment of canine spontaneous intracranial gliomas. *J Neurosurg.* 2015;123(4):1008–1025. <http://dx.doi.org/10.3171/2014.12.JNS141768>
29. Bagley RS, Gavin PR, Moore MP, Silver GM, Harrington ML, Connors RL. Clinical signs associated with brain tumors in dogs: 97 cases (1992–1997). *J Am Vet Med Assoc.* 1999;215:818–819.
30. Iliopoulou MA, Kitchell BE, Yuzbasiyan-Gurkan V. Development of a survey instrument to assess health-related quality of life in small animal cancer patients treated with chemotherapy. *J Am Vet Med Assoc.* 2013;242(12):1679–87.
31. Lipsitz D, Higgins RJ, Kortz ZD, Dickinson PJ, Bollen AW, Nayadan DK, et al. Glioblastoma multiforme: Clinical findings, magnetic resonance imaging, and pathology in five dogs. *Vet Pathol.* 2003;40:659–69. <http://dx.doi.org/10.1354/vp.40-6-659>
32. Stoica G, Kim HT, Hall DG, Coates JR. Morphology, immunohistochemistry, and genetic alterations in dog astrocytomas. *Vet Pathol.* 2004;41:10–19. <http://dx.doi.org/10.1354/vp.41-1-10>
33. Stoica G, Levine J, Wolff J, Murphy K. Canine astrocytic tumors: A comparative review. *Vet Pathol.* 2011;48(1):266–75. <http://dx.doi.org/10.1177/0300985810389543>
34. Young BD, Levine JM, Porter BF, Chen-Allen AV, Rossmeisl J, Platt SR, et al. Magnetic resonance imaging features of intracranial astrocytomas and oligodendrogliomas in dogs. *Vet Radiol Ultrasound.* 2011;52:132–41. <http://dx.doi.org/10.1111/j.1740-8261.2010.01758.x>
35. Rossmeisl JH, Clapp K, Pancotto TE, Emch S, Robertson JL, Debinski W. Canine butterfly glioblastomas: A neuroradiological review. *Front Vet Sci.* 2016;3:40.
36. Louis DN, Ohgaki H, Wiestler OD, Cavenee WK, Burger PC, et al. The 2007 WHO classification of tumours of the central nervous system. *Acta Neuropathologica.* 2007;114:97–109. <http://dx.doi.org/10.1007/s00401-007-0243-4>
37. Ostrom QT, Gittleman H, Fulop J, Liu M, Blanda R, Kromer C, et al. CBTRUS statistical report: Primary brain and central nervous system tumors diagnosed in the United States in 2008–2012. *Neuro Oncol.* 2015;17(S4):iv1–iv62. <http://dx.doi.org/10.1093/neuonc/nov189>
38. Verhaak RG, Hoadley KA, Purdom E, Wang V, Qi Y, Wilkerson MD, et al. Integrated genomic analysis identifies clinically relevant subtypes of glioblastoma characterized by abnormalities in PDGFRA, IDH1, EGFR, and NF1. *Cancer Cell.* 2010;17:98–110. <http://dx.doi.org/10.1016/j.ccr.2009.12.020>
39. Cancer Genome Atlas Research Network. Comprehensive genomic characterization defines human glioblastoma genes and core pathways. *Nature.* 2008;455:1061–1068. <http://dx.doi.org/10.1038/nature07385>
40. Boudreau CE, York D, Higgins RJ, LeCouteur RA, Dickinson PJ. Molecular signalling pathways in canine gliomas. *Vet Comp Oncol.* 2017;15(1):133–50. <http://dx.doi.org/10.1111/vco.12147>
41. York D, Higgins RJ, LeCouteur RA, Wolfe AN, Grahn R, Olby N, et al. TP53 mutations in canine brain tumors. *Vet Pathol.* 2012;49:796–801. <http://dx.doi.org/10.1177/0300985811424734>
42. Ide T, Uchida K, Kikuta F, Suzuki K, Nakayama H. Immunohistochemical characterization of canine neuroepithelial tumors. *Vet Pathol.* 2010;47:741–50. <http://dx.doi.org/10.1177/0300985810363486>
43. Higgins RJ, Dickinson PJ, Lecouteur RA, Bollen AW, Wang H, Corely LJ, et al. Spontaneous canine gliomas: Overexpression of EGFR, PDGFRalpha and IGF2 demonstrated by tissue microarray immunophenotyping. *J Neuro Oncol.* 2009;98:49–55. <http://dx.doi.org/10.1007/s11060-009-0072-5>
44. Dickinson PJ, Roberts BN, Higgins RJ, Leutenegger CM, Bollen AW, Kass PH, et al. Expression of receptor tyrosine kinases VEGFR-1 (FLT-1), VEGFR-2 (KDR), EGFR-1, PDGFRalpha and c-Met in canine primary brain tumours. *Vet Comp Oncol.* 2006;4:132–40. <http://dx.doi.org/10.1111/j.1476-5829.2006.00101.x>
45. Dickinson PJ, Sturges BK, Higgins RJ, Roberts BN, Leutenegger CM, Bollen AW, et al. Vascular endothelial growth factor mRNA expression and peritumoral edema in canine primary central nervous system tumors. *Vet Pathol.* 2008;45:131–9. <http://dx.doi.org/10.1354/vp.45-2-131>

46. Rossmeisl JH, Duncan RB, Huckle WR, Troy GC. Expression of vascular endothelial growth factor in tumors and plasma from dogs with primary intracranial neoplasms. *Am J Vet Res.* 2007;68:1239–45. <http://dx.doi.org/10.2460/ajvr.68.11.1239>
47. Gibo DM, Debinski W, Bonomo J, Rossmeisl J, Robertson J, Dickinson P, et al. Interleukin 13 receptor alpha-2 is widely over-expressed in human and canine primary brain tumors as detected by novel bispecies-specific monoclonal antibodies. *Neuro Oncol.* 2012;14:vi47.
48. Debinski W, Dickinson P, Rossmeisl JH, Robertson J, Gibo DM. New agents for targeting of IL-13RA2 expressed in primary human and canine brain tumors. *PLoS One.* 2013;8:e77719. <http://dx.doi.org/10.1371/journal.pone.0077719>
49. Sturges BK, Dickinson PJ, Aina OH, York D, LeCouteur RA, Lam KS. Identification of novel targeting peptides for canine glioma. *J Vet Intern Med.* 2008;22:771.
50. Mariani CJ, Mariani CJ. Matrix metalloproteinase-2 and -9 in canine central nervous system tumors. In: *Proceedings of the American College of Veterinary Internal Medicine Forum, New Orleans, LA, May 30–June 2, 2012*, p. 421.
51. Rossmeisl JH. Exploiting proteases and their inhibitors as targets for the treatment of canine brain tumors. In: *Proceedings of the American College of Veterinary Internal Medicine Forum, Denver, CO, June 8–11, 2016*, pp. 518–21.
52. Platt S, Nduom E, Kent M, Freeman C, Machaidze R, Kaluzova M, et al. Canine model of convection-enhanced delivery of cetuximab-conjugated iron-oxide nanoparticles monitored with magnetic resonance imaging. *Clin Neurosurg.* 2012;59:107–13. <http://dx.doi.org/10.1227/NEU.0b013e31826989ef>
53. Betensky RA, Louis DN, Cairncross JG. Influence of unrecognized molecular heterogeneity on randomized clinical trials. *J Clin Oncol.* 2002;20:2495–9. <http://dx.doi.org/10.1200/JCO.2002.06.140>
54. Reitman ZJ, Olby NJ, Mariani CL, Thomas R, Breen M, Bigner DD, et al. IDH1 and IDH2 hotspot mutations are not found in canine glioma. *Int J Cancer.* 2010;127:245–6. <http://dx.doi.org/10.1002/ijc.25017>
55. Thomas R, Duke SE, Wang HJ, Breen TE, Higgins RJ, Linder KE, et al. “Putting our heads together”: Insights into genomic conservation between human and canine intracranial tumors. *J Neurooncol.* 2009;94:333–49. <http://dx.doi.org/10.1007/s11060-009-9877-5>
56. Pluhar GE, Grogan PT, Seiler C, Goulart M, Sanatcruz KS, Carlson C, et al. Anti-tumor immune-response correlates with neurological symptoms in a dog with spontaneous astrocytoma treated by gene and vaccine therapy. *Vaccine.* 2010;28:3371–8. <http://dx.doi.org/10.1016/j.vaccine.2010.02.082>
57. CBS Interactive, Inc. Man’s best friend: Key to brain cancer cure? CBS News (www.cbsnews.com). 2011. Available from: <http://www.cbsnews.com/video/watch?id=7390631n&tag=cbsnewsMainColumnArea> (accessed January 5, 2017).
58. Andersen BM, Pluhar GE, Seiler CE, Goulart MR, Sanatacruz KS, Schutten MM, et al. Vaccination for invasive canine meningioma induces in situ production of antibodies capable of antibody-dependent cell-mediated cytotoxicity. *Cancer Res.* 2013;73:2987–97. <http://dx.doi.org/10.1158/0008-5472.CAN-12-3366>
59. Dickinson PJ, LeCouteur RA, Higgins RJ, Bringas JR, Roberts B, Larson RF, et al. Canine model of convection-enhanced delivery of liposomes containing CPT-11 monitored with real-time magnetic resonance imaging: Laboratory investigation. *J Neurosurg.* 2008;108:989–98. <http://dx.doi.org/10.3171/JNS/2008/108/5/0989>
60. Dickinson PJ, LeCouteur RA, Higgins RJ, Bringas JR, Larson RF, Yamashita Y, et al. Canine spontaneous glioma: A translational model system for convection-enhanced delivery. *Neuro Oncol.* 2010;12:928–40. <http://dx.doi.org/10.1093/neuonc/noq046>
61. Varenika V, Dickinson PJ, Bringas J, LeCouteur R, Higgins R, Park J, et al. Detection of infusate leakage in the brain using real-time imaging of convection-enhanced delivery. *J Neurosurg.* 2008;109:874–80. <http://dx.doi.org/10.3171/JNS/2008/109/11/0874>
62. Bobo RH, Laske DW, Akbasak A, Morrison PF, Dedrick RL, Oldfield EH. Convection-enhanced delivery of macromolecules in the brain. *Proc Natl Acad Sci U S A.* 1994;91:2076–80. <http://dx.doi.org/10.1073/pnas.91.6.2076>
63. Vogelbaum MA. Convection-enhanced delivery for treating brain tumors and selected neurological disorders: A review. *J Neurooncol.* 2007;83:97–109. <http://dx.doi.org/10.1007/s11060-006-9308-9>

64. Debinski W, Tatter SB. Convection-enhanced delivery for the treatment of brain tumors. *Exp Rev Neurother*. 2009;9:1519–27. <http://dx.doi.org/10.3171/jns.1995.82.6.1021>
65. Lieberman DM, Laske DW, Morrison PF, Bankiewicz KS, Oldfield EH. Convection-enhanced distribution of large molecules in gray matter during interstitial drug infusion. *J Neurosurg*. 1995;82:1021–9.
66. Sampson JH, Archer G, Pedain C, Wembacher-Schroder E, Westphal M, Kunwar S, et al. Poor drug distribution as a possible explanation for the results of the PRECISE trial. *J Neurosurg* 2010;113:301–9. <http://dx.doi.org/10.3171/2009.11.JNS091052>
67. Kunwar S, Chang S, Westphal M, Vogelbaum M, Sampson J, Barnett G, et al. Phase III randomized trial of CED of IL13-PE38QQR vs Gliadel wafers for recurrent glioblastoma. *Neuro Oncol*. 2010;12(8):871–81. <http://dx.doi.org/10.1093/neuonc/nop054>
68. Gibo DM, Dickinson P, Robertson J, et al. Highly potent toxin targeting IL-13Ra2 in canine and human glioblastoma. *Neuro Oncol*. 2012;14:vi31–2.
69. Debinski W, Dickinson PJ, Rossmeisl JH, Robertson JL, Gibo DM. Canine gliomas over-express IL-13Ralpha2, EphA2 and Fra-1 in common with human high-grade astrocytomas. *Neuro Oncol*. 2009;9:535.
70. Sampson JH, Raghaven R, Brady ML, Provenzale JM, Herndon JE, II, Croteau D, et al. Clinical utility of a patient-specific algorithm for simulating intracerebral drug infusions. *J Neurocol*. 2007;9:343–53. <http://dx.doi.org/10.1215/15228517-2007-007>
71. Rosenbluth KH, Martin AJ, Mittermeyer S, Eschermann J, Dickinson PJ, Bankiewicz KS. Rapid inverse planning for pressure-driven drug infusions in the brain. *PLoS One*. 2013;8(2):e56397. <http://dx.doi.org/10.1371/journal.pone.0056397>
72. Rossmeisl JH, Garcia PA, Daniel GB, Bourland JD, Debinski W, Dervisis N, et al. Invited review—Neuroimaging response assessment criteria for brain tumors in veterinary patients. *Vet Radiol Ultrasound*. 2014;55:115–132. <http://dx.doi.org/10.1111/vru.12118>
73. Davalos RV, Mir LM, Rubinsky B. Tissue ablation with irreversible electroporation. *Ann Biomed Eng*. 2005;33:223–31. <http://dx.doi.org/10.1007/s10439-005-8981-8>
74. Al-Sakere B, Andre F, Bernat C, Connault E, Opolon P, Davalos RV, et al. Tumor ablation with irreversible electroporation. *PLoS One*. 2007;2:e1135. <http://dx.doi.org/10.1371/journal.pone.0001135>
75. Rubinsky B. Irreversible electroporation in medicine. *Technol Cancer Res Treat*. 2007;6:255–9. <http://dx.doi.org/10.1177/153303460700600401>
76. Neal RE, II, Rossmeisl JH, Jr, Garcia PA, Lanz OI, Henao-Guerrero N, Davalos RV. Successful treatment of a large soft-tissue sarcoma with irreversible electroporation. *J Clin Oncol*. 2011;29:e372–7. <http://dx.doi.org/10.1200/JCO.2010.33.0902>
77. Garcia PA, Pancotto TE, Rossmeisl JH, Jr, Henao-Guerrero N, Gustafson NR, Daniel GB, et al. Non-thermal irreversible electroporation (N-TIRE) and adjuvant fractionated radiotherapeutic multimodal therapy for intracranial malignant glioma in a canine patient. *Technol Cancer Res Treat*. 2011;10:73–83. <http://dx.doi.org/10.7785/tcrt.2012.500181>
78. Thomson KR, Cheung W, Ellis SJ, Fdereman D, Kavnoudias H, Loader-Oliver D, et al. Investigation of the safety or irreversible electroporation in humans. *J Vasc Interv Radiol*. 2011;22(5):611–21. <http://dx.doi.org/10.1016/j.jvir.2010.12.014>
79. Ellis TL, Garcia PA, Rossmeisl JH, Henao-Guerrero N, Robertson J, Davalos RV. Nonthermal irreversible electroporation for intracranial surgical applications: Laboratory investigation. *J Neurosurg*. 2011;114:681–8. <http://dx.doi.org/10.3171/2010.5.JNS091448>
80. Arena CB, Sano MB, Rossmeisl JH, Caldwell JL, Garcia PA, Rylander MN, et al., High-frequency irreversible electroporation (H-FIRE) for non-thermal ablation without muscle contraction. *Biomed Eng Online*. 2011;10(1):102. <http://dx.doi.org/10.1186/1475-925X-10-102>
81. Arena CB, Sano MB, Rylander MN, Davalos RV. Theoretical considerations of tissue electroporation with high-frequency bipolar pulses. *IEEE Trans Biomed Eng*. 2011;58(5):1474–82. <http://dx.doi.org/10.1109/TBME.2010.2102021>
82. Ivey JW, Latouche EL, Sano MB, Rossmeisl JH, Davalos RV, Verbridge SS. Targeted cellular ablation based on the morphology of malignant cells. *Sci Rep*. 2015;5:17157. <http://dx.doi.org/10.1038/srep17157>
83. Garcia PA, Rossmeisl JH, Jr, Robertson JL, Olson JD, Johnson AJ, Ellis TL, et al. 7.0-T magnetic resonance imaging characterization of acute blood-brain-barrier disruption achieved with

- intracranial irreversible electroporation. *PLoS One*. 2012;7:e50482. <http://dx.doi.org/10.1371/journal.pone.0050482>
84. Hjouj MD, Last D, Guez D, Daniels D, Sharabi S, Lavee J, et al. MRI study on reversible and irreversible electroporation induced blood brain barrier disruption. *PLoS One*. 2012;7:e42817. <http://dx.doi.org/10.1371/journal.pone.0042817>
 85. Arena CB, Garcia PA, Sano MB, Olson JD, Rogers-Cotrone T, Rossmeisl JH, Jr, et al. Focal blood-brain-barrier disruption with high-frequency pulsed electric fields. *Technology*. 2014;2(3):206–13. <http://dx.doi.org/10.1142/S2339547814500186>
 86. Rossmeisl JH, Jr, Garcia PA, Pancotto TE, Robertson JL, Henao-Guerrero N, Neal RE, et al. Safety and feasibility of the Nanoknife system for irreversible electroporation ablative treatment of canine spontaneous intracranial gliomas. *J Neurosurg*. 2015;123(4):1008–25. <http://dx.doi.org/10.3171/2014.12.JNS141768>
 87. Zupanic A, Kos B, Miklavcic D. Treatment planning of electroporation-based medical interventions: Electrochemotherapy, gene electrotransfer and irreversible electroporation. *Phys Med Biol*. 2012;57(17):5425. <http://dx.doi.org/10.1088/0031-9155/57/17/5425>
 88. Corovic S, Lackovic I, Sustaric P, Sustar T, Rodic T, Miklavcic D. Modeling of electric field distribution in tissues during electroporation. *BioMed Eng Online*. 2013;12(1):1–27. <http://dx.doi.org/10.1186/1475-925X-12-16>
 89. Rossmeisl JH, Garcia PA, Robertson JL, Ellis TL, Davalos RV. Pathology of non-thermal irreversible electroporation (N-TIRE) induced ablation of the canine brain. *J Vet Sci*. 2013;14(4):433–40. <http://dx.doi.org/10.4142/jvs.2013.14.4.433>
 90. Garcia PA, Kos B, Rossmeisl Jr., JH, Pavliha D, Miklavcic D, Davalos RV. Predictive therapeutic planning for irreversible electroporation treatment of spontaneous malignant glioma. *Med Phys* 2017; e-pub 6/8/17; doi:10.1002/mp.12401
 91. Marčan M, Pavliha D, Kos B, Forjanič T, Miklavčič D. Web-based tool for visualization of electric field distribution in deep-seated body structures and planning of electroporation-based treatments. *BioMed Eng Online*. 2015;14(Suppl 3):S4. <http://dx.doi.org/10.1186/1475-925X-14-S3-S4>
 92. Garcia PA, Davalos RV, Miklavcic D. A numerical investigation of the electric and thermal cell kill distributions in electroporation-based therapies in tissue. *PLoS One*. 2014;9:e103083. <http://dx.doi.org/10.1371/journal.pone.0103083>
 93. Kranjc M, Bajd F, Sersa I, Woo EJ, Miklavcic D: Ex Vivo and in silico feasibility study of monitoring electric field distribution in tissue during electroporation based treatments. *PLoS One*. 2012;7:e45737. <http://dx.doi.org/10.1371/journal.pone.0045737>
 94. Lynn JG, Zwemer RL, Chick AJ, Miller AE. A new method for the generation and use of focused ultrasound in experimental biology. *J Gen Physiol*. 1942;26:179–93. <http://dx.doi.org/10.1085/jgp.26.2.179>
 95. Barnard JW, Fry WJ, Fry FJ, Krumins RF. Effects of high intensity ultrasound on the central nervous system of the cat. *J Comp Neurol*. 1955;103:459–84. <http://dx.doi.org/10.1002/cne.901030304>
 96. Fry WJ, Brennan JF, Barnard JW. Histological study of changes produced by ultrasound in the gray and white matter of the central nervous system. *Ultrasound Med Biol*. 1957;3:110–30.
 97. Astrom KE, Belle, Ballantine HT, Heidensleben E. An experimental neuropathological study of the effects of high-frequency focused ultrasound on the brain of the cat. *J Neuropathol Exp Neurol*. 1961;20:484–520. <http://dx.doi.org/10.1097/00005072-196120040-00002>
 98. Meyers R, Fry WJ, Fry FJ, Dreyer LL, Schultz DF, Noyes RF. Early experiences with ultrasonic irradiation of the pallidum and nigral complexes in hyperkinetic and hypertonic disorders. *J Neurosurg*. 1959;16:32–54. <http://dx.doi.org/10.3171/jns.1959.16.1.0032>
 99. Hickey RC, Fry WJ, Meyers R, Fry FJ, Bradbury JT. Human pituitary irradiation with focused ultrasound. An initial report on effect in advanced breast cancer. *Arch Surg*. 1961;83:620–33. <http://dx.doi.org/10.1001/archsurg.1961.01300160132016>
 100. Tung YS, Marquet F, Teichert T, Ferrera V, Konofagou EE. Feasibility of noninvasive cavitation-guided blood-brain barrier opening using focused ultrasound and microbubbles in nonhuman primates. *Appl Phys Lett*. 2011;98:163704. <http://dx.doi.org/10.1063/1.3580763>

101. Fry FJ, Goss SA. Further studies of the transskull transmission of an intense focused ultrasonic beam: Lesion production at 500 kHz. *Ultrasound Med Biol.* 1980;6:33–8. [http://dx.doi.org/10.1016/0301-5629\(80\)90061-7](http://dx.doi.org/10.1016/0301-5629(80)90061-7)
102. Leinenga G, Langton C, Nisbet R, Gotz J. Ultrasound treatment of neurological diseases-current and emerging applications. *Nat Rev Neurol.* 2016;12:161–74. <http://dx.doi.org/10.1038/nrneurol.2016.13>
103. Ishihara Y, Calderon A, Watanabe H, Okamoto K, Suzuki Y, Kuroda K. A precise and fast temperature mapping using water proton chemical shift. *Magn Reson Med.* 1995;34:814–23. <http://dx.doi.org/10.1002/mrm.1910340606>
104. Xu Z, Ludomirsky A, Eun LY, Hall TL, Tran BC, Fowlkes JB, et al. Controlled ultrasound tissue erosion. *IEEE Trans Ultrason Ferroelectr Freq Control.* 2004;51(6):726–36. <http://dx.doi.org/10.1109/TUFFC.2004.1308731>
105. Hynynen K. Focused ultrasound for blood-brain disruption and delivery of therapeutic molecules to the brain. *Expert Opin Drug Deliv.* 2007;4(1):27–35.
106. Zhi R, Cohen ZR, Harnof S, Tal S, Faibel M, Nass D, et al. Magnetic resonance image-guided, high-intensity focused ultrasound for brain tumor therapy. *Neurosurgery.* 2006;59(5):949–56.
107. Hynynen K, Jolesz FA. Demonstration of potential noninvasive ultrasound brain therapy through an intact skull. *Ultrasound Med Biol.* 1998;24:275–83. [http://dx.doi.org/10.1016/S0301-5629\(97\)00269-X](http://dx.doi.org/10.1016/S0301-5629(97)00269-X)
108. Sun J, Hynynen K. The potential of transskull ultrasound therapy and surgery using the maximum available skull surface area. *J Acoust Soc Am.* 1999;105:2519–27. <http://dx.doi.org/10.1121/1.426863>
109. Coluccia D, Fandino J, Schwyzer L, O’Gorman R, Remonda L, Anon J, et al. First non-invasive thermal ablation of a brain tumor with MR-guided focused ultrasound. *J Ther Ultrasound.* 2014;2:17. <http://dx.doi.org/10.1186/2050-5736-2-17>
110. Marquet F, Teichert T, Wu Y-S, Downs M, Wang S, Chen C, et al. Real-time transcranial monitoring of safe blood-brain barrier opening in non-human primates. *PLoS One.* 2014;9:e84310. <http://dx.doi.org/10.1371/journal.pone.0084310>

Index

¹⁸FET-PET, 163
¹⁸F-Fluorodeoxyglucose PET, 180
¹⁸F-Fluoromethylcholine, 185
¹⁸F-Fluorothymidine, 186
1p/19q, 32
3D reconstruction, 386
5-ALA, 199, 200, 246–248, 289, 290

A

Acoustic energy, 416
Actin rearrangement, 79
Adhesion complexes, 79
Age, 145
Age at recurrence, 287
Amino-acid PET, 182
Anatomic prevalence, 29
Angiogenesis, 5–9, 95–97, 99, 101–104,
114, 306, 318, 319, 323–325
Angiogenesis inhibitors, 20, 306
Animal trials, 387
Apoptosis, 118
Arborizing catheter, 359
ATRX, 32
Autophagy, 61
Auxonal guidance molecules, 80
Axial T2-weighted MRI, 265

B

Bevacizumab, 203, 207–209, 216
Biomarkers, 16, 18, 100
Biopsy, 160
Bipolar probe, 376
Blood-brain barrier, 343, 395

Blood-brain barrier disruption, 380
Blue excitation light, 248
Brachytherapy, 206

C

Cadherins, 83
Cathereters, 362
Cell proliferation, 112, 118
Cell sorting, 65
Cell-line xenografts, 132
Cellular protrusions, 79
Cerebral gliomas, 263
Chemotherapy, 223, 292, 305
Chondroitin sulfate proteoglycans, 78
Classification, 9, 146
Clinical features, 302
Clinical outcome, 283
Clinical practice, 155
Clinical trials, 16, 203, 208, 209,
211–214, 217–221
Clinically relevant model, 405
Combination regimens, 207, 210, 216
Combination treatment, 206
Complementary treatment, 200
Complications, 290
Confusion, 226
Contrast-enhanced MRI, 181
Controllable drug delivery, 397
Convection-enhanced delivery,
359, 411
Copy number aberrations, 13
Cortical mapping, 263
Current standards, 197
Cytoreduction, 291

Cytoskeleton, 78

Cytotoxic therapy, 341

D

Depression, 226

Deregulated lncRNAs, 109

Deregulated miRNAs, 101

Differential diagnosis, 157

Differentiation, 178

Diffuse glioma, 74

Direct cortical stimulation, 276

DNA methylation, 44, 63

Dose-fractionation schedule, 201

Drug resistance, 115

E

EA5-Fc-PE38QQR, 349

ECM, 322

Effect of treatment, 35

EGFR/PTEN/AKT/mTOR pathway, 34

Electric stimulation mapping, 275

Eloquent cortex, 270

EMT, 82

EOL care, 226

Eph receptors, 349

EphA2, 344, 345

EphA3 receptor, 346

Ephrins, 81

Epidemiology, 29, 143, 298

Epigenetic mechanisms, 43

Epigenetic regulation, 62

Epigenome, 10

Epithelial to mesenchymal transition, 8

Ethnicity, 146

Extent of resection, 246, 289

External beam radiation, 201

Extracellular matrix, 76

F

FET-PET, 163

Fluorescence-guided surgery, 246

Fluorophores, 247

Follow-up, 162

Fractionated radiation, 206

Functional MRI, 266

Functional tests, 64

Future perspectives, 165

G

Galectins, 78

GBM vasculature, 318

G-CIMP, 33

Gender, 145

Gene ontology, 46

Genetic alterations, 5

Genetically engineered mouse
models, 134

Genetics, 34

Genome, 10

Genomic abnormalities, 9

Genomic landscape, 12

Genomics, 3

Gliadel wafer, 19

Glial cell compartment, 320

Glioblastoma, 3, 27, 43, 59, 73, 95, 131,
143, 155, 175, 243

Glioblastoma in the elderly, 222

Glioblastoma models, 327

Glioblastoma therapy, 197

Glioma cell migration, 80

Glioma cell motility, 73

Glioma extent, 159

Glioma initiation, 32

Glioma progression, 34

Glioma stem cells, 319

Glioma subtypes, 12
Glioma transformation, 35
Gliomagenesis, 31
Glutamate signaling, 80
Glycoproteins, 78
Go or grow, 75
Growth factor receptor inhibitors, 19
GSC differentiation, 119
GSCS, 108

H

Heterogeneous nature, 316
High-frequency irreversible
 electroporation, 373, 415
High-intensity focused
 ultrasound, 396
Histone modifications, 62
Hydrodynamic model, 80
Hypermethylated genes, 46
Hypermethylation, 47
Hypomethylation, 48, 53
Hypoxia, 75
Hypoxia-PET, 186

I

IDH, 32
IL-13RA2, 344
IL-13RA2, 345
Image-guided, 395
Immune cells, 321, 331
Immune evasion, 115
Implantable wafers, 201
Improving resection, 290
Incidence, 144
IncRNAs, 118
Indocyanine green, 247
Infiltration, 74

Infusion distribution, 367
Inherent section bias, 283
Intertentorial approaches, 253
Integrins, 77
Interstitial fluids, 323
Intracranial pressure, 226
Intraoperative technologies, 246
Intraoperative videoangiography, 249
Intratumor heterogeneity, 6
Intravenous anesthetics, 245
Invasion, 114, 119
Ion channels, 80
Irreversible electroporation, 373, 413

K

Karnofsky performance scale, 284

L

LNCRNA, 53
Long Coding RNAs, 117

M

MacDonald criteria, 175, 177,
 178, 207
Magnetic resonance imaging, 264
Magnetoencephalography, 267
Maintenance therapy, 201
MassARRAY, 49
Material properties, 385
Matrix metalloproteinases, 77
Maximizing local access, 341, 357,
 373, 395, 405
MeDIP-Chip, 46
Methylomes, 44
Microenvironment, 315
MicroRNAs, 97

Microscopic features, 299
 Migration, 114, 119
 Minimal residual disease, 292
 miR-101, 53
 miRNA, 51, 53
 MiRNA biogenesis, 98
 MiRNA deregulation, 97
 miRNA therapeutics, 116
 Miscellaneous agents, 20
 Molecular biology, 299, 300
 Molecular classification, 30
 Molecular genetics, 27
 Molecular landscape, 30
 Molecular mechanisms, 73
 Monopolar probe, 376
 Monotherapy, 207, 210, 216
 Mouse models, 131
 Multimodality, 165
 Muscle relaxants, 246
 Mutated genes, 13

N

Netrins, 81
 Neuroimaging, 302
 Neuronavigation, 250
 Neuropsychological assessment, 268
 New therapeutic approaches, 405
 Newer drugs, 307
 Nitrosourea, 207–209
 Noncoding RNA, 95
 Novel PET tracers, 187
 Novel Radiotracers, 165

O

Opening of the BBB, 396
 Optimization of catheters, 361
 Outcome, 143, 149, 307

P

PI61NK4A/RB1 pathway, 35
 Park bench position, 255
 Pathogenesis, 4
 Pathological variants, 300
 Pathology, 299
 Patient position, 250
 Patient-derived xenografts, 133
 Pediatric glioblastoma, 297
 Perioperative evaluation, 245
 PET, 175
 PET imaging, 155
 Pore formation, 376
 Positron emission tomography, 268
 Postoperative care, 257
 Preclinical, 387, 411
 Preoperative planning, 264
 Primary diagnosis, 157
 Primary GBM, 10
 Prognostic factors, 148, 149
 Prognostication, 165
 Progression, 162
 Prone position, 253
 Pseudoprogression, 162

Q

QUAD-CTX, 350, 351

R

Radiation, 37, 161
 Radiation therapy, 305
 Radiological diagnosis, 282
 Radionecrosis, 162
 Radiotherapy, 223
 RANO criteria, 175, 178, 185, 283
 Recurrence, 178
 Recurrent glioblastoma, 204

Recurring glioblastoma, 281
Re-irradiation, 205
Remote-controlled, 395
Reoperation, 281
Resection, 160, 263
Resistance, 119
Reversible electroporation, 375
Risk factors, 148

S

Scales to predict survival, 289
Secondary GBM, 10
Secondary glioblastoma, 27
Second-line chemotherapy, 207
Secreted mRNAs, 100
Sedimentation field-flow
 fractionation, 65
Seizures, 225
Semaphorins, 81
Seven ports, 365
Shadowgraphy, 364
Single port, 365
Single-port microneedle catheter, 363
Site, 145
Sitting position, 254
SLIT/ROBO, 81
SLUG, 83
Small GTPases, 78
SNAIL, 83
Soluble factors, 323
Somatic mutation, 12
Somatosensory evoked potentials, 275
Spontaneous canine gliomas, 407
Standards of care, 197
Stem cell identification, 61
Stem cells, 397
Stem-like cells, 59
Stemness, 112

Stereostatic glioblastoma ablation, 414
Stereostatic radiosurgery, 205
Stupp protocol, 60, 243
Subclassification, 291
Supine position, 251
Supportive care, 225
Supportive environment, 317
Supratentorial approaches, 251
Surface anatomical landmarks, 269
Surgery, 198, 223, 304
Surgical considerations, 268
Surgical management, 243
Surgical navigation, 274
Surgical risks, 290
Surgical series, 284
Surgical technique, 273
Survival, 148
Syngenic mouse models, 135
Systemic brain tumor therapy,
 395, 396

T

Targeted therapeutic agents, 17
Targeted therapy, 202, 306
Temozolamide, 18, 19, 36, 200, 201,
 203, 210, 211
Temperature profile, 385
TERT, 33
TGF- β , 82
Therapeutic deliveries, 341, 359, 373,
 395, 405
Therapeutic prediction, 16
Therapeutic response, 119
Therapeutic targeting, 330
Therapy, 395
Therapy response assessment, 175, 177
Tissue diagnosis, 291
Tissue mechanics, 322

Tissue phantoms, 359
TP53, 32
TP53/MDM2/P14ARF pathway, 35
Transcortical magnetic stimulation, 267
Transcriptome, 10
Treatment, 176
Treatment planning, 160, 382
Treatment response, 162
Treatment routes, 325
Treatment-related effects, 178
Tumor cell, 315
Tumor microenvironment, 318, 328, 329
Tumor-treating electric fields, 221
TWIST, 83

V

Vascular endothelial growth factor, 301
Vasculature, 330
Viability, 112

W

White light, 248

X

Xenografts, 132

Z

ZEB, 83

Doi: <http://dx.doi.org/10.15586/codon.glioblastoma.2017.ind>